An investigation of Macroamphiphile Composition and Biosynthesis in Representative Actinomycete Bacteria

MD. OBAIDUR RAHMAN

Doctor of Philosophy
(PhD)

2008

An investigation of Macroamphiphile Composition and Biosynthesis in Representative Actinomycete Bacteria

MD. OBAIDUR RAHMAN
Supervisor: Professor Iain Sutcliffe

A thesis submitted in partial fulfillment of the requirements of the University of Northumbria at Newcastle for the degree of Doctor of Philosophy

Research undertaken in the School of Applied Science

2008

DEDICATION

I would like to dedicate my thesis to my beloved parents

Your talent is God's gift to you,

What you do with it is your gift back to God.

-Leo Buscaglia

Declaration

I declare that the work contained in this thesis has not been submitted for any other award and that it is all my own work.

Name: Md. Obaidur Rahman

Signature:

Date:

Acknowledgment(s)

This thesis is dedicated to my parents who taught me to love learning and always made my education prior to their top priorities.

My gratitude to everyone in the School of Applied Science, Northumbria University, especially the lab A307, A301 and A310 for being friendly and supportive during my three and half year's studies. Everyone in the lab A307 has been selflessly supportive to my own particular research interests. My supervisor, Prof. Iain C. Sutcliffe, not only found me a project that fits my interest but also encouraged me to become an independent and confident researcher and providing me with all educational and financial requirements for my project. For his support I am exceptionally grateful owing to the fact few supervisors had given their students more trust and freedom. Iain has also shrewdly guided my bioinformatics analysis and research; he recognised the significance of my matching bioinformatics work and provided the ideas for its applications in this thesis and still guiding me for my future work.

The rest of the Bio-applied science faculty and staff have also supported my education and research. Dr. Stephen Cummings and Dr. Amanda L. Jones (Newcastle University, UK) has helped me to produce phylogenectic tree. Dr. Justin Perry has helped me with chemistry and Dr. Meng, Dr. Anna and Dr. Mandy who were not only my well wishers but were also advisers of my different practical works. My fellow PhD students (Ben, Yang, Claire and Lakshmy and other present students in Lab A307) have also greatly contributed to my success by sharing data, ideas, suggestions for paper revisions, and meaningful friendship. Yang has also been very kind in helping me to complete my 2D gels data...my sincere and magnanimous thanks to them.

I would like to thank Dr JérômeNigou (CNRS, Inst Pharmacol & Biol Struct, UPR 9062, F-31077 Toulouse, France) for MALDI/MS analysis and Dr Markus Pfitzenmaier (Philipps-Universität Marburg, Germany) for doing NMR analysis for me. Professor David Wilson and Dr Diane Irwin (Department of Molecular Biology and Genetics, Cornell University, U.S.A.), Professor Milton da Costa (Departamento de Bioquímica, Universidade de Coimbra, Portugal), Dr. Christopher Bagwell (Environmental Biotechnology, Savannah River National Laboratory, Aiken, SC, USA) and Dr Dean Harrington (University of Bradford, UK) have helped in my research by providing me the organisms. Professor Ken Knox (Institute of Dental Research, Sydney, Australia) and Prof. Walsh also played an extremely important role in my research for supplying me with the polyclonal and monoclonal anti-LTA.

Finally, I would like to thank Northumbria University for providing an opportunity and financial support for my research.

Abstract

Studies of the distribution of macroamphiphiles in Gram-positive bacteria are interesting in relation to understanding their functions and are of chemotaxonomic value at the supergeneric level. Previous studies have revealed the distribution of lipoteichoic acid (LTA) in the low G+C phylum Firmicutes and typically parallel that of teichoic acid as a secondrary cell wall polymer (SCWP). The present study has focussed on the distribution of macroamphiphiles in the high G+C phylum Actinobacteria, where most previous studies have revealed lipoglycans as the macroamphiphiles in various different lineages of the phylum.

The present study has, for the first time, investigated macromaphiphiles in a thermophilic Actinobacterium, *Thermobifida fusca*. The study detected the presence of LTA, with detailed structural analysis. This confirms the compatibility of these macromolecules with membrane adaptation at higher temperatures. A second thermophilic Actinobacteria, *Rubrobacter xylanophilus* (which has been moved recently to the most distant lineage of the phylum) was found to lack of typical macroamphiphiles.

The present study also detected a novel LAM-like molecule in *Kineococcus radiotolerans* suggesting a close relationship between the distribution of LAM or LAM-like molecules and that of the SCWP, arabinogalactan (AG). The study also identified the presence both LTA and lipoglycan in two representatives of the genus *Streptomyces* (*Streptomyces coelicolor* and *Streptomyces* sp. DSM40537). This allows a re-evaluation of the hypothesis (Fischer, 1994) that a single type of major macroamphiphile is normally present in a single organism.

Extending these findings, comparative genomic analyses suggest that the LTA biosynthesis pathway in Actinobacteria might be different from that in the Firmicutes. The alanine substitution pathway for LTA and teichoic acids (TA) was also found to be absent from the phylum Actinobacteria. Moreover, the comparative genomic analyses for *Kineococcus radiotolerans* were consistent with the practical results for this organism, illustrating the potential of predicting macroamphiphile composition utilizing genome databases. The study has also confirmed that the distribution of macroamphiphiles and SCWPs has importance chemotaxonomic value especially at the supra-generic level; it can be hypothesised from the study that: ***LTA containing Actinobacteria contain TA as a SCWP, whilst lipoglycan containing Actinobacteria generally contains other SCWPs, such as AG, rather than TA.***

List of Contents

List of Tables

List of Figures

CHAPTER ONE

INTRODUCTION

1. Bacterial cell envelope: staining characteristics

The bacterial cell envelope is mainly defined by the bilayer membrane surrounding the cytoplasm; its multifunctional characteristics can be classified generally in two categories. The first category is the rigid characteristic allowing the cell to resist turgor pressure and maintaining physical integrity and the second category is the permeability, elasticity and fluidity characteristics of the cell envelope required for the cell growth, division and passaging of nutrients, proteins and ions (Bhavsar and Brown, 2006). These properties have made the study of bacterial cell envelopes an attractive and stimulating part of microbiology.

Depending on their staining characteristics, the Danish pharmacologist and physician Hans Christian Jaochim Gram (1884) classified bacteria into two groups, Gram-negative and Gram-positive bacteria. Gram-negative bacteria do not retain stains because of their complex envelope structure composed of a thin cell wall and an outer membrane surrounding the cytoplasmic membrane. Conversely, the simpler structure of the Gram-positive bacterial cell envelope is composed of a thicker cell wall which retains the stain (Desvaux *et al.*, 2006, Gupta, 1998).

According to Bergey's Manual, Gram-positive bacteria can be further divided into two groups, low G+C (containing Guanine and Cytosine <50% of the total DNA), i.e. phylum *Firmicutes* and high G+C (>50%), i.e. phylum *Actinobacteria* (Garrity, 2001). For the purpose of the present study, typical Gram-positive cell envelopes shall be discussed, especially emphasizing the high G+C Gram-positive Actinobacteria.

Though the Gram-positive and Gram-negative bacteria can be easily classified by the Gram staining process, there are some exceptions in some Gram-positive bacteria because of their different cell envelope structure. Some members of *Clostridium* and *Mycoplasma* do not retain the Gram stain as their peptidoglycan layer is too thin or they lack cell walls, respectively (Desvaux *et al.,* 2006). Also, there are some bacteria closely related to the Gram-positive bacteria that do not retain the Gram stain as they possess a Gram-negative-like cell envelope, such as *Fusobacterium nucleatum* (Snel *et al.,* 2005, Desvaux *et al.*, 2006). On the other hand, there are members of the phylum *Deinococcus-Thermus* that retain the Gram stain although they are not closely related to the Gram-positive bacteria (Desvaux *et al.,* 2006). Moreover, some phyla such as *Chloroflexi* or *Thermomicrobia* contain bacteria of both types of Gram staining characteristic (Botero *et al.*, 2004). Even the Gram-negative cell envelope structure has been observed in the deep branches of the phylum Firmicutes (Shatalkin, 2004). So to classify bacteria depending on the single characteristic of Gram staining is useful but not conclusive, which makes the microbiologist depend on other additional characteristics of the cell envelope.

1.1. Structure of the cell envelope of Gram-Positive bacteria

The Gram-positive bacterial cell envelope is composed of a plasma membrane and peptidoglycan or murein layer. The plasma membrane, surrounding the cells cytoplasm, is composed of a phospholipid bilayer which acts as a permeability barrier and carries a vast collection of proteins involved in important and essential functions of the cell.

Weidel and Pelzer (1964) used the word 'murein' first time to describe the bacterial layer surrounding the inner membrane, which has been replaced by the word 'peptidoglycan', which describes the biochemical characteristics of the wall rather than the functional aspects. The peptidoglycan (PG) serves as the major stress-bearing component of the cell envelope (Dmitriev *et al.*, 2005).

Beside these two layers, the bacterial cell envelope contains different macromolecules such as secondary cell wall polymers (SCWPs) and macroamphiphiles, anchored in the PG and cytoplasmic membrane, respectively. Moreover different types of proteins are also present on the surface of the Gram-positive bacteria.

1.2. Inner membrane or cytoplasmic membrane

The cytoplasmic membrane acts as the boundary between the cell and its environment. In bacteria it is composed generally of a phospholipid bilayer, with varying amounts of glycolipids, and many different types of integral and peripheral proteins.

1.2.1. Phospholipids

Phospholipids are the basic matrix of the plasma membrane. These molecules have both hydrophilic (water soluble) and hydrophobic (water insoluble) groups, giving the molecules an amphoteric (amphiphilic) characteristic. This characteristic allows the molecules to form a bilayer in an aqueous environment, where the hydrophobic and hydrophilic ends of the molecules are arranged on the inside and outside of the bilayer, respectively (Figure 1.1).

The primary function of phospholipids is to provide a permeability barrier for cells and organelles and also to provide metabolic precursors for other important cellular components. Phospholipids also influence the properties of integral and peripheral membrane proteins which are involved in essential and important functions of the cells, such as energy transduction, signal transduction, solute transport, deoxyribonucleic acid (DNA) replication, protein targeting and trafficking, cell-cell recognition, secretion, etc. (Dowhan, 1997b).

Phospholipids can be classified into two major groups depending on their total charge characteristics, zwitterionic (uncharged) and anionic phospholipids.

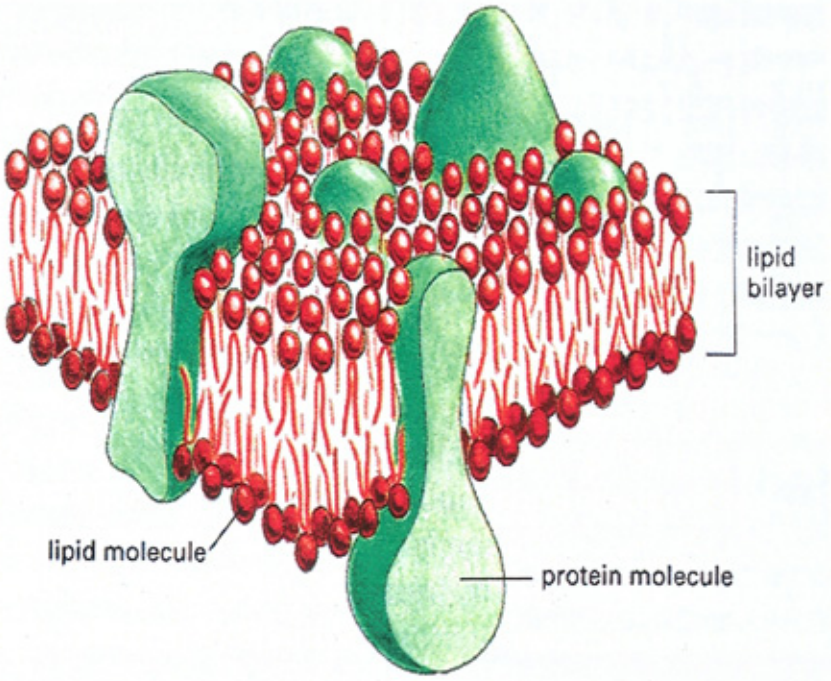

Figure 1.1. Structural representation of the arrangement of phospholipids and proteins based on the Singer-Nicholson 'fluid-mosaic model'. (Taken from http://math.lanl.gov/~yi/lipid.html).

Zwitterionic phospholipids' balanced charge is more favourable than anionic phospholipids in most membrane systems (Dowhan, 1997b).

Phosphatidylethanolamine (PE) is the major zwitterionic phospholipid in Gram-negative bacteria such as *Escherichia coli* (70-80% of the total phospholipids) and some Gram-positive bacteria such as *Bacilli* (Cronan, 2003, Sonenshein *et al.,* 1993). PE is synthesized from the central liponucleotide intermediate CDP-diacylglycerol (CDP-DAG) by the enzymes PssA and Psd (Dowhan, 1997a). CDP-DAG also can be converted into the major anionic phospholipids, phosphatidylglycerol (PtdG) and cardiolipin (CL) via the intermediate phosphatidylglycerol-3-phosphate (PGP) as shown in Figure 1.2 (Cronan, 2003). Most Gram-positive bacteria lack PE and instead contain derivatives of PtdG as zwitterionic or net positive charged phospholipids formed by substituting one of the glycerol hydroxyl groups with amino acids (Nesbitt and Lennarz, 1968). These derivatives have been identified in several species of Bacilli in addition to PE (Sonenshein *et al.,* 1993). Gram-positive bacteria lacking PE usually contain large amount of diacylglycerol (DAG) with sugar unit(s) substituted at the *sn*-3 position (Dowhan, 1997b), helping in formation of macroamphiphiles and SCWPs, which will be discussed later. Photosynthetic Gram-negative organisms like *Rhodobacter sphaeroides* contain phosphatidylcholine (PC), which is formed by methylation of PE via S-adenosylmethionine (Goldfine, 1984, Iba *et al.,* 1993, Zhang and Rock, 2008).

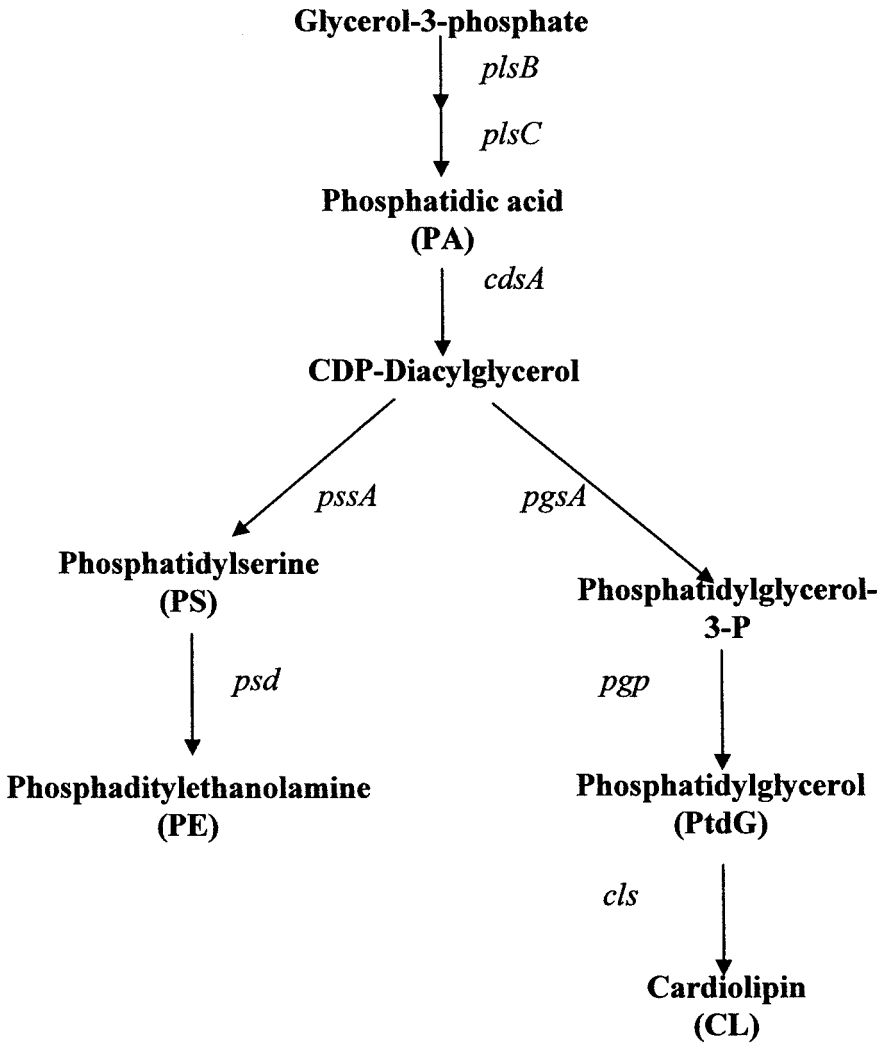

Figure 1.2. Schematic presentations of the phospholipids biosynthesis pathway and the associated genes. The genes encoding the enzymes catalyzing each step are indicated in italics. The genes encoding the enzymes catalyzing each step are indicated in italics. P*lsB*: sn-glycerol-3-phosphate acyltransferase, PlsC: 1-acyl-glycerol-P acyltransferase, CdsA: CDP-diacylglycerol synthase, PssA: Phosphatidylserine synthase, PgsA: Phopahtidyl glycerol synthase, Psd: phosphatidylserine decarboxylase, Pgp: Phosphatidyl glycerol synthase, Cls: Cardiolipin synthas. Data taken from Dalen & Kruijff (2004).

The zwitterionic phospholipid PE, which has no net charge at physiological pH, has a specific involvement in supporting active transport systems; these include the high affinity for proline transport protein and the melibiose transport protein of *E. coli*, the sodium-dependent leucine transport system of *Pseudomonas aeruginosa*, the branched chain amino acid carrier of *E. coli*, and several transport systems of *Bacillus* species. PE is also associated with the assembly of membrane proteins like the lactose permease (Dowhan, 1997b).

The second group of phospholipids constitutes the negatively charged lipids PtdG and CL which are essential for the translocation of proteins (especially proteins of the Sec-machinery) across the inner membrane, also other anionic phospholipids promoted translocation (Schatz and Dobberstein, 1996, Diamond *et al.*, 1995, Zhang and Rock, 2008). They are also important during insertion and functional assembly of membrane proteins (Cronan, 2003).

1.2.2. Organisation of the membrane lipids

The organisation of bacterial cell membranes is extremely complex subject and still an on-going area of research. The most accepted paradigm regarding this was the fluid-mosaic membrane model of Singer-Nicolson (1972), also known as S-N model, which predicted that phospholipids forms a lipid bilayer and membrane components like proteins and other lipids are distributed randomly in both dimensions with lateral and rotational freedom (Figure 1.1) (Singer and Nicolson, 1972). At present, a considerable amount of experimental and theoretical data suggests that rather than lateral random distribution, the membrane components are distributed in domains with distinct lipid and protein composition, and the domains are known as rafts (Somerharju *et al.*, 1999, Matsumoto *et al.*, 2006, Vereb *et al.*, 2003). The phenomenon came from the study of mammalian cell caveolae, which are important for signal transduction and cholesterol efflux, and the main components of which are the protein caveolin (having a high affinity for cholesterol) which enriched the cholesterol level in its surrounding and may also enrich the glycosphingolipids and sphingomyelin levels *(Lisanti et al., 1995, Murata et al.*, 1995, Simons and Ikonen, 1997). The interaction between lipid-lipid and lipid-protein molecules in the plasma membrane have suggested to produce these rafts or domains, especially for polar chemoreceptor proteins and proteins involved in cell division; the cell membrane have been found to be laterally polarized to create an environment for the function of certain membrane proteins (Shapiro *et al.*, 2002). Moreover, lipid domains or heterogeneity of lipid molecules has been identified in a variety of studies such as cardiolipin (CL) membrane domains, present in the polar and septal region during the cell division or growth, again

creating a specific environment for the function of different protein complexes in the cell membrane (Mileykovskaya, 2007). These studies suggest that rather than random localization, mobility and distribution of cell surface lipids and protein molecules throughout the membrane, they are distributed in domains or rafts and free diffusion can only occur within the domain borders, where molecular interaction do not interfere. This has shifted the S-N model from fluidity to mosaicism and this is now known as the dynamically structured mosaic model (Vereb *et al.*, 2003).

1.2.3. Glycolipids

Glycolipids are generally composed of carbohydrates and long chain fatty aliphatic acids or alcohols, and can be directly extracted from bacteria rather than using any hydrolytic procedures (Shaw, 1970). Depending on their chemical composition, bacterial glycolipids can be classified into two groups, glycosyl diglycerides and acylated sugar derivatives.

Glycosyl diglycerides glycolipids are derivatives of 1,2-diacyl-sn-glyceride with an attachment of carbohydrate residues at the 3-position of the glycerol. They are generally distributed widely in Gram-positive bacteria, but are not typically found in Gram-negative bacteria (Shaw, 1970; 1975; Zhang & Rock, 2008). They are the most common types of glycolipid with a wide range of structural diversity and composition. Among them, α-diglucosyl-, β-diglycosyl-, digalactosyl-, dimannosyl- and galactosylglucosyl- diglycerides are the most prevalent and distributed among several genera of Gram-positive bacteria (Shaw, 1970; 1975). Uronic acid containing glycolipids, such as glycosylglucouronyl diglyceride and glucosylglactouronyldiglyceride have been identified from *Pseudomonas diminuta* and *Streptomyces* strains, respectively (Wilkinson, 1969, Bergelson *et al.,* 1970). Moreover many organisms have been identified with more than one type of glycolipid.

In most cases, monoglycosyl diglycerides are thought to be a precursor in the biosynthesis of glycosyl diglycerides and found in lower amount, but a glucose containing monoglycosyl diglyceride has been identified in *Treponema zuelzerae* in high amounts (Meyer and Meyer, 1971, Zhang and Rock, 2008). In some organisms, such as *Mycoplasma* and *Acholeplasma* species, glycolipids have been identified with more than two sugar residues diglycerides (Oshima and Yamakawa, 1972, Plackett, 1967, Mayberry *et al.*, 1974).

The second class of glycolipids are the acylated sugar derivatives. Rather than containing a glycerol as a linker, the acyl groups are directly esterified to the carbohydrate residues. Much less attention has been provided to this kind of glycolipids as they are often present in very small amounts which may depend upon the age and composition of the culture (Shaw, 1970). However, they may be more widely distributed among bacteria than glycosyl diglycerides. The most familiar member of this group is the diacyl trehalose of members of the genus *Mycobacterium* and close relatives (Shaw, 1975).

1.2.4. Glycophospholipids

Glycophospholipids are molecules located in the membrane and according to the Shaw and Stead (1972) nomenclature, this term is used for any lipid macromolecules containing carbohydrate and phosphate residues. On the other hand, phosphoglycolipids are those lipids which are derived from the addition of phosphate-containing residues to glycolipids. There are several types of glycophospholipids, such as phosphatidylinositol mannosides (PIMs), phosphatidylglycerol glycerides and phosphatidylglucose.

PIMs are a family of macromolecules containing one or more mannose units attached to phosphatidylinositol (PI) and can be classified into two main groups depending on the mannose numbers, apolar and polar. Generally, the smaller PIMs, which have fewer sugar residues, are known as apolar PIMs (PIM_1 to PIM_4) (Discussed later in section 1.7.5) (McCarthy *et al.,* 2005). These smaller PIMs, along with PI, have been found to be essential for the growth of the organisms that produce them (Kordulakova *et al.,* 2002, Haites *et al.,* 2005). They also function as the precursors of polar PIMs and lipoglycans, such as lipomannan (LM) and lipoarabinomannan (LAM). The polar PIMs (PIM_5-PIM_8) have more mannose residues than apolar PIMs (Furneaux *et al.,* 2005, Garton and Sutcliffe, 2006, Gilleron *et al.,* 2003, Kordulakova *et al.,* 2002). These higher PIMs (PIM_5-PIM_8) are believed to be synthesized and displayed on the outer surface of the cytoplasmic membrane, whereas apolar PIMs are synthesized at the inner leaflet (Discussed later in section 1.7.5). PIM_2 and PIM_6 are found to be the predominant PIMs in *Mycobacterium spp.* (Gilleron *et al.,* 2001, Gilleron *et al.,* 2003). PIMs are also found in other

members of the mycolata, such as the suborder Corynebacterineae (Shaw, 1975), members of which have cell envelopes containing mycolic acids (discussed later in section 1.4). PIMs may have functional interactions with the mycolic acids in mycolate cell envelopes, although there are many examples of genera where PIMs are present and mycolic acids are absent (for example, *Streptomyces* spp.). PIMs may also be used as a precursor for lipoglycan biosynthesis (discussed later in Section 1.7.5).

1.2.5. Isoprenoid quinones

Isoprenoid quinones are cytoplasmic membrane components of bacteria, which play important roles in electron transport, oxidative phosphorylation, and also possibly in active transport (Collins and Jones, 1981). They are mainly classified into two groups, the naphthoquinones and the benzoquinones. The former has been subdivided into two main types; the phylloquinones occur less commonly in bacteria, whereas the menaquinones are present in almost all bacteria. The large variation of side chain length, saturation, and hydrogenation allowed them to used as taxonomic markers for characterizing bacteria (Collins and Jones, 1981).

1.3. Peptidoglycan (PG) or murein layer

PG plays a vital role in maintaining cell shape and integrity by creating a three-dimensional meshwork surrounding the cells and resists the internal osmotic pressure of the cells (Schiffer and Holtje, 1972, Nanninga, 1998). The glycan chain of PG is composed of alternating units of N-acetyl-glucosamine (NAcGlc) and N-acetyl-muramic acid (NAcMur) joined by β, 1→4 linkages; PG also contains short peptides composed of alternating L- and D- amino acid which are linked to the carboxyl group of NAcMur (Figure 1.3). The glycan chain forms a helical structure in physiological conditions and two or more chains together form a three dimensional meshwork by creating short peptide bridges between a peptide subunit of one glycan chain and that of another glycan chain, either directly or via a short peptide bridge between the two peptide subunits (Heijenoort, 2001a, Bhavsar and Brown, 2006).

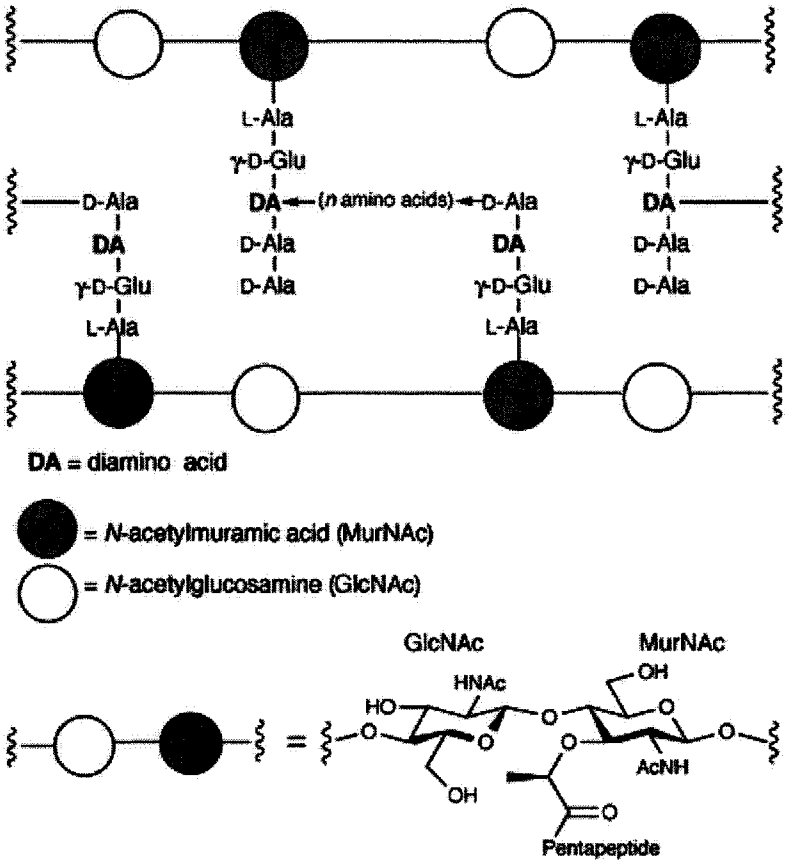

Figure 1.3. Scheme of the primary structure of bacterial peptidoglycan. Abbreviations: GlcNAc: *N*-acetylglucosamine; MurNAc: *N*-acetylmuramic acid; DA: diamino acid (generally diaminopimelic acid or L-lysine); D-Glu:D-glutamyldiaminopimelyl; *n*: number of amino acids in the cross-bridge depending on the organism; (D-Ala): often missing in the peptidoglycan of many organisms →. Taken from Heigenoort (2001a).

1.3.1. Biosynthesis of Peptidoglycan

Both Gram-positive and Gram-negative bacteria peptidoglycan biosynthesis have been investigated and found to be similar. The first stage involves six well known cytoplasmic steps for the formation of a UDP-MurNAc-pentapeptide precursor from UDP-GlcNAc by *mur (AA)BCDEF* encoded enzymes as shown in Figure 1.4. The next stage occurs at the cytosolic surface of the inner membrane where Lipid I is formed by translocating the MurNAc-pentapeptide to the membrane compartment via covalent linkage with undecaprenyl-phosphate (an unsaturated lipid carrier) by the *mraY* encoded enzyme (Figure 1.4). Lipid I is converted to lipid II, which is formed by addition of GlcNAc to the 4-hydroxyl of MurNAc by the *murG* encoded enzyme as shown in Figure 1.4 (Heijenoort, 2001b, Bhavsar and Brown, 2006).

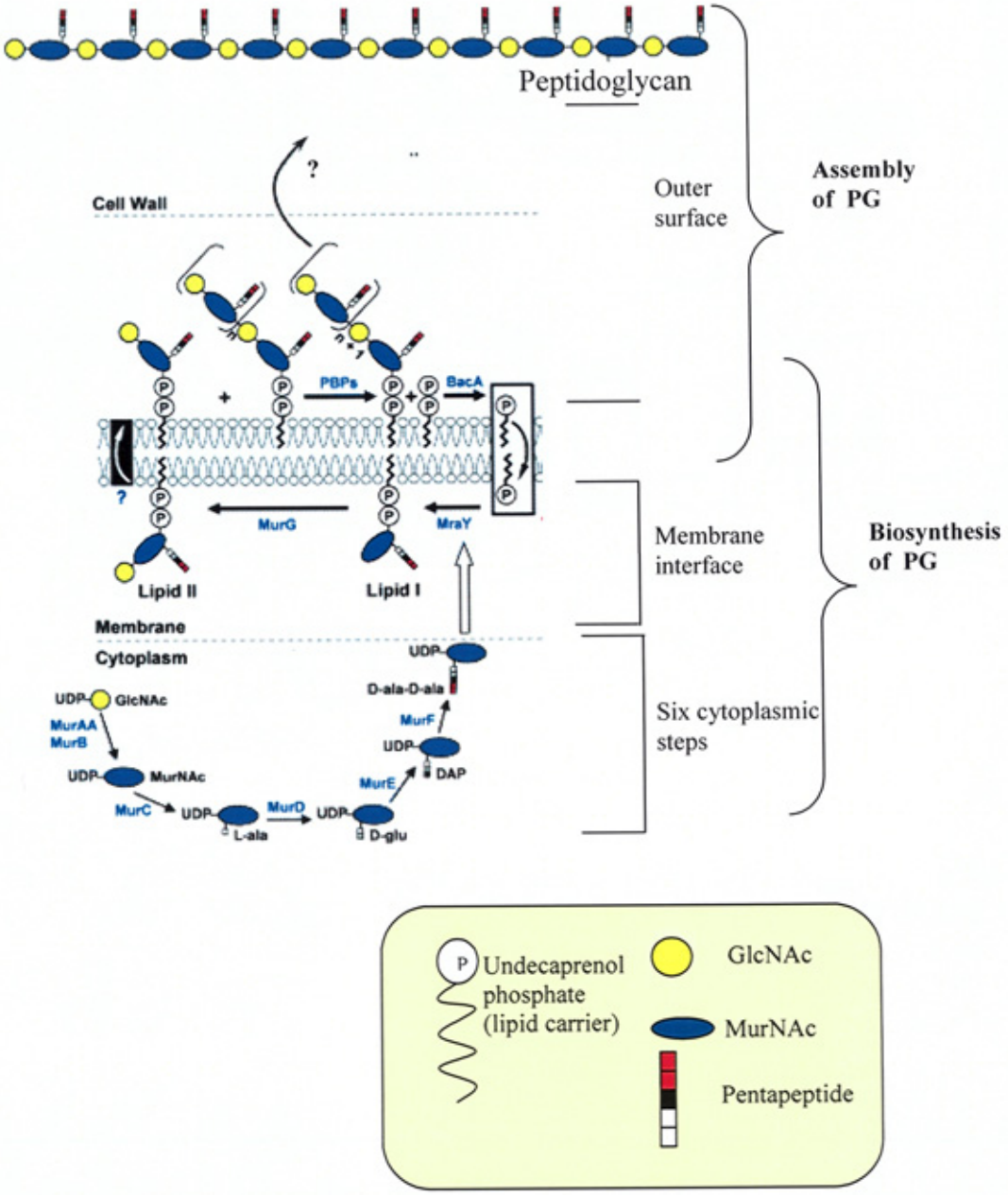

Figure 1.4. Transcompartmental biosynthesis of Peptidoglycan. Unknown enzymatic reactions are denoted by question mark. Modified from Bhavasar & Brown (2006).

1.3.2. Assembly of PG

In the second stage, the movement of Lipid II across the cell membrane is believed to be carried out by an unknown flippase enzyme (Figure 1.4). After extrusion through the membrane, Lipid II is subjected to two types of enzyme activities. Class A high molecular weight penicillin binding proteins (HMW PBPs), bifunctional proteins that contain both glycosyltransferase and transpeptidase activities, catalyze the formation of linear glycan chains by transglycosylation. This step also liberates the undecaprenyl-pyrophosphate which recycles to act as a carrier (Figure 1.4). The second enzyme, Class A HMW PBPs, attach the newly synthesized glycan chain to an adjacent chain by transpeptidation, which may occur after or simultaneously with the previous step (Bhavsar and Brown, 2006).

1.3.3. Arrangement of PG strands on the cell surface

The classical or "textbook" model postulated that the glycan chains in PG run parallel to the plasma membrane surface, whereas the peptide bridges are arranged in perpendicular, which provides networks (layers) of glycan strands forming the sacculus (Dmitriev *et al.*, 2003). However, this model conflicts with the tensile force, release of proteins via the cell membrane and features such as branched cell morphology. Recently, a new model with a different concept has been proposed, known as the scaffold model. The model proposes that the glycan chains run perpendicular to the plasma membrane and cross-linked peptide bridges are parallel with the membrane, forming a continuous sponge-like matrix (not layers) that can function as an elastic external cytoskeleton (Dmitriev *et al.*, 2005, 2003). The proposed scaffold-like principles agree with the stress-bearing construction, enabling the wall to be simultaneously porous and elastic, compact and stretchable and also show how bacteria can shrink and swell by retaining large amounts of water in the porous matrix (Dmitriev *et al.*, 2005). Though the Scaffold model has clear advantages over the traditional model, the traditional model is more consistent with understanding of the Gram-negative cell division process (Dmitriev *et al.*, 2003). Another model has been recently suggested by Meroueh *et al.* (2006), known as honey comb model. The model suggest that the cross-linking between the glycan does not occur between all chains, rather they are incomplete which allow them to produce variable pore sizes within peptidoglycan layer and this agrees with the *Staphylococcus aureus* cell surface pore sizes which vary from 50 to 500 °A (Touhami *et al.*, 2004). This model may explain the different pores size observed in peptidoglycan and also give an

idea about the orientation of membrane-bound enzymes. Though this model doesn't distinguish between the arrangement of peptidoglycan chains proposed by the other two models it favours the orthogonal glycan orientation of Scaffold model, which allows the production of small to large pores on the bacterial cell surface, especially explaining the location of penicillin binding proteins (PBP) transpeptidase active site in the periplasm and also explaining the holding of the TolC protein by peptide cross-link of PG (Meroueh *et al.*, 2006). Recently, Hayurst *et al.* (2008) calculated the length of the longer glycan strands in rod-shaped *Bacillus subtilis* which were longer than the width or length of the bacteria, so they proposed peptidoglycan "ropes", which were formed by polymerization and cross-linking of glycan strands, coiled into a helix forming the inner surface cable structures as shown in Figure 1.5. This architecture agrees with the "text book" model. Consequently, there are still extensive debates around these models and further studies are needed to create an accurate model for PG arrangement.

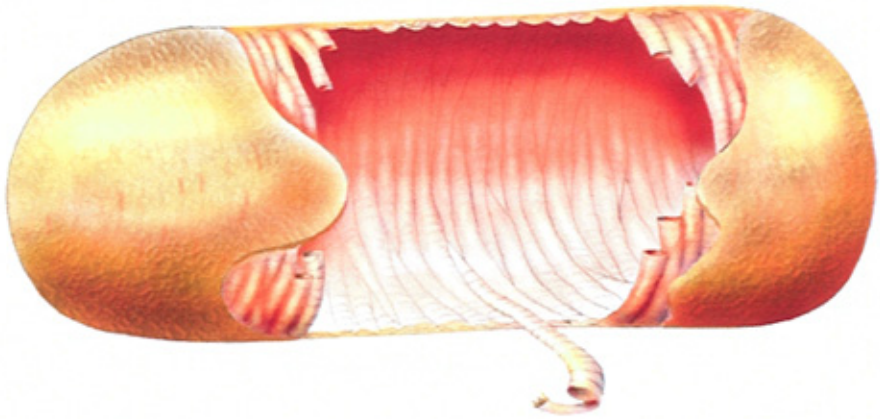

Figure 1.5. Model of *B. subtilis* cell wall peptidoglycan architecture. The image shows the cell wall cylinder with the peptidoglycan depicted as cables with a coiled substructure. Both cables and cross striations are shown. Taken from Hayhurst *et al.* (2008).

1.4. Outer surface layers of Gram-positive bacteria

Generally, Gram-positive bacteria do not contain any outer cell membrane like Gram-negative bacteria but many Gram-positive bacteria possess outer surface layers. The presence of different surface layers in Gram-positive bacteria is described briefly in below.

The members of suborder Corynebacterineae of Actinobacteria phylum contains a outer layer composed of mycolic acids, along with meso-diaminopimelic acid in the PG and arabinose and galactose in their cell wall polysaccharides (Chun *et al.,* 1996). For this reason the suborder is also known as the mycolata. Mycolic acids are high molecular weight, long chain, 3-hydroxy fatty acids with an alkyl branch at position 2. The mycolic acids are believed to form an outer lipid permeability barrier analogous to the outer membranes of Gram-positive bacteria (Sutcliffe, 1998, Chun *et al.,* 1996, Mcneil *et al.,* 1991).This layer increases resistance to chemical injury and prevent the activity of hydrophobic antibiotic substances, which help bacteria to survive in hostile environments (Barry *et al.,* 1998).

The second type of outer cell layer is the crystalline bacterial cell surface layer known as S-layer. Presently, this layer is recognized as the most widely distributed outer most cell envelope layer of archeae, Gram-positive and Gram-negative bacteria (Schaffer *et al.,* 2007). This layer can constitute up to 20% of the total bacterial cell proteins, with components forming a regular two dimensional structure on the supporting envelope layer (Sleytr *et al.,* 2007). S-layers produce a smooth outer surface (Figure 1.6) with an uneven inner

surface and the alignment of these supramolecular structures form lattices with oblique, square or hexagonal symmetry, along with different pores in the layer; these alignments and pore sizes are found to be species specific (Sleytr *et al.*, 2007). Another major characteristics of S-layers is the glycosylation of S-layer proteins (1-15% by weight), linking a glycan chain as shown in Figure 1.6. This layer also enables bacteria to survive in competitive environments (Sleytr *et al.*, 2005).

Some Gram-positive bacteria synthesize large polysaccharide capsules, rather than producing S-layer proteins, but some may contain both layers (Navarre and Schneewind, 1999). *Streptococcus agalactiae* (Group B *Streptococcus* or GBS) synthesise capsules, generally composed of D-galactose, D-glucose, N-acetyl-D-glucosamine, and N-acetylneuraminic acid and contain complex repeating units built from five to seven monosaccharides (Kogan *et al.*, 1996). *Streptococcus pyogenes* possesses a hyaluronic acid composed capsule (Navarre and Schneewind, 1999) , whereas *Bacillus anthracis* contain both poly-gamma-D-glutamic acid polysaccharide capsules and an S-layer. Capsules also help organisms to survive hostile environments and also play a vital role in the virulence of the organisms (Mesnage *et al.*, 1998).

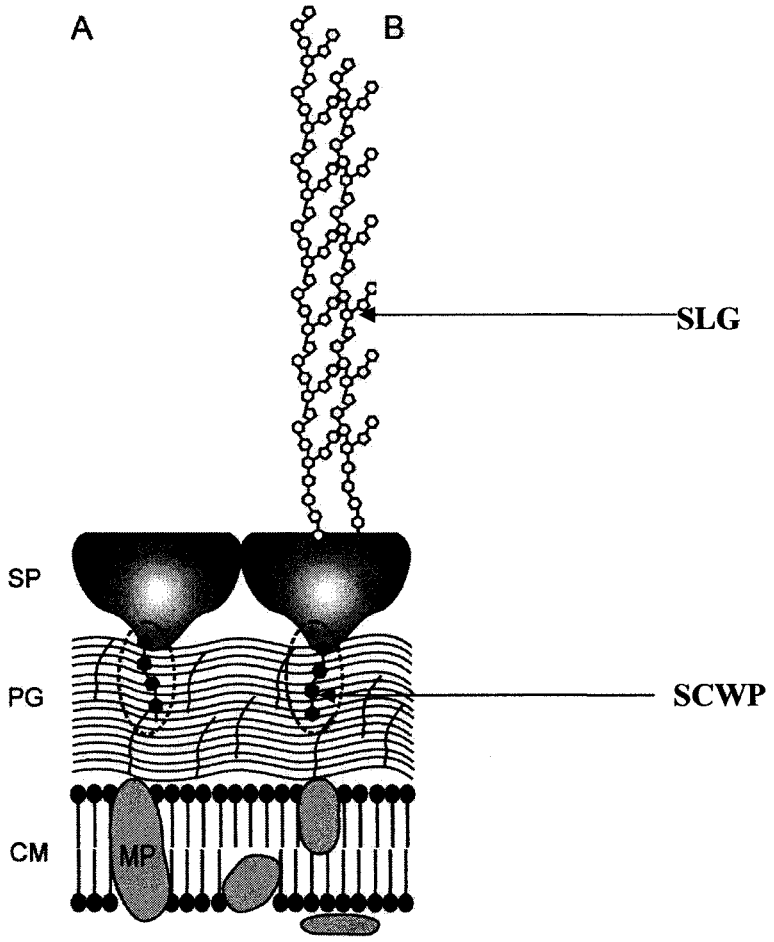

Figure 1.6. Schematic presentation of (**A**) S-layer protein and (**B**) S-layer-glycoprotein in Gram-positive *Bacillus* indicating the cellular location of 'non-classical' SCWP. The dotted ovals indicate the SCWP. CM, cytoplasmic membrane; MP, membrane protein; PG, peptidoglycan; SP, S-layer protein; SLG, S-layer glycoprotein; SCWP, secondary cell wall polymer. Figure is taken from Schaffer & Messner (2005).

1.5. Cell envelope proteins of Gram-positive bacteria

Cell envelope protein of Gram-positive bacteria must be attached to the cell envelope, i.e. either in/at the cytoplasmic membrane or as cell wall components. Moreover, there is no guarantee of these proteins being exposed on the cell surface because of the thickness of the peptidoglycan and the presence of other surface layers (as described in Section 1.4). Based on these two characteristics, four major types of cell envelope proteins have been classified in Gram-positive bacteria:

1.5.1. Transmembrane proteins

These proteins are anchored into the cytoplasmic membrane by hydrophobic transmembrane domain(s) and have a large variety of functions, ranging from metabolism of carbohydrates, proteins, lipids, nucleotides to signal transduction or virulence factors (Tjalsma *et al.*, 2000). The integration of these proteins into the lipid bilayer may occur in two ways: (i) insertion of the hydrophobic segments one at a time and/or (ii) by pairs forming helical hairpins model.

1.5.2. Lipoproteins

Lipoproteins are covalently attached to membrane lipids and characterized by a specific signal peptide of a conserved lipobox sequence (Desvaux *et al.*, 2006) and also involved in a large variety of physiological functions, such as acting as adhesins, transporters, receptors, enzymes or virulence factors (Sutcliffe and Russell, 1995).

1.5.3. LPXTG-like proteins

These proteins contain a C-terminal LPXTG-like motif and are covalently attached to the peptidoglycan by an enzyme called sortase (Navarre and Schneewind, 1999, Ton-That *et al.,* 2004, Bierne and Cossart, 2007). These proteins may play major roles in bacterial pathogenicity and also may act as adhesins, antigens, receptors and enzymes (Desvaux *et al.,* 2006).

1.5.4. Cell wall binding proteins

These proteins bind to the cell envelope by recognizing specific cell wall domains. This basic mechanism can serve as the foundation for assembly of much more complex macromolecular structures, such as S-layers (see Section 1.4), pili, flagella and cellulosomes (Sara, 2001, Koebnik, 2001, Jonson *et al.,* 2005, Desvaux, 2005).

1.6. Secondary cell wall polymers (SCWPs)

Gram-positive bacterial cell walls contain a variety of polysaccharides, covalently linked to PG. These cell wall polysaccharides can be classified on the basis of their structural characteristics into three groups:

1) Teichoic acids (TA)

2) Teichuronic acids

3) Other neutral or acidic polysaccharides.

They are also known as secondary cell wall polymers (SCWPs) for their apparently secondary role in cell wall functions. TA and teichuronic acid are also known as 'classical' SCWPs, and may play essential roles in normal cell function and as a result considerable energy is used in their biosynthesis. On the other hand SCWPs that provide anchors for S-layer proteins (Sleytr, 1976, Sleytr *et al.,* 2007) are the novel class of 'non-classical' or third group of SCWPs.

1.6.1. Classical SCWPs of Gram-positive bacteria

Teichoic acid (TA) and teichuronic acids are the best characterised SCWPs. The SCWPs' anionic groups occur in the polymers as phosphate (TA) or carboxyl (teichuronic acid) groups and they may also differ in containing acidic side chains, such as phosphate, organic acids (e.g. pyruvic acid and succinic acid) or sulphate (Araki and Ito, 1989, Schaffer and Messner, 2005, Naumova and Shashkov, 1997).

Though the structures of different types of TA are well studied (Fischer, 1988), only a few of the teichuronic acids have been subjected to full chemical analysis. These anionic polymers can account for 10-60% (by weight) of the bacterial cell wall, but this amount depends on the cultural conditions of the bacteria (Schaffer and Messner, 2005, Ellwood and Tempest, 1969). The exact biological function of these negatively charged SCWPs is not fully understood but several general functions have been, such as binding of divalent cations; roles in the balance of metal ions for membrane function and folding of extracellular metallo-proteins; binding of proteins; providing a source of phosphate under phosphate starvation conditions: interactions with cell wall lytic enzymes and the formation of a barrier to prevent diffusion of nutrients and metabolites (Hancock and Baddiley, 1972, Fischer, 1994b, Navarre and Schneewind, 1999). Thus SCWPs contribute to make up a complex meshwork with other carbohydrate-containing membrane polymers and peptidoglycan which is important for a variety of cellular functions, including growth, division, maintenance of shape and protection from osmotic stress (Hancock, 1997, Bhavsar *et al.,* 2004, Kobayashi *et al.,* 2003, Ginsberg *et al.,* 2006)

1.6.2. Teichoic acid (TA)

The general composition of TA is repeated units of alditol-phosphate linked to the peptidoglycan via a phosphodisaccharide core (Figure 1.7). Although their exact function(s) are unknown, TA likely play an important role in general physiology (as noted above) and also some times function as virulence factors as has been proven for *Staphylococcus aureus* infection (Weidenmaier *et al.*, 2004, Weidenmaier *et al.*, 2005). Though previous studies have suggest the TA is essential for the cells (Kobayashi *et al.*, 2003, Bhavsar and Brown, 2006, Ginsberg *et al.*, 2006), more recent studies have revealed it can be dispensable for cell viability *in vitro* (D'Elia *et al.*, 2006a, 2006b), which will be briefly discussed later in Section 1.6.2.2. TAs are attached to the peptidoglycan and the distribution of these attachments occurs initially along the inner surface of the PG layer, followed by the movement of covalent linked TA-peptidoglycan through the thickness of the cell wall, a process known as 'inside-to-outside' growth mode (Neuhaus and Baddiley, 2003, Anderson *et al.*, 1978). These chains of TAs are likely arranged perpendicular to the cell surface (although see Section 1.3.3 above with respect to the issue of peptidoglycan architecture), extended throughout the peptidoglycan and approximately 50% of the TAs may form a 'fluffy' layer beyond the cell wall (Birdsell *et al.*, 1975, Doyle *et al.*, 1975, Archibal *et al.*, 1973).

Figure 1.7. Schematic presentation of teichoic acid.

Structural diversity of TA occurs due to the diversification of repeating units (constituting 30 to 60% of the cell wall mass), glycosyl substituents and D-alanyl esters (Archibald *et al.,* 1993, Baddiley, 1970, Endl *et al.,* 1983, Naumova and Shashkov, 1997, Neuhaus and Baddiley, 2003). TA can be classified into two major types depending on the composition of their repeating units: 1,3-glycerol-phosphate (Gro-P) and 1,5-D-ribitol-phosphate (Rbo-P) (Neuhaus and Baddiley, 2003). In either case, the repeating unit is linked to the C-6 MurNAc residues of peptidoglycan with a linkage unit generally composed of $(Gro\text{-}P)_{2\ or\ 3}ManNAc(\beta 1\text{-}4)GlcNAc\text{-}P$ (Figure 1.8) (Araki and Ito, 1989, Coley *et al.,* 1978, Kojima *et al.,* 1985, Neuhaus and Baddiley, 2003).

Teichoic acids can be further characterized into four types depending on the main chains structural pattern of repeating units. Type I consists of polyol phosphate polymers whereas type II is composed of glycosylpolyol phosphate residues; type III is composed of alternating units of teichoic acid type I and II; and type IV contains alternating units of poly(polyol phosphate) and poly(glycosylpolyol phosphate). In all four types, the structural units of the polymers are joined by phosphodiester bonds (Naumova *et al.,* 2001, Naumova and Shashkov, 1997). The four types of polymers are shown in next page:

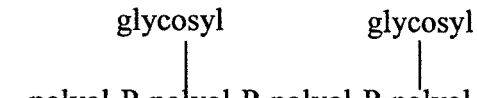

- polyol-P-polyol-P-polyol-P-polyol-P-polol-P (Type I)

-glycosylpolyol-P-glycosylpolyol-P-glycosylpolyol-P (Type II)

-polyol-P-glycosyl-P-polyol-P-glycosyl-P-polyol-P- (Type III)

- polyol-P-glycosylpolyol-P polyol-P-glycosylpolyol-P- (Type IV)

These can be further classified into subtypes. The details of the subtypes are given in Table 1.1, with their distribution with in the Gram-positive bacteria.

The distribution of TA can be genus and species specific. For example those of *Bacillus subtilis* 168, *B. subtilis* W23 and *Bacillus coagulans* contain the monomers –Gro-P-, -Rbo-P- (Figure 1.8) and -6-Gal(α1-2)GroP-, respectively (Archibald *et al.,* 1993, Iwasaki *et al.,* 1986). However, exceptions can be observed in the chemical composition of repeating units or monomers within some genera (Table 1.1) or even in different strain of same species (Figure 1.8). Moreover, a single species or strain can contain more than one teichoic acid, as in *B. subtilis* 168, which contains D-alanyl-[α-D-glucosylated poly(-Gro-P)] as a major teichoic acid (Doyle *et al.,* 1974, Pollack and Neuhaus, 1994), with a minor poly(3-O-β-Glucosyl-N-Acetylgalactosamine) teichoic acid (Archibald *et al.,* 1993, Iwasaki *et al.,* 1986). It should also be noted the bacteria such as *B. subtilis* may be able to switch between the synthesis of TA and teichuronic acids (Neuhaus and Baddiley, 2003).

Similarly, members of the genus *Staphylococcus* contain either –Gro-P- or –Rbo-P- repeating units in their TA. For example, *S. aureus* H and *S. aureus* Copenhagen contains –Rbo-P-, whereas *Staphylococcus cohnii* strains contain poly(Gro-P) TA (Neuhaus and Baddiley, 2003).

Another diversification of the TA structure is caused by the glycosylation pattern of the main chain structure, which can also be species and genus specific, though the degree of glycosylation can depend on the age of the cell and phosphate (P_i) concentration of the growth medium (Grant, 1979). For example, glycosyl substituents are observed in all species of *Staphylococcus* but the substitution pattern may differ within the same species. For example *S. aureus* contains D-alanyl-[α,β-GlcNAc-poly(Rbo-P)] TA glycosylated on position 4 of the D-ribitol in either and α- or β-linkage (Neuhaus and Baddiley, 2003).

In the case of alanyl-esterification, unlike glycosylation, the alanine has been found to be always constant in stereochemistry: D-configuration (Neuhaus and Baddiley, 2003). The only thing different regarding alanyl-esterification is the position in the repeat unit of the TA. In *S. aureus* H, the D-alanyl ester is found at position C2 of the –Rbo-P-monomer and a phosphodiester anionic linkage with the vicinal 3'-OH of the ribitol flanks the D-alanyl ester (Mirelman *et al.*, 1970, Neuhaus and Baddiley, 2003). In all poly(Gro-P) TAs the D-alanyl ester on position C2 is flanked by two phosphodiester linkages and when the 2'-OH

of glycerol is substituted by a glycosyl unit the D-alanyl may substitute onto the sugar (Neuhaus and Baddiley, 2003).

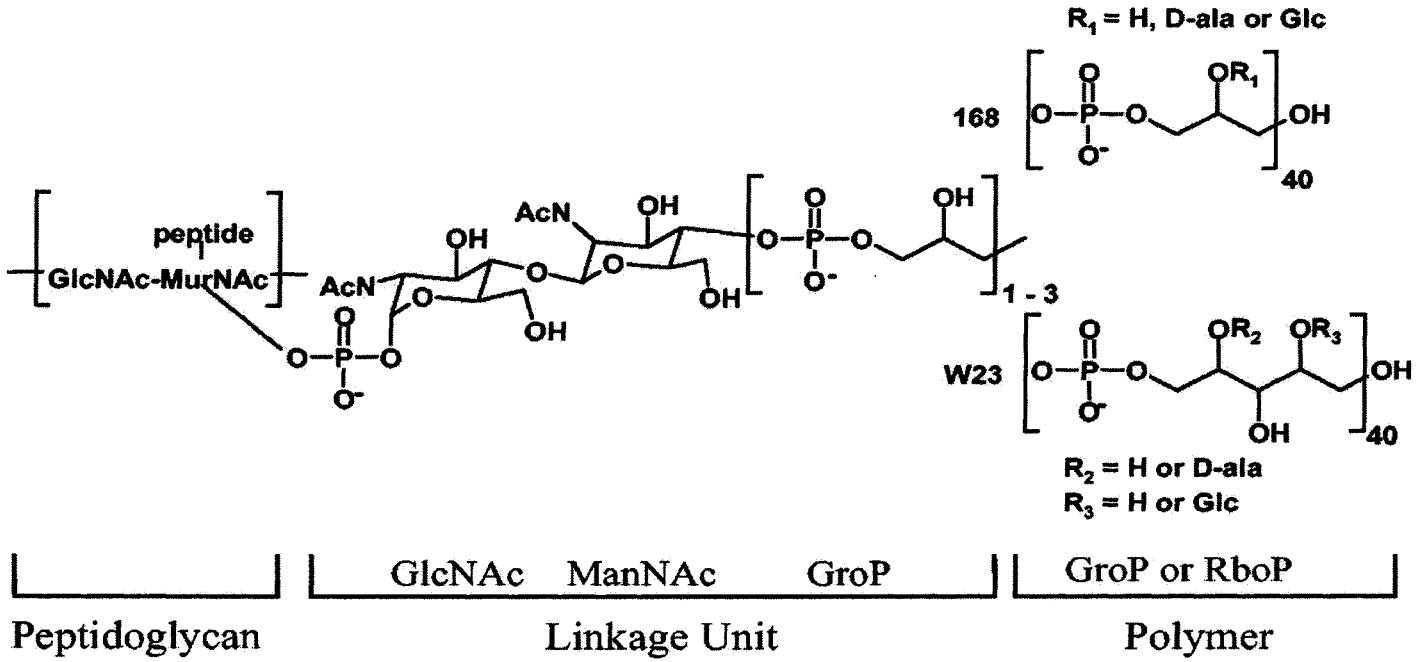

Figure 1.8. Chemical structures of the two types of predominant teichoic acid in *B. subtilis*, taken from Bhavsar *et al.*, 2004. Poly(Gro-P) and poly(Rbo-P) are attached to peptidoglycan via a highly conserved linkage unit in strains 168 and W23, respectively.

Table 1.1. Types and subtypes of teichoic acid and distribution in different Gram-positive bacteria genera. Modified from Naumova & Shaskov, 1997; Naumova *et al.*, 2001.

Type	Subtype	Polyol of main chain	Presence of sugar in main chain	Occurrence in genera of different Gram-positive bacteria
Type I Poly(polyol phosphates)	1,3-poly(glycerol phosphate)	Glycerol	No	**High G+C:** *Arthrobacter, Brevibacterium, Glycomyces, Herbidospora, Microbispora, Nocardiopsis, Nonomuraea, Planotetraspora, Spirilliplanes, Streptomyces, Thermobifida* **Low G+C:** *Bacillus, Lactobacillus, Staphylococcus*
	2,3-poly(glycerol phosphate)	Glycerol	No	**High G+C:** *Glycomyces, Planotetraspora, Streptomyces* **Low G+C:** *Bacillus*
	1,5 polymers (phosphodiester bonds link C-1 and C-5 of ribitol)	Ribitol	No	**High G+C:** *Brevibacterium, Nocardioides, Nocardiopsis, Streptomyces* **Low G+C:** *Bacillus, Lactobacillus, Listeria, Staphylococcus*
	3,5 polymers (phosphodiester bonds link C-3 and C-5 of ribitol)	Ribitol	No	**High G+C:** *Nocardiopsis*
	Poly(erythritol phosphate)	Erythritol	No	**High G+C:** *Brachybacterium, Glycomyces*
	Poly(mannitol phosphate) (phosphodiester bonds link C-1 and C-6 of mannitol)	Mannitol	No	**High G+C:** *Brevibacterium*
	Poly(mannitol phosphate) (phosphodiester bonds link C-4 and C-6 of mannitol)	Mannitol	No	**High G+C:** *Bifidobacterium*
	Poly(arabitol phosphate)	Arabitol	No	**High G+C:** *Agromyces*

Type	Subtype	Polyol of main chain	Presence of sugar in main chain	Occurrence in genera of different Gram-positive bacteria
Type II Poly(glycosylpolyol phosphates)	II-GS 3,3	Glycerol	Yes	**High G+C:** *Actinomadura, Nocardioides* **Low G+C:** *Bacillus,*
	II-GS 3,4	Glycerol	Yes	**High G+C:** *Streptomyces*
	II-GS 3,6	Glycerol	Yes	**High G+C:** *Actinocorallia, Actinomadura, Actinoplanes, Spirilliplanes, Streptomyces* **Low G+C:** *Bacillus, Lactobacillus*
	II-RS 5.3	Ribitol	Yes	**High G+C:** *Agromyces*
	II-RS 5,6	Ribitol	Yes	**Low G+C:** *Streptococcus*
Type III **Poly(polyol phosphate-glycosyl phosphates), mixed structures**		Glycerol	Yes	**Low G+C:** *Staphylococcus*
Type IV **Poly(polyol phosphate-glycosylpolyol phosphates)**		Glycerol	Yes	**High G+C:** *Nocardiopsis*

1.6.2.1. Comparison of glycerol and ribitol teichoic biosynthesis

The biosynthesis of TA has similarities to peptidoglycan synthesis and can be divided into five phases: i) synthesis of a linkage unit carrier ii) polymerization of the poly(alditol-P) on the lipid intermediate iii) flipping across the membrane iv) linkage unit attachment to the peptidoglycan, and v) substitution of the polymerized chain by glycosylation and D-alanylation. The first two phases occur at the cytosol side of the membrane and CDP-glycerol or CDP-ribitol is the source of repeated units of monomer alditol-P (Neuhaus and Baddiley, 2003). The last two phases occur on the outer surface of the membrane as the carrier lipid carries the intermediate TA to the peptidoglycan (Figure 1.9). An unsaturated 55-carbon 'carrier' lipid known as undecaprenol phosphate acts as a carrier for TA, which also act as the carrier for peptidoglycan as discussed earlier (Yokoyama *et al.*, 1989, Ginsberg *et al.*, 2006).

In *B. subtilis* 168 the *tagABDEGHO* genes were found to be involved in poly(Gro-P) TA and in *S. aureus* or *B. subtilis* W23 the *tarABDFIJKL* genes are involved in poly(Rbo-P)TA biosynthesis (Figure 1.9) (Lazarevic *et al.*, 2002, Qian *et al.*, 2006). Both the *tag* and *tar* genes are organized in divergently transcribed operons: *tagAB-tagD(E)F*, and *tarABIJKL-tarDF*, respectively (Lazarevic *et al.*, 2002). A non essential gene, *tagE* is responsible for the glycosylation of the polymer (Mauel *et al.*, 1991). The *tagA* and *tagD* genes of 168 and their counterparts *tarA* and *tarD* of W23, located on the each side of the regulatory region by 399 and 509 nucleotides, respectively, are

involved in linkage unit synthesis on the undecaprenol phosphate (Figure 1.9 & 1.10). The TagA, TagB, TagF, and TagD proteins which synthesise the linkage unit, the alditol phosphate chain and CDP-glycerol exhibit high similarity to their Tar counter parts (Lazarevic *et al.,* 2002). Though TagF exhibits high similarity with TarF, their functions are different. In strain *B. subtilis* 168, TagF polymerizes the main glycerol-P chain on the linkage unit: (Gro-P)$_2$ManNAc(β1-4)GlcNAc-P; whereas TarF is possibly limited to the addition of the second Gro-P to the linkage unit in *B. subtilis* W23 (Bhavsar and Brown, 2006). To complete the Rbo-P polymer, four more hypothetical steps, i.e. four genes are required. Two are required for the synthesis of CDP-ribitol from ribulose-P by *tarJ* and *tarI*, followed by the addition of ribitol-P onto the second Gro-P by *tarK* and finally, polymerization of the ribitol-P by *tarL* (Figure 1.9). These four genes are located downstream of *tarAB* and also very specific for poly(Rbo-P) (Lazarevic *et al.,* 2002). In *B. subtilis* 168, TagO, which is responsible for the addition of GlcNAc-P (to initiate linkage unit synthesis), and the proteins encoded by the *tagGH* operon, which are believed to act as a 'flippase' (involved in teichoic acid translocation from cytoplasm side to the outer surface of the membrane), are independent from the divergon (Neuhaus and Baddiley, 2003), but these steps are still to be identified for *B. subtilis* W23. Moreover, the enzyme involved in the translocation of teichoic acid from the lipid carrier to the peptidoglycan is still unknown.

Two promoters have been identified for the regulation of the *tag* genes expression whereas four promoters have been identified for the *tar* divergon (Mauel *et al.,* 1995). In *B. subtilis* W23, the position of the additional

promoters are located on a 100 nt DNA segment between the two *B. subtilis*168 homologue promoters (Lazarevic *et al.*, 2002).

Some TA containing organisms also contain another operon *ggaAB* encoding proteins for the synthesis of a minor teichoic acid. For example, *B. subtilis* 168 produces poly(glucosylN-acetylgalactosamine-1-phosphate) [poly(GlcGAlNac-1-P] as a minor wall teichoic acid (Freymond *et al.*, 2006).

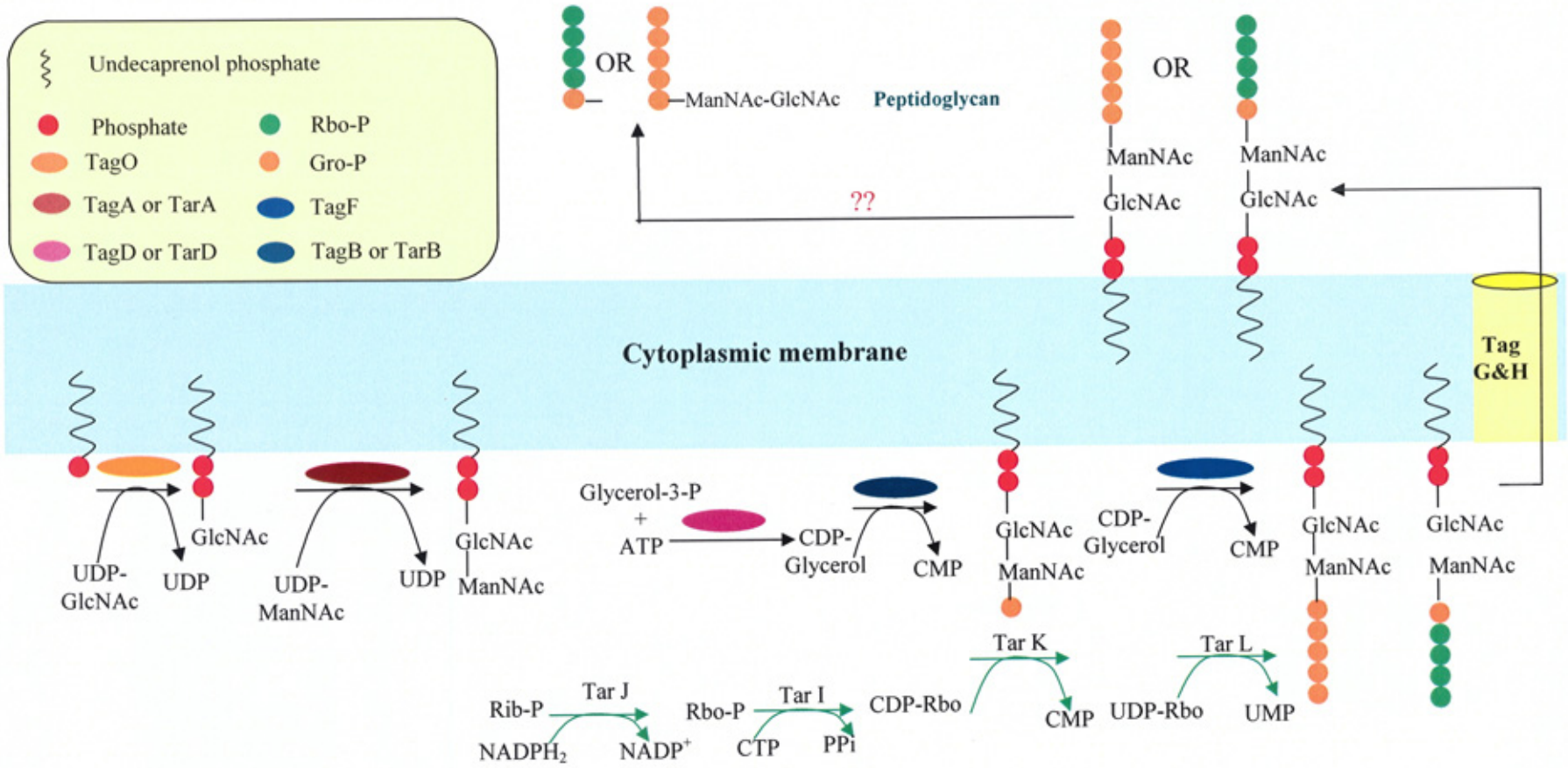

Figure 1.9. Comparison between biosynthesis pathway for the Gro-P TA of *B. subtilis*168 represented by Tag proteins and black arrows; and proposed pathway of poly(Rbo-P) by Tar enzymes and green arrows. ? mark not identified. The data have been taken from Lazarevic *et al.,* 2002; Bhavsar & Brown, 2006; Qian *et al.,* 2006. Cytoplasmic TagE use UDP-glucose to add glycosyl substituents to growing TA has been omitted for clarity.

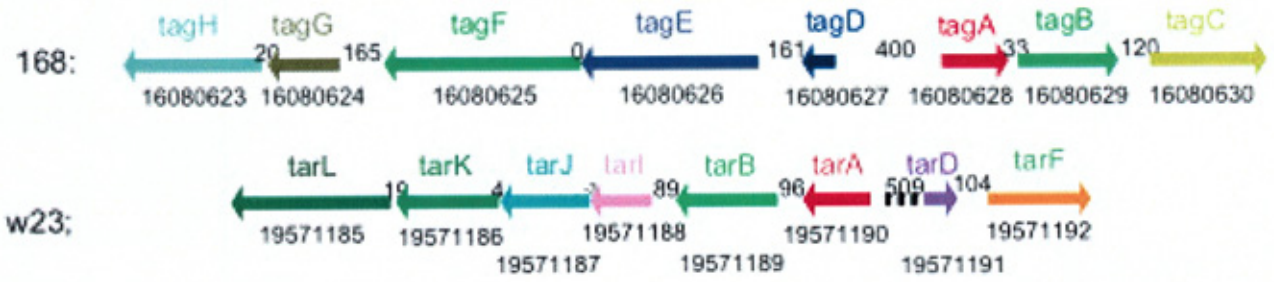

Figure 1.10. Genomic organizations of tag/tar genes of *Bacillus subtilis* 168 and W23 strains, taken from Qian *et al.* (2006). Abbreviation encoded enzymes for, tagA: N-acetylmannosaminyltransferase; tagB: CDP-glycerol:glycerophosphate glycerophosphotransferase; tagC: Major teichoic acid biosynthesis protein C, tagD: Glycerol-3-phosphate cytidylyltransferase; tagE: Poly(glycerol-phosphate) alpha-glucosyltransferase; tagF: CDP-glycerol:poly(glycerophosphate) glycerophosphotransferase; tagG: Teichoic acid translocation permease protein; tagH: Teichoic acids export ATP-binding protein tagH; tarA: N-acetylmannosaminyltransferase; tarB: CDP-glycerol:glycerophosphate glycerophosphotransferase; tarL: Polyribitolphosphotransferase; tarD: Glycerol-3-phosphate cytidylyltransferase; tarF: CDP-glycerol:glycerophosphate glycerophosphotransferase; tarI: Ribitol-5-phosphate cytidylyltransferase; tarJ: Ribitol-5-phosphate dehydrogenase; tarK: Ribitolphosphotransferase; tarL: Polyribitolphosphotransferase

1.6.2.2. Essentiality of *tag* and *tar* genes

Previous studies (Bhavsar *et al.*, 2004, Ginsberg *et al.*, 2006, Weidenmaier e*t al.*, 2005) have suggested that mutations in *tag* genes are lethal for the cell and concluded that TA is essential for cell viability. However, D'Elia *et al.* (2006a, 2006b) were able to show that wall TA biogenesis is dispensable in *S. aureus* and *B. subtilis*. In these studies they were able to delete the *tagO* and *tarO* genes, which are responsible for the first step in TA synthesis of *B. subtilis* and *S. aureus*, respectively. The mutations had no effect in the viability of the cells *in vitro*. However, the later genes of the TA synthesis pathway (which are responsible for the polymer formation and export) were found to be essential for the cell viability. The study suggested, since *tagO* or *tarO* is essential in TA synthesis and deletion of the gene is not lethal for bacterial growth, then TA may not be essential for cell viability. On the other hand, lethality of the deletion of later genes could suggest two things: i) that TA is essential for the cell viability and in the *tagO* or *tarO* mutants, the first step may be bypassed by other enzymes. ii) lipid-liked precursor of TA (synthesised downstream from the TagO step) may be toxic to the cells or accumulation of the polyprenol linked precursors of TA may decrease the availability of the free polyprenols which are also required for PG biosynthesis and this eventually cause cell lysis (D'Elia *et al.*, 2006a).

1.6.3. Teichuronic acid

Teichuronic acid is a phosphate-free glucuronic acid polymer attached to the PG of bacterial cell walls (Wright and Heckels, 1975) and is synthesized by enzymes encoded in the *tua* operon (Soldo *et al.,* 1999). The distribution of teichuronic acids is less widespread in Gram-positive bacteria compared to TA. It has been found in members of both low G+C Gram-positive genera (*Bacillus, Staphylococcus* and *Streptococcus*) and high G+C genera such as *Actinoplanes*, *Catellotospora*, *Corynebacterium, Micrococcus* and *Propionibacterium,* (Naumova and Shashkov, 1997).

Ellwood & Tempest (1969) have reported that during phosphate limited growth, the anionic glucuronic acid components of teichuronic acid are substituted for the anionic phosphate groups of TA in order to satisfy the cellular requirement for an anionic polymer *(Soldo et al., 1999, Archibald et al.,* 1993), and to liberate phosphate from the TA for reutilisation for more urgent uses such as nucleic acid synthesis (Bhavsar *et al.,* 2004). However, there is a debate with this accepted hypothesis, as a significant amount of TA has been detected in the cell walls of *B. subtilis* 168 under phosphate limited condition (Soldo *et al.,* 1999) and also because the bacterium was found to be compromised in culture density rather than depleting its TA as phosphate became increasingly limited, which raised the possibility that TA may still be essential for growth during phosphate limitation and may play a unique role that teichuronic acid cannot play (Bhavsar *et al.,* 2004, Lang *et al.,* 1982). Both TA and teichuronic acid polymers have been shown to bind magnesium ions

with nearly identical affinities (Heckels *et al.,* 1977) and also regulate autolysis (Calamita and Doyle, 2002), which suggests that the teichuronic acid can play most of the roles of TA and during phosphate limited conditions may allow a decrease in the TA amount rather than fully substituting for it.

Sequence analysis has revealed the *tua* operon (*tua ABCDEFGH*) of *B. subtilis 168* encoding enzymes required for the teichuronic acid and its precursor UDP-glucuronate (Soldo *et al.,* 1999). The organization of the *tua* operon and roles of the different genes are shown on Figure 1.11.

A

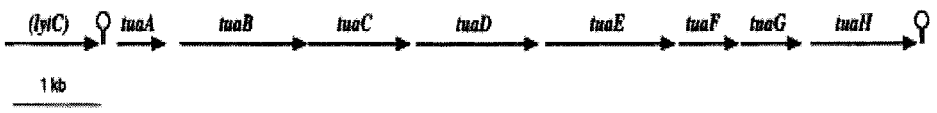

B

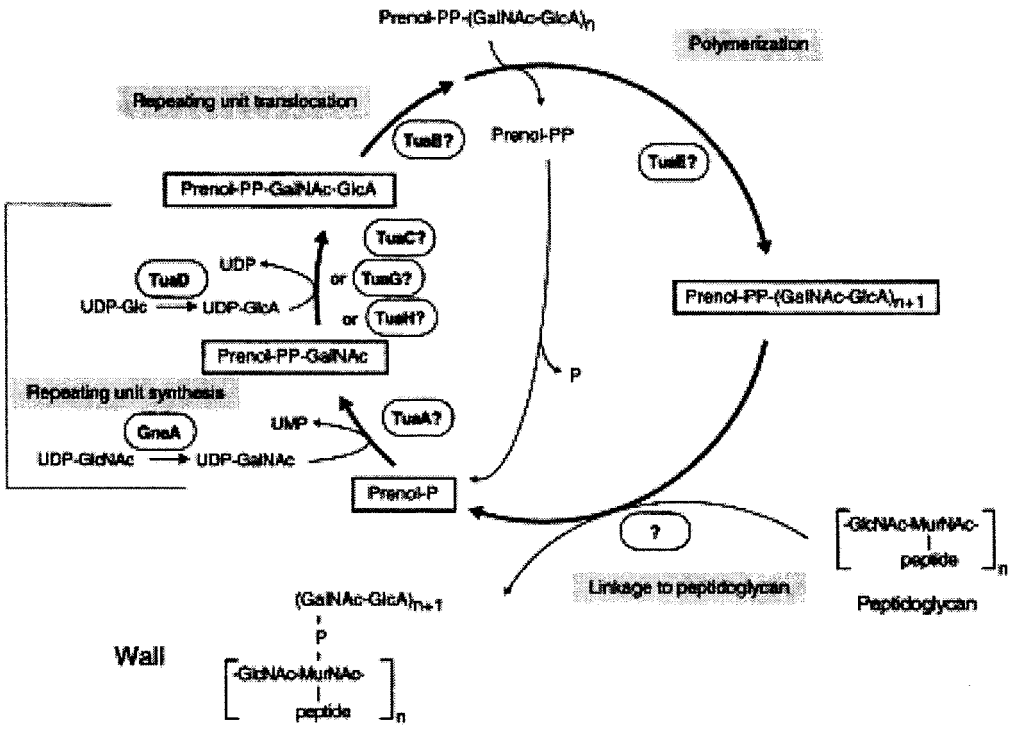

Figure 1.11(A). Organization of the *tua ABCDEFGH* operon. Thick arrows correspond to ORFs. ⚲ represents a putative transcriptional terminator. Taken from Soldo *et al.,* 1998. (**B**) Putative metabolic pathway and role of *tua* gene products in the synthesis of *B. subtilis* stain 168 teicuronic acid. Taken from Soldo *et al.,* 1998.

1.6.4. 'Non-classical' SCWPs

Binding of SCWPs to PG is a common characteristic for both classical and non-classical SCWPs. The main difference between them is that classical SCWPs are thought to play a direct role in cell function, whereas non-classical SCWPs are thought to play indirect roles, such as providing a scaffold for S-layer proteins (Schaffer and Messner, 2005). In Gram-positive bacteria two well characterized 'non-classical' SCWPs are arabinogalactan (AG) and SCWPs of S-layer protein.

Arabinogalactan (AG) is the linking structure between the PG and the mycolic acids in members of the mycolata group of high G+C Gram-positive bacteria (discussed in Section 1.4). AG may represents ~ 35% of the mass of cell walls (Daffe *et al.,* 1993). In most mycolic acid containing organisms, this linking structure is composed of two linked polysaccharide segments, homogalactan and arabinan. In *Mycobacterium tuberculosis* the homogalactan portion is composed of alternating 5-linked β-galactosyl furanosyl (β-Gal*f*) and 6-linked β-Gal*f* units and the arabinan composed of three major domains, a linear 5-linked arabinosyl furanosyl (Ara*f*), a β- Ara*f*-(1→2)-α-Ara*f* disaccharide branched on both 3 and 5 positions of an Ara*f* unit and a 5-linked-α-Ara*f* unit branched position on both 3 and 5 position of an Ara*f* unit (Daffe *et al.,* 1993, Tropis *et al.,* 2005). The arabinan chains are attached to the galactan segment through the C-5 of some of the 6-linked Gal*f* units (Mcneil *et al.,* 1991). In *M. tuberculosis*, AG contain a branched hexa-arabinoside (Ara_6) terminus at the non reducing end, which distinguishes it from another arabinose containing cell

envelope macromolecule, lipoarabinomannan (LAM) which contain a linear terminal tetra-arabinoside (Ara_4) (Zhang *et al.,* 2003). The mycolic acids are attached to this Ara_6 non-reducing end of AG as [5-O-mycolyl-β-D-Ara*f*-(1→2)-5-O-mycolyl-α-D-Ara*f*]-3,5-α-D-Ara*f* (Mcneil *et al.,* 1991). At the reducing end, a special diglycosylphosphoryl bridge (linkage unit), L-Rhap-(1→3)-D-GlcNAc(1→P) links the galactan of AG to the C-6 of some of the muramyl residues of PG (Mcneil *et al.,* 1991, Brennan and Crick, 2007).

Emb proteins encoded by the genes in the operon of *embCAB* were found to be involved in the arabinan segment of these molecules (Belanger *et al.,* 1996, Cole *et al.,* 1998). Knockout mutants of *embA* and *embB*, individually, showed that their gene products were involved in the AG biosynthesis, as each mutant considerably reduced the formation of non-reducing terminal disaccharide of AG, but the mutation had no effect on LAM biosynthesis (Escuyer *et al.,* 2001). The arabinose source on the outer surface of the cell membrane will be discussed later in section 1.7.5.2.

The second example of 'non-classical' SCWPs is the SCWP associated with S-layer proteins (Figure 1.6). These cell wall polymers act as a link between S-layer protein and PG. The SCWP is bound to the N-terminal region of S-layer proteins by two types of motifs in these proteins. Firstly, S-layer homology (SLH) motifs in an SLH domain (composed of approximately 55 amino acids, containing 10-15 conserved residues at the N-terminus of S-layer proteins)

bind to a distinct type of pyruvylated SCWP, which has been identified in *B. anthracis* (Schaffer and Messner, 2005). Alternatively, in *Geobacillus thermophilus* wild type strains, where S-layer protein lacks an SLH domain, a non-pyruvylated SCWP containing a negatively charged 2,3-dideoxydiacetamidomannosamine uronic acid interacts with a highly conserved N-terminal region of the S-layer protein (Sleytr *et al.,* 2007). A lectin-type binding has also been identified between a SCWP and the C-terminal region of the S-layer protein of *Lactobacillus acidophilus* ATCC 4556 and *Lactobacillus crispatus* (Sleytr *et al.,* 2005, Sleytr *et al.,* 2007).

1.7. Macroamphiphiles (MA)

The term 'macroamphiphile' is used to describe a diverse range of macromolecules or large polysaccharide polymers in the cell membranes of bacteria. Unlike SCWPs, these molecules are anchored into the cell membrane instead of covalently bound to the PG. The general feature of these molecules is that they contain both hydrophilic and hydrophobic regions (Figure 1.12A). The hydrophobic region is composed of fatty acids which is anchored into the cell membrane (orange region in the Figure 1.12A), whilst the hydrophilic region is composed of variable carbohydrate or polysaccharide structures (blue region of the Figure 1.12A). Such amphiphiles or amphiphatic molecules are distributed in many membranes but bacterial membrane macroamphiphiles have been of considerable interest for their serological and biological properties and their possible role in the pathogenesis of disease. In the case of Gram-positive bacteria, these amphiphiles are anchored in the cytoplasmic membrane and the hydrophilic part is extended from the membrane/wall interface through the peptidoglycan and, to a lesser extent, to the external surface of the cell (Figure 1.12B) (Wicken and Knox, 1980).

In the case of Gram-negative bacteria these macroamphiphiles are detectable in the outer leaflet of the outer membrane and also to a lesser extent in the external environment (Figure 1.12C).

A

B

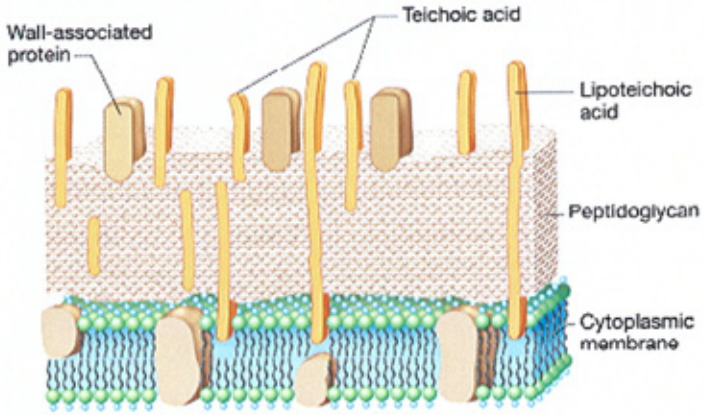

C

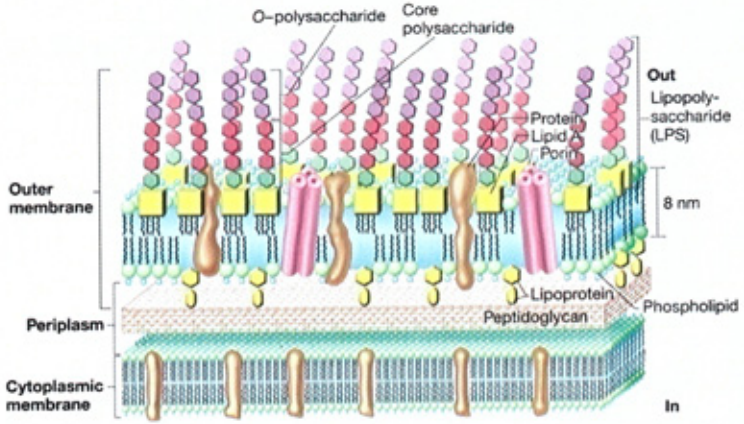

Figure 1.12. Schematic presentation of (**A**) a generalised macroamphiphile structure (**B**) Teichoic acid (SCWP) and LTA (macroamphiphile) in Gram-positive bacteria and (**C**) LPS (macroamphiphile) in Gram-negative bacteria. The pictures in parts B and C have been taken from Madigan *et al.* (2003).

1.7.1. Classification of the major macroamphiphiles

Macroamphiphiles can be classified into different groups depending on the chemical composition of the molecules. The major macroamphiphiles are (Figure 1.13):

1) Lipopolysaccharides (LPS) of Gram-negative bacteria
2) Lipoteichoic acids (LTA) of Gram-positive bacteria
3) Lipoglycans (LCHO) of Gram-positive bacteria

Lipoglycans can be further classified into lipoglucogalactans, lipomannans (LM), lipoarabinomannans (LAM) and LAM-like compounds etc, which will be described in later sections. The schematic presentations of the major macroamphiphiles with their general chemical composition are shown in Figure 1.13.

1.7.2. Distribution of the macroamphiphiles

The general distributions of the major macroamphiphiles are summarised in Table 1.2 (Wicken and Knox, 1980, Sutcliffe, 1994b, Sutcliffe and Shaw, 1991). It has been generalised that "LPS, LTA and lipoglycan do not occur together in the same organism and may replace each other functionally" (Fischer, 1994b). Generally, Gram-negative bacteria possess lipopolysaccharide (LPS), which is anchored into the outer leaflet of the outer membrane as shown in the Figure 1.12 (C) (Wicken and Knox, 1980). The present study deals with the distribution and characteristics of the Gram-positive bacterial macroamphiphiles, so the following sections describe the

major macroamphiphiles in Gram-positive bacteria, especially LTA and lipoglycans.

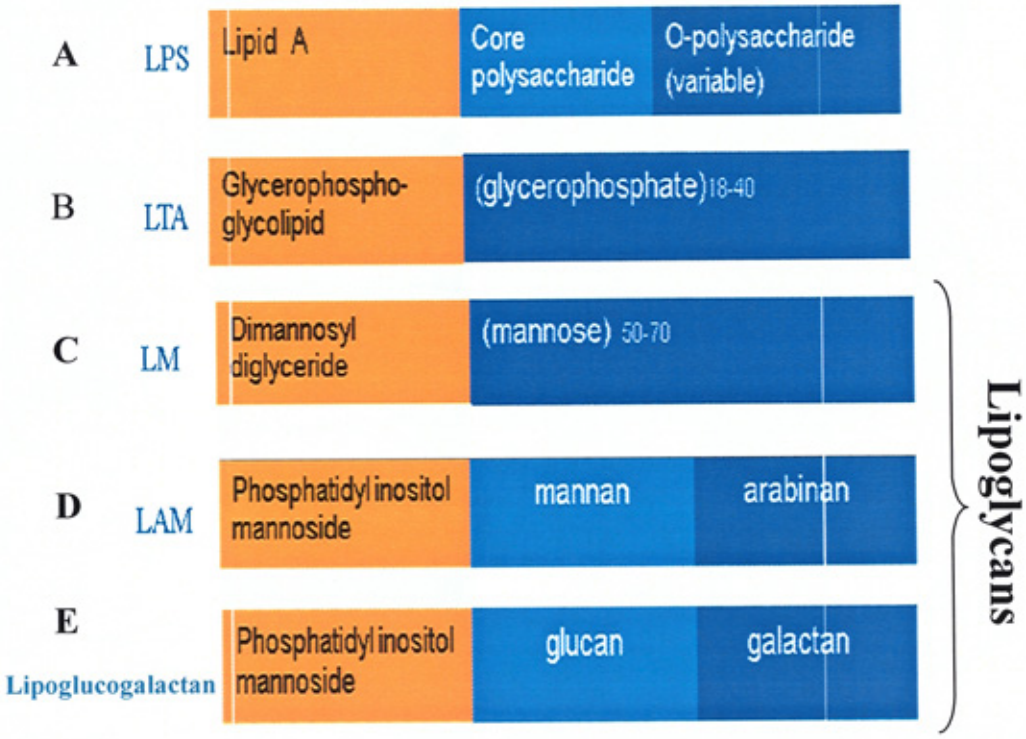

Figure 1.13. Schematic presentation of (A) LPS: Lipopolysaccharide (B) LTA: Lipoteichoic acid (C) LM: Lipomannan and (D) LAM: Lipoarabinomannan (E) Lipoglucogalactan

Table 1.2. General distribution of macroamphiphiles in bacteria

Subgroup	**Macroamphiphiles**
Gram-negative	Lipopolysaccharide (LPS)
Gram-positive (Low G+C)	Lipoteichoic acid (LTA) Lipoglycans (*Mollicutes*)
Gram-positive (High G+C)	**Lipoglycan:** Lipoglucogalactans Lipomannan (LM), Lipoarabinomannan (LAM) LAM-like Other lipoglycans **LTA***

* The presence of LTA in actinomycetes is discussed in the text

1.7.3. Lipoteichoic acid (LTA)

In analogy to TA, LTA contain alditolphosphates as integral parts of their hydrophilic chain, but unlike TA rather than being bound to the PG, LTA are anchored to the cytoplasmic membrane of the cell via their hydrophobic fatty acids. Moreover the alditolphosphate in LTA and TA are sterochemically different (see below). LTA and TA have been considered as more or less secondary cellular components but at present this view is changing as clear evidence of TA as important components of *B. subtilis* and *S. aureus* (which has been described in the TA sections 1.6.2.2) and also LTA lacking mutants could not be detected either in *S. aureus* or in *Lactobacillus casei* by chemical mutagenesis (Fischer, 1994a). Indeed LTA appears to be an essential component in *S.* aureus (Grundling and Schneewind, 2007) as discussed in the section on LTA biosynthesis in Section 1.7.3.3.

The distribution of LTA has been generalised to be restricted to the Low G+C subgroup of Gram-positive bacteria, *Firmicutes* (Sutcliffe, 1994b), though some studies (Gnilozub *et al.,* 1994b, Potekhina et al., 1983) suggest that LTA may also be present in members of the high G+C subgroup of Gram-positive *Actinobacteria.*

1.7.3.1. Chemical composition and occurrences of LTA

The chemical composition of LTA can be viewed as a fusion of two molecules: a glycolipid or lipid anchor and a hydrophilic chain structure which is composed of repeated unit of alditolphosphates (Figure 1.14). Even though the polymer chain structure of LTA and TA both possess a poly(glycerophosphate) chain, they are structurally and metabolically unrelated. The glycerol-phosphate (GroP) residues of LTA are derived from UDP-glycerol (phosphatidyglycerol) and have a *sn*-glycero-1-phosphate stereochemistry; GroP in TA is derived from CDP-glycerol (discussed in section 1.6.2.1) and has a *sn*-glycero-3-phosphate stereochemistry i.e. two different enantiomeric stereochemical configurations.

1.7.3.1.1. Chain structure

The chain is typically composed of a single unbranched chain of GroP linked by a phosphodiester bond to the glycolipid moiety. The structure variation of this chain in different species and genera occurs in respect to length of the chain and substitution on C-2 of its glycerol residues. The length of the chain is fairly constant between 16 to 40 GroP units in different strains of the species (Iwasaki *et al.,* 1986, Fischer *et al.,* 1978b, Fischer *et al.,* 1978a, Nakano and Fischer, 1978). The substituents are generally D-alanyl ester or glycosyl residues, as in TA, which can be classified into four groups according to substituent: Group I lacks any substituents; Groups II and III carry D-alanyl esters or glycosyl residues, respectively; and the group IV contains both these substituents (Table 1.3). D-alanine has been the only amino-acid residue detected so far, while a narrow range of common monosaccharide residues

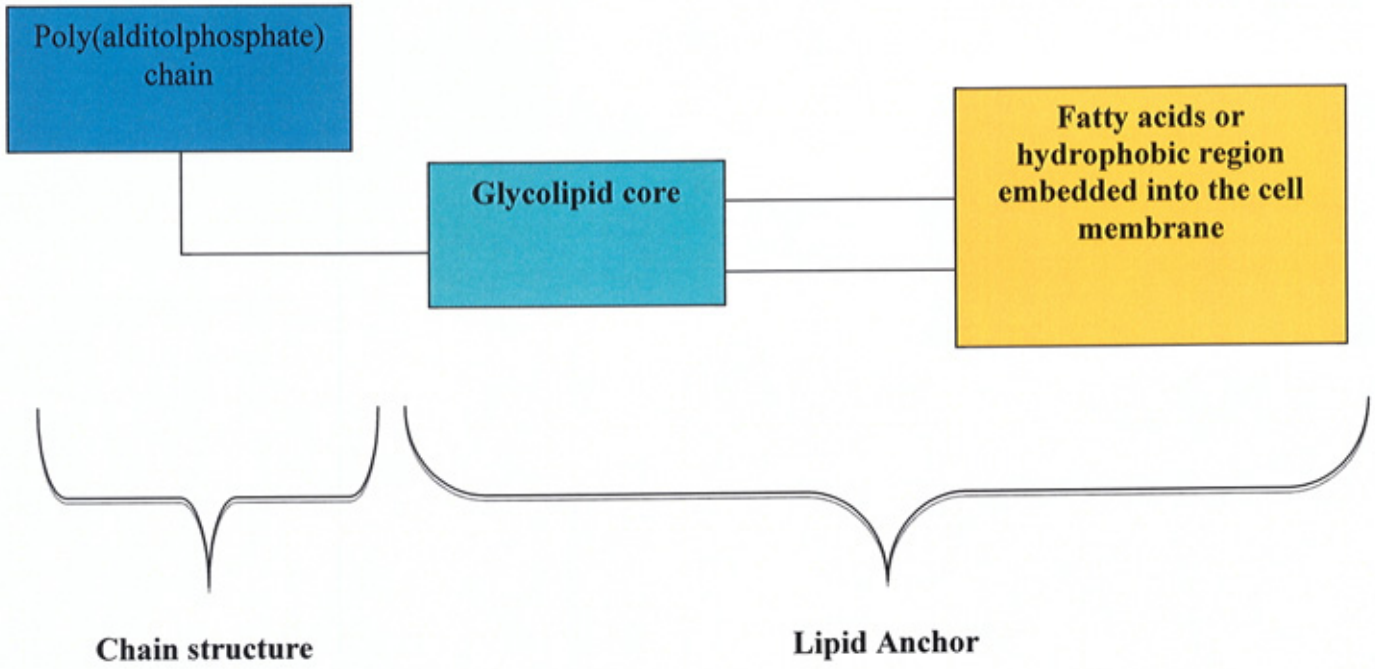

Figure 1.14. Schematic presentation of the Lipoteichoic acid (LTA).

Table 1.3. Grouping of poly(GroP)LTA from *Firmicutes* based on substitution type. Modified from Fischer, 1988.

Groups	Substituent		LTA from
	D-alanine	Glycosyl	
I	None	None	'*Micrococcus varians*' ATCC 29750 (*Staphylococcus* sp.); *Bacillus megaterium*, various strains
II	Present	None	*Lactobacillus casei, Lactobacillus helveticus*, Streptococci group A, *Lactococcus plantarum, Lactococcus raffinolactis, Staphylococcus xylosus, Staphylococcus aureus* H
III	None	Present	*Bacillus coagulans, Enterococcus faecalis* ATCC 9790
IV	Present	Present	*Enterococcus faecalis* Kiel 277738, DSM 20478, NCIB 8191, NCIB 39; *Lacotcoccus lactis*, *Listeria* various species, *Bacillus licheniformis*, *Bacillus subtilis* various strain.

have been found, with an exception of LTA from *Enterococcus faecalis* strains containing mono-, di-, tri- and tetrahexosyl residues as substituents (Fischer, 1988). The degree of glycosylation and alanylation of the poly(GroP) chain differs from strain to strain, though whether an organism contain mixtures of substituted and unsubstitued LTA or whether all chains are partially substituted is still unknown (Fischer, 1988). These variations can be used to identify different group of bacteria by antigen grouping or lectin affinity chromatography (Fischer and Rosel, 1980, Wicken and Knox, 1975).

Another type of LTA contains a poly(glycosylalditolphosphate) chain structure, found in few species of Low G+C Gram-positive bacteria. For example, the LTA of *Lactococcus garvie*ae is chains composed of α(1→6)-linked digalactosyl residues between the GroP moieties, and position 2 of the later is substituted with another α-D-galactopyranosyl (Gal*p*) residue (Fischer, 1994b) and D-alanine substituents are absent. *Clostridium innocuum* contains LTA which has β-Gal*p* residues intercalated between the GroPs moieties.

In the lipoteichoic acid of *Streptococcus pneumoniae* a unique situation occurs with the replacement of GroP by tetrasaccharide-ribitol-phosphate repeated unit and also phosphocholine substitutions are found on the two N-acetylgalactosamine residues of the tetrasaccharide (Behr *et al.,* 1992). The repeated units are identical to the structure of the TA of the organism and the presence of ribitol-phosphate defined it as a LTA rather than a lipoglycan (Sutcliffe, 1994b, Fischer *et al.,* 1993).

Another type of LTA which has been found in 'nutritionally variant' steroptococci serotypes I and II which has been reclassified as *Streptococcus defectiveus* and *Streptococcus adjacens*, respectively (Bouvet *et al.*, 1989) found to be lacking in PGP-LTA and compositional analysis of *S. defectiveus* showed the presence of a lipidated poly(RboP) with galactose and alanine sustituents (Sutcliffe, 1994b). *Streptococcus mitis* and *Streptococcus oralis* which were also considered to have a close relationship with 'nutritionally variant' steroptocci found to be lack in PGP-LTA (Sutcliffe, 1994b).

1.7.3.1.2. Lipid Anchor

The lipid moiety of the LTA acts as an anchor in the cytoplasmic membrane. The anchor is typically composed of fatty acids, in the form of diacylglycerol, and a carbohydrate unit, as in glycolipids and phosphoglycolipids. As the distribution of glycolipids and phosphoglycolipids among Gram-positive bacteria is usually genus and species-specific, so the LTA anchor structure varies accordingly (Fischer, 1994a).

The structure and occurrence of different kinds of lipid anchor for poly(GroP) LTA, depending on the sugar moiety, are listed in Table 1.4 where dihexosyldiacylglycerols are common and trihexosyldiacylglycerols occur rarely, whereas monoheoxosyldiacylglycerol have not been detected but are believed to be present as the precursor of dihexosyldiacylglycerols (Fischer, 1988). In a number of genera such as *Enterococcus, Lactobacillus, Lactococcus, Streptococcus,* either a third fatty acid ester (acyl) or a *sn*-3-phosphatidyl (Ptd) residue was detected in the LTA anchor, in addition to the

Table 1.4. Lipid anchors (linkage unit) of poly(GroP)LTA. Taken from Fischer, 1994b.

Glycolipid	Derivative	Occurrence (Gram-positive Low G+C)
Glc(α1-2)Glc(α1-3)acyl$_2$Gro	-	*Streptococci, Leuconstoc*
Glc(α1-2)Glc(α1-3)acyl$_2$Gro	Glc(α1-2)Glc(α1-3)acyl$_2$Gro 6 └acyl	*Lactococci*
Glc(α1-2)Glc(α1-3)acyl$_2$Gro	Glc(α1-2)Glc(α1-3)acyl$_2$Gro 6 └Ptd	*Enterococci*
Glc(β1-6)Glc(β1-3)acyl$_2$Gro	-	*Bacilli, Staphylococci*
Gal(α1-2)Glc(α1-3)acyl$_2$Gro	Gal(α1-2)Glc(α1-3)acyl$_2$Gro 6 └acyl	*Streptococci, Lacotbacilli*
Gal(α1-2)Glc(α1-3)acyl$_2$Gro	Gal(α1-2)Glc(α1-3)acyl$_2$Gro 6 └Ptd	*Listeria*
Glc(β1-6)Gal(α1-2)Glc(α1-3)acyl$_2$Gro	Glc(β1-6)Gal(α1-2)Glc(α1-3)acyl$_2$Gro 6 └acyl	*Lactobacilli*
	acyl$_2$Gro	*Bacilli*

* Ptd represents phosphatidyl residues and acyl represents fatty acid

glycolipid, which may be expected to anchor the LTA more firmly in the membrane, but they represent less than 50% of the total LTA of the representative organism (Fischer, 1988).

The fatty acid composition of LTA is usually quite similar to that of the total cellular lipids, thus reflecting the origin of the lipid moiety from membrane lipids (see below). However, the amounts of the fatty acids may differ, with the absence of some fatty acids in LTA compared to the total membrane lipids, which may be due to lower accessibility of these fatty acids to the location in the outer layer of the membrane. For example, *Enterococcus faecalis* total lipids contained 3.4% C14:0, 37.7% C16:0, 7.5% C16:1, 35.8% C18:1 and 15.5% Cis-11,12-methylene-octadecanoic acid whereas the LTA contained these fatty acids in the proportions 5.7% C14:0, 37.7% C16:0, 8.7% C16:1, 40% C18:1 and 7.9% Cis-11,12-methylene-octadecanoic acid (Toon *et al.,* 1972). In *Lactococcus lactis,* the cell membrane contained C14:1 but this fatty acid was absent from the LTA (Fischer, 1994a). However, there has not been any evidence for fatty acids being present in the LTA but absent from the cell membrane lipids.

1.7.3.2. Functions of LTA

Although many functions have been attributed to LTA, its specific functions are still unknown. LTA, along with TA and PG, makes up a polyanionic network or matrix which provides the cell envelope with elasticity, porosity, tensile strength, and electrostatic characteristics and also affects the permeability of the membrane and binding of cell surface proteins (Archibald *et al.,* 1993, Buckland and Wilton, 2000, Dijkstra and Keck, 1996, Doyle and Marquis, 1994, Labischinski and Maidhof, 1994, Marquis, 1988, Thwaites and Mendelson, 1991).

The ion-exchange properties of the polyanionic matrix has the capability to bind divalent cation like magnesium or calcium ions, which are required for the functions of membrane associated enzymes such as autolysins (Foster and Popham, 2002, Shockman and Holtje, 1994). Autolysins bind to the bacterial cell surface and degrade the peptidoglycan layer, which is required for the cell growth and cell division (Holtje and Tuomanen, 1991, Oshida *et al.,* 1995). Mutation in the *ypfp* gene (discussed later in section 1.7.3.3.2) of *S. aureus* lead to a marked decrease in LTA production and a clear reduction was also found in the activity or substrate accessibility of the autolytic enzymes (Fedtke *et al.*, 2007). This affect has also been identified by mutating the *ltaS* gene (discussed later in section 1.7.3.3.3) of *S. aureus* (Grundling and Schneewind, 2007a) and may occur due to two reasons. Firstly, this may be due to a decreased concentration of divalent cations like magnesium or calcium ions which are require for the autolytic enzymes at low ionic strength (Bierbaum and Sahl, 1987). The second reason may be a decrease in the non-covalent binding of

these proteins to LTA on the surface of the membrane by a non-covalent binding motif known as GW motif (Desvaux *et al.,* 2006). Internalin B (InlB), an autolysin in *Listeria monocytogenes* was found to interact with LTA by this motif of ~80 amino acids long containing Glycine-Tryptophan (Gly-Trp) dipeptide known as GW module (Jonquieres *et al.,* 1999). Autolysin activity may also be affected by the D-Ala substitution of LTA or TA, as this substitution decreases the negative charge of these macromolecules and with that their capacity for binding divalent cation required for the enzymatic activity and also the interaction with the GW module of the enzyme *(Fischer et al.,* 1981). So, D-alanylation of LTA may play a vital part in autolysin activity and regulate the cell growth and division.

D-alanylation of LTA also play a vital role in the pathogenicity of the organism, which has been established for *L. monocytogenes, S. agalactiae* and *S. aureus* (Abachin *et al.,* 2002, Collins *et al.,* 2002, Poyart *et al.,* 2003). This role may depend on two factors. Firstly, increasing polyanionic surface charge may weaken the adherence of these bacteria to host surfaces. The second factor may be altering the binding characteristics of adhesins (Neuhaus and Baddiley, 2003), which are bacterial cell surface proteins which may form complexes with LTA (Beachey and Simpson, 1982). The binding of these proteins with LTA determines the cell surface hydrophobicity. Decreasing the amount of cellular LTA by *ypfp* mutation of *S. aureus* reduced its capability to form a biofilm on hydrophobic polystyrene plates, due to its loss of capability to adhere to the surface (Fedtke *et al.,* 2007).

The elastic capacity of the polyanionic matrix occurs due to the charge-charge repulsion of the phosphodiester anionic linkages of LTA or TA. This elasticity has a correlation between the rigid-rod and random coil conformations of the LTA during interactions with PG that may determine the expansion and contraction of the cell wall (Neuhaus and Baddiley, 2003). The interchange between TA conformations (from helical structure to random coil) at low ionic strength is disrupted by the addition of either Ca^{2+} or Mg^{2+} (Pal *et al.,* 1990). On the other hand, due to increases in charge-charge repulsion on removal of D-alanyl esters from TA, the *S. aureus* cell wall has found to expand in volume from 5.1 to 10.1 mL/g (Ou and Marquis, 1970).

The capacity of the membrane for trafficking of ions, nutrients, proteins and antibiotics depends on the proton gradients (Kemper *et al.,* 1993, Ou and Marquis, 1970). The proton gradient which is formed due to the charge distribution in the envelope of the respiring cell and can possibly extend approximately 2 nm into the wall matrix (Kemper *et al.,* 1993, Koch, 1986). However this may be affected by the presence of counter ions such as potassium.

LTA may also influence the fluidity and permeability of the cell membrane and also may involved in the membrane separation during cell division and thermotropic membrane properties (Fischer, 1988, Fischer, 1990, Gutberlet *et al.,* 1997). These functions of LTA can be influenced by the supramolecular organization of the LTA.

The LTAs has the ability to form micelles in aqueous media, where the glycolipid forms the centre of the micelle and the hydrophilic chains occupy the outer water-filled shell (Fischer, 1994b, Wicken *et al.,* 1986). This is a common supramolecular organization for LTA or lipoglycans but is different from LPS. The ratio of the cross-sectional area for the hydrophobic and hydrophilic regions of LPS with its six or seven appropriately spaced fatty acid residues is approximately 1, making the overall shape cylindrical (Figure 1.15A) and ordered in a lamellar arrangement (Figure 1.15B). On the other hand, the molecular shape of LTA is conical (Figure 1.15C) since it has only two or three fatty acids making the hydrophobic cross-sectional area smaller than hydrophilic region and this causes its micellar arrangement, which is also similar for lipoglycan. Thus, in contrast to formation of surface layer like LPS, instead LTA or lipoglycan have to be inserted into membranes, formed by phosopholipid or DAG-type lamellar-phase lipids (Figure 1.15D) (Fischer, 1994b, Fischer, 1988).

The distribution of LTA in cell membranes can also affect the fluidity and permeability characteristics of the membrane. The presence of high concentration of LTA, decreasing the mean area per molecule of LTA, may possibly squeeze out micellar LTA from monolayers (Fischer, 1988). Moreover, the rigid rod (extended) and coil conformation of LTA caused due to low and high-ionic strength medium, respectively, may also play an important part in the fluidity and permeability of the membrane (Neuhaus and Baddiley, 2003). In vesicles of dipalmitoyl-sn-glycero-3-phospho-1-glycerol (DPPG) at high ionic strength, the glycolipid anchor of LTA interaction with

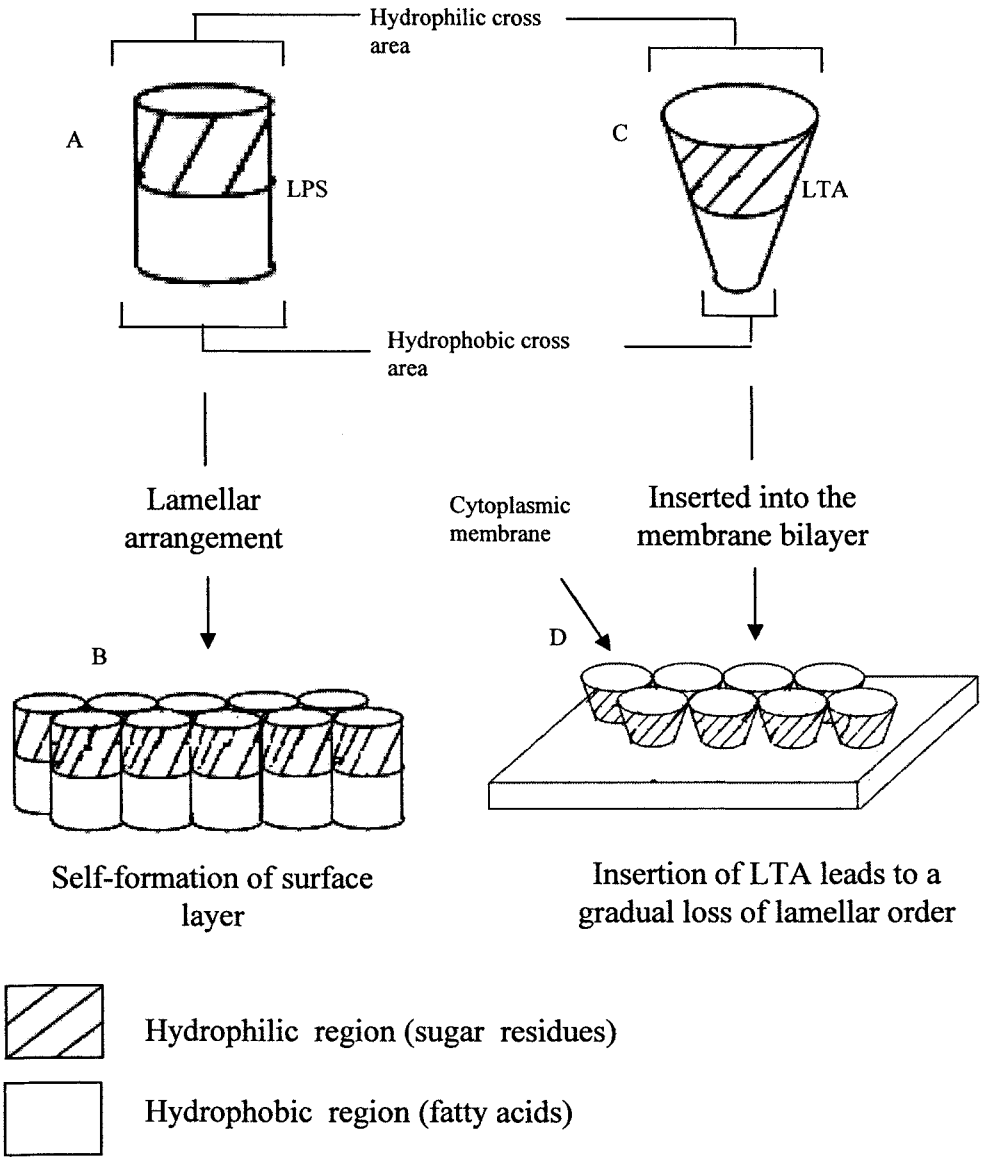

Figure 1.15. Model of LPS and LTA. The ratio of the cross-sectional areas of the hydrophobic and the hydrophilic regions for LPS are approximately 1 and for LTA <1 which gives cylindrical (**A**) and conical shape (**C**), respectively. (**B**) LPS has the capacity to arrange as a surface layer, (**D**) LTA instead needs to be inserted into a membrane and then may change the fluidity and permeability of the membrane.

the GroP moiety of adjacent DPPG, and long distance interactions between the DPPG headgroup and LTA poly(GroP) chains in a random-coil conformation was hypothesized to stabilize the fluidity of the membrane (Gutberlet *et al.*, 1997).

1.7.3.3. LTA biosynthesis

Understanding of LTA biosynthesis is still incomplete, and there is debate about the synthesis steps and their cellular compartmentisation. This section discusses the different proposed pathways and presents models for the LTA biosynthesis pathway.

The biosynthesis of LTA can be divided into four parts a) providing a source of GroP b) lipid anchor biosynthesis c) polymerisation of the GroP chain and d) substitution of the GroP chain by alanylation and glycosylation.

1.7.3.3.1. Source of glycerolphosphate (Gro-P)

The Gro-P required for LTA biosynthesis is derived from PtdG, rather than CDP-glycerol which serves as the donor in the synthesis of TA (Fischer, 1994a, Fischer, 1994b, Fischer, 1988). The synthesis of the poly(GroP) LTA chain probably occurs on DAG or PtdG and the chain is then transferred on to the specific glycolipid anchor (Table 1.4; see section 1.7.3.3.3), a step which likely occurs on the outer surface of the cytoplasmic membrane (Fischer, 1994b). On the other hand, PtdG synthesis occurs at the inner surface of the cytoplasmic membrane by four reactions (Cronan, 2003, Dowhan, 1997b) catalyzed by: 1) DAG kinase 2) CdsA 3) PgsA and 4) an unknown phosphatase. PtdG is finally transfered to the outer leaflet of the membrane by an unknown flippase enzyme as shown in Figure 1.16. After transfer of the GroP from the PtdG, the released diacylglycerol (DAG) is returned to the inner leaflet and is reused for further PtdG synthesis (Cronan, 2003).

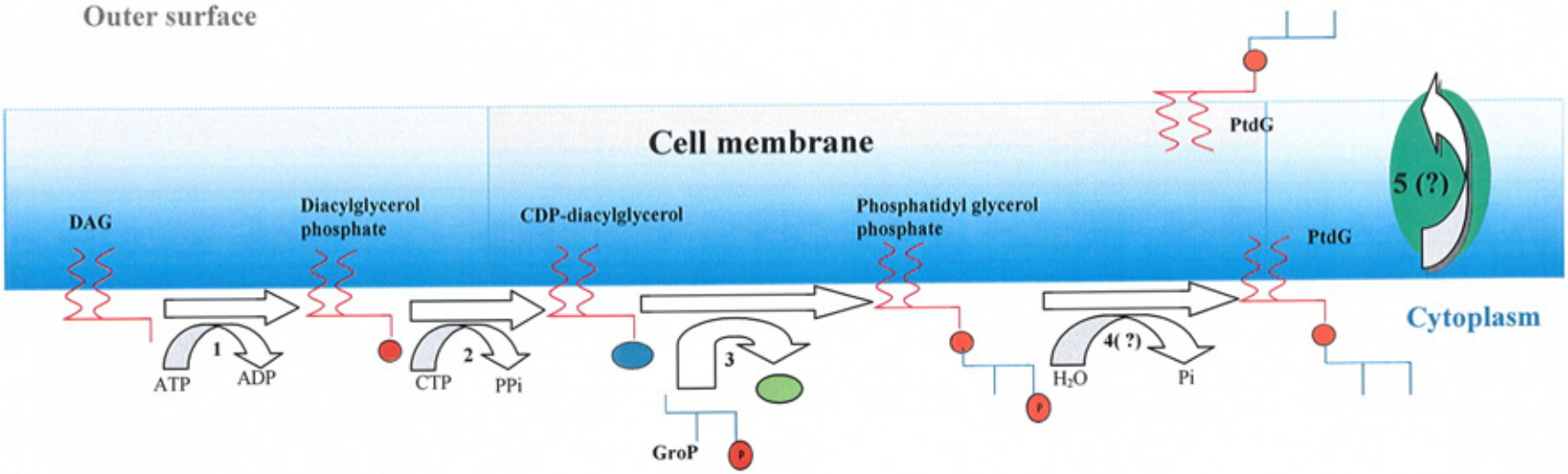

Figure 1.16. Schematic presentation of PtdG biosynthesis, the source of GroP as a source poly(GroP) LTA chain elongation. DAG, CTP and ATP represent DAG, CTP and ATP. The enzyme responsible for the steps are 1)DAG kinase 2)CdsA 3)PgsA 4)Unknown phosphatase 5)Unknown flippase.  represents CDP, CMP is represented by  and  represents phosphate. The chemical structure for DAG is 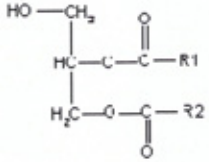 where R1 and R2 are the fatty acyl group. Data has been adapted from Cronan, 2003.

1.7.3.3.2. Biosynthesis of lipid anchor

The biosynthesis of the lipid anchor originates from DAG. The biosynthetic pathways are shown in Figure 1.17. One possible pathway involves the formation of the lipid anchor at the outer surface of the membrane by a glycosylation process (pathway 1 in Figure 1.17). The process involved the delivery of sugar units from UDP-Glc or UDP-sugar units, the glycosyl units of which would need to be translocated via undecaprenol phosphate (as discussed previously in PG biosynthesis, Section 1.3.1) to the outer surface of the membrane and added to diacylglycerol for the formation of Glc_2-DAG glycolipid. This pathway is designated as the 1st proposed pathway in Figure 1.17 and described in detail later in the section 1.7.3.3.3.

Recently in *B. subtilis* and *S .aureus*, a prossessive cytoplasmic glycosyltransferase YpfP, has been identified which is required for glycolipid biosynthesis, along with PgcA and GtaB enzymes (Jorasch *et al.*, 2000, Jorasch *et al.*, 1998, Kiriukhin *et al.*, 2001, Grundling and Schneewind, 2007a). In *B. subtilis*, glucose-6-phosphate is converted to α-glucose-1-phosphate, a reaction catalyzed by α-phosphoglucomutase (PgcA; previously known as GtaC and GtaE) (Lazarevic *et al.*, 2005, Grundling and Schneewind, 2007a); then a UTP: α-glucose-1-phosphate uridyltransferase (GtaB) synthesises UDP-glucose from the α-glucose-1-phosphate and finally YpfP enzymes of *S. aureus* or IagA of *S. agalactiae* transfers glucose from the UDP-glucose to DAG (Pooley *et al.*, 1987, Grundling and Schneewind, 2007a, Doran *et al.*, 2005) for the synthesis of Glc_2DAG (lipid anchor). Since YpfP is a cytoplasmic enzyme, this gives rise to the 2nd pathway in Figure 1.17, where the Glc_2-DAG is synthesised at the

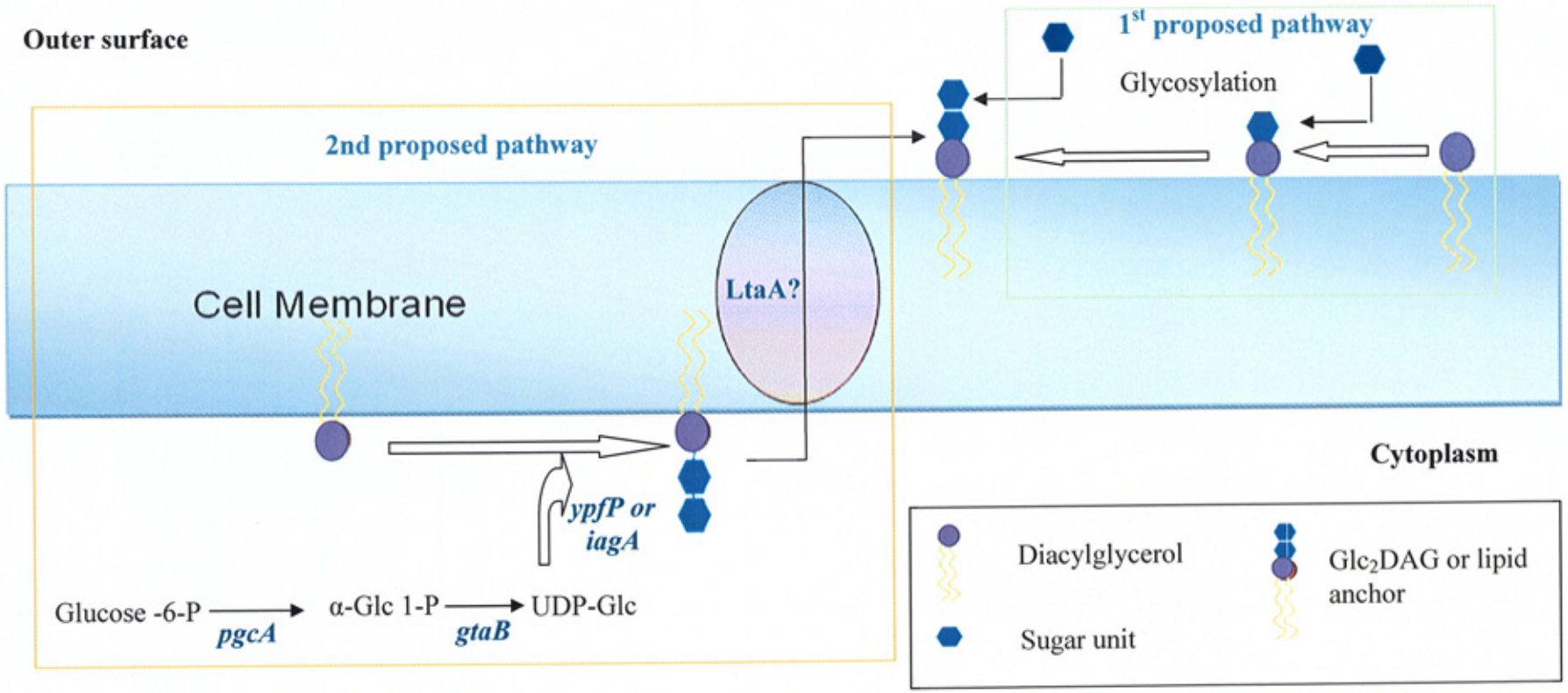

Figure 1.17. Schematic presentation for the biosynthesis of the lipid anchor of LTA. The 1st pathway proposed assumes transfer of the glycosyl units to the outer surface of the plasma membrane by undecaprenolphosphate. The 2nd pathway, which is supported by recent evidence, has been adapted from Doran *et al.* (2005), Grundling & Schneewind (2007 a;b). The question mark represents the steps in the pathway that is still poorly understood.

inner leaflet of the membrane and then transfered to the outer surface via a flippase, known as LtaA. It has been proven that in *S. aureus*, YpfP, PgcA or GtaB are essential for the synthesis of the lipid anchor but LtaA is not essential for this glycolipid synthesis (Grundling and Schneewind, 2007a, Grundling and Schneewind, 2007b). On the other hand, mutation in *ltaA* showed, there was no difference in the total amount of glycolipid in the membrane but the lipid anchor (Glc_2-DAG) of LTA was decreased compared to the wild-type and increased amounts of DAG were present as the lipid anchor, suggesting LtaA may be involved in glycolipid transport across the membrane (Grundling and Schneewind, 2007a, Grundling and Schneewind, 2007b). Moreover it has been demonstrated that in absence of LtaA, YpfP synthesised Glc_3-DAG when expressed in *E. coli* membranes. This pathway agrees with the Fischer model for polyGroP synthesis at the bacterial surface (Fischer, 1994a). The LtaA function is shown on Figure 1.17.

1.7.3.3.3. Polymerisation of the poly(GroP) chain

There are two proposed pathways for the polymerisation of the GroP chain which likely occurs on the outer surface of the cell membrane. The first proposed pathway (Figure 1.18) suggests that the biosynthesis starts with the transfer of GroP from PtdG to the preformed lipid anchor, such that the chain is polymerised by successive addition of individual GroP residues to the lipid anchor. This observation is consistent with the *in vivo* pulse-phase experiments that implicated PtdG as the donor of the GroP in LTA (Fischer, 1994a, Fischer, 1994b, Koch *et al.,* 1984, Taron *et al.,* 1983). On the other hand, the detection of oligophosphoglycerophospholipids derived from PtdG-GroP in *Streptococcus sanguis* (Chiu *et al.,* 1993) suggested that these lipids may be intermediates in the assembly of LTA, and the second pathway (Figure 1.18) has been proposed. The pathway proposed rather than successive addition of GroP directly onto the lipid anchor, the polymerisation occurs on a PtdG anchor and later the whole poly(GroP) chain is transferred to the glycolipid anchor (Chiu *et al.*, 1993, Neuhaus and Baddiley, 2003).

The mutation of *ypfP* has an effect on glycolipid synthesis which indirectly effects LTA synthesis by removing Glc_2-DAG (Grundling & Schneewind, 2007a) so the cell uses or retains DAG or PtdG moieties as the LTA lipid anchor. On the other hand, mutations of *ltaA* caused structural changes in staphylococcal LTA by decreasing the amounts of Glc_2-DAG anchor and increased the amount of DAG as the anchor unit (Grundling and Schneewind, 2007a). However, these studies fail to distinguish whether pathway 1 (Figure 1.18) operates and the lipid anchor is switched in response to the mutations or

whether pathway 2 (Figure 1.18) operates and the variant anchored LTA builds up due to lack of preformed anchor units.

In both the cases, two glycerophosphate transferase may be involved, one to recognize the glycolipid, other to polymerize the main chain. One of the transferases appears to be the LTA synthase (LtaS) enzyme, which has been found necessary and sufficient for the polymerization of LTA poly(GroP) in *S. aureus*, a reaction that presumably uses PtdG as substrate and proceeds in the presence or absence of Glc_2-DAG (Grundling and Schneewind, 2007b). The lack of LTA in a *S. aureus, ltaS* mutant strongly suggests that LtaS is one of the transferase enzymes responsible for the polymerization of GroP in LTA (Grundling and Schneewind, 2007b).

LtaS is predicted to assemble as a membrane protein with a large C-terminal domain located on the outer surface of the bacterial membrane. The C-terminal domain (LtaS, amino acids 245-604) presumably functions as a catalytic domain and was annotated as a sulfatase domain (Figure 1.19) in the Pfam database (www.sanger.ac.uk/Software/Pfam) (Grundling and Schneewind, 2007b), but still it is unclear whether the glycerophosphate transfer as single units or as a whole chain. The interaction of LtaS with LtaA and the enzymes responsible for glycolipid synthesis are described in Figure 1.19. Further studies are needed to untangle whether LtaS assembles GroP on the DAG or the glycolipid anchor.

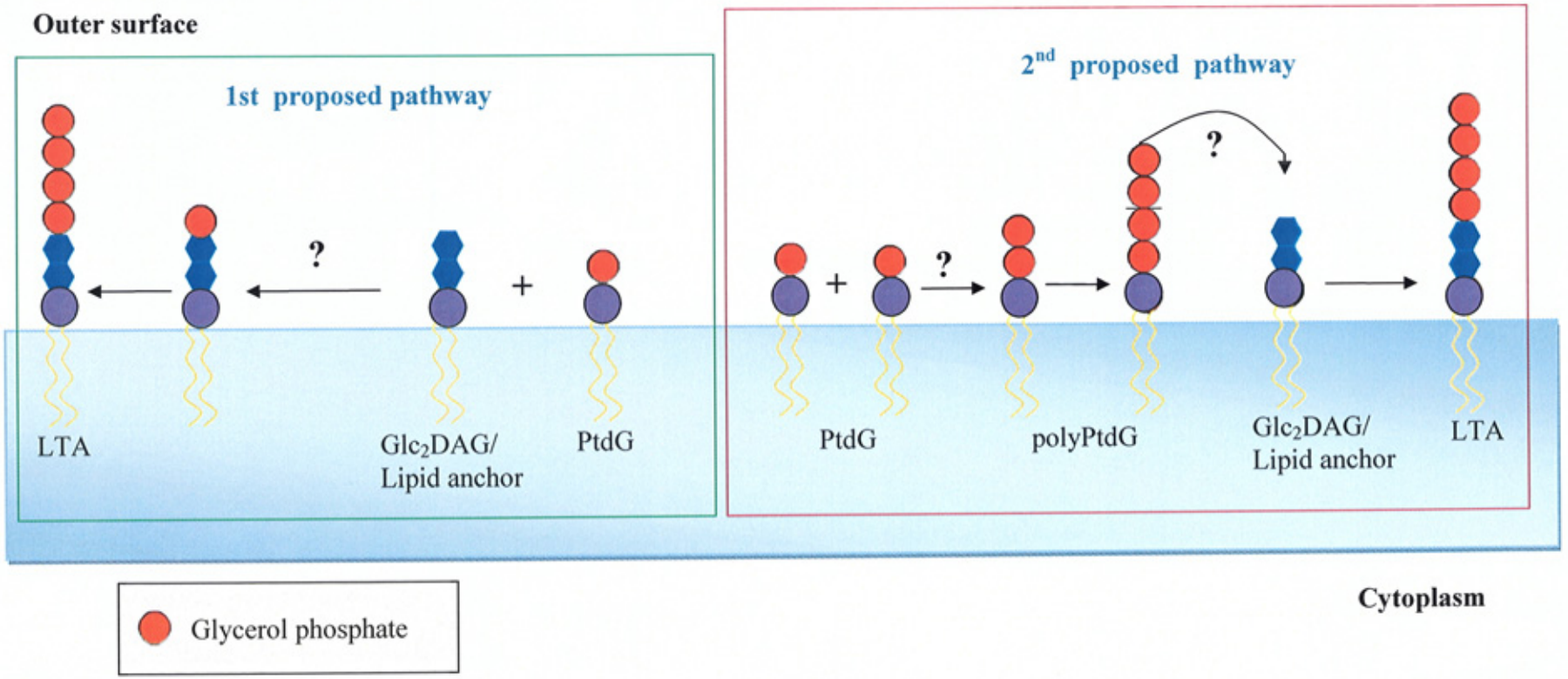

Figure 1.18. Schematic presentation for the polymerisation of the polyGroP LTA chain. 1st proposal pathway has been adapted from Taron *et al.* (1983), Koch *et al.* (1984) and Fischer (1994a;b) and the 2nd proposal pathway adapted from Chiu *et al.* (1993). Question marks (?) represent the responsible enzyme is still unknown.

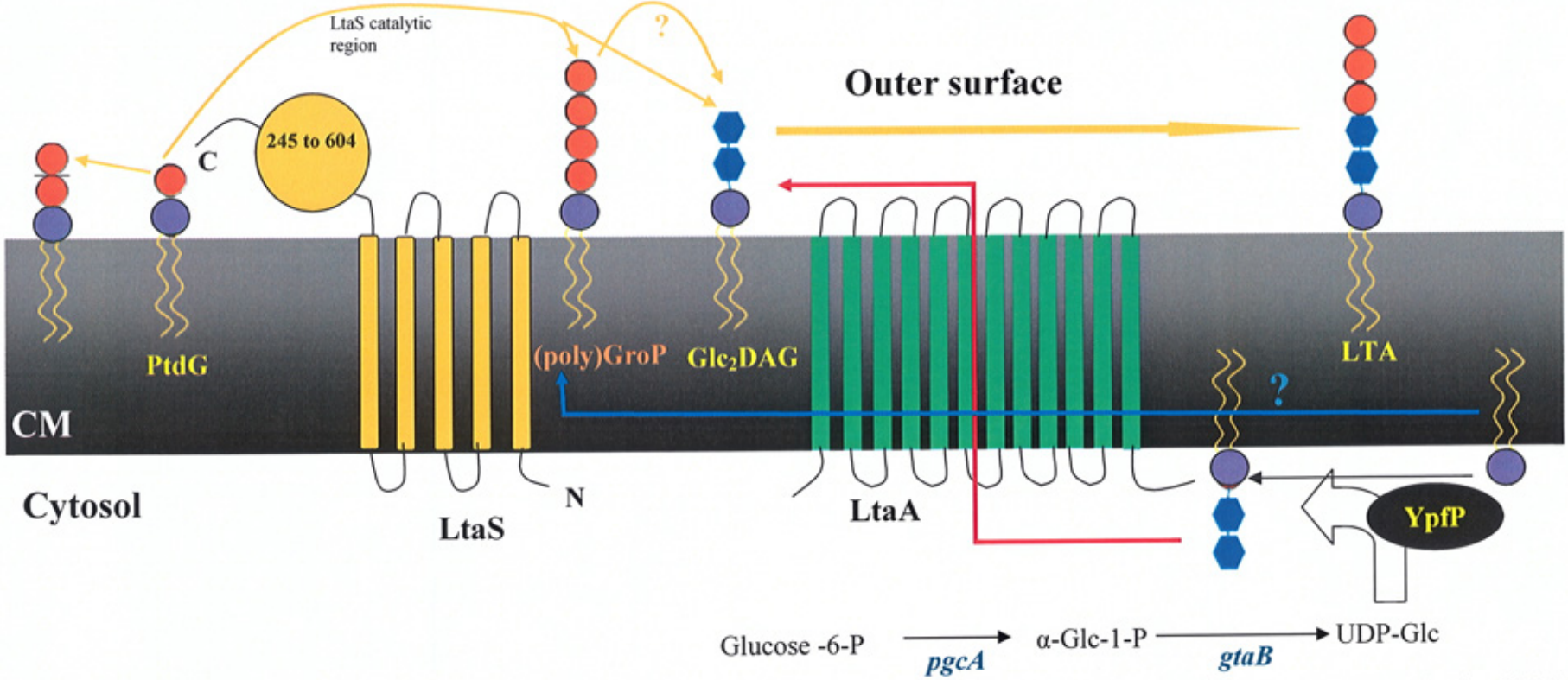

Figure 1.19. Schematic presentation of the function of LtaA and LtaS, representing the recent findings concerning the biosynthesis of LTA. Orange lines (⟶) and orange question mark (?) represent LtaS function and that the precise pathway are still to be defined, respectively. The red line (⟶) and blue line (⟶) represent the LtaA's function and that the pathway is still to be defined, respectively. The black line shows the biosynthesis of Glc_2-DAG by PgcA, GtaB and YpfP enzymes. The data has been adapted from Grundling & Schneewind (2007a;b).

1.7.3.3.4. Substitution of LTA

Generally LTA chains are substituted by D-alanyl ester and sugar residues, and based on this, LTA can be classified into four groups as discussed previously (Table 1.3 and section 1.7.3.2). The following sections describe the substitution processes.

1.7.3.3.4.1. Addition of D-Alanyl Residues

The synthesis of D-alanyl-LTA or TA is similar and requires four proteins that are encoded by the *dlt* operon (Neuhaus and Baddiley, 2003). The four proteins are Dcl, Dcp, DltB and DltD encodes by the *dltA, dltC, dltB* and *dltD* genes (Figure 1.20). Dcl activates D-alanine and also ligates the activated ester to a 4′-phosphopanteheine prosthetic group of the Dcp carrier; this protein is designated as D-alanine:Dcp ligase (AMP forming). It has been proposed that DltD facilitates the binding of Dcp and Dcl for ligation of Dcp with D-alanine (reaction 2, Figure 1.21), and also functions in the final esterification step, though the later function was not successfully demonstrated in *in vitro* conditions (Neuhaus and Baddiley, 2003).

The fourth protein's DltB hydrophobic profile shows a pattern of 12 putative membrane-spanning domains (Neuhaus *et al.,* 1996). Blast searches identified regions of the DltB protein with similarities to a variety of transport proteins in the major facilitator superfamily and ATP-binding cassette family, including proton antiporters that pump compounds (e.g. tetracycline, glycerol-3-phosphate, and gluconate) from cytosol at the expense of the proton motive force. Based on this, it has been suggested that the function of DltB could be

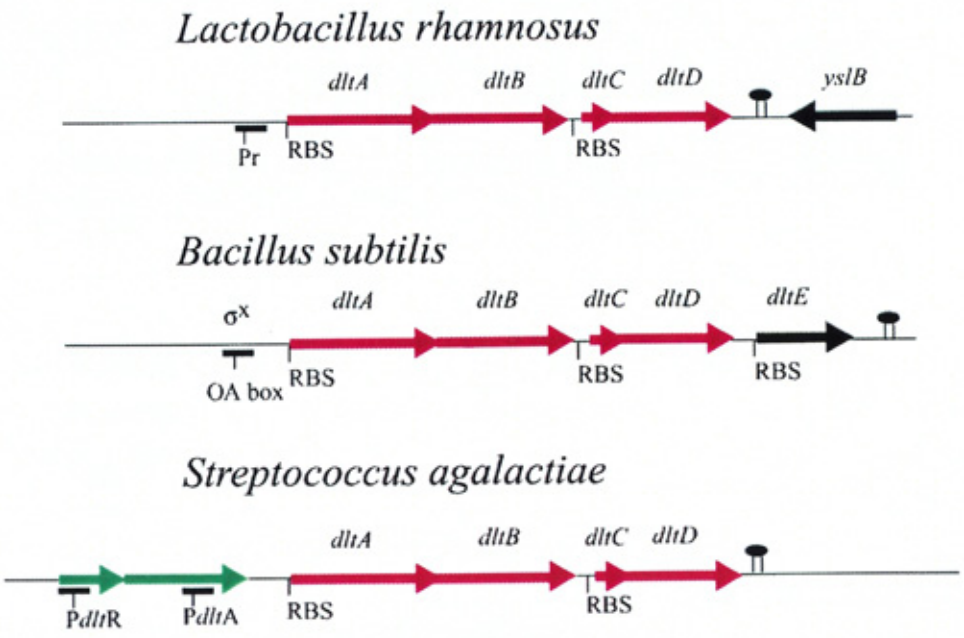

Figure 1.20. Comparison of the dlt operons from *L. rhamnosus*, *B. subtilis 168*, and *S. agalactiae*. The red genes (*dltA, dltB, dltC* and *dltD*) are common to all *dlt* operons. The green genes in *S. agalctiae* a novel two-component regulatory system. The genes in black neither are nor required for D-alanylation. ⊤ is the rho-independent terminator. The figure is taken from Neuhaus & Baddiley (2003).

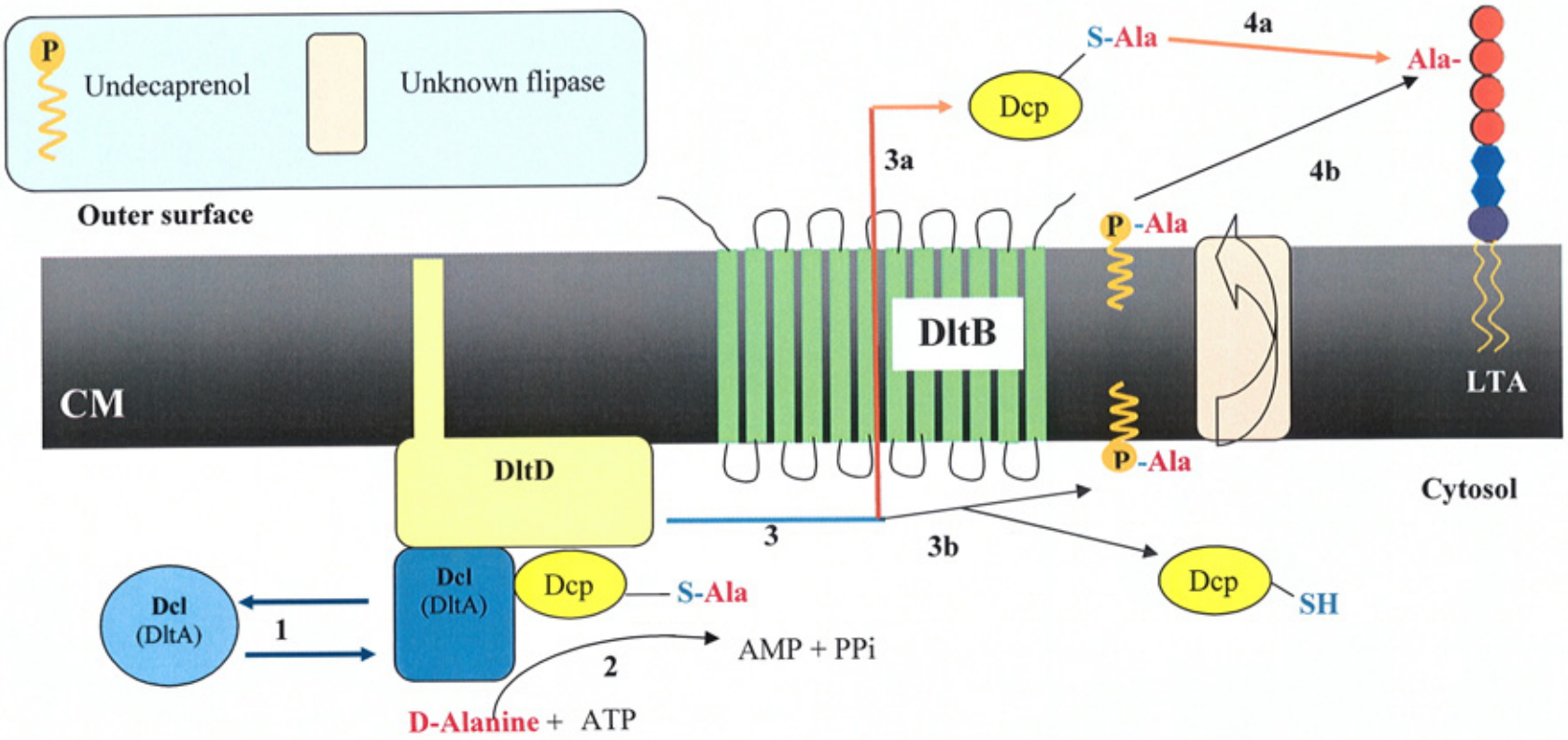

Figure 1.21. Model for the incorporation of D-alanyl ester residues into membrane-associated LTA. The blue arrows (→) represents the reactions which has been established. The brown arrows (→) and black arrows (→) represent the DltB possible functions: actual secretion of D-alanyl-Dcp and acyltrasferase, respectively. Whether DltB is bifunctional or single functional is not known. Data adapted from Neuhaus & Baddliey (2003)..

the secretion of D-alanyl-Dcp to the outer surface (Figure 1.21, reaction 3a) (Neuhaus *et al.,* 1996). However, the DltB sequence also contain regions in which two conserved motifs of *O*-acyltransferases were identified, which may link DltB to a superfamily of membrane-bound-*O*-acyltransferases which have been proposed to require undecaprenol-P (described in peptidoglycan biosynthesis section 1.3.1) as a membrane acceptor (Heaton and Neuhaus, 1994, Neuhaus and Baddiley, 2003). Use of this lipid carrier an intermediate in the incorporation system would give rise to a second pathway for D-alanine transport to the LTA or TA as shown in reactions 3b and 4b in Figure 1.21. However, Neuhaus and Baddiley (2003) concluded that undecaprenol-P lipid is not an intermediate in D-alanine incorporation as they could not detect any D-alanyl-P-polyprenol in cell membranes. Thus it is still unknown whether DltB functions in the actual secretion of D-alanyl-Dcp or functions as an acyltransferase or is bifunctional. It has been proven that the proposed mechanism for reaction 4a in Figure 1.21 does not require any transferase enzyme; only D-alanyl-Dcp and membrane-associated LTA are required (Neuhaus and Baddiley, 2003, Kiriukhin and Neuhaus, 2001).

A fifth gene *dltE* encoding an oxidoreductase has been identified in *B. subtilis* in addition to *dlt ABCD* (Figure 1.20) (Glaser *et al.,* 1993), but inactivating *dltE* did not inhibit the D-alanylation (Perego *et al.,* 1995) which suggests that this enzyme does not take part in the alanylation process. The above process for D-alanylation is also similar for TA alanylation.

1.7.3.3.4.2. Glycolsylation

The glycosylation process is thought to be occurred at the outer-surface of the cell membrane and the sugar residues for substitution originate from cytoplasmic UDP-sugar residues. These must be transported across the membrane, presumably via undecaprenol phosphate lipid carrier as has been discussed in Section 1.3.1 of peptidoglycan biosynthesis and Figure 1.4.

1.7.4. Lipoglycans of Gram-positive bacteria

Lipoglycans are the second major type of macroamphiphile in the membranes of Gram-positive bacteria and seem generally widely distributed within the Gram-positive High G+C organisms, especially in the phylum Actinobacteria, and also in the Mollicutes class of Low G+C Firmicutes (Sutcliffe, 1994b, Smith, 1987). These macroamphiphiles can be distinguished from LTA mainly on the basis of their hydrophilic chain, where the GroP or RboP chain is replaced by homo- or heteropolysaccharide chains. The general structure of lipoglycans is similar to the LTA, i.e. it has an anchor to the cytoplasmic membrane via hydrophobic fatty acids and also contains a hydrophilic chain, which is likely to be elongated through the peptidoglycan and may protrude on the surface of the cells. The functions of lipoglycans may be similar to LTA, as they show similar supramolecular organisation as LTA and are found to be present in organisms which do not contain LTA or LPS (Fischer, 1994b). Lipoglycans can be further subgrouped on the basis of their polysaccharide chain types. These subgroups are described in sections following a brief review of the classification of the Gram-positive bacteria and the distribution of lipoglycans in the phylum Actinobacteria.

1.7.4.1. Lipoglucogalactan

Lipoglucogalactan is a lipoglycan reported in different members of the genus *Bifidobacterium* (Dencamp *et al.,* 1985, Iwasaki *et al.,* 1990). The anchor unit of the lipoglucogalactan of *Bifidobacterium bifidum* subspecies *pennsylvancum* DSM 20239 has a lipid anchor composed of Gal-α(1→3)-diacyglycerol, which is attached to a glucogalactofuranan polymer chain that carries monomeric *sn*-glycerol-phosphate side chains. The GroP side-chain configuration is stereochemically similar to that in LTA, suggesting that the GroP is derived from PtdG. 20-50% of the GroP units are found to be substituted by ester linked L-alanine. The presence of this L-alanine is very unusual for Actinobacteria which has been discussed detailed later in Chapter 8. This type of lipoglycan was also identified in different species of the genus *Bifidobacterium* (Iwasaki *et al.,* 1990).

1.7.4.2. Lipomannan (LM)

Depending on their lipid anchor moiety, LM can be classified into two main groups: DAG-containing LM (DAG-LM; diglyceride anchored) and PI-anchored LM (PI-LM; which have a PI anchor unit).

DAG-LM has been identified in representatives of several genera of the Actinobacteria. The most studied DAG-LM among them is that of *Micrococcus luteus* (Powell *et al.*, 1974) which contains a dimannosylgylceride anchor with a mannose chain, generally containing ca. 50 units of mannose and substituted by succinate. This substitution give the DAG-LM an overall negative charge, which allows it to bind divalent cations such as Mg^{2+} (Owen and Salton, 1975). Similar LMs have been identified also in *Micrococcus agilis* CCM1744, *Rothia dentocariosa* and *Stomatococcus mucilaginosus* (another member of the Micrococcineae suborder), although apparently without any succinyl ester substitution (Lim and Salton, 1985, Sutcliffe, 1994a, Sutcliffe and Old, 1995a). Indeed, DAG-LM appears widely distributed throughout the genus *Micrococcus* (Sutcliffe and Alderson, 1995).

The second LM type, PI-LM, have also been identified in representatives of several families of the Actinobacteria, where this lipoglycan may be either the main macroamphiphile in some organisms or as a precursor of LAM or LAM-like molecules. The latter include the well characterised PI-LM/LAM of members of the genus *Mycobacterium* (see Section 1.7.4.3 below). These PI-LM or MPI-like lipoglycans are most likely derived from PIM_3-PIM_4 on the basis of their mannose chain structure, as PI-LM contain $\alpha(1\rightarrow6)$ linked-

mannose, and may be further mannosylated to form mature, branched PI-LM, where the branched chain is formed by α(1→2) linked-mannose (Nigou *et al.*, 2003). In contrast to PI-LM, the polar PIMs do not contain any branched chains; PIM_5 and PIM_6 contain terminal linear α(1→2)-Man*p*, which is not found in PI-LM or LAM (Khoo *et al.*, 1995). These PI-LMs are distributed among several genera of the Actinobacteria and are described briefly in the following sections. Similar PI-LM molecules have also been tentatively identified in members of the genera *Corynebacterium* and *Gordonia* that produce LAM-like lipoglycans (Puech *et al.*, 2001; Flaherty and Sutcliffe, 1999; Gibson *et al.*, 2005; Sutcliffe and Garton, 2006).

In *Saccharothrix aerocolonigenes* (now called *Lechevalier aerocolonigenes*), a PI-LM has been identified, which has an PI anchor and whose α(1→6)-Man*p* backbone is 80% substituted by side chains composed of Man*p*-α(1→2)-Man*p*-α(1→2) (Gibson *et al.*, 2005). Another example is the genus *Propionibacterium* as *Propionibacterium freudenreichii* was found to lack LTA and contain a unique inositol-containing LM, proposed to be a PI-LM of approximately 30 mannose residues (Sutcliffe & Shaw, 1989).

1.7.4.3. Lipoarabinomannan (LAM)

Mycobacterial LAMs are the classical examples of LAM molecules, which are generally composed of three structural components: the membrane anchor which is similar to that of both PIMs and PI-LM; the backbone, which consists of two homopolysaccharides: mannopyranose (Man*p*), in a structure similar to MPI, and arabinofuranose (Ara*f*), the unique characteristic of LAM; and the unique capping motifs of LAM, which vary among the mycobacterial species (Chatterjee and Khoo, 1998, Nigou *et al.,* 2003).

The anchor structure is based on PI with one α-D-Man*p* unit linked at 2-positon of the inositol to form PIM_1. Though inositol is an essential polyol in eukaryotes, in prokaryotes, inositol derivatives are important in osmotic protection of archaebacteria and absent from most of the eubacteria (Haites *et al.,* 2005). However, inositol is found to be an essential component of mycothiol, lipoglycans and PIMs of different genera of Actinobacteria, (Movahedzadeh *et al.,* 2004).

The polysaccharidic backbone is composed of D-mannan and D-arabinan domains. These domains seem to be strongly conserved among the different mycobacterial species. The D-mannan domain has a similar structure to the mature PI-anchored lipomannan as discussed previously. The D-arabinan domain consist of an α(1→5) linked-Ara*f* backbone and branching occurs by β(1→2) linked-Ara*f*. The attachment site(s) between the two domains still remains unknown (Nigou *et al.,* 2003). The main backbone of *Araf* can be substituted by two kinds of arrangements, tetra-arabinofuranoside (Ara_4) and

hexa-arabinofuranosides (Ara_6) in mycobacteria depending on the capping motif (Briken *et al.,* 2004).

The capping motifs differentiate LAM from AG, the other arabinan-containing heteropolysaccharide of the mycobacterial cell wall discussed in section 1.4. The capping motifs present on the non-reducing termini of the arabinosyl side-chains can be classified into three groups, ManLAM, PILAM and AraLAM (Briken *et al.,* 2004). ManLAM occurs in the slow-growing mycobacteria such as *Mycobacterium tuberculosis, Mycobacterium leprae*, *Mycobacterium bovis* and *Mycobacterium avium*, where the caps consist of a single Man*p*, a dimannoside Man*p* (predominant) or a trimannoside (Nigou *et al.,* 1997, Vercellone *et al.,* 1998, Guerardel *et al.,* 2003b). On the other hand, PILAM caps are characteristic of fast growing mycobacteria such as *Mycobacterium smegmatis* and *Mycobacterium fortuitum*, where the cap is composed of a phosphoinositide unit. The third class, known as AraLAM, has been identified in *Mycobacterium chelonae*, is defined as lacking in either of the other types of capping (Nigou *et al.,* 2003). Additional substituents such as 5-methylthiopentosyl and succinate have been identified in the LAM of *M. tuberculosis* and *Mycobacterium kansasii* (Joe *et al.,* 2006, Turnbull *et al.,* 2004, Guerardel *et al.,* 2003a, Treumann *et al.,* 2002)

In lipoglycan and PIM, anchor variations occur by the acylation with fatty acids in two aspects: i) the nature of the fatty acids ii) the number of acylation. The nature of the fatty acids of LAM is usually quite similar to that of the total cellular lipids in the cell membrane, thus reflecting the origin of the lipid

moiety from membrane lipids, as with LTA (Kordulakova *et al.*, 2003). Unlike LTA, a large number of different acyl forms exist in the LAM, e.g. four acylation sites have been identified in ManLAM, they are positon 1 and 2 of glycerol (the acylation form found in LTA), position 6 of the mannose linked to position 2 of myo-inositol (Khoo *et al.*, 1995, Nigou *et al.*, 1997) and position 3 of myo-inositol (Nigou *et al.*, 1999, Nigou *et al.*, 2003).

LAM or LAM-like molecules have also been identified in representatives of other genera of Actinobacteria, such as, *Corynebacterium, Rhodococcus, Gordona, Tsukamurella, Dietzia,* and *Turicella* (Sutcliffe, 1994b, Sutcliffe and Shaw, 1991). Brief descriptions of these LAMs are given below.

Different species of *Corynebacterium*, such as *Corynebacterium diphtheriae, Corynebacterium xerosis* and *Corynebacterium matruchotti* were found to lack LTA and presence of arabinose was serologically detectable (Misaki *et al.*, 1977, Mc. Carty, 1959) Moreover, a lipoglycan phenol extracted from *C. diphtheriae* was found to contain mannose with lesser amount of arabinose and minor amount of glycerol and phosphate (Kokeguchi *et al.*, 1987). This is also consistent with analysis of the lipoglycan of *C. matruchotti*, suggesting the lipoglycan is a LAM or LAM-like molecule (Sutcliffe, 1995). Finally Tatituri *et al.* (2007) identified LAM from *C. glutamicum*, which shows Cg-LAM is much smaller version of LAM characterised by single t-Ara*f* residues linked to the mannan $\alpha(1\rightarrow6)$ backbone, proving *Corynebacterium* genera contains LAM or LAM-like molecules.

In the family Nocardiaceae, only members of the genus *Rhodococcus* have been subjected to macroamphiphile studies. Two species of the genus, *Rhodococcus equi* and *Rhodococcus ruber,* were found to contain LAM-like molecules (Garton *et al.,* 2002, Gibson *et al.,* 2003c, Nigou *et al.,* 1999). The main feature of these LAM-like molecule is the presence of an MPI anchor similar to mycobacterial LAM, but their molecular weight is significantly lower than ManLAM with a linear α(1→6)-mannan occasionally substituted (approximately 44-45%) at *O*-2 by a single Man*p* unit and some of these side chain are substituted at *O*-2 position by t-Ara*f* units. A LAM-like molecule, along with a putative MPI, has also been identified in *Rhodococcus rhodnii* N445 (Flaherty *et al.,* 1996).

Ikeda-Fujita *et al.* (1987) have shown *Gordona rubropertincus* ATCC 27863, *Gordona terrae* ATCC 25594 and *Tsukamurella paurometabolum* ATCC 25938 contain biologically active lipoglycans composed of mannose and smaller amount of arabinose. Later, Flaherty & Sutcliffe (1999) demonstrated the presence inositol, mannose and arabinose in a lipoglycan from *G. rubropertincta* and by anti-LAM blotting proved the macroamphiphile is a LAM-like molecule. Similarly, in *Gordonia bronchialis,* a LAM-like molecule has been identified (Garton and Sutcliffe, 2006). MPI-like molecules were also detected along with these LAM-like molecules, which may be consistent with the finding that *Gordonia sputi* synthesises phosphatidylinositol octamannoside (PIM_8, Furneaux *et al.*, 2005. Gibson *et al.,* 2004). *T. paurometabola* contains a smaller LAM (12.5 KDa) compose of an MPI anchor, glycosylated by a linear α(1→6)-mannan domain, which is further substituted by α(1→3)-Ara*f*

chains and half of these chains are further substitute at *O*-2 position by a dimannoside motif. The above data suggest LAMs are widely distributed in both the genera *Gordonia* and *Tsukamurella,* which are representative of the families Gordoniaceae and Tsukamurellaceae.

A lipoglycan, unusually small and predominantly PI-LM in nature has been isolated from *Dietzia maris*; the presence of minor levels of arabinose along with a predicted PI anchor and weak cross-reaction with a polyclonal anti-LAM antiserum suggested the macroamphiphile may be a PI-LM/LAM like molecule (Sutcliffe, 2000). *Turicella otitidis*, the only member of the monospecific genus *Turicella*, was found to contain a truncated LAM which is closely related in structure to the *R. ruber* LAM (RruLAM), composed of an α(1→6)-Man*p* chain substituted at all *O*-2 positions by t-α-Ara*f* units (Gilleron *et al.*, 2005). The presence of LAM in *Turicella* has chemotaxonomic value as the absence of mycolic acids has made it difficult to classify this genus within the Corynebacteriaceae subgroup.

Amycolatopsis sulphurea was found to contain a novel ManLAM which is composed of a short mannan domain and a multi-branched arabinan domain. The α-1-5 linked arabinan domain is substituted by a single β- Ara*f* at the *O*-2 position for the formation of branch. The LAM also contains a manno-oligosaccharide caps similar to that of the ManLAM of *M. tuberculosis* and *M. bovis BCG* (Gibson *et al.*, 2003b).

LAM-like lipoglycans can be broadly classified as 'truncated LAM' with single t-Ara substitutions (as in *T. otitidis,* Gilleron, *et al.,* 2005) or more elaborate fully arabinosylated LAM, as in *A. sulphurea* and mycobacteria (Gibson *et al.,* 2003b) . LAM or LAM like lipoglycans are typical of the mycolata but also present in members of the sub-order *Pseudonocardiaceae* (e.g. *A. sulphurea* and *L. aerocologinenes*), suggesting they may be widely distributed in Actinobacteria (Embley *et al.,* 1988, Gibson *et al.,* 2003b).

1.7.4.4. Other lipoglycans

Although *P. freudenereichii* apparently contained PI-anchored LM (discussed previously), in *Propionibacterium acnes a* lipoglycan with a different carbohydrate composition was identified (Whale *et al.,* 2004). In this case, the hydrophilic chain was reported to be composed of mannose, galactose, glucose and an unidentified amino sugar (Whale *et al.,* 2004). Two lipoglycan fractions were recovered, one of which also contained inositol, perhaps indicating a PI anchor. The composition of the polysaccharide was also noted to be similar to that of the *P. acnes* cell wall polysaccharide.

Within the suborder Actinomycineae, only the genus *Actinomyces* has been investigated for the presence of macroamphiphiles. *Actinomyces pyogenes*, *Actinomyces naesulundii* ATCC 12104 and *Actinomyces viscousus* ATCC 19246 and OM2105 have been found to be lack in LTA (Hamada *et al.,* 1976). Moreover a heteropolysaccharide lipoglycan containing mannose, glucose, and galactose as major components was extracted from *A. viscosus* NY1, which was also detectable in *A. naeslundii* ATCC 12104, *Actinomyces israelli* C65 and *A. viscosus* WVU-626 (Wicken *et al.,* 1978).

In the family Jonesiaceae, *Jonesia dentificans* of the monospecific genus *Jonesia* has been found to contain a lipoglycan composed of galactose and glucosamine, which has not been characterised in detail (Rocourt *et al.,* 1987, Ruhland and Fiedler, 1987).

Finally, lipoglycans have been detected in the class Mollicutes of the Low G+C Gram-positive bacteria, especially in all species of *Acholeplasma, Anaeroplasma* and *Ureaplasma* and in selected species of *Mycoplasma* (Smith, 1984). Though the structures of these lipoglycans are still to be revealed, the chemical composition shows that the lipoglycan has significant amount of glycerol, neutral sugars and amino sugar (Totsuka *et al.,* 1990, Smith, 1985). For example, the lipoglycan of *Ureaplasma urealyticum* found to contain mannose, glucose and galactose as neutral sugar and fatty acids, glycerol and significant amount of phosphorus (Smith, 1985). The presence of lipoglycan in the Mollicutes has significant chemotaxonomic value, as in the low G+C Firmicutes phylum LTA appears to be the most widely distributed macroamphiphile. Recently, it has been proposed to move this class from the phylum Firmicutes to the phylum Tenericutes, which will be published in the next edition of the *Bergey's Manual of Systematic Bacteriology* (K.H. Schleifer and W. Ludwig, reported at http://www.bacterio.cict.fr/classifphyla.html).

1.7.5. Lipoglycan biosynthesis

As reviewed above, lipoglycans are diverse macromolecules which occur in many different genera of actinobacteria. The most studied lipoglycans are the mycobacterial lipoglycans, PI-LM and LAM. Although the structures of these macromolecules are well documented, relatively little is known about the biosynthesis of these molecules. Since, these molecules share a conserved glycosylated phosphatidylinositol anchor, it has been hypothesized that the biosynthesis sequence is PI→PIM→ PI-LM→LAM (Chatterjee and Khoo, 1998, Nigou *et al.,* 2003) and this hypothesis is supported by recent direct biosynthetic evidence. The present understanding of the synthesis of LAM will be reviewed briefly in the following sections.

1.7.5.1. Phosphatidylinositol (PI) anchor biosynthesis

The inositol required for PI synthesis can be obtained in two distinct ways, either as exogenously acquired inositol or from the glycolytic pathway by the conversion of glucose-6-phosphate (Glc-6-P) to inositol-1-P (Ino-1-P) by inositol-3-phosphate synthase (IPS) encoded by the *ino1* gene (Haites *et al.,* 2005). Ino-1-P is then converted to inositol (Ino) by inositol monophosphatase (IMP) (Parish *et al.,* 1997) (Figure1.22). PI biosynthesis occurs by transfer of myo-inositol to CDP-diacylglycerol, a reaction catalyzed by the enzyme phosphatidylinositol synthase (PgsA) enzyme, which has been identified in *M. tuberculosis* as the *pgsA* (Rv2612c) gene product (Jackson *et al.,* 2000). The synthesis of CDP-diacylglycerol is described in Figure 1.16 and PI synthesis in Figure 1.22.

It has been hypothesized (Schaeffer *et al.,* 1999, Alexander *et al.,* 2004) that lower PIM (PIM_1 to PIM_4) are synthesised on the inner leaflet of the cytoplasmic membrane by sequential mannosylation of PI (Figure 1.22); and the higher PIM (e.g. PIM_6), LM or LAM are synthesised by mannosylation of smaller PIM on the outer surface of the membrane (Figure 1.23). Consequently, the synthesis of these molecules requires three things: i) activated mannose residues are required at both the outer and inner surfaces of the plasma membrane ii) activated arabinose is required at the outer surface of the plasma membrane, and iii) various specific mannosyltransferase enzymes required for the different mannosylation reactions.

1.7.5.2. Mannose and Arabinose sources

GDP-mannose has shown to be the primary donor species at the cytosol side of the membrane (McCarthy *et al.,* 2005), which can be produced by two distinct pathways: either by hexokinase which converts exogenously acquired mannose to mannose-6-phosphate (M6P), or from the glycolytic pathway (Figure 1.22), where glucose-6-phosphate (G-6-P) is converted to M6P. Fructose-6-P, which is converted to mannose-1-phosphate (M1P) by phosphomannose isomerase (PMI) and phosphomannomutase (PMM), respectively (McCarthy *et al.,* 2005). Finally, GDP-mannose is produced by GDP-mannose pyrophosphorylase (GDPMP) from mannose-1-phosphate. In *M. tuberculosis*, ManA (Rv3255c) (Patterson *et al.,* 2003) and ManC (Ning and Elbein, 1999, Ma *et al.,* 2001) (Rv3264) have been identified as the PMI and GDPMP enzymes, respectively, and the former of these was found to be essential for the growth of mycobacteria.

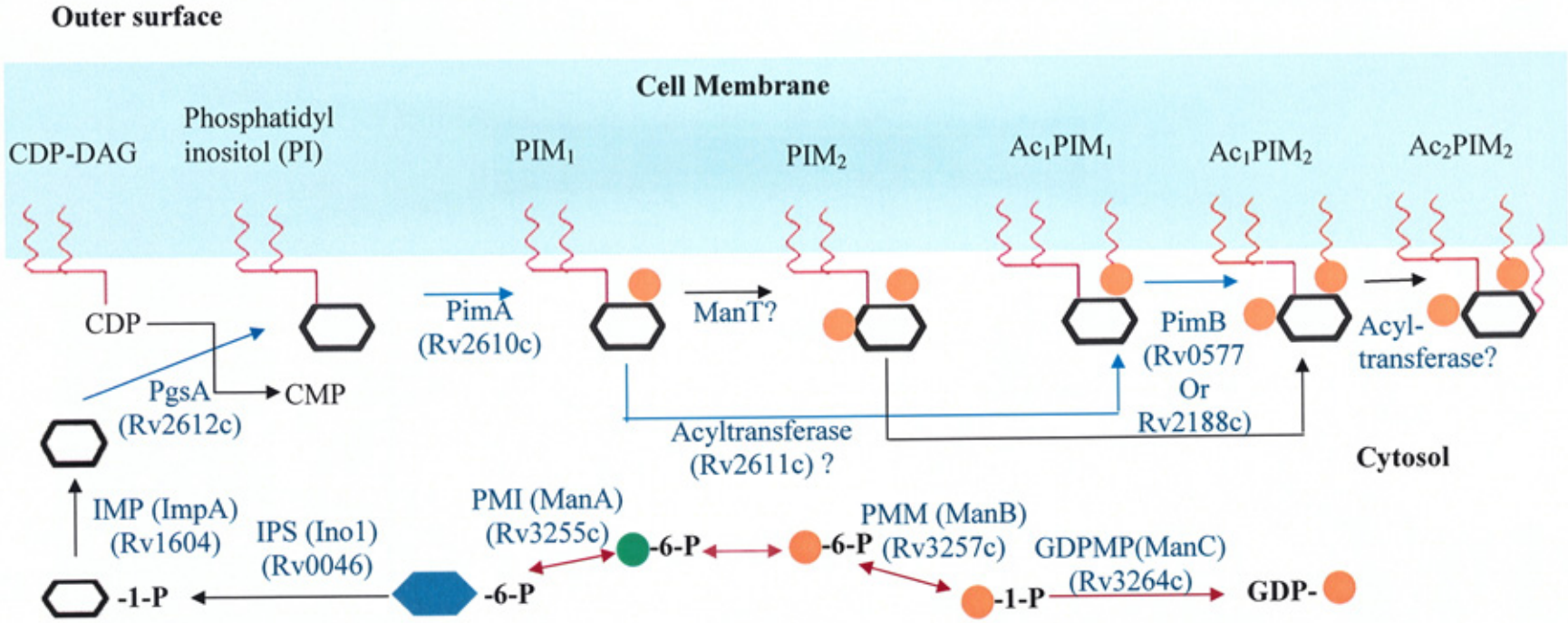

Figure. 1.22. Schematic presentation of smaller PIMs biosynthesis and source of Inositol and Mannose in the inner surface of the cell. GDMP:GDP-mannose pyrophosphorylase, PMM: Phosphomannomutase, PMI: Phosphomannose isomerase, IPS: Inositol-1-P-synthase, IMP: Inositol-1-P phosphatase, PgsA: PI synthase, represents glucose, represents inositol, represents fructose and represents mannose. Rv number represents the gene identified in *M. tuberculosis.* GDP-Mann is the only source of mannose for the above mannosylation reactions. Adapted from data in Takayama & Goldman (1969), Parish *et al.* (1997) Ning & Elbein (1999), Scheffer *et al.* (1999) ; Jackson *et al.* (2000) ; Kremer *et al.* (2002) ; Kordulakova *et al.* (2003) ; Patterson *et al.* (2003) ; Alexander *et al.* (2004) ; Haites *et al.* (2005) and McCarthy *et al.* (2005).

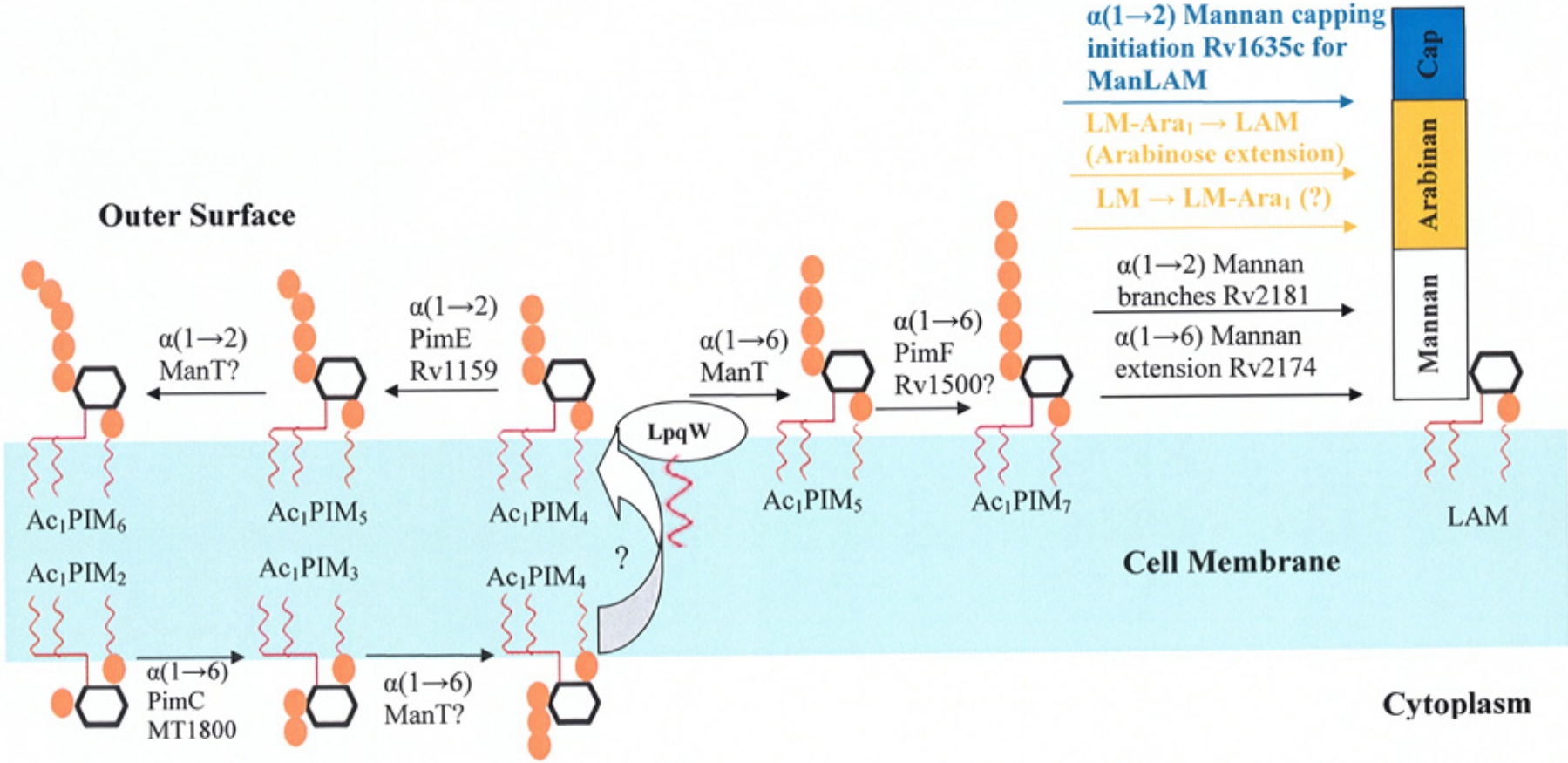

Figure 1.23. Schematic presentation of the proteins identified for the biosynthesis of polar PIM, PI-LM and LAM in *M. tuberculosis*. ManT represent mannosyl transferase and ● represent mannose residue. The mannose source at the inner surface of cell membrane is GDP-mannose and at the outer surface is polyprenol-mannose; the arabinose source at the outer surface is polyprenol-arabinofuranose. LpqW is a lipoprotein, which may direct Ac_1PIM_4 to the relevant ManT. Adapted from data in Zhang *et al.*, 2003; Alexander *et al.*, 2004; Dinadayala *et al.*, 2006; Koyacevic *et al.*, 2006 ; Morita *et al.*, 2006 ; Mishra *et al.*, 2007.

On the other hand, polyprenyl-phosphate sugars are found to be the only primary donor sources for mannose and arabinose sugars at the outer surface of the cell membrane. Due to the lack of a transporter, GDP-mannnose is unable to cross biological membranes, rather there is transfer of its mannose to a unsaturated polyprenol phosphate to form polyprenol phosphate mannose, a reaction which has been found to be carried out by the C-terminal domain of the *Mt*Ppm1 enzyme of *M. tuberculosis*, *Ms*Ppm1 enzyme of *M. smegmatis* and Cg-Ppm1 of *C. glutamicum* (Baulard *et al.*, 2003, Gibson *et al.*, 2003a). Comparative genomic studies showed the transmembrane N-terminal of MtPpm1 domain has an orthologue in both *M. smegmatis* and *C. glutamicum* as MsPpm2 and Cg-Ppm2, respectively, but in both cases rather than fusion with the Ppm1 protein, Ppm2 are present as separate proteins, suggesting MtPpm1 is the result of the fusion of two ancestral neighbouring open reading frames. After the formation of polyprenol-P-mannose, the molecule is flipped by an unknown flippase and this makes the mannose available at the outer surface of the cell membrane.

Arabinose is required for the synthesis of both LAM and the cell wall arabinogalactan (AG) polymer. Furanose is the common configuration for arabinose in both LAM and AG, and decaprenylphosphoryl-D-Ara*f* (DPA) is the only known source identified in mycobacteria for Ara*f* (Wolucka *et al.*, 1994). DPA is synthesized from 5-phosphoribose diphosphate (pRpp) shunt by three biosynthetic reactions rather than being synthesised from a sugar nucleotide precursors (Klutts *et al.*, 2002, Scherman *et al.*, 1995). The three steps are the transfer of 5-phosphopentose from pRpp to decaprenyl phosphate

(Huang *et al.,* 2005) producing the compound 5-phospho-α-D-ribose-1-phosphate-decaprenyl-phosphate (DPPR), then, removal of the 5' phosphate from the product to form α-D-ribose-1-phosphate-decaprenyl (DPR) and finally the epimerization of DPR for the formation of DPA (Mikusova *et al.,* 2005). The UbiA protein of *C. glutamicum*, which is orthologus to Rv3806 of *M. tuberculosis*, acts as the 5-phosphoribosyltransferase enzyme in the first step and the second step, which requires a phosphatase enzyme, has been predicted to a gene encoded directly upstream of the *ubiA* gene (Alderwick *et al.,* 2005). The third epimerization step has been shown to catalyzed by Rv3790 and Rv3791, two proteins of *M. tuberculosis* are found to be essential for this reaction (Mikusova *et al.,* 2005). DPA is presumably 'flipped' to the membrane surface in the same way as DPM. Recently, however, alternative pathways for arabinose delivery have been suggested by the characterisation of a LAM variant in *C. glutamicum* (Tatituri *et al.,* 2007).

1.7.5.3. Biosynthesis of the apolar smaller PIMs (PIM_1 to PIM_3)

The first step of glycosylated phosphatidylinositol or PIM synthesis involves in the formation of PIM_1 from PI by transferring of a mannose residue from GDP-mannose to the PI's 2-position of the myo-inositol ring. This reaction is essential for the growth of mycobacteria and catalyzed by the PimA (Rv2610c) mannosyltransferase (ManT) enzyme (Kordulakova *et al.*, 2002). PIM_1 is further mannosylated to PIM_2 and PIM_3 by PimB and PimC (PimC is not be present in all strains which must be substituted by other ManT to synthesise PIM_3), respectively (Schaeffer *et al.*, 1999, Kremer *et al.*, 2002). These enzymes are the only well characterized enzymes in the early steps of LAM or PI-LM biosynthesis. They all function as α(1→6) mannosyltransferases, where PimB adds mannose on the 6-position of myo-inositol ring and PimC on the *O*-6 of mannose-α(1→6)-myo-inositol of PIM_2. These enzymes are characterized as belonging to the glycosyltransferase-A (GT-A) superfamily and to family 4 of the CAZy classification of GTs (http://afmb.cnrs-mrs.fr/CAZY). They use GDP-Mann as the sugar donor, suggesting the enzyme presence at the cytosol side of the cytoplasmic membrane. However, it is noted that recent paper has suggested that Rv2188c is involved in synthesising PIM_2 (Lea-Smith *et al.*, 2008) instead of PimB.

These smaller PIMs are known to be acylated by different acyltransferases and found in different acylation forms. In mycobacteria, the Rv2611c protein was found to be an acyltranferase responsible for the formation of Ac_1PIM_1 and Ac_1PIM_2 by acylating the 6-positon of the Man*p* residue linked to positon 2 of myo-Ins (Kordulakova *et al.*, 2003). It is notable that PgsA (Rv2612c) for PI

biosynthesis, PimA (Rv2610c) and the Rv2611c acyltransferase are located in the same operon (Kordulakova *et al.*, 2003). Takayama and Goldman (1969) suggested that the Ac_1PIM_1 is more preferable substrate for mannosylation than Ac_1PIM_2, and this step may constitute a key regulatory event in the PIM, PI-LM and LAM biosynthesis. The acylation of both PIM_1 and PIM_2 have been proved to occur in mycobacteria with the formation of the final product Ac_2PIM_2, which is present in the mycobacterial cell membrane and is formed by the acylation at the position-5 of myo-Ins by an unidentified acyltransferase (Kordulakova *et al.*, 2003). Both Ac_1PIM_2 and Ac_2PIM_2 have found to participate in the biosynthesis of higher mannose containing polymers (Figure 1.22) (Kordulakova *et al.*, 2003, Kordulakova *et al.*, 2002).

1.7.5.4. Polar PIMs, PI-LM and LAM biosynthesis

Though the above details are known about the synthesis of the lower PIMs, comparatively little is known about the synthesis of the higher hypermannosylated compounds (higher PIMS, PI-LM and LAM). Recently, PIM_4 which is formed by the mannosylation of PIM_3 by an unidentified α(1→6)- ManT, has been identified as the point at which the PIM and LAM biosynthetic pathways diverge (Morita *et al.*, 2006)

The commitment of $AcPIM_4$ to either polar PIM or PI-LM/LAM biosynthesis requires at least two enzymes activities: a putative α(1→2)-mannosyltransferase and an α(1→6)-mannosyltransferase, respectively. Two proteins, PimE and LpqW have been recently identified in mycobacteria, which are responsible for the divergence in the pathways (Morita *et al.*, 2006, Marland *et al.*, 2006, Kovacevic *et al.*, 2006). PimE is a polyprenol-phosphate-mannose (PPM) dependent ManT which catalyzes the α(1→2)-mannosyl transfer for $AcPIM_5$ synthesis, and may also be responsible for the mannosylation of $AcPIM_5$ to $AcPIM_6$, suggesting this enzyme may be responsible for the diverting of PIM_4 to the synthesis of PIM_6 or higher PIMs (Morita *et al.*, 2006). On the other hand, a highly conserved gene *lpqW* responsible for the production of a lipoprotein LpqW, which lacks glycosyltransferase motifs, is believed to take part indirectly in the transfer of mannose for the synthesis of $AcPIM_5$ in an α(1→6) linkage. LpqW is believed to form an LpqW-PIM_4 complex and present the PIM_4 to a specific unknown α(1→6) ManT for the formation of $AcPIM_5$ containing an α(1→6) linkage (Kovacevic *et al.*, 2006). Deletion of PimE and LpqW have no effect on the

growth and viability of the mutant strains and the accumulation of PIM_4 in the cell membrane supports this junction point in PIM and LAM biosynthesis and also shows PIM_6 can be replaced by PIM_4 functionally (Morita *et al.*, 2006).

Recently, *Rv1500* gene (named *pimF*) has been identified in *Mycobacterium marinum,* which may be responsible for the transfer of mannose to Ac_4PIM_5, leading to the formation of Ac_4PIM_7 (Alexander *et al.*, 2004). Though the linkage manner and the mannose donor have not been identified, mutation of PimF caused no effect on the PIM_6 synthesis, which suggest the enzyme may be α(1→6) ManT and since the higher PIM are synthesised on the outer surface of the membrane, the enzyme may use PPM as mannose donor. However Burguiere *et al.* (2005) have named the *Rv1500* gene product as LosA rather than PimF and suggested to be responsible for synthesis of highly polar lipooligosaccharides (LOSs), a broad class of trehalose-based lipids distributed widely in mycobacteria. Another ManT belonging to the GT-C family of glycosyltransferases, identified at the *Ncgl2093* and *Rv2174* loci of *C. glutamicum* and *M. tuberculosis* respectively, named MptA, has been found to be a PPM-dependent α(1→6) mannosyltransferase involved in the later stage of LM biosynthesis (Mishra *et al.*, 2007). MptA appears to be involved in main chain LM synthesis and this chain serves as the template for branching by another PPM-dependent α(1→2) ManT, which may be Rv2181 of *M. tuberculosis* (another member of the GT-C family) (Kaur *et al.*, 2006).

For LAM biosynthesis, no enzyme has been identified which is responsible for the addition of the first arabinose residues to LM and even the type of linkage

between the mannose and arabinose is unknown. Another GT-C family member, the EmbC arabinosyltransferase (*M. tuberculosis* Rv3793) elongates the arabinose chain and uses DPA as the arabinose donor (Zhang *et al.,* 2003, Berg *et al.,* 2005). For the capping of LAM macromolecules different ManTs have been suggested to be involved for PILAM and ManLAM synthesis which may belongs to different GT-C families. Among them MT1671 (*M. tuberculosis* Rv1635c) has been identified as necessary for the capping of ManLAM and responsible for first step of capping by functioning as an α(1→2) ManT (Dinadayala *et al.,* 2006). Though the mannose donor is unknown, it seems likely that the Man*p* donor is PPM, as the enzyme is in the GT-C superfamily. Moreover, at least one or more enzyme is still to be identified which are responsible for the complete synthesis of the Man*p* caps of ManLAM in *M. tuberculosis* and understanding of PILAM biosynthesis is in its early stage. The biosynthesis pathway of LAM is summarised in Figure 1.23.

There are still many steps required to understand the synthesis of these hypermannosylated macroamphiphiles. Moreover, organisms like *Micrococcus luteus*, which produce DAG-LM with a DAG anchor rather than PI have different biosynthetic pathways (Pakkiri *et al.,* 2004), where the anchor α-D-mannosyl-(1→3)-α-D-mannosyl-(1→3)-diacylglycerol is formed by at least two enzymes at the inner leaflet of the membrane, utilizing the GDP-Mann as the mannose donor. This glycolipid is then likely to be transfer by a flippase to the outer leaflet of the membrane. Further elongation of the Man_2-DAG is believed to be achieved by the transfer of mannose from a polyprenolmannose

donor on the outer surface of the membrane by unknown mannosyltransferase(s). Also the DAG-LM chain is then esterified with succinyl esters by an unknown pathway which is yet to be revealed.

1.8. The phylum Actinobacteria

The Actinobacteria is a large phylum of high G+C Gram-positive bacteria, which used to be considered as an intermediate between bacteria and fungi (Mims *et al.,* 1998). The major characteristic of the organisms of this group are that they contain more than 55 mol percent guanine and cytosine in their total genome (Fox *et al.,* 1980, Gao *et al.,* 2006). The phylum Actinobacteria was classified into five subclasses (Figure 1.24), although the subclass Sphaerobacteridae has subsequently been proposed to belong within the phylum Chloroflexi (Hugenholtz and Stackebrandt, 2004). The largest subclass in the phylum Actinobacteria is the Actinobacteridae, which has two order: Bifidobacteriales and Actinomycetales (Stackebrandt *et al.,* 1997). The latter order has further been classified into eleven suborders (Figure1.25). The morphological characteristics of the actinomycetes are highly diverse, as the group contains genera like *Corynebacterium* which divide by binary division, *Mycobacterium* and *Nocardia spp.* which have unusual cell envelopes and some branching, to extensively branching and filamentous species like *Streptomyces* (Atlas, 1997). These diverse morphological characteristics have made the study of cell envelopes of these organisms an interesting subject, especially in the search for chemotaxonomic markers to classify organisms which cannot be resolved solely on the basis of 16S rRNA phylogenetic characteristics (Ventura *et al.,* 2007). Moreover, this group contain secondary metabolite producing organisms, such as *Streptomyces spp.*; pathogenic organisms, including members of the genera *Mycobacterium, Rhodococcus,* and *Corynebacterium*; and also thermophilic organisms such as *Rubrobacter spp.*, *Thermobifida fusca* and different species of *Streptomyces* are scattered

through out the phylum. This has made the study of the phylum one of the most interesting topics for microbiologists.

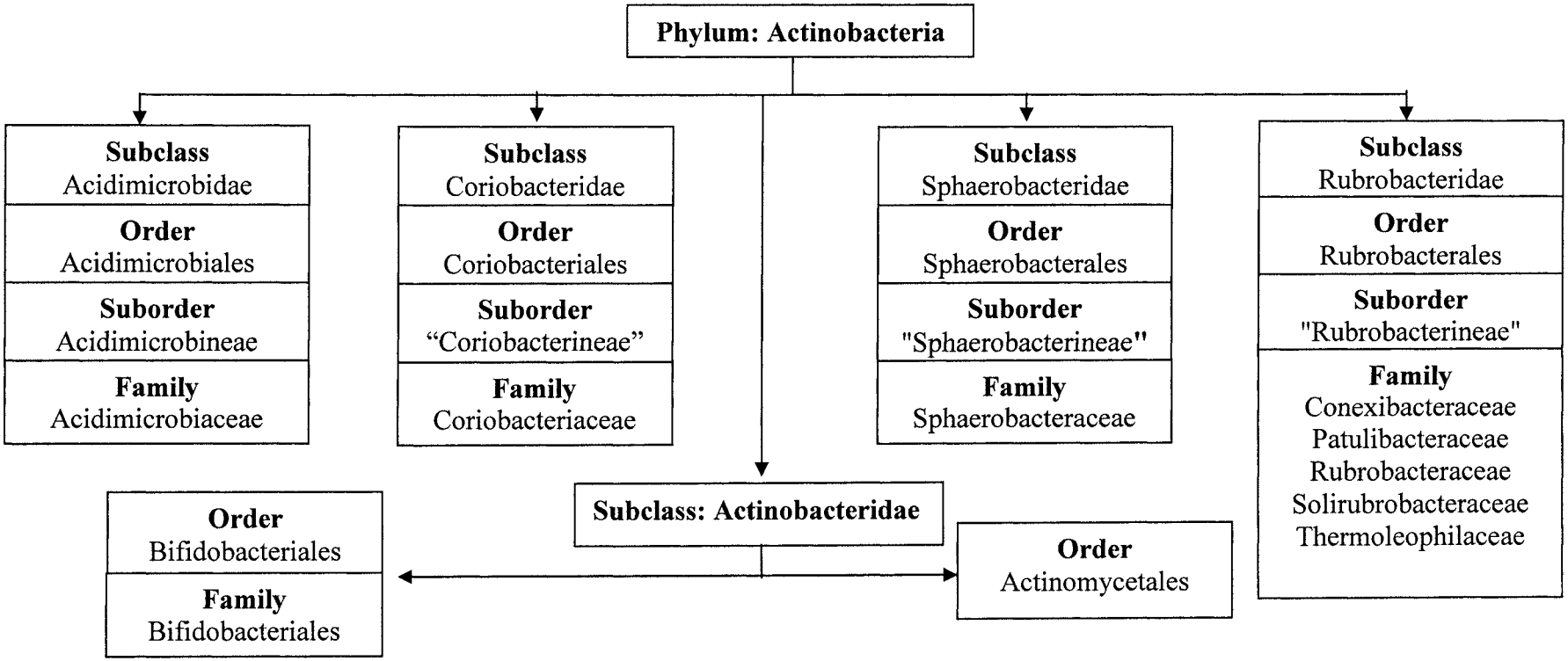

Figure 1.24. Flowchart for the classification of Gram-positive high G+C: Actinobacteria phylum. The data taken from URL: http://www.bacterio.net & Stackebrandt, Rainey & WardRainey, 1997. Note that subclass Sphaerobacteridae has been proposed to belong to the phylum Chloroflexi Hugenholtz & Stackebrandt, 2004.

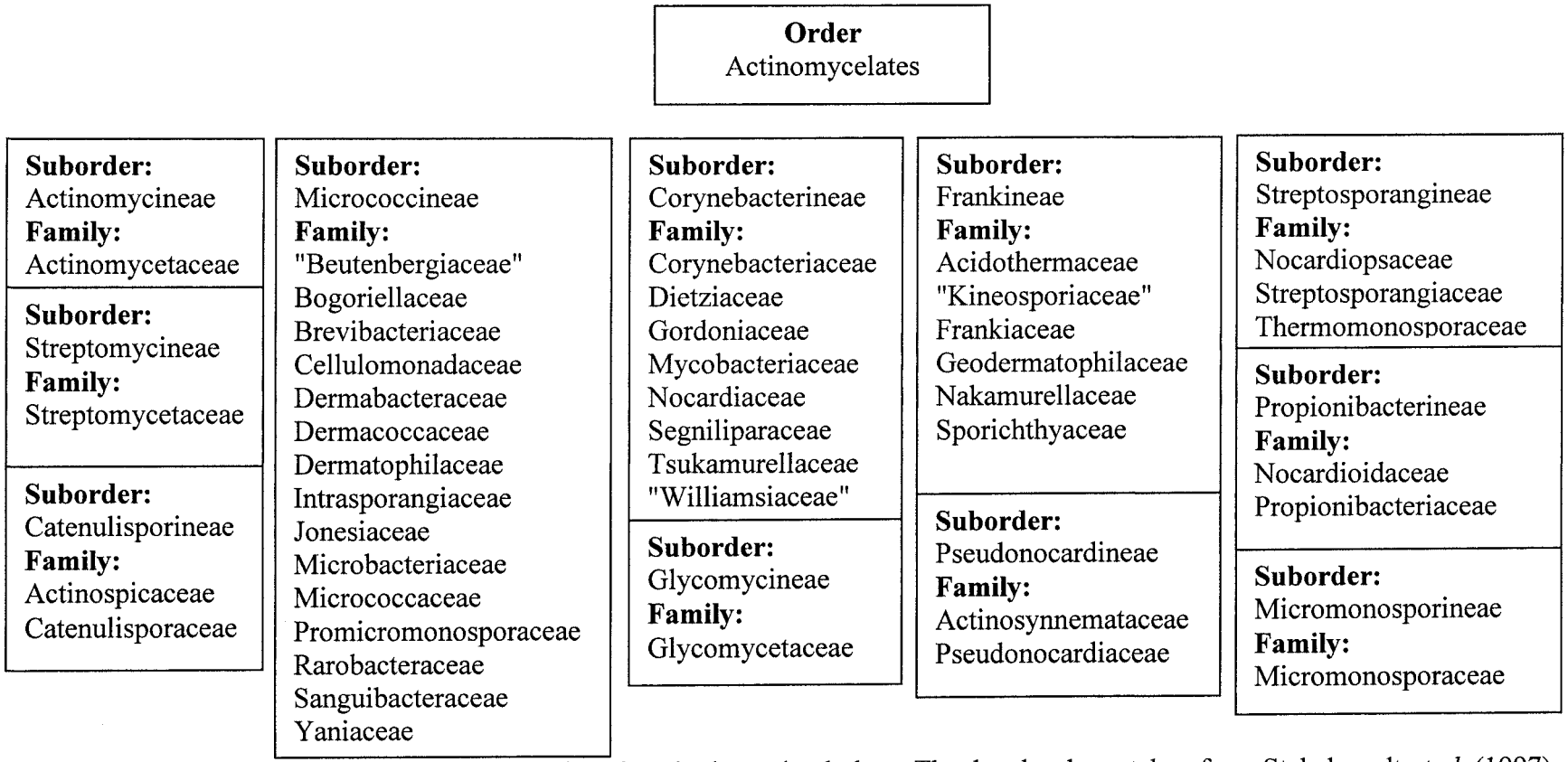

Figure 1.25. Classification of Actinomycelates order of Actinobacteria phylum. The data has been taken from Stakebrandt *et al.* (1997) & http://www.bacterio.net.

1.9. Distribution of macroamphiphiles in Actinobacteria

The organisms in the phylum Actinobacteria are high G+C Gram-positive bacteria and according to the hypothesised distribution pattern of macroamphiphiles, they are generally predicted to contain lipoglycans (Table 1.2). Lipoglycans, previously described as 'atypical LTA' (Sutcliffe and Shaw, 1991) as they are present in Gram-positive bacteria which lack LTA, may replace LTA functionally. Moreover, the distribution of LTA and diverse lipoglycans has been found to be discontinuous within the Gram-positive bacteria. These criteria allowed the proposal that the distribution pattern of macroamphiphiles may have chemotaxonomic value (Sutcliffe, 1994b), which may help to classify the bacterial domain more precisely. In this section, a summary of the distribution of macroamphiphiles in Actinobacteria will be briefly presented and also it will be shown that a large number of organisms are still left to be studied.

Out of five subclasses of the phylum Actinobacteria, macroamphiphiles have only been studied in the members of the subclass Actinobacteridae (Figure 1.24), the distribution of macroamphiphiles in the subclass Actinobacteridae is shown in Table 1.5. Comparison of Table 1.5 with the taxonomic diversity in the subclass Actinobacteridae (Figures 1.24 and 1.25) clearly demonstrates that many Actinomycete taxa have yet to be investigated for their macroamphiphiles. Moreover, most studies for macroamphiphiles have only focused on a limited range of taxa e.g. Mycolata; micrococci and relatives as shown in the Table 1.5 and still a wide range of lineages are left to be investigated.

Table 1.5. Distribution of macroamphiphiles in subclass Actinobacteridae.

Order	Suborder	Family	Macroamphiphile	References
Bifidobacteriales		Bifidobacteriales	Lipoglucogalactan	Dencamp *et al.*, 1985, Iwasaki *et al.*, 1990
Actinomycelates	Actinomycineae	Actinomycetaceae	Lipoglycan	Hamada *et al.*, 1976, Wicken *et al.*, 1978
	Micrococcineae	Jonesiaceae	Lipoglycan	Rocourt *et al.*, 1987, Ruhland and Fiedler, 1987
		Micrococcaceae	DAG-LM	Powell *et al.*, 1974, Lim and Salton, 1985, Sutcliffe and Old, 1995b, Sutcliffe, 1994aSutcliffe and Alderson 1995
	Corynebacterineae	Corynebacteriaceae	PI-LM & LAM	Mc. Carty, 1959, Misaki *et al.*, 1977, Kokeguchi *et al.*, 1987, Tatituri *et al.*, 2007
		Turicella	LAM	Gilleron *et al.*, 2005
		Dietziaceae	PI-LM/ LAM-like	Sutcliffe, 2000
		Gordoniaceae	PI-LM/LAM-like	Flaherty and Sutcliffe, 1999, Garton and Sutcliffe, 2006
		Mycobacteriaceae	PI-LM & LAM	Briken *et al.*, 2004, Nigou *et al.*, 2003
		Nocardiaceae	LM & LAM	Nigou *et al.*, 1999, Garton *et al.*, 2002, Gibson *et al.*, 2003c, Flaherty *et al.*, 1996
		Tsukamurellaceae	LAM-like	Gibson *et al.*, 2004
	Pseudonocardineae	Actinosynnemataceae	PI-LM	Gibson *et al.*, 2005
		Pseudonocardiaceae	LAM	Gibson *et al.*, 2003b
	Propionibacterineae	Propionibacteriacea	PI-LM or/& lipoglycan	Shaw and Dinglinger, 1969, Whale *et al.*, 2004

1.10. Aims of the project

This project was mainly focussed on determining the distribution of macroamphiphiles in the phylum Actinobacteria, based on which the chemotaxonomic value, the biosynthetic pathways and functional characteristics of these large macromolecules was tried to be resolved. From the previous section, it has been established that most of the studies regarding macroamphiphiles have been done within specific regions of the phylogenetic tree of Actinobacteria and thus there are still large gaps in the phylogenetic tree which remain uninvestigated. As the study of macroamphiphiles is a laborious and time-consuming process, so the organisms chosen for this project were selected based on two criteria:

1. Filling the gaps in phylogenetic tree, so the distribution pattern and functions of the macroamphiphiles within the tree could be better understood.
2. Organisms' whose whole genome sequences have been finished, so that these genome sequences can be used for comparative genomic studies to understand the pathways for macroamphiphile biosynthesis.

Previously, no thermophilic actinobacteria have been subjected to study for their macroamphiphile composition, so this criteria was also considered while choosing the organisms. Moreover, organisms outside the Actinobacteridae subclass have been considered for first time in this project.

Depending on the above criteria four organisms were chosen for study in this project:

1. *Thermobifida fusca* (thermophile, member of the suborder Streptosporangineae)
2. *Rubrobacter xylanophilus* (thermophile, member of the subclass Rubrobacteridae)
3. *Kineococcus radiotolerans* (member of the suborder Frankineae)
4. *Streptomyces coelicolor* M145 (member of the suborder Streptomycineae)

The aim of the project can therefore be summarised as follows:

1. To identify the macroamphiphiles present in these organisms.
2. To determine the chemical and structural characteristics of these macroamphiphiles.
3. To analyse the distribution pattern of these macroamphiphiles in comparison with previously studied macroamphiphiles and to identify the chemotaxonomic value of these molecules.
4. To understand the distribution pattern of the macroamphiphiles in comparison with SCWPs (especially TA) and to try to understand their functions.
5. By comparative genomic studies, to resolve the biosynthetic pathway of these macromolecules, especially LTA.

CHAPTER TWO

METHODS AND MATERIALS

The analysis of macroamphiphiles from microorganisms is a time consuming and laborious procedure. It ranges from the extraction and purification of macroamphiphiles to the chemical and structural characterisation of the macromolecules (Figure 2.1).

2.1. Purification of macroamphiphiles

Purification of macroamphiphiles typically requires purifying macroamphiphiles from at least 1.0 g dry weight of cells of the organisms, which requires large scale culture and harvesting of cells, followed by an appropriate extraction method. This is followed by separating these macromolecules based on their hydrophobicity, ionic and chemical characteristics, which not only separate them from nucleic acid, proteins or carbohydrates, but also separate the different types of macroamphiphiles.

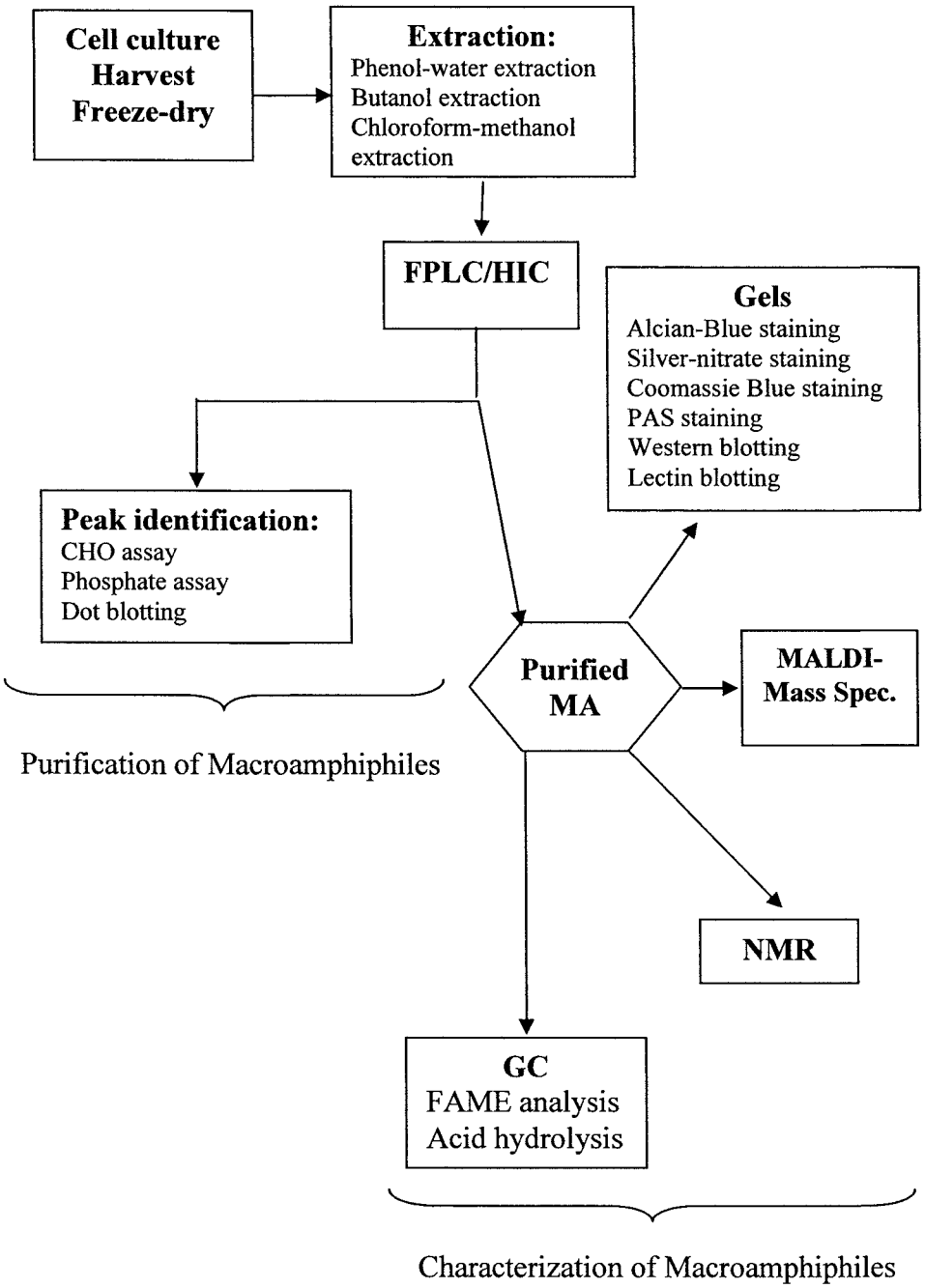

Figure 2.1. Diagram presenting the methods involved in the analysis of macroamphiphiles.

2.1.1. Bacterial strain used in this study

The bacterial strains used in this project were all high G+C Gram-positive bacteria, belong to the phylum Actinobacteria. *T. fusca* strain YX (Lykidis *et al.,* 2007) was kindly supplied by Professor David Wilson and Dr Diane Irwin (Department of Molecular Biology and Genetics, Cornell University, U.S.A.). *R. xylanophilus*, DSM 9941^{T} (Carreto *et al.,* 1996), was kindly supplied by Profesor Milton da Costa (Departamento de Bioquímica, Universidade de Coimbra, Portugal). *K. radiotolerans* strain SRS30216 (the genome sequenced strain) was kindly supplied by Dr Christopher Bagwell (Environmental Biotechnology, Savannah River National Laboratory, Aiken, SC, USA). *Streptomyces coelicolor* M145, was supplied by Dr. Stephen Cummings (School of Applied Science, Northumbria University, Newcastle Upon Tyne, UK) and *Streptomyces* sp. strain DSM40537 was purchased from Deutsche Sammlung von Mikroorganismen und Zellkulturen GmbH (DSMZ, German Collection of Microorganisms and Cell Cultures). The low G+C, Gram-positive bacterium (phylum Firmicutes) *S. agalactiae* (GBS) strain A909 was used as a reference organism for LTA positive organism and was provided by Dr Dean Harrington (University of Bradford, UK).

2.1.2. Media preparation

2.1.2.1. Hagerdahl medium

This liquid medium was used for the growth of *T. fusca* (Hagerdal *et al.*, 1978). Macro salts (10X) (Table 2.1) and Micro salts (50X) (Table 2.1) prepared as autoclaved stocks. For 100 mL medium the additions for carbon source (yeast extract; glucose or cellobioise) were autoclaved in 88 mL distilled water and then the autoclaved Macro salts (10X; 10 mL per 100 mL medium), Micro salts (50X; 2 mL per 100 mL medium) were added into the mixture separately. Medium was completed by the addition of 10 µL thiamine stock and 400 µL of biotin stock. The ingredients for Macro salts, Micro salts, carbon sources and additional supplements are shown in Table 2.1.

2.1.2.2. Tripticase soya media (TM)

This solid medium was used for the growth of *T. fusca* and *R. xylanophilus.* Medium contained 3.0 g Tripticase soya (MERCK, S.N: 1.00525) and 1.5 g bacteriological agar per 100 mL distilled water (dH_2O). For liquid culture of *R. Xylanophilus*, agar was omitted from the medium.

2.1.2.3. Thermus media (ATCC medium: 697)

This solid media (Table 2.2) was used for the growth of *R. xylanophilus.* For liquid culture of *R. xylanophilus*, agar was omitted from the medium (Kilbane *et al.*, 2002).

Table 2.1. Ingredients of Hagerdahl medium

Macro Salts 10X (per litre)	
Ingredient	Amount (g)
Sodium Chloride, NaCl	15.0
Ammonium sulphate, $(NH_4)_2SO_4$	31.0
Sodium biphosphate, Na_2HPO_4*	91.0
Potassium biphosphate, KH_2PO_4	9.0
Micro Salts 50X (per 500 ml)	
Ingredient	Amount (g)
EDTA	1.25
Magnesium sulphate, $MgSO_4.7H_2O$	5.0
Zinc sulphate, $ZnSO_4.7H_2O$	0.2
Ferrous sulphate, $FeSO_4$	0.5
Manganese sulphate, $MnSO_4.7H_2O$	0.38
Calcium chloride, $CaCl_2.2H_2O$	0.66
Carbon Source (Any one, per litre)	
Ingredient	Amount (g)
Cellobiose	5.0
Glucose	5.0
Xylan	7.5-10.0
Addition supplement per litre	
Ingredient	Amount (mg)
Biotin (stock 10 mg/mL, filter sterilised)	1.0
Thiamine (stock 0.25 mg/mL, filter sterilised)	1.0
Yeast extract**	200

*$Na_2HPO_4.7H_2O$ solution adjusts to pH 7.4 +/- 0.2.

** Yeast extract ingredient is optional.

Table 2.2. Ingredients for Thermus media

Ingredient	**Amount**
Yeast extract	4.0 g
Peptone	8.0 g
NaCl	2.0 g
Agar	30 g
dH_2O	1 Litre (L)
Adjust the culture at pH 7.5 before autoclave.	

2.1.2.4. TGY Medium

This solid media was used for the growth of *K. radiotolerans* (Table 2.3). For liquid culture of *K. radiotolerans*, agar was omitted from the medium (Bagwell *et al.,* 2008).

2.1.2.5. PTYG Medium

This solid medium was used for the growth of *K. radiotolerans.* For liquid culture of *K. radiotolerans*, agar was omitted from the medium and the ingredients has shown in Table 2.4 (Bagwell *et al.,* 2008).

2.1.2.6. Mannitol Soya Flour Media or MS Media

This solid medium was used as a sporulating medium for *S. coelicolor* M145 and *Streptomyces* strain DSM40537 and the ingredients of the medium are showed in Table 2.5 (Kieser *et al.,* 2000). To collect the spores, nitrocellulose membranes (pore size 0.45 μm, radius 82 mm; Whatman) were placed on the surface of the agar plates.

2.1.2.7. Non-sporulating Media

This solid medium was used as a non-sporulating medium for *S. coelicolor* M145 and *Streptomyces* strain DSM40537 (Table 2.6) (Kieser *et al.,* 2000).

2.1.2.8. Yeast extract-malt extract media (YEME)

This liquid medium was used for the culture of *S. coelicolor* M145 and *Streptomyces* strain DSM40537. The ingredients are shown in Table 2.7 (Kieser *et al.,* 2000).

Table 2.2. Ingredients for Thermus media

Ingredient	**Amount**
Yeast extract	4.0 g
Peptone	8.0 g
NaCl	2.0 g
Agar	30 g
dH_2O	1 Litre (L)
Adjust the culture at pH 7.5 before autoclave.	

Table 2.3. Ingredients for TGY medium

Ingredient	**Amount**
Tryptone	1.0 g
Yeast extract	0.5 g
Glucose	0.1 g
Agar	1.5 g
dH_2O	100 ml
Adjust the culture at pH 7.2 before autoclave.	

Table 2.4. Ingredients for PTGY medium

Ingredient	**Amount**
Peptone	0.5 g
Tryptone	0.5 g
Yeast extract	0.5 g
Glucose	1.0 g
Agar	1.5 g
dH_2O	100 ml
$MgSO_4$. $7H_2O$ (stock of 60 mg/ml) prepared and autoclaved separately and added 100 µl into the auclaved broth	60 mg
Adjust the culture at pH 7.2 before autoclave.	

Table 2.5. Ingredients Mannitol Soya Flour medium

Ingredient	**Amount**
Agar	20.0 g
Mannitol	20.0 g
Soya flour (source)	20.0 g
dH_2O	1 L

Table 2.6. Ingredients non-sporulating medium

Ingredient	**Amount**
Agar	20.0 g
Malt extract	10 g
Yeast extract	10 g
dH_2O	1 L

Table 2.7. Ingredients YEME medium

Ingredient	**Amount**
Yeast extract	3 g
Peptone	5 g
Malt extract	3 g
Glucose	1 g
dH_2O	800 ml
Magnesium chloride ($MgCl_2.6H_2O$), stock solution (2mM) and autoclaved separately.	2 ml
Sucrose 34 g added in 150 ml of water and autoclaved separately.	200 ml

2.1.3. Cell harvesting and freeze drying (large culture volume)

At the time of harvesting, each culture was streaked onto an agar plate of an appropriate medium to get single colonies after overnight incubation, in order to check the purity of the culture. The broth was harvested by 800 mL of broth culture dispensing into 4x200 mL centrifuge pots. The pots were centrifuged at 4000 x g for 15 min at 4°C. Then the supernatant was decanted carefully without disturbing the cell pellet.

Fresh broth culture (800 mL) was dispensed again into the 4 x 200 mL centrifuge pots and again centrifuged using the same conditions as before. These steps were repeated until the broth culture was completely harvested. 10-15 mL phosphate buffer saline (PBS) was added to the final cell pellet in each centrifuge pot. Cell pellets were resuspended using a 5 mL Gilson by repeated drawing up and expelling the PBS onto the pellet. Once the pellet had been resuspended, the final volume was adjusted to approximately 50 mL in each centrifuge tube by adding PBS. The pots were centrifuged again at 4000 x g for 15 min at 4°C.

The supernatant was decanted carefully without disturbing the cell pellet and each cell pellet was resuspended again into 10 mL cold PBS. The washed cell suspensions were transferred into a single 50 ml 'Falcon' centrifuge tube which was centrifuged again at 4000 x g for 15 min at 4°C and the supernatant discarded. A second purity was checked for contamination by Gram staining (described later in section 2.3.1) before the washed cell pellets were frozen and lyophilized using a Christ, Alpha 1-2 Lo Plus freeze drier.

2.1.4. Delipidation of the lyophilized cell

The lyophilized cells were suspended in water to 50 mg cells/mL. The suspended cells were subjected to sonication using a Soniprep150 sonicator, Amplitude micron20 (10 sec x 3 times) to disrupt the cells. Then the disrupted cells were delipidated by adding an equal volume of Chloroform ($CHCl_3$): Methanol (CH_3OH) 2:1 solution. The solution was shaken overnight (100 x g) at room temperature.

The cell solution was centrifuged at 150 x g for 10 min or left on the desk for half an hour, so that the water and the $CHCl_3$ phase separated. The cells pellet was recovered and subjected to the extraction process to recover macroamphiphiles.

2.1.5. Macroamphiphiles Extraction Processes

There are several methods for extracting macroamphiphiles of which the three extraction methods used in this project were phenol extraction, butanol extraction and chloroform-methanol extraction methods.

2.1.5.1. Phenol extraction methods

For hot phenol-water extraction (Westphal and Jann, 1965; Fischer *et al.*, 1983), lyophilised bacterial cells were resuspended at 50 mg/mL into distilled water and mixed with equal volume of hot (68°C) 90% (w/v) phenol and extracted for 1 h at 68°C in a shaking water bath (120 x g). The single phase extract was separated into distinct aqueous and phenol phases by centrifugation (1 h, 4000 x g, 4°C) and the upper aqueous phase withdrawn. The phenol phase was washed by shaking with an equal volume of water and the aqueous wash recovered by centrifugation as before. The combined aqueous extracts were extensively dialysed to remove phenol traces and freeze-dried. All dialysis steps were performed with low molecular weight cut-off dialysis tubing (SnakeSkin^{TM} pleated dialysis tubing, Pierce).

2.1.5.2. Butanol extraction method

The modified butanol extraction method of Morath *et al.* (2001) and Theilacker *et al.* (2006) was used to extract macroamphiphiles. For butanol extraction (Morath *et al.*, 2001; Theilacker *et al.*, 2006), wet bacterial cells were suspended in 0.1 M sodium citrate buffer pH 4.7 at 0.66 mg/mL. The cells were disrupted by sonication using sonicator Soniprep150, Amplitude micron20 (10 sec pulse for two min, on ice). The disrupted cells were mixed with an equal volume of n-butanol and stirred for 30 min at room temperature. After centrifugation at 13,000 x g for 20 min, the lower aqueous phase was recovered and extensive dialysis was performed to remove butanol and the extract freeze-dried.

2.1.5.3. Chloroform-methanol extraction method

Chloroform-methanol extraction of *R. xylanophilus* was performed using an adaption of the method of Behr *et al.* (1992). Briefly, cells, suspended at 50 mg/mL in sodium acetate buffer pH 4.7 and cells were disrupted by sonication (10 sec pulse for 2 min). After adjusting the pH to 5.5 with 1 M $NaHCO_3$, 2 vol. MeOH and 1 vol. $CHCl_3$ were added and the mixture was stirred at room temperature for 3 h. After centrifugation (600 x g, 30 min), the supernatant was withdrawn, the pellet resuspended in 4 vol. of 0.05 M sodium acetate pH 5.5/MeOH/$CHCl_3$ (0.8:2.0:1.0; by vol.) and stirred overnight. After centrifugation, the supernatant were combined in a final $CHCl_3$/MeOH/H_2O proportion of 1.0:1.0:0.9. After centrifugation, the combined supernatants were extracted twice with chloroform, freed from methanol by rotary evaporation

(both at 20° C) and dialyzed against three 5-L changes of distilled water and freeze dried.

2.1.6. Separating macroamphiphiles

2.1.6.1. Hydrophobic interaction chromatography (HIC)

Crude cell extracts were subjected to hydrophobic interaction chromatography (HIC) using previously described methods (Fisher, 1996; Sutcliffe, 2000). The crude extracts was loaded onto a 1.75 X 20 cm Octyl-Sepharose CL-4B (Sigma-Aldrich) column in 8 mL of equilibration buffer (100 mM sodium acetate pH 4.5 containing 15% v/v n-propanol) and the column was eluted with 48 mL of this buffer. Hydrophobically retained material was then eluted with a 192 mL gradient of 15-65% v/v n-propanol in 100 mM sodium acetate pH 4.5 buffer using an automated flow-pressure liquid chromatography (FPLC) system (Pharmacia Biotech) to generate the gradient. The FPLC collection profile is shown in Figure 2.2.

2.1.6.2. Anion exchange chromatography

Crude cell extracts were first subjected to HIC as described in section 2.1.6.1. The crude extracts was loaded onto a 0.46 X 10 cm column of 30Q beads (Amersham Pharmacia Biotech) in 10 mL of equilibration buffer (1 M sodium acetate pH 4.5 containing 45% v/v n-propanol and 0.0 M NaCl) and the column was eluted with 100 mL of this buffer. Retained material was then eluted with a 800 mL gradient of 0.0 to 0.8 M NaCl in 1 M sodium acetate pH 4.5 containing 45% v/v n-propanol buffer using an automated FPLC system (Pharmacia Biotech). The FPLC collection profile is shown in Figure 2.3.

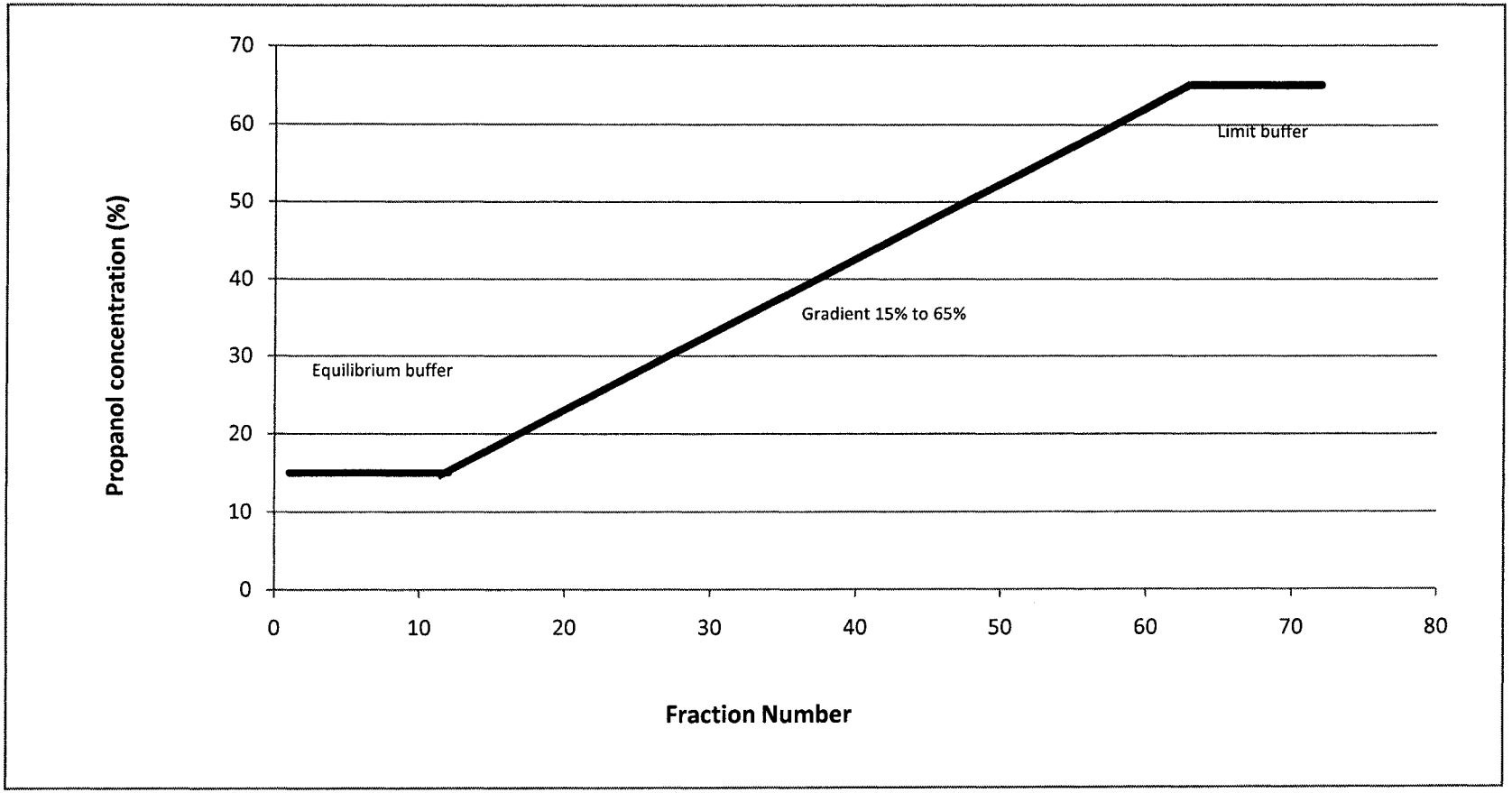

Figure 2.2. Schematic presentation of the HIC profile. The crude extract was loaded the column with equilibration buffer until fraction 12, after which gradient elution with an increasing concentration of propanol was begun. Each fraction was collected at 4 ml at a flow rate of 0.2 mL/min.

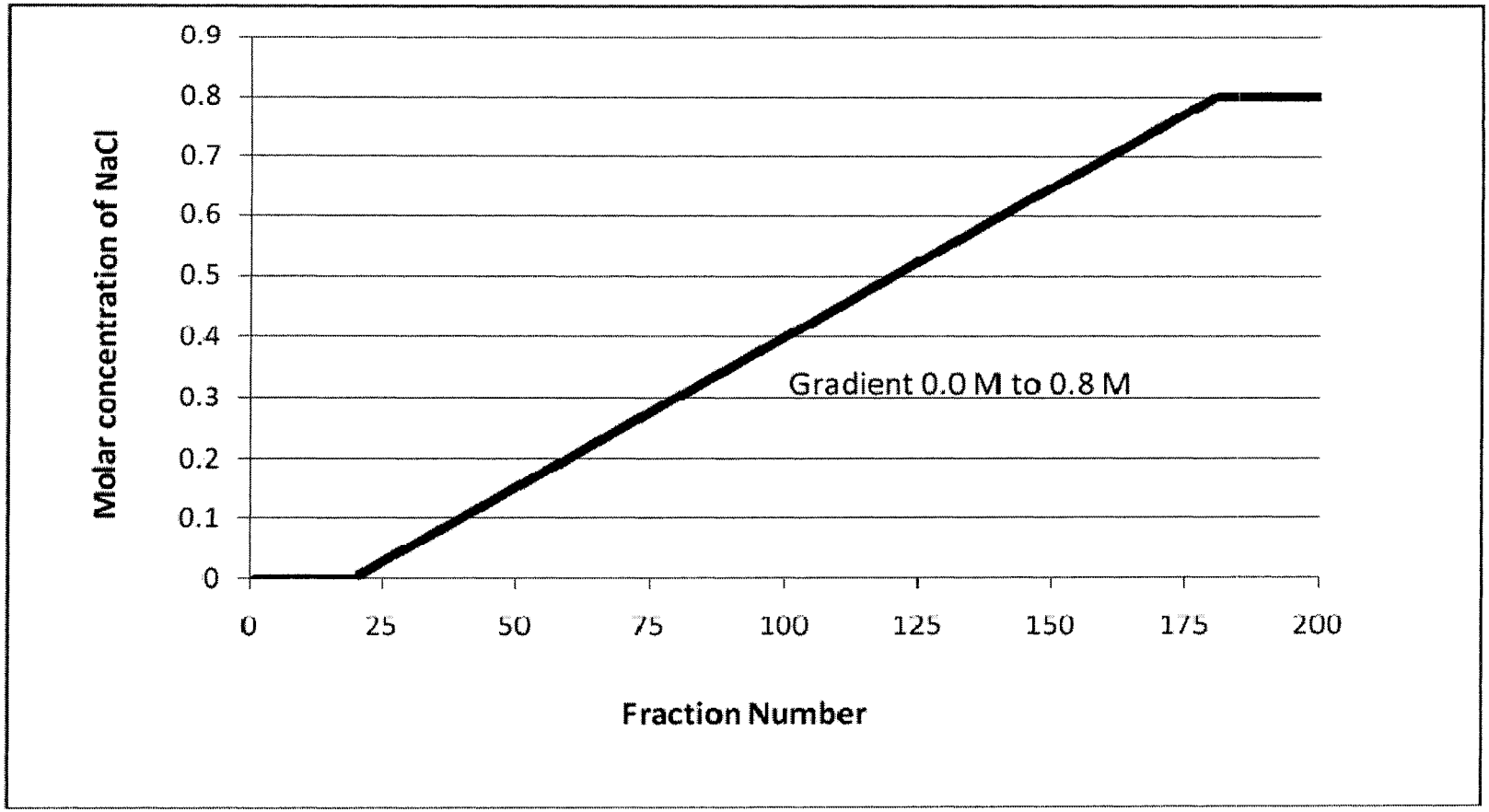

Figure 2.3. Schematic presentation of the anion exchange profile. The crude extract was loaded the column with equilibration buffer until fraction 20, after which gradient elution with an increasing molarity of NaCl was begun. Each fraction was collected at 5 ml at a flow rate of 0.5 mL/min.

2.1.6.3. Mannose-Binding protein column for purification of mannose containing molecules.

An ImmunoPure® IgM purification kit (PIERCE) was used for separating mannose containing molecules/macroamphiphiles from purified macroamphiphile extracts according to the manufacturers protocol. Generally this method has been used to isolate and purify immunoglobulin M (IgM) but this method has also been used for purification of mannosyl-lipoarabinomannan and lipomannan from *Mycobacterium avium* (Polotsky *et al.*, 1997), *Micrococcus luteus* and *Enterococcus spp.* (Polotsky *et al.*, 1996).

The ImmunoPure® MBP Column was prewashed and equilibrated with 5 mL ImmunoPure® MBP Column Preparation Buffer and 20 mL of the ImmunoPure® IgM Binding Buffer at 4°C, respectively. Freeze dried macroamphiphiles in cold 1 mL ImmunoPure® IgM binding buffer (provided by PIERCE) was loaded onto the column. A further 0.5 mL of ImmunoPure® IgM binding buffer was loaded and incubated at 4°C for 30 min. The column was then eluted with 42 mL of IgM binding buffer to remove the unbound macromolecules and the buffer was collected in 4 mL fractions. The column was loaded with 4 mL of ImmunoPure® IgM Elution Buffer and incubated for 1 h at room temperature. Then the column was eluted with elution buffer (64 mL) and 4 mL fractions were collected.

2.1.7. Detection of macroamphiphiles in column fractions

Macroamphiphiles containing fractions were identified by carbohydrate and phosphate assay and sometimes via dot immunoblotting.

2.1.7.1. Carbohydrate assay

i) **Phenol-Sulphuric Acid "total" Carbohydrate Micro-method**

The method is ideal for detecting carbohydrate in column fraction, though not suitable for analytical process and adapted from Fox and Robyt (1991). 40 µL of sample were added from fractions obtained from chromatography or MBP column purification in 96-well titre plate as triplicate aliquots. After overnight incubation at room temperature to evaporate solvents, 40 µL of 2.5% (v/v) phenol was added to each of the wells. After careful vortex for approximately 30 sec the plates were kept on ice for at least 5 min and 125 µL concentrated sulphuric acid (H_2SO_4) added to each well. The mixture was vortexed again carefully, sealed with plate sealer, and then incubated for 30 min at 80°C. The plate was then cooled to room temperature and the absorbance was measured at 492 nm using a plate reader (FL600 FAC, Bio-TEK Instruments. Ind.).

ii) **Scale-down tube method**

This method was adapted from Rao and Pattabiraman (1989) and, generally used for the quantification of carbohydrate in samples. Standard dilutions (250 μg/mL, 200 μg/mL, 150 μg/mL, 100 μg/mL, 75 μg/mL, 50 μg/mL and 25 μg/mL) were prepared from stock solutions of 1.0 mg/mL glucose or mannose. 200 μL of standards and appropriate diluted samples were aliquoted into Eppendorf tubes in duplicate and 600 μL concentrated H_2SO_4, (95-97%, v/v) added. Tubes were then subjected to vigorous vortex mixing for 10-15 sec and incubated at 80°C for 10 min. The tubes were then kept in the ice for 10-15 min to cool down below room temperature and 10 μL 80% (v/v) phenol was added into each tube and vortex gently. After 30 min of incubation at room temperature the colour developed in the tubes, triplicate 200 μL samples from which were then aliquoted into rows of a titre plate and the absorbance were measured at 492 nm (CECIL CE2030 spectrophotometer, Scientific & Medical product Ltd.).

2.1.7.2. Phosphorus analysis

The method was derived from Chen *et al.* (1956). Samples containing 1-5 μg phosphorus (samples were diluted appropriately if they contained more than this range) were evaporated to dryness in glass test tubes, using a hot-plate or oven. Blank and standard tubes containing 0-5 μg phosphorus tubes were treated identically. 100 μL digestion mixtures (15 mL concentrated H_2SO_4 mixed with 10 mL of 60% v/v, perchloric acid) was added to each tube and heated for 30 min using a hot-plate. After cooling down the tubes to room temperature, 3.9 mL 18 mΩ/cm distilled water was added to each tube and then 4.0 mL freshly prepared colour reagent (20 mL 3M sulphuric acid, H_2SO_4, 20 mL 2.5% (w/v) ammonium molybdate, 60 mL 18 MΩ/cm distilled water and 2 g of ascoribic acid were mixed to prepare 100 mL of colour reagent) and incubated at 37 °C for 1.5 for 2 h. After the incubation, the absorbance was measured at 820 nm (CECIL CE2030 spectrophotometer).

2.1.7.3. Dot blotting

This is a modified western blotting method in which the presence of specific antigen is identified without running any electrophoresis gels, using only the blot process. 1 μL of sample was pipetted directly onto the nitrocellulose membrane from each fractions of the FPLC-HIC column, with positive controls (serial diluted LTA or LAM) in rows, as dots. The membrane was allowed to dry at room temperature (approximately 1 h). Then the non-specific binding sites on the membrane were blocked by incubating overnight in 5% (w/v) milk powder (Marvel) in PBS-Tween (0.05% w/v). The blocking solution was discarded and the membrane was incubated with primary antibody solution for 2-3 h, which was then washed with 5 changes of PBS-Tween buffer (5-10 min each wash). After washes, the membrane was incubated with secondary antibody for 2-3 h and again washed with 5 changes of PBS-Tween buffer. The colour of the blot was developed using the BCIP/NBT alkaline phosphatase reagent (Zymed kit; prepared according to manufacturers instructions) and incubating at 37°C. After development of the colour the blot was transferred in distilled water and rinsed thoroughly with several changes of water to prevent excessive background colour developing. The blot was stored by drying on tissue.

2.2. Characterisation of the Macroamphiphiles

2.2.1. Sodium dodecyl sulfate – Polyacrylamide gel electrophoresis (SDS-PAGE)

The method was taken from Laemmli (1970) and the gel was prepared using a discontinuous electrophoresis system (Laemmli 1970) with 15% (w/v) resolving gels in a minigel format (Mini-Protean® II, BIORAD).

Tris-HCl 2 M, pH 6.8 (100 mL) stacking or upper gel buffer was prepared by dissolving 24.2 g Tris base (Sigma Trizma) in 70 mL 18 MΩ/cm water and pH was made 6.8 by adding concentrated HCl (37%, v/v). Buffer was stored at 4°C in a brown glass bottle.

3M Tris-HCl pH 8.8 (100 mL) resolving or lower gel buffer was prepared by dissolving 36.3 g Tris base (Trizma) in 70 mL 18 MΩ/cm water and pH was made 8.8 by adding concentrated HCl. Buffer was stored at 4°C in a brown glass bottle.

Sample buffer (x 5) was prepared by adding 0.3 mL of 2 M Tris-HCl pH 6.8, 5 mL of 50% (v/v) glycerol, 2 mL of 10% (w/v) SDS, and a small spatula tip of bromophenol blue was added at the end. Finally, 0.5 mL of 2-mercaptoethanol was added and the buffer stored at 4°C. One volume of sample buffer was added to 4 volumes of sample and the sample was boiled for 4 min in a water bath.

Tris-Glycine-SDS running buffer (10x) ingredients are shown in Table 2.8. Alternatively, Biorad pre-prepared T10x running buffer was used. The gel casting protocol is given in Table 2.9 for the lower resolving gel and Table 2.10 for the upper stacking gel. Gels were assembled and run using the Mini-Protean® II (BIORAD) system, following the manufacturer's instructions. 10X running buffer were diluted to 1X concentration immediately before use. Gels were electrophoresed at constant voltage (typically 120V) until the bromophenol blue dye front was about to leave the bottom of the gel (typically after ca. 90 min).

Table 2.8. Ingredients for Tris-Glycine-SDS running buffer (10x concentrate).

Ingredient	**Amounts**
Trizma base	30 g
Glycine	144 g
SDS	10 g
ddH_2O	1 L

Table 2.9. Lower resolving gel recipes

Ingredients	**Amount for 10% lower gel**	**Amount for 12% lower gel**	**Amount for 13% lower gel**	**Amount for 15% lower gel**
ddH_2O	6.14 mL	5.64 mL	5.39 mL	4.89 mL
3M Resolving buffer	1.25 mL	1.25 mL	1.25 mL	1.25 mL
Acrylogel (40%)	2.5 mL	3.0 mL	3.25 mL	3.75 mL
Ammonium persulfate (APS)*	100 µL	100 µL	100 µL	100 µL
TEMED	10 µL	10 µL	10 µL	10 µL

**APS was made freshly by dissolving APS at 20 mg/mL in ddH_2O.*

**TEMEDis N,N,N',N'-Tetramethylethylenediamine.*

Table 2.10. Upper Stacking gel recipes (5%)

Ingredient	**Amounts**
ddH_2O	3.953 mL
2M Stacking buffer	3.12 µL
Acrylogel (40%)	625 µL
APS	100 µL
TEMED	10 µL

**ddH_2O means 18 MΩ/cm water*

2.2.3. Gel Staining

2.2.3.1. 0.05% Alcian Blue staining

The method was adapted from Min & Cowman (1986). The gel was washed with water and put into glass staining dishes with the 0.05% w/v Alcian Blue 8GX (Sigma) solution (approximately 50 mL of Alcian Blue staining solution required for each gel). The gel was incubated for 1 h at room temperature in a shaker. The gel was then washed with 2 to 3 times with water and the bands were documented before the gels were subjected to silver nitrate staining.

2.2.3.2. Silver nitrate staining

The method was adapted from Tsai and Frasch (1982). The samples and reference macromolecules were fixed in the gel after gel electrophoresis by treating the gel with 40% ethanol-5% acetic acid , in a glass staining dishes and placing it in a shaker for overnight. The gel was then treated with 0.7% (w/v) periodic acid in 40% ethanol-5% acetic acid (each v/v) for 30 min for oxidation. The gel was then transferred into a new staining dish and has been washed with 3 changes of 18 MΩ/cm water O (15 min/wash). After washing, the gel was stained with freshly prepared staining solution (Table 2.11). The gel was again washed with 3 changes of 18 MΩ/cm water (15 min/wash) and washed with freshly prepared developing solution (5 mg/mL citric acid was prepared then this stock diluted 1:100 and then 50 μL formaldehyde was added into the diluted citric acid solution). Several changes of developing solution heightened development. 10% (v/v) acetic acid for 1 to 5 min was used to stop the development and washed repeatedly with distilled water.

Table 2.11. Staining solution ingredients

Reagent	**Amount for 1 gel**	**Amount for 2 gels**
0.88 s.g. ammonia	0.352 mg (~400 µl)	0.704 mg (~800 µL)
100 mM NaOH	5.6 mL	11.2 mL
20% w/v Silver nitrate, added dropwise	1 mL	2 mL
18 MΩ/cm water	23 mL	46 mL
Final volume	30 mL	60 mL

2.2.3.3. Coomassie Blue staining

Bio-Safe™ Coomassie (Coomassie® G250, BIO-RAD) was used for Coomassie Blue staining and the protocol described is the manufacturer's instruction.

The gel was washed 3 times for 5 min (each time) in 200 mL of 18 MΩ/cm water for each gel. All water was then removed from the staining container and 50 mL Bio-Safe Coomassie Stain was added and shaken for 1 h. The staining bands generally appeared within 20 min and reached maximum intensity within 1 h. The gel was rinsed in 200 mL ddH_2O again and kept for storage in 18 MΩ/cm water.

2.2.3.4. Periodic acid-Schiff staining

Schiff's reagent Fuchsin-sulfite reagent (Sigma, S5133) was used for the Periodic acid-Schiff staining method, adapted from Segrest *et al.* (1972). Each gel was fixed in 40% ethanol-5% acetic acid (each v/v) overnight. 50 mL freshly prepared 0.7% (w/v) periodic acid in 5% (v/v) acetic acid was then used for the oxidizing reaction for 2 to 3 h. The reagents were then discarded and the gel was transferred to freshly prepared 0.2% (w/v) sodium metabisulphite in 5% acetic acid, which was discarded after 30 min. Another 50 mL of the same reagent was added and the gel incubated for 2 to 2.5 h. The gel was then transferred into Schiffs reagents (Sigma) for 12-18 h at room temperature. The Schiffs reagent was then discarded and the gel was rinsed with abundant water. The gel was then destained by several changes of 5% (v/v) acetic acid and also stored in 5% (v/v) acetic acid.

2.2.4. Western blotting

Macroamphiphiles were further analysed following electrophoretic transfer (Western blotting; Transblot apparatus, Bio-Rad; UK) onto nitrocellulose membranes (0.2 μm, BIORAD). After transfer, the membranes were incubated overnight with a blocking solution of 5% (w/v) skimmed milk in phosphate buffered saline containing 0.05% w/v Tween 80 (PBST). Blots were subsequently incubated for 2 h with primary antibody diluted in 5% (w/v) skimmed milk in PBST. After thorough washing with five change of PBST, the blots were incubated with secondary antibody diluted in 5% (w/v) skimmed milk (Marvel) in PBST. After thorough washing with five changes of PBST, the blots were developed with BCIP/NBT alkaline phosphatase substrate solution (Zymed, California, USA).

Table 2.12. List of primary and secondary antibiotic used in western blotting.

Primary Antibody	**Dilution**	**Secondary antibody**	**Dilution**
Polyclonal anti-LTA antibody, supplied by Professor Ken Knox (Institute of Dental Research, Sydney, Australia).	**1:5000**	Alkaline phosphatase-conjugated anti-human IgG (Dako A/S, Denmark)	**1:2000**
Monoclonal anti-LTA antibody BSYX-A110 (Walsh *et al.* 2004)	**1:2000**	Alkaline phosphatase-conjugated anti-human IgG (Dako A/S, Denmark)	**1:2000**
Polyclonal anti-LAM antibody, supplied by Colarado State University as part of NIH, NIAID Contract No. HHSN266200400091C, entitled "Tuberculosis Vaccine Testing and Research Materials"	**1:750**	Alkaline phosphatase-conjugated anti-rabbit IgG (Sigma)	**1:30000**
Monoclonal anti-LAM antibody, supplied by Colarado State University as part of NIH, NIAID Contract No. HHSN266200400091C, entitled "Tuberculosis Vaccine Testing and Research Materials,"	**1:20**	Alkaline phosphatase-conjugated anti-rabbit IgG (Sigma)	**1:30000**

2.2.5. Lectin blotting

Macroamphiphiles were further analysed by lectin blotting following electrophoretic transfer (Transblot apparatus, Bio-Rad; UK) onto nitrocellulose membranes (0.2 μm, BIORAD). After transfer, the membranes were incubated overnight with a blocking solution of 5% (w/v) skimmed milk in PBST. Blots were subsequently incubated for 2 h with Concavilin A-Biotin conjugate: 2 mg/mL Concavalin A-Biotin (Sigma, from *Canavalila ensiformis*, [Jack Bean], type IV), diluted 1:100 into PBST. To ensure lectin binding, $CaCl_2$ and $MnCl_2$ were added, each diluted 1:1000 from 100 mM stocks. After thorough washing with five change of PBST, the blots were incubated with Streptavidin-alkaline phosphatase (Sigma 'ExtraAvidin') conjugate diluted 1:70000 in PBST. After thorough washing with five changes of PBST, the blots were developed with BCIP/NBT alkaline phosphatase substrate solution (Zymed, California, USA).

2.2.6. Chemical composition analysis of macroamphiphiles

The chemical composition of a typical macroamphiphile consists of two parts, fatty acids (hydrophobic region) and a carbohydrate polymer (hydrophilic region). To analyse these regions, Gas Chromatography (GC) with a ATI UNICAM 610 series Gas Chromatograph were performed.

2.2.6.1. Fatty acid derivatisation for gas chromatography

The method was adapted from Komagata and Suzuki (1987). Fatty acids in the macroamphiphiles (typically 1-2 mg purified product) and lyophilised bacterial whole cells (ca. 30 mg) were analysed by GC following derivatisation to their fatty acid methyl esters (FAMEs) by acid catalysed methanolysis using 1 mL 1.5% (v/v) sulphuric acid in anhydrous methanol (16 h, 50°C). FAMEs were recovered by three extractions into 3 mL hexane. The pooled hexane phases (ca. 9 mL) were backwashed with an equal volume of water, removed to a clean glass tube and dried over anhydrous sodium sulphate. Finally, the pooled hexane phases were concentrated under nitrogen. Identification of major fatty acids was made by comparison of retention times with authentic FAME standards (Sigma Chemical Co) as shown in Figure 2.4.

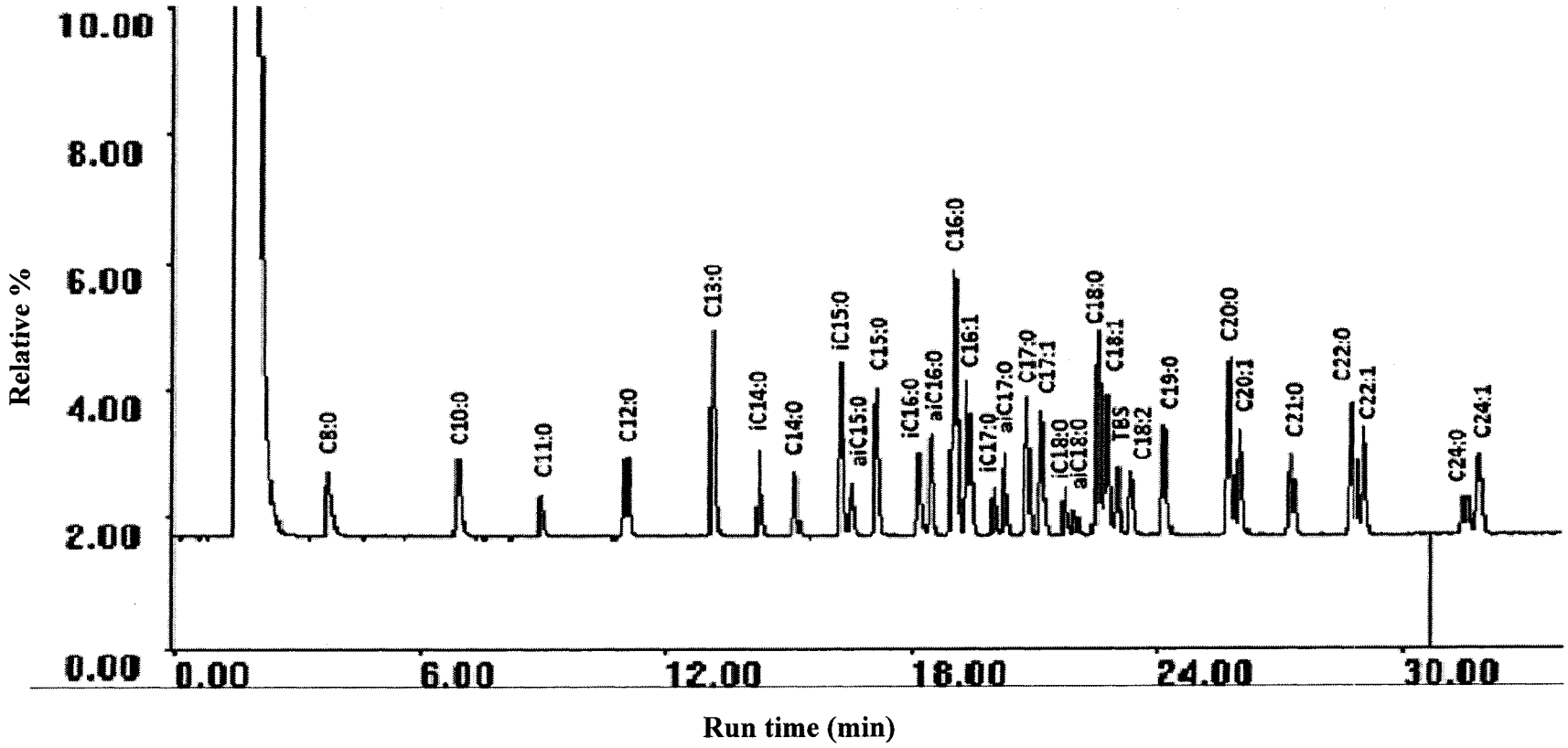

Figure 2.4. The GC profile for the analysis of 32 authentic fatty acid methyl ester standards.

Table 2.13. Fatty acids were analysed by GC of their methyl esters and identified by comparison with a mixture of 32 authentic standards (Sigma), the list of which is given below:

Designation	Systematic Name	Common name
C8:0	Octanoic acid	Caprylic
C10:0	Decanoic acid	Capric
C11:0	Undecanoic	-
C12:0	Dodecanoic acid	Lauric
C13:0	Tridecanoic	-
iC14:0	12-methyl tridecanoic	-
C14:0	Tetradecanoic acid	Myristic
iC15:0	13-methyl tetradecanoic acid	-
aiC15:0	12-methyl tetradecanoic	-
C15:0	Pentadecanoic	-
iC16:0	14-methylpentadecanoate	-
aiC16:0	13-methylpentadecanoate	-
C16:0	Hexadecanoic	Palmitic acid
C16:1	hexadec-9-enoic acid or 9-*cis*-Hexadecenoic acid	Palmitoleic
iC17:0	15-methyl hexadecanoate	-
aiC17:0	14-methyl hexadecanoate	-
C17:0	Heptadecanoic	Margaric
C17:1	Heptadecenoic	-
iC18:0	16-methyl heptadecanoic	-

Designation	Systematic Name	Common name
aiC18:0	15-methyl heptadecanoic	-
C18:0	Octadecanoic acid	Stearic
C18:1	cis-Δ9-octadecenoic acid	Oleic acid
TBS	10-methyl octadecanoic	Tuberculostearic
C18:2	*cis, cis*-9,12-octadecadienoic acid.	Linoleic acid
C19:0	Nonadecanoic	-
C20:0	Eicosanoic acid	Arachidic
C20:1	cis-9-eicosenoic	Gadoleic
C21:0	Heneicosanoic	-
C22:0	Docosanoic acid	Behenic
C22:1	*cis*-13-docosenoic	Erucic
C24:0	Tetracosanoic acid	Lignoceric
C24:1	*cis*-15-tetracosenoic	Nervonic

2.2.6.2. Carbohydrate or sugar determination by GC

For analysis of carbohydrate composition, samples (typically 1-2 mg of macroamphiphile) were acid hydrolysed with 2 M hydrochloric acid (2h, 120°C) in sealed glass ampoules. Hydrolysates were neutralised by drying *in vacuo* over sodium hydroxide pellets and the released carbohydrates were converted to their alditol acetate derivatives by the method of Saddler *et al.* (1991). Freeze dried hydrolysate were dissolved into 3M ammonium hydroxide (150 μL) and freshly prepared 10% (w/v) sodium borohydride at 37°C for 1 h, later neutralized by glacial acetic acid. The hydrolysate was then treated with 0.3 mL 1-methylimidazole and 2 mL acetic anhydride and incubated for 15 min at room temperature. Alditol acetate then added with 4 mL of 18 MΩ/cm water and 1 mL of dichloromethane and, after vigorous shaking and centrifugation on a low speed, the dichoromethane phase was recovered and removed to a clean glass tube and dried over anhydrous sodium sulphate. Finally, the pooled dichloromethane phase was concentrated under nitrogen. Identification of sugars was made by comparison of GC retention times with authentic alditol and sugar standards (Sigma Chemical Co., UK) derivatised by the same method. The standard carbohydrate are shown in Figure 2.5 and Table 2.14.

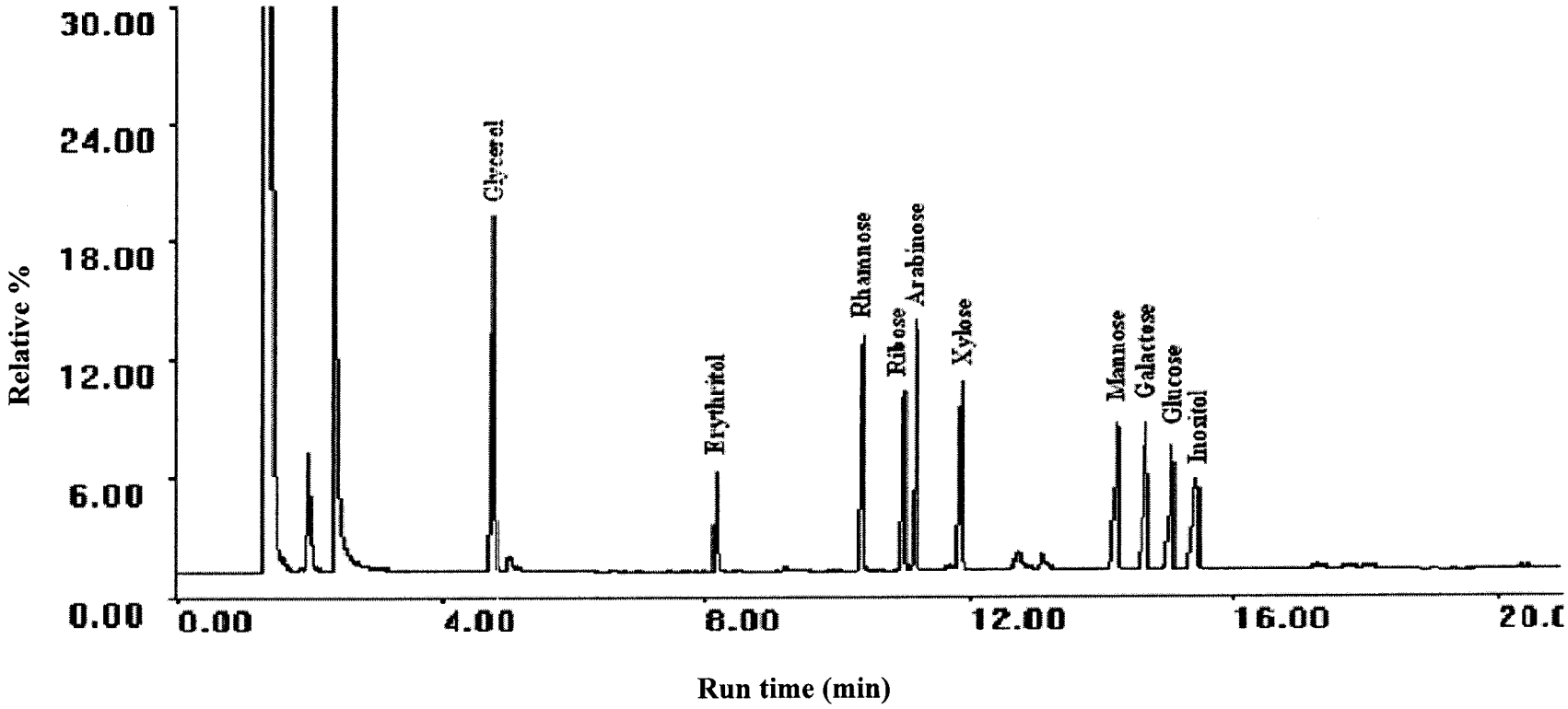

Figure 2.5. The GC analysis for their alditol acetate derivatives and identified by comparison with a mixture of 10 authentic standards (Sigma).

Table 2.14. Sugars were analysed by GC of their alditol acetate derivatives and identified by comparison with a mixture of 10 authentic standards (Sigma), which are given below in elution order:

Carbohydrate Name	**Chemical structure**
Glycerol	$CH_2(OH)\text{-}CH(OH)\text{-}CH_2(OH)$
Erythritol	$CH_2(OH)\text{-}CH(OH)\text{-}CH(OH)\text{-}CH(OH)\text{-}CH_2(OH)$
Rhamnose	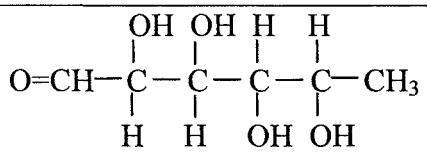
Ribose	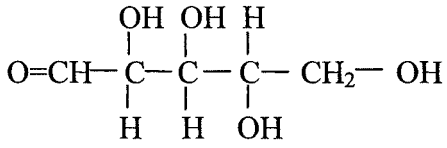
Arabinose	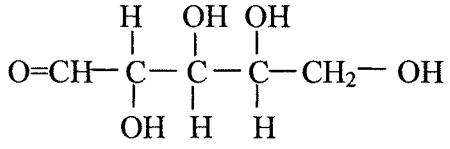
Xylose	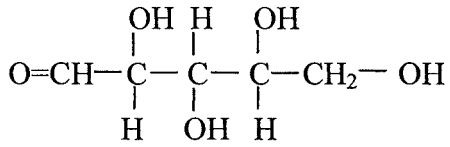
Mannose	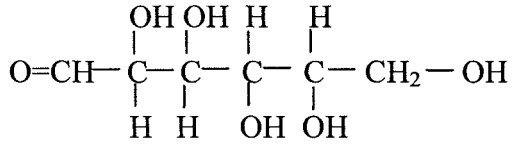
Galactose	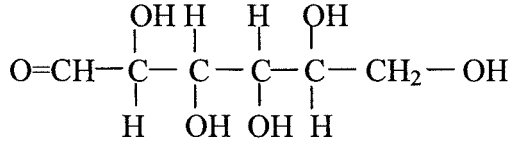
Glucose	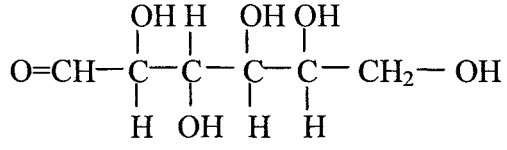
Inositol	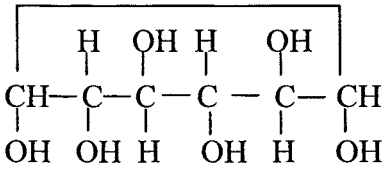

2.2.7. Structural analysis

2.2.7.1. MALDI-Mass spec.

Purified K. *radiotolerans* macroamphiphile (ca. 8 mg) was prepared and sent to Dr Jérôme Nigou (CNRS, Inst Pharmacol & Biol Struct, UPR 9062, F-31077 Toulouse, France) for MALDI/MS analysis. The matrix used was 2,5-dihydroxybenzoic acid at a concentration of 10 μg/μL, in a mixture of water/ethanol (1:1, v/v). 0.5 μL of lipoglycan, at a concentration of 10 μg/μL, was mixed with 0.5 μL of the matrix solution. Analyses were performed on Voyager DE-STR MALDI-TOF instrument (PerSeptive Biosystems, Framingham, MA) using linear mode detection. Mass spectra were recorded in the negative mode using a 300 ns time delay with a grid voltage of 80% of full accelerating voltage (20 kV) and a guide wire voltage of 0.15%. The mass spectra were mass assigned using external calibration.

2.2.7.2. Nuclear magnetic resonance (NMR)

Purified LTA from *T. fusca* (ca 8 mg) was sent to Dr Markus Pfitzenmaier (Philipps-Universität Marburg, Germany) where it was analysed by NMR using previously described methods (Henneke *et al.*, 2005), in collaboration with Siegfried Morath from the laboratory of Professor Thomas Hartung. NMR spectra were determined using a Bruker Avance 600 MHz spectrometer and standard acquisition software. Spectra were recorded at 300 K using 3-(trimethylsilyl) 3,3,2,2-tetradeuteropropionic acid Na salt (d_4-TSPA) as the shift reference (δ = 0.00 parts per million). Homonuclear assignments were taken from double-quantum filtered correlation spectroscopy (DQF-COSY), total correlation spectroscopy (TOCSY), rotating frame Overhauser enhancement spectroscopy (ROESY). ^{13}C assignments were based on heteronuclear multiple-quantum correlation (HMQC).

2.2.7.3. Two-dimensional gel analysis

This gel analysis involved two types of separation of the macromolecules represented by the two dimensions of the electrophoresis: 1) the first dimension involved separating the molecules based on their pI value (Iso-electric pH), 2) second dimension separates the molecules based on their molecular weights.

2.2.7.3.1. First Dimensional electrophoresis

2.2.7.3.1.1. Preparation of the sample

Freezed-dried purified sample of *T. fusca* LTA (Tfu-LTA) was re-suspended into 350 µL rehydration solution (urea 8M, CHAPS (3-[(3-Cholamidopropyl) dimethylammonio]-1-propanesulfonate) 2%) with 0.001 g Dithiothreitol (DTT), 3.5 µl Bromophenol Blue (1% w/v) and 7 µL IPG buffer (pH 3-10), for reswelling of immobline drystrip supplied by Amersham Bioscience, UK.

2.2.7.3.1.2. Rehydration of IPG strips

The reswelling tray was levelled on the table and the prepared samples were pipetted into each slot slowly and carefully, so that air bubbles were minimized. One Immobiline Drystrip gel (pH 3-10, 18 cm supplied by Amersham Bioscience, UK) with 3 mL Drystrip cover fluid was gently laid down to prevent evaporation. The reswelling tray was covered by a sliding lid. The gels were kept hydrating overnight at room temperature.

2.2.7.3.1.3. Running the first dimension

A Multiphor II apparatus (Amersham Bioscience, UK) was used for this. The cooling plate was levelled. Oil was poured over to cover the cooling plate. The plate with the anodic (red) electrode was placed at the top and large bubbles from underneath the plate were removed to connect anode (red) and cathode (black) electrode strip tray leads to the unit. 15 mL cover fluid was pipetted onto the Drystrip tray. The Drystrip aligner was placed (groove side up) on to the surface of the Drystrip tray. IEF electrode contact strips (11 cm) were cut from the main strip and each strip moistened with 0.5 mL ddH_2O. The IPG strip was removed from the reswelling tray and the rehydrated strips placed into wells of the Drysrip aligner, the strips were placed next to each other in the centre lanes of tray. The moistened electrode contact strips (Amersham Bioscience, UK) were placed across the cathodic and anodic ends of the strips. The electrodes were placed and pressed down on the top of electrodes strips. Oil was poured over the strip to cover the strip (100 mL), lid was placed on the unit and power supply was connected to the unit. The Multiphor II/EPS 3501 XL power supply was set on gradient mode with the current check option deselected. The voltage programme for first dimension isoelectric focusing is shown in Table 2.15. After running the first dimension the strips were stored at -70°C.

Table 2.15. The voltage progamme for first dimension isoelectric focusing for Immobline™ DryStrip pH3-10, 18 cm (GE healthcare, www. gehealthcare.com).

Step	Volt	mA	W	Time (h)	KVh
1	500	2	5	0:01	
2	3500	2	5	1:30	3
3	3500	2	5	4:50-6:20	17-22
Total				**6:20-7:50**	**20-25**

2.2.7.3.2. Second dimensional electrophoresis

Gels (20 x 20 cm) were cast using a discontinuous systems as follows:

2.2.7.3.2.1. 13% (w/v) Resolving gel

65 mL 18 MΩ/cm water, 37.5 mL resolving gel buffer (as described in Section 2.2.1), and 52.2 mL Acrylamide (40%, w/v), 750 µL APS (1%, w/v), 75 µL TEMED.

2.2.7.3.2.2. Stacking gel

19.2 mL 18 MΩ/cm water, 8 mL stacking gel buffer (described in Section 2.2.1), 2.95 mL Acrylamide (40%, w/v), 150 µL APS (1%, w/v), 30 µL TEMED.

2.2.7.3.2.3. Equilibration of IPG strips

Prior to the second dimension SDS-PAGE, the IPG strips were equilibrated for 15 min with gentle shaking in 10 mL equilibration solution containing 0.1 g DTT and after that again equilibrated for 15 min with 10 mL equilibration stock containing 0.45 g iodoacetamide (IAA). After equilibration, the IPG strips were aligned on one edge of a filter paper for 1 min to remove excess liquid, before they were applied to SDS-PAGE gels.

2.2.7.3.2.4. Preparation of agarose

20 mL of running buffer, 0.1 g agarose and 10 µL Bromophenol Blue were heated. The equilibrated strips were soaked by 18 MΩ/cm water then the strips were transferred immediately to the plates and covered by agarose solution. After, the agarose became solid one end of the gel was cut to allow the addition of the protein standards.

2.2.7.3.2.5. Run the second dimension

After attaching the plates to the electrophoresis unit and placing the lid on the top of the tank, the electrical leads were attached to suitable power supply. Power supply was turned on to begin the electrophoresis at 100-400 voltage, 80 mA for 2 gels and run for 5-6 h. After electrophoresis was complete, the gel was stained with Alcian Blue and Western blotted with monoclonal anti-LTA as described in section 2.2.2 and 2.2.3.1, respectively.

2.2.7.3.2.6. Scanning the gels

The gel was scanned by Scanner GS-710, the images were saved digitally and manually analyzed.

2.3. Other Microbiological methods

2.3.1. Gram-staining protocol

2.3.1.1. Preparation of a heat-fixed film

A microscope slide was cleaned and labelled with a glass etching pen. A small droplet of tap water was spread on the centre of the slide. The bacteria from a single colony was mixed with the droplet of water using a sterile wire loop and spreaded over the central part of the slide to produce a thin film. The film was then allowed to air-dry at room temperature. The film was fixed by passage through the Bunsen flame. The film was finally allowed to cool at room temperature.

2.3.1.2. The Gram staining procedure

A heat fixed film was flooded with methyl violet (30 to 40 sec). The film was then rinsed with tap water and then flooded with Gram's iodine (30 to 40 sec). Again the film rinsed with tap water, then decolourised with acetone (2-3 s). Immediately, the film was rinsed with tap water, under running tap again. Then the film was counterstained with Safranin (15-20 s) and rinsed with tap water and blotted dry with a paper towel and examined with or without a cover-slip, using the oil immersion (x 100) lens.

2.3.2. Storing bacteria in glycerol

Various microorganisms grown in broth cultures and stored frozen using 10-20% glycerol (v/v) as a cryoprotectant. 1.5 mL 'Nalgene' Cryoware vials were used as storage containers.

2.3.2.1 Preparation of glycerol stock (30% w/v)

A small amount of glycerol was weighed out in a small Duran flask. The required total volume was then calculated by the following equation:

30% volume needed mL = (weight in grams/30) X 100

The volume of the glycerol present was calculated from its density by the equation:

Volume mL = weight in grams / 1.26

The volume of the glycerol was subtracted from the total volume and this volume of distilled water added to the glycerol. The solution was finally mixed well and autoclaved.

2.3.2.2. Preparing bacterial stocks

Aseptically, 500 μL of sterile 30% (v/v) glycerol was added to a series of Nalgene tube and 500 μL of broth culture was then added to each of the tube, sealed firmly and labelled and stored at -20°C for medium-term or -80 °C for long-term storage.

2.4. Other biochemical analysis

2.4.1. Purification of Teichoic acid from bacterial cells

The method was adapted from the method of Archibald *et al.* (1968a,b). Approximately 500 mg of lyophilised cells was placed in a screw-capped glass tube. 10% (v/v) Trichloroacetic acid (TAA) was added to give a ca. 50 mg/mL cell suspension and kept at 4 °C for 48 h. The cell debris was spun down and the supernatant extract collected and freeze dried. The freeze dried supernatant is expected to contain the TA.

2.4.2. Protein assay

Bradford reagent (Sigma, B6916) was used for protein assay of the samples, notably to detect protein contamination.

96 Well Plate Assay Protocol (taken from the Sigma product information):

The assay was performed in 96 well plates. With this assay it was possible to quickly assay multiple protein samples, while using a small volume (5 μL).

Gently Bradford Reagent was mixed in the bottle and brought to room temperature. Protein standards were prepared in buffer ranging from 0.1-1.4 mg/mL using a Bovine Serum albumin (BSA) protein standard. 5 μL of the protein standards were added to separate wells in the 96 well plates. To the blank wells, 5 μL of 18 MΩ/cm water was added. The samples were prepared from the purified freeze-dried macroamphiphiles with an approximate protein concentration between 0.1-1.4 mg/mL. To each well being used, 250 μL of the

Bradford Reagent were added and mixed on a shaker for approximately 30 sec. The samples were incubated at room temperature for 5 to 45 min (the protein dye complex is stable for up to 60 min). The absorbance was measured at 595 nm within the 60 min. time limit. The net absorbance vs. the protein concentration was plotted for each standard. The protein concentration of the sample(s) was obtained by comparing the net A_{595} values against the standard curve determined.

2.4.3. Detection of protein on nitrocellulose membrane

Ponceau's solution (Sigma, P7170) were used to detect protein band on nitrocellulose membrane after Western blotting.

After finishing the protein transfer steps of Western blotting (Section 2.2.4), the nitrocellulose membrane was washed with water. Ponceau's solution (approximately 10 mL) was then added to the container so that the solution covered the membrane and the container was shaken for 5-10 min. The staining solution was discarded and the membrane washed with 18 MΩ/cm water, gently. Protein bands (e.g. molecular weight markers) appear on the membrane at this stage and can be marked with pencil. The staining was reversible and could be removed with further water washes. The nitrocellulose membrane was then used for further analysis by Western blotting.

2.5. Molecular biology techniques

2.5.1. 16S rDNA sequencing

For sequencing of 16S rDNA several stages required

1) DNA extraction
2) 16S rDNA gene amplification method
    i) Polymerase chain reaction (PCR)
    ii) Agarose Gel to identify amplified products
    iii) Purification of PCR product
3) Ligation into pGEM-T Easy plasmid.
4) Transformation
5) Sequencing

2.5.1.1. DNA extraction

A Qiagen Purification of Genomic DNA from Gram-Positive bacteria Kit was used. Bacterial cells were harvested (max. 2 x 10^9 cells) in a microcentrifuge tube by centrifuging for 10 min at 5000 x g. Supernatant was discarded (0.5 mL media). The bacterial cell pellet was resuspended in 180 µL enzymatic lysis buffer and incubated for at least 30 min at 37°C. 25 µL proteinase K and 200 µL of Buffer AL were added and the suspension incubated at 70°C for 30 min. 200 µL ethanol (96-100%, v/v) was added to the samples and mixed thoroughly by vortexing. The mixture was pipetted for into a DNeasy Mini spin column placed in the collection tube provided. The samples were centrifuged at ≥ 6000 x g for 1 min and flow-through discarded into the collection tube. The DNeasy Mini spin column was placed in a new 2 mL collection tube (provided) and 500 µL Buffer AW1 was added and centrifuged for 1 min at ≥ 6000 x g. Flow-through to the collection tube was discarded. The DNeasy Mini spin column was again placed in a 2 mL collection tube, 500 µL buffer AW2 was added and centrifuged for 3 min at 20,000 x g to dry the DNeasy membrane. Flow-through to the collection tube was discarded. The DNeasy Mini Spin column was placed in a clean 1.5 mL or 2 mL microcentrifuge tube and was 200 µL Buffer AE pipette directly onto the DNeasy membrane. The membrane was incubated at room temperature for 1 min, and then centrifuged for 1 min at ≥ 6000 x g to recover eluted DNA. The elution step was repeated once as described above.

2.5.1.2. 16S rDNA gene amplification method

2.5.1.2.1. Polymerase chain reaction (PCR)

Each PCR reaction contained the reagents shown in Table 2.16 and the conditions for the PCR are shown in Table 2.17. PCR was done in the presence of 1, 2, 3 and 4 mM $MgCl_2$. Primers S1: $^{5'}$AGAGTTTGATCCTGGCTCAG$^{3'}$ and S2: $^{5'}$GGCTACCTTGTTACGACTT$^{3'}$ were used to specifically amplify the near full length 16S rRNA gene sequence (Muyzer *et al.*, 1993).

Table 2.16. Ingredients for each PCR reaction.

Ingredients	**Final amount or concentration**
Taq Buffer (10X)	1 X concentration
dNTPs	0.2 mM
Primers (each)	0.5 μM
Sample/Genomic DNA	1 μg
Taq DNA polymerase	2.5 Unit

Table 2.17. Conditions of the PCR reaction

Steps	**Time**	**Temperature**	**Cycle**
Denaturation	3 min	95°C	
Denaturation	2 min	95°C	1 cycle
Primer annealing	1 min	35, 38, 42 and 46°C	35 cycles
Elongation	4 min	72°C	
Elongation	20min	72°C	1 cycle

2.5.1.2.2. Analysis of amplified DNA by agarose gel electrophoresis

1% (w/v) agarose and 1X TAE buffer (Table 2.18) were mixed and melted in a 600 W microwave oven for one min, on full power. The gel was cast in a agarose gel mini (35 mL) or midi (100 mL) gel electrophoresis tray. 15 µL well spacers were inserted into the molten agarose and the gel allowed to set. The samples were prepared in DNA loading buffer (Table 2.18) and loaded into the wells along with a lane containing READY-LOAD ™ λDNA *Hind III* Fragments used as DNA size standards. 150 mV was applied to the gels and the tracking dye was allowed to travel two-thirds of the way down the gel. The gel was stained by immersing it in Ethidium bromide (EtBr) solution for 5 min, with shaking at 50 x g. The gel was then viewed under UV light.

Table 2.18. Materials of Agarose gel electrophoresis

Ingredients	**Amount**
50 x TAE buffer	
Trizma base, pH 8.0	242 g
Glacial acetic acid	57.1 mL
EDTA (0.5M; pH8.0)	100 mL
Total volume (with 18 MΩ/cm water)	1000 mL
6 x DNA Loading Buffer (Solution is stored at 4°C)	
Bromophenol Blue	2.5% (w/v)
Sucrose	40% (w/v)
Agarose gel	
SeaKem LE agarose	1 g
1 x TAE buffer	100 mL

2.5.1.2.3. Purification of PCR products from PCR mixtures

A QIAquick® Spin PCR purification kit (Qiagen) was used. The microcentrifuge protocol was adapted from the QIAquick® Spin PCR book: 5 volumes of Buffer PBI was added to 1 volume of the PCR sample and mixed. The colour of the mixture was checked to be yellow (similar to Buffer PBI without the PCR sample). A QIAquick spin column was placed in a 2 mL collection tube provided with the kit. To bind DNA, the sample was applied to the QIAquick column and centrifuged for 30-60 sec. Flow-through was discarded. The QIAquick column was placed back into the same tube. To wash, 0.75 mL Buffer PE was added to the QIAquick column and centrifuged for 30-60 sec. Flow-through was discarded and the QIAquick column was placed back in the same tube. The column was centrifuged for an additional 1 min. The QIAquick column was placed in a clean 1.5 mL microcentrifuge tube. To elute DNA, 50 µL Buffer EB (10 mM Tris-HCl, pH 8.5) or water was added to the centre of the QIAquick membrane; the column was stood for 1 min and the column centrifuged for 1 min.

2.5.1.3. Ligation of DNA into plasmids

The pGEM®-T Easy Vector System (Promega) was used for the cloning of purified PCR products. The vector contains T7 and SP6 RNA polymerase promoters flanking a multiple cloning site (MCS) within the α-peptide coding region of the enzyme β-galactosidase. Therefore, the insertion can be determined by the colour screening of the indicator plates. The following method is taken from technical manual for the pGEM®-T and pGEM®-T Easy Vector systems. pGEM®-T Easy Vector and Control insert DNA tubes were briefly centrifuged to collect the contents at the bottom of the tubes. Ligation reactions were set up as Table 2.19. The reactions were mixed by pipetting and incubated overnight at 4 °C.

Table 2.19. Ligation reaction set up.

Reagents	**Standard reaction**	**Positive control**	**Background control**
2X Rapid ligation buffer, T4 DNA ligase	5 µL	5 µL	5 µL
pGEM®-T Easy Vector	1 µL	1 µL	1 µL
PCR Product	X* µL	-	-
Control insert DNA	-	2 µL	-
T4 DNA ligase (3 Weiss units/µl)	1 µL	1 µL	1 µL
18 MΩ/cm water of final volume of	10 µL	10 µL	10 µL

*Molar unit of PCR product required optimization:

{(ng of Vector x Kb size of DNA)/ Kb size of the vector} x insert : vector molar ratio

= ng of insert

Insert : vector molar ratio 1:3 to 3:1 provide good initial parameter.

pGEM®-T Easy Vectors are 3 Kb and are supplied at 50 ng/µL.

16S rRNA for microorganisms is 200 bp or 0.2 Kb.

PCR product = {(50 ng x 0.2 Kb)/3.0 Kb} x (3 x1) = 10 ng DNA.

The PCR product concentration was measure by the following equation:

Absorbance at 260 nm x 14 x 50 = Concentration of DNA (ng/ µL)

2.5.1.4. Protocol for transformation using the pGEM®-T Easy Vector ligation reaction products

JM109 High Efficiency Competent *E. coli* Cells (Cat.#L2001, Promega) were used for the transformation.

Two LB agar plates (Table 2.20) with ampicillin/IPTG/X-Gal supplements were prepared for each ligation reaction and two plates for determining the ligation efficiency. The plates were equilibrated to room temperature prior to plating. The tubes containing the ligation reactions were centrifuged to collect contents at the bottom of the tube. Another tube on ice was set with 0.1 ng uncut plasmid for determination of the transformation efficiency of the competent cells. A tube of frozen JM109 High Efficiency Competent *E. coli* cells was removed from storage and placed in an ice bath until just thawed (about 5 min). The cells were mixed by gently flicking the tube. Carefully, 50 µL of cells were transferred into each tube prepared above. Gently the tubes were flicked to mix and placed them on ice for 20 min. The cells were heat-shocked for 40-50 sec in a water bath at exactly 42 °C. Immediately the tubes were returned to ice for 2 min. 950 µL room temperature SOC medium (Table 2.20) was added to the tubes containing cells transformed with ligation reactions and 900 µL to the tube containing cells transformed with uncut plasmid. The tubes were incubated for 1.5 h at 37 °C with shaking (150 x g). 100 µL of each transformation culture was plated onto duplicate LB/ampicillin/IPTG/X-Gal plates (Table 2.20). For the transformation control, a 1:10 dilution with SOC medium was recommended for plating. For higher number of colonies, the cells were pelleted by centrifugation at 1000 x g for 10

min, and then resuspended in 200 µL SOC medium, and 100 µL was plated on each of two plates. The plates were incubated overnight (16-24 h) at 37 °C. Generally, white colonies are expected from cells that contained the inserts. 2-3 white colonies were inoculated onto ampicillin containing LB plates and the plates were incubated overnight (16-24 h) at 37°C. From these plates, 2-3 white colonies were inoculated into 250 mL LB media and incubated overnight (16-24 h) at 37 °C and 200 x g. The broth was subjected to plasmid extraction and used to make glycerol stocks.

Table 2.20. Materials for transformation using the pGEM®-T Easy Vector ligation reaction products

Ingredients	**Amount**
Isopropyl β-D-1-thiogalactopyranoside (IPTG) stock solution (0.1 M), filter sterilize and stored at 4°C	
IPTG	1.2 g
ddH_2O	50 mL (final volume)
X-Gal (2 mL), stock covered with aluminum foil and stored at -20 °C	
5-bromo-4-chloro-3-indolyl-β-D-galactoside	100 mg
N,N′-dimethyl formamide	2 mL
Luria-Bertani (LB) medium (per Litre)	
Tryptone	10 g
Yeast extract	5 g
NaCl	5 g
ddH_2O	800 mL
pH adjusted to pH 7.0 with NaOH and the final volume was made 1 Litre by adding ddH_2O.	
LB plates with ampicillin/IPTG/X-Gal	
Agar	15 g
LB medium	15 mL
Ampicillin	100 µg/mL
IPTG	0.5 mM
X-Gal	80 µg/mL
Ampicillin was added after the autoclaved of the Agar and LB medium cool down to 50 °C; and IPTG and X-Gal was added after the plates were poured.	
SOC medium (100 mL)	
Tryptone	2 g
Yeast-extract	0.5 g
NaCl (1M)	1 mL
KCl (1 M)	0.25 mL
Mg^{2+} (sterilized 2M)	1 mL
Glucose (sterilized 2M)	1 mL
18 MΩ/cm water	100 mL (Final volume)

2.5.1.5. Plasmid DNA purification using QIAprep Spin Miniprep Kit and a microcentrifuge tube

The process purified up to 20 μg of high-copy plasmid DNA from 1-5 mL overnight cultures of *E. coli* in LB medium. The protocol was taken from the QIAprep® Miniprep Handbook (second edition, Qiagen). A single colony was picked from a freshly streaked selective plate and used to inoculate a culture of 1-5 ml LB medium containing the appropriate antibiotic (ampicillin). The culture was incubated for 12-16 h at 37 °C with vigorous shaking. The bacterial cells were harvested by centrifugation at 6000 x g in a conventional, table-top micorcentrifuge for 3 min at room temperature. The pelleted bacterial cells were resuspended in 250 μL Buffer P1 (Qiagen) and transferred to a microcentrifuge tube. 250 μL Buffer P2 (Qiagen) was added and mixed thoroughly by inverting the tube 4-6 times. 350 μl Buffer N3 (Qiagen) was added and mixed immediately and thoroughly by inverting the tube 4-6 times. The tube was centrifuged for 10 min at 10000 x g. The supernatants from this step were applied to a QIAprep spin column by decanting or pippeting. The column was centrifuged for 30-60 sec. The flow-through was discarded. The QIAprep spin column was washed by adding 0.5 mL Buffer PB and centrifuging for 30-60 sec. The flow-through was discarded and the column centrifuged for an additional 1 min to remove residual wash buffer. The QIAprep column was placed in a clean 1.5 mL microcentrifuge tube. To elute DNA, 50 μL Buffer EB (Qiagen) or water was added to the centre of each QIAprep spin column, the column was kept standing for 1 min and then centrifuged for 1 min. The DNA eluted was retained and its concentration was

measured by measuring the absorbance at 260 nm (A_{260}) by Heλios α, Spectronic Unicam, using the following equations:

Concentration of DNA sample= 50 µg/mL X A_{260} X Dilution factor

The liquid was evaporated using CHRiST RVC 2-18 centrifuge evaporator and the dried DNA was sent to Lark Technologies, Inc., Comprehensive Pharmacogenomics & Molecular Services(tm), Hope End, UK., for sequencing.

2.6. Bioinformatics Analysis

2.6.1. Preliminary bioinformatics

Protein sequences were obtained from UniProt ExPASY (expert protein analysis system), a protein identification and characterisation tool (www. Expasy.org). The rRNA gene sequences were taken from National Centre for Biotechnology Information, GenBank (NCBI, http://www.ncbi.nlm.nih.gov/) and the Ribosomal Database Project-II (RDP-II, http://rdp.cme.msu.edu/).

2.6.2. Alignment of sequences

All alignments were performed using ClustalW software from www.ebi.ac.uk/Tools/clustalw. Multiple sequences were entered and the alignment runs. The alignment was used for the phylogenetic tree construction.

2.6.3. BLAST Analysis

To identify possible similar homologues proteins or similar sequences to genes, BLAST searches were performed. DNA blasts (BLASTN) were used when searching for similar gene sequences and protein blasts (BLASTP) were used when looking for protein homologues. Both were used from the NCBI server (http://www.ncbi.nlm.nih.gov/blast/Blast.cgi).

2.6.4. Phylogenetic tree construction

MEGA3: Integrated software for molecular evolutionary genetic sequence analysis and sequence alignment (Kumar *et al.*, 2003, *et al.*, 2004) was used for drawing phylogenetic trees.

2.7. Reference LTA of *Streptococcus agalactiae* A909 (GBS) purification

The GBS-LTA used as an reference LTA in the present study which obatained by phenol-extraction (described in Section 2.1.5.1) and the macroamphiphile purified by HIC column (described in Section 2.1.6.1). The HIC profiles are shown in Appendix I.

CHAPTER 3

Investigation of macroamphiphiles in *Thermobifida fusca*

3.1. Classification

Thermobifida fusca was first isolated from composted horse manure by Henssen in 1957 and classified in the genus *Thermomonospora* as *Thermomonospora fusca.* At that time this genus comprised thermophilic aerobic actinomycete strains, which were characterized on the basis of formation of single spores on aerial mycelium (Henssen, 1957). In 1973, Cross and Goodfellow moved this organism, along with *Thermomonospora alba* to the new genus *Thermobifida* (Cross and Goodfellow, 1973, McCarthy and Cross, 1984). Recently the genus *Thermobifida* has been reclassified in the family *Nocardiopsaceae,* within the suborder of Actinobacteria, on the basis of 16S rRNA gene sequenced-based phylogenetic, chemotaxonomic and phenotypic characteristics (Zhang *et al.*, 1998). The genera, has three members following the addition of a new species, *Thermobifida cellulytica* (Kukolya *et al.*, 2002). Presently the classification of *Thermobifida fusca* is as follows:

Phylum: Actinobacteria

Order: *Actinomycetales*

Suborder: *Streptosporanginae*

Family: *Nocardiopsaceae*

Genus: *Thermobifida*

Species: *Thermobifida fusca*

3.2. Morphological characteristics

The primary phenotypic characteristics of the genus *Thermobifida* are Gram-positive, non acid-fast, chemo-organotrophic and aerobic organisms that form an extensively branched substrate mycelium. They produce single, smooth surface, oval to round (0.5-2.0 μm in diameter), heat-sensitive spores (aleuriospores) on aerial hyphae alone, or both aerial and substrate hyphae (Kukolya *et al.*, 2002).

The filamentous soil bacterium *T. fusca* is a typical thermophilic actinomycete with an optimal growth temperature of 50-55°C (Crawford, 1975) with a pH range for growth of 7-9 (Zhang *et al.*, 1998) and with the ability to use simple sugars and carboxylic acids as carbon sources (http://genome.jgi-psf.org/draft microbes/thfu/thefu.home.html), as a consequence of *T. fusca* using chemo-organotrophic and aerobic metabolism (Zhang *et al.*, 1998, Lykidis *et al.*, 2007). In using carbohydrates for carbon and energy metabolism, rather than peptides and proteins, *T. fusca* is considered a typical cell wall degrading organisms (Crawford, 1975).

T. fusca belongs to the microflora of organic materials, which produces many kinds of hydrolytic enzymes that degrade cellulose and other plant cell wall polymers such as compost heaps, rotting hay, manure piles or mushroom growth medium (Bachmann and Mccarthy, 1991, Zhou *et al.*, 2004). Characterized cellulases from *T. fusca* include three endocellulases (Cel9B, Cel6A and Cel5A), two exocellulases (Cel6Band Cel48A), and an unusual

cellulases (Cel9A) have been studied extensively because of their thermostability, broad pH range (4-10) and high activity (Zhou *et al.*, 2004).

Generally the organism takes 3-4 days to develop colonies on Tryptone-Yeast extract-Glucose (TYG) or Brain Heart Infusion (BHI) agar plates, at 55°C and sporulation occurs after about 3 days, as the evidenced by the appearance of an abundant white aerial mycelium (Crawford, 1975). The colonies are thin and transparent and sporulation occurs only at the edge of the colonies. Although the culture does not produce any diffusible pigments on the agar media, there is evidence of production of soluble pigment while growing in liquid media containing yeast extract, as the broth is converted from slightly yellowish to golden brown as a result of growth of *T. fusca* (Crawford, 1975).

3.3. Chemotaxonomic characteristics

Thermobifida alba and *T. fusca* were placed in the new genus *Thermobifida* for their unique chemotaxonomic characteristics. Their cell walls contain meso-diaminopimelic acid as the murein diamino acid and no characteristic sugar was detected, which are the characteristics of cell wall type III and sugar pattern type C (Kukolya *et al.*, 2002). The genus menaquinone type is 4D: the major isoprenoid quinonones were octa- and hexahydrogenated menaquinones with 10 isoprenoid units [MK-10(H_8), MK-10(H_6)] (Zhang *et al.*, 1998, Kukolya *et al.*, 2002). Substantial amounts of MK-11(H_6) and MK-11(H_8) were recorded in *T. fusca,* besides the dominant menaquinones (Kroppenstedt and Goodfellow, 1992).

All strains of the genera *Thermobifida* have been identified with phosphatidylethanolamine and glycolipid as the major lipids with some unidentified phospholipids, which are the characteristics of phospholipid type-II pattern polar lipid containing organisms (Lechevalier *et al.*, 1981, Zhang *et al.*, 1998). However, studies by Henssen (1957), McCarthy & Cross (1984), Kroppenstedt *et al.* (1990) and Kudo (1997) suggest that the genus *Thermobifida* contains phospholipid type I (PIM, PI, PtdG and DAG). The fatty acid pattern type 3e (iC15:0 and aiC17:0, 30%) was characterised in *T. fusca*, with the absence of mycolic acids (Kukolya *et al.*, 2002).

Two types of teichoic acids have been identified in *T. fusca* from chemical analysis and NMR studies: unsubstituted 1,3-poly(GroP) and β-glucosylated 1,3-poly(GroP) (Potekhina *et al.*, 2003).

3.4. Physiology and Genomic characteristics

The Joint Genome Institute has sequenced the complete genome of *T. fusca* which is deposited in GenBank with the accession number, CP000088. The genome consists of a single circular chromosome with 3,642,249 bp, 67.5% G+C and 3,117 predicted coding sequences (CDS) (Lykidis *et al.*, 2007). The organisms genome contain 413 unique genes compared to 32 other Actinobacteria genomes, out of which 83 are CDSs and rest of them are hypothetical proteins with no functions that have been identified. The comparison between genomes of Actinobacteria shows the *T. fusca* is closely related to *Streptomyces coelicolor* and *Nocardia farcinica* (Lykidis *et al.*, 2007). The comparative genomics also found that two of the three subunits of exonuclease V are notably absent in these mycelial Actinobacteria: streptomycetes, Frankia and *T. fusca*, which are seems to be present in other actinobacteria (Ventura *et al.*, 2007). The genome analysis of *T. fusca* showed the ability to utilizie a similar fatty acid synthesis system as in *Streptomyces*. Moreover, the organism has all the genes for biosynthesis of phophatidylglycerol, phosphatidylserine, phosphatidylethanolamine and PI. Also, a phosphatidylinositol mannosyltransferase homolog (Tfu2101) has been identified which suggest the organism has the ability to synthesize apolar PIMs which agree with the chapter 8 genome analysis, Table 8.4 and also consistent with the previous studies (Lykidis *et al.*, 2007). The genome analysis also shows the presence of a cardiolipin synthase (Tfu2817) gene (Lykidis *et al.*, 2007).

3.5. The significance of studying *T. fusca*'s macroamphiphiles

Studying the cell membranes of thermophiles is an interesting and significant aspect of microbiology, especially regarding the mechanisms for their adaptation to high temperatures. Previously, *T. fusca* has been mainly studied for the presence of cell wall degrading enzymes but very few studies have been done with the cell envelope of this or other thermophilic actinomycetes.

The production of spores, which may be allergenic and associated with a condition called farmers lung (especially for mushroom workers) has also made the study of the *T. fusca* cell envelope medically significant (Vandenbogart *et al.*, 1993).

This organism is interesting from the point of view of its macroamphiphiles since this is the first actinomycete thermophile which has been studied in this regard. Moreover, the presence of cell wall teichoic acid is intriguing, since this is typically present as the SCWP in those Firmicutes (low G+C Gram positive) which also synthesise LTA as a macroamphiphile. This makes this high G+C Gram-positive organism an interesting subject for studying the distribution of macroamphiphiles throughout the phylum Actinobacteria.

Moreover, *T. fusca* is closely related to the *S. coelicolor* (Chater and Chandra, 2006, Lykidis *et al.*, 2007), which is another organism from the phylum Actinobacteria under investigation in this project. The study of the macroamphiphile in *T. fusca* will help us not only to understand the distribution of macroamphiphiles, but also to understand the function of the

macroamphiphiles by comparing the membrane structure of closely related genera.

3.6. Results

3.6.1. Organism and culture conditions

The type strain of *T. fusca*, YX was kindly provided by David Wilson and Diane Irwin (Cornell University, New York). *T. fusca* failed to grow on non-defined media such as tryptone-yeast-glucose based (TYG), yeast extract-malt extract (YEME) or GYM *Streptomyces* medium (medium 65; DSMZ, 2004). The bacteria were successfully grown in semi-defined liquid Hagerdahl medium (see section 2.1.2.1) containing 0.5% (w/v) cellobiose or glucose (as carbon source) at 50°C with shaking (100 xg). The yield of harvested cells was typically 0.7 g and 0.5 g dry cells per L when using glucose and cellobiose as carbon source in Hagerdahl media, respectively.

Time scale experiments has showed that after 16 h the organism grew as small white cotton-like clumps (puffballs) within the clear medium, but the colour of the medium changed to slightly yellow with spreading of the clumps after 24 h. The colour of the medium intensified with more dispersed or floating cells and spore like-objects appeared after 48 h. When the cells were grown for more than two days, sedimentation of the cells increased and also the intensity of the colour change was more apparent in glucose-containing media than that with cellobiose as carbon source.

Gram staining of the cells was observed at 100x magnification under an oil immersion lens as shown in the Figure 3.1. The observation of purple-stained hair like structures confirmed that the bacterium is a filamentous Gram positive organism.

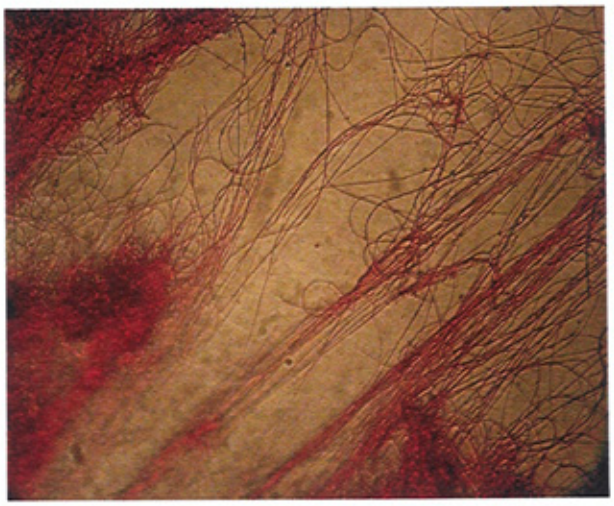

Figure 3.1. Gram staining of *T. fusca* showing hair-like filaments, taken at 100X magnification under oil immersion lens.

3.6.2. Purification of the *T. fusca* macroamphiphiles

Macroamphiphilic material was extracted from *T. fusca* in two ways, the standard hot phenol-water extraction method (described in Chapter 2, section 2.1.5.1) and a recently described butanol extraction method (described in Chapter 2, section 2.1.5.2). In both cases, the extracted macroamphiphile was purified by HIC-FPLC (Chapter 2, section 2.1.6.1). The column fractions from the HIC were subjected to carbohydrate and phosphate assay (methodology described in Chapter 2, sections 2.1.7.1 & 2.1.7.2, respectively), as shown in Figure 3.2 and Figure.3.3 for FPLC runs 3 and 4, respectively. Hydrophilic contaminants (nucleic acids and polysaccharides) not retained by the HIC column were recovered during the elution with equilibration buffer as peak 1. Subsequent gradient elution with an increasing concentration of propanol recovered a single major macromphiphilic carbohydrate and phosphate containing peak (Peak 2, Figure 3.2 and 3.3). In both cases, the material in peak 2 contained a significant amount of phosphate compared to carbohydrate. The HIC profile of the cells when cellobiose was used as carbon source in the growth medium gave a similar pattern shown in Figure II.2 and II.6 (Appendix II). The other FPLC runs are also shown in Appendix II.

Dot-immunoblotting (method described in Chapter 2, section 2.1.7.3) with a monoclonal anti-LTA antibody (Table 2.12) reacted positively across the peak 2 as shown in Figure 3.4.

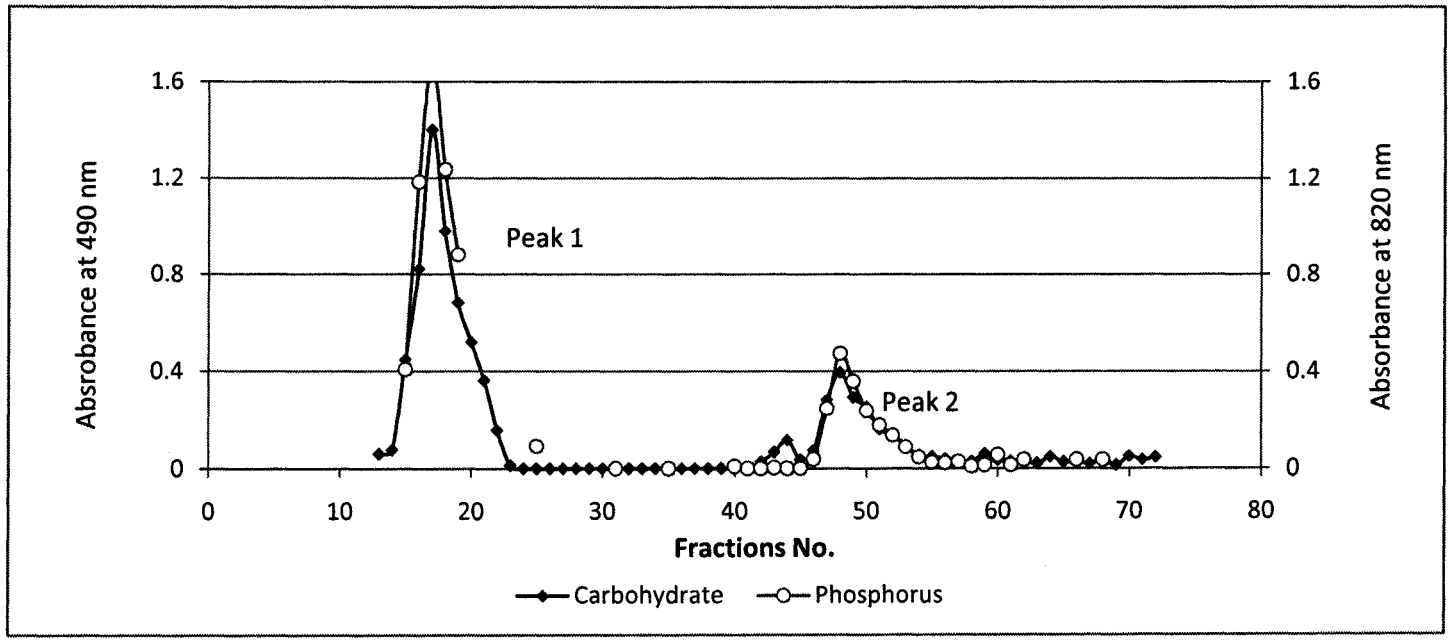

Figure 3.2. Representative HIC profile for the purification of a crude phenol extract (FPLC run 3) from *T. fusca*. The crude extract was loaded to the column with equilibration buffer until fraction 12, after which gradient elution with an increasing concentration of propanol was begun. Column fractions (4 mL) were analyzed for carbohydrate and phosphorus and by dot immunoblotting.

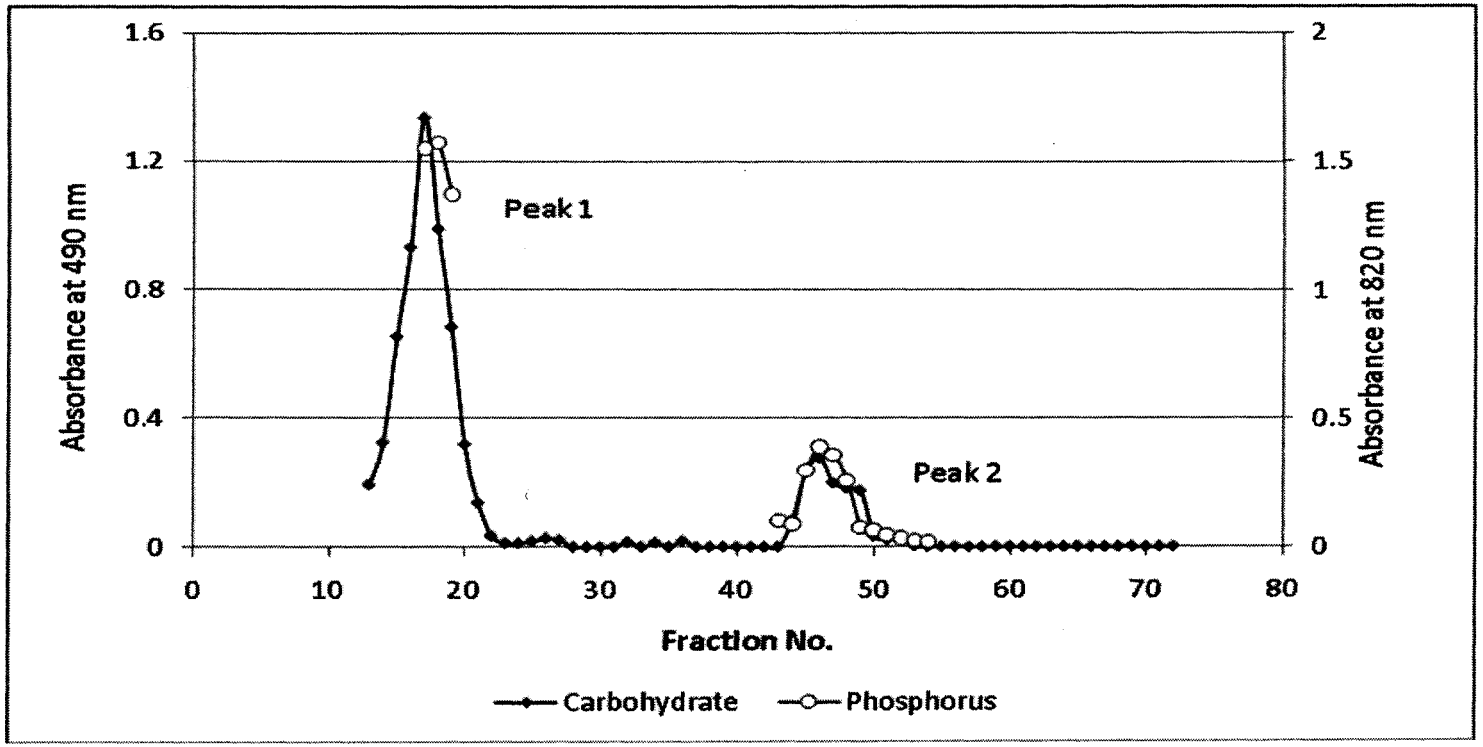

Figure 3.3. HIC profile for the purification of a crude butanol extract (FPLC run 4) from *T. fusca*. The crude extract was loaded to the column with equilibration buffer until fraction 12, after which gradient elution with an increasing concentration of propanol was begun. Column fractions (4 mL) were analyzed for carbohydrate and phosphorus.

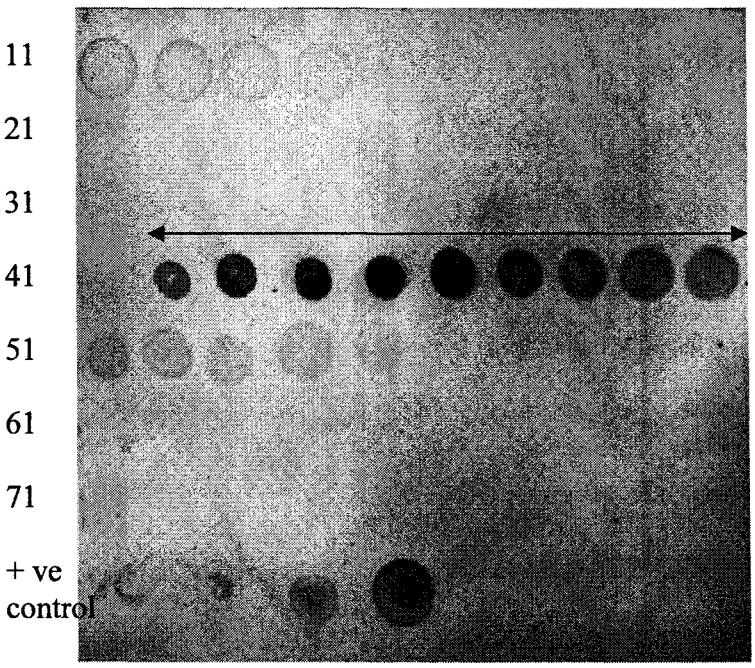

Figure 3.4. Dot immunoblotting with monoclonal anti-LTA. The number at the left hand side represents the fraction number. Fractions 42-50 (◄⟶►), which correspond to peak-2 of Figure 3.2, show a clear positive reaction with the monoclonal anti-LTA. Positive control spots are serial 10-fold dilutions of an approximately 1 mg/mL LTA preparation from *Streptococcus sanguis* (Sigma).

Peak-2 fractions were recovered by freeze-drying after extensive dialysis and represented 0.15% of the dry cell weight when using the hot phenol-water extraction method and cells grown with glucose as carbon source in Hagerdahl medium. For the butanol extraction method approximately 9.5 g of wet weight cell was used, which represent approximately 1 g of dry cells (assumed to be 10% , w/v, of wet cells) and following purification by HIC, approximately 4 mg of crude butanol extract has been obtained, which represent approximately 0.4% (w/w) of the cell weight. However, when using cellobiose as a carbon source for growth in Hagerdahl medium, the amount of phenol-water extracted HIC-purified material decreased to 0.02% (w/w).

3.6.3. Chemical composition of the macroamphiphiles

Chemical analysis indicated a carbohydrate : phosphorus ratio of at least 1:3 for the *T. fusca* macroamphiphile. Phosphate in the HIC purified macroamphiphile was estimated using the method of Chen *et. al.* (1956) and carbohydrate assayed by the method of Rao & Pattabiraman (1989), a scaled down method for use of Eppendorf tube, as described in Chapter 2, Section 2.1.7.1, respectively. Protein contamination was assayed using a commercial kit (Chapter 2, section 2.4.2), and determined to be below the level of detection.

Fatty acid composition of the whole cells and macroamphiphile of *T. fusca* was determined by FAME derivatisation and GC analysis (described in Chapter 2, Section 2.2.6.1), and is summarised in Table 3.1 and Figures 3.5 to 3.8. The major fatty acids detected in the whole bacterial cells (using glucose or cellobiose as carbon source in the media) were iC16:0 and aiC17:0 (Figure 3.5, Table 3.1). Fatty acid profiles were obtained for the macroamphiphiles, with only iC16:0 and trace amounts of the other fatty acids present in the whole bacterial cells of *T. fusca* (Figure 3.6, 3.7, Table 3.1). The butanol extracted macroamphiphile showed, in addition to the major fatty acid iC16:0, possibly a 13-methyl branched fatty acid, C16:0 and iC18:0 and traces amount of the other fatty acids also found in whole bacterial cells (Figure 3.8, Table 3.1).

The sugar composition of the macroamphiphile was determined following acid hydrolysis to release monosaccharide components and derivatisation to alditol acetates for GC, as described in Chapter 2, section 2.2.6.2. As shown in Figure

3.9 and Table 3.2, the macroamphiphile was predominantly glycerol and glucose in nature, in all the cases, whether cellobiose or glucose was used as carbon source for the growth, or whether material was extracted by butanol or the phenol-water extraction methods.

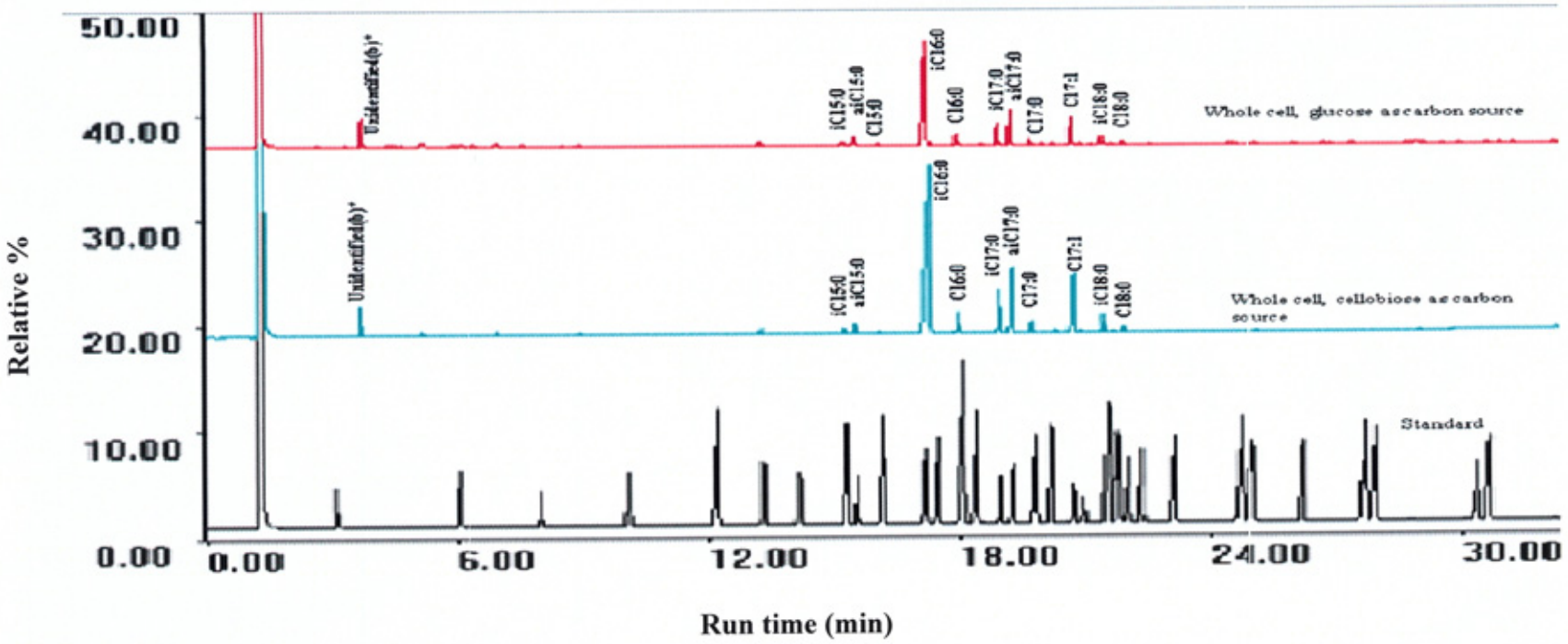

Figure 3.5. FAME analysis results for whole cells of *T. fusca* grown in glucose or cellobiose as carbon sources. The labelling of the standard fatty acids has been shown in Chapter 2, Figure 2.4.

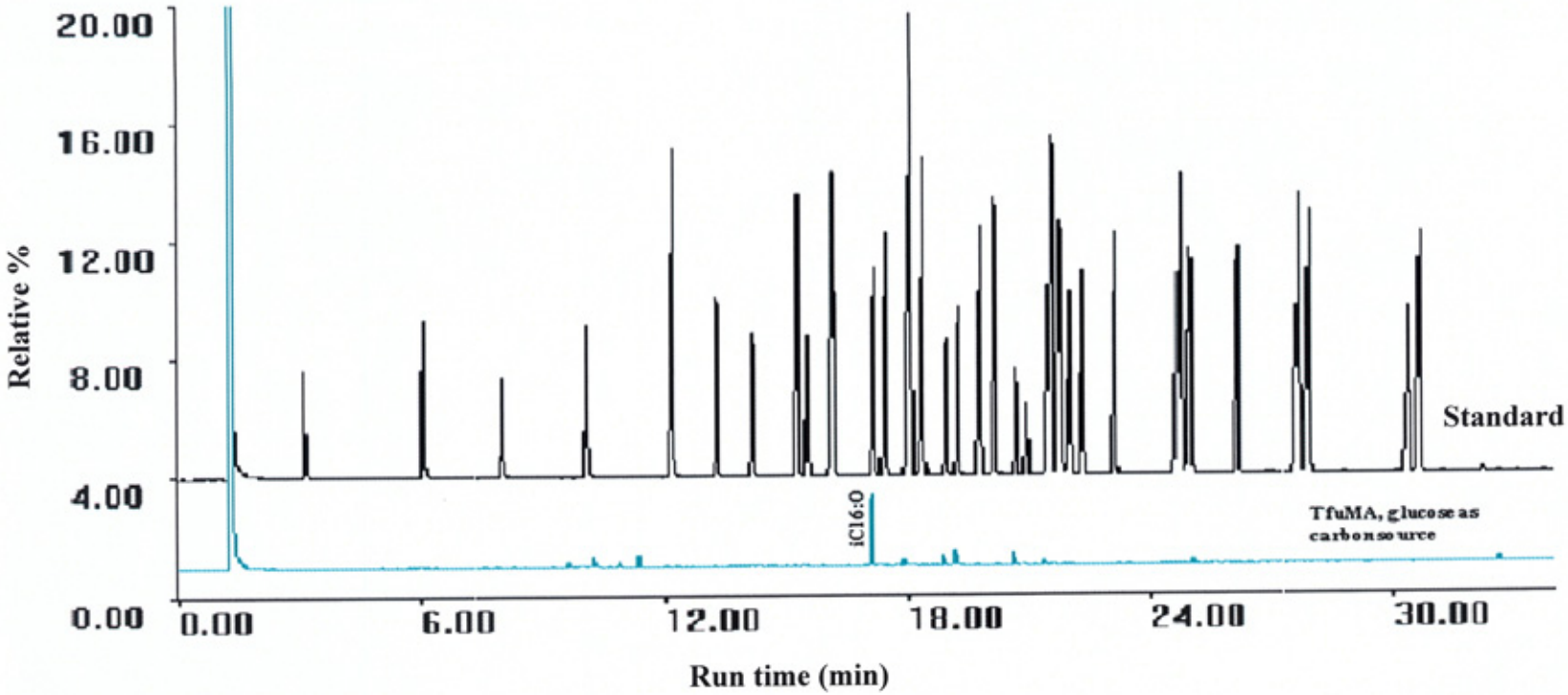

Figure 3.6. FAME analysis results for macroamphiphile (TfuLTA) of *T. fusca* grown with glucose as carbon source and extracted using the phenol-water method. The labelling of the standard fatty acids has been shown in Chapter 2, Figure 2.4

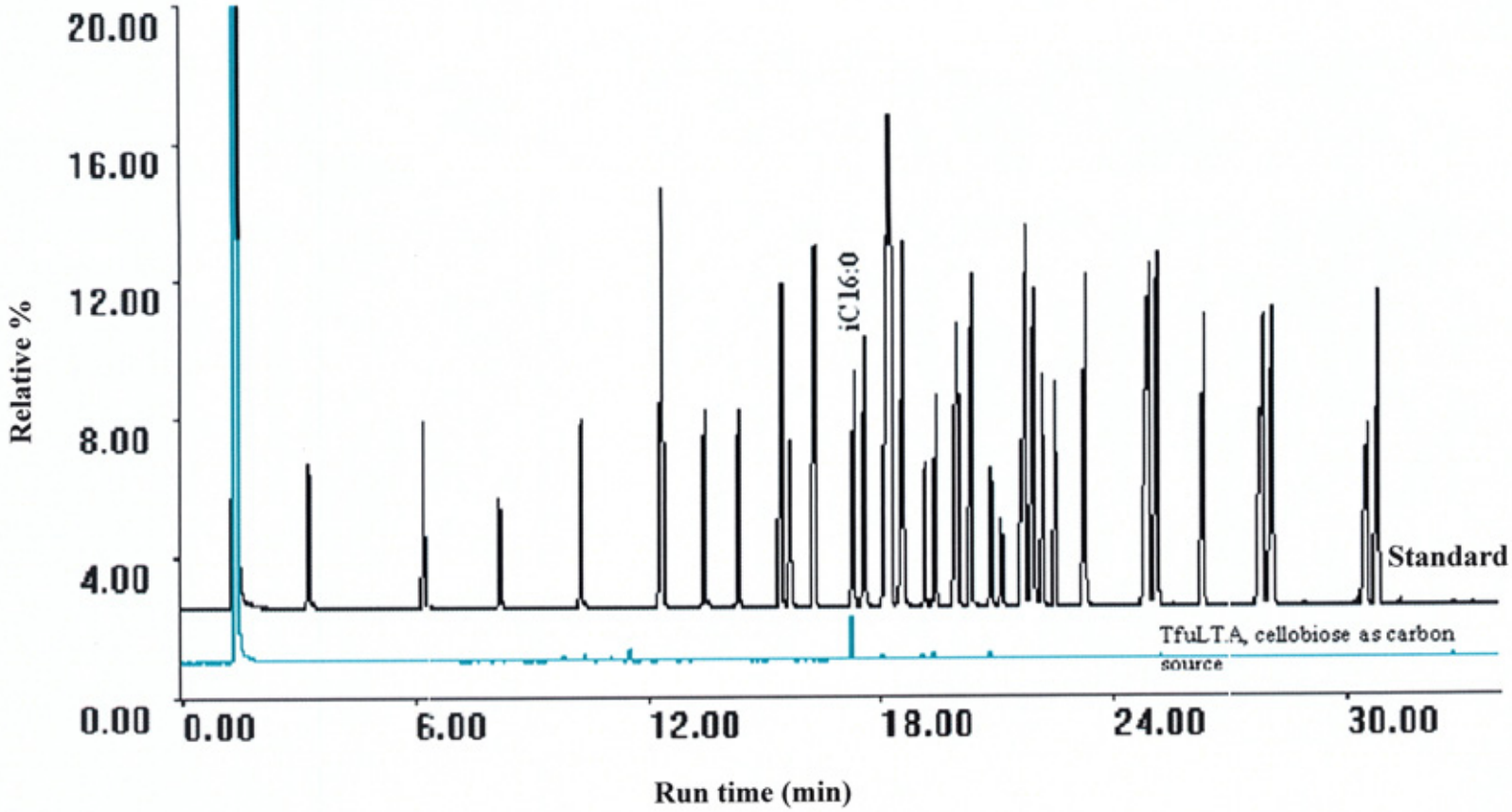

Figure 3.7. FAME analysis results for macroamphiphile (TfuLTA) of *T. fusca* grown on cellobiose as carbon source and extracted using the phenol-water method. The labelling of the standard fatty acids has been shown in Chapter 2, Figure 2.4

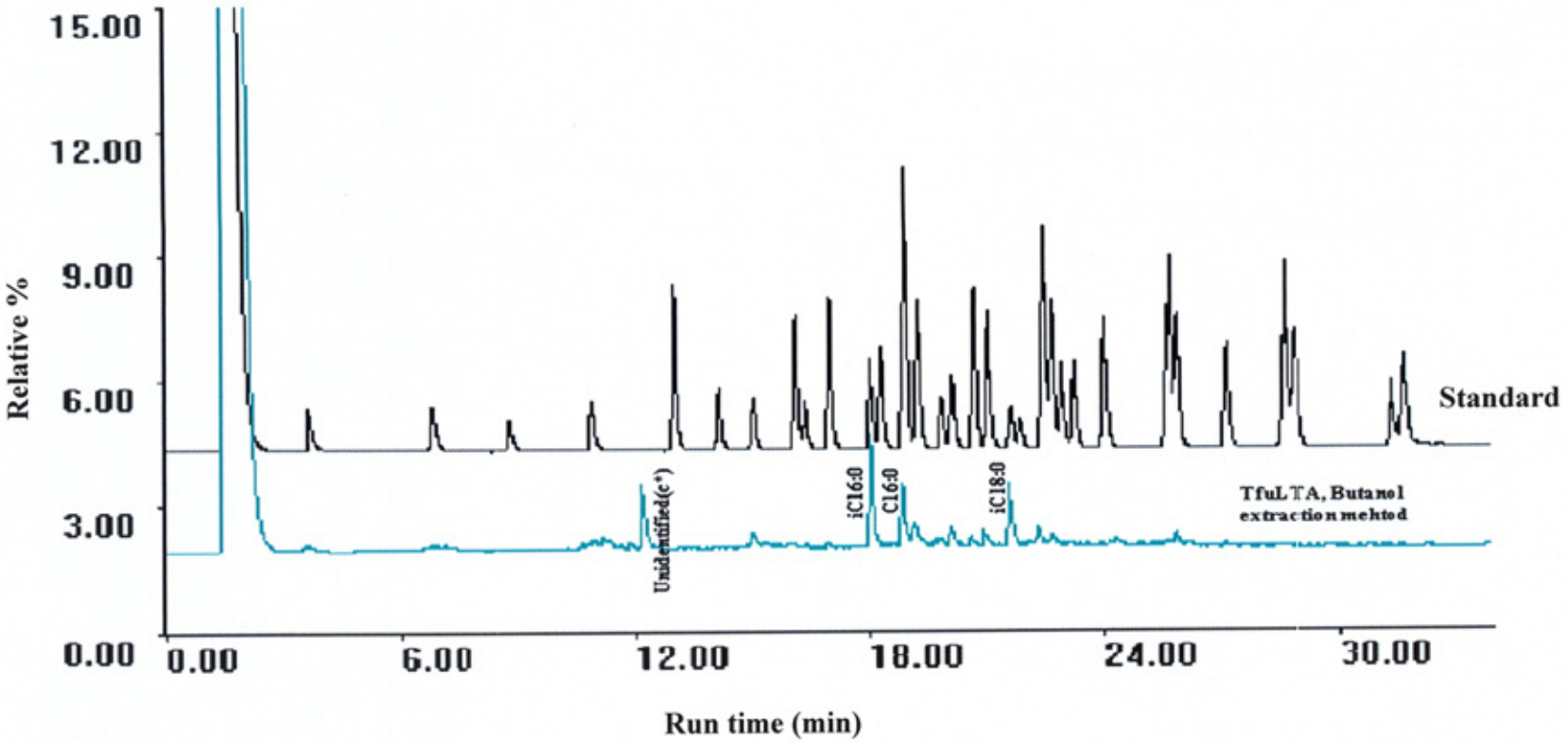

Figure 3.8. FAME analysis results for macroamphiphile (TfuLTA) of *T. fusca* grown on cellobiose as carbon source and extracted using the butanol extraction method. The labelling of the standard fatty acids has been shown in Chapter 2, Figure 2.4

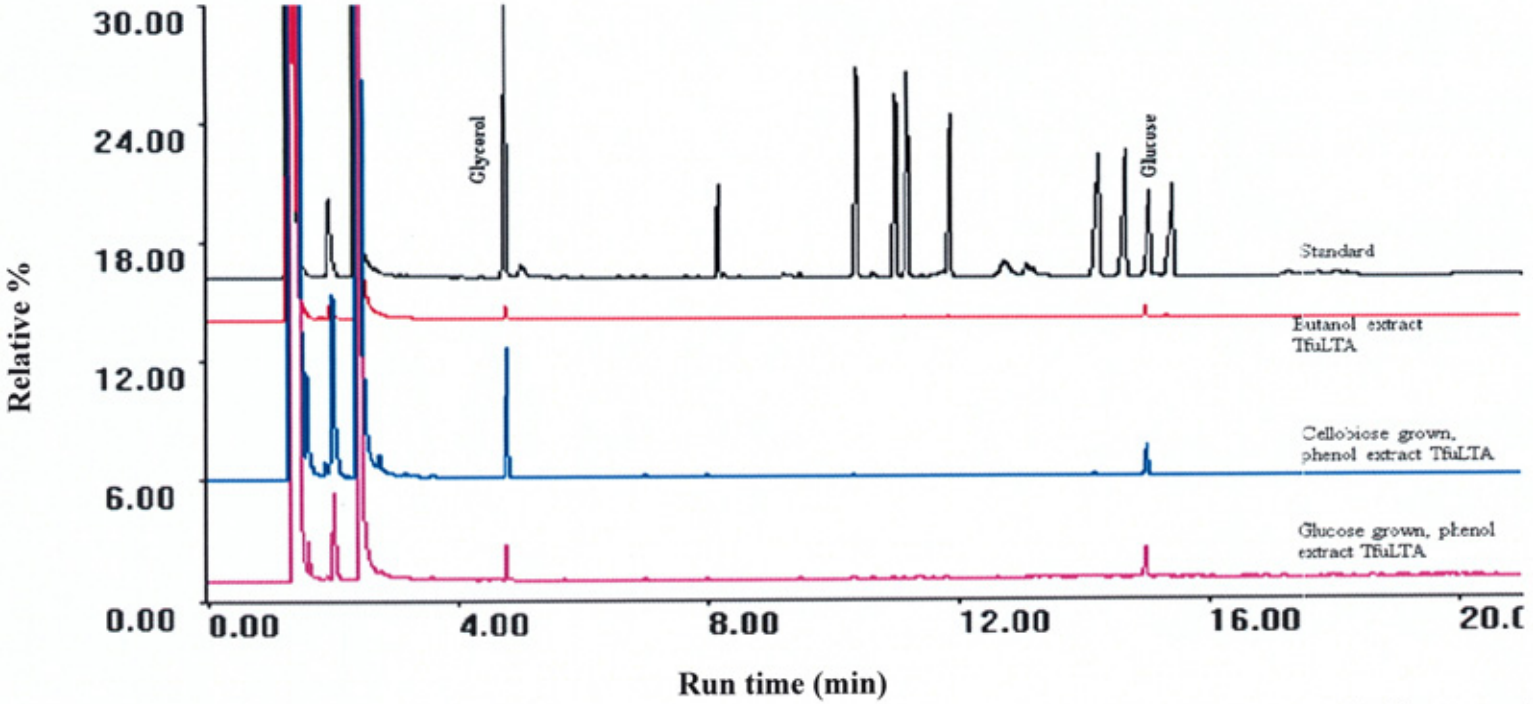

Figure 3.9. Carbohydrate analysis results for macroamphiphiles (TfuLTA) of *T. fusca* grown in either glucose or cellobiose as carbon source and extracted using the phenol-water extraction method. Analysis of a butanol extracted macroamphiphile is also shown. The labelling of the standard sugars have been shown in Chapter 2, Figure 2.5 and Table 2.14.

Table 3.1. Comparison of macroamphiphile fatty acid composition with the whole cell fatty acids of *T. fusca* YX.

FAME identified[a]	Whole cells (glucose grown)	Whole cells (cellobiose grown)	TfuLTA, (glucose grown; phenol -water extraction)	TfuLTA, (cellobiose grown; phenol -water extraction)	TfuLTA (glucose grown; butanol extraction)
Unidentified[b]	5.888	7.272	0	0	0
Unidentified[c]	Trace	Trace	Trace	Trace	15.99
iC15:0	1.173	Trace	0	0	0
aiC15:0	2.037	Trace	0	0	0
C15:0	0.395	0	0	0	0
iC16:0	55.776	58.913	100	100	58.913
C16:0	3.473	2.820	Trace	Trace	11.3
iC17:0	6.356	4.154	Trace	Trace	Trace
aiC17:0	10.282	9.932	Trace	Trace	Trace
C17:0	1.39	Trace	0	0	0
C17:1	0.587	0	0	0	0
iC18:0	7.616	13.999	Trace	Trace	14.3
aiC18:0	3.60	Trace	0	0	0
C18:0	1.715	2.909	0	0	0
C18:1	0.740	0	0	0	0

[a]Fatty acids were analysed by GC of their methyl esters and identified by comparision with a mixture of 32 authentic standards (Sigma Chemical Co.). Composition is given as the percentage of total integrated chromatographic peak areas. [b]Possibly C10 methyl branched fatty acid, [c]Possibly C13 methylbranched fatty acid. Composition is given as the percentage of total integrated chromatographic peak areas.

Table 3.2. Carbohydrate composition of the HIC-purified acid hydrolysed macroamphiphiles of *T. fusca* YX

Carbohydrate identified[a]	***T.fusca* macroamphiphile (glucose as carbon source)**	***T.fusca* macroamphiphile (cellobiose as carbon source)**	***T.fusca* macroamphiphile (butanol extraction)**
Glycerol	64.3	82.3	59.2
Glucose	35.7	17.7	41.8

[a] Carbohydrates were analysed by GC of their alditol acetate derivatives and identified by comparision with a mixture of authentic standards (alditol acetates of glycerol, erythritol, rhamnose, ribose, arabinose, xylose, mannose, galactose, glucose and inositol; shown in Figure 2.5). Composition is given as the percentage of total integrated chromatographic peak areas.

3.6.4. Electrophoretic analyses of the *T. fusca* macroamphiphile

The *T. fusca* macroamphiphile was examined by electrophoresis followed by staining with Alcian Blue 8GX, silver-nitrate, Coomassie Blue and periodate Schiffs reagent (described in Chapter 2, Sections 2.2.3.1, 2.2.3.2, 2.2.3.3 and 2.2.3.4, respectively). The Coomassie Blue, Periodate Schiffs reagent and Alcian Blue 8GX staining each revealed broad band around the 15 KDa region (data shown in Figures 3.10-3.12). However, silver-nitrate staining was unable to stain either *T. fusca* samples or an LTA standard (GBS LTA or commercial LTA of *S. sanguis,* Sigma); instead silver-nitrate showed a negative stain against the light brown stained gel background around the 15 KDa region (data not shown).

As shown in Figure 3.11, the electrophoretic mobility of the *T. fusca* macroamphiphile was similar to that of a reference GBS LTA. Moreover, on Western blotting the *T. fusca* macroamphiphile reacted with a polyclonal and monoclonal anti-LTA (Table 2.12) which was visualised as a broad smear over a range of approx. 15 kDa as compared with protein standard molecular-weight markers (Figure 3.13). A similar smear was also visualised for both commercial LTA and GBS LTA. This evidence strongly suggested that LTA was present as the macroamphiphile in *T. fusca* and so this macroamphiphile was designated as TfuLTA. From these data and the above chemical characterisation this LTA can be provisionally concluded to be a poly(GroP) backbone LTA (PGP-LTA).

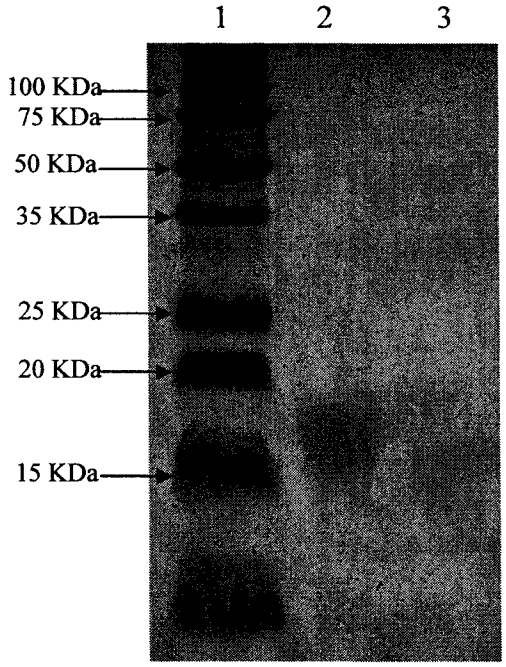

Figure 3.10. Coommasie Blue staining: Lane 1, protein standard ladder; Lane 2: *T. fusca* macroamphiphile; Lane 3: GBS LTA.

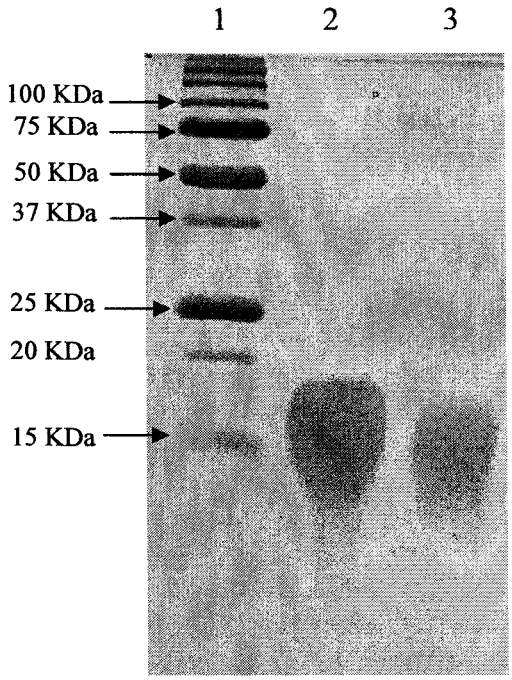

Figure 3.11. Alcian Blue staining: Lane 1, protein standard ladder; Lane 2: *T. fusca* macroamphiphile; Lane 3: GBS LTA.

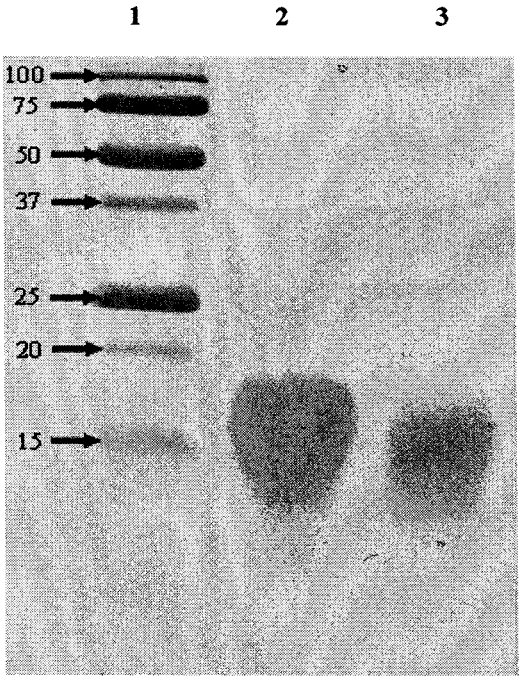

Figure 3.12. Periodate Schiffs reagent staining: Lane 1, protein standard ladder; Lane 2: *T. fusca* macroamphiphile; Lane 3: GBS LTA

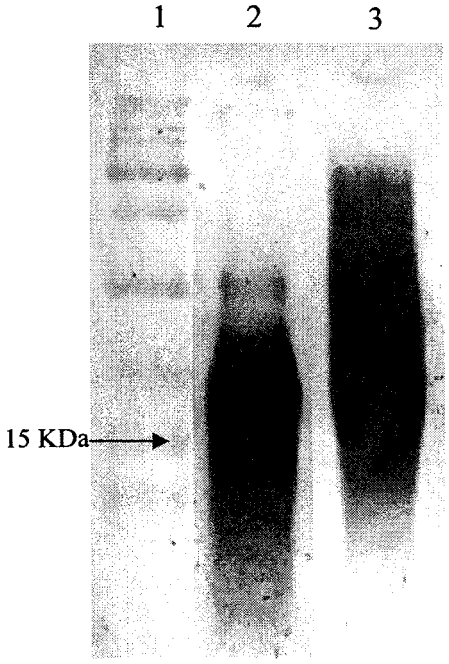

Figure 3.13 (a)

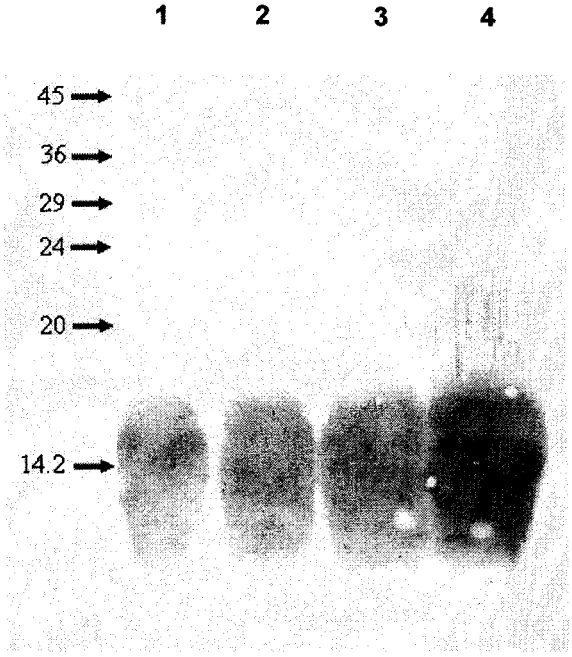

Figure 3.13 (b)

Figure 3.13. Electrophoretic analyses of the *T.fusca* macroamphiphile followed by Western blotting. (**a**) blot probed with polyclonal anti-LTA. Lane 1 is protein ladder, lane 2 is *T. fusca* LTA and lane 3 is GBS LTA (**b**) blot probed with monoclonal anti-LTA. Samples were separated by SDS-PAGE, blotted onto nitrocellulose and probed with anti-LTA antibodies to detect LTA. In part B, lanes 1, 2 and 3 are different preparations of the *T. fusca* macroamphiphile and lane 4 is the reference GBS LTA.

3.6.5. Distinguishing Lipoteichoic acid (LTA) from teichoic acid (TA)

T. fusca is known to contain polyGroP wall TA as SCWP (Section 1.6.2) which could explain the cross-reaction with the monoclonal anti-LTA antibody described above. However, hot phenol-water extracts or butanol extracts do not typically contain significant amounts of wall TA since they are covalently anchored to the peptidoglycan. Moreover, further purification of the macroamphiphile by HIC reduces the possibility of contamination of the preparation with TA due to the absence of a hydrophobic moiety in mature TA. However, teichoic acids are biosynthesised at the cytoplasmic face of the plasma membrane on a polyprenol-phosphate carrier lipid, before flipping to the outer leaflet of the plasma membrane and transfer onto the growing cell wall as described in Chapter 1, section 1.6.2.1 and Figure 1.9. It was therefore considered as a possibility that the Tfu-LTA described here was in fact a polyprenol-linked biosynthetic intermediate from TA biosynthesis. Consequently, additional experiments were done to prove that the positive anti-LTA reaction for the *T. fusca* macroamphiphile was not a false positive reaction of membrane-anchored TA precursors. The experimental design is shown in flowchart of Figure 3.14.

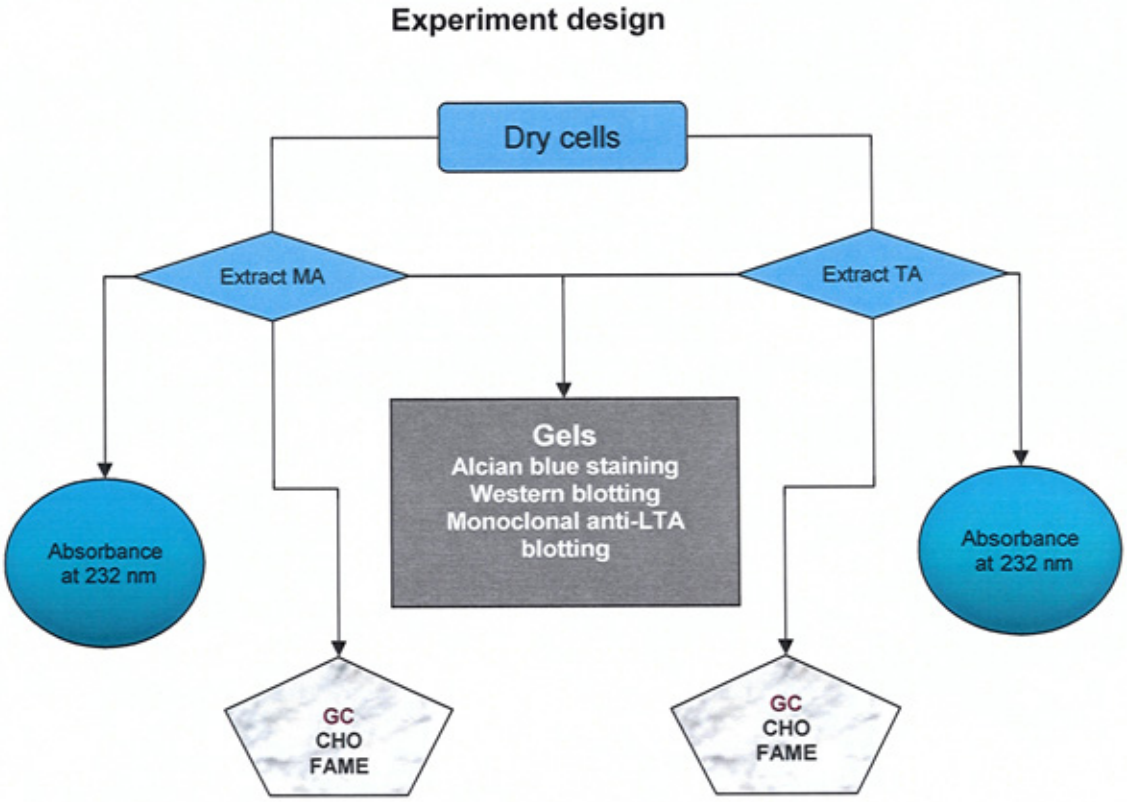

Figure 3.14. Experimental design for proving the LTA of *T. fusca* is not a false positive reaction for TA precursor. GC represents Gas Chromatography and CHO represents alditol acetates analysis of carbohydrates. FAME is fatty acid analysis & MA, macroamphiphile.

TA material was extracted from *T. fusca* using the TA extraction method (describes in Chapter 2, Section 2.4). There was no peak identified for either macroamphiphile or teichoic acid at 232 nm on UV spectrometry, which strongly suggests that neither of the molecules is attached to a polyprenol membrane carrier (Mcarthur *et al.*, 1980, Ginsberg *et al.*, 2006), as polyprenols have multiple carbon-carbon double bonds and should have absorbed light at this wavelength (Collmer *et al.*, 1988). The alditol acetates derivatisation for analysis of carbohydrate showed that both the macroamphiphile and teichoic acid preparation contained glycerol and glucose (Figure 3.15), consistent with a glycerol-phosphate backbone present in each. However, the fatty acid analysis again demonstrated that the macroamphiphile preparation contained branched chain fatty acids (consistent with a diacylglycerol hydrophobic moiety), which were absent from the TA preparation as expected (data not shown). Cumulatively, these data were consistent with the assumption that the extracted macroamphiphile is an LTA rather than a polyprenol-anchored TA precursor as described in Chapter 1, section 1.6.2.1. and Figure 1.9.

The presence of LTA in *T.fusca* was further demonstrated by electrophoresis followed by Alcian Blue staining and Western blotting with monoclonal anti-LTA. Alcian Blue staining showed the position of the MA was similar to the position of commercial LTA preparations and both gave positive reactions with the monoclonal anti-LTA (Figures 3.13 and 3.16). However, for the TA preparation of *T. fusca*, the material stained with Alcian Blue was observed in a different electrophoretic position from that of the commercial LTA and also gave no reaction with the monoclonal anti-LTA (Figure 3.16). The results for

this section have been summarized in Table 3.3. These data strongly suggest the macroamphiphile identified as TfuLTA is not an artefact arising from the extraction of polyprenol-linked TA precursors.

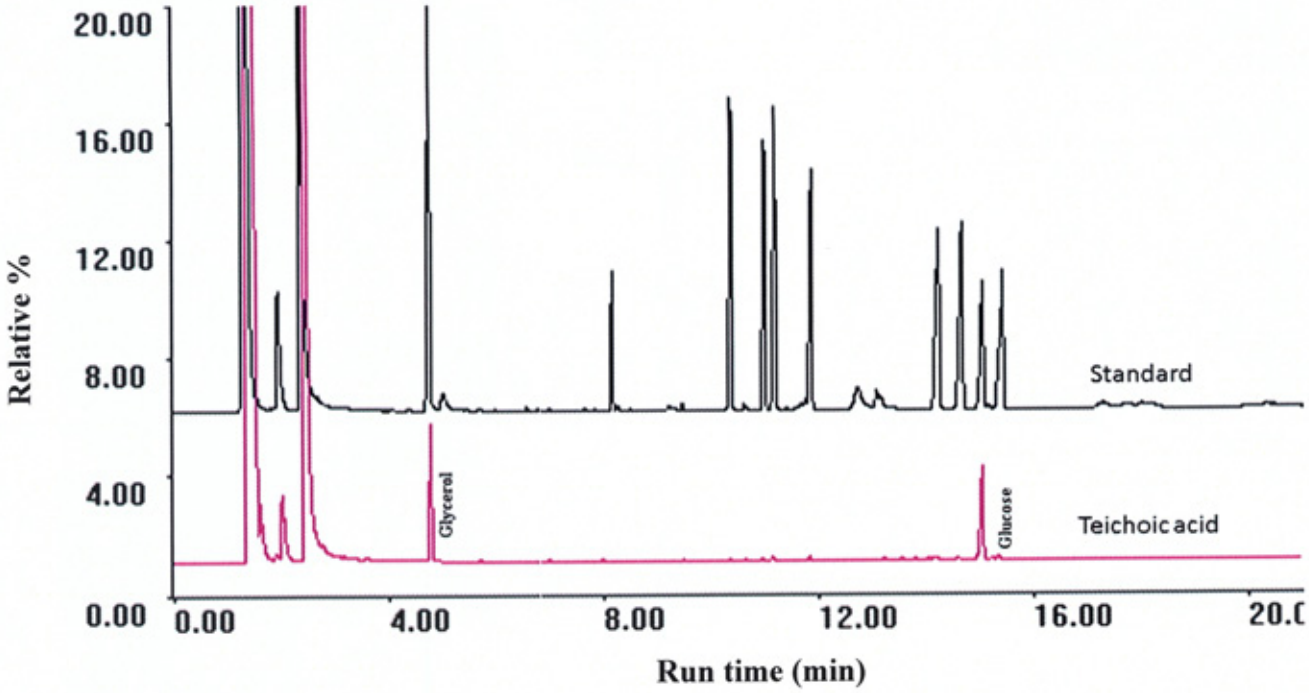

Figure 3.15. Carbohydrate analysis results for TA extracted from *T. fusca* grown on glucose as carbon source. The labelling of the standard sugars has been shown in Chapter 2, Figure 2.5 and Table 2.14.

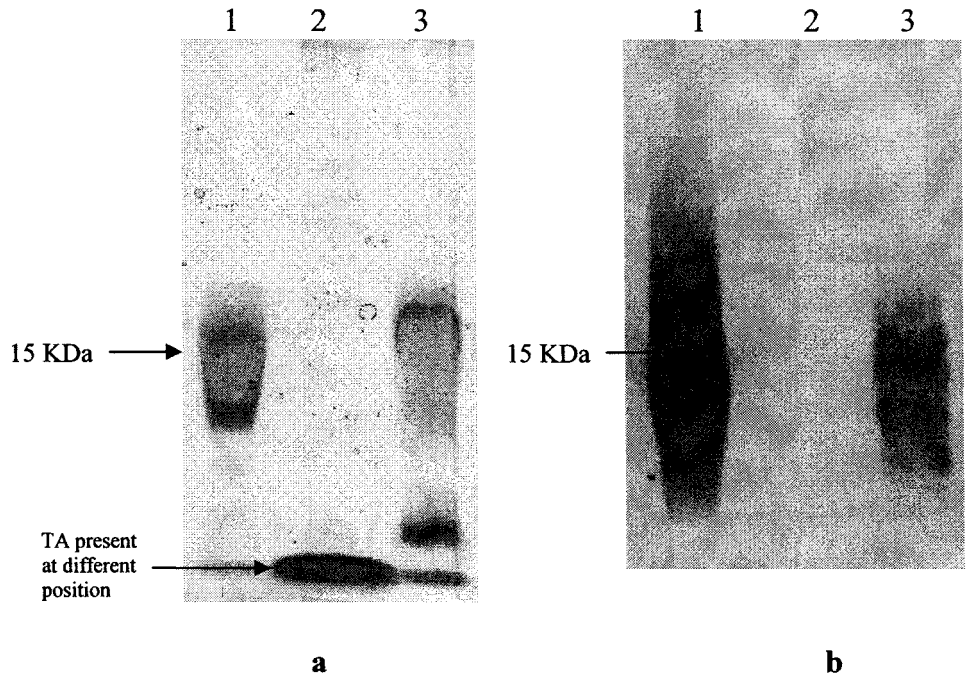

Figure 3.16. Electrophoretic analysis of the TfuLTA and extracted TA. (a) by alcian blue staining: Lane 1, commercial LTA; Lane 2: *T. fusca* TA; Lane 3: TfuLTA **(b)** by Western blotting using monoclonal anti-LTA. Samples were separated by SDS-PAGE, blotted onto nitrocellulose and probed with anti-LTA to detect LTA. Lane 1, commercial LTA; Lane 2: *T. fusca* TA; Lane 3: TfuLTA.

Table 3.3. Results for the experiment design of the Figure 3.14. GC represents the gas chromatography, CHO represents alditol acetates test in GC and FAME represents the fatty acid analysis test. MA, macroamphiphile (putative Tfu-LTA).

Experiment		***Thermobifida fusca***	
		MA	TA
Absorbance at 232 nm		No peak	No peak
GC	**CHO**	Glycerol from GP Backbone	Glycerol from GP Backbone
	FAME	Branched chain FAME present	No FAME
SDS-PAGE Gel Analysis	**Alcian blue stain (Figure 3.16a)**	MA stains in similar position to the standard LTA.	Staining position was different from standard LTA
	Anti-LTA blotting (Figure 3.16b)	Positive reaction at a similar positon to the standard LTA.	No reaction

3.6.6. NMR

Further structural analysis of the TfuLTA was done by NMR analysis, described in Chapter 2, section 2.2.7.2. Purified ca. 8 mg LTA of *T. fusca* was prepared and sent to Dr Markus Pfitzenmaier (Department of Organic Chemistry, University of Marburg, Germany) for NMR analysis. The following is a summary of the data generated from his analysis, in collaboration with Siegfried Morath and Thomas Hartung (EU Joint Research Centre, European Centre for the Validation of Alternative Methods, Ispra, Italy).

NMR analysis of ca. 8 mg HIC-purified Tfu-LTA confirmed the presence of poly(GroP)-LTA structure (Figure 3.17 and 3.18; Tables 3.4 & 3.5). Figures 3.17 and 3.18 and Table 3.4 confirmed the fatty acid signals and the poly(GroP) signals, although it is noted that the NMR couldn't definitively confirm whether both the fatty acids and the polyGroP are in the same molecule or not. The main component of the sample consisted of a 1,3-linked polyglycerophosphate chain, which is characteristic of most LTA backbones (described in Chapter 1, section 1.7.3.1.1). The NMR also showed the fatty acids present in the sample were branched alkyl chains without any double bonds (consistent with the lack of absorbance at 232 nm). The number of GroP repeat units phosphate may be approximately 19, although this was hard to determine accurately because of the very broad CH_3 signal (Figure 3.17 and Tables 3.4 & 3.5).

The NMR also identified three types of substituent for the hydroxyl group at position 2 of glycerol (Figure 3.19): glucosyl, acetate and lactate. The glucosyl substituents were β-linked to the C2 hydroxyl of the poly(GroP) repeating unit. The acetyl groups were acetylated to both the C2 of the poly(GroP) repeat unit and to the C6 of the β-glucosyl-substituents (Figure 3.17-3.19 and Table 3.5). Lactyl groups were also detected but at present their localisation within the TfuLTA molecule cannot be precisely determined. The suggested structure of TfuLTA is shown in Figure 3.19.

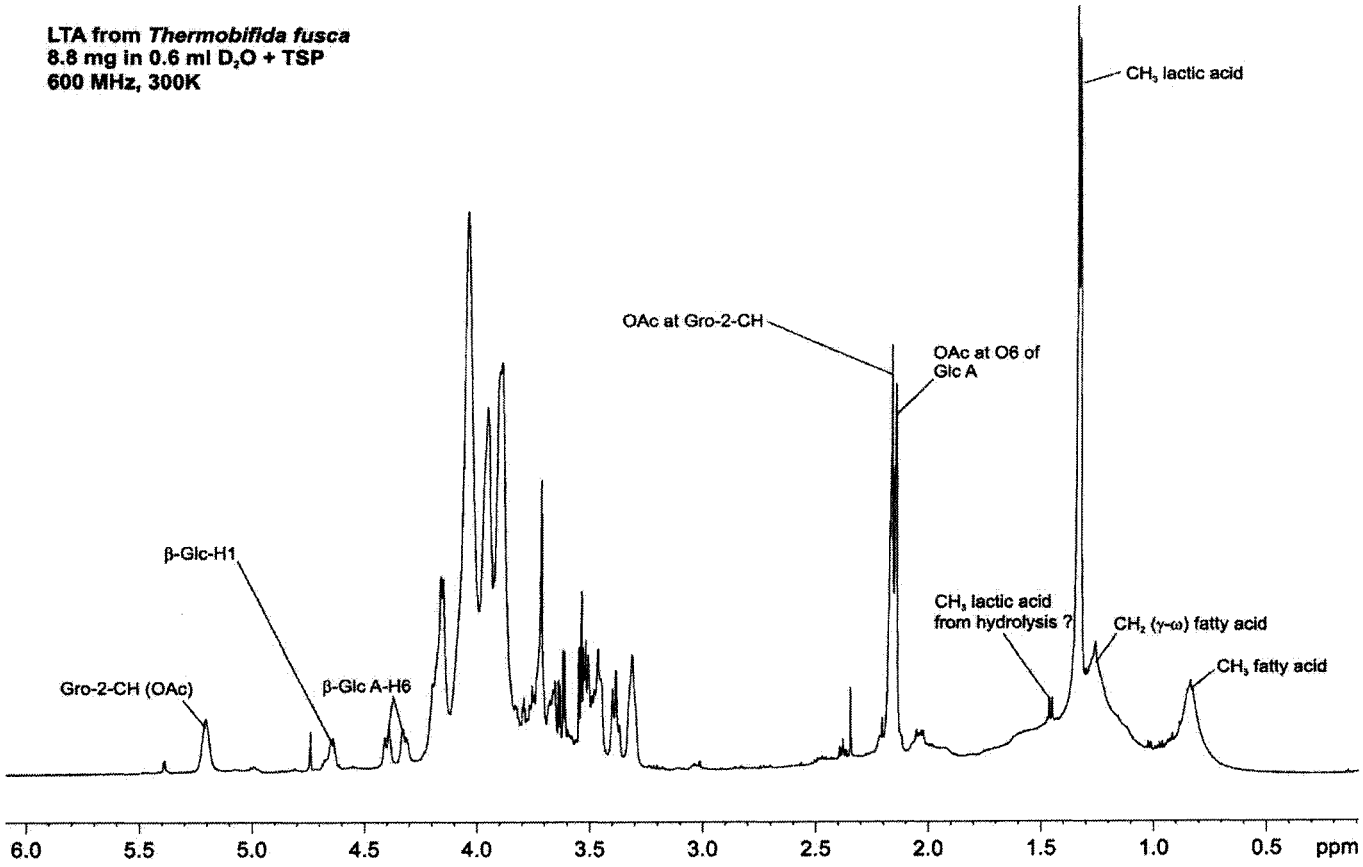

Figure 3.17. 1D NMR analysis of Tfu-LTA showing the signals attributed to key components. Data from Dr Markus Pfitzenmaier.

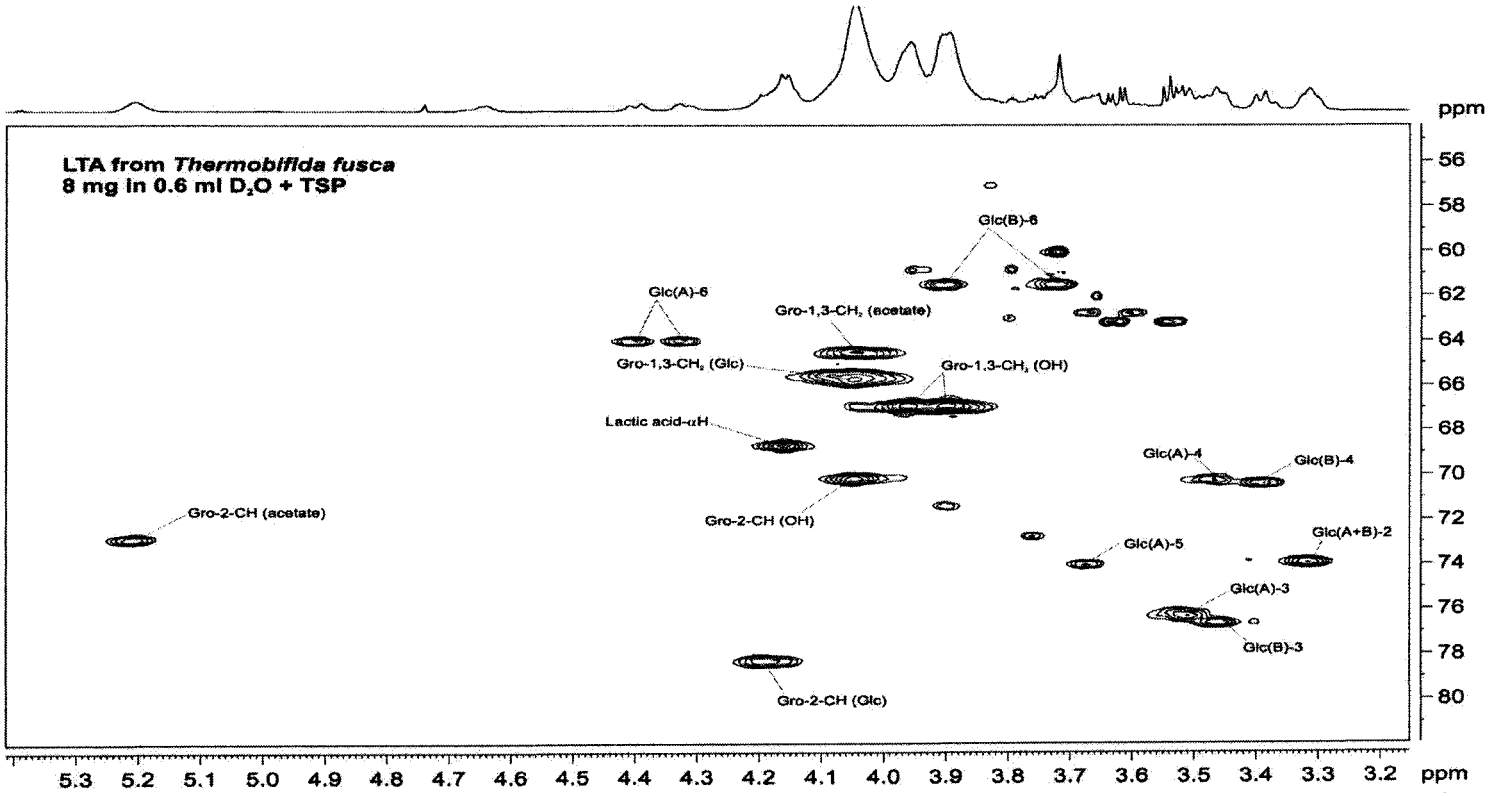

Figure 3.18. 2D NMR analysis of Tfu-LTA showing the signals attributed to key components. Data from Dr Markus Pfitzenmaier

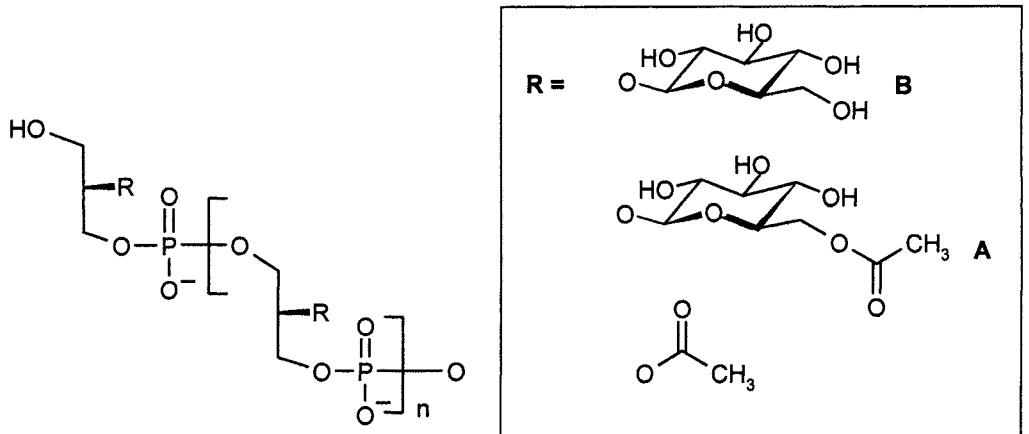

Glycerol repeating units: n = 19 (calculation based on the very broad CH_3 signal with a value of 6 protons)
Acetate substitution: 11 %
Glc A substitution: 6 %
Glc B substitution : 12 %
Unsubstituted: 73 %
Fatty acid chain: no double bonds, mainly branched alkyl chains

Figure 3.19. Structure of the *T. fusca* LTA as suggested by chemical and electrophoretic analysis and confirmed by NMR

Table 3.4. Additional signals in the NMR of TfuLTA. Data from Dr Markus Pfitzenmaier.

Substituent	δ_H	δ_C
CH_3 fatty acids linear	0.828	12.8
CH_3 fatty acids linear	0.847	15.4
CH_3 fatty acids branched	0.826	20.6
CH_3 fatty acids branched	0.845	24.1
CH_2 (γ-ω) fatty acids	1.14-1.28	30.9-31.7
CH_2 (α) fatty acids ?	2.382	31.2
CH_2 (β) fatty acids ?	1.592	24.8
CH_2 (γ) fatty acids ?		
Lactic acid -βH Hydrolysis ?	1.457	17.6
Lactic acid-αH Hydrolysis ?	3.762	52.1
D/L-Lactic acid-βH	1.333	21.4
D/L-Lactic acid -αH	4.157	69.6
free glycerol ?	3.598, 3.667	63.6
free glycerol ?	3.896	72.3

calibrated on TSP in ^{1}H and ^{13}C

Table 3.5. Main substituent signals in the NMR of TfuLTA. Data from Dr Markus Pfitzenmaier

Substituents	**δ_H (in ppm)**	**δ_C (in ppm)**
Acetate	2.166	22.2
Gro-2-CH (acetate)	5.205	73.7
Gro-1,3-CH_2 (acetate)	4.039	65.4
β-Glc(A)-1H	4.676	103.9
β-Glc(A)-2H	3.320	74.8
β-Glc(A)-3H	3.508	77.2
β-Glc(A)-4H	3.464	71.1
β-Glc(A)-5H	3.670	74.9
β-Glc(A)-6H	4.326, 4.398	64.9
Acetate at O6	2.146	22.0
Gro-2-CH (β-Glc A)	4.161	79.1
Gro-1,3-CH_2 (β-Glc A)	4.034	66.5
β-Glc(B)-1H	4.644	103.8
β-Glc(B)-2H	3.312	74.8
β-Glc(B)-3H	3.456	77.5
β-Glc(B)-4H	3.386	71.2
β-Glc(B)-5H		
β-Glc(B)-6H	3.721, 3.900	62.3
Gro-2-CH (β-Glc B)	4.188	79.1
Gro-1,3-CH_2 (β-Glc B)	4.042	66.5
Gro-2-CH (OH, unsubst.)	4.043	71.0
Gro-1,3-CH_2 (OH, unsubst.)	3.894, 3.957	67.8

3.6.7. Two-dimensional gel electrophoresis of Tfu-LTA

One-dimensional SDS-PAGE coupled with different staining or Western blotting with monoclonal anti-LTA antibody was useful in assessing the LTA in relation to protein size standards and it was noted that LTA typically displays a broad diffuse band (Figures 3.10-3.13). Previous studies by Torreles *et al.* (2004) showed that if SDS-PAGE analysis was preceded by a first-dimensional IEF separation, LAM from *M. leprae* (LepLAM) and *M. tuberculosis* (RvLAM) can be resolved into several discrete isoforms equilibrating at different pH values instead of a horizontal spread. They also showed the mycobacterial LM yielded only one isoform. Therefore the present study has studied the isoforms present in the LTA of *T. fusca* and *S. agalactiae* (GBS) by developing the 2D-gel electrophoresis method.

The data (Figure 3.20) revealed that the LTA of *T.* fusca produced three isoforms but these isoforms were found in different positions according to the molecular weight, which was not noted previously in Torreles *et al.* (2004). On the other hand, GBS-LTA yielded only one isoform (Figure 3.21). It was notable that the position of the major isoform from the TfuLTA was very similar to that of GBS LTA in both the molecular weight dimension (as previously observed on 1D SDS-PAGE) and in the IEF dimension. Repeated gels run were shown in Appendix II. However, further studies are needed to confirm these results.

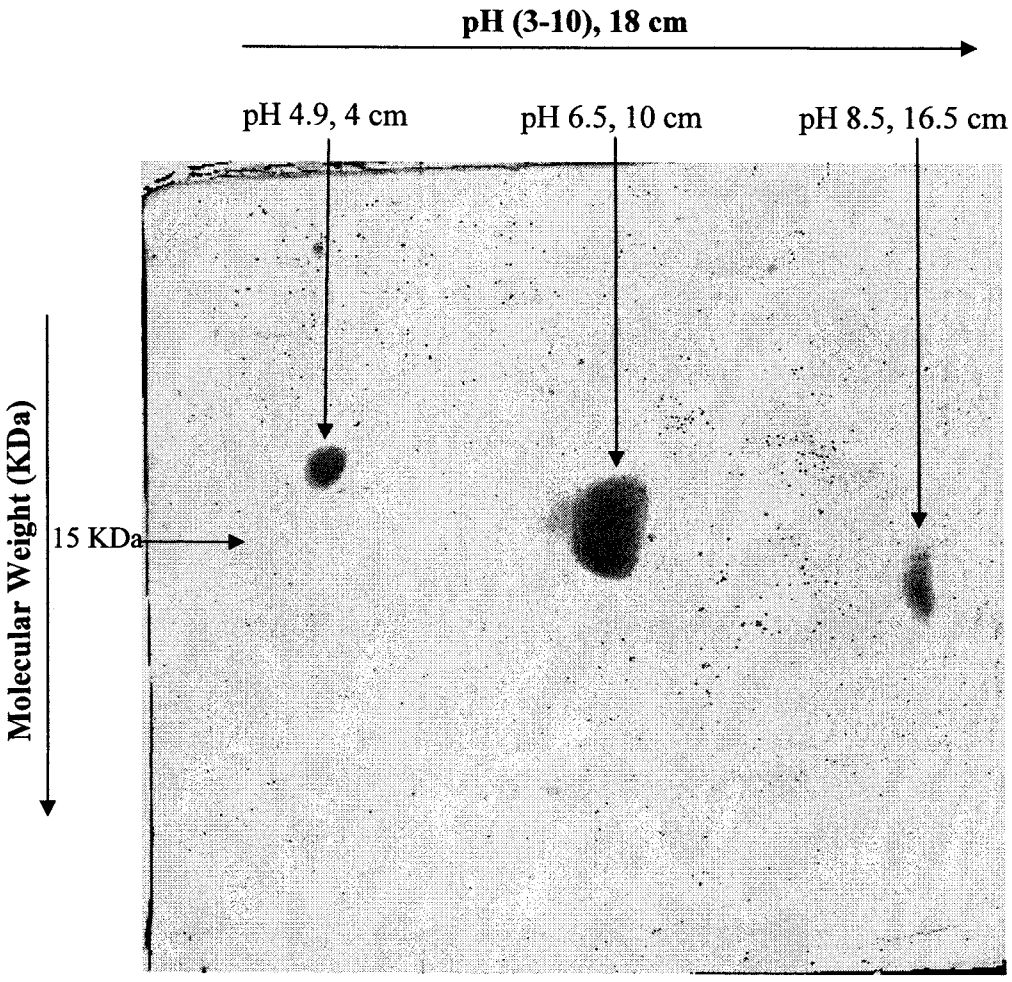

Figure 3.20. Two-dimensional gel electrophoresis of Tfu-LTA.

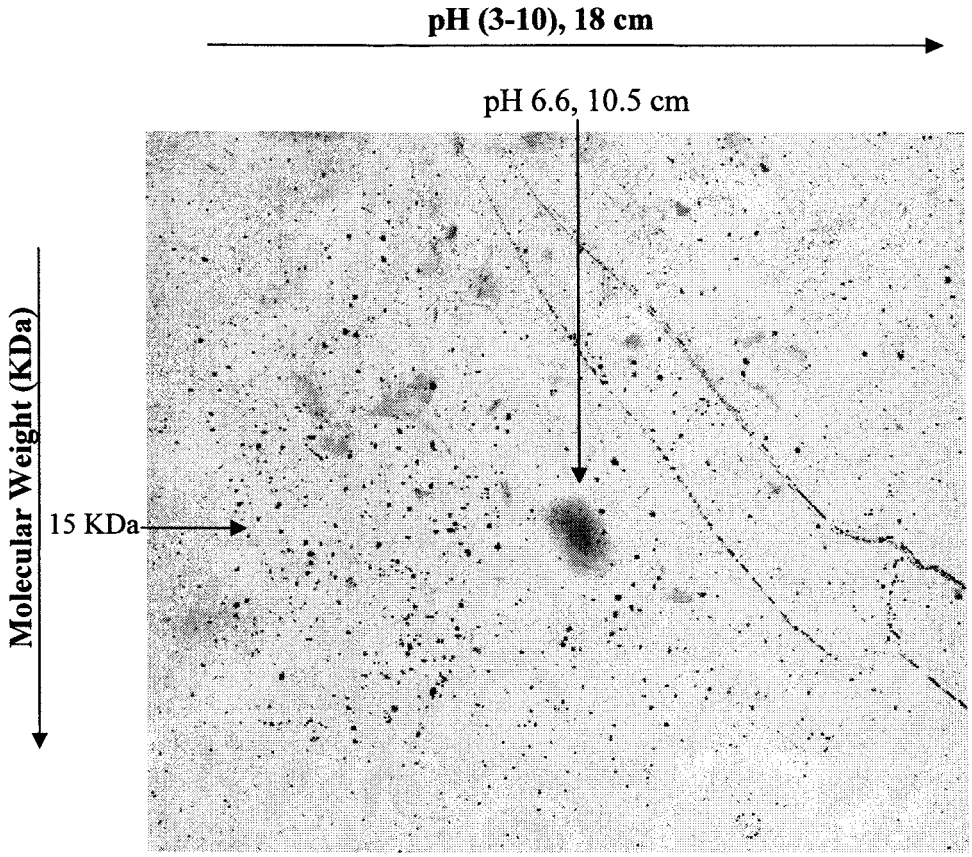

Figure 3.21. Two-dimensional gel electrophoresis of GBS-LTA.

3.7. Discussion

3.7.1. Growth characteristics

Previous studies (Crawford, 1975) have shown that amino acids can neither be used as a carbon and energy source nor as a nitrogen source by *T. fusca*. Even proteins like casein and gelatin can't be used, showing the bacteria is not adapted for growth at the expense of proteinaceous substrates, either intact or hydrolyzed (McCarthy and Cross, 1984). Carbohydrates, both sugars and polymers, are the only sources for carbon and energy during growth of *T. fusca*. Glucose or cellulose were found to be the best sources of carbon and energy for the growth, along with ammonia as the best nitrogen source (McCarthy and Cross, 1984). Biotin and a mixture of amino acids can fulfil the culture's trace nutrient requirements, but good growth has been obtained in a non-defined media containing yeast extract (Crawford, 1975). Consequently, good media for the growth of *T. fusca* is a semi-defined medium which contain defined sugars and ammonia as carbon, energy and nitrogen sources and non-defined compounds like yeast extract and biotin for other nutrient requirements. This has been confirmed in the present study by growing the bacteria successfully in Hagerdahl medium, whereas it was found to be unable to grow in TYG, YEME or GYM media.

The intensity of the colour change from yellowish to golden brown with time for *T. fusca* culture has been noticed previously in liquid culture by Crawford (1975) and suggested to be the result of soluble pigment production by the organism. This result is consistent with the presence of the cluster encoding

genes which are predicted to participate in carotene biosynthesis, which is a soluble isoprenoid pigment found in different micoroorganisms and plant (Lykidis *et al.*, 2007). The production of this soluble pigment may differ due to use of different carbon sources, which has also found to affect the mycelial surface of *T. fusca*. A smooth mycelial surface was observed when *T. fusca* was grown on basal medium containing glucose, whereas a scabrous mycelial appearance was observed when medium containing cellobiose as sole carbon source was used (Kukolya *et al.*, 2001). Though the previous studies showed that cellobiose was better carbon source for *T. fusca* (Crawford, 1975), the yield of the harvest in the present studies suggested that glucose was a better carbon source.

The purple, hair-like structure of *T. fusca* observed after Gram staining was as expected as the organism is a filamentous Gram positive bacteria and spores were found to be attached on the surface of these mycelia, which is consistent with the previous electronic microscopic study of Kukolya, Szabo & Hornod (2001), where they shown that *T. fusca* formed highly branched mycelium and heat-sensitive spores on aerial hyphae.

3.7.2. Identification of the *T. fusca* macroamphiphile as an LTA

Both phenol-water extraction and butanol extraction followed by HIC purification have allowed the identification of an abundant macroamphiphile at the same region of the propanol gradient elution in *T. fusca*. The amount of material extracted by the butanol extraction process was higher than that from the phenol extraction process, which might have occured due to the presence of other contaminants within the extract and this can also be observed from the fatty acid profile of the macroamphiphiles (Figure 3.8 and Table 3.1), suggesting the presence of distinct fatty acid containing contaminants in the butanol extracted material. Therefore, the present study suggest that the hot phenol-water extraction method is better extraction process compared to the butanol extraction method, which is consistent with previous studies (Fischer, 1990, Fischer, 1988, Fischer, 1994b).

The low amount of carbohydrate detected in both the HIC fractions and the purified macroamphiphiles (CHO:P ratio approximately 1:3) represent characteristics of an LTA rather than a lipoglycan since LTA has a high phosphorus content due to the polyGroP chain, with hexose:phosphorus ratios of $\leq$ 1:1 typical. Further evidence for the presence of LTA was provided by the positive results obtained from the *T. fusca* preparations on dot immunoblotting and also by SDS-PAGE/Western blotting with purified macroamphiphile, using the monoclonal anti-LTA antibody BSYX-A110, which was developed as a chimeric, monoclonal antibody (mAb) for binding *S. aureus* LTA (Walsh *et al.*, 2004) and kindly provided by Biosynexus (http://biosynexus.com/productsbsyx.html).

The analysis of fatty acids can be useful to differentiate *Thermobifida* species from other actinomycete species with similar morphology, such as members of the genus *Thermomonospora*. *Thermobifida* species are characterized by a high amount of *iso*- and *anteiso*-branched fatty acids, namely, 15-methyl-hexadecanoic acid (iso-C17:0; 15–30%) and 14-methyl-hexadecanoic acid (aiC17:0; 15–30%), whereas *Thermomonospora* and *Actinomadura* species synthesize only traces of these fatty acids (Greinermai *et al.*, 1987). In contrast, these latter taxa synthesize significant amounts of 10-methyl branched fatty acids, whereas this fatty acid is only a minor component in *Thermobifida* (1–5%). 2-hydroxy fatty acids (a diagnostic fatty acid in *Microbispora*) could not be detected in *Thermobifida* species (Greinermai *et al.*, 1987). The data in Table 3.2 shows the presence of branched chain fatty acids i.e. iC16:0, iC17:0, aiC17:0 and aiC18:0 as major fatty acids, consistent with the previous literature. cyclo9-10 C17:0, the predominant fatty acid in one report for *T. cellulytica* (Kukolya *et al.*, 2002), was not detected in our study. This may be due to species-specific differences between *T. fusca* and *T. cellulytica* or the result of our using different media (semi-defined Hagerdahl media and Luria-Bertani medium or saccharose broth, respectively). Also the derivatisation methods employed may affect detection of cyclopropane FAMEs.

After SDS-PAGE, the staining of the *T. fusca* macroamphiphile with Coomassie Blue gave a broad band around 15 KDa (Figure 3.10, lane 2) but this was negatively stained with the highly sensitive silver-nitrate stain (data not shown), which suggested that the molecule is highly negative charged but not necessarily a lipoglycan compound. Alcian Blue staining proved to be a

better staining reagent for the detection of negatively charged macromolecules as it showed better staining of commercial and reference LTA preparations (Figure 3.11). Likewise, Alcian Blue stained the *T. fusca* macroamphiphile clearly (Figure 3.11). Positive staining with periodate Schiff's reagent suggested that the *T. fusca* LTA contained carbohydrate, consistent with the presence of the glucose molecules which were subsequently identified by GC and NMR.

Since both TA and LTA have similar glycerol-phosphate repeated hydrophilic backbones, although of different stereochemistry (discussed in section 1.7.3.1), and the anti-LTA antibody binds to this backbone in staphylococcal LTA (Walsh *et al.*, 2004), the dot blotting and Western blotting results may have been a false-positive reaction with a membrane-anchored wall TA precursor (shown in Figure 1.9 and described in section 1.6.2.1)

However, the precursor TA is an intermediate in TA synthesis (Figure 1.9) and expected to turnover rapidly and not to accumulate to significant levels. Moreover the polyprenol presenting the TA precursor has C=C double bonds (described in section 1.3.1) which were found to be absent from the purified LTA by measuring the OD at 232 nm (Collmer *et al.*, 1988). Moreover the presence of fatty acids in the purified HIC sample (and which help to attach the molecule to the HIC column until eluted by propanol) also separate LTA from TA or a precursor TA, which do not contain fatty acids. The specificity of the monoclonal anti-LTA antibody towards LTA was examined by extracting teichoic acid (TA) from the cell wall (Figure 3.16). Staining with Alcain Blue

and silver-nitrate staining showed that the electrophoretic mobility of TA is different to that of the extracted LTA (Figure 3.16). Significantly, the anti-LTA antibody failed to cross-react with the TA extract. This also proves that the antibody is very specific for LTA only, even though the backbone structure of both the molecule is similar but stereochemically different as described in Section 1.6.3.

Cumulatively these data distinguish allow the TfuLTA to be confidently distinguished from a lipid-linked TA precursor.

The presence of high amounts of glycerol with glucose, along with the amount of phosphorus (notably a CHO:P ratio of 1:3) and the absence of other sugars such as mannose, arabinose or inositol suggested that the hydrophilic part of the macroamphiphile is most likely a poly(GroP) polymer, which represents the typical backbone of LTA. Glucose might be present as a substituent on this backbone or derive from a glycolipid anchor.

The NMR result also showed the major backbone of the LTA is a poly(GroP) repeating unit. The chain length analysis suggested the chain length is 19 repeat units. The fatty acid signals in the glycolipid anchor of the LTA was consistent with the GC analysis. Moreover, the NMR identification of glucosyl substituents was also consistent with the GC analysis. Interestingly, the β-configuration of the glucose linkage was unusual, as most organisms LTA reported found glucose in α-configuration (discussed in section 1.7.3.1.1). However this result was consistent with the reported poly(GroP) wall TA of *T. fusca* also containing β-linked glucolsyl substitutents (Potekhina *et al.*, 2003).

D-alanine substituents, which are typical of many poly(GroP)-LTA (Fischer, 1994b, Neuhaus and Baddiley, 2003) were not detected. In Firmicutes such as *B. subtilis* and *Lactobacillus rhamnosus*, the Dlt system provides dedicated systems for the activation, relay and ligation of D-alanine to TA and LTA (discussed in section 1.7.3.3.4.1). The absence of D-alanine in the Tfu-LTA as determined by NMR was consistent with the failure to detect significant homologues of the DltB, DltC and DltD proteins encoded in the *T. fusca* genome (discussed later in Chapter 8), which was also consistent with the failure to detect any D-alanine substituents on the TA of *T. fusca* (Potekhina *et al.*, 2003). However, acetyl groups were detected to be linked to both the C2 of the poly(GroP) repeat units and to the C6 of the β-glucosyl-substituents. The presence of lactyl groups within the Tfu-LTA molecule, although without their precise location in the structure, was unusual for an LTA. However lactyl groups have been previously detected in the LAM of *M. leprae* (Hunter *et al.*, 1986). The lactate might provide additional acidic characteristics to the LTA, as with succinate and pyruvate substitution of lipoglycans (Fischer, 1994b).

Further studies by 2D gel electrophoresis of LTA suggested that TfuLTA shows a different number of isoforms. Tfu-LTA forms three isoforms at different pI values. pI differencs among the isoforms might be caused by the presence or absence of glucose, lactate or both as substituents in the GroP backbone of LTA. Different isoforms of LAM were found to be due to heterogenous molecular composition (Torrelles *et al.*, 2004). In contrast, the GBS reference LTA was uniform, suggesting that LTA isoforms differ among the bacterial sources although the position of the major isoform from the

TfuLTA was very similar to that of GBS LTA. Despite the apparent similarity in pI, other LTA from different bacterial sources may not be the same (e.g. differing in extent and type of substituents) and further studies are needed to delineate their structure-function correlation. Also the present study has to be repeated again to confirm these results (studies which were unable to be completed due to lack of time).

The above data that have shown that *T. fusca* synthesises a PGP-LTA are of interest given the evident need for thermophiles to regulate their membrane composition to counteract the fluidising effects on membrane lipids of growth at high tempreratures (Russell and Fukunaga, 1990, Konings *et al.*, 2002). Notably, LTA are not inherently bilayer forming lipids and so form micelles in aqueous solutions (Labischinski *et al.*, 1991, Fischer, 1994b, Gutberlet *et al.*, 1997). However, biophysical studies have suggested that appropriate regulated amounts of poly(GroP)-LTA may help stabilise the membrane surface due to interactions between the poly(GroP) and membrane lipid head groups (Gutberlet *et al.*, 1997). The present study, along with previous studies of *Bacillus coagulans* (Iwasaki *et al.*, 1986) and *Bacillus stearothermophilus* (Card and Finn, 1983), presently known as *Geobacillus stearothermophilus*) is significant in confirming that the presence of LTA is clearly compatible with effective membrane function during growth at high temperatures.

The distribution of LTA and lipoglycans has some chematoxonomic utility, typically at the generic and suprageneric level (Sutcliffe, 1994b, Sutcliffe and Alderson, 1995). The present finding of poly(GroP)-LTA in *T. fusca*

corroborates previous finding that a *Streptomyces* sp. (Potekhina *et al.*, 1983) and four representative of the genus *Agromyces* (Gnilozub *et al.*, 1994b) produce poly(GroP)-LTA, i.e. that some Actinobacteria synthesise LTA. Moreover, the present project has also identified a putative LTA in the model acitnomycete *S. coelicolor* M145 (discussed later in Chapter 6 & 8). This gives us evidence that the genera *Thermobifida* and *Streptomyces* are closely related to each other, and this result is consistent with orthologue gene studies (Chater and Chandra, 2006, Lykidis *et al.*, 2007), which will be discussed later in Chapter 6 & 8.

The present finding highlights the need of further studies of the distribution of LTA in Actinobacteria and also reinforces the need for further consideration of the roles of LTA in the membrane adaptation of thermophiles. Further comparative genomics studies should be done to understand the structure-function correlation, in conjunction with the application of new analytical and genetic tools.

CHAPTER FOUR

Investigation of macroamphiphiles in *Rubrobacter xylanophilus*

4.1. Introduction

The first described species of the genus *Rubrobacter*, *Rubrobacter radiotolerans*, a highly radiotolerant, Gram-positive, polymorphic rod bacteria, was originally assigned to the genus *Arthrobacter* primarily on the basis of morphological considerations and named *Arthrobacter radiotolerans* (Suzuki *et al.*, 1988). Later it was proven that the organism was misclassified and on the basis of chemotaxonomic characteristics and molecular phylogenetic analyses the organism was reclassified in a new genus, *Rubrobacter*, as *R. radiotolerans* comb. nov (Stackebrandt *et al.*, 1997). The genus was placed as a deep-rooting member of the class Actinobacteria based on 16S rRNA and this position was also found to be consistent with two signature indel sequences (cytochrome-c-oxidase subunit 1, Cox1 and CTP synthetase) of the Actinobacteria, whereas two other signature indel sequences (23S rRNA and glutamyl-tRNA synthetase, GluRS) were found to be absent suggesting the genus is distantly related to other Actinobacteria in the phylogenetic tree (Gao and Gupta, 2005, Stackebrandt *et al.*, 1997, Carreto *et al.*, 1996). The presence of signature proteins and the genomic organisation of several marker genes is also consistent with *R. xylanophilus* being a deep rooted member of the actinobacteria (Gao *et al.*, 2006, Kunisawa, 2007).

R. xylanophilus was isolated from a heat polluted runoff from a carpet factory in the United Kingdom was placed into the genus *Rubrobacter* on the basis of morphological, biochemical characteristics, chemotaxonomic parameters and 16S rRNA gene sequence data (Carreto *et al.*, 1996). The levels of 16S rRNA gene sequence similarity between *R. xylanophilus* and *R. radiotolerans* are 90%; though this is relatively low for species belonging to the same genus, the high similarity between the phenotypic and chemotaxonomic characteristics was considered to justify placing the *R. xylanophilus* in the genus *Rubrobacter* (Carreto *et al.*, 1996). Recently, another member, *Rubrobacter taiwanensis*, has been introduced into this genus (Chen *et al.*, 2004).

Presently the classification of *R. xylanophilus* can be summarised follows (LPSN: http;//www.bacterio.cict.fr/):

Phylum: Actinobacteria

Class: Actinobacteridae

Subclass: Rubrobacteridae

Order: Rubrobacterales

Suborder: "Rubrobacterineae"

Family: Rubrobacteraceae

Genus: *Rubrobacter*

Species: *Rubrobacter xylanophilus*

4.2. Morphological, cultural and physiological characteristics of *R. xylanophilus*

R. xylanophilus is a Gram-positive, aerobic bacterium with relatively small, non-motile, rod-shaped cells (0.9 to 1.0 μm wide and 1.0 to 3.0 μm long), whilst a few of them appear as spherical or coccoid cells. Depending on the growth temperature, the colony appears light pink (60°C) or pink (45°C) which is a characteristic distinct from *R. radiotolerans*, producing light pink colonies on solid medium (Carreto *et al.*, 1996). Pink-pigmentation is one of the common characteristics of the genus *Rubrobacter* , which is also found in new species *R. taiwanensis* (Chen *et al.*, 2004). Schabereiter-Gurtner *et al.* (2001) identified *Rubrobacter* spp. from rosy discoloured paint layer materials, where the temperature was neither over 15°C nor exposed to any kind of irradiation. Since the study was done with culture-independent methods the physiological properties or species of the *Rubrobacter* spp. still remain to be identified. Subsequent studies have also identified *Rubrobacter* spp. associated with discolored paintings (Imperi *et al.*, 2007).

Another two common characteristics between *Rubrobacter* species are thermophilic growth and extreme resistance to gamma radiation. *R. xylanophilus* grows between 40°C and 70°C with an optimum growth temperature of about 60°C and did not grow at temperature above 70°C. *R. taiwanensis* (Chen *et al.*, 2004) has a similar optimum temperature but can be grown at lower temperatures (30°C). Growth temperature is one of the most outstanding differential characteristics between *R. xylanophilus* and *R. radiotolerans*, since the optimum growth temperature of *R. radiotolerans* is

between 45 and 50 °C and this species does not grow at temperatures above 55°C (Carreto *et al.*, 1996).

Optimal growth of *R. xylanophilus* occurs in Thermus Basal salts medium containing ammonium sulphate and an appropriate carbon source with an optimum pH 7.5 to 8, like other members of the genus *Rubrobacter*, but the organism can not grow below pH 6.0 and above pH 8.0. The organism also grows well in nutrient broth and tryptic soya broth. At 60°C on *Thermus* agar plates, the organism may take 7 days to appear as colonies (Carreto *et al.*, 1996).

R. xylanophilus has the capability to hydrolyze xylan, which distinguishes the organism from *R. radiotolerans*, and this characteristic gave the species name 'xylanophilus' (Carreto *et al.*, 1996). *R. xylanophilus* has other distinguishable phenotypic characteristics from *R. radiotolerans*, such as utilisation of inositol, ribose, galactose, succinate and acetamide. The other phenotypic characteristics of this organism are: non-fermentative, presence of cytochrome oxidase, catalase and β-galactosidase, capability of reducing nitrate to nitrite, hydrolizing capability of gelatine, hide powder azure, arbutin, esculin and hippurate (Carreto *et al.*, 1996).

4.3. Biochemical analysis and radiation resistance abilities of *R. xylanophilus*

R. xylanophilus has only one respiratory lipoquinone: menaquinone 8, which is similar to the *R. radiotolerans* isoprenoid compositon. The organisms polar lipids and peptidoglycan type (lysine, glutamate and alanine molar ratio 1:1:3 for *R. xylanophilus*) are also identical to *R. radiotolerans*. Five similar phospholipids, including PtdG and diphosphatidylglycerol, one phosphoglycolipid and one glycolipid have been identified by thin-layer chromatography in these two species (Carreto *et al.*, 1996, Suzuki *et al.*, 1988).

Among the chemotaxonomic characteristics there is an unusually high proportion of branched chain fatty acids in the cell membrane. The fatty acid composition between *R. xylanophilus*, *R. radiotolerans* and *R. taiwanensis* were also qualitatively very similar. The major fatty acids reported for *R. xylanophilus* following growth at 60°C were aiC18:0 (53%), C18:0 (20%) and iC16:0 (12%) which is similar for the other two species (Carreto *et al.*, 1996, Chen *et al.*, 2004). Moreover the fatty acid profile of these three species (Table 4.1) showed the proportion of branched chain fatty acids generally increased as the temperature increased from 40° to 60° C (Chen *et al.*, 2004).

Members of the genus *Rubrobacter* possess a remarkable resistance to acute and chronic exposure to ionizing γ-radiation (Chen *et al.*, 2004, Suzuki *et al.*, 1988, Yoshinak.T *et al.*, 1973, Ferreira *et al.*, 1999). *R. radiotolerans* is more resistant to gamma radiation than the *R. xylanophilus* (Ferreira *et al.*, 1999), though *R. xylanophilus* has exhibited variable resistance in different studies

(Chen *et al.*, 2004, Ferreira *et al.*, 1999). The genus *Rubrobacter* showed higher gamma radiation resistant than the genus *Deinococcus* (Chen *et al.*, 2004). Even though they were isolated in thermal environment or irradiated samples, DNA markers for this genus were also identified in desert soil along with species of *Deinococcus*, suggesting that the organism may grow in abundance during sporadic rainy periods and survive for long period in deserts soil (Holmes *et al.*, 2000; http://genome.jgi-psf.org/finished_microbes/rubxy/rubxy.home.html).

As well as the adaptation of *R. xylanophilus* to extremely radiation, the bacterium is also adapted to other inhospitable environments, like moderate salinity (<7% NaCl) and higher temperature (80° C) (Carreto *et al.*, 1996). Adaptation to inhospitable environments often requires accumulation of small organic molecules known as compatible solutes (Brown, 1976). Trehalose is one of the general stress protectants believed to be involved in the response to stress conditions like temperature, desiccation, freezing, oxygen deprivation, nutrient starvation, toxic compounds and oxidative agents (Hoelzle and Streeter, 1990, da Costa *et al.*, 1998, Santos and da Costa, 2002b, Elbein *et al.*, 2003) and is found to be widely distributed in nature (Empadinhas *et al.*, 2007). *R. xylanophilus* was found to synthesize trehalose in minimal medium (De Smet *et al.*, 2000, Wolf *et al.*, 2003, Empadinhas *et al.*, 2007). Unexpectedly, mannosyl glycerate (MG) has also been found to accumulate as a compatible solute in *R. xylanophilus* (Empadinhas *et al.*, 2007). MG generally occurs in thermophilic organisms which have a higher growth range than this bacteria, like *Thermus thermophilus* and *Rhosothermus marinus* (Santos and da Costa,

2002a, Martins *et al.*, 1999, Empadinhas *et al.*, 2007). MG has even been detected in *R. xylanophilus* grown at 43 °C and this result is consistent with the presence of MG in marine red algae and identification of genes for the synthesis of MG in mesophilic bacteria and in low temperature environment archeal metagenomes (Empadinhas *et al.*, 2007). This suggests that MG may not only accumulate in thermal shock but rather may be present in other stress conditions also (Empadinhas and da Costa, 2006). Moreover, two biosynthetic pathway has been identified for MG: direct conversion of GDP-mannose and D-glycerate into MG by mannosylglycerate synthetase (MgS) and another pathway involved in formation of the intermediate mannosyl-3-phosphoglycerate (MPG) by the enzyme MpgS from GDP-mannose and 3-phosphatidyl-glycerol acetate and conversion of MPG to MG by MpgP (Martins *et al.*, 1999, Empadinhas *et al.*, 2001). In *R. xylanophilus* a highly divergent MpgS has been identified as being involved in the second pathway as both GDP-mannose and 3-phosphatidyl-glycerol acetate have been identified in this bacterium (Empadinhas *et al.*, 2005).

Di-myo-inositol-phosphate (DIP), the most widespread small-molecular weight solute in hyperthermophilic archaea and bacteria; has been identified in *R. xylanophilus*, which is unexpected as the molecule hasn't been detected in organisms with optimal temperatures below 80 °C (Santos and da Costa, 2002a). A minor amount of di-N-acetyl-glucosamine phosphate (DAGAP, a novel compound) was detected in all conditions along with DIP in *R. xylanophilus* (Empadinhas *et al.*, 2007).

Other than the above mentioned studies, relatively few studies have looked at the physiology and biochemistry of *R. xylanophilus*. However, the genome of *R. xylanophilus* DSM9941 strain has been sequenced by the DOE Joint Genome Institute (http://genome.jgi-psf.org/finished microbes/rubxy/rubxy .home.html) and been published in GenBank (CP000386). The genome sequence of *R. xylanophilus* was of particular interest due to the position of the genus as the deepest branch of the Actinobacteria (Suzuki *et al.*, 1988), and thus distantly related to several organisms of medical importance such as members of the genus *Mycobacterium* and also antibiotic producing bacteria such as members of the genus *Streptomyces*. The organism possesses a single 3.22575 Mbp genome with 3140 protein coding genes identified. The G+C content of this organism is 70.5 mol% which is slightly higher than the *R. radiotolerans* (67.9 mol%) and *R. taiwnaensis* (68.5 mol%) (http://genome.jgi-psf.org/finished_microbes/rubxy/).

Table 4.1. Fatty acid compositions at different temperatures of *R. xylanophilus, R. radiotolerans and R. taiwanensis.* Data taken from Chen *et al* (2004).

Fatty acid	***R. xylanophilus***		***R. radiotolerans***		***R. taiwanensis***	
	45 °C	**60 °C**	**37 °C**	**45 °C**	**45 °C**	**60 °C**
16:0 alcohol	2.8	ND	12.6	4.5	ND	ND
C16:0	7.6	2.7	4.5	6.8	4.6	2.8
17:0 alcohol	3.1	ND	8.0	5.0	3.6	ND
iC16:0	10.4	11.6	39.2	48.9	10.3	12.3
Unknown[a]	1.4	2.3	ND	ND	3.4	3.8
C17:0	2.4	2.1	ND	ND	1.4	2.4
iC17:0	4.0	1.9	ND	ND	10.8	13.2
18:0 alcohol	7.5	3.7	17.6	11.6	8.8	5.5
C18:0	11.4	21.4	3.6	5.7	7.9	7.9
19:0 alcohol	7.8	2.8	4.8	3.6	8.6	6.3
iC18:0	3.2	3.4	ND	ND	4.2	3.2
aiC18:0	37.5	46.6	8.5	12.8	25.3	33.3
C19:0	ND	ND	ND	ND	10.3	8.4

NB. Values are percentages of total fatty acids. ND, Not detected. Unknown fatty acids with equivalent chain-length of 21.714 and 23.714.

4.4. The significance of studying *R. xylanophilus* macroamphiphiles

The cell envelopes of thermophilic bacteria play an important role in their adaptation to growth at high temperatures. Specifically, the maintenance of membrane structure and function are important aspects of adaptation to thermophilic conditions (Russel, and Fukunaga, 1990; Konings *et al.*, 2002; Charlier and Groomans; 2005). One of the main aims of this study was therefore to investigate the presence of macroamphiphiles in the cell envelopes of the thermophilic actinomycetes *R. xylanophilus* and *T. fusca* (Chapter 3). Moreover, the phylogenetic position of the subclass Rubrobacteridae is one of the interesting aspects as this lineage represents one of the earliest branches of the phylum Actinobacteria (Carreto *et al.*, 1996; Stackebrandt *et al.*, 1997; Goa *et al.*, 2006). Furthermore, the capacity of degrading hemicellulose and xylan make the organism significant for playing important role in environmental biodegradation (Ferreira *et al.*, 1999). Consequently, it was of interest to begin the study of the cell envelope of *R. xylanophilus*.

4.5. Results

4.5.1. Organism and culture characteristics

Serial dilution and plating of *R. xylanophilus* showed the bacteria grew to a high yield on Thermus medium agar plates at 55°C (Section 2.1.2.3). The colonies were pink-cloudy in appearance on the plate and appeared relatively small, coccoid or spherical, some times rod-shaped on Gram staining, constitute with the species description. The appearance of colonies took up to four to five days on TM-agar plates.

R. xylanophilus grows to a maximal level after 48 h in liquid TM media at 55°C and 100 x g shaking. After 24 h the pink organism could be observed in the bottom of non-shaking flasks. The organism appeared to become stickier and lighter in its colour (pink) with time.

Gram staining of the cells was observed at 100x magnification under an oil immersion lens showing typical Gram-positive bacteria purple staining as shown in Figure 4.1 which confirmed that the bacterium is a Gram-positive organism.

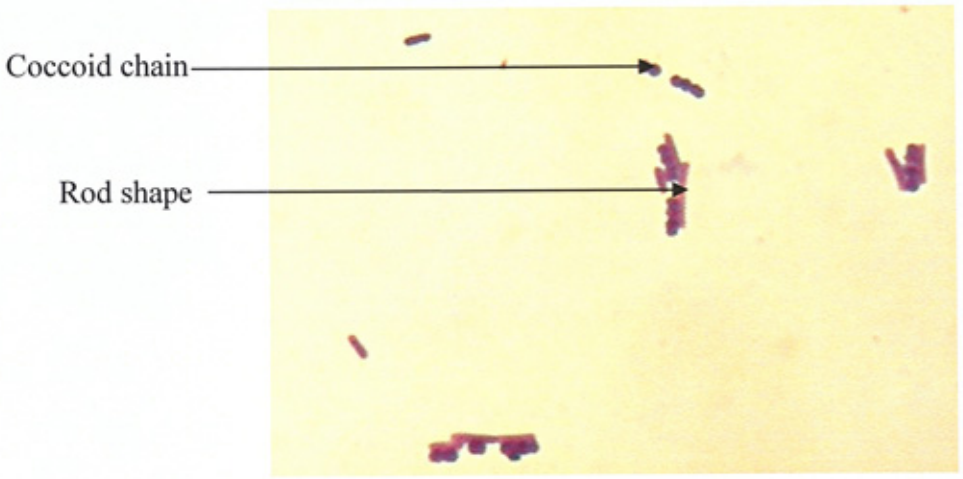

Figure 4.1. Gram staining picture of *R. xylanophilus* showing both coccoid and rod shaped, taken at 100X magnification under oil immersion lens.

4.5.2. Purification of the *R. xylanophilus* macroamphiphiles

It was attempted to extract macroamphiphilic materials from *R. xylanophilus* using three methods, the standard hot phenol-extraction (described in Chapter 2, Section 2.1.5.1), the butanol extraction method (Section 2.1.5.2) and a methanol-chloroform extraction method (Section 2.1.5.3). Following dialysis and lyophilisation, the extracts were purified by HIC column chromatography and the fractions were subjected to carbohydrate and phosphate assays (Section 2.1.6.1; 2.1.7.1 and 2.1.7.2), as shown in Figures 4.2-4.4. With all three extraction methods hydrophilic contaminants (likely nucleic acids, proteins and polysaccharides) not retained by the HIC column were recovered by the elution with equilibration buffer or starting of the gradient, represent by the peak 1 region. However, in all cases, the subsequent gradient elution with an increasing concentration of propanol failed to elute any significant carbohydrate and/or phosphate-containing material (Figures 4.2-4.4). It was concluded from these observations that *R. xylanophilus* does not synthesise significant quantities of any typical macroamphiphilic carbohydrate and/or phosphate containing material. Repetition of the hot phenol-water extraction method showed similar results (data shown in Appendix III).

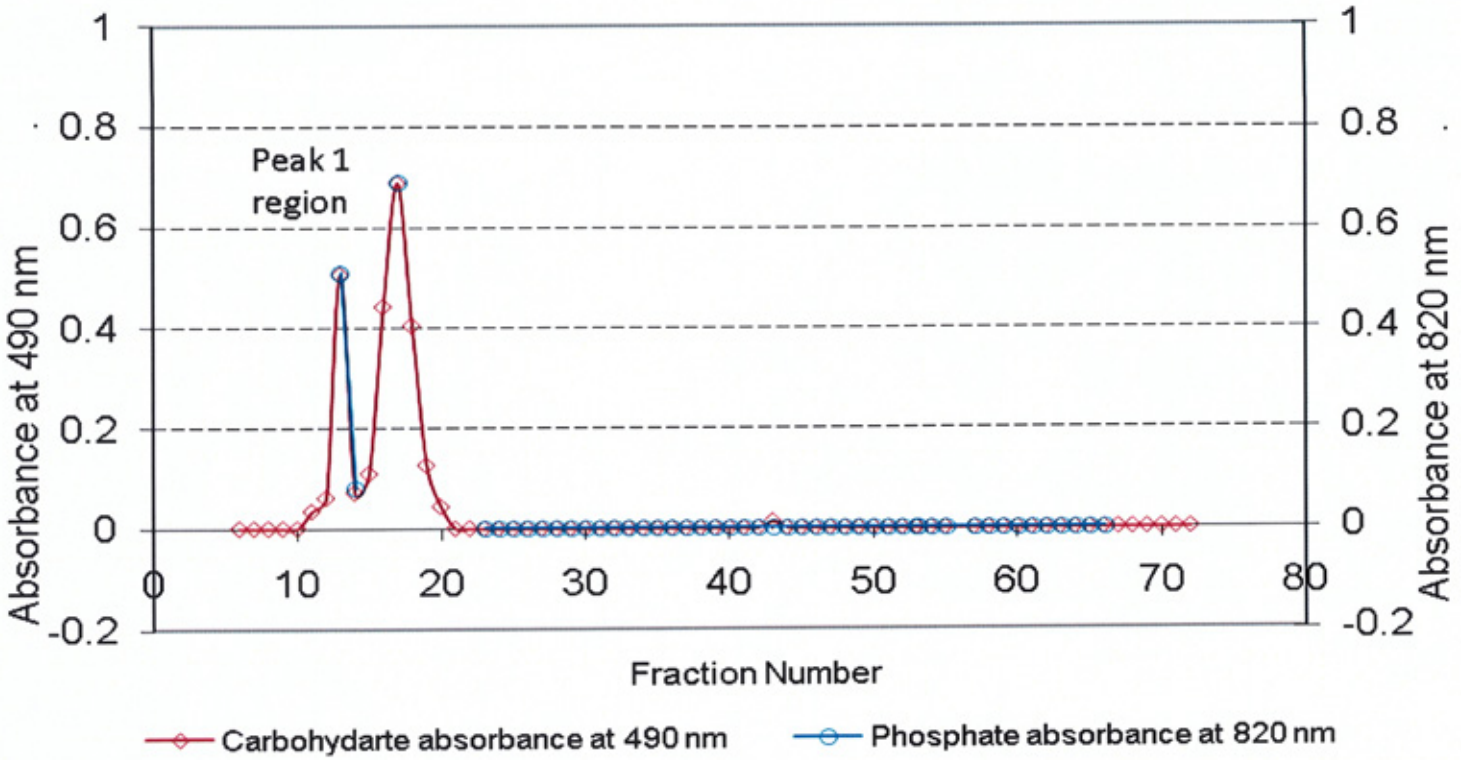

Figure 4.2. HIC profile for the purification of a crude phenol extract from *R. xylanophilus*. The crude extract was loaded the column with equilibration buffer until fraction 12, after which gradient elution with an increasing concentration of propanol was begun. Column fractions (4 mL) were analyzed for carbohydrate and phosphorus.

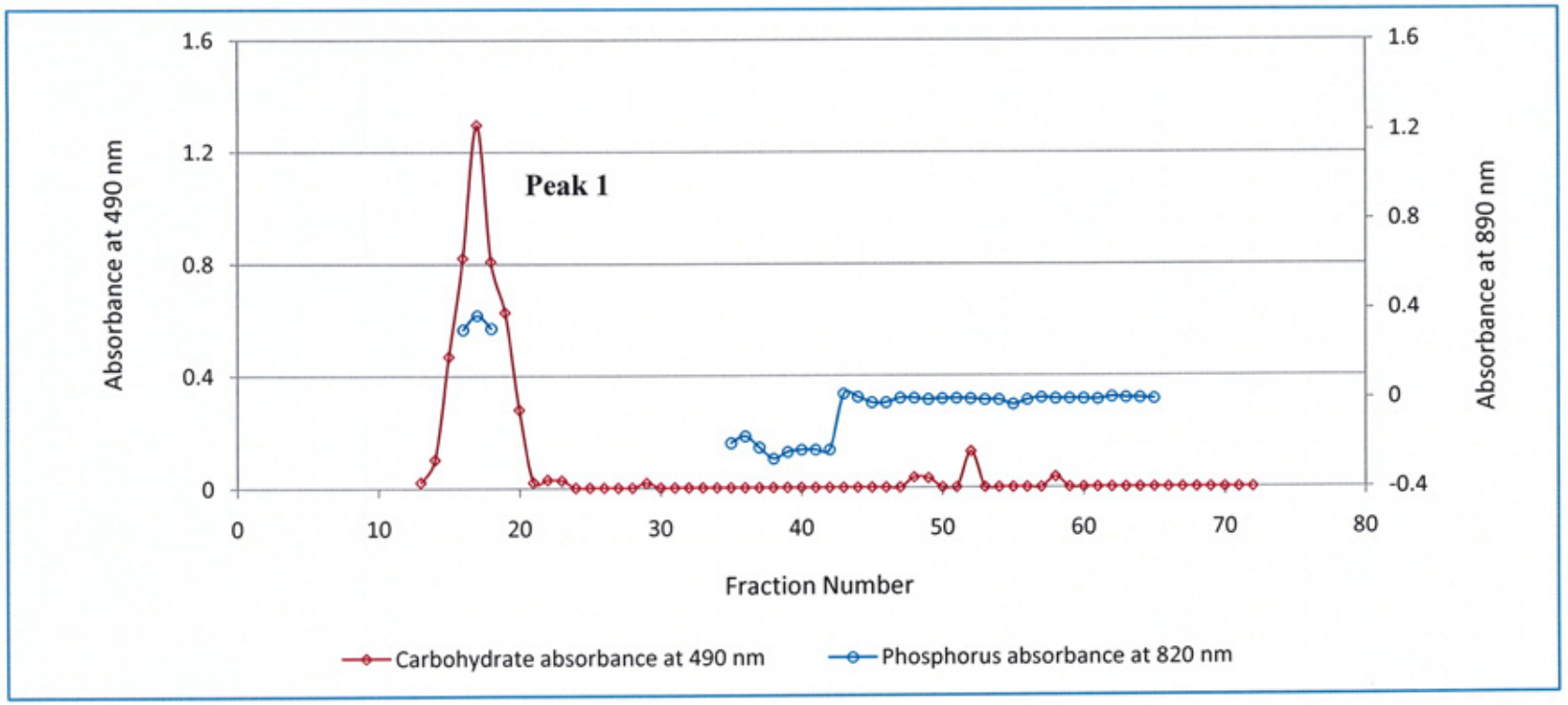

Figure 4.3. HIC profiles for the purification of a crude butanol extract from *R. xylanophilus*. The crude extract was loaded the column with equilibration buffer until fraction 12, after which gradient elution with an increasing concentration of propanol was begun. Column fractions (4 mL) were analyzed for carbohydrate and phosphorus.

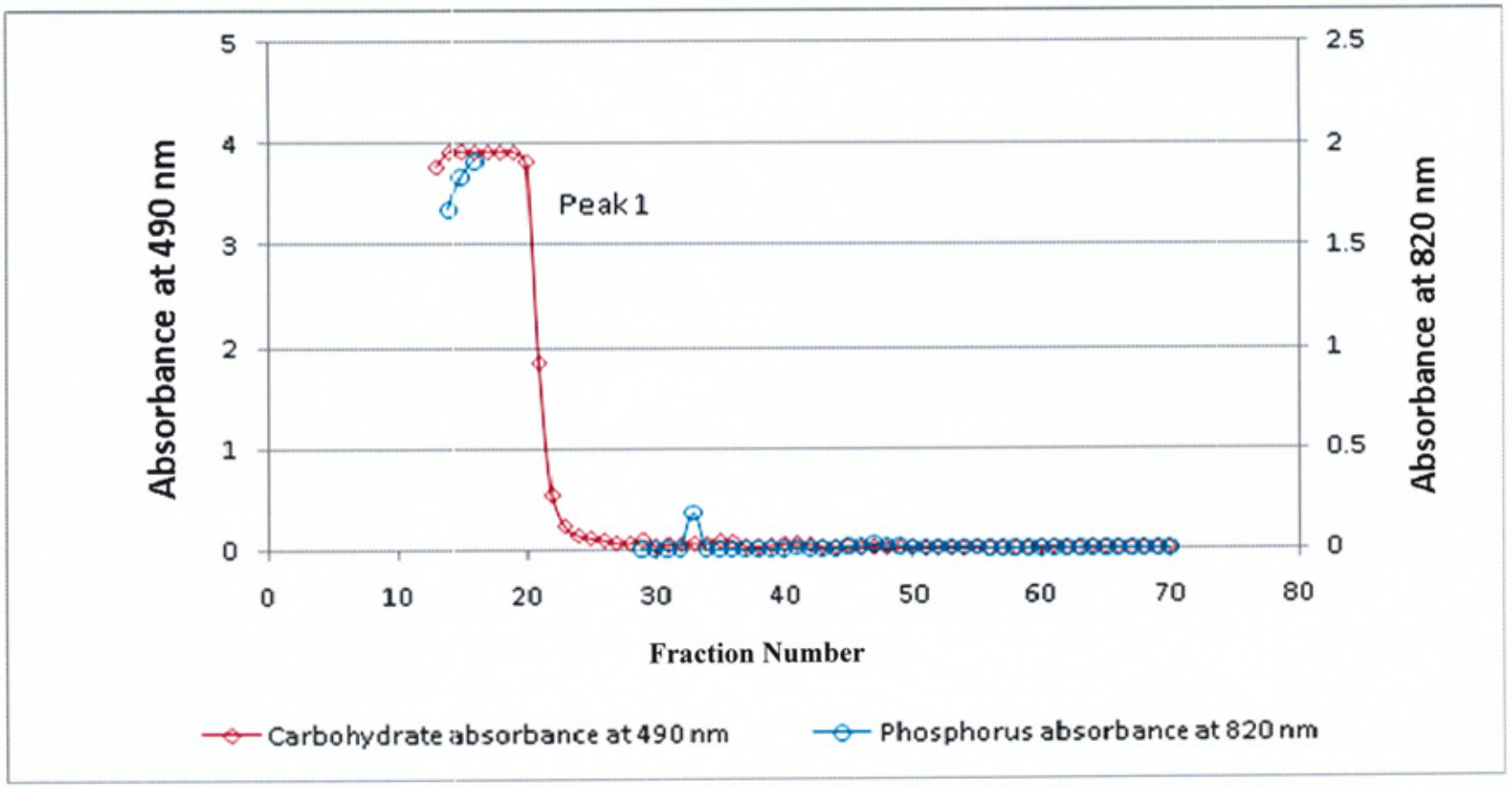

Figure 4.4. HIC profiles for the purification of a crude chloroform-methanol extract from *R. xylanophilus*. The crude extract was loaded the column with equilibration buffer until fraction 12, after which gradient elution with an increasing concentration of propanol was begun. Column fractions (4 mL) were analyzed for carbohydrate and phosphorus.

4.5.3. Fatty acid profile of *R. xylanophilus*

The fatty acid composition of the whole cells from *R. xylanophilus* was determined by FAME derivatisation and GC analysis (as described in chapter 2, Section 2.2.6.1), and the results are summarised in Table 4.2. The major fatty acids detected in whole cells were iC16:0, aiC18:0 and C18:0. These results are consistent with those of previous studies (Table 4.1). Comparison with the data of Carreto *et al.* (1996) is shown in Table 4.3. In previous studies, fatty acids including iC17:0, C17:0 and iC18:0 were identified which couldn't be identified by the present study. The present study detected minor amounts of the fatty acid TBS which hasn't been reported by previous studies although they have reported various different 'unknown' fatty acids to be present.

Table 4.2. Fatty acid composition of the whole cell fatty acids of *R. xylanophilus*.

FAME identified[a]	Sample 1	Sample 2	Sample 3
Unknown[b]	trace	4.8	4.5
iC16:0	17.7	10.9	15.2
C16:0	1.7	Trace	1.6
aiC17:0	1.8	Trace	2.4
aiC18:0	57.7	55.5	54.1
C18:0	19.4	28.8	19.8
TBS	2.2	Trace	2.4

[a] Fatty acids were analysed by GC of their methyl esters and identified by comparision with a mixture of 32 authentic standards, list has been given in Chapter 2, Table 2.13 (Sigma Chemical Co.; those FAMEs marked*) . Composition is given as the percentage of total integrated chromatographic peak areas. [b]Possibly 13 Methyl branched fatty acid, which is not present in standard (Chapter 2, Table 2.13). Composition is given as the percentage of total integrated chromatographic peak areas.

Table 4.3. Comparison of fatty acids composition with the whole cell fatty acids of *R. xylanophilus* at different temperature.

FAME identified[a]	**45 °C (Carreto, *et al.*, 1996)**	**55 °C (Experimental work; Table 4.2)**	**60 °C (Carreto, *et al.*, 1996)**
Unknown[b]	Not reported	tr-5	Not reported
iC16:0	9.8	11-18	12.4
C16:0	5.3	Tr-2	2.3
aiC17:0	1.9	Tr-2	1.7
aiC18:0	37.1	54-58	53.0
C18:0	13.1	19-29	20.0
TBS	Not reported	Tr-2	Not reported

[a] Fatty acids were analysed by GC of their methyl esters and identified by comparision with a mixture of 32 authentic standards for experimental work, list has been given in Chapter 2, Table 2.13 (Sigma Chemical Co.; those FAMEs marked*). [b]Possibly 13 Methylbranched fatty acid, which is not present in the standard mixture (Chapter 2, Table 2.13). Composition is given as the percentage of total integrated chromatographic peak areas.

4.5.4. The phylogenetic position of *Rubrobacter* genus within Gram positive bacteria

Almost complete 16S rRNA gene sequences of 72 organisms were collected from GenBank, assembled, compared and aligned using Molecular Evolutionary Genetics Analysis (MEGA) software version 4.0. (Tamuma, et al, 2007) as described in Section 2.6.4. The number of nucleotides (nt) included in the analysis for each organism are shown in Appendix III together with the corresponding GenBank accession numbers and species names.

The 16S rRNA gene tree based on the neighbour-joining algorithm shows the positions of the *Rubrobacter* (*R. xylanophilus*) within the evolutionary radiation encompassed by the 51 type species which represent 51 genera of Gram positive high G+C bacteria and 14 type species representing 14 genera of Gram positive low G+C bacteia. Seven other sequences representing the type genera and type species of *Deinococcus*, Cyanobacteria, two Proteobacteria, *Nitrospira*, *Thermotoga* and the phylum Aquificae are shown as out groups (Figure 4.5).

The position of the suborder *Rubrobacter* was found to be the earliest branch of the class Actinobacteria (Gram-positive , High G+C) and the position is not shown to be included within the Gram positive low G+C organisms as shown in Figure 4.5.

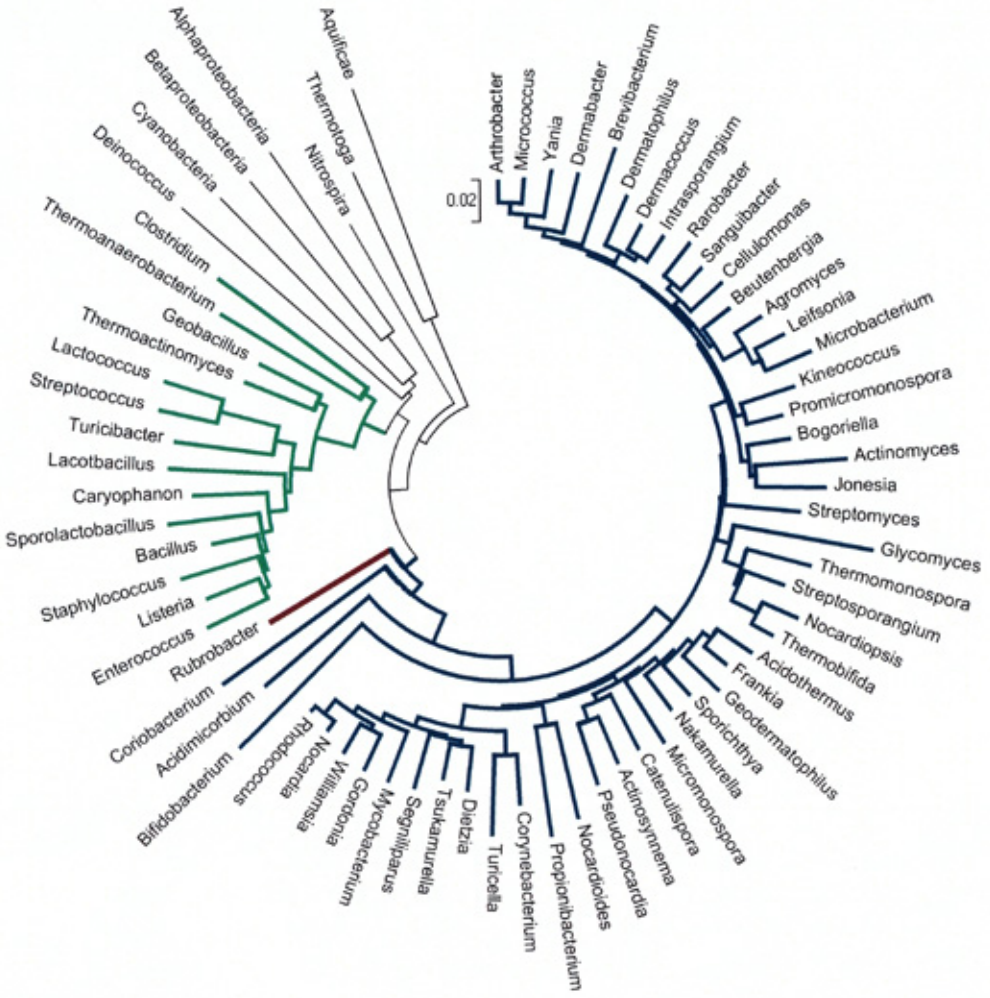

Figure 4.5. Neighbour–joining tree (Saitou & Nei, 1987) based on complete 16S rRNA gene sequences showing the position of *Rurbrobacter* (brown branch) with in the Gram positive high G+C (Actinobacteria, blue branches), Gram positive low G+C (Firmicutes, Green branches) and other branches represents Deinococcus, Cyanobacteria, Proteiobacteria, Nitrospira, Thermotoga and Aquificae phylum (black branches). The tree has been done using Molecular Evolutionary Genetics Analysis (MEGA) software version 4.0 (Tamuma, et al, 2007).

4.6. Bioinformatics analysis of the *R. xylanophilus* genome

The position of *Rubrobacter* as the deepest lineage of the phylum Actinobacteria (Stackebrandt *et al.*, 1997; Gao *et al.*, 2006; Kunisawa, 2007; Figure 4.5) with the bioinformatic studies of Gao and Gupta (2005) that demonstrated the absence of two signature sequences out of four signature sequences of Actinobacteria (described in Section 4.1) and present study, which showed the absence of any typical macroamphiphiles in *R. xylanophilus,* all reflect that the proposal that *Rubrobacter* is not a typical genus of the Actinobacteria.

To confirm the absence of typical macroamphiphiles, such as LTA and lipoglycans, genomic analyses were done by utilizing bioinformatics tools with the deposited genome sequence.

Since the LTA is a typical macroamphiphile and found to be present in *T. fusca* and some other thermophilic Gram-positive bacteria (discussed in Chapter three) and *R. xylanophilus* is an thermophilic actinobacteria, a BlastP search using NCBI Blast (http://www.ncbi.nlm.nih.gov/sutils/genom_table.cgi) was used to identify homologues of the proteins responsible for LTA biosynthesis, LtaA and LtaS (described detailed in Chapter one and section 1.7.3.3.2, Figure 1.19).

As shown in Table 4.4, although homologues of both proteins are present in the genomes of LTA containing Gram-positive low G+C bacteria (Firmicutes, which were used as a positive control), neither of these protein were encoded in the available genomes of Actinobacteria, except *R. xylanophilus.* The absence of both the genes in *T. fusca* and also *S. coelicolor* which have been proven to be LTA containing organisms, in the present project (Chapters 3, 6 and 8), could suggests that these genes may not be responsible for LTA biosynthesis or there may be an alternative biosynthesis pathway for LTA in the phylum Actinobacteria.

When LtaS was used a query, three distant hits were identified in *R. xylanophilus* genome, Rxyl_0662, Rxyl_0864 and Rxyl_0661, all of them were reported as sulfatase enzymes in the database annotation (EMBL and NCBI). LtaS also has been annoted as sulfatase enzyme in *S. aureus* and *S. agalactiae* (Grundling and Schneewind, 2007b). The significance of these homologues is therefore hard to define and they may not be orthologues of LtaS. Similarly, the presence of LtaA homologues may not be significant since it functions as a transporter in the cell membrane and so the homologues may be responsible for transport of other molecules rather than LTA biosynthesis precursors.

Generally, organisms where LTA is present have been reported to contain TA as SCWP (Sutcliffe, unpublished observations; Weidenmaier & Peschel, 2008), which has been also shown to be true for *T. fusca* (discussed in Chapter three) and *S. coelicolor* (discussed later in Chapter 6) of the phylum Actinobacteria. The TA biosynthetic pathway has been well established as discussed in

Chapter one, Section 1.6.2.1. A Blast search for TA biosynthesis genes was done against the *R. xylanophilus* genome and identified homologue for TagA, TagO , TagD and TagE. Homologues of these were also found in also TA lacking organisms, presumably for other related functions. However, there was no homologues found for TagB and TagF, which are responsible for the synthesis of the poly(GroP) polymer (Bhavsar *et al.*, 2004) and thus for TA biosynthesis (Chapter one, section 1.6.2.1). From the results in Table 4.5, it can be concluded that *R. xylanophilus* doesn't synthesis poly-GroP TA, which is consistent with the experimental results (data not shown). The experimental analysis following TA extraction (Chapter 2, section 2.4.1) was unable to detect any glycerol or any other sugar containing macromolecules by GC in *R. xylanophilus*.

The absence of LTA (experimental results presented here) with the absence of TA (experimental results and absence of *tag* gene homologues), also suggests that the LtaS homologues of *R. xylanophilus* are more likely to be homologues responsible for functions other than LTA biosynthesis.

To analyse for the presence of PI-LM or LAM lipoglycan, the *R. xylanophilus* genome was searched for homologues of the genes identified for lipoglycan biosynthesis in *M. tuberculosis*, (Table 4.6 & 4.7). For biosynthesis of PI and apolar PIMs, homologues of most of the *M. tuberculosis* proteins were detected in the *R. xylanophilus* genome, suggesting the species may have the capacity to synthesise PI and apolar PIMs. The presence of homologues of Rv3806 and Rv3791 (Table 4.6) also suggests the species may have the capacity to produce

undecaprenol-arabinose to provide an arabinose source at the outer surface of the membrane (discussed in Chapter one, section 1.6.5.2). However the absence of an EmbC (Rv3793) homologue in *R. xylanophilus* (Table 4.7), responsible for the initiation of LAM biosynthesis from LAM (Discussed in Chapter one, Section 1.7.5.2) suggest the species lacks the capacity to synthesise LAM. Undecaprenol-arabinose may be needed to synthesise a cell wall polymer but these have not yet been characterised in *R. xylanophilus*.

The only significant but different homologue of various mannosyl transferases involved in polar PIM/LM biosynthesis was Rxyl_0872 (Table 4.7), suggest R. xylanophilus lacks the range of glycosyl transferases needed to synthesis PI-LM, consistent with the experimental data.

Table 4.4 LtaS and LtaA (*S. aureus,* LTAS_STAA3, 646 a.a. and LTAA_STAA3, 396 a.a. respectively) homologues in the genomes of *R. xylanophilus* and other representative bacteria.

Organism	LtaS homologue	LtaA homologue
***R. xylanophilus* DSM 9941**	**Rxyl_0662** (630 a.a.) sulfatase Identities = 78/303 (25%) Expect = 1e-16 **Rxyl_0854** (674 a.a.) sulfatase Identities = 73/312 (23%) Expect = 1e-11 **Rxyl_0661** (646 a.a.) sulfatase Identities = 78/337 (23%) Expect = 5e-10	**Rxyl_0374** (433 a.a.) major facilitator superfamily MFS_1 Identities = 74/305 (24%) Expect = 6e-06 **Rxyl_0507** (450 a.a.) major facilitator superfamily MFS_1 Identities = 72/360 (20%) Expect = 1e-04
***B. subtilis* subsp. subtilis str. 168**	**BSU07260** (639 a.a.) Hypothetical protein Identity: 358/625 (57%) Expect = 0.0	**BSU07910** (391a.a.) Hypothetical protein Identities = 88/383 (22%) Expect = 1e-10
***S. agalactiae* A909**	**SAK_1414** (714 a.a.) (sulfatase) Identities = 268/658(40%) Expect = 2e-131	**SAK_1515** (389 a.a.) Drug:H+ antiporter-1 (DHA1) family protein Identities = 75/363 (20%) Expect = 3e-09
***L. monocytogenes* EGD-e**	**lmo0927** (653 a.a.) Hypothetical proteins Identities = 334/638(52%) Expect = 0.0	**lmo2826** (382 a.a.) Hypothetical proteins Identities = 85/374 (22%) Expect = 8e-14
***L. lactis* subsp. lactis Il1403**	**L13927** (722 a.a.) Hypothetical protein Identities = 251/671(37%) Expect = 2e-119	**L157472** (393 a.a.) ybfD, (Transporter) Identities = 76/373 (20%) Expect = 3e-09
***Enterococcus faecalis* V583**	**EF1264** (702 a.a.) Sulfatase Identities = 292/645(45%) Expect = 2e-155	**EF1078** (384 a.a.) Multidrug resistance protein Identities = 86/374 (22%) Expect = 2e-11
M. tuberculosis* H37Rv *as negative control (non LTA producer	**None**	**Rv1410c** (518 a.a.) Aminoglycosides/Tetracycline-transport integral membrane protein Identities = 40/178 (22%), Expect = 2e-04

Nt. a.a. means amino acids, only the closest homologue has been taken in account.

Table 4.5. TA biosynthesis genes homologue(s) in *R. xylanophilus* genome

Proteins name (*B. subtilis*)	***R. xylanophilus* homologue(s)**
BSU35690 (446 a.a.) **ggaA**	None
BSU35680 (900 a.a.) ggaB	None
BSU35750 (256 a.a.) **tagA**	**Rxyl_2691** (256 a.a.) Glycosyl transferase, WecB/TagA/CpsF family Identities = 59/211 (27%) Expect = 1e-19
BSU35760 (381 a.a.) **tagB**	None
BSU35770 (442 a.a.) **tagC**	None
BSU35740 (129 a.a.) **tagD***	**Rxyl_0711** (455 a.a.) RfaE bifunctional protein, domain II Identities = 45/133 (33%), Expect = 6e-11
BSU35730 (673 a.a.) **tagE***	**Rxyl_1939** (384 a.a.) glycosyl transferase Identities = 39/149 (26%), Expect = 3e-08
BSU35720 (746 a.a.) **tagF**	None
BSU35530 (358 a.a.) **tagO***	**Rxyl_3091** (327 a.a.) glycosyl transferase Identities = 82/300 (27%) Expect = 3e-23

** More homologues are present in R. xylanophilus, only the closest one has been mentioned.*

Table 4.6. PI and apolar PIMs biosynthesis enzyme (*M. tuberculosis*) homologue(s) in *R. xylanophilus*.

Reactions	**Gene name (*M. tuberculosis*)**	***R. xylanophilus* homologue(s)**
PI/precursor synthesis		
Phosphomannomutase	Rv3257c (465 a.a.)	**Rxyl_1134** (472 a.a.) Identities = 210/445 (47%) Expect= 2e-106
Ins-1-phosphate synthase	Rv0046, Ino1 (367 a.a.)	**Rxyl_0688** (443 a.a.) Identities = 30/107 (28%) Expect = 6e-04
Inos-1-P phosphatase	Rv1604, ImpA (270 a.a.)	**Rxyl_1545** (259 a.a.) Identities = 85/246 (34%) Expect = 2e-25
PI synthase CDP-DAG + inositol → PI	Rv2612c, PgsA (217 a.a.)	**Rxyl_2978** (201 a.a.) Identities = 63/189 (33%) Expect = 4e-20
PI/precursor synthesis		
DAG → Phosphatidate	Rv2252 (309 a.a.)	**Rxyl_1713** (312 a.a.) Identities = 92/304 (30%), Expect = 4e-23
	Rv3218 (321 a.a.)	**Rxyl_1713** (312a.a.) Identities = 83/326 (25%), Expect = 9e-09
PI to PIMs cytoplasmic (apolar PIM biosynthesis)		
PI → PIM_1	Rv2610c, PimA (378 a.a.)	**Rxyl_2620** (385 a.a.) Identities = 157/393 (39%) Expect = 3e-59
PIM_1 acyltransferase	Rv2611c (316 a.a.)	Absent
PI to PIMs cytoplasmic (apolar PIM biosynthesis)		
PIM_1→ PIM_2	Rv2188c, PimB' (385 a.a.)	**Rxyl_0383** (377 a.a.) Identities = 159/359 (44%) Expect = 6e-61
PIM_2→ PIM_3/ PIM_4	PimC, MT1800 (381 a.a.) or other Mannosyl transferase	**Rxyl_1298** (374 a.a.) Identities = 77/238 (32%) Expect = 2e-19

Table 4.7. Polar PIMs, LM and LAM biosynthesis genes (*M. tuberculosis*) homologue(s) in *R. xylanophilus*

Reactions	**Gene name (*M.. tuberculosis*)**	***R. xylanophilus* homologue(s)**
Lipid linked precursor synthesis (for transfer from the inner membrane to outer surface)		
C35P (polyprenol) → C35P-mannose	Rv2051c (874 a.a.)	Absent
	MSMEG_3860 (615 a.a.) CN hydrolase domain (≡ N-terminus of Rv2501c)	Absent
	MSMEG_3859 (265 a.a.) (≡ C-terminus of Rv2501c)	**Rxyl_1238** (340 a.a.) Identities = 80/242 (33%) Expect = 2e-18
Lipid linked precursor synthesis (for transfer from the inner membrane to outer surface)		
C35P-ribose synthase	Rv3806 (302 a.a.)	**Rxyl_1966** (301 a.a.) Identities = 95/279 (34%) Expect = 3e-39
C35P-ribose → C35P-arabinose epimerase	Rv3790 (461 a.a.)	**Rxyl_3087** (752 a.a.) Identities = 50/187 (26%) Expect = 3e-09
	Rv3791 (254 a.a.)	**Rxyl_2474** (263 a.a) Identities = 63/216 (29%) Expect = 4e-10
Convert apolar PIMs to Polar PIMs or LM (extracytoplasmic)		
LpqW feeds PIM_4 to LM	Rv1166 (635 a.a.)	**Rxyl_0872** (541 a.a.) Identities = 57/284 (20%) Expect = 2e-07
PIM_4→ PIM_5 (PIM branch rather than LAM)	Rv1159, PimE (431 a.a.)	**Rxyl_2872** (393 a.a.) Identities = 90/339 (26%) Expect = 6e-07
Mannan extension	Rv2174, MptA (516 a.a.)	**Rxyl_2872** (393 a.a.) Identities = 77/318 (24%) Expect = 6e-06
	Rv1459c (591 a.a.)	Absent
Convert apolar PIMs to Polar PIMs or LM (extracytoplasmic)		
Mannan branches	Rv2181(427 a.a.)	**Rxyl_2872** (393 a.a.) Identities = 93/389 (23%) Expect = 5e-10
Arabinan addition		
LM-$Arabinose_1$→ LAM	Rv3793,EmbC (1094 a.a.)	Absent
Capping/ substituents		
Mannose capping	Rv1635c (556 a.a.)	Absent

4.7. Discussion

The purpose of the present study was to identify any macroamphiphiles in *R. xylanophilus* and compare this phenotypic characteristic with other Actinobacteria and thermophilic Gram-positive bacteria.

The coccoid, spherical or rod shape and pink colony appearance of *R. xylanophilus* on TM-agar plates was observed also in previous studies (Ferreira *et al.*, 1999, Chen *et al.*, 2004). More over uniform pink colour colonies in the plates and higher optimum temperature prevent the growth of other lab contaminant organisms, e.g. *E. coli* with *R. xylanophilus* broth and the microscopic Figure 4.1 is distinct from the filamentous thermophilic organism of *T. Fusca*, the only likely contaminant in the lab at higher temperature. Furthermore FAME profile shows similarity with previous studies of *R. xylanophilus* suggesting the organism hasn't been contaminated. Growth on agar-plates was difficult due to the evaporation of the liquid from the plate at the high temperature of incubation: plates were therefore sealed with cellophane tape to resist the evaporation, but growth was still very poor, possibly due to the restricted aeration.

In liquid culture, the growth took 48 h to produce maximal amounts of cells and the yield was quite good (1.5 g dry cell/ litre). The pink colour of the organism made it easy to determine the purity of the organism; though the colour became lighter with time; the Gram staining and the fatty-acid profile by GC proved that there were no contamination in the lighter pink colour samples.

Growth at 55°C should also reduce the possibility of contamination with mesophilic bacteria.

The major fatty acid profile obtained here (Table 4.2) was consistent with previous studies (Table 4.3), although some of the minor fatty acids were not identified. Notably, the significant content of aiC18:0 is a distinguishing characteristic of *R. xylanophilus*. The increased branched chain fatty acid content with temperature was observed in present study compared to the data previously reported by Carreto *et al.* (1996) and Chen *et al.* (2004) study for cells grown below 55°C.

The dry cells of *R. xylanophilus* were subjected to the hot phenol-water procedure to extract macroamphiphiles. Following dialysis and lyophilisation, and purification by HIC using FPLC machine showed that hydrophilic contaminants were washed through the column with the equilibrium buffer and some starting of the gradient (Peak 1 in Figure 4.2). However, unusually, the propanol gradient failed to elute any significant carbohydrate and/or phosphate containing material, suggesting that no macroamphiphilic component was present (e.g. compare Figure 3.2, peak 2) and to ensure this result the experiment was repeated several times (Appendix III). To explore this possibility further, freeze-dried cells of *R. xylanophilus* were also extracted using the butanol-water method which has been used previously to extract LTA from Gram-positive bacteria and LPS from various Gram-negative bacteria (Morrison and Leive, 1975, Morath *et al.*, 2001, Theilacker *et al.*, 2006). Again, following application of the extract to the HIC column, elution with an

increasing propanol gradient failed to elute any significant carbohydrate and/or phosphate-containing material (Figure 4.3). Finally, the F antigen (LTA) of *Streptococcus pneumoniae* has been shown to partition anomalously during standard phenol-water extraction (Behr *et al.*, 1992). Therefore, a modification of the chloroform-methanol based extraction method which has been used to extract pneumococcal F antigen (Behr *et al.*, 1992) was used with *R. xylanophilus* cells. As with previous attempts, chemical analysis of fractions following HIC purification indicated that this method had also failed to recover macroamphiphilic carbohydrate and/or phosphate containing material from freeze-dried cells of *R. xylanophilus* (Figure 4.4). Therefore, it can be concluded that *R. xylanophilus* does not synthesise significant quantities of a carbohydrate and/or phosphate containing macroamphiphile. This is a highly unusual finding: virtually all studies that have examined extracts of Gram-positive bacteria for LTA or lipoglycans have recovered one or other of these macroamphiphiles. The only previous reports of the absence of LTA or related macroamphiphile from Gram-positive bacteria are studies of some *Bacillus* spp. *Bacillus* sp. A007 failed to turnover radiolabelled phosphatidylglycerol into PGP-LTA although the presence of an alternative macropamphiphile was not investigated (Koga *et al.*, 1984). Likewise, strains of *Bacillus polymyxa* (now *Paenibacillus polymyxa*) and *Bacillus circulans* lack PGP-LTA (Iwasaki *et al.*, 1989). However, neither of these studies used HIC to distinguish macroamphiphiles from other non-lipidated cellular components and so the absence of structurally variant (non-PGP) LTA or lipoglycans in these species needs definitive confirmation.

The absence of LTA or lipoglycan or any other typical macroamphiphiles in *R. xylanophilus* is a very unusual and distinctive finding, especially for justifying the present taxonomic position of this bacterium. Moreover, the genomic analysis via bioinformatics agrees with the experimental results for the absence of typical macroamphiphiles. The bioinformatics analysis suggests the likely presence of apolar PIMs which may compensate to some extent for the function of a macroamphiphile. Therefore, studies of the glycolipids (especially PIMs) and their functions in cell membrane will be an interesting project for this organism lacking of macroamphiphiles.

The phylogenetic tree based on 16S rRNA gene sequences shown in Figure 4.5 shows the position of *R. xylanophilus* as the deepest lineage of Actinobacteria phylum but the position doesn't intermingle with representatives of the phylum Firmicutes. The chemotaxonomic data regarding cell envelope, such as that presented herein, are useful for defining the classification of many taxa of both Firmicutes and Actinobacteria. It is notable that representative of most lineages phylogenetically placed within the Firmicutes contain LTA (discussed in Section 1.7.2). The absence of LTA and the 16S rRNA gene sequence analysis suggest that the organism does not belong to this Gram-positive subgroup. On the other hand, the placement of *R. xylanophilus* in the class Actiobacteria in Figure 4.5 agrees with previous studies (Carreto *et al.*, 1996, Stackebrandt *et al.*, 1997, Gao and Gupta, 2005). The lack of macroamphiphiles in *R. xylanophilus* suggest the members of this genus are not typical actinobacterial species, which agree with the studies of Gao & Gupta (2005), which showed that out of four signature sequences (Cox1, CTP synthetase, 23S rRNA and

GluRS) of Actinobacteria two of them (Cox1, CTP synthetase) are missing. So, the present data agrees with the position of the genus *Rubrobacter* as the deepest lineage of the Actinobacteria.

Thus the apparent absence of either LTA or lipoglycan in the membranes of *R. xylanophilus* is intriguing given the presumed functional importance of macroamphiphiles in the membranes of Gram-positive bacteria and notable given the phylogenetic position of the genus *Rubrobacter*. The result also contradicts the presence of LTA in *T. fusca* and other thermophilic Gram-positive bacteria (Iwasaki *et al.*, 1986, Card and Finn, 1983), suggesting LTA is not essential for membrane function during growth of Gram-positive bacteria at higher temperatures. These findings regarding *R. xylanophilus* are of obvious significance when considering the physiological functions of LTA and lipoglycans, which as yet remain to be fully determined (Fischer, 1994a, Sutcliffe, 1994b, Sutcliffe, 2005, Grundling and Schneewind, 2007b).

CHAPTER FIVE

Investigation of macroamphiphiles in

Kineococcus radiotolerans

5.1. Introduction

5.1.1. Isolation and Taxonomy

Kineococcus radiotolerans was first isolated from a high level radioactive environment, the Savannah River Site in Aiken, South Carolina, USA (Phillips *et al.*, 2002). BLAST analysis of the 16S rRNA gene sequence showed 93% similarity with the only validly published species of the genus *Kineococcus*, *Kineococcus aurantiacus* RA 333^T (Yokota *et al.*, 1993) though the DNA-DNA hybridization analysis revealed only 31% similarity between the strains. The *K. radiotolerans* 16S rRNA gene sequence also showed a high level of similarity with uncharacterized and validly published Mojave Desert isolates AS3635, AS2960, AS3641, AS3079 and AS2987 (GenBank accession numbers AF060694, AF060673, AF060695, AF060682 and AF060672, respectively) (Phillips *et al.*, 2002).

The high (93%) 16S rRNA sequence identity and low DNA similarity (revealed by DNA-DNA hybridization) with the type species *K. aurantiacus*, allowed *K. radiotolerans* to be classified into genus *Kineococcus* as a separate species (Phillips *et al.*, 2002). In a subsequent study of Lee (2006), the 16S rRNA similarity showed a higher similarity value (98.9%) for *K. aurantiacus* and *K. radiotolerans* and also another novel species, *Kineococcus marinus*,

was identified with 93.0-93.4% similarity values to the other members of the genus *Kineococcus* and slightly lower similarity values (93.1~93.8%) to the members of the genus *Kineosporia*. *K. aurantiacus*, the type species of the genus *Kineococcus* was originally included in the family Pseudonocardiaceae based on the production of majority iso- and anteiso- branched chain fatty acids (Embley *et al.*, 1988), which were also reported in *K. radiotolerans* (mainly aiC15:0) (Phillips *et al.*, 2002). However, phylogenetic analysis led to the proposal that the signature sequence of the 16S rRNA of suborder Pseudonocardiaceae was not conserved in *K. radiotolerans* and also poorly matched with *K. aurantiacus*, and that the members of the genus were more closely related to the suborder Frankineae (Stackebrandt *et al.*, 1997). For this reason the *Kineococcus* had been reconsidered as a novel genus and included in the suborder Frankineae, suggested as a new family "Kineosporiaceae" with two other genera, *Cryptosporangium* and *Kineosporia* (Stackebrandt *et al.*, 1997, Euzéby, 2008). However, the position of the genera *Kineococcus* and also *Kineosporia* still remains uncertain at the hierarchic classification above the family level. Thus further studies are required, especially for the investigation of the phenotypic characteristics of the members of these genera.

Presently, *K. radiotolerans* had been classified as follows (Euzéby, 2008):

Phylum: Actinobacteria

Class: Actinobacteridae

Order: Actinomycetales

Suborder: Frankineae

Family: Kineosporiaceae

Genus: *Kineococcus*

Species: *Kineococcus radiotolerans*

The *K. radiotolerans* genome has been sequenced by the DOE Joint Genome Institute but has yet to be formally published. It apparently possesses a single 4.89396 Mbp genome with 4559 protein coding genes (NCBI, URL: http://www.ncbi.nlm.nih.gov/sites/entrez?Db=genomeprj&Cmd=Search&TermToSearch=txid266940[orgn]). The G+C content of the *K. radiotolerans* genome is 74.2 mol% (Bagwell *et. al.*, 2004), which is slightly higher than the G+C content (73.3 mol %) of *K. aurantiacus* (Yokota *et al.*, 1993).

5.1.2. Morphological, Cultural and Physiological Characteristics

Virtually the only information on *K. radiotolerans* is that in the species description (Phillips *et al.*, 2002). *K. radiotolerans* is an orange pigmented, aerobic, coccus shaped bacterium with 1.0-1.5 μm in diameter. The cells occur in pairs, tetrads and in larger symmetrical clusters (10 mm in diameter). Approximately 1% of the cells were observed to be motile within a broth and produced polar flagella which were observed by electron microscopy (Phillips *et al.*, 2002).

One major characteristic feature of *K. radiotolerans* is the dramatic change observed in colony morphology with age on plating medium. Young colonies were moist, smooth and round, but there was a transition into a rough, dry, raised colony mass of irregular shape over prolonged incubation. The mature colony morphology was considered strikingly similar to that of *M. tuberculosis*. *K. radiotolerans* thin sections revealed a thick extracellular polymer shell surrounding individual cells within cluster formations (Phillips *et al.*, 2002).

The physiological characteristics of *K. radiotolerans* were quite similar or comparable to *K. aurantiacus*. Both the species showed no cytochrome C oxidase, urease activity but the catalase activity was positive (Phillips *et al.*, 2002). The temperature range for growth of *K. radiotolerans* was 11 to 41 °C in PTYG medium, with an optimum temperature of 32°C (doubling time 2.5 h) (Phillips *et al.*, 2002), which was comparable to those of *K. aurantiacus*

(Yokota et al., 1993). Though both the species grew between pH 5 and 9, and in the presence of up to 5% NaCl (w/v) and 20% glucose (w/v) (Phillips *et al.*, 2002), *K. aurantiacus* grew at a broader pH range between pH 4.5 and pH 9.5 (Yokota *et al.*, 1993). *K. radiotolerans* can utilise glucose, galactose, L-arabinose, sucrose, mannose, xylose, glycerol, mannitol, inositol and sorbitol as carbon sources but was unable to utilize ribose and citrate, which differentiated it from *K. aurantiacus* (Phillips *et al.*, 2002). On the other hand, the inabililty to utilise lactose, maltose, rafinose, rhamnose and ribose differentiated it from *K. marinus* (Lee, 2006). The positive urease enzyme activity in *K. aurantiacus* was absent in both *K. radiotolerans* and *K. marinus* (Lee, 2006) .

The fatty acid profile of *K. radiotolerans* was characterised by the predominance of aiC15:0 (90%), which was similar to the value of 88.7% reported for *K. aurantiacus* by Yokota *et al.* (1993), with other minor fatty acids of chain length between C14 and C18. Though the fatty acid pattern in the new species of *K. marinus* was similar and aiC15:0 was the major fatty acid, the relative percentage was only 54.4%, quite low compared to the other two species (Lee, 2006). Surprisingly, the GC analysis originally suggested the presence of arachidonic acid (C20:4) and 19-24 carbon chain length alkenes (approximately 70% were 21- and 22-C chain length alkenes) in *K. radiotolerans*, but subsequent GC-MS could not detect any C20:4 (Phillips *et al.*, 2002).

The nature of the isoprenoid present in *K. radiotolerans* is still to be revealed but all three *Kineococcus* species produce an orange pigment (Phillips *et al.*, 2002, Lee, 2006). The orange pigment of the cells was found to be soluble in methanol and the extracted pigment contained absorption peaks at approximately 444, 471 and 501 nm, as with pigment which was also extracted from *K. aurantiacus*, suggesting the pigment was a carotenoid (Kleinig *et al.*, 1970).

The other general biochemical characteristics, like presence of meso-diaminopimelic acid in the peptidoglycan and apparently AG polymer present in the cell wall, along with the absence of mycolic acids, in all these three species defined the members of the genera *Kineococcus* and differentiates them from the members of the closely related genus *Kineosporia (Phillips et al., 2002, Yokota et al., 1993, Itoh et al., 1989, Kudo et al., 1998, Lee, 2006)*. For *K. marinus,* MK-9 was found to be the predominant menaquinone and PtdG, PI were detected as polar lipids (Lee, 2006), but for the other two species the menaquinones and apolar PIM precursor have yet to be revealed.

5.1.3. Radiation & dessication resistance abilities

K. radiotolerans possesses a remarkable resistance to acute and chronic exposure to ionizing γ-radiation and prolonged desiccation (Phillips *et al.*, 2002). This species was more resistant to radiation than *K. aurantiacus* but showed an intermediate level of radiation resistance compared with *Deinococcus radiodurans* and *Escherichia coli* (Phillips *et al.*, 2002). However, *K. radiotolerans* had retained relatively higher viability than *D. radiodurans* following long term desiccation. A relation was observed between uptake of transition metals, ionizing radiation resistance and oxidative stress. During chronic radiation, copper supplementation increased the colony formation of *K. radiotolerans*, which was also weakly induced by both iron and manganese supplementation, whereas cobalt was inhibitory to the growth in presence or absence of irridation (Bagwell *et al.*, 2008). *Kineococcus*-like organism 16S rRNA gene sequences were also reported to be found in arid environments like the Mojave desert (Garrity and Searles, 1998) and samples collected in the northern Caribbean following African dust storm events (Griffin *et al.*, 2003). This suggests that resistance to desiccation may be an important feature of these organisms. Moreover, high resistance to ionizing radiation, desiccation, and oxidative stress may make *K. radiotolerans* potentially useful for *in situ* biodegradation of problematic organic contaminants from highly radioactive environments.

5.2. The significance of studying *K. radiotolerans* macroamphiphile composition

Characteristics of the cell membrane have always been an important consideration for the classification of bacteria, especially the major menaquinones, phospholipid composition and fatty acid profiles. It has been proposed that the discontinuous distribution of macroamphiphilic components within the Gram-positive phylum may have chemotaxonomic value (Sutcliffe, 1994b), which suggests that identifying the macroamphiphile in *K. radiotolerans* may have a value in clarifying the position of the genus *Kineococcus* in the phylum Actinobacteria.

Secondly, studying the cell membranes of radiotolerant organisms is of biotechnological interest. The present study will give us opportunities for functional and comparative genomic exploration into macroamphiphile biosynthesis, since it may be possible to correlate the chemical composition of the macroamphiphile with the presence of specific glycosyltransferases in the sequenced *K. radiotolerans* genome.

Moreover, due to the completion of whole genome sequences for other radioresistant microorganisms such as *D. radiodurans*, the study of macroamphiphiles may give an opportunity to find out the functional aspects of these macromolecules in cell membrane of radiotolerant organisms.

5.3. Results

5.3.1. Organism and culture conditions

K. radiotolerans strain SRS30216 (the genome sequenced strain) was successfully grown in liquid tryptone-yeast-glucose based (TYG) medium at 32°C and 100 x g. On agar plates (TYG medium, Section 2.1.2.4), the orange colonies appeared after 48 h at 32°C but the growth took place at the heavily inoculated part of the plate only.

Growth curve experiments showed the growth of the *K. radiotolerans* reached its maximum level after 24 h in small scale cultures (100 ml), Figure 5.1 & Table 5.1. The dispersed cells appeared after 8 h of the inoculation, but pellets or clumps appeared after 20 h. With time, the dispersed cells decreased and the cell pellet increased and became sticky.

Gram staining of the cell was observed at 100x magnification under an oil immersion lens as shown in the Figure 5.2. The purple-stained cells of *K. radiotolerans* proved the bacterium was Gram-positive and also confirmed the purity of the culture and the coccoid shape represented the classical shape of the bacterium.

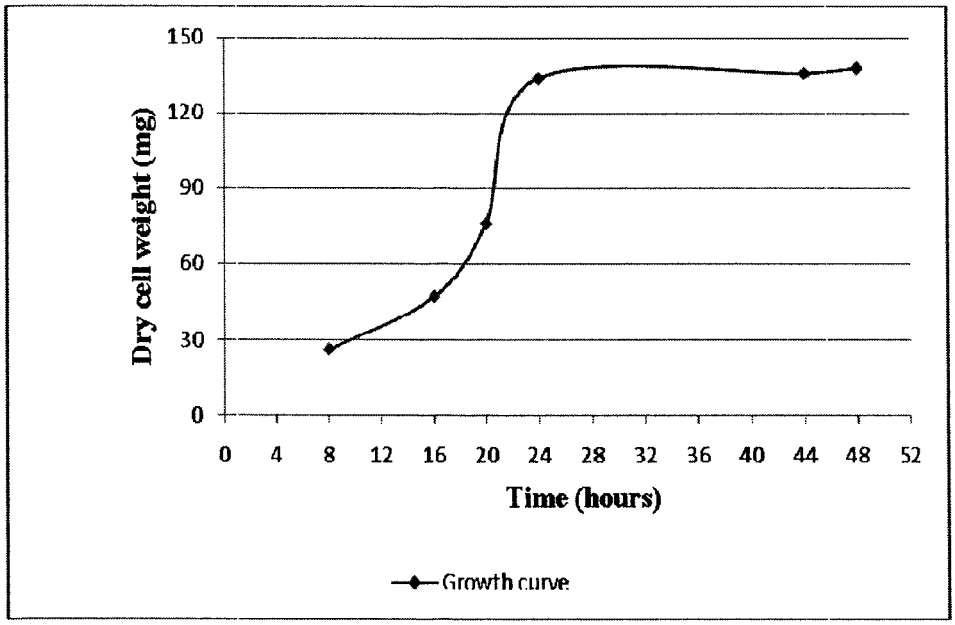

Figure 5.1. Growth curve depending on the dry cell weigh (mg) yielded vs time (h). The exponential phase was between 16 and 24 h after inoculation.

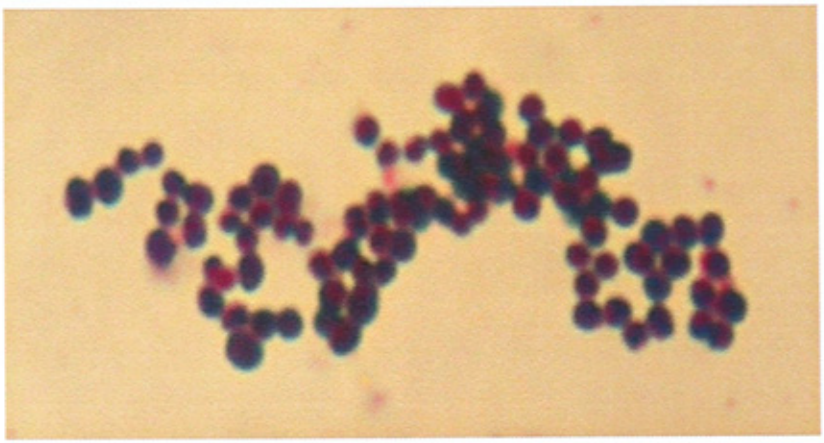

Figure 5.2. Gram staining picture of *K. radiotolerans* showed coccoid shape bacterium and classical purple colour of the Gram-positive bactieria, taken at 100X magnification under oil immersion lens.

Table 5.1. Time scale experiment for *K. radiotolerans,* small culture (100 ml) TYG media at 30°C and 100 x g.

Time (h)	**TYG media amount (ml)**	**Physical properties**		
		Colour	**Appearance**	**Dry weight (mg)**
8	100	Orange	Disperse	26
16	100	Orange	Disperse	47
20	100	Orange	Clump, floating	76
24	100	Orange	Clump, pellet	134
44	100	Orange	Clump, pellet	136
48	100	Orange	Clump, pellet, sticky	138
72	100	Orange	Clump, pellet, sticky	137

5.3.2. Purification of the *K. radiotolerans* macroamphiphiles

Macroamphiphilic material was extracted from *K. radiotolerans* in two ways, the standard hot phenol-water extraction method (described in Chapter 2, Section 2.1.5.1) and the recently described butanol extraction method (Section 2.1.5.2). Following the hot phenol-water extraction method, the extracted macroamphiphiles were purified by HIC-FPLC column chromatography (methodology section 2.1.6.1), fractions from which were subjected to carbohydrate and phosphate assays (methodology described in Section 2.1.7.1 & 2.1.7.2). The HIC elution profile for a representative hot phenol-water extraction is shown in Figure 5.3. Hydrophilic contaminants (nucleic acids, proteins and polysaccharides) not retained by the HIC column were recovered during the elution with equilibration buffer as the peak 1 region. Subsequent gradient elution with an increasing concentration of propanol recovered a minor and a major macroamphiphilic carbohydrate and phosphate containing peaks (Peak 2 and Peak 3; Figure 5.3). In both the peaks, the amount of phosphate was minimal compared to the amount of carbohydrate, which was consistent with the presence of lipoglycan (Sutcliffe, 1995, Sutcliffe, 1997, Fischer, 1994b). The experiments were repeated several times and the results were consistent between HIC runs (Data shown in Appendix IV).

Dot-immunoblotting (method described in Chapter 2, Section 2.1.7.3) with a polyclonal anti-LAM (Table 2.12) was done for the recovered fractions and no reaction was observed (data not shown).

Following the butanol extraction method, the extract was also purified by HIC column chromatography and fractions were also subjected to carbohydrate and phosphate assay. Hydrophobic contaminants not retained by HIC column were recovered in the peak 1 region, as shown in the Figure 5.4, and the single macroamphiphile peak contained significant amounts of carbohydrate and minimal amounts of phosphate, which was consistent with the hot phenol-water extraction (the peak is similar to peak 3 in Figure 5.3).

Peak 3 fractions from the hot phenol-water extraction were recovered by freeze-drying after extensive dialysis and represented 0.08% of the dry cell weight but the peak 2 material recovered was insufficient to quantify. In the butanol extraction method, approximately 13.4 g wet weight of cells was used, which represents approximately 1.34 g of dry cells (assumed to be 10% of wet cells), and following purification by HIC, approximately 4.3 mg of crude butanol extract was obtained from peak 2, which thus represents approximately 0.34% of the cell weight.

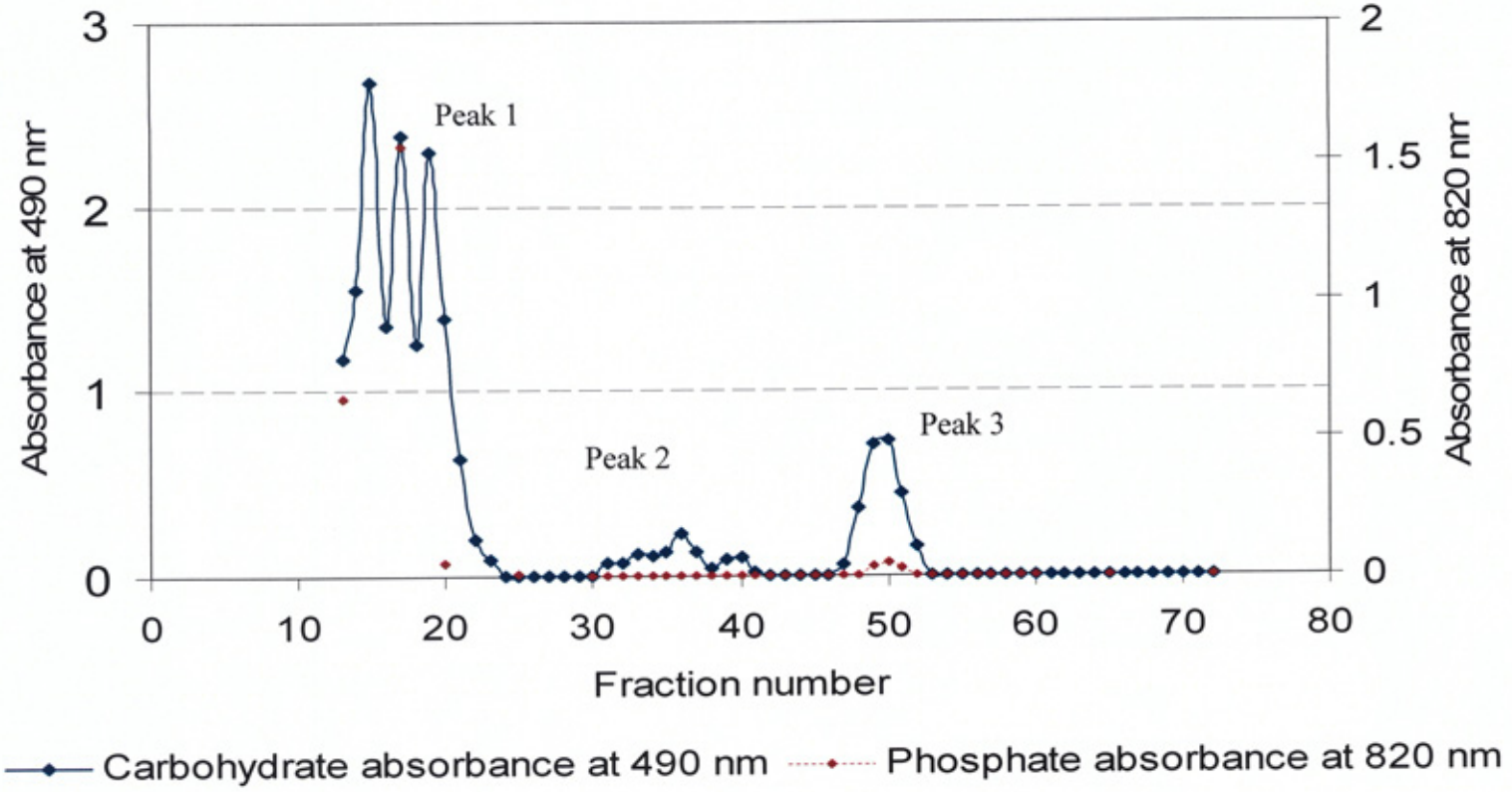

Figure 5.3. HIC profile for the purification of a representative crude hot phenol-water extract from *K. radiotolerans*. The crude extract was loaded the column with equilibration buffer until fraction 12, after which gradient elution with an increasing concentration of propanol was begun. Column fractions (4 mL) were analyzed for carbohydrate (—◆—) and phosphorus (···◆···).

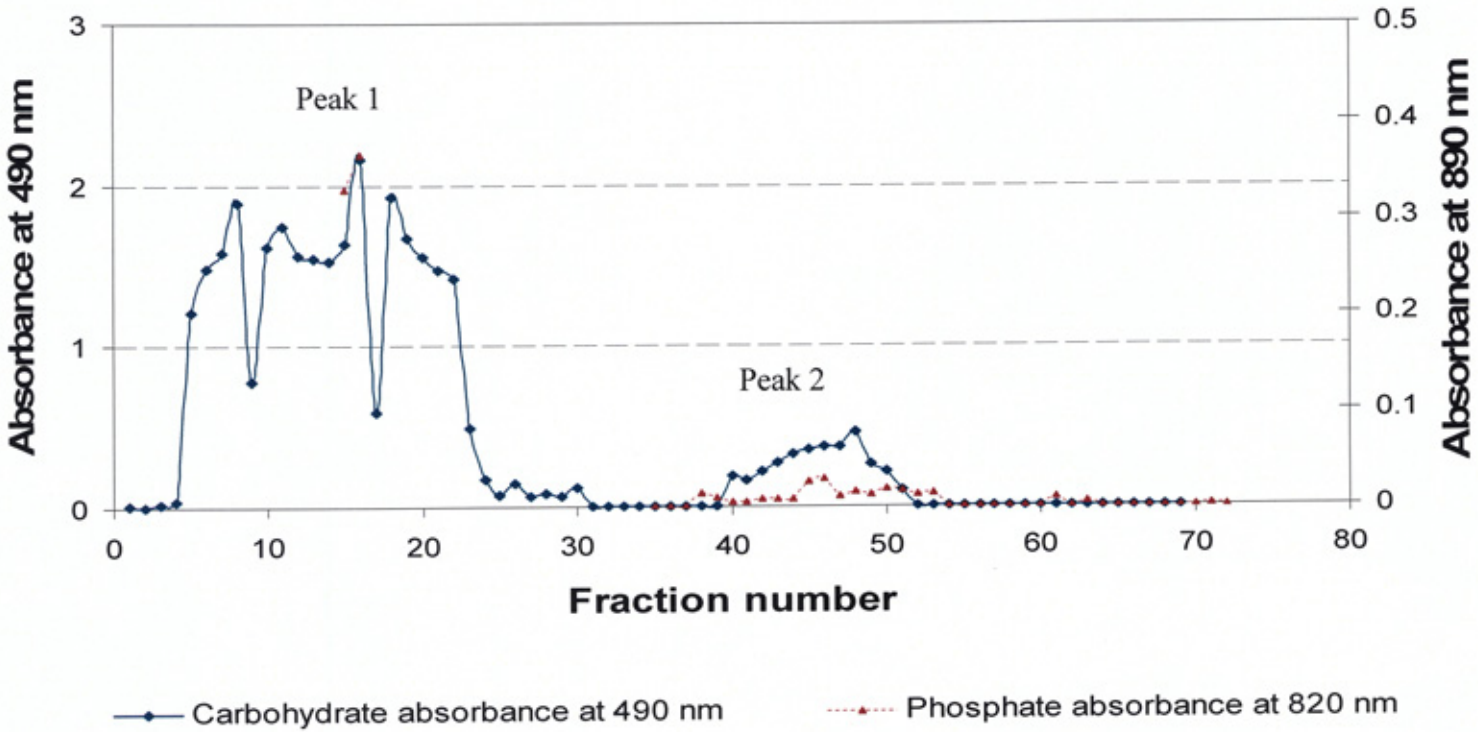

Figure 5.4. HIC profile for the purification of a crude butanol extract from *K. Radiotolerans*. The crude extract was loaded the column with equilibration buffer until fraction 12, after which gradient elution with an increasing concentration of propanol was begun. Column fractions (4 mL) were analyzed for carbohydrate (—◆—) and phosphorus (···▲···).

5.3.3. Chemical composition of the macroamphiphilies

Chemical analysis from carbohydrate and phosphate tests indicated that the *K. radiotolernas* macroamphiphile contained minimal phosphorus compared to the amount of carbohydrate. Protein contamination was assayed using a commercial kit (Section 2.4.2) for purified lyophilized peaks and determined to be below the level of detection.

The fatty acid composition of the whole cells and macroamphiphiles from *K. radiotolerans* were determined by FAME derivatisation and GC analysis (described in chapter 2, Section 2.2.6.1), and summarised in Table 5.2. The major fatty acid detected in the whole bacterial cells was aiC15:0. Peak 2 from the phenol-water extraction HIC purified column (Figure 5.3) did not contain any detectable fatty acid which suggests the peak may not contain any macroamphiphile and might be a hydrophilic contaminant, although the amount of material may have been below the level of detection. FAME analysis of Peak 3 from the hot phenol-water extraction (Figure 5.3) and peak 2 from the butanol extraction method (Figure 5.4) showed aiC15:0 as the major fatty acid, similar to the whole cells GC profile (Figure 5.5, Figure 5.6 and Table 5.2).

The sugar composition of the macroamphiphile(s) from Peak 3 of the phenol extracted (Figure 5.3) and peak 2 of the butanol extracted HIC-purified material (Figure 5.4) was determined following acid hydrolysis to release monosaccharide components and derivatisation to alditol acetates for GC, as described in Chapter 2, Section 2.2.6.2. As shown in Figure 5.7 & Table 5.3 in

both cases, the macroamphiphile(s) contained glycerol, arabinose, mannose, galactose and glucose as their predominant sugars.

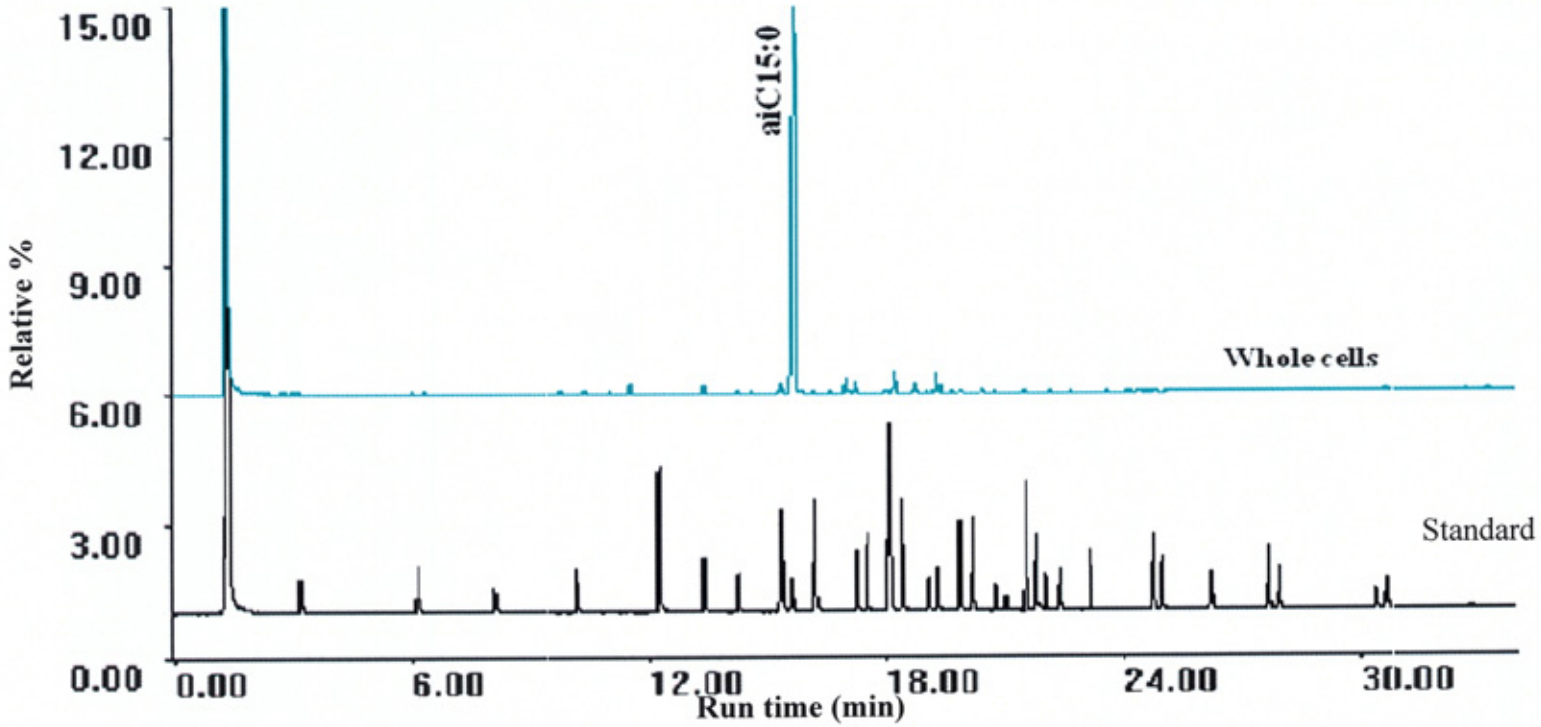

Figure 5.5. FAME analysis results for whole cells of *K. radiotolerans*. The identities of the standard fatty acids are shown in Chapter 2, Figure 2.4.

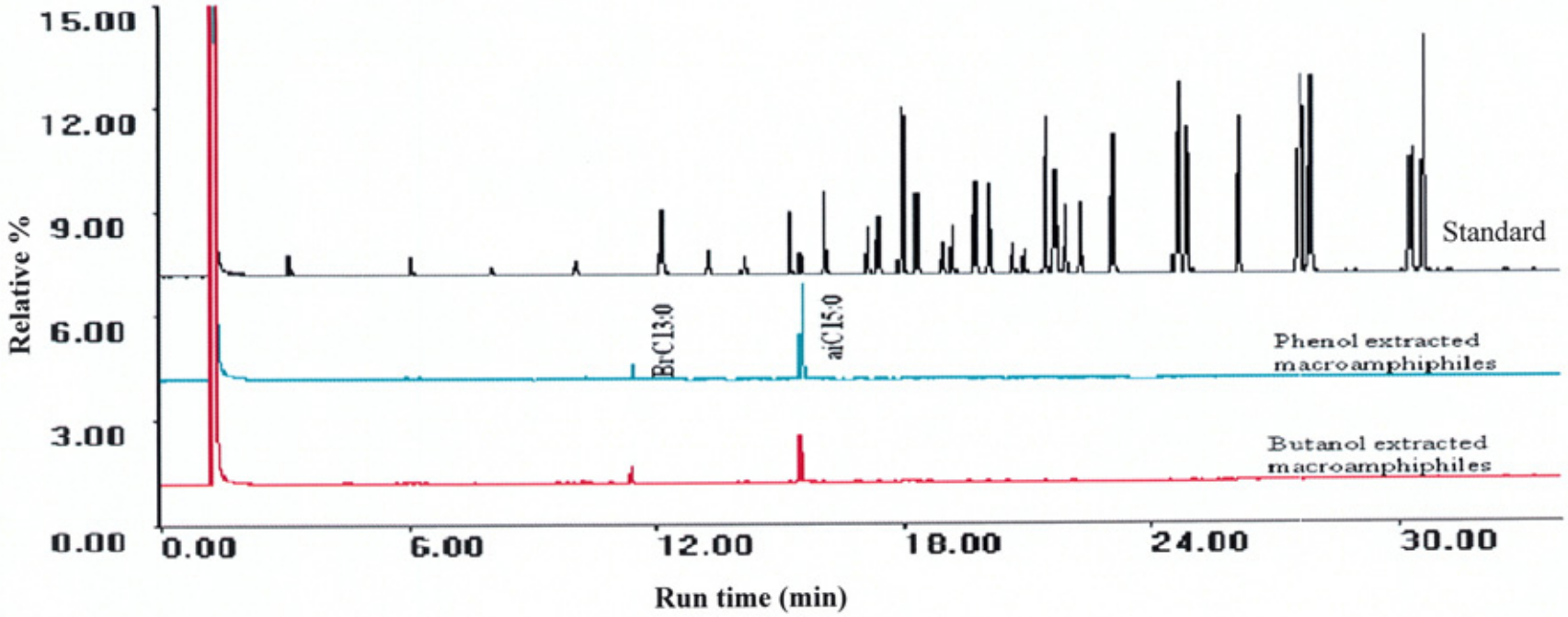

Figure 5.6. FAME analysis results for macroamphiphiles of *K. radiotolerans*. The identities of the standard fatty acids are shown in Chapter 2, Figure 2.4.

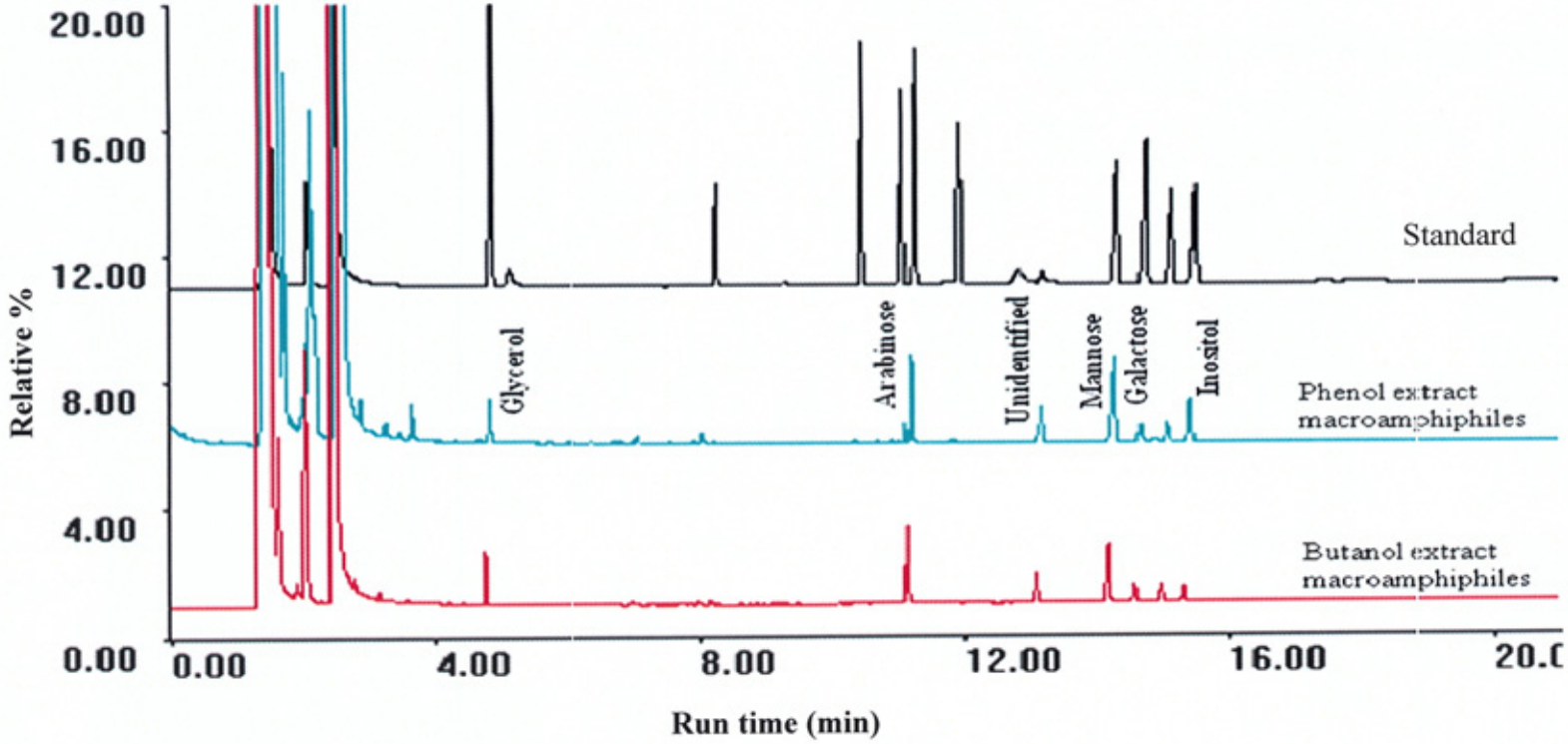

Figure 5.7. Carbohydrate analysis results for macroamphiphilies of *K. radiotolerans* extracted using phenol-water and butanol extraction method. The labels of standard sugars have been shown in Chapter 2, Figure 2.5 and Table 2.14.

Table 5.2. Comparison of macroamphiphile fatty acid composition with the whole cell fatty acids of *K. radiotolerans.*

FAME identified[a]	**Whole cells**	***K. radiotolerans* macroamphiphiles (phenol extracted; peak 3)**	***K. radiotolerans* macroamphiphiles (butanol extracted)**
Unidentified[b]	3.0	9.9	25.082
aiC15:0	90.1	90.1	74.918
iC16:0	1.4	0	0
C16:0	3.0	0	0
iC17:0	1.3	0	0
C17:0	1.3	0	0

[a] Fatty acids were analysed by GC of their methyl esters and identified by comparison with a mixture of 32 authentic standards. Composition is given as the percentage of total integrated chromatographic peak areas. [b] define what b represents e.g. "tentatively identified as aiC13:0 or iC13:0"

Table 5.3 Carbohydrate composition of the HIC-purified acid hydrolysed macroamphiphiles of *K. radiotolerans*.

Carbohydrate identified[a]	***K. radiotolerans* macroamphiphiles for FPLC run 3 sample (phenol-water extracted peak 3, Appendix IV, Figure V.3)**	***K. radiotolerans* macroamphiphiles for FPLC run 7 sample (phenol-water extracted peak 3, Figure 5.3)**	***K. radiotolerans* macroamphiphiles for FPLC run 8 sample (butanol extracted sample, peak 2, Figure 5.4)**
Glycerol	15.1	11.6	31.25
Arabinose	23.1	17.4	29.9
Unidentified[b]	11.7	11.3	Trace
Mannose	29.8	32.9	38.9
Galactose	6.9	5.7	Trace
Glucose	7.7	5.3	Trace
Inositol	5.8	13.3	Trace

[a] Carbohydrates were analysed by GC of their alditol acetate derivatives and identified by comparision with a mixture of authentic standards (alditol acetates of glycerol, erythritol, rhamnose, ribose, arabinose, xylose, mannose, galactose, glucose and inositol). Composition is given as the percentage of total integrated chromatographic peak areas. [b] an unknown sugar, run time Rf ca. 13.28.

5.3.4. Electrophoretic analysis of the *K. radiotolerans* macroamphiphiles

The *K. radiotolerans* macroamphiphile fractions (phenol extracted, HIC purified) was examined by electrophoresis followed by staining with Silver-nitrate, Alcian-Blue 8GX, periodate Schiffs reagent and Commassie Blue (Described in Chapter 2, Sections 2.2.3.1, 2.2.3.2, 2.2.3.3 and 2.2.3.4, respectively). Peak 2 from the hot phenol-water extract (Figure 5.3) did not stain with any of the staining reagents, suggesting that the amount of material molecule recovered in this HIC fraction was insufficient to do further analysis. Alcian blue 8GX, Coomassie Blue, and combined Alcian Blue and silver nitrate staining each revealed a broad staining band with a ladder-like region around 20 KDa and 10 KDa (Figures 5.8, 5.9 and 5.10, respectively) for the material in peak 3 of Figure 5.3. Figure 5.8 and 5.9 show the relative position of reference LTA (from Group B *Streptococcus*) and standard LAM positions, respectively, compared to the position of the ladder-like staining of the *K. radiotolerans* macroamphiphiles. The LTA (Figure 5.8) ran at a similar position to the ladder-like staining (around the 15 KDa region) of the *K. radiotolerans* macroamphiphile(s), whereas standard LAM (Figure 5.9) ran in the region of 25 to 35 KDa. Periodate Schiffs reagent only reacted with the material around the 15 KDa regions of the gels very weakly (Figures 5.11 and 5.12). Also shown in Figure 5.12 is the position of PIMs, which ran to a noticeably lower (<10 KDa) position, which differentiated it from the *K. radiotolerans* macroamphiphiles. Staining with the periodate Schiffs reagent suggests the macroamphiphiles contain hexose sugar. Silver-nitrate staining showed that there might be a minor protein contaminant band at the tip of the

ladder near the 10 KDa (Figure 5.10), though chemical analysis was unable to detect any protein (see above).

The electrophoretic mobility of the *K. radiotolerans* macroamphiphile(s) was not similar to the reference LTA, LAM or PIM observed by the different staining of electrophoresis gels (Figures 5.8-5.12). Moreover, on Western blotting the *K. radiotolerans* macroamphiphile reacted with neither anti-LTA (Figure 5.13 a and b, monoclonal and polyclonal antibodies) nor with monoclonal or polyclonal anti-LAM antibodies (Figure 5.14 and data not shown), suggesting that the macroamphiphile was neither LTA nor a typical fully arabinosylated LAM molecule, as the arabinan is the immunodominant epitope in LAM (Kaur *et al.*, 2002). Lectin blotting showed a negative reaction (Figure 5.15), i.e. a clear zone was visible amongst the general background development and showed reaction with the presumed contaminant protein band around 10 KDa, suggesting this might be a mannosylated glycoprotein. From this it can also be assumed that the mannose observed by GC was not present as terminal mannose residues in the macroamphiphiles, since concanavalin A lectin binds to terminal mannose (Sutcliffe, 2000, Reeke *et al.*, 1974, Gunther *et al.*, 1973).

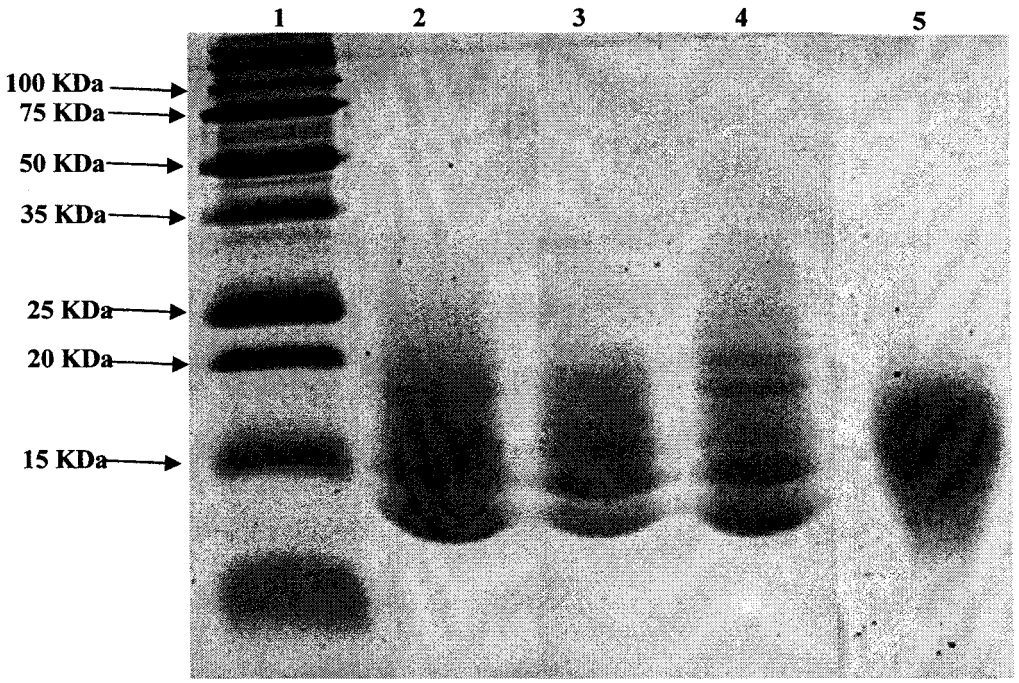

Figure 5.8. Alcian Blue staining: Lane 1, protein standard ladder; Lane 2 to 4: different preparation of *K. radiotolerans* macroamphiphiles (peak 3) and Lane 5: GBS LTA. Note that irrelevant sample lanes between samples shown in lanes 4 and 5 have been digitally removed.

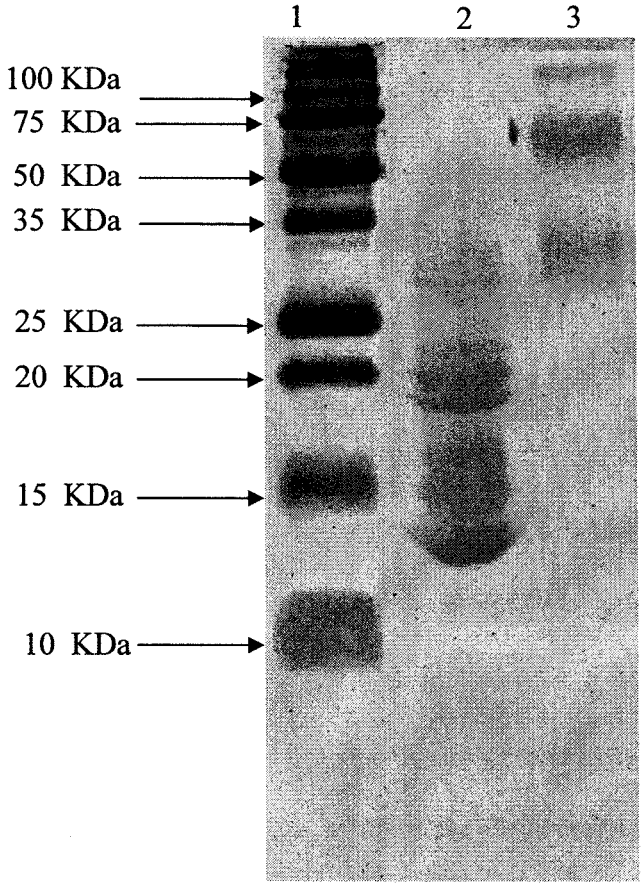

Figure 5.9. Coomassie Blue staining: Lane 1, protein standard ladder; Lane 2: *K. radiotolerans* macroamphiphiles and Lane 3: Standard LAM.

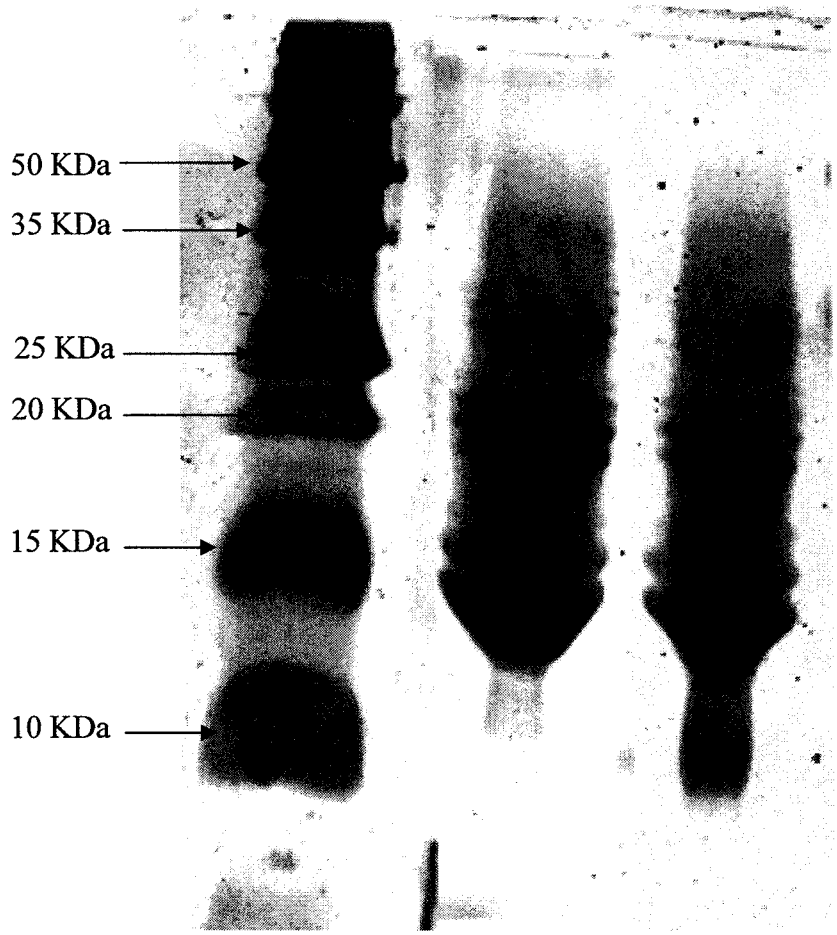

Figure 5.10. Alcian blue and Silver-nitrate staining: Lane 1, protein standard ladder; Lane 2 and 3: different preparation of *K. radiotolerans* macroamphiphiles.

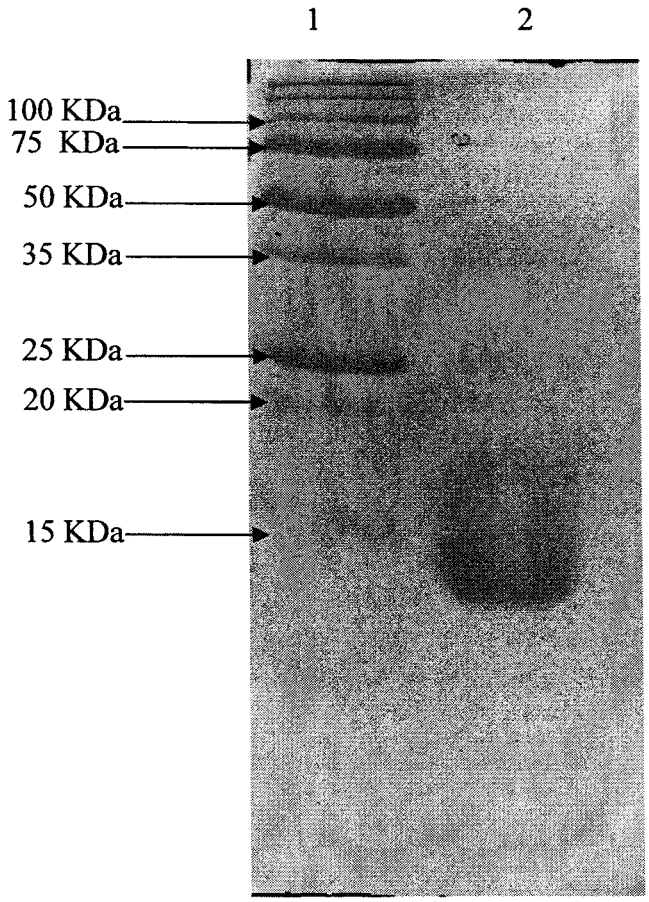

Figure 5.11. Periodate Schiffs reagent staining: Lane 1, protein standard ladder, Lane 2: *K. radiotolerans* macroamphiphiles (peak 3).

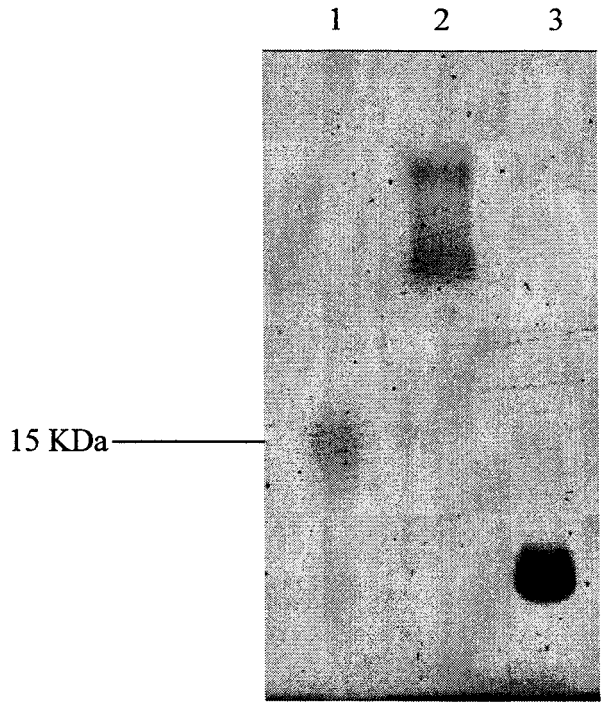

Figure 5.12. Relative position of *K. radiotolerans* macroamphiphiles with in comparison with LAM and PIM, following periodate Schiffs reagent staining: Lane 1: *K. radiotolerans* macroamphiphiles, Lane 2: LAM standard and Lane 3: PIM standard.

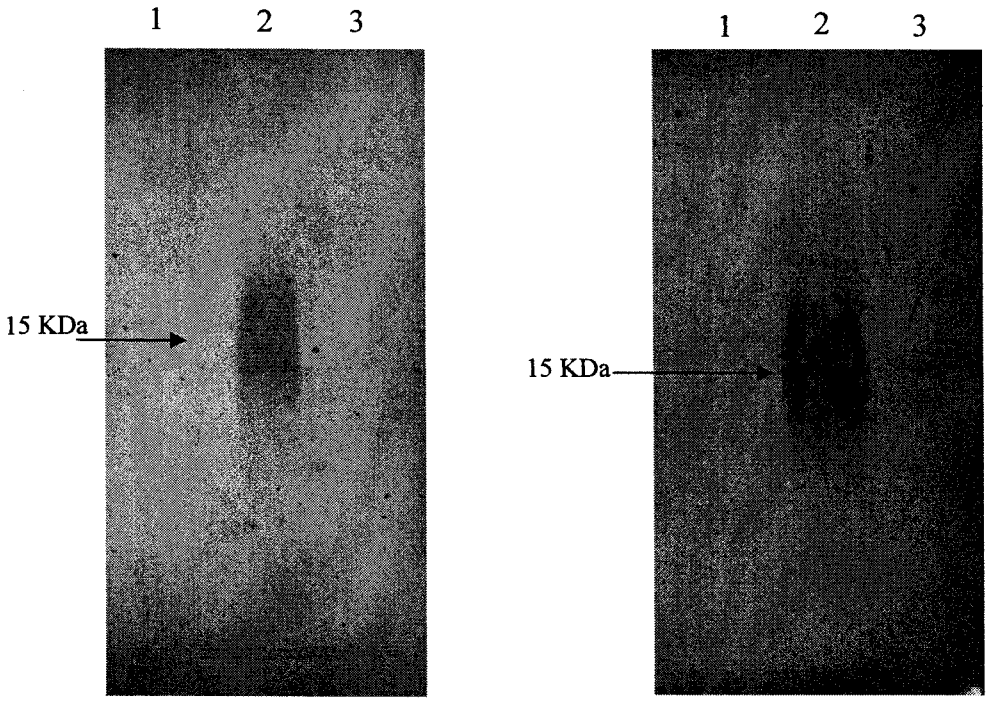

Figure 5.13. (a) Polyclonal anti-LTA blotting **(b)** monoclonal anti-LTA blotting. Lane 1: *K. radiotolerans* macroamphiphile, Lane 2: LTA standard Lane 3: LAM standard. The 15 KDa position indicated was determined by refence to protein molecular weight markers during blot processing.

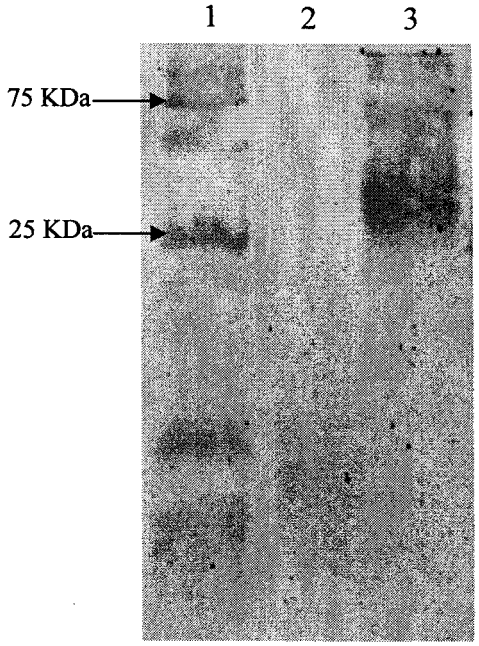

Figure 5.14. Anti-LAM blotting, Lane 1: Protein standard ladder, Lane 2: *K. radiotolerans* macroamphiphiles and Lane 3: LAM standard.

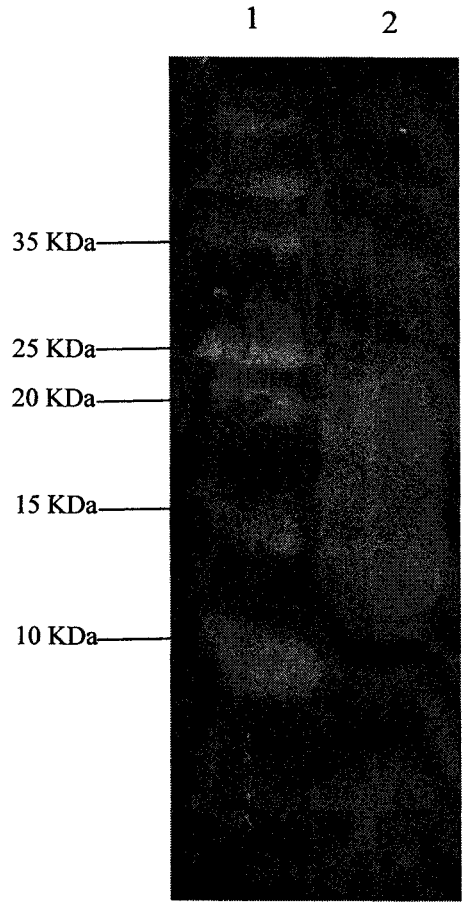

Figure 5.15. Lectin blotting, Lane 1: Protein standard ladder, Lane 2: *K. radiotolerance* macroamphiphiles. Negative staining of the macroamphiphiles appears light against the background, with a presumptive protein band cross-reacting at around 10 KDa.

5.3.5. MALDI/MS analysis

The ladder like appearance while staining with Coomassie Blue, Alcian Blue and Silver staining (Figure 5.8-5.10) suggested a repeating unit structure may be present in the *K. radiotolerans* macroamphiphile, as has also been observed with many lipopolysaccharide (LPS). In order to determine if there was a repeating unit, further analysis was done with MALDI mass spectrometry. Purified macroamphiphiles (ca. 8 mg) of *K. radiotolerans* were prepared and sent to Dr Jerome Nigou (CNRS, Institut de Pharmacologie & Biologie Structurale, Toulouse, France) for MALDI/MS analysis. The method has been described in section 2.2.7.1.

Suprisingly, the MALDI Mass spectrum showed a major peak around 5 KDa and a minor peak around 6 KDa, but no sign of a repeat unit, as shown by the even mass distribution around 5 KDa in Figure 5.16.

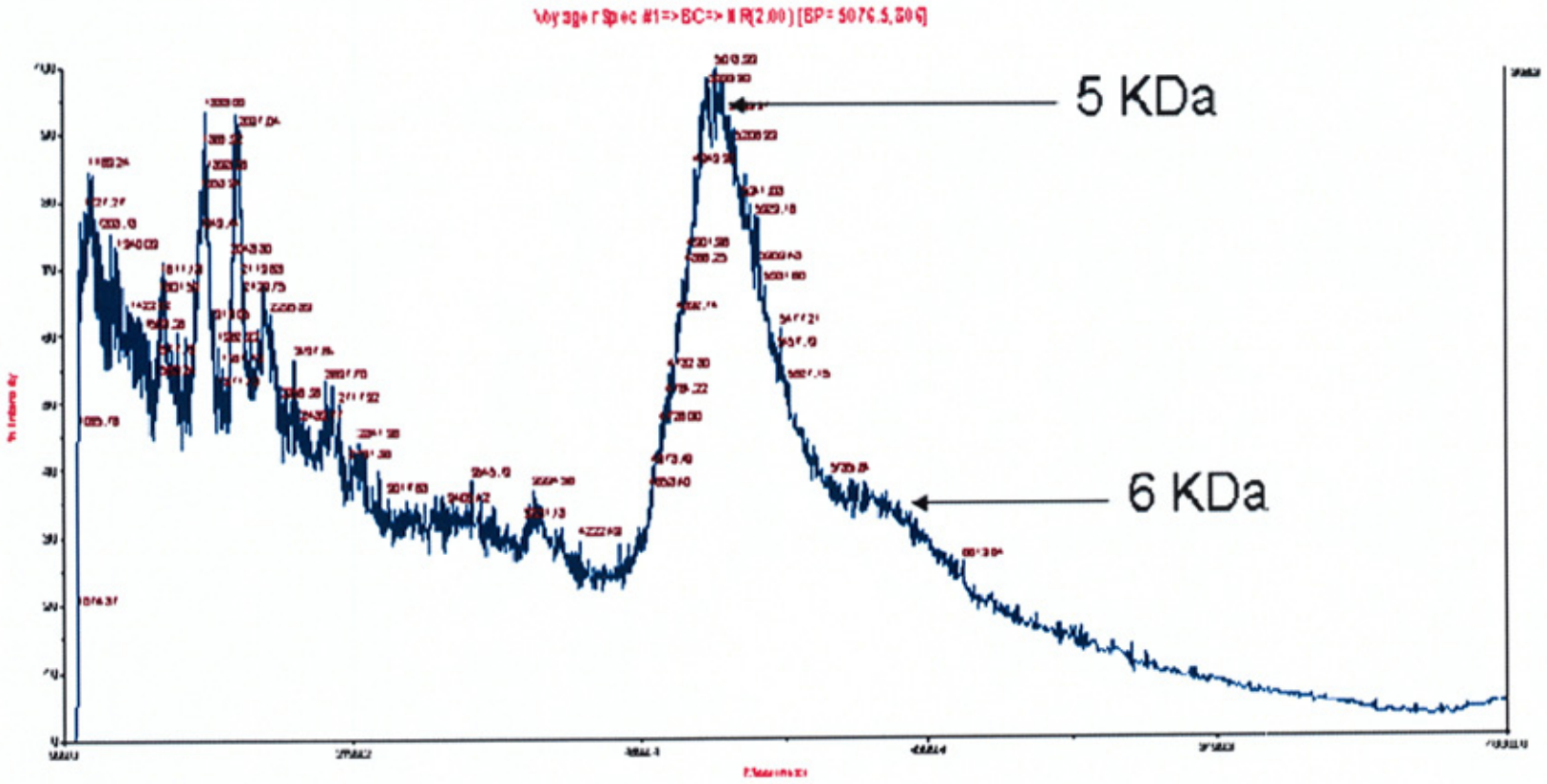

Figure 5.16. MALDI-MS data for the *K. radiotolerans* macroamphiphile. The analysis was performed by Jérôme Nigou (Toulouse, France).

5.3.6. Separating the macroamphiphilic materials by anion exchange chromatography

From MALDI/MS analysis, the *K. radiotolerans* macroamphiphiles was revealed to contain two molecules, a major component and a minor fraction. Since the macroamphiphilic materials may contain different sugar units, and possibly substituents, anion exchange chromatography was attempted to separate the macromolecules on the basis of possible charged group differences. The purified phenol extracted macroamphiphiles obtained from the HIC column were dialysed and lyophilised and subjected to anion exchange chromatography as described in Chapter 2, Section 2.1.6.2. The fractions were subjected to carbohydrate assay, as shown in Figure 5.17. The anion exchange chromatography was unable to adequately separate the macromolecules, presumably due to relatively small differences in the ionic characteristics between the macromolecules.

Fractions 95-112, 113-126, 127-142 and 152-170 were collected separately, dialyzed and lyophilized, the recovered purified products were subjected to SDS-PAGE analysis. However Alcian Blue, Silver-nitrate and Coomassie Blue staining failed to reveal the macroamphiphiles as resolved into fractions, presumably because the sample recovered in each fraction were below the level of detection (data not shown).

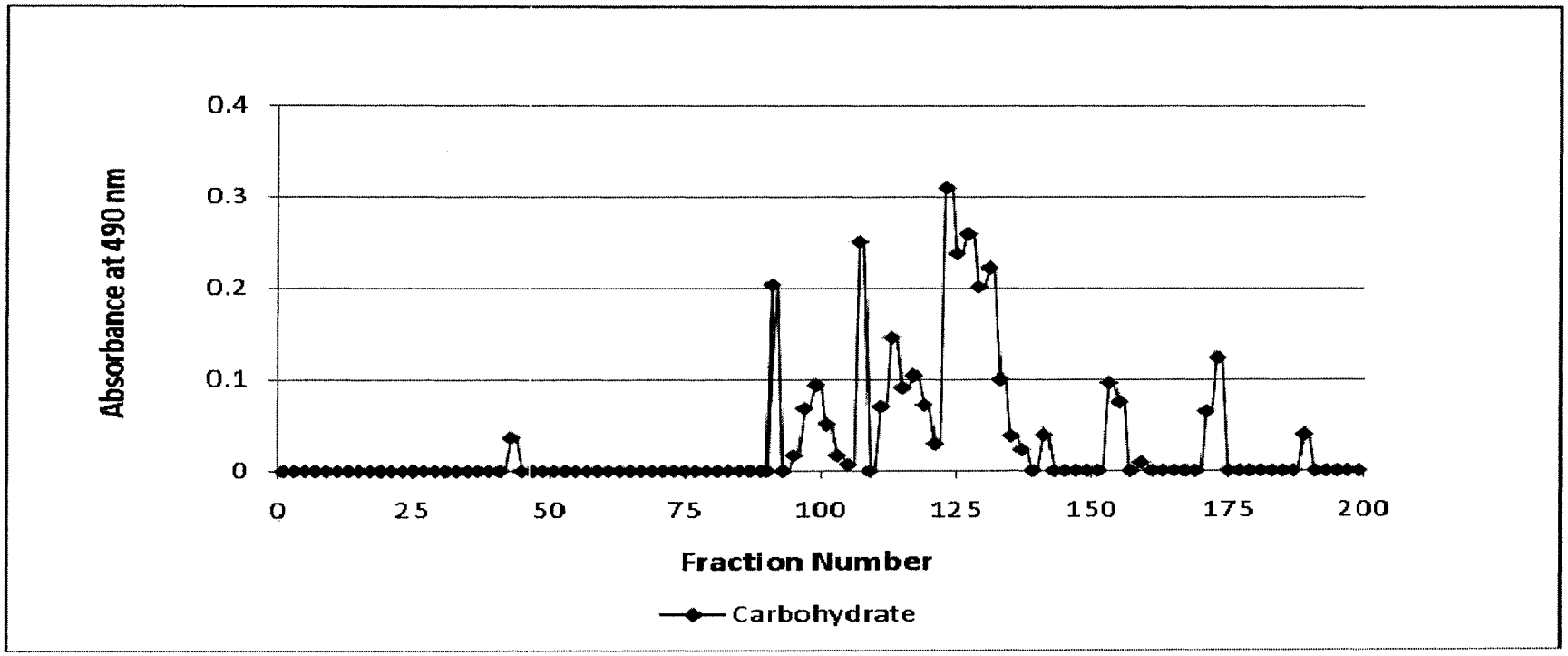

Figure 5.17. Anion exchange chromatography profile for the purification of a HIC purified macroamphiphile preparation from *K. radiotolerans*. The sample was loaded onto the column with equilibration buffer until fraction 20, after which gradient elution with an increasing concentration of NaCl was begun. Column fractions (5 mL) were analyzed for carbohydrate.

5.3.7. Purification of mannose containing molecules

Since the anion exchange chromatography had failed to adequately separate the macroamphiphilic fraction, the HIC purified molecule(s) were subjected to Mannose-Binding protein (MBP) column chromatography in order to separate them on the basis of their mannose content, as the carbohydrate anyalysis by GC showed the presence of mannose residues (15-30% of the total sugar), as shown in Table 5.3.

MBP column chromatography was performed as described in Chapter 2, Section 2.1.6.3. The fractions were subjected to carbohydrate and phosphate assays, which revealed three peaks, as shown in Figure 5.18 (Peak 1, Peak 2 and Peak 3). Since the peak 1 material did not bind to the column, the peak 1 containing molecule should not contain any mannose residues. On the other hand, peak 2 and 3 are revealed to contain mannose due to their binding to the column.

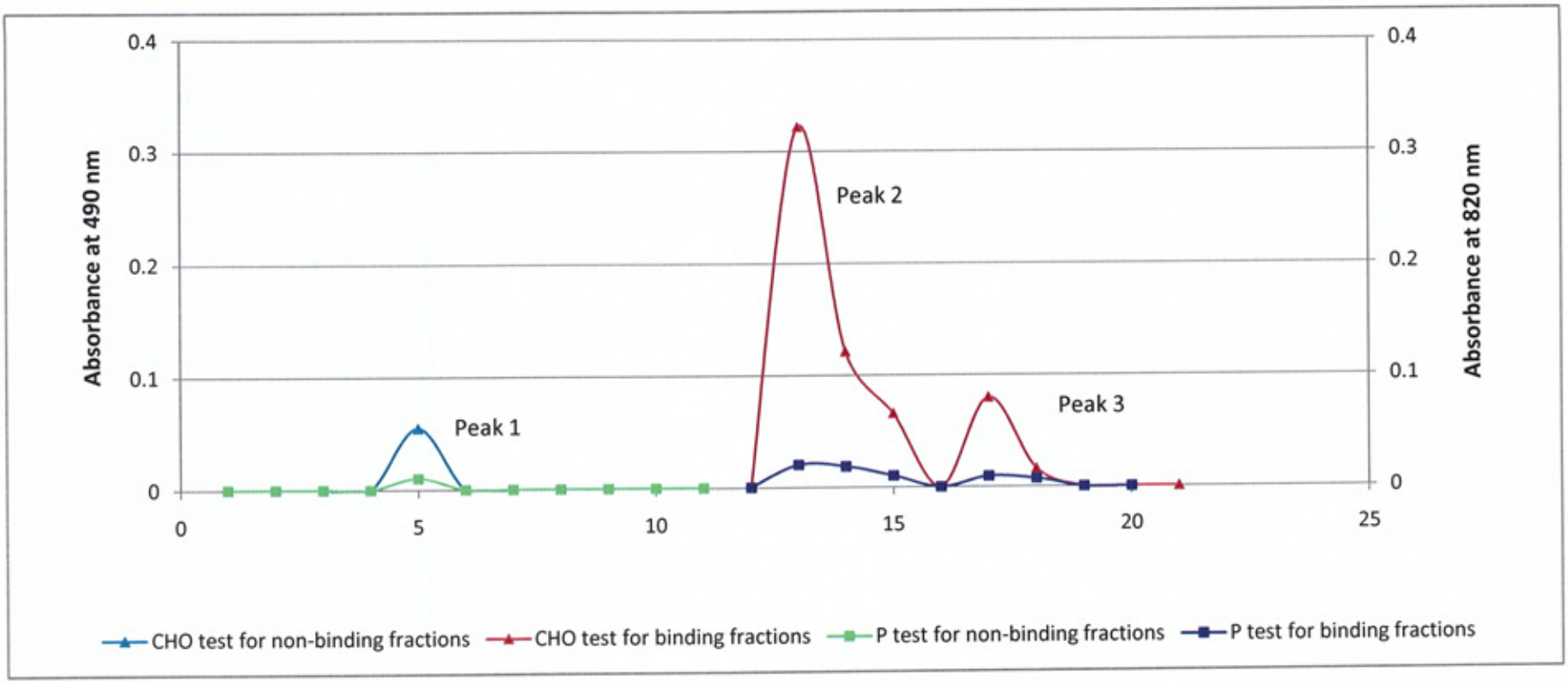

Figure 5.18. MBP column profile for HIC purified *K. radiotolerans* macroamphiphiles. The purified macroamphiphiles was loaded into the column with binding buffer until fraction 11, after which the column was washed with elution buffer 4 mL of 14 fractions (12 to 25). Column fractions (4 mL) were analyzed for carbohydrate and phosphorus.

5.3.8. Chemical analysis of MBP column peaks

The sugar composition of the MBP purified column peaks 1, 2 and 3 (Figure 5.18) were determined following acid hydrolysis to release monosaccharide components and derivatisation to alditol acetates for GC, as described in Chapter 2, section 2.2.6.2. Table 5.4 presents a summary of carbohydrate composition of the peaks obtained by MBP purification. Peak 1 contained glycerol and galactose with an unidentified sugar residue which was also observed in purified macroamphiphiles after HIC purification (Table 5.3). The absence of mannose in this peak demonstrated that the MBP column separation had worked effectively.

Peak 2 was composed of mainly of mannose, glycerol, galactose and arabinose with trace amount of inositol. Phosphate analysis showed the presence of minor amount of phosphate.

Peak 3 was composed of glycerol, mannose and glucose with presence of a minor amount of xylose, the latter of which was also identified in macroamphiphiles extracted by the butanol extraction process (Table 5.3).

Table 5.4 Carbohydrate composition of the MBP-purified acid hydrolysed macroamphiphilic peaks of *K. radiotolernas*.

Carbohydrate identified[a]	***K. radiotolerans* MBP purified Peak 1**	***K. radiotolerans* MBP purified Peak 2**	***K. radiotolerans* MBP purified Peak 3**
Glycerol	81.5	32.1	81.3
Arabinose	_	3.1	_
Xylose	_	_	1.5
Unidentified[b]	5.4	_	_
Mannose	_	55.1	7.6
Galactose	4.8	3.3	_
Glucose	_	_	3.1
Inositol	_	Trace	_

[a] Carbohydrates were analysed by GC of their alditol acetate derivatives and identified by comparision with a mixture of authentic standards (alditol acetates of glycerol, erythritol, rhamnose, ribose, arabinose, xylose, mannose, galactose, glucose and Inositol as shown in Figure 2.5). Composition is given as the percentage of total integrated chromatographic peak areas. [b] an unknown sugar, run time 13.43.

5.3.9. Electrophoretic analysis of the *K. radiotolerans* MBP purified peaks

A *K. radiotolerans* macroamphiphile preparation (phenol extracted, HIC purified) and MPB purified column peaks were examined by electrophoresis followed by staining with silver-nitrate, Alcian Blue 8GX, periodate Schiffs reagent. The periodate Schiffs reagent did not react with the material recovered from the MBP column (data not shown), but reacted with the HIC-purified macroamphiphiles (Figures 5.11 and 5.12). Alcian blue and Silver-nitrate staining reacted with the peak 2 and faintly with peak 3 (Figure 5.19) and the characteristic laddering was still observed. Lectin blotting showed a negative staining reaction with the peak 2 (Figure 5.20), similar to the pattern of the HIC purified macroamphiphiles (Figure 5.15). The MBP Peak 3 material showed two bands on Alcian blue and Silver-nitrate staining which also appeared as negatively stained bands on lectin blotting (Figures 5.19 and 5.20). Although at lower yield and load the pattern of reaction resembled that of the molecules present in peak 2 (Figure 5.19 and 5.20). Staining or lectin blotting failed to detect components of Peak 1 from the MBP column profile, due to the insufficient amount of material recovered.

Lectin blotting revealed that the presumptive protein band of ca. 10 KDa was still present, suggesting there might be a mannosylated protein contaminating the preparation but no protein detected using the Bradford reagent protein assay (Chapter 2, Section 2.4.2) or when detecting any protein bands on the nitrocellulose membrane by Ponceau's staining solution (Chapter 2, Section 2.4.3).

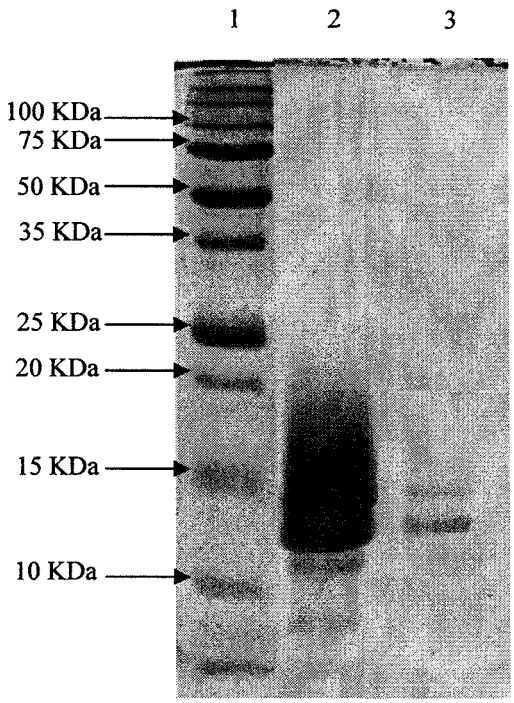

Figure 5.19. Alcian Blue staining of MBP purified macroamphiphile fractions: Lane 1, Protein standard ladder; Lane 2: MBP peak 2 and Lane 3: MBP peak 3.

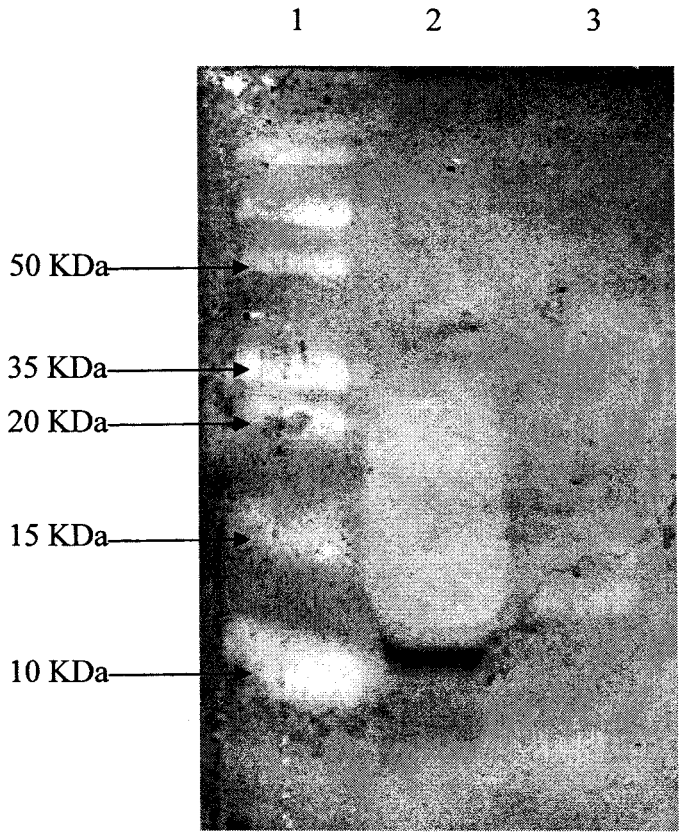

Figure 5.20. Lectin blotting of MBP purified macroamphiphile fractions. Lane 1: Protein standard ladder, Lane 2: MBP peak 2 and Lane 3: MBP peak 3. Note negative staining of the macroamphiphiles and positive reaction with a likley protein band around 10 KDa.

5.3.10. Bioinformatics analysis of *K. radiotolerans* genome

Although *K. auranticus* and *K. marinus* were identified as having arabinose and galactose as cell wall sugars (Yokota *et al.*, 1993; Lee, 2006), strongly suggesting AG as a SCWP, the genes from the well established pathway for TA biosynthesis were searched for in the *K. radiotolerans* genome. The BlastP results for genes responsible for TA biosynthesis showed the presence of clear homologues for the protein TagB, TagD, TagE, TagF and TagO (Table 5.5), suggesting the organism may be capable of producing a TA, especially given the presence of homologues of TagB and TagF, which are responsible for poly(glycerol phosphate) polymer synthesis (Bhavsar *et al.*, 2004).

To analyse the presence of lipoglycan biosynthesis pathway genes in *K. radiotolerans,* the homologue(s) for the enzymes/proteins identified for *M. tuberculosis* LAM biosynthesis (as discussed in Chapter one, Sections 1.7.5, 1.7.5.1, 1.7.5.2, 1.7.5.3 & 1.7.5.4) were searched via BlastP. The results are shown in Table 5.6 and 5.7.

Table 5.6 shows the organism has homologue(s) for enzymes on the pathway for PI and apolar PIM biosynthesis, which is consistent with the experiment as results of Lee (2006). Table 5.7 shows that most of the genes for enzymes responsible for LM and LAM biosynthesis are present in the *K. radiotolerans* genome, which suggests that *K. radiotolerans* has the capacity to synthesise LAM or LAM-like macroamphiphiles.

Table 5.5. TA biosynthesis genes of *B. subtilis* homologue(s) in *K. radiotolerans* genome

Genes name of *B. subtilis*	**Size of *B. subtilis* protein a.a.**	***K. radiotolerans* homologue(s)**	**Size a.a.**	**Amino acid identity**	**E number**
ggaA	446	Krad_3285	296	29/94 (30%)	4e-05
ggaB	900	Krad_3986	358	41/208 (19%)	1e-06
tagA	256	Absent	-	-	-
tagB*	381	Krad_1574*	404	77/310 (24%)	1e-20
tagC	442	Absent	-	-	-
tagD	129	Krad_1824	146	42/125 (33%)	1e-10
tagE	673	Krad_1062	400	42/156 (26%),	7e-10
tagF*	746	Krad_3986*	358	138/366 (37%)	9e-67
tagO	358	Krad_1261	394	108/322 (33%)	2e-41

* Note: TagF is also significantly homologue to Krad_1574 and TagB significantly homologous to Krad_3986.

Table 5.6. PI and apolar PIMs biosynthesis genes (*M. tuberculosis*) homologue(s) in *K. radiotolerans*.

Reactions	**Gene name (*M. tuberculosis*)**	***K. radiotolerans* homologue(s)**
PI/precursor synthesis		
Phosphomannomutase	Rv3257c (465 a.a.)	**Krad_3841**(497 a.a.) Identities=282/479 (58%) Expect = 4e-147
Ins-1-phosphate synthase	Rv0046, Ino1 (367 a.a.)	**Krad_3509** (360 a.a.) Identities=275/352 (78%) Expect = 8e-156
Inos-1-P phosphatase	Rv1604, ImpA (270 a.a.)	**Krad_2135** (260 a.a.) Identities = 72/211 (34%) Expect = 8e-18
PI synthase CDP-DAG + inositol → PI	Rv2612c, PgsA (217 a.a.)	**Krad_3064** (206a.a.) Identities = 94/192 (48%) Expect = 2e-39
PI/precursor synthesis		
DAG → Phosphatidate	Rv2252 (309 a.a.)	**Krad_1884** (293 a.a.) Identities = 118/294 (40%), Expect = 2e-47
	Rv3218 (321 a.a.)	**Krad_0248** (366 a.a.) Identities = 90/337 (26%), Expect = 7e-12
PI to PIMs cytoplasmic (apolar PIM biosynthesis)		
PI → PIM_1	Rv2610c, PimA (378 a.a.)	**Krad_3062** (371 a.a.) Identities = 197/371 (53%) Expect = 3e-97
PIM_1 acyltransferase	Rv2611c (316 a.a.)	**Krad_3063** (311 a.a.) Identities = 125/306 (40%) Expect = 6e-47
PI to PIMs cytoplasmic (apolar PIM biosynthesis)		
PIM_1→ PIM_2	Rv2188c,PimB' (385 a.a.)	**Krad_3243** (396 a.a.) Identities = 195/383 (50%) Expect = 3e-103
PIM_2→ PIM_3/ PIM_4	PimC, MT1800 (381 a.a.) or other Mannosyl transferase	**Krad_3070** (403 a.a.) Identities = 108/374 (28%) Expect = 8e-13

Table 5.7. Polar PIMs, LM and LAM biosynthesis genes (*M. tuberculosis*) homologue(s) in *K. radiotolerans*

Reactions	**Gene name (*M. tuberculosis*)**	***K. radiotolerans* homologue(s)**
Lipid linked precursor synthesis (for transfer from the inner membrane to outer surface)		
C35P (polyprenol) → C35P-mannose	Rv2051c (874 a.a.)	**Krad_1890** (593 a.a.) Identities = 210/545 (38%) Expect = 3e-87
	MSMEG_3860 (615 a.a.) CN hydrolase domain (≡ N-terminus of Rv2501c)	**Krad_1890** (593 a.a.) Identities = 226/532 (42%) Expect = 7e-91
	MSMEG_3859 (265 a.a.) (≡ C-terminus of Rv2501c)	Krad_ 0328 (270 a.a.) Identities = 115/237 (48%) Expect = 1e-53
Lipid linked precursor synthesis (for transfer from the inner membrane to outer surface)		
C35P-ribose synthase	Rv3806 (302 a.a.)	**Krad_3882** (300 a.a.) Identities = 158/299 (52%) Expect = 1e-77
C35P-ribose → C35P-arabinose epimerase	Rv3790 (461 a.a.)	**Krad_4160** (481 a.a.) Identities = 257/457 (56%) Expect = 2e-147
	Rv3791 (254 a.a.)	**Krad_3873** (257 a.a.) Identities = 135/255 (52%) Expect = 3e-70
Convert apolar PIMs to Polar PIMs or LM (extracytoplasmic)		
LpqW feeds PIM_4 to LM	Rv1166 (635 a.a.)	**Krad_3863** (523 a.a.) Identities = 83/385 (21%) Expect = 1e-07
PIM_4→ PIM_5 (PIM branch rather than LAM)	Rv1159, PimE (431 a.a.)	**Krad_0243** (417 a.a.) Identities = 119/376 (31%) Expect = 2e-33
Mannan extension	Rv2174 (516 a.a.) MptA	**Krad_0171** (473 a.a.) Identities = 138/523 (26%) Expect = 4e-15
	Rv1459c (591 a.a.)	**Krad_0171** (473 a.a.) Identities = 73/234 (31%) Expect = 5e-12

Reactions	**Gene name (*M . tuberculosis*)**	***K. radiotolerans* homologue(s)**
Convert apolar PIMs to Polar PIMs or LM (extracytoplasmic)		
Mannan branches	Rv2181(427 a.a.)	**Krad_0243** (417 a.a.) Identities = 136/425 (32%) Expect = 2e-46
Arabinan addition		
LM-Arabinose$_1$→ LAM	Rv3793,EmbC (1094 a.a.)	**Krad_0769** (590 a.a.) Identities = 89/331 (26%) Expect = 3e-07
Capping/ substituents		
Mannose capping	Rv1635c (556 a.a.)	**Krad_3874** (523 a.a.) Identities = 126/421 (29%) Expect = 1e-26

5.3.11. Secondary cell wall polymer (SCWP) analysis for *K. radiotolerans*

Kineococci have been implicated to contain AG polymer as their SCWP, along with absence of mycolic acid *(Phillips et al., 2002, Yokota et al., 1993, Itoh et al., 1989, Kudo et al., 1998, Lee, 2006)*. However, in the present study analysing the genome via Blast searches has identified most of the TA biosynthesis genes in *K. radiotolerans* genome, which contradicts with the presence of an AG polymer. In order to determine the SCWP, a general procedure for extracting TA as described in Chapter 2, Section 2.4.1, was used.

The extracted materials' sugar composition were determined following acid hydrolysis to release monosaccharide components and derivatisation to alditol acetates for GC, as described in Chapter 2, section 2.2.6.2. From Figure 5.21 and Table 5.8, it is evident that the SCWP materials contained mannose and glucose as major components, with lesser amounts of arabinose and galactose. The presence of galactose and arabinose would be consistent with the presence of an AG polymer as a SCWP and the notable absence of glycerol also suggests the presence of a SCWP that was not TA. However, the predominance of mannose and glucose was unexpected.

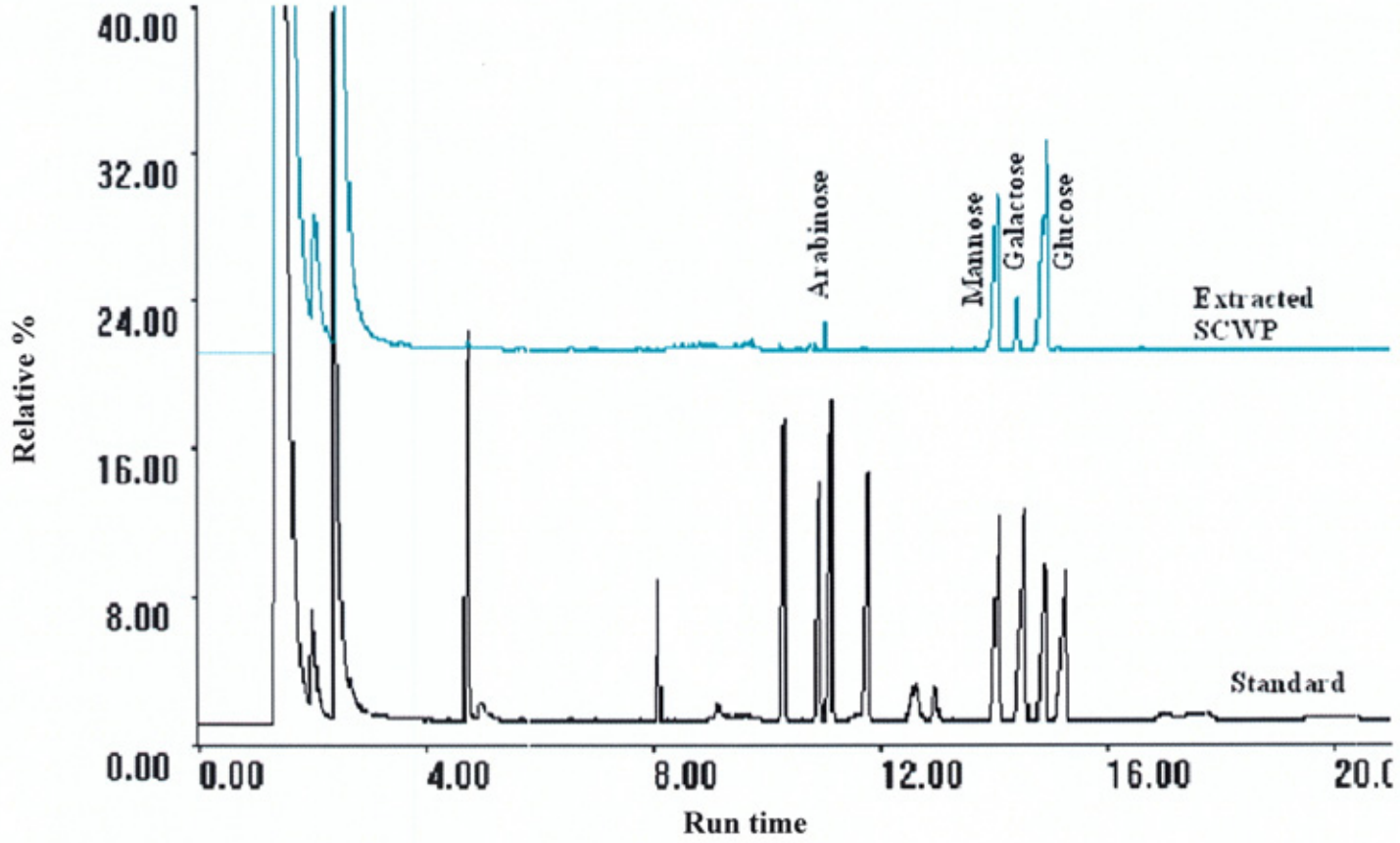

Figure 5.21. Carbohydrate analysis results for extracted SCWP of *K. radiotolerans*. The labelling of the sugar standards has been shown in Chapter 2, Figure 2.5 and Table 2.14.

Table 5.8. Carbohydrate composition of the acid hydrolysed SCWP materials of *K. radiotolerans*.

Carbohydrate identified[a]	***K. radiotolerans* SCWP materials**
Arabinose	2.5
Mannose	34.8
Galactose	6.9
Glucose	55.8

[a] Carbohydrates were analysed by GC of their alditol acetate derivatives and identified by comparision with a mixture of authentic standards (alditol acetates of glycerol, erythritol, rhamnose, ribose, arabinose, xylose, mannose, galactose, glucose and Inositol as shown in Figure 2.5). Composition is given as the percentage of total integrated chromatographic peak areas.

5.4. Discussion

The purpose of this study was to investigate the macroamphiphiles in *K. radiotolerans,* and if possible, to use this chemotaxonomic characteristic to justify the present position of the genus *Kineococcus* in the phylum Actinobacteria.

5.4.1. Growth characteristics

K. radiotolerans culture was found to be Gram-positive, coccoid shaped and orange in colour which were consistent with previous studies (Phillips *et al.*, 2002). The orange pigment is a characteristic of the common genus and is attributed to the presence of carotenoids (Phillips *et al.*, 2002). The growth curve showed that the organism's exponential phase was between 16 to 24 h and that clumps were produced after the exponential phase.

In liquid culture, growth took 36 h for producing optimal amount of cells, yielding 0.87 g dry cells/litre. The orange colour of the organism made it easy to determine the purity of the organism, which were further reinforced by the fatty acid profile of the whole cells of *K. radiotoloerans* as determined by GC (Figure 5.5).

5.4.2. Identification of the *K. radiotolerans* macroamphiphile(s)

Both hot phenol-water and butanol extraction, followed by HIC purification, allowed the identification of a peak around fraction number 40 to 50 in the FPLC profiles, which are represented by peaks 3 and 2, respectively in Figures 5.3 and 5.4. The amount of material recovered from the butanol extraction process was higher than that from the phenol extraction process, which is presumed to be due to extraction of other contaminants by the butanol extraction method. This was also suggested by the carbohydrate composition of the macroamphiphiles (Table 5.3). This is consistent with the conclusion from the *T. fusca* study (Chapter 3), that the hot phenol-water extract method was a more convenient and effective method to extract macroamphiphiles than the butanol extraction method.

The low amount of phosphate detected in the purified macroamphiphiles presented the characteristics of a lipoglycan rather than LTA, since lipoglycans contain a high proportion of sugar residues, whilst dot immunoblotting with polyclonal anti-LAM antibody suggested the lipoglycan might not be a typical LAM.

The fatty acids profile of the *K. radiotolerans* whole cells showed the presence of aiC15:0 as more than 90%, consistent with this fatty acid being the predominant fatty acid for members of the genus *Kineococcus* (Yokota *et al.*, 1993, Lee, 2006).

The fatty acid composition of the macroamphiphile(s) of *K. radiotolerans* showed a very similar fatty acid profile to the whole cells with predominant aiC15:0 and minor amounts of a fatty acid tentatively identified as iso- or anteiso- C13:0. The relative percentages of the fatty acids differed between the phenol-water and butanol extracted macromaphiphile(s), which might be due to contaminants in the butanol extraction, as mentioned earlier.

After SDS-PAGE, the staining of the *K. radiotolerans* macroamphiphiles with Coomassie Blue, Alcian Blue and Silver staining showed a broad range of ladder-like bands between 20 and 10 KDa region (Figure 5.8-5.10), suggesting the macroamphiphiles might contain repeated polymer units, as has been observed for some LPS. However, the MALDI-MS data showed that the macroamphiphile material contained a major macromolecule producing a peak with a uniform distribution around 5 KDa, with a minor amounts of a macromolecule producing a peak around 6 KDa (Figure 5.16) , rather than revealing any polymer repeating unit. The relative positions of the stained macroamphiphilic material in comparison with LAM, LTA and PIM reference standards showed the material only ran in the same gel region as LTA. However, the low phosphate content and the negative reaction with polyclonal and monoclonal anti-LTA antibodies (Figure 5.13) indicate the organism did not contained any typical LTA. Moreover, the negative reaction with lectin blotting (Figure 5.11) suggested the macroamphiphile did not contain any terminal mannose residues. A discrete band produced around 10 KDa might be a mannosylated protein, though overall the level of protein contamination was below that detectable by protein assay.

The sugar composition of the macroamphiphiles showed the presence of mannose, arabinose, galactose, glucose and inositol suggesting the molecule might be a LAM or LAM like molecule as observed in mycolata organisms and members of the Pseudonocardiaceae (discussed in Chapter one, Section 1.7.4.3). However, no reaction with polyclonal or monoclonal anti-LAM antibodies (Figure 5.16) was observed, suggesting that the macroamphiphile might be a novel LAM-like macroamphiphile. As the arabinan is the major epitope in LAM (Kaur et al, 2002) the structure may present as a 'truncated LAM' as in *R. equi* and *T. otitidis* (Garton *et al.*, 2001; Gilleron *et al.*, 2005). It is noted that other truncated LAM-like lipoglycans fail to react with anti-LAM antibodies (Gilleron *et al.*, 2005).

The anion exchange chromatography did not efficiently separate the macromolecules (Figure 5.17) suggesting that the macromoleucles were not well charged (as in LTA) and suggested the characteristics of a lipoglycan, generally composed of pentose and hexose sugars.

The MBP column chromatography (Figure 5.21) was effective in separating the molecules depending on the presence of mannose, separating the HIC purified macroamphiphile materials into three separate peaks. The first peak did not contain mannose, consistent with the observation that it did not bind to the MBP column. The sugar analysis showed the presence of a high proportion of glycerol in this material but further analysis could not be done due to the small amount of material recovered. The second peak represented the major macroamphiphile and sugar analysis showed the presence of mannose,

arabinose, inositol and glycerol, a classical sugar composition for LAM or LAM-like macroamphiphiles. The negative reaction with the lectin blotting suggested that the macroamphiphile might be a novel LAM-like macroamphiphiles with no terminal mannose residues. The small amount of galactose detected in this fraction (Table 5.3) could suggest either the persistence of a contaminant or a novel substituent, as galactose has never previously been reported in LAM type lipoglycans. A persistent band was observed around 10 KDa and attributed to a glycoprotein contaminant. The third peak showed the presence of glycerol, xylose, mannose and glucose which might be represent a second type of macroamphiphile. Lectin blotting and Alcian Blue staining showed that the peak 3 might contain the peak 2 molecule, concluding that MBP column might not separate the molecules totally.

The staining of peak 2 from the MBP column chromatography suggested that this macromolecule was the major macroamphiphile and from the sugar composition its seemed to be a LAM-like molecule. Moreover, negative stain with lectin blotting suggested that mannose residues were not present in the terminal end of these macroamphiphiles and suggested to be a novel LAM-like macroamphiphile.

The presence of AG as a SCWP had been observed in other mycolata oraganisms of Actinobacteria phylum and in members of the Pseudonocardiaceae. Where investigated, these organisms have always been found to biosynthesise LAM or LAM-like macroamphiphiles (discussed in

Chapter one, Section 1.7.4). In the present study *K. radiotolerans* found to be synthesising a SCWP with minor components typical of an AG (Table 5.8). The presence of major amounts of mannose and glucose may reflect the presence of other abundant cell envelope polysaccharides in *K. radiotolerans* such as the extracellular matrix/slime layer observed previously (Phillips *et al.*, 2002). The present study found no evidence for *K. radiotolerans* producing TA, in spite of the presence of homologues of TA biosynthetic genes in the *K. radiotolerans* genome (Table 5.5). Proteins necessary for LAM biosynthesis proteins (homologues of those identified in *M. tuberculosis* and other mycobacteria) were identifed in the genome (Table 5.6 & 5.7), consistent with the conclusion that *K. radiotolerans* synthesises a LAM-like macroamphiphile.

5.4.3. Conclusion

It is concluded that *K. radiotolerans* appears to produce a novel LAM-like macroamphiphile, possibly with another novel lipoglycan as a minor macroamphiphile. Further analysis is required to separate these macromolecules so they can be subjected to detailed structural analysis.

In producing a novel LAM-like macroamphiphile, *K. radiotolerans* extends the apparent correlation between the distribution of AG and LAM or LAM-like molecules, supporting the significance of SCWP and macroamphiphile as chemotaxonomic markers. Moreover, the position of the genus *Kineococcus* within the Frankineae suborder as determined by 16S rRNA gene analysis, is justified by this result as the suborder is closely related to genera of the mycolata (Stackebrandt *et al.*, 1997).

Further comparative genomics studies, along with biochemical and structural analyses, are required to understand the distribution-function correlation between the *K. radiotolerans* macroamphiphile(s) and those of other Actinobacteria which are related to this organism.

CHAPTER SIX

Investigation of macroamphiphiles in *Streptomyces coelicolor* M145

6.1. Introduction

6.1.1. Isolation and Taxonomy

S. coelicolor strain M145 is the plasmid-free derivative of *S. coelicolor* strain A3(2), the genome of which has been completely sequenced and annotated (Bentley *et al.*, 2002). The 8.67 Mb linear genome with 7825 annotated genes represents one of the largest genomes of all sequenced bacteria (and is twice the size of the *E. coli* and *B. subtilis* genomes), also reflecting the complex life style of the organism (Hesketh *et al.*, 2002). The early development of genetic systems and its production of at least four chemically distinct antibiotics have made *S. coelicolor* A3(2) the model organism of the genus *Streptomyces* (Hopwood, 1999).

Streptomycetes are Gram-positive aerobic bacteria which differ from most other bacteria in their morphology and life cycle characteristics, which in many ways resemble the filamentous fungi (Flardh, 2003, Anderson and Wellington, 2001).

The genus *Streptomyces* is presently situated in the order Actinomycetales within the class Actinobacteria (Stackebrandt *et al.*, 1997). The genus is defined on the basis of chemotaxonomic and phenotypic characteristics, in

which the 16S rRNA homology has been emphasized mostly (Stackebrandt *et al.*, 1997), along with fatty acid and lipid patterns of the cell envelope (Williams *et al.*, 1989).The G+C content of the DNA in the members of this genus was found to be 69-78% (Kornwendisch and Kutzner, 1992).

Presently, *S. coelicolor* A3(2) had been classified as follows (Stackebrandt *et al.*, 1997):

Phylum: Actinobacteria

Class: Actinobacteridae

Order: Actinomycetales

Suborder: Streptomycineae

Family: Streptomycetaceae

Genus: *Streptomyces*

Species: "*Streptomyces coelicolor*" A3(2)

Taxonomically, recent studies based on 16S rDNA sequencing (Baylis and Bibb, 1988, Witt and Stackebrandt, 1990), ribosomal AT-L90 protein (Ochi, 1995b, Ochi and Hiranuma, 1994) and L11 protein sequencing (Kawamoto and Ochi, 1998), DNA-DNA homology (Hatano *et al.*, 1994) and phage typing (Kornwendisch and Schneider, 1992) support the conclusion of Kutzner & Waksman (1959) and Monson *et al.* (1969) that *S. coelicolor* A3(2) belongs to the species of *Streptomyces violaceoruber* rather than being a validly described separate species, or being placed with common members of *S. coelicolor* (Muller 1908), which has very little taxonomic similarity with the strain (Ochi,

1995a). However, the name is too deeply conserved in the literature to justify making the correction.

6.1.2. Morphological, Cultural and Physiological Characteristics

S. coelicolor A3(2) is a soil bacterium like other members of the genera *Streptomyces*, though a significant number of the members of this genus are also found in aquatic habitats (Manteca *et al.*, 2005). This soil bacterium, like other members of Streptomycetes, possesses a complex life cycle similar to fungi (Elliot and Talbot, 2004), which starts by the germination of spores, followed by the development of branched hyphae or vegetative mycelium, which is then followed by the production of aerial hyphae which eventually undergo septation to yield chains of unigenomic spores as shown in Figure 6.1 (Chater and Losick, 1997).

Generally, the colonies of *Streptomyces* are produced by the mycelium of branching hyphae filaments. During adverse conditions, like drought, the hyphal growth becomes limited and much of the biomass converted into spores, which is the semi-dormant stage in the life cycle and allows the organism to survive in soil for long periods (Ensign, 1978). The study of Karagouni *et al.* (1993) has proved the spores are resistant to low nutrient and water availability whereas the mycelium is sensitive to drought. The conversion of *S. coelicolor* A3(2) mycelium to tough, desiccation-resistant spores occurs through the growth of a fluffy white aerial mycelium, which undergo multiple cell division to generate a string of unigenomic compartments (Kelemen and Buttner, 1998). *S. coelicolor* forms aerial mycelia and spores only when grown on solid media (Chater, 2001).

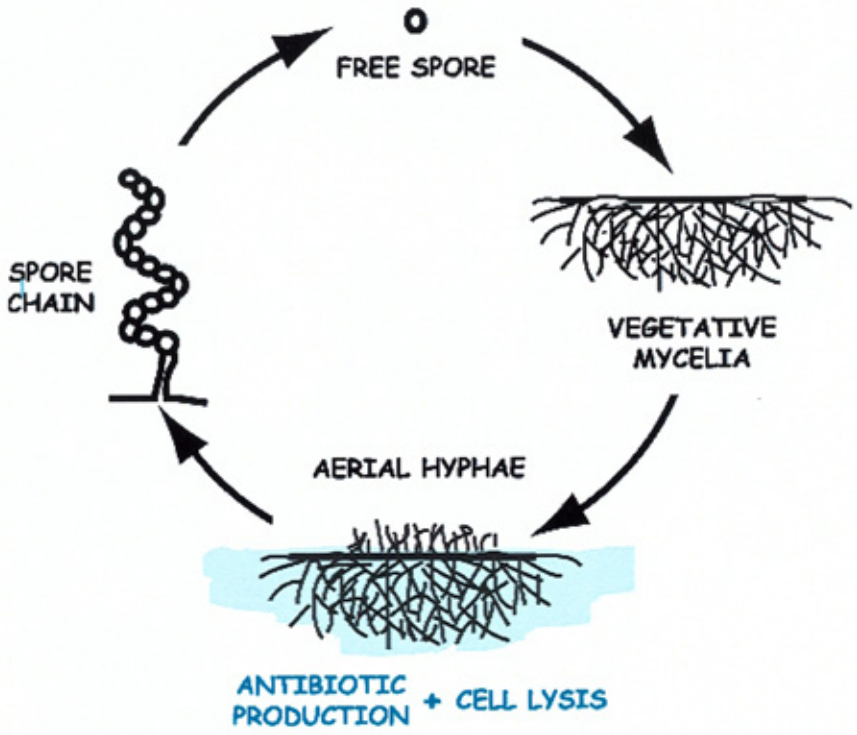

Figure 6.1. Complex life cycle of the genus *Streptomyces*. Taken from http://biology.kenyon.edu/courses/biol114/Chap11/Chapter_11A.html.

As a soil bacterium *S. coelicolor* A3(2) has the capability to degrade various organic compounds which include xylan, chitin and cellulose. The genome sequence of the organism revealed 172 genes encoding secreted proteins for carbon utilization, such as hydrolases, chitinases (19 have been identified of Family 18), cellulases, lipases and proteases (Kawase *et al.*, 2006, Bentley *et al.*, 2002, Bertram *et al.*, 2004) and also 81 ATP binding cassette (ABC) permeases has been identified which are possibly used for the uptake of sugars, oligopeptides and nucleosides as well as drug export (Schneider, 2001, van Veen and Konings, 1998).

6.1.3. Biochemical characteristics

Biochemical analysis indicates that the genus *Streptomyces* should be restricted to strains that have peptidoglycan composed of N-acetylglucosamine, N-acetylmuramic acid, alanine, D-glutamic acid and glycine with L-DAP as the diaminoacid (Azuma *et al.*, 1970, Uchida and Aida, 1977, Uchida and Aida, 1979). The fatty acid profile shows the major fatty acids in *Streptomyces* spp. are saturated, iso- and anteiso fatty acids (Kroppenstedt and Kutzner, 1976). For *S. coelicolor* iC14:0, C14:0, iC15:0, aiC15:0, C15:0, iC16:0, C16:0, iC17:0 and aiC17:0 have been detected, along with C16:1 unsaturated fatty acid (Li *et al.*, 2005). Members of the genus have a phospholipid type II pattern, i.e. consisting of diphosphatidylglycerol, phophatidylethanolamine, PI and PIMs (Lechevalier *et al.*, 1977), and menaquinone MK-9 has been detected as the major isoprenoid (Collins *et al.*, 1984, Alderson *et al.*, 1985). *Streptomyces* also contain TA but lack mycolic acids. For example, *S. coelicolor* was found to contain a ribitol-phosphate backbone TA (Naumova *et al.*, 1980b).

6.1.4. Antibiotic production

The genus *Streptomyces* has been identified with the production of more than 50 antibiotics; in *S. coelicolor* A3(2) 20 clusters responsible for antibiotic production have been identified and each cluster is believed to produce a different antibiotic chemical (Donadio *et al.*, 2002). An extensive study regarding the genetic control of antibiotic production and its connection to morphological and physiological development has been made (Hopwood *et al.* 1995). More recently, microarray analysis regarding growth phase and regulation of antibiotic synthetic pathways in *S. coelicolor* A3(2) has been reported by Huang *et al.* (2001). Hopwood (1999) has identified two pigmented antibiotics: tripyrrole undecylprodigiosin (Red) and actinorhodin (Act), which are blue yellow and blue, respectively, at high pH and both are red at low pH. The blue colour of Act is responsible for the *S. coelicolor* name. Another two non-pigmented antibiotics are the calcium-dependent antibiotic (CDA) and methylenomycin (Mmy), both of which can be assayed in simple plate culture inhibition assays (Anderson *et al.*, 2001). The pigmented *S. coelicolor* antibiotics can easily be observed in both plate and liquid cultures during growth as most of the secondary metabolite production was found to occur in the substrate (vegetative) mycelium (Anderson *et al.*, 2001).

6.2. Significance of investigating *S. coelicolor* M145 macroamphiphiles

The genome project of *S. coelicolor* A3(2) has revealed one of the largest sequences among the bacteria, whose genome sequence have been completed. Though this antibiotic producing industrially important organism has been studied intensely with regard to genetics, metabolism and antibiotic production, very little is known about its cell envelope. The present study of the macroamphiphiles will not only give insight into the nature of the cell envelope but may also reveal the function or necessity of the macroamphiphiles' function at different stages of its complex life cycle, i.e., spore, aerial mycelium and vegetative mycelium, for the first time.

The present study can compare the macroamphiphiles distribution between *S. coelicolor* A3(2) and *T. fusca* (another organism investigated in this project, discussed in Chapter 3). Both are filamentous mycelium and spore producing organisms of the phylum Actinobacteria. Though the two genera are phylogenetically well separated based on 16S rRNA sequence analysis, comparative genomic studies have shown a comparatively high orthology value for genes for these two organisms and suggested them to be more closely related (Chater and Chandra, 2006). Therefore, the present study will allow the comparison between macroamphiphiles distribution among these two genera, which may have value as chemotaxonomic markers. Finally, the distribution of macroamphiphiles may have further chemotaxonomic value, as the current classification systems has not yet solved the taxonomy within the genus. The present study might therefore aid subsequent investigations of the relationship between *S. coelicolor* A3(2) and *S. violaceoruber*.

6.3. Results

6.3.1. Organism and culture conditions

S. coelicolor M145 was supplied by Dr. Stephen Cummings (School of Applied Science, Northumbria University, Newcastle Upon Tyne, UK) and originally obtained from the John Innes Centre, Norwich. *S. coelicolor* M145 was successfully grown in sporulating, nonsporulating agar media and also in YEME liquid media (described in chapter 2, sections 2.1.2.6, 2.1.2.7 & 2.1.2.8, respectively).

The growth of the spores or mycelium of *S. coelicolor* M145 on sporulating agar plates were observed at different times. Figure 6.2 showed the culture plates grown for different times in sporulating agar media, along with the Gram stains of the cells which were observed at 100X magnification under an oil immersion lens. After 24 h the colour of the culture turns to reddish and vegetative mycelium can be observed in the Gram staining slide (Figure 6.2a), which gradually forms a white layer on the surface of the plate (Figure 6.2b) and mycelium can be observed in the Gram staining slide and this white layer finally turned to grey color after 5-6 days (Figure 6.2c), which has been found to be a spore rich culture. This stage was suitable for the preservation of the *Streptomyces* spores. The mycelium observed in Figure 6.2b and c are more likely to be aerial mycelium.

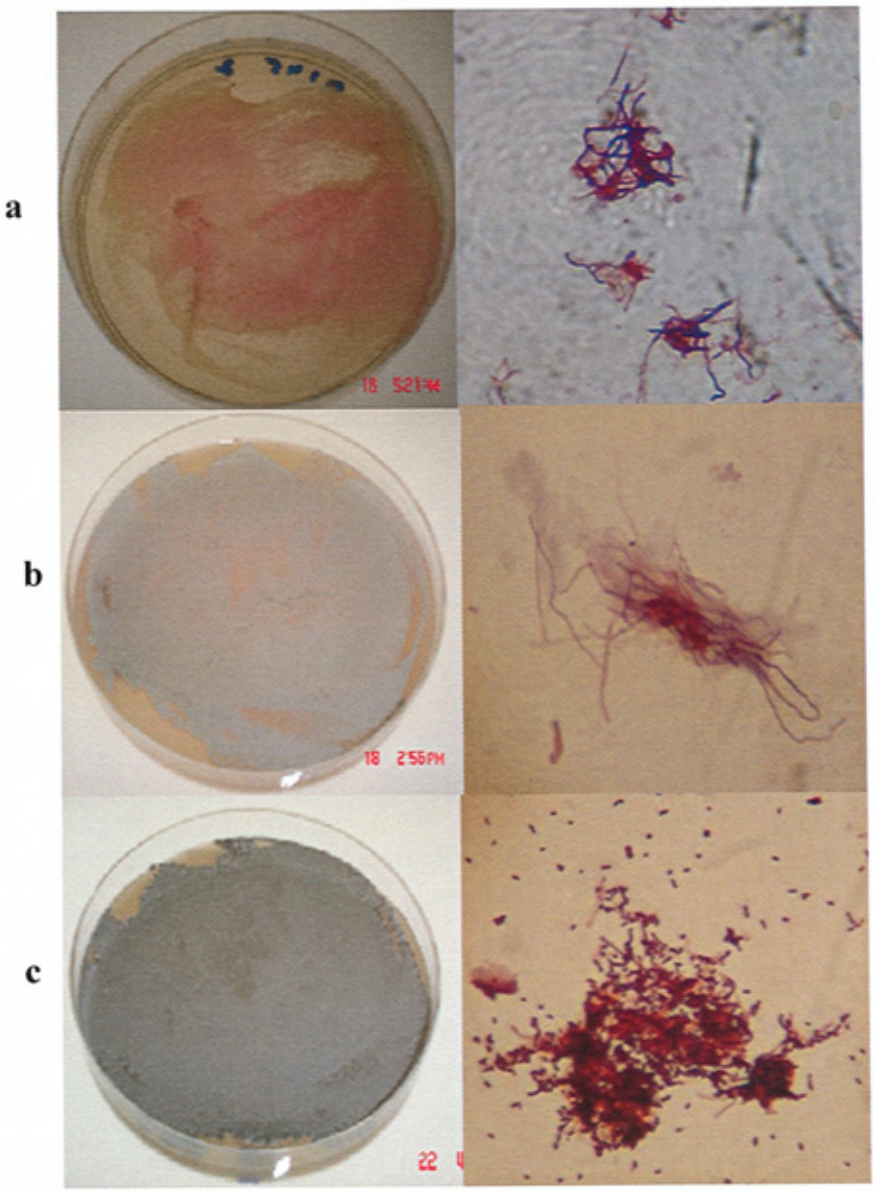

Figure 6.2(a-c). *S. coelicolor* M145 sporulating plate after (a) 24 h, (b) 72 h and (c) 144 h, showing the characteristic colour development and corresponding pictures of Gram stains, taken at 100X magnification under oil immersion lens.

6.3.2. Process optimization

Yeast extract-malt extract based (YEME) media has been used as a liquid culture media for the growth of *S. coelicolor* M145 (Kieser *et al.*, 2000). Mycelium was the best biomass for the physiological and biochemical studies, so it was essential to optimize the cultures condition to gain higher yields, as macroamphiphile studies require at least ca. 1 g of dry cells. Since the organism is highly aerobic, the culture needs to be shaken at 30°C at high speed (5 xg) and with sufficient air space for good aeration (2:5 v/v). *S. coelicolor* M145 tends to grow as rather compact masses or pellets of mycelium, so steps like adding polyethylene glycol (PEG), high concentration of sucrose (34 g/100 ml) in the media or physical changes such as using flasks containing baffles or inserting a stainless steel spring into ordinary Erlenmeyer flasks were taken to encourage a more dispersed growth. To optimize the process of higher yield a series of experiments was done. In the first stage of the optimization, high concentration sucrose, PEG and spring inserts were used to determine the optimal disperse growth conditions for *S. coelicolor* M145. Table 6.1 and Figure 6.3 show the observations of the culture and yield. These data suggested that dispersed growth, which increased the yield, was favored mostly by using a high concentration of sucrose with spring inserts.

In the second stage, the inoculation amount of spores was optimized by the weight of the dry cell yield in 200 mL YEME media. The result suggested (Table 6.2) that the inoculation of higher amount spores increased the yield, but the increase was not substantial.

Growth curves were performed by inoculating 1 Petri dish of spores (gross collection) in 200 mL YEME media using sucrose at 30°C and 300 x g. Figure 6.4 and the data in Table 6.3 suggested the increase in absorbance and dry cell weight (mg) had a good correlation and both of them gave similar growth curves. The highest growth was observed in both curves around 12 to18 h and then there were a decrease in the amount of yield. These results therefore suggested that the harvesting time of the culture was optimum around 18 h after the inoculation of the spores.

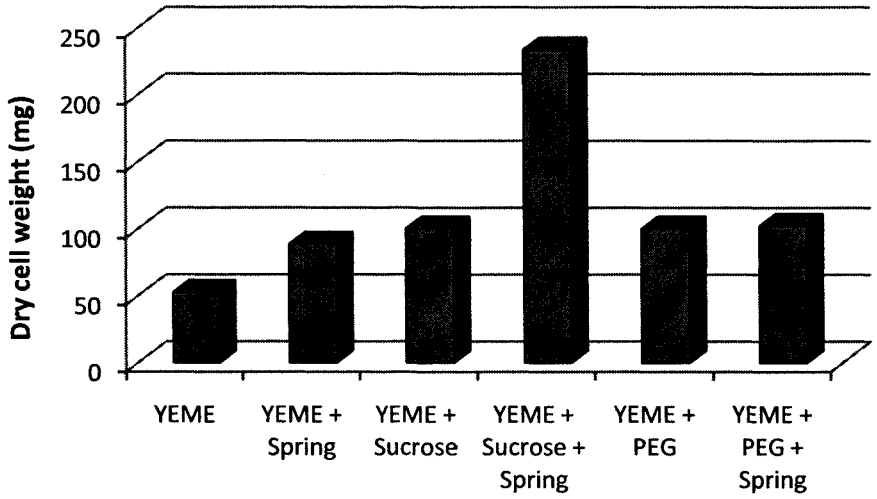

Figure 6.3. Optimizing dispersed growth condition for *S. coelicolor* M145 growth. Dry cell weight (mg) represented yields for each conditions and petridishes used reflects the gross amount of spores.

Table 6.1. Optimizing the growth conditions for dispersed growth of *S. coelicolor* M145. 200 ml (total volume) of YEME media and 0.5 ml of spore suspension was used as inoculums for each condition.

Process	Observation	Yield dry cell weight (mg)
Only YEME	• Clumping together (clumps can be seen) • No foam produced • Two layers produced after centrifugation, black (spore): white (mycelium) approx 1:1	52.6
YEME + Spring	• Clumping size smaller (hard to see) • Foam produced • Two layers produced after centrifugation, black (spore): white (mycelium), less than 1:1.	88.7
Sucrose	• No clumping • No foam • White layer is present in significant amounts after centrifugation	100.3
Sucrose + Spring	• No clumping with cloudy appearance • Foam produced • White layer is quite a significant amount after centrifugation	234.1
PEG	• No clumping with cloudy appearance • No foam • Both white and grey layer are present in significant amounts after centrifugation	100.2
PEG + Spring	• No clumping with most cloudy appearance • No foam • Both white and grey layer are present in significant amounts after centrifugation	102.3

Table 6.2. Optimization of the inoculation of spores in 200 mL YEME media containing 34 g/100 mL sucrose and using springs in the flask.

Number of Petri dish	**Yield in 200 mL media (mg)**
1	192.3
2	202.0
3	224.4

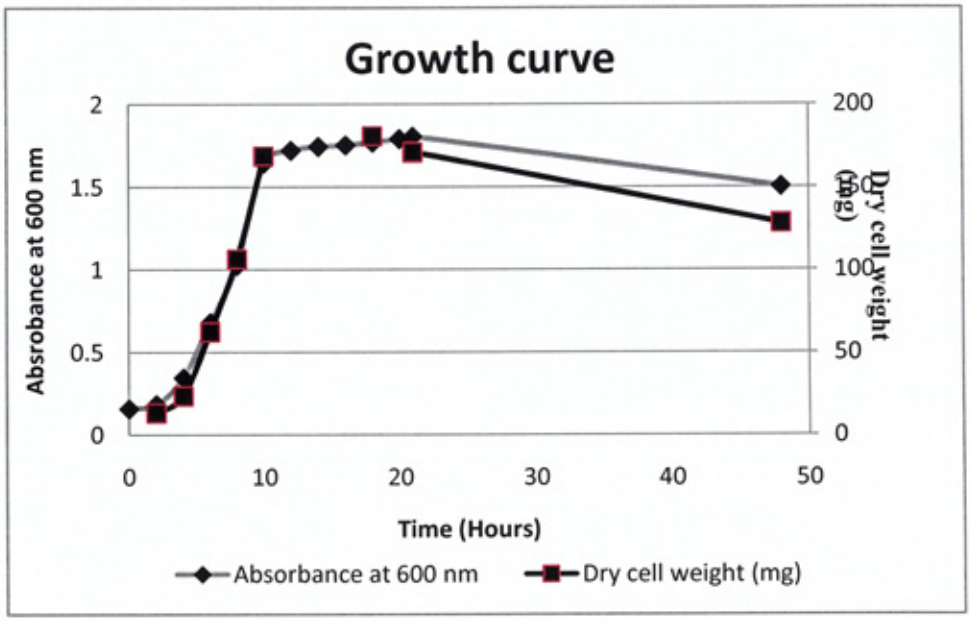

Figure 6.4. Growth curve of *S. coelicolor* M145. Growth was measured as increased absorbance at 600 nm over time or by weighing the dry cell weight obtained.

Table 6.3. Growth curve data for *S. coelicolor* M145, inoculation of 1 petridish spores in 200 mL YEME media containing 34 g/100 mL sucrose the flask.

Time (h)	Absorbance at 600 nm	Dry cells weight (mg)
0	0.158	-
2	0.183	13.28
4	0.346	23.55
6	0.679	62.33
8	1.026	106.56
10	1.644	168.84
12	1.72	-
14	1.743	-
16	1.752	-
18	1.768	180.87
20	1.79	-
21	1.804	171.12
48	1.503	128.25

6.3.3. Purification of the *S. coelicolor* M145 macroamphiphiles

Macroamphiphilic material was extracted from *S. coelicolor* M145 by the standard hot phenol-water extraction method (described in Chapter 2, section 2.1.5.1). The extracted macroamphiphile(s) was purified by HIC-FPLC (Chapter 2, section 2.1.6.1). The column fractions from the HIC were subjected to carbohydrate and phosphate assay (methodology described in Chapter 2, sections 2.1.7.1 & 2.1.7.2, respectively), as shown in Figure 6.5. Hydrophilic contaminants (nucleic acids and polysaccharides) not retained by the HIC column were recovered during the elution with equilibration buffer as peak 1. Subsequent gradient elution with an increasing concentration of propanol recovered two carbohydrates and phosphate containing peaks (Peak 2 and 3 in Figure 6.5). Peak 2 contained a significant amount of phosphate compared to carbohydrate, and peak 3 contained lesser amounts of phosphate compared to peak 2. The HIC-FPLC runs for subsequent repeat experiments shown on Appendix V.

Dot-immunoblotting (method described in Chapter 2, section 2.1.7.3) with a monoclonal anti-LTA (Table 2.12) reacted positively with fractions just before and across peak 2 but didn't react with the fractions across peak 3 as shown in Figure 6.6.

Peak 2 fractions were recovered by freeze-drying after extensive dialysis and represented 0.23 to 0.24 % of the dry cell weight extracted when using the hot phenol-water extraction method; the peak 3 represented 0.09 to 0.10% of the dry cell weight extracted. However, introducing a delipidation step (described

in Chapter 2 and Section 2.1.4) before the phenol extraction method decreased the quantity of peak 3 recovered to below a measurable level and increased the yield of peak 2 to 0.7 to 0.8% of the dry cell weight extracted. The change in the HIC profile which was observed is shown in Figure 6.7.

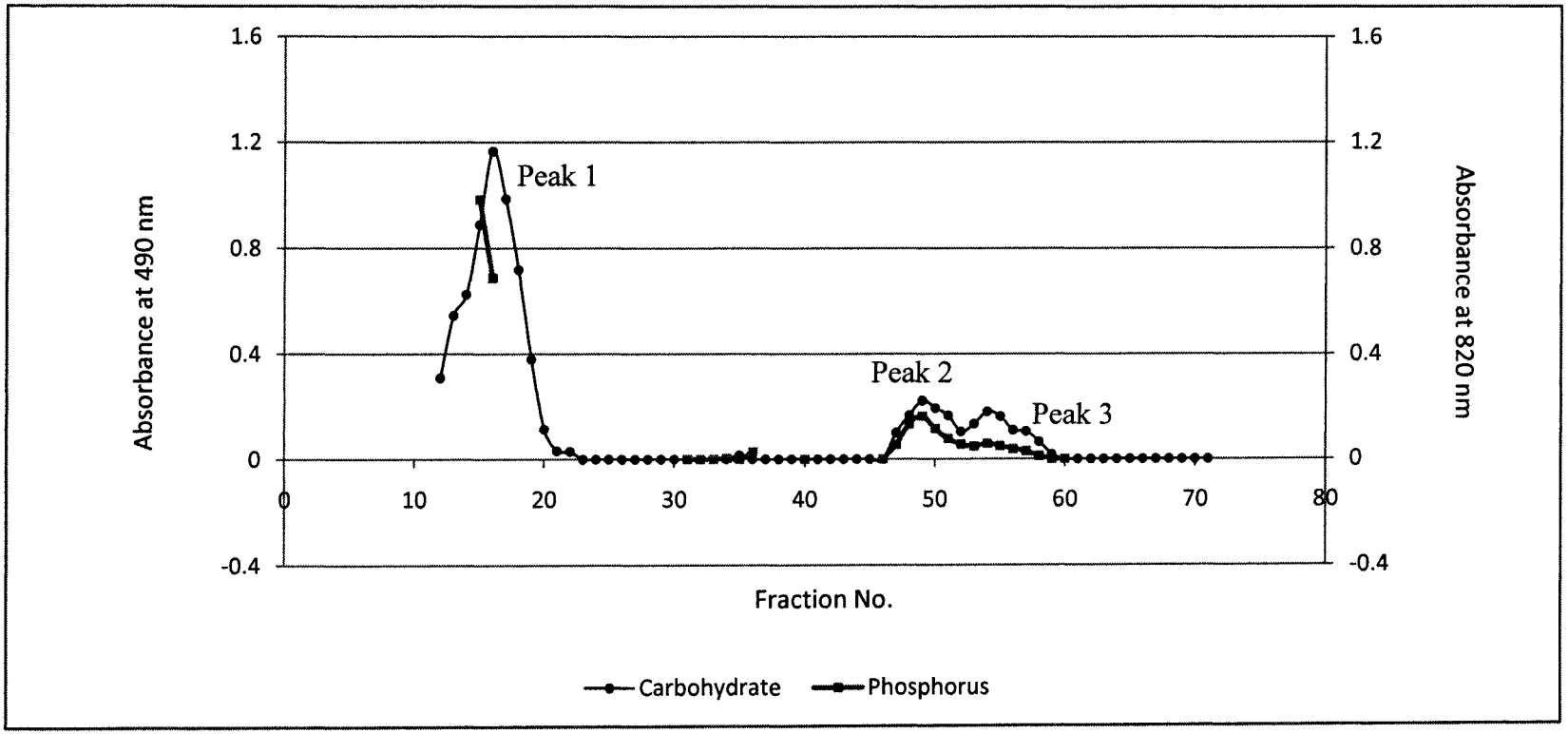

Figure 6.5. HIC profile for the purification of a crude phenol extract from *S. coelicolor* M145. The crude extract was loaded to the column with equilibration buffer until fraction 12, after which gradient elution with an increasing concentration of propanol was begun. Column fractions (4 mL) were analyzed for carbohydrate and phosphorus. Peak 2 (fractions 44-52) and Peak 3 (fractions 53-61) were pooled, dialysed and recovered by freeze drying.

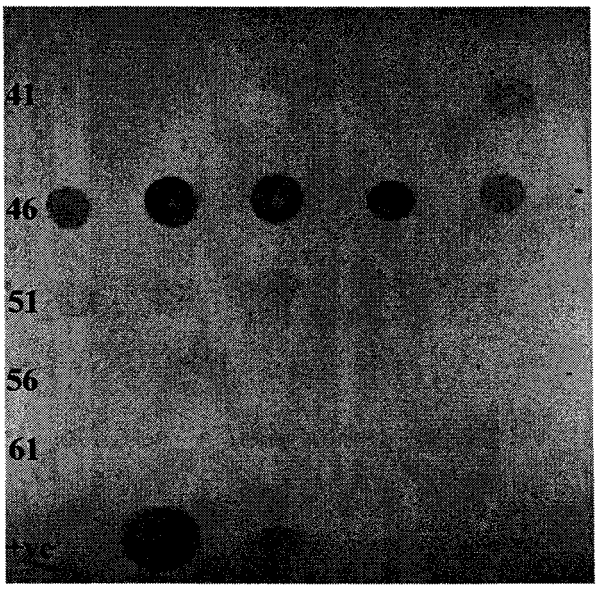

Figure 6.6. Dot immunoblotting of HIC column fractions with monoclonal anti-LTA. The number represents the fractions number. Fractions 45-53 showed a positive reaction with the monoclonal anti-LTA which represented the fractions slightly earlier than and across peak 2 of Figure 6.5. Positive control spots are serial 10-fold dilutions of an approximately 1 mg/mL LTA preparation from *Streptococcus agalactiae*.

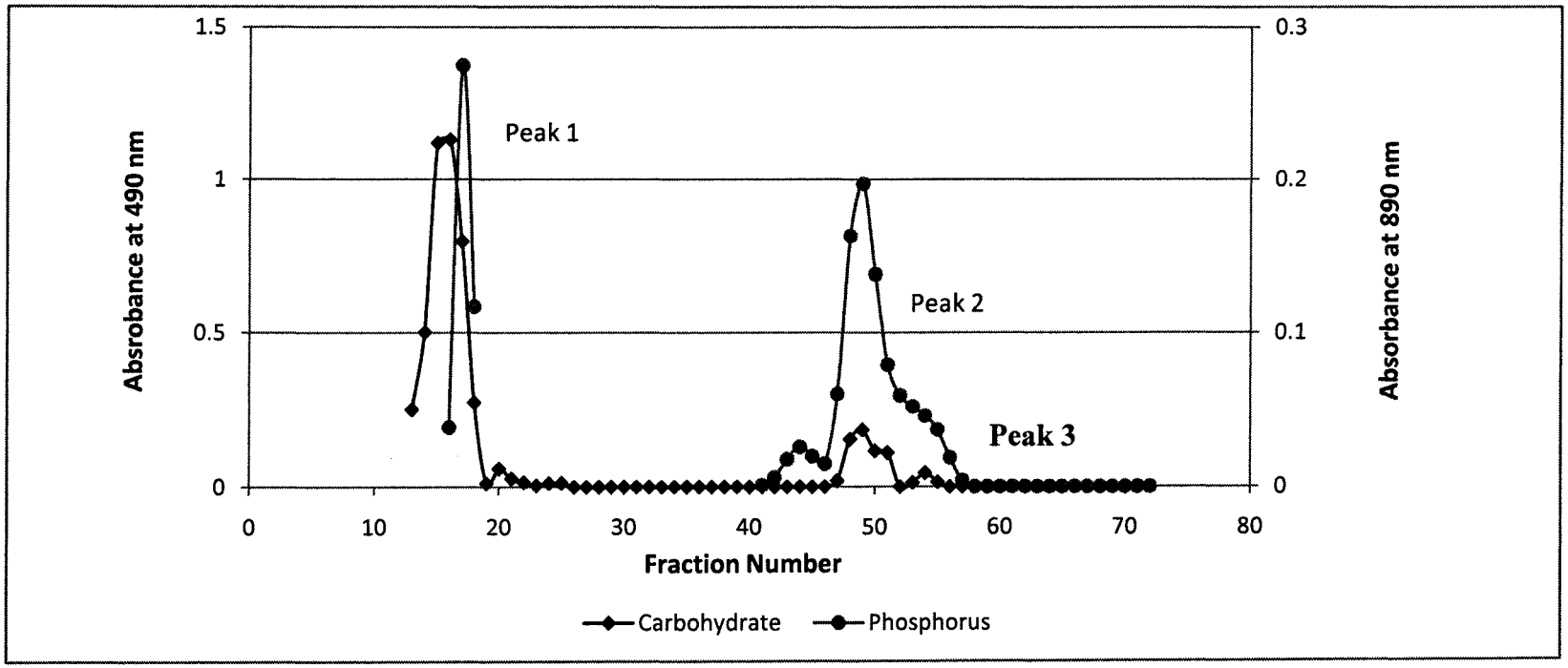

Figure 6.7. HIC profile for the purification of a crude phenol extract from *S. coelicolor* M145 showing the effect of the introduction of a delipidation step prior to the phenol extraction. The crude extract was loaded to the column with equilibration buffer until fraction 12, after which gradient elution with an increasing concentration of propanol was begun. Column fractions (4 mL) were analyzed for carbohydrate and phosphorus. Peak 2 (fractions 43-50) and Peak 3 (fractions 52-55) were pooled, dialysed and recovered by freeze drying.

6.3.4. Chemical composition of the macroamphiphiles

Chemical analysis indicated the presence of notable amounts of phosphorus in the peak 2 materials of *S. coelicolor*. Protein contamination was assayed using a commercial kit (Chapter 2, section 2.4.2), and determined to be below the level of detection.

The fatty acid composition of the whole cells and macroamphiphiles of *S. coelicolor* was determined by FAME derivatisation and GC analysis (described in Chapter 2, Section 2.2.6.1) and is summarised in Table 6.4 and Figure 6.8. The major fatty acids detected in the whole bacterial cells were aiC15:0, iC16:0, C16:0 and aiC17:0 with minor amounts of iC14:0, iC15:0, C15:0, iC17:0, C17:0 and C17:1 (Figure 6.8, Table 6.4). Cell samples collected throughout the whole growth cycle were taken (at 36, 72 and 144 h growth) and displayed the same fatty acid pattern (data not shown). Fatty acid profiles were obtained for the macroamphiphilic materials of Peak 2 and 3, which showed of the same fatty acid profiles although with increases and decreases of the relative percentage of some fatty acids as shown in Figure 6.8 and Table 6.4.

The sugar composition of the macroamphiphile fractions were determined following acid hydrolysis to release monosaccharide components and derivatisation to alditol acetates for GC, as described in Chapter2, section 2.2.6.2. As shown in Figure 6.9 and Table 6.5, the macroamphiphilic materials of Peak 2 and 3 contained predominantly glycerol, mannose and glucose, and the ratio of inositol and arabinose decreased in peak 3. Notably, there was a

significant amount of galactose in Peak 2, whereas this was barely detectable in peak 3.

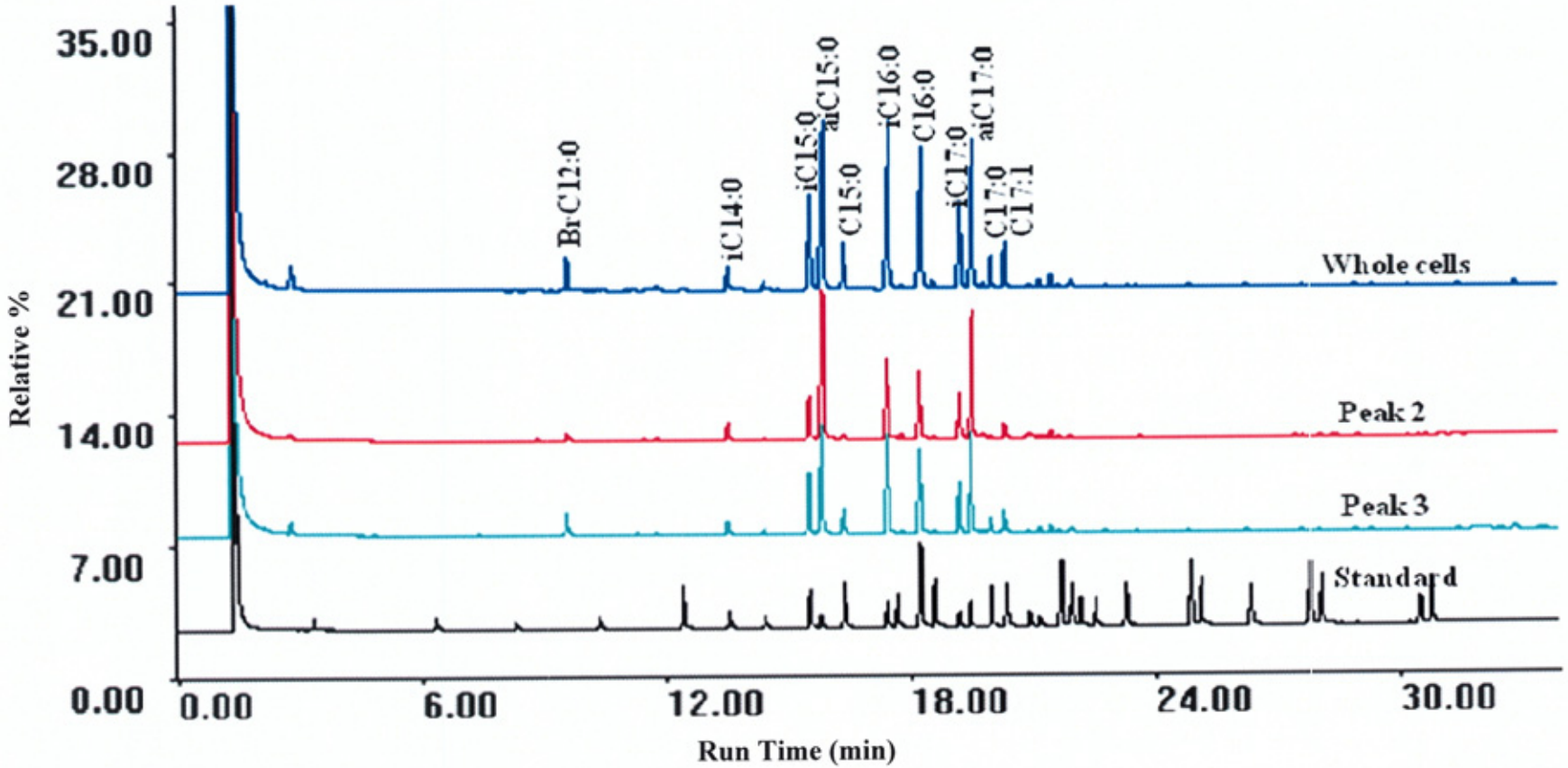

Figure 6.8. FAME analysis results for whole cells and peak 2 & 3 macroamphiphilic materials of *S. coelicolor*. The label of standard fatty acids has been shown in Chapter 2, Figure 2.4.

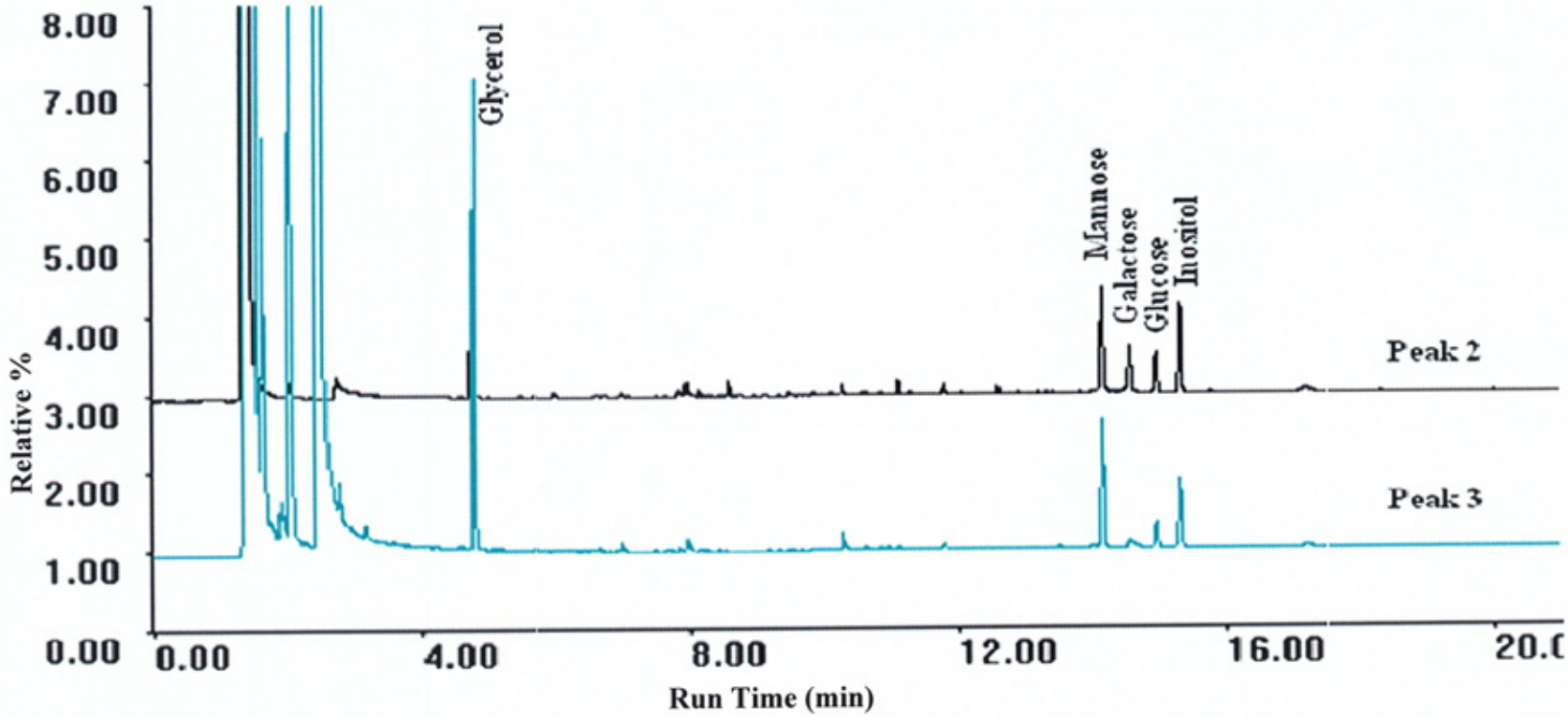

Figure 6.9. Carbohydrate analysis results for peak 2 & 3 macroamphiphilic materials of *S. coelicolor*. The peaks were identified in comparison to standard sugars as has been shown in Chapter 2, Figure 2.5 and Table 2.14.

Table 6.4. Comparison of the Peak 2 & 3 macroamphiphile fatty acid composition with that of the whole cell fatty acids of *S. coelicolor* M145.

FAME identified[a]	**Whole cells**	**Peak 2 macroamphiphile**	**Peak 3 macroamphiphile**
Unknown[b]	0.91	Trace	trace
iC14:0	3.2	1.5	0.9
iC15:0	9.6	9.1	5.8
aiC15:0	22.6	16.4	10.3
C15:0	2.2	1.8	2.1
iC16:0	26.9	23.9	14.3
C16:0	12.9	17.2	23.2
iC17:0	6.7	8.2	6.9
aiC17:0	15.8	18.4	12.4
C17:0	trace	1.8	2.0
C17:1	trace	2.1	trace

[a] Fatty acids were analysed by GC of their methyl esters and identified by comparison with a mixture of 32 authentic standards (Sigma Chemical Co.) Composition is given as the percentage of total integrated chromatographic peak areas. [b]Unknown is possibly a branched chain C12:0 fatty acid.

Table 6.5. Carbohydrate composition of the HIC-purified acid hydrolysed macroamphiphiles of *S. coelicolor* M145

Carbohydrate identified[a]	**Peak 2 macroamphiphile**	**Peak 3 macroamphiphile**
Glycerol	23.818	58.040
Arabinose	2.017	trace
Mannose	26.105	23.522
Galactose	11.317	ND
Glucose	10.539	4.351
Inositol	23.272	3.017

[a] Carbohydrates were analysed by GC of their alditol acetate derivatives and identified by comparison with a mixture of authentic standards (alditol acetates of glycerol, erythritol, rhamnose, ribose, arabinose, xylose, mannose, galactose, glucose and inositol) shown in Figure 2.5. Composition is given as the percentage of total integrated chromatographic peak areas. ND means not detected.

6.3.5. Electrophoretic analysis of the *S. coelicolor* macroamphiphiles

The *S. coelicolor* M145 macroamphiphile fractions (phenol extracted, HIC purified) were examined by electrophoresis followed by staining with Silver-nitrate, Alcian-Blue 8GX and periodate Schiffs reagent (described in Chapter 2, Sections 2.2.3.1, 2.2.3.2 and 2.2.3.3 respectively). Alcian blue 8GX, and combined Alcian Blue and silver nitrate staining each revealed a broad staining band around 25 KDa and 20 KDa region and also another broad band around 10 KDa (Figures 6.10 and 6.11, lane 2, respectively) for the material in peak 2 of Figure 6.5 and 6.7. On the other hand, the peak 3 material from Figure 6.5 showed similar electrophoresis pattern but introducing delipidation steps prior to phenol extraction reduced the amount of the band around 10 KDa and the 25-20 KDa broad band was not evident in this sample (Lane 5, Figures 6.10 and 6.11).

Periodate Schiffs reagent stained the band in the 10 KDa regions of both Peak 2 and Peak 3 quite intensely, while for the bands in the 25 to 20 KDa region, the staining was not as intense and again not evident in Peak 3 (Figure 6.12). Moreover, the data in Figure 6.12 shows that the 10 KDa region band was in similar position with a PIM_6 standard.

Though the staining did not detect any macromolecules which were similar to reference LTA in electrophoretic mobility, on Western blotting the Peak 2 material reacted with a polyclonal anti-LTA (data not shown) and monoclonal anti-LTA (Figure 6.13). It was noted that the cross-reaction was in a very

similar position to that of the reference LTA suggesting peak 2 contained LTA with other two macromolecules (i.e. those at ca. 10 kDa and at ca. 20-25 kDa).

Lectin blotting showed a negative reaction (Figure 6.14), i.e. a clear zone was visible amongst the general background development, around the 20-25 KDa region. From this it could also be assumed that the mannose observed by GC was not abundantly present as terminal mannose residues in the macroamphiphiles, since this lectin binds to terminal mannose.

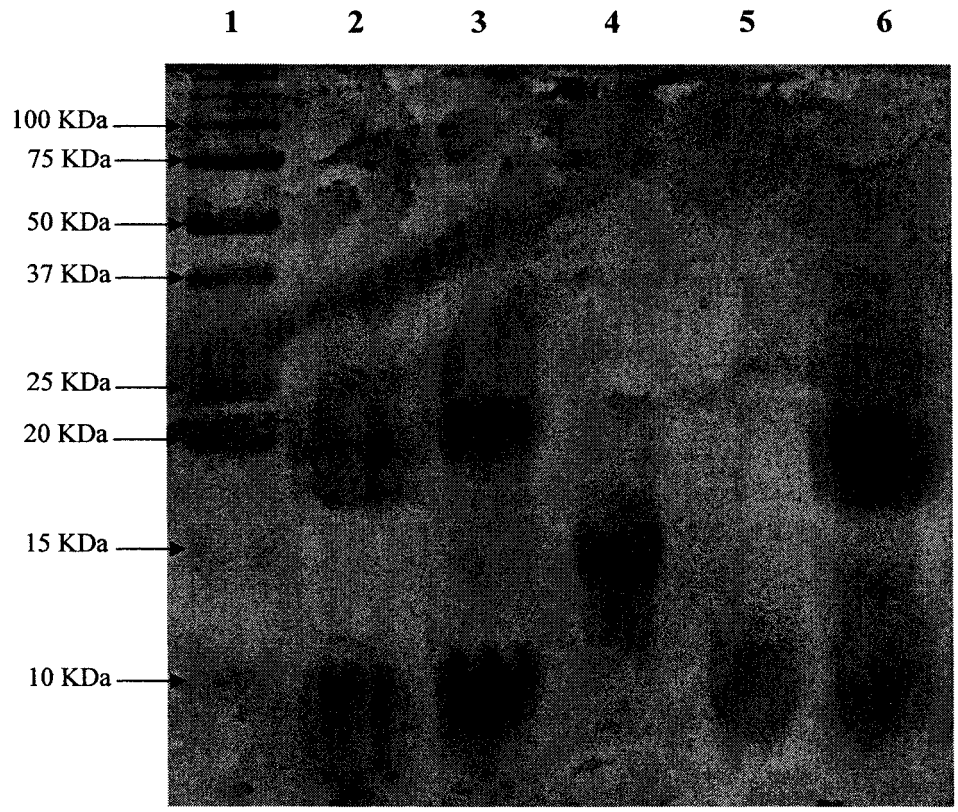

Figure 6.10 Alcian Blue staining of *S. coelicolor* M145 macroamphiphile preparations. Lane 1: Protein standards ladder; Lane 2: Peak 2; Lane 3: Peak 3; Lane 4: GBS LTA (standard); Lane 5: Peak 3 (from cells subjected to delipidation prior to phenol extraction); Lane 6: Peak 2 (from cells subjected to delipidation prior to phenol extraction).

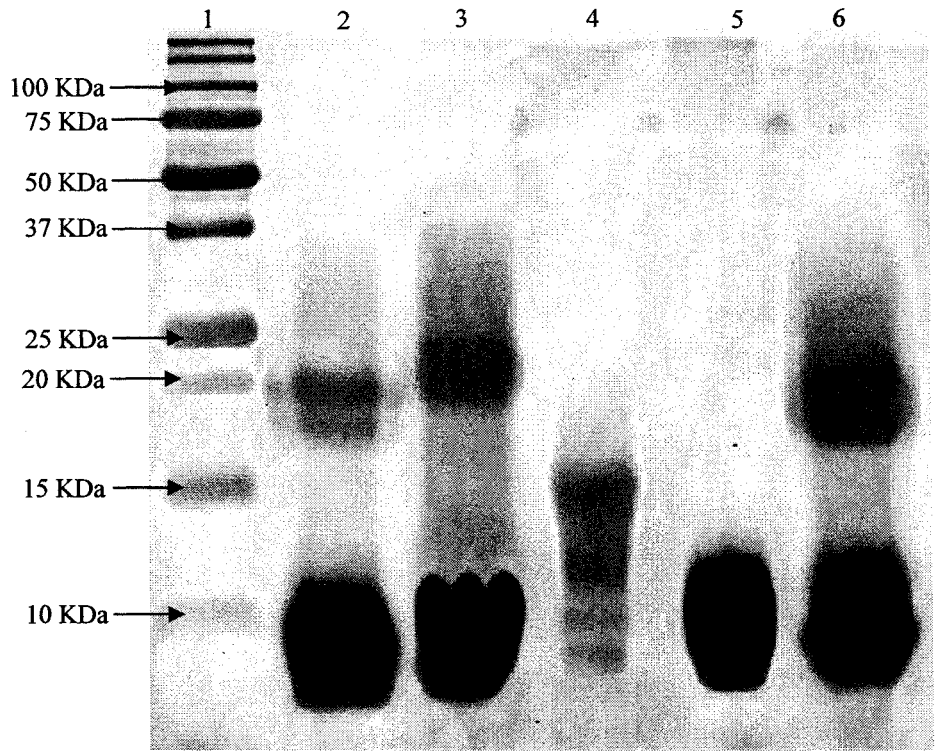

Figure 6.11. Alcian Blue & Silver-nitrate staining of *S. coelicolor* M145 macroamphiphile preparations. Lane 1: Protein standard ladder; Lane 2: Peak 2; Lane 3: Peak 3; Lane 4: GBS LTA (standard); Lane 5: Peak 3 (from cells subjected to delipidation prior to phenol extraction); Lane 6: Peak 2 (from cells subjected to delipidation prior to phenol extraction)

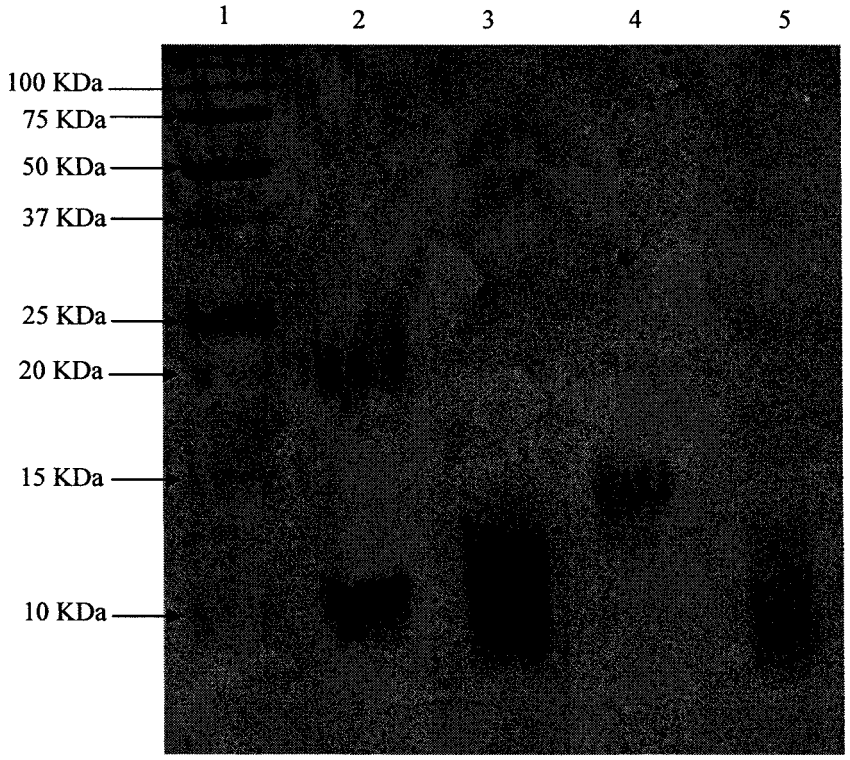

Figure 6.12. Periodate Schiffs reagent staining of *S. coelicolor* M145 macroamphiphile preparations. Lane 1: Protein standard ladder; Lane 2: Peak 2; Lane 3: Peak 3; Lane 4: GBS LTA (standard); Lane 4: PIM_6 standard.

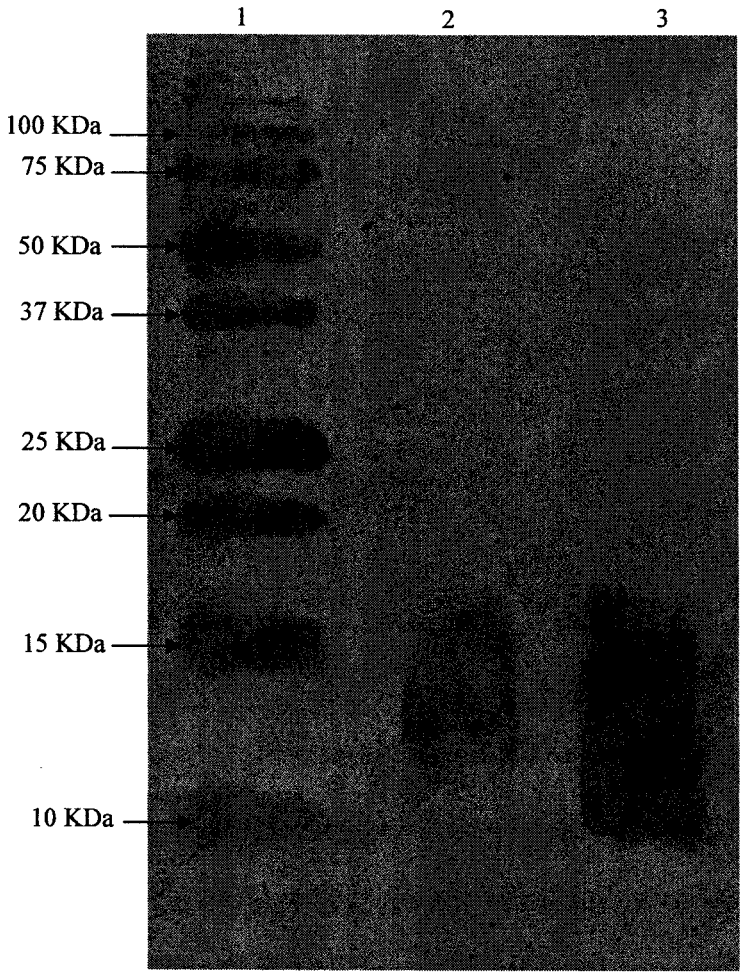

Figure 6.13. Western blotting of *S. coelicolor* M145 macroamphiphile preparations using a monoclonal anti-LTA antibody. Lane 1: Protein standard ladder; Lane 2: Peak 2; Lane 3: GBS LTA (standard).

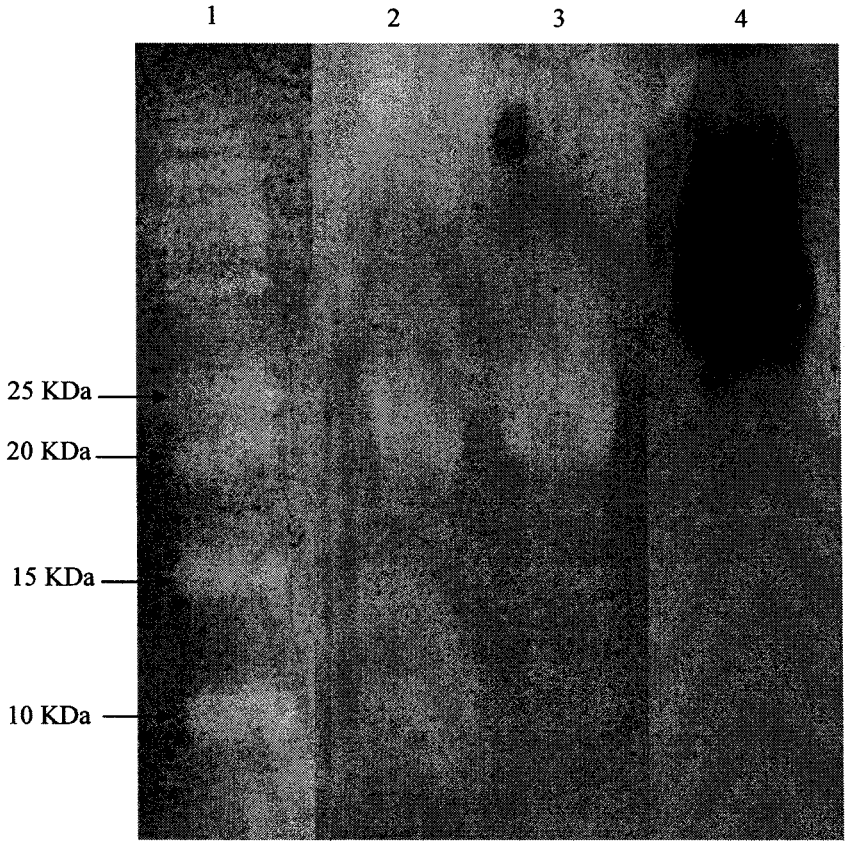

Figure 6.14. Lectin blotting of *S. coelicolor* M145 macroamphiphile preparations. Lane 1: Protein standard ladder, Lane 2: *S. coelicolor* Peak 2 macroamphiphiles Lane 3: *S. coelicolor* Peak 3 macroamphiphiles; Lane 4: LAM standard (overloaded). Negative staining of the macroamphiphiles appears light against the background. Irrelevant sample lanes between samples shown in lanes 1 and 2 & lanes 3 and 4 have been digitally removed.

6.3.6. Distinguishing Lipoteichoic acid (LTA) Vs Teichoic acid (TA)

S. coelicolor M145 may contain polyGroP wall teichoic acids as SCWP (Section 1.6.2) which could explain the cross-reaction with the monoclonal anti-LTA antibody described above. Consequently, additional experiments were done to prove that the positive anti-LTA reaction for the *S. coelicolor* M145 macroamphiphile was not a false positive reaction of a membrane-anchored TA precursor, using an experimental design similar to that shown in Figure 3.11.

TA materials were extracted from *S. coelicolor* M145 using the TCA extraction method (describes in Chapter 2, Section 2.4). There was no peak identified for either macroamphiphile or TA materials at 232 nm, by UV spectrometry, which proves that neither molecule is bound to the membrane carrier undecaprenyl (Mcarthur *et al.*, 1980, Ginsberg *et al.*, 2006), which has multiple carbon-carbon double bonds and should have absorbed light at this wave length (Collmer *et al.*, 1988). The alditol acetate GC method for the analysis of carbohydrate showed that both the macroamphiphile and TA contained mainly glycerol, but the TA preparation also contained ribose or ribitol, consistent with a possible ribitol-phosphate backbone in a TA (Figure 6.15). The fatty acid analysis again demonstrated that the macroamphiphile preparation contained fatty acids (consistent with a hydrophobic moiety), which were absent in the TCA-extracted TA materials as expected. Cumulatively, these data were consistent with the assumption that one of the extracted macroamphiphiles in Peak 2 from the HIC purification is an LTA rather than a

membrane-anchored TA precursor (as described in Chapter 1, section 1.6.2.1. and Figure 1.9).

The presence of TA in *S. coelicolor* was further analysed by electrophoresis followed by Combined Alcian Blue and Silver nitrate staining and Western blotting with the monoclonal anti-LTA antibody (Table 2.12). Combined Alcian Blue and silver-nitrate staining showed the position of the TA was similar to the position of LTA (GBS) as shown in Figure 6.16, but the TCA extracted TA did not give a positive reaction with the monoclonal anti-LTA (Figure 6.17), again strongly suggesting the HIC Peak 2 containing anti-LTA positive reaction was not due to a TA. This also indicated that the antibody was very specific for LTA only, even though the backbone structure of both the TA and LTA are similar but stereochemically different as described in Section 1.7.3. The results for this section has been summarised in Table 6.6.

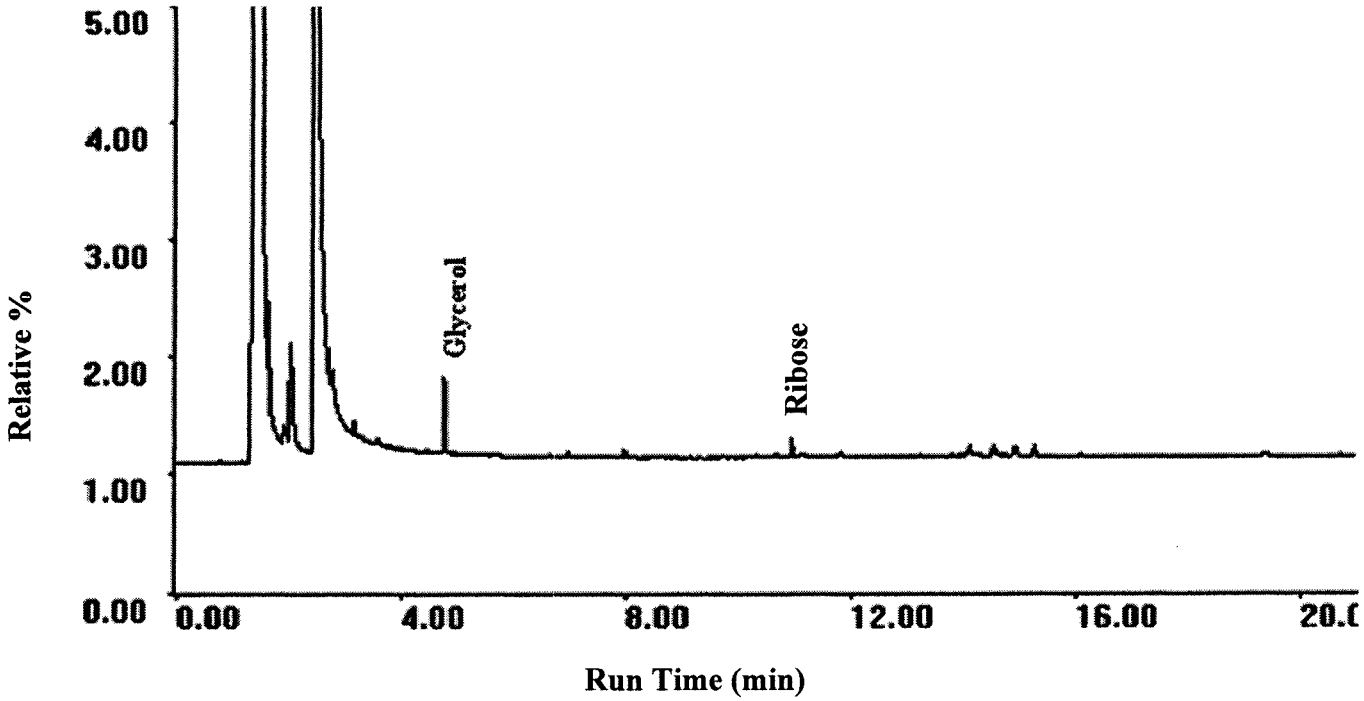

Figure 6.15. Carbohydrate analysis results for the TA extract from *S. coelicolor* M145. The peaks were identified by reference to the standard sugars as shown in Chapter 2.

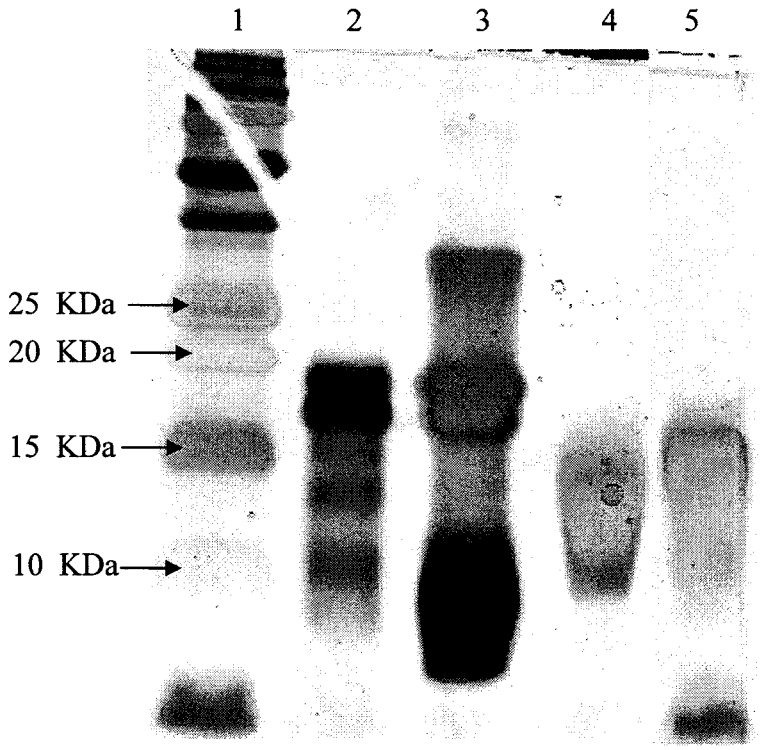

Figure 6.16. Alcian Blue & Silver-nitrate staining of *S. coelicolor* M145 extracts. Lane 1: Protein standard ladder; Lane 2 & 3: HIC Peak 2 fractions from different macroamphiphile preparations; Lane 4: TCA extracted TA material; Lane 5: GBS LTA (standard).

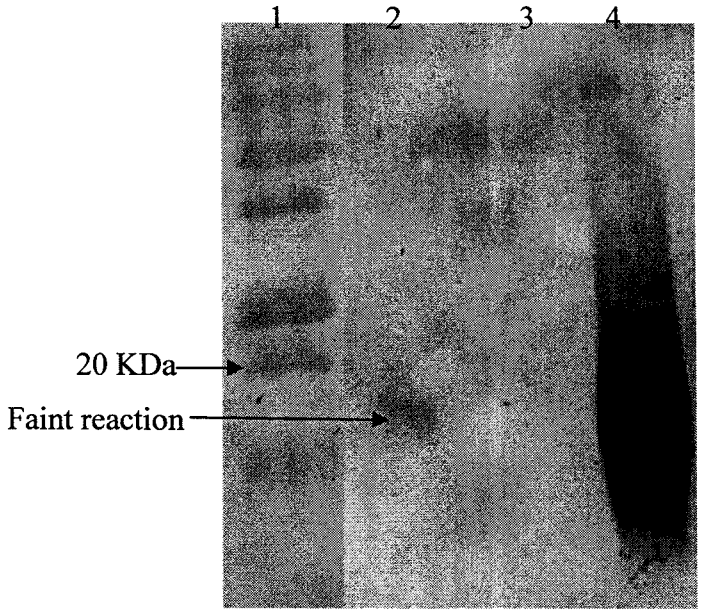

Figure 6.17. Monoclonal anti-LTA blotting of *S. coelicolor* M145 preparations. Lane 1: Protein standard ladder; Lane 2: HIC Peak 2 macroamphiphile; Lane 3: TCA extracted TA; Lane 4: LTA (standard, overloaded). Irrelevant sample lanes between samples shown in lanes 1 and 2 have been digitally removed.

Table 6.6. Results for the analysis of TCA extractable materials from *S. coelicolor*. GC represents the gas chromatography, CHO represents alditol acitates test in GC and FAME represents the fatty acid analysis test.

Experiment		***Streptomyces coelicolor***	
		Macroamphiphile (Peak 2)	**Precursor TA**
Absorbance at 232 nm (prenyl presence)		**No peak**	Should give peak
GC	FAME	**FA present**	No fatty acids
	CHO	GroP backbone	GroP backbone (different stereochemistry)
Gel	Anti-LTA blotting	**+ve at similar position to . GBS-LTA std**	**TA prep gave no reaction**

6.3.7. Separating the macroamphiphilic materials by anion exchange chromatography

From the gel electrophoresis analysis, *S. coelicolor* M145 macroamphiphiles (peak 2, Figure 6.5) was revealed to contain three molecules i.e. material that stains at ca. 20-25 kDa; material that cross-reacts with the monoclonal anti-LTA; and the low molecular weight (≤ ca 10 kDa) material which may be glycolipids as this component was diminished by prior delipidation of the whole cells. Since LTA is anionic whereas other macroamphiphilic materials may contain different sugar units, and possible substituents, anion exchange chromatography was attempted to separate the macromolecules on the basis of possible charged group differences, as previously described for *K. radiotolerans* (Section 5.3.6). The purified phenol-extracted macroamphiphiles obtained from the HIC column were dialysed and lyophilised and subjected to anion exchange chromatography as described in Chapter 2, Section 2.1.6.2. The fractions obtained were subjected to carbohydrate assay, as shown in Figure 6.18. As shown, the anion exchange chromatography was unable to adequately separate the macromolecules.

Consistent with the phosphate peak detected (Figure 6.18), LTA blotting showed a positive reaction across 45-57 fractions regions (Figure 6.19). Fractions 3-5, 35-61, 66-68 and 82-88 were collected separately, dialyzed and lyophilized, the recovered purified products were subjected to SDS-PAGE analysis. However, Alcian Blue, Silver-nitrate stain or anti-LTA blotting failed to reveal the macroamphiphiles as being resolved into separate fractions, presumably because the sample recovered in each fraction were below the level

of detection (data not shown). The anion exchange chromatography was performed several times but on each occasion was unsuccessful in separating. The macroamphiphiles chromatography profiles of repeated anion-exchange have been shown in Appendix V.

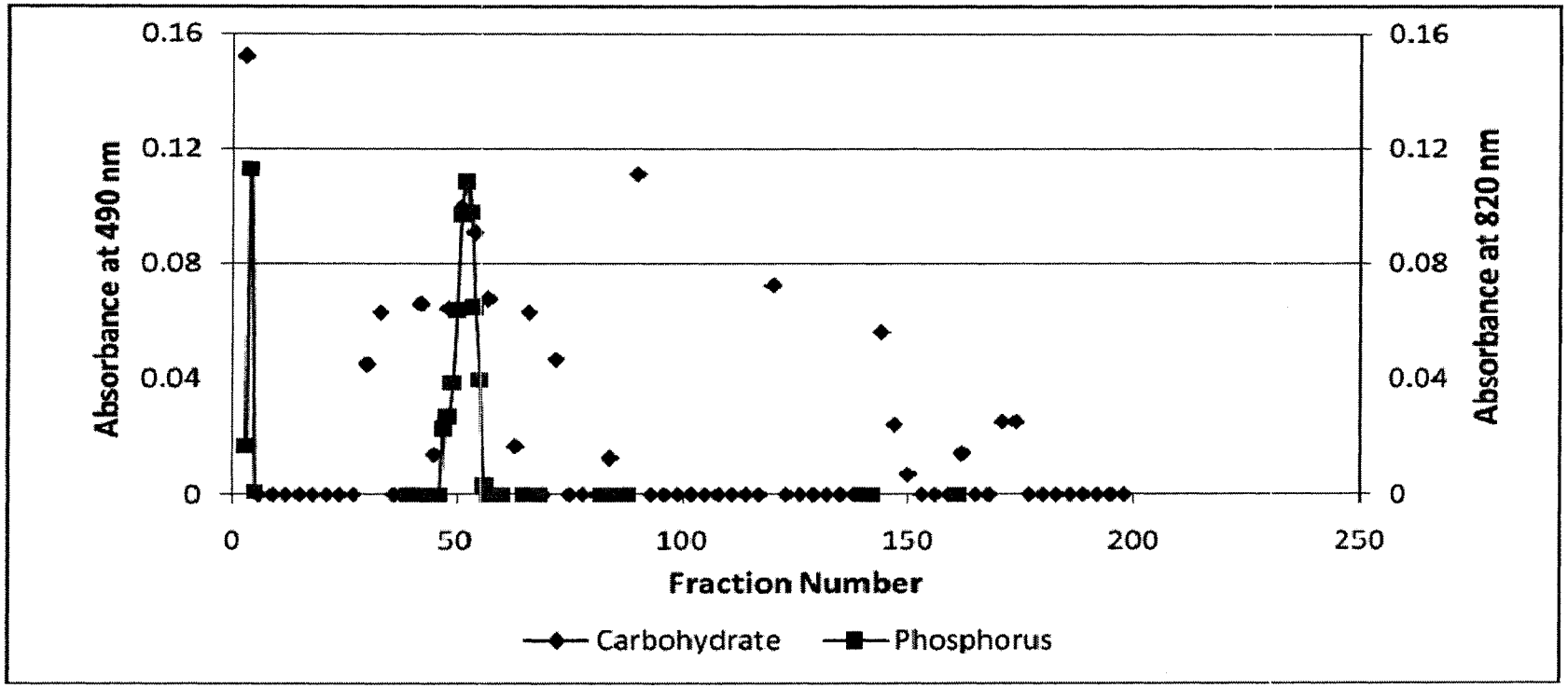

Figure 6.18. Anion exchange chromatography profile for the purification of a HIC purified macroamphiphile preparation from *S. coelicolor*. The sample was loaded onto the column with equilibration buffer until fraction 20, after which gradient elution with an increasing concentration of NaCl was begun. Column fractions (5 mL) were analyzed for carbohydrate and phosphorus.

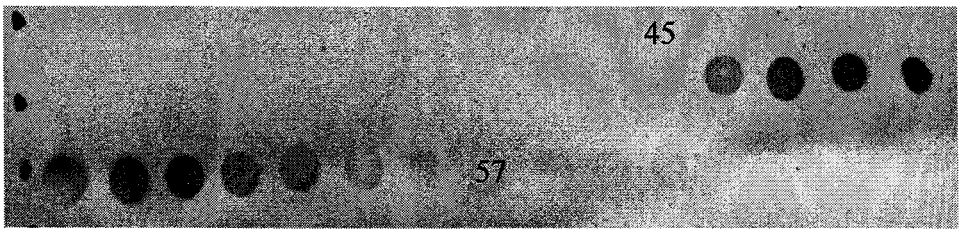

Figure 6.19. Dot immunoblotting of anion exchange column fractions with monoclonal anti-LTA. The number represents the fractions number. Fractions 45-57 showed a positive reaction with the monoclonal anti-LTA, consistent with positive fractions previously detected by HIC (Figure 6.6).

6.3.8. Purification of mannose containing molecules

Since the anion exchange chromatography had failed to adequately separate the macroamphiphilic fraction, the HIC purified molecules (comparable to peak 2, Figure 6.5) were subjected to Mannose-Binding protein (MBP) column chromatography in order to separate them on the basis of their mannose content, as the carbohydrate analysis by GC showed the presence of mannose residues as shown in Table 6.5.

MBP column chromatography was performed as described in Chapter 2, Section 2.1.6.3. The fractions were subjected to carbohydrate and phosphate assays, which revealed two peaks, as shown in Figure 6.20 (Peak 1 & 2). Since the peak 1 material did not bind to the column, this suggested that the macromolecule present did not contain any mannose residues. On the other hand, peak 2 material was revealed to contain mannose, due to the binding to the column.

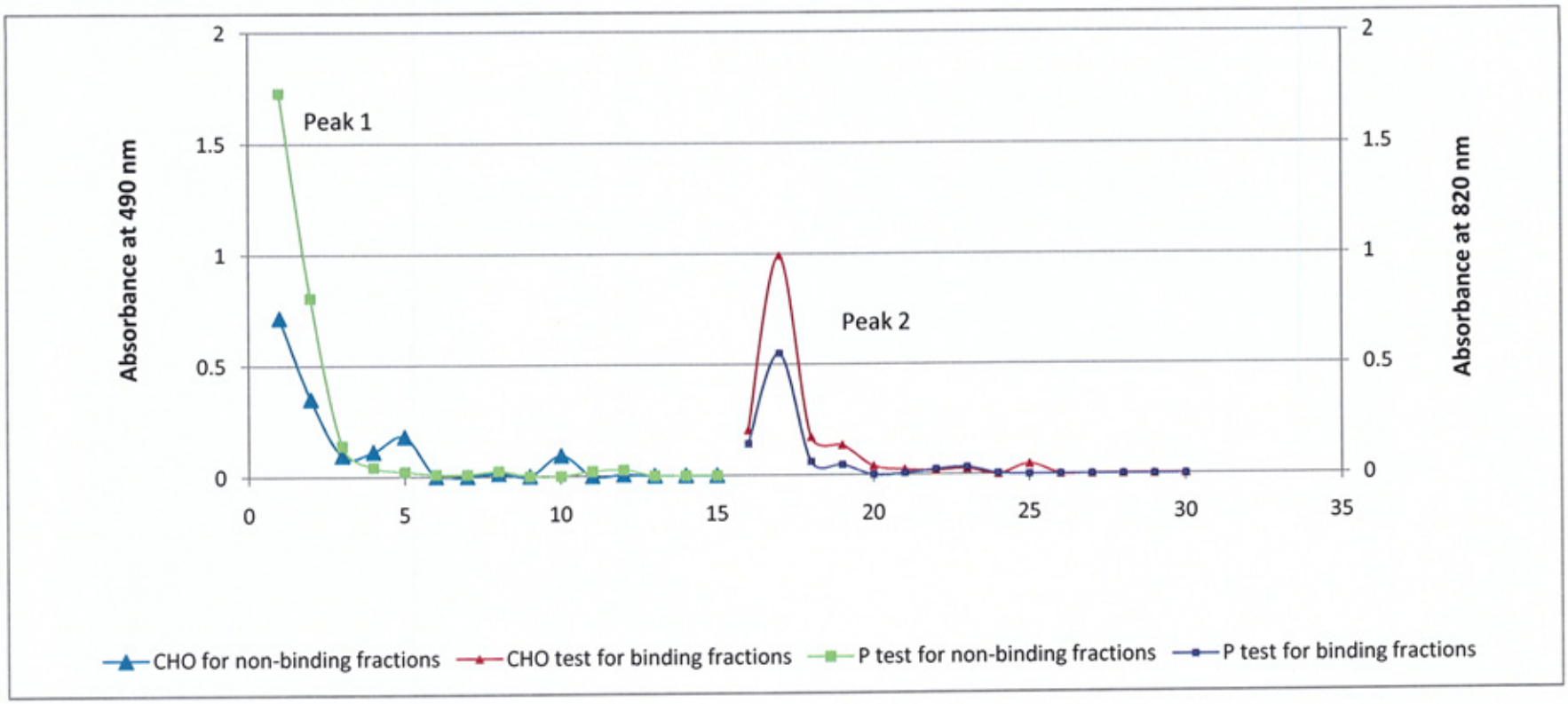

Figure 6.20. MBP column profile for HIC purified *S. coelicolor* macroamphiphiles. The purified macroamphiphiles (peak 2 of Figure 6.11) was loaded onto the column with binding buffer until fraction 11, after which the column was washed with elution buffer for 14 fractions (12 to 25). Column fractions (4 mL) were analyzed for carbohydrate and phosphorus.

6.3.9. Chemical analysis of MBP column peaks

The sugar composition of the MBP purified column peaks 1 and 2 (Figure 6.20) were determined following acid hydrolysis to release monosaccharide components and derivatisation to alditol acetates for GC, as described in Chapter 2, section 2.2.6.2. Table 6.7 presents a summary of the carbohydrate composition of the peaks obtained following MBP purification. Peak 1 contained glycerol and glucose, which were also observed in purified macroamphiphiles after HIC purification (Table 6.5). The absence of mannose in this peak demonstrated that the MBP column separation had worked effectively.

Peak 2 was composed of glycerol, mannose, galactose, glucose and inositol. Significant amounts of mannose were present in this peak, which demonstrated that the MBP column separation had worked (Table 6.7). Arabinose was not observed in either peak, contrary to the previous detection of very minor amounts of this sugar (Table 6.5).

Table 6.7. Carbohydrate composition of the MBP-purified acid hydrolysed macroamphiphilic peaks of *S. coelicolor*.

Carbohydrate identified[a]	***S. coelicolor* MBP purified Peak 1**	***S. coelicolor* MBP purified Peak -2**
Glycerol	89.4	46.9
Mannose	Trace	17.9
Galactose	Trace	7.5
Glucose	10.6	18.7
Inositol	Trace	10.0

[a] Carbohydrates were analysed by GC of their alditol acetate derivatives and identified by comparision with a mixture of authentic standards (alditol acetates of glycerol, erythritol, rhamnose, ribose, arabinose, xylose, mannose, galactose, glucose and Inositol as shown in Figure 2.5). Composition is given as the percentage of total integrated chromatographic peak areas.

6.3.10. Electrophoretic analysis of the *S. coelicolor* MBP purified peaks

S. coelicolor macroamphiphile MPB purified column peaks (peak 1 & 2, Figure 6.20) were examined by electrophoresis followed by staining with combined Alcian Blue 8GX and silver nitrate stains and by monoclonal anti-LTA antibody blotting. Alcian blue and Silver-nitrate staining reacted with both peak 1 and 2 in similar patterns, around the 20 to 10 KDa region (Figure 6.21). Anti-LTA blotting showed a positive reaction with both peak 1 and 2 at the similar region 20 to 10 KDa (Figure 6.22).

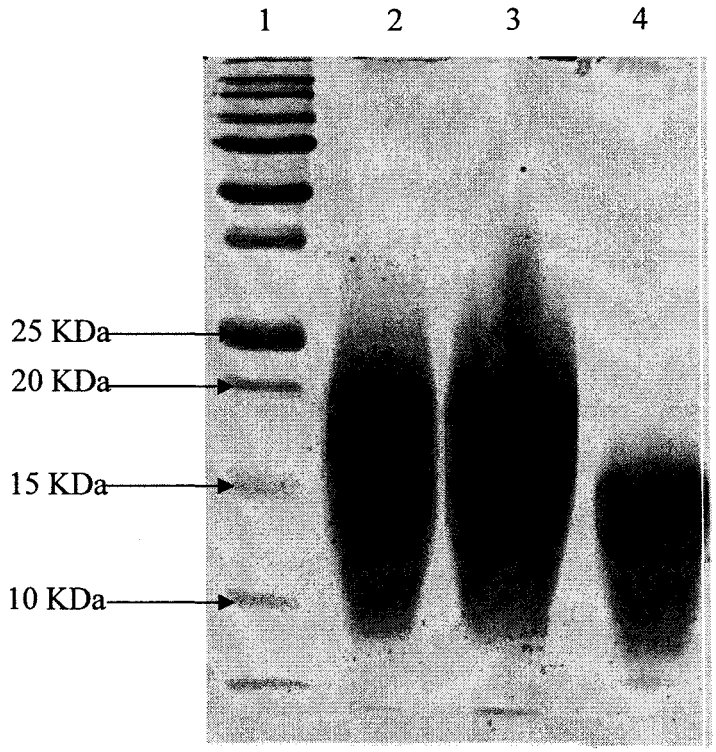

Figure 6.21. Alcian Blue & Silver-nitrate staining of *S .coelicolor* M145 MBP purified macroamphiphile materials. Lane 1: Protein standard ladder; Lane 2: MBP Peak 1; Lane 3: MBP Peak 2; Lane 4: GBS LTA (standard).

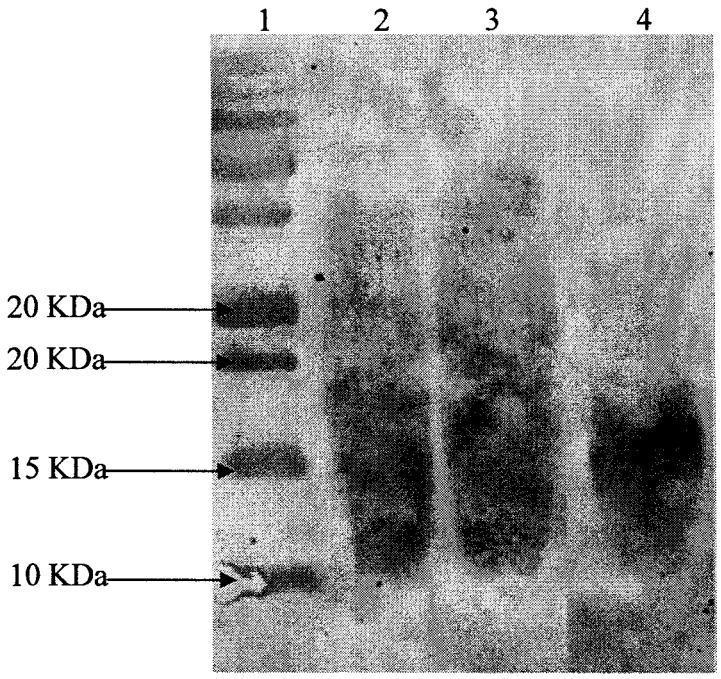

Figure 6.22. Monoclonal anti-LTA Western blotting of *S. coelicolor* M145 MBP purified macroamphiphilic materials. Lane 1: Protein standard ladder; Lane 2: MBP Peak 1; Lane 3: MBP Peak 2; Lane 4: GBS LTA (standard). Irrelevant sample lanes between samples shown in lanes 3 and 4 have been digitally removed.

6.3.11. Correlation between macroamphiphiles biosynthesis and different stage of the life cycle of S. *coelicolor* M145

The intensity of the anti-LTA reaction on Western blotting with the *S. coelicolor* macroamphiphiles varied with different sample preparations, which suggested that there might be a correlation between the extracted LTA amount and the life cycle of the organism. To determine very approximately the amount of LTA present at different stages of growth, crude phenol extracts from cells grown for different times were analyzed by dot blotting. The intensity of the LTA reaction with the monoclonal-anti-LTA antibody was determined using samples adjusted to a constant phosphate concentration (1 μg of phosphorus/μL of sample) as shown in Figure 6.23. The results suggested that LTA production varied at different stages of mycelium growth and that it was highest around 48 h.

To further determine the LTA amount in spores, aerial mycelium and mycelium of *S. coelicolor*, crude phenol extraction were done from the freeze dried spores, aerial mycelium and mycelium and dot blot was performed with samples containing a constant amount of phosphate (1 μg of phosphorus/μL of sample). Figure 6.24 showed that the mycelium samples reacted intensely with the anti-LTA monoclonal antibody, whereas only a moderate reaction was found with aerial mycelium and a faint reaction with spore samples.

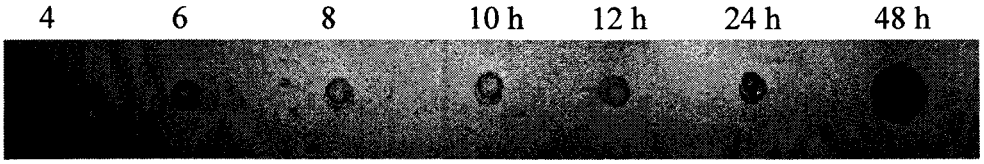

Figure 6.23. Dot blotting with monoclonal anti-LTA antibody using crude phenol extracts from cells at different times of liquid culture (YEME media) or mycelium growth. Dots were taken from 1 μg/μL phosphorus concentrated crude phenol extracted samples at different time scale of the growth.

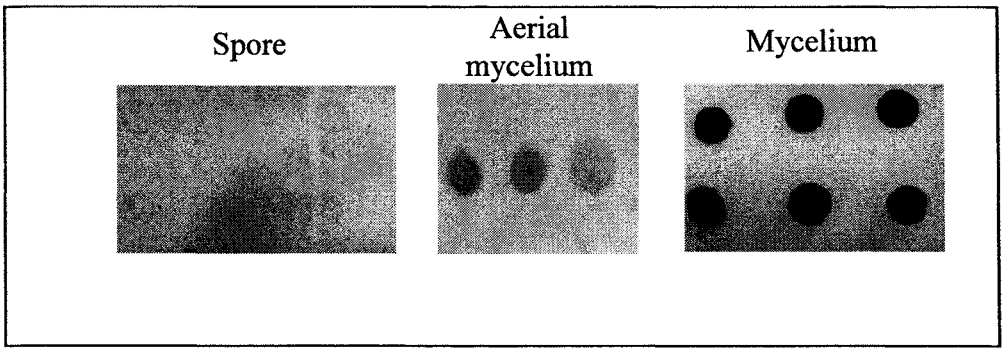

Figure 6.24. Dot blotting with monoclonal anti-LTA antibody against crude phenol extracts obtained from biomass at different stages of the *S. coelicolor* M145 lifecycle. Dots were taken from 1 μg/μL phosphorus concentrated crude phenol extracted samples at different stages.

6.4. Discussion

The purpose of this study was to investigate the macroamphiphiles present in *S. coelicolor* M145, try to understand the presence of macroamphiphiles at different stages of the life cycle of the organism and also to compare the results with those for other closely related genera such as *Thermobifida.*

6.4.1. Growth characteristics and optimisation of biomass yield

The spore and aerial mycelium was observed on sporulating agar plates as shown in Figure 6.3. The lifecycle showed the classical progression to the formation of spores, as described in previous studies (Kieser *et al.*, 2000).

Approximately 1 g or more dry cells is required for the investigation of the macroamphiphile in an organism. Therefore, vegetative mycelium grown in liquid culture was found to be the best source for obtaining higher yields of *S. coelicolor* M145. Since the organism was highly aerobic, the cultures were shaken at 300 x g and with sufficient space, i.e. 200 mL culture in 500 mL flasks (ratio 2:5). 34% (w/v) sucrose (which can not be catabolised by *S. coelicolor*), with springs and a complex media like YEME was found to yield the highest amount of cells (Figure 6.3 and Table 6.1), due to favouring dispersed growth of the cells (Discussed in section 6.1.2).

Moreover, since the yield may also depend on the amount of the inoculum, the amount of spores was also optimised. Due to contamination and difficulty of measuring the inoculum, spores were quantified as the number of petri dishes from which the spores were grown and collected. Table 6.2 showed that an

increase in the inoculum increased the amount of yield (dry cell weight), but the increase was not economically and practically significant, suggesting that spores collected from a single Petri dish would be sufficient or economically sensible for 200 ml culture inoculation.

Finally the growth curve in Figure 6.4, showed that the growth curve derived from absorbance data matched that derived from the dry cell weight data. Due to the formation of clumps, *S. coelicolor* did not form a homogeneous suspension, so by using two variables the growth curved had been defined. The growth curve showed that the culture should be harvested between 18 to 20 h after inoculation to achieve the highest yield of biomass.

6.4.2. Identification of the *S. coelicolor* macroamphiphiles

The phenol extraction process followed by HIC purification allowed the identification of two peaks typically around fractions 46 to 59 in the FPLC profiles, which are represented as peak 2 and 3 in Figure 6.5. The higher amount of phosphate present in Fractions 46 to 50 represents the characteristics of an LTA rather than a lipoglycan since LTA has higher phosphorus content due to its polyalditol-phosphate chain (described in section 1.6.3.1). Further evidence for the presence of LTA was provided by the positive results obtained from the immunodot blotting, using a monoclonal anti-LTA antibody (Figure 6.6). Introducing a delipidation step prior to hot-phenol extraction decreased the amount of Peak 3 (Figure 6.7) suggesting that Peak 3 might be rich in glycolipids (such as PIMs), which were found to be removed from cell membrane by the delipidation process. Due to the overlap of the two peaks, it was inevitable that the two preparations might contain molecules from both peaks in different concentrations.

The analysis of fatty acids can be useful to differentiate *Streptomyces* species from species of other genera with similar morphology. The major fatty acid profiles of the whole cells and macroamphiphilic materials showed similar patterns with slight changes in the percentage of some fatty acids (Table 6.4). Importantly, the whole cell fatty acid profiles obtained matched that from the previous studies of *S. coelicolor* A3(2) (Li *et al.*, 2005). After SDS-PAGE, the staining of the *S. coelicolor* M145 macroamphiphiles with Alcian Blue, combined Alcian Blue & Silver-nitrate, or periodate Schiffs reagents suggested peak 2 contained two molecules, which were also observed in peak 3,

producing two broad bands around 25 to 20 KDa and 10 KDa in comparison to the protein standards. However, introducing a delipidation step prior to phenol extraction decreased the relative amount of the band around 10 KDa, which reacted strongly with periodate Schiffs reagent, suggesting the molecule contains hexose sugar. This band had a similar electrophoretic mobility to the PIM_6 reference. Together, these data suggested the macromolecule was a glycolipid (such as PIM). However, it was notable that this molecule was not detected on lectin blotting, which is expected to give a positive reaction with the terminal mannose in PIMs. This observation has yet to be explained.

The broad band around 20-25 KDa reacted with Alcian Blue, and lower part of the band around 20 KDa with periodate Schiffs base, suggesting the molecule is negatively charged and contains sugar, respectively. The failure to react with the poly- or monoclonal anti-LTA and negative blotting with lectin blotting (a similar pattern to the *K. radiotolerans* macroamphiphilic material, Chapter 5), suggested that the molecule might be a novel lipoglyan with no terminal mannose.

Finally, the poly- and monoclonal anti-LTA reacted with material around 15 KDa (i.e. at a similar position as the standard LTA) suggesting the presence of LTA as third component in peak 2 (Fig. 6.13). However, it was unusual that the molecule did not stain with Alcian Blue (Fig 6.10).

In conclusion the electrophoretic analyses suggested that phenol-water extraction of *S. coelicolor* extracts at least three major fractions: a lipoglycan

like fraction (detected at 20-25 kDa), a presumptive LTA (detected at ca 15 kDa) and a glycolipid-like fraction (detected at <10kDa).

The sugar composition of the macroamphiphiles showed the presence of glycerol, mannose, glucose and inositol in both the peaks, along with presence of galactose and minor amounts of arabinose in peak 2 only. From the gel electrophoresis and Western blotting analysis, it was observed that the 20-25 KDa and 10 KDa components were present in both the peaks but only peak 2 contained materials that cross-reacted with the anti-LTA. This suggested that the LTA specifically might contain galactose as component, e.g. as a substituent on the main chain.

Since both TA and LTA have similar glycerol-phosphate repeated hydrophilic backbones, although of different stereochemistry (Discussed in section 1.7.3.1), and the anti-LTA binds to this backbone (Walsh *et al.*, 2004), the dot blotting and Western blotting results may have been a false-positive reaction with a membrane-anchored wall TA precursor (shown in Figure 1.9 and described in section 1.6.2.1). However, intermediates in TA synthesis (Figure 1.9) are expected to turnover rapidly and not to accumulate to significant levels. Moreover the polyprenol present in the precursor has C=C double bonds (described in section 1.3.1) which were found to be absent in the purified LTA by measuring the OD at 232 nm. Conversely, the presence of fatty acids in the purified HIC sample would explain the attachment of the molecule to the HIC column and also distinguishes the putative LTA from TA or a precursor TA, which do not contain fatty acids. Although TCA extracted TA stained with

Alcain Blue and silver-nitrate at an electrophoretic position similar to the extracted LTA (Figure 6.16), the monoclonal anti-LTA antibody failed to react with this TCA extracted TA but was positive towards LTA (Figure 6.17).These data strongly suggested that the molecule identified among the *S. coelicolor* macroamphiphiles was an LTA rather than a TA.

The component which stained around 20-25 KDa might be a novel lipoglycan (notably due to the detection of significant glucose) or one composed of glycerol, inositol, mannose and minor amount of arabinose. However, the complicating presence of other components means this can not be definitively concluded.

6.4.3. Separating the macroamphiphile(s) extracted from *S. coelicolor*

The anion exchange chromatography did not efficiently separate the macroamphiphiles (Figure 6.18). Although the dot immunoblotting showed the presence of LTA between fractions 45-57, gel electrophoresis followed by staining with Alcian Blue and Silver nitrate staining and Western blotting with monoclonal anti-LTA antibody failed to detect macroamphiphiles, most likely be due to the minute amount of the molecules recovered. The process was repeated several times with higher amounts of harvested and extracted cells but the procedure was still unsuccessful.

The MBP column chromatography (Figure 6.20) was effective in separating the molecules depending on the presence of mannose; the chromatography separated the peak 2 material from the HIC profile into two separated peaks. In the MBP profile (Figure 6.24), the first peak contained almost no mannose which is consistent with the observation that it did not bind to the MBP column. The peak showed higher amounts of glycerol with lesser amounts of glucose and traces of galactose, inositol and mannose. On the other hand peak 2, which bound to the MBP column, showed the presence of significant amount of glycerol, mannose, glucose, galactose and inositol (Table 6.7). Further gel electrophoresis analysis with these peaks showed that both the peaks stained with Alcian blue, in a similar position to LTA and also positively reacted with the monoclonal anti-LTA antibody (Figure 6.21 and 6.22). These results suggest that *S. coelicolor* might contain two types of LTA, one with a mannose substituent and another with non-mannose substituents. Peak 2 from the MBP column might also contain some mannose containing macroamphiphile

(lipoglycan) along with mannose containing LTA. For both peaks from the MBP column, the broad smears (around 10-20 kDa) obtained on gels stained with Alcian blue (Figure 6.21) or Western blotted with monoclonal anti-LTA (Figure 6.22) were in contrast to the previous gels showing a more defined banding pattern (e.g. Figures 6.10, 6.11 and 6.13). This suggests components introduced during the MBP purification step (e.g. buffer salts) affect the electropohoretic mobility of the extracted materials. This phenomenon complicates interpretation of the present data and will require further study.

6.4.4. LTA biosynthesis in different stages of *S. coelicolor* M145 life cycle

The reaction intensity with the monoclonal anti-LTA antibody differed in different sample preparation, which lead to the hypothesis of varying levels of LTA biosynthesis at different stages of the *S. coelicolor* life cycle. To determine the LTA amount, crude phenol extracts containing a constant amount of phosphorus (1 μg/μL) was used for immunodot blotting using monoclonal anti-LTA to show the proportion of the phosphorus involved in LTA biosynthesis in 1 μg. The results suggested that in the early stages of the life cycle the intensity was high (4-6 h), but then it decreased around 8h but then it increase further and became highest at 48 h of the growth curve (Figure 6.23). A second set of results using crude phenol extracts from spores, aerial mycelium and vegetative mycelium and a constant load phosphorus in each sample (1 μg/μL) suggested that LTA production increased in ascending order from spore, aerial mycelium to vegetative mycelium (Figure 6.24). These result possibly reflect the dormant stage, i.e. spores do not require the cell membrane to produce these large molecule (LTA) in high amounts as at this stage energy is required for other purposes in an adverse environment. Similarly for aerial mycelium also more energy is required for the spore production. On the other hand, vegetative mycelium showed the most positive cross-reaction suggesting LTA may be most needed during the maximal growth stage of the organism.

6.4.5. Comparative studies between *S. coelicolor* M145 and *T. fusca*

S. coelicolor A3(2) and *T. fusca* are two representative species in the phylum Actinobacteria which produce mycelia and spores on aerial hyphae. The spores of *T. fusca* are formed as clumps and for *S. coelicolor* as chains on the aerial hyphae (Chater and Chandra, 2006). Moreover, a comparative genomics study between *S. coelicolor* and *T. fusca* by Chater & Chandra (2006) showed the two genera might be more closely related than indicated by the phylogenetic distance between these two genera based on 16S rRNA gene analysis (Figure 4.4).

The present study has focussed on the phenotypic characteristics of the cell envelope, especially on the macroamphiphiles and SCWPs. For SCWPs it has been revealed from previous and present studies that *T. fusca* possesses poly(GroP) TA (Potekhina *et al.*, 2003) and *S. coelicolor* most likely possesses either a ribitol-phosphate backbone TA (Naumova *et al.*, 1980a) and/or a poly(GroP) TA (this study). Both types of TA may be synthesised by the same *Streptomyces* spp. (Streshinskaya *et al.*, 2004) and it is clear from recent work that *Streptomyces* spp. can synthesise many types of SCWP, with distinctive substituents and both poly-alditol-phosphate and more complex TA backbone structures (Shashkov *et al.*, 2006, Naumova *et al.*, 1980a, Shashkov *et al.*, 2002, Kozlova *et al.*, 2006). Furthermore the present study has shown the presence of LTA in both the organisms in agreement with the suggestion (Charter & Chandra, 2006) that the two genera are more closely related than as presented by the phylogenetic tree based on 16S rRNA.

6.5. Conclusion

Three phenol extractable amphiphilic components have been identified in *S. coelicolor* M145 (Figure 6.25), of which the major macroamphiphile runs as a broad band around 25-20 KDa in gel electrophoresis (Figure 6.25, Lane 2), stains with Alcian-blue, silver-nitrate and periodate Schiffs reagents and negatively stains on lectin blotting, which suggested the molecule is a novel lipoglycan. The second macroamphiphile is a presumptive LTA, which runs around 15 KDa, i.e. in a similar position to the standard LTA (GBS) and reacts positively with a monoclonal anti-LTA antibody (Figure 6.25, Lane 3). Finally, the component detected around 10 KDa, behaved like glycolipid as it runs to a similar position as the standard PIM_6 and stained with periodate Schiffs reagent. However, the lack of reaction on lectin-blotting remains unexplained. The sugar residues detected in the HIC purified preparations agree with the above conclusions.

The LTA present in *S. coelicolor* appeared to occur with and without mannose residues as substituents (Figure 6.22). However further techniques need to be developed to separate the macroamphiphiles and to study the structure of the molecules by mass spectrometry and NMR.

There was an apparent variation in the presence of LTA at different stages of the *S. coelicolor* life cycle (Figures 6.23 & 6.24). Further study is required to understand the requirement or function of the LTA at the different stages of the growth. *S. coelicolor* is therefore potentially useful as a model organism to understand the function of this macromolecule as the stages of the life cycle of

this organism can be easily separated and analysed. Moreover, the presence of LTA in filamentous and aerial hyphae/spore forming organisms, like *Thermobifida* and *Streptomyces* is an interesting observation as most studies of LTA have focussed on rod or coccus shaped unicellular *Firmicutes*. Further understanding of the biosynthesis and function of these macromolecules may be gained from comparative genomic and phenotypic studies between *S. coelicolor* and *T. fusca* as complete genome sequences are available for both organisms.

Though the present study has revealed novel findings regarding the cell envelope of *S. coelicolor*, further studies are needed to resolve the apparent presence of two major biosynthetically unrelated macroamphiphiles (LTA and lipoglycan) in a single organism, which hasn't been reported previously in any studies.

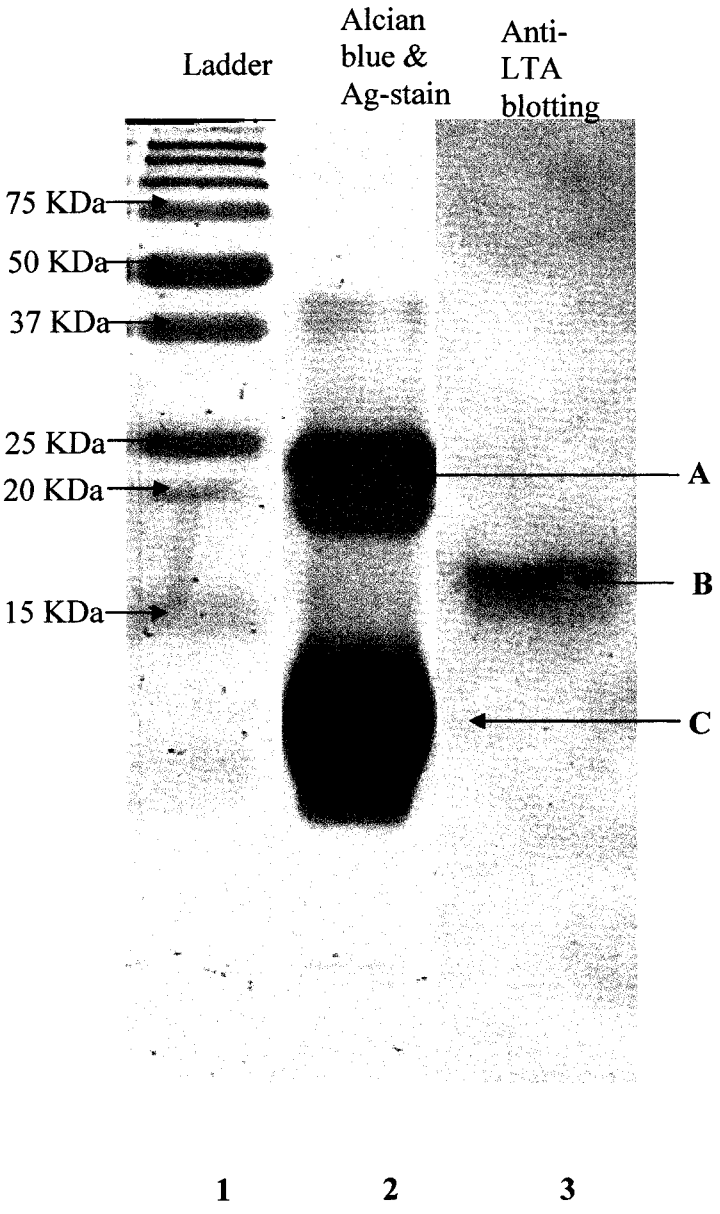

Figure 6.25. The position of the macroamphiphiles detected by gel electrophoresis for *S. coelicolor* M145. 'A' represents the major macoroamphiphiles (lipoglycan), 'B' represents the LTA and C represents the PIM-like molecule. Lane 1: Protein standard ladder. Lane 2 and 3 both contain Peak 2 of HIC profile of Figure 6.5. Lane 3 is digitally introduced from the scan of a western blot with anti-LTA antibody.

CHAPTER SEVEN

Characterisation of *Streptomyces* sp. DSM 40537 and investigation of its macroamphiphile

7.1. Introduction

The strain *Streptomyces* sp. DSM 40537 (equivalent to the strains deposited as ATCC 3351 and ISP 5537) was identified originally as *Actinomyces saprophyticus* or *Streptomyces griseus*, and was deposited by Waksman in 1947 under the name *Streptomyces albus* (Shirling and Gottlieb, 1972).

Very little research has been done regarding this strain, with the following description taken from Shirling and Gottlieb (1972). The morphological characteristics of the strain showed mature spore chains generally containing 3-10 smooth surface spores, although some long chains (>50 spores) were also reported. The spore morphology was observed on yeast-malt agar, oatmeal, salt-starch agar and glycerol-asparagine agar. Spores of "*Streptomyces albus*" ATCC 3351 were reported to belong to the yellow colour group (Tresner *et al.*, 1961) and the colour of the mycelium was reported to be yellow, with immature or poorly developed aerial mycelium coloured white (Shirling and Gottlieb, 1972). No pigment was observed on the reverse of the colony or released to the medium on any of the media tested. The strain was found to utilize D-Glucose, L-arabinose, D-xylose, D-mannitol and D-fructose for their growth (Shirling and Gottlieb, 1972).

Although there has been minimal study of *Streptomyces* sp. DSM 40537 (ATCC 3351), Naumova *et al.* (1980) reported the presence of a glycerol TA in a strain they described as *Streptomyces levoris* K-3056 (ATCC 3351). Subsequently, Potekhina *et al.* (1983) studied the macroamphiphile present in "*Streptomyces levoris*" K-3056. A cold (4°C) phenol-water extraction method was used, followed by gel filtration purification on a Sepharose 6B column. This strategy was reported to recover a poly-GroP LTA. The fatty acid profile of the LTA showed the presence of C15:0, iC16:0, C16:0 and C17:0 as major fatty acids, along with lesser amounts of C14:0 and iC15:0. In addition to poly-GroP, the study also identified glucose and small quantities of mannose and galactose in the chain poly-GroP chain of LTA. The glucose was provisionally attributed to the glycolipid anchor of the LTA.

Confusingly, this preliminary study contradicted their earlier report (Naumova *et al.*, 1980a) by stating that they did not detect any polyol-phosphate type TA; instead, a polysaccharide composed of mainly mannose and galactose, along with phosphorus, was reported to be present (Potekhina *et al.*, 1983).

7.2. The significance of present study

As the Potekhnia *et al.* (1983) study had provisionally identified LTA in "*S. Levoris*" K-3056 (ATCC 3351), the present study was done to reconfirm their results and to use the data in comparison to the results from studies of *S. coelicolor* M145 (Chapter Six). However, a search of the ATCC catalogue (http://www.lgcpromochem-atcc.com/) indicated that strain ATCC 3351 is no longer available. Therefore, *Streptomyces* sp. strain DSM 40537 (= ATCC 3351) was obtained instead from the Deutsche Sammlung von Mikroorganismen und Zellkulturen GmbH (DSMZ, German Collection of Microorganisms and Cell Cultures). The aim of this study was help produce a hypothesis regarding the presence of LTA in the genus *Streptomyces*.

Moreover, as the strain *Streptomyces* sp. DSM 40537 (ATCC 3351) had not yet been identified at the species levels, the present study has sequenced the 16S rDNA in order to reconfirm the position of this strain within the genus *Streptomyces*.

7.3. Results

7.3.1. Morphological and Physiological characteristics

Streptomyces sp. strain DSM 40537 was bought from DSMZ. The freeze dried biomass supplied by DSMZ was rehydrated into YEME medium and inoculated in liquid YEME media and onto sporulating agar plates. Following growth, stocks from both the cultures were stored as glycerol stocks and designated as DSM1 and DSM2, respectively. These glycerol stocks from both cultures were inoculated onto sporulating plates, non-sporulating plates and YEME media. However, unfortunately the cultures obtained from each of these stocks were observed to have different phenotypes (Figure 7.1, 7.2 &7.3); the strains had distinct characteristics which were consistent on repeated inoculations using different media. For clarity, these two stocks and the 'strains' derived from them are here described as strain DSM1 and DSM2.

On sporulating agar plates, strain DSM1 formed a cloudy transparent layer, whereas strain DSM2 grew as single colonies with an orange colour after 24 h (Figure 7.1A). After 72 h the DSM1 strain layer turned yellow with no pigment secretion on the plate whereas the DSM2 strained colonies turned white, with the release of orange pigment into the plate (Figure 7.1B). After 144 h, the DSM1 strain layer turned a more yellowish colour whilst colonies of strain DSM2 turned to grey colour (Figure 7.1C).

On non-sporulating agar plates, strain DSM1 again grew as a transparent layer and strain DSM2 grew as single scattered light orange coloured colonies after

24 h (Figure 7.2A). After 72 h, the DSM1 strain remained the same colour instead of turning yellow but the layer was thicker than at 24 h; for strain DSM2, the colour did not change to white but rather turned light orange colour with larger sized colonies (Figure 7.2B). After 144 h (Figure 7.2C), the DSM1 strain remain the same colour with a denser layer evident and the DSM2 strain colonies became deep orange, along with the secretion of orange pigment into the medium.

In liquid YEME media (Figure 7.3A) after 24 h the DSM1 strain showed scattered/dispersed, rough-surfaced white clumps, whereas the DSM2 strain showed smooth, dense white clump formation. After 72 h, the strain DSM1 culture became cloudy without changing any colour, whilst the strain DSM2 culture clumps became denser and orange in colour along with changing the media to an orange colour (Figure 7.3B). After 144 h, these changes were even more pronounced (Figure 7.3C).

The Gram-staining for both the strains showed the typical purple colour of Gram-positive bacteria in filaments, with spores depending on the stage of the growth (data not shown).

Cumulatively, these experiments suggested that two stable, phenotypically distinct strains, DSM1 (stored as glycerol stocks derived from the original YEME broth culture) and DSM2 (stored as glycerol stocks derived from the original culture on sporulating agar plates), had been recovered from the single vial received from DSMZ as strain *Streptomyces* sp. DSM 40537. It was noted

that strain DSM1 showed phenotypic and morphological characteristics most similar to those described by Shirling & Gottlieb (1972) for *Streptomyces* sp. ATCC 3351.

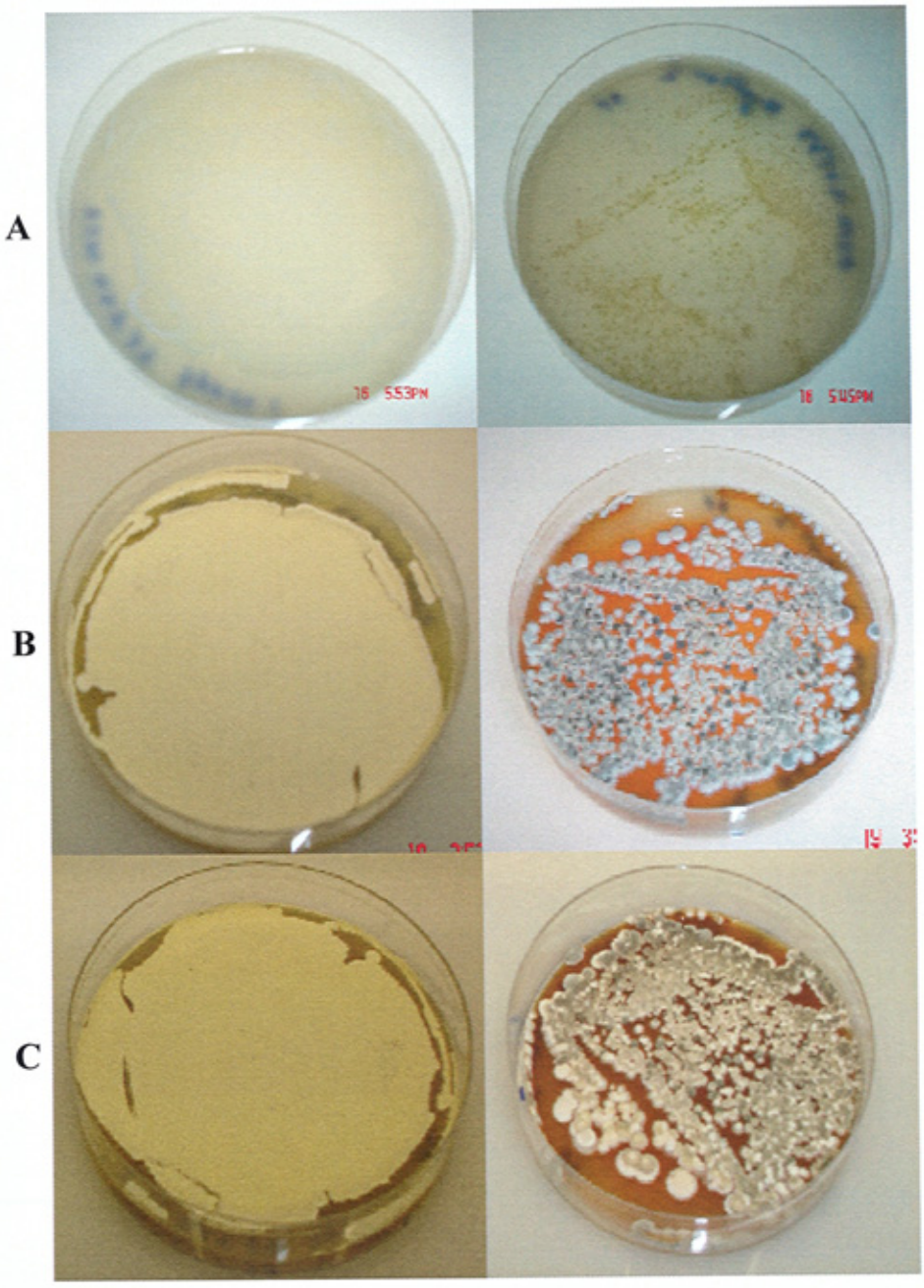

Figure 7.1. *Streptomyces* DSM40537 derived strains cultured on sporulating agar plate medium. Cultures are shown after (A) 24 h (B) 72 h and (C) 144 h growth on sporulating agar plates. The left hand plates show strain DSM1 and the right hand plates show strain DSM2.

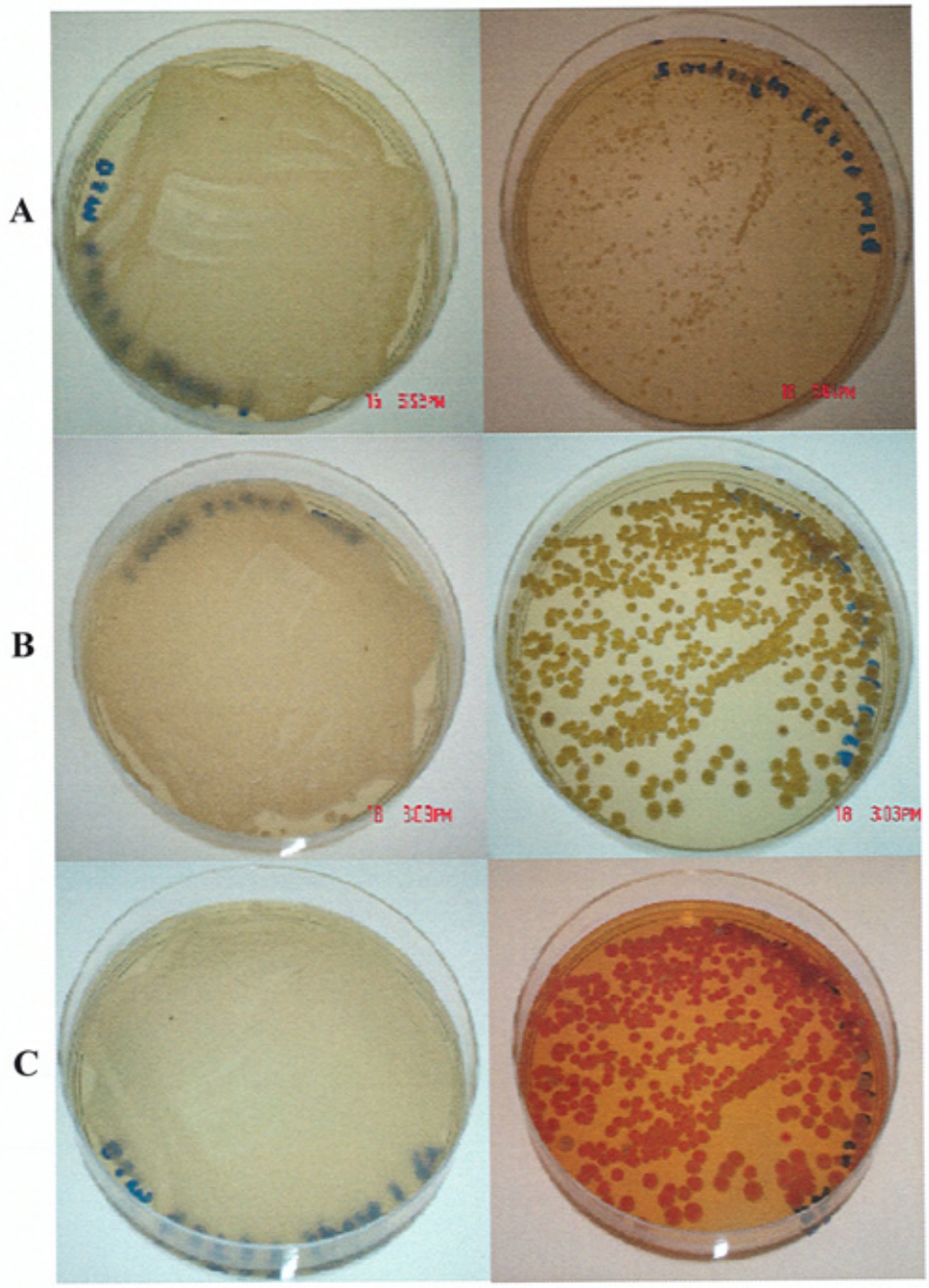

Figure 7.2. *Streptomyces* DSM40537 derived strains cultured on non-sporulating agar plate medium. Cultures are shown after (A) 24 h (B) 72 h and (C) 144 h growth. The left hand plates show strain DSM1 and the right hand plates show strain DSM2.

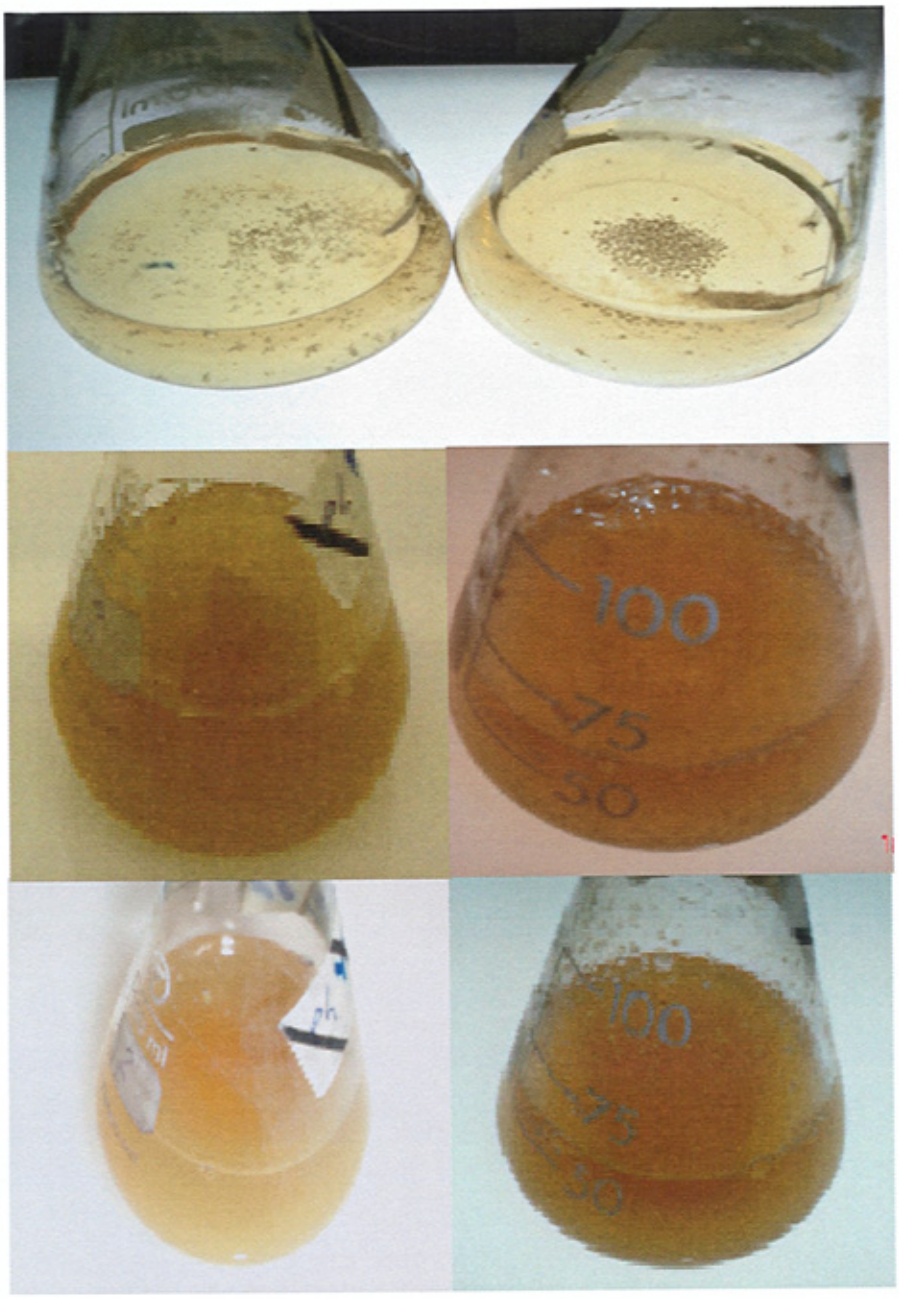

Figure 7.3. *Streptomyces* DSM40537 derived strains grown in YEME liquid medium. Cultures are shown after (A) 24 h (B) 72 h and (C) 144 h growth. The left hand flask shows a culture of strain DSM1 and the right hand flask shows a culture of strain DSM2.

7.3.2. 16S rDNA sequencing of the two distinct phenotype strains

To help confirm the likely relationship between the DSM1 and DSM2 strains16S rDNA sequencing was performed for both, using the method described in detail in Chapter 2, Section 2.5.1. 1404 and 1398 base pairs of good quality sequence (forward and reverse strand) were obtained for strain DSM1 and strain DSM2 respectively. The sequences for each of the strains were 100% identical strongly suggesting them to be derived from the same species. The sequence obtained is shown in Figure 7.4 and has been deposited in Genbank (Accession Number to be supplied). A NCBI Blast search (http://www.ncbi.nlm.nih.gov/blast/Blast.cgi) with the 16S rRNA gene sequence clearly showed that the organism belongs to the genus *Streptomyces* and that among the closest matches to this strain were the sequences from *S. albus* sub sp. albus (NBRC3711=IFO=3711=ATCC3351=DSM40537) and *S. saprophyticus* (NBRC 13440=ATCC3351=DSM 40537). From the tracking of the ATCC strain numbers, both of these strains are suggested to be the same as *Streptomyces* DSM 40537. A summary of the Blast search results are given in Table 7.1. Although the Blast results identified a great number of 'hits' with unspeciated "*Streptomyces* sp." strains, the closest type strains of members of the genus *Streptomyces* were found to be *Streptomyces sampsonii, Streptomyces champavatii, Streptomyces golbisporus subsp. caucasicus, Streptomyces odorifer, Streptomyces albidoflavus, Streptomyces canescens, Streptomyces coelicolor* [sensu stricto rather than the A3(2) strain], *Streptomyces limosus* and *Streptomyces fellus*. Figure 7.5 shows the phylogenetic position of *Streptomyces* DSM 40537 with other type strains of *Streptomyces* obtained from the Ribosomal Database Project II (RDP II,

http://rdp.cme.msu.edu/). The tree shows the presence of the strain with the type strains of *S. fellus, S. coelicolor, S. limosus, S. odorifer, S. canescens, S. sampsoni* and *S. alvidoflavus,* which agrees with the data in Table 7.1 from the NCBI Blast search and this subgroup has also been previously shown by Lee *et al.* (2005).

AGTGGCGAACGGGTGAGTAACACGTGGGCAATCTGCCCTGCACTCTGGGACAA
GCCCTGGAAACGGGGTCTAATACCGGATATGACCGTCTGCCGCATGGTGGATG
GTGTAAAGCTCCGGCGGTGCAGGATGAGCCCGCGGCCTATCATCTTGTTGGTG
AGGTAGTGGCTCACCAAGGCGACGACGGGTAGCCGGCCTGAGAGGGCGACCGG
CCACACTGGGACTGAGACACGGCCCAGACTCCTACGGGAGGCAGCAGTGGGGA
ATATTGCACAATGGGCGAAAGCCTGATGCAGCGACGCCGCGTGAGGGATGACG
GCCTTCGGGTTGTAAACCTCTTTCATCAGGGAAGAAGCGAAAGTGACGGTACC
TGCAGAAGAAGCGCCGGCTAACTACGTGCCAGCAGCCGCGGTAATACGTAAGG
CGCAAGCGTTGTCCGGAATTATTGGGCGTAAAGAGCTCGTATGCGGCTTGTCA
CGTCGGTTGTGAAAGCCCGGGGCTTAACCCCGGGTCTGCAGTCGATACGGGCA
GGCTAGAGTTCGGTAGGGGAGATCGGAATTCCTGGTGTAGCGGTGAAATGCGC
AAATATCAGGAGGAACACCGGTGGCGAAGGCGGATCTCTGGGCCGATACTGAC
GCTGAGGAGCGAAAGCGTGGGGAGCGAACAGGATTAGATACCCTGGTAGTCCA
CGCCGTAAACGGTGGGCACTAGGTGTGGGCAACATTCCACGTTGTCCGTGCCG
CAGCTAACGCATTAAGTGCCCCGCCTGGGGAGTACGGCCGCAAGGCTAAAACT
CAAAGGAATTGACGGGGGCCCGCACAAGCGGCGGAGCATGTGGCTTAATTCGA
CGCAACGCGAAGAACCTTACCAAGGCTTGACATACACCGGAAACGTCTGGAGA
CAGGCGCCCCCTTGTGGTCGGTGTACAGGTGGTGCATGGCTGTCGTCAGCTCG
TGTCGTGAGATGTTGGGTTAAGTCCCGCAACGAGCGCAACCCTTGTCCCGTGT
TGCCAGCAGGCCCTTGTGGTGCTGGGGACTCACGGGAGACCGCCGGGGTCAAC
TCGGAGGAAGGTGGGGACGACGTCAAGTCATCATGCCCCTTATGTCTTGGGCT
GCACACGTGCTACAATGGCCGGTACAATGAGCTGCGATACCGTGAGGTGGAGC
GAATCTCAAAAAGCCGGTCTCAGTTCGGATTGGGGTCTGCAACTCGACCCCAT
GAAGTCGGAGTCGCTAGTAATCGCAGATCAGCATTGCTGCGGTGAATACGTTC
CCGGGCCTTGTACACACCGCCCGTCACGTCACGAAAGTCGGTAACACCCGAAG
CCGGTGGCCCAACCCCTTGTGGGAGGGAGCTGTCGAAGGTGGGACTGGCGATT
GGGACGAAGTCGTAACAAGGTATCCA

Figure 7.4. The 16S rRNA gene sequence determined for strains DSM1 and DSM2. 1404 nucleotides of sequence are shown which exhibited 100% identity for each strain.

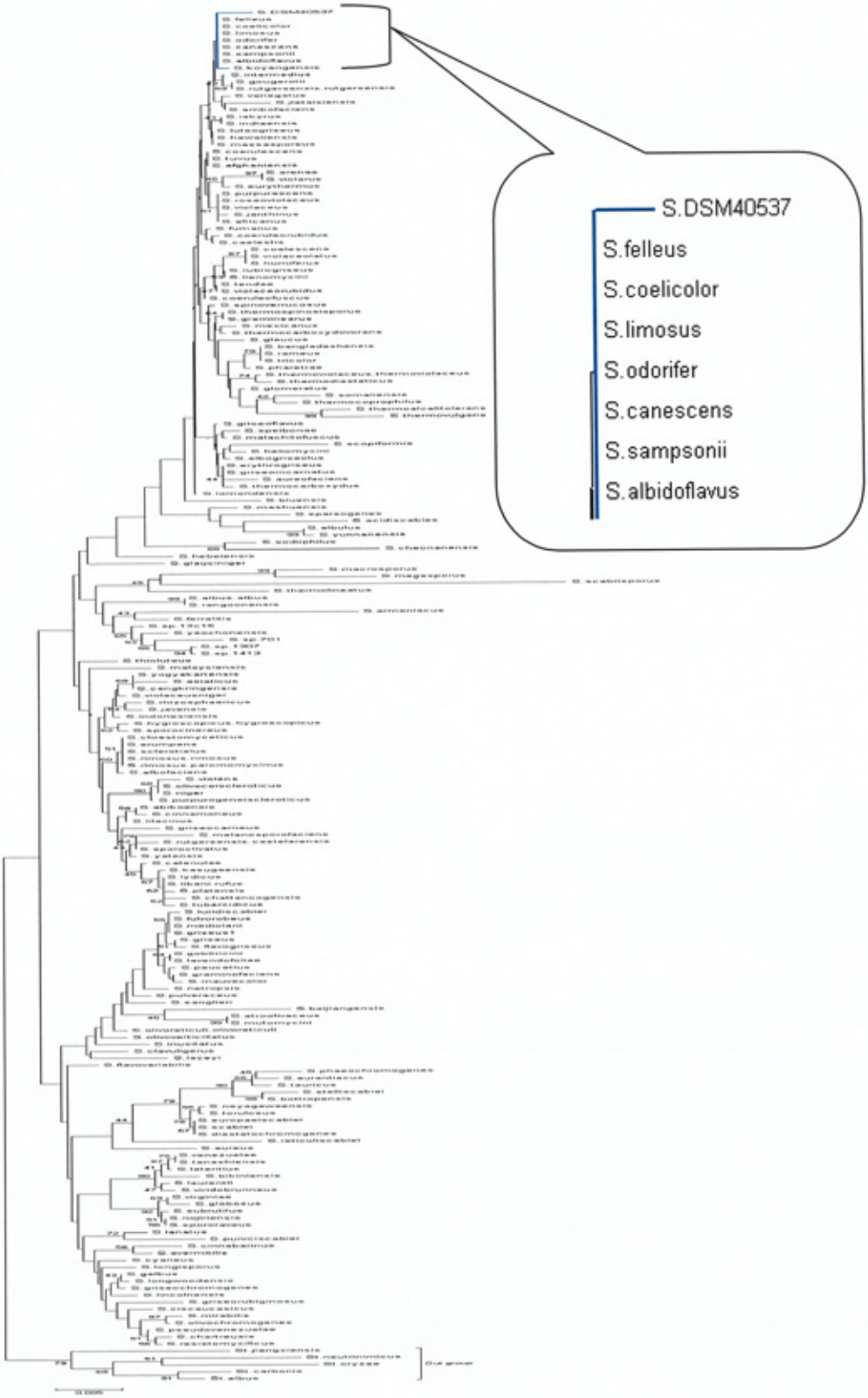

Figure 7.5. *Streptomyces* DSM40537 position with the type strain 16S rRNA of *Streptomyces* obtained from the RDP II (Appendix VI). The tree has been made using the programme MGMA 4.

Table 7.1. NCBI Blast results for Streptomyces DSM 40537 16S rDNA. Only the major relevant strains and type strains are presented from the Blast results, as many hits to uncharacterised "Streptomyces sp." are also recovered.

Accession No.	Strain description	Score	Identities	Expect	Type strain
AB184782.1	*Streptomyces albus* subsp. albus Strain: NBRC3711=IFO=3711=ATCC3351=DSM40537	2558 bits (1385)	1395/1400 (99.643%)	0.0	These strains have the same 16S rRNA sequences (100% identity) as found by ClustalW alignment and shown in Appendix VI, proving the three strains are for same species.
AB184773.1	*Streptomyces albus* subsp. albus Strain: NBRC 3422= ATCC 3381 (same source for previous strain suggesting they are same)	2558 bits (1385)	1395/1400 (99.643%)	0.0	
AB184404.1	*Streptomyces saprophyticus* Strain: NBRC 13440=ATCC3351= DSM 40537	2558 bits (1385)	1395/1400 (99.643%)	0.0	
AB184278.1	*Streptomyces krainskii* Strain: NBRC 13053^{T} = ATCC 25465=DSM 40321	2558 bits (1385)	1395/1400 (99.643%)	0.0	Type strain suggested: "*Streptomyces krainskii*"
AY636155.1	*Streptomyces fungicidicus* Strain: "YH04". No culture collection record identified.	2558 bits (1385)	1395/1400 (99.643%)	0.0	
DQ026642.1	*Streptomyces champavatii* Strain: IFO 15392=DSM 40841	2536 bits (1373)	1391/1400 (99.357%)	0.0	
AB184643.1	*Streptomyces champavatii* Strain: NBRC 15392=IFO 15392=DSM 40841	2536 bits (1373)	1391/1400 (99.357%)	0.0	Type strain
D63871.1	*Streptomyces sampsonii* Strain: NBRC 13083=IFO 13083=ATCC 25495=DSM 40394	2536 bits (1373)	1391/1400 (99.357%)	0.0	Type strain

Accession No.	Strain description	Score	Identities	Expect	Type strain
AB249937.1	*Streptomyces globisporus* subsp. caucasicus Strain: NBRC 100770=ATCC 19907=DSM 40814	2532 bits (1371	1390/1400 (99.236%)	0.0	Type strain
AB184355.1	*Streptomyces odorifer* Strain=NBRC 13365=IFO 13365=ATCC 6246=DSM 40347	2532 bits (1371	1390/1400 (99.236%)	0.0	Type strain
AB184255.1	*Streptomyces albidoflavus* Strain: NBRC 13010=IFO 13010=ATCC 25422=DSM 40455	2532 bits (1371	1390/1400 (99.236%)	0.0	Type strain
Z76684.1	*Streptomyces canescens* (DSM 40001T)	2532 bits (1371	1390/1400 (99.236%)	0.0	Type strain
AB184196.1	*Streptomyces coelicolor* Strain: NBRC 12854=IFO 12854=ATCC 23899=DSM 40233	2531 bits (1370)	1390/1400 (99.236%)	0.0	Type strain
AB184147.1	*Streptomyces limosus* Strain: NBRC 12790=IFO 12790=ATCC 19778=DSM 40131	2531 bits (1370)	1390/1400 (99.236%)	0.0	Type strain
AB184129.1	*Streptomyces felleus* Strain: NBRC 12766=ATCC 19752=DSM 40130	2531 bits (1370)	1390/1400 (99.236%)	0.0	Type strain
AY079156.1	*Streptomyces koyangensis* strain VK-A60	2531 bits (1370),	1390/1400 (99.236%)	0.0	

7.3.3. Purification of the *Streptomyces* DSM 40537 macroamphiphiles

Macroamphiphilic material was extracted from both strain DSM1 and DSM2 by the standard hot phenol-water extraction method (described in Chapter 2, section 2.1.5.1). The extracted macroamphiphile(s) were purified by HIC-FPLC (Chapter 2, section 2.1.6.1). The column fractions from the HIC were subjected to carbohydrate and phosphate assay (methodology described in Chapter 2, sections 2.1.7.1 & 2.1.7.2, respectively), as shown in Figures 7.6 and 7.7. Hydrophilic contaminants (nucleic acids and polysaccharides) not retained by the HIC column were recovered during the elution with equilibration buffer as peak 1 in both the purifications. Subsequent gradient elution with an increasing concentration of propanol recovered two peaks (peak 2 & 3) from the DSM1 strain extract and one peak (peak 2) from the DSM2 strain extract (Figures 7.6 and 7.7), respectively. For both strains Peak 2 contained a significant amount of phosphate compared to carbohydrate, whilst peak 3 from strain DSM1 contained a lesser amount of phosphate compared to peak 2.

Dot-immunoblotting (method described in Chapter 2, section 2.1.6.3) with a monoclonal anti-LTA reacted positively with fractions across the peak 2 for both the strains (Figures 7.8 and 7.9), but did not react with the peak 3 fractions from strain DSM1, as shown in Figure 7.8.

For each strain, the Peak-2 fractions were recovered by freeze-drying after extensive dialysis and represented 0.46% of the dry cell weight extracted for

strain DSM1 and 0.23% for strain DSM2. The peak 3 material of strain DSM1 was too minor to quantitate or to do further analysis.

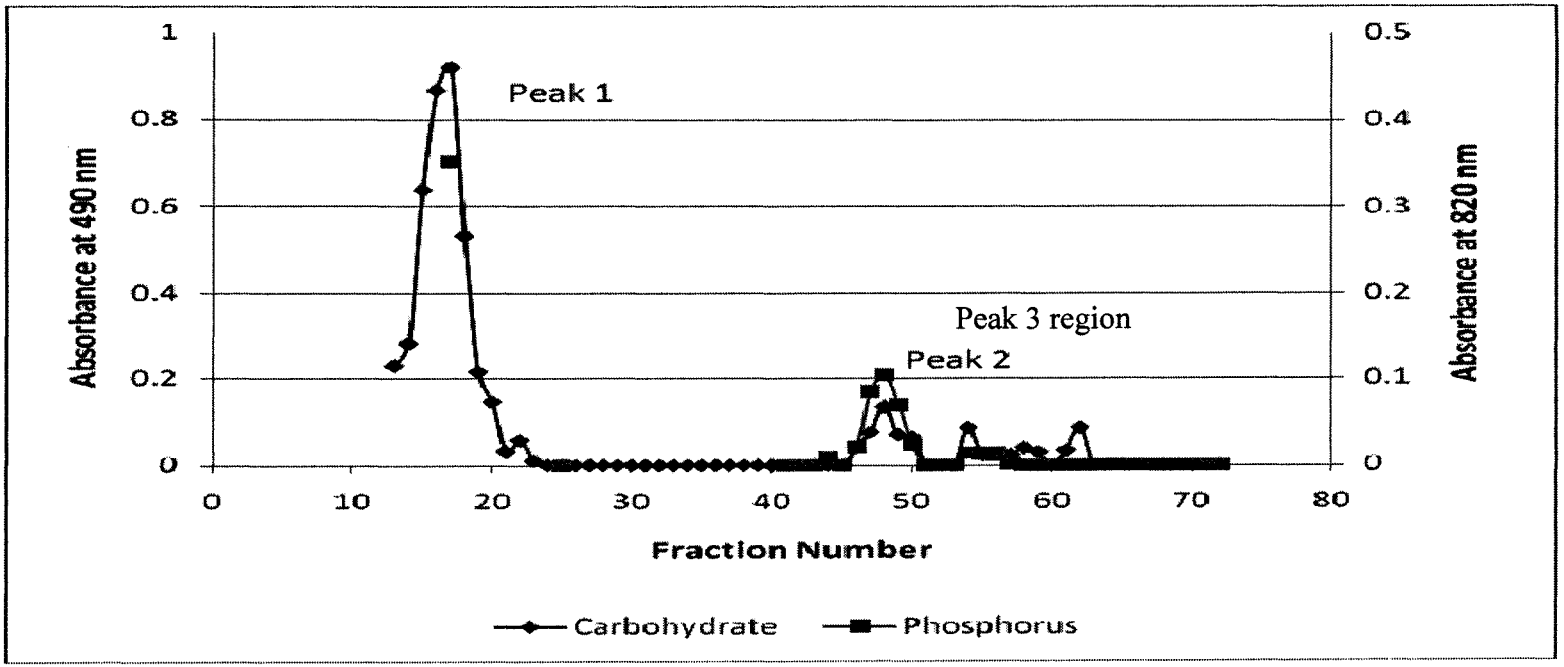

Figure 7.6. HIC-FPLC profile for the purification of a crude phenol extract from *Streptomyces* strain DSM1. The crude extract was loaded to the column with equilibration buffer until fraction 12, after which gradient elution with an increasing concentration of propanol was begun. Column fractions (4 mL) were analyzed for carbohydrate and phosphorus.

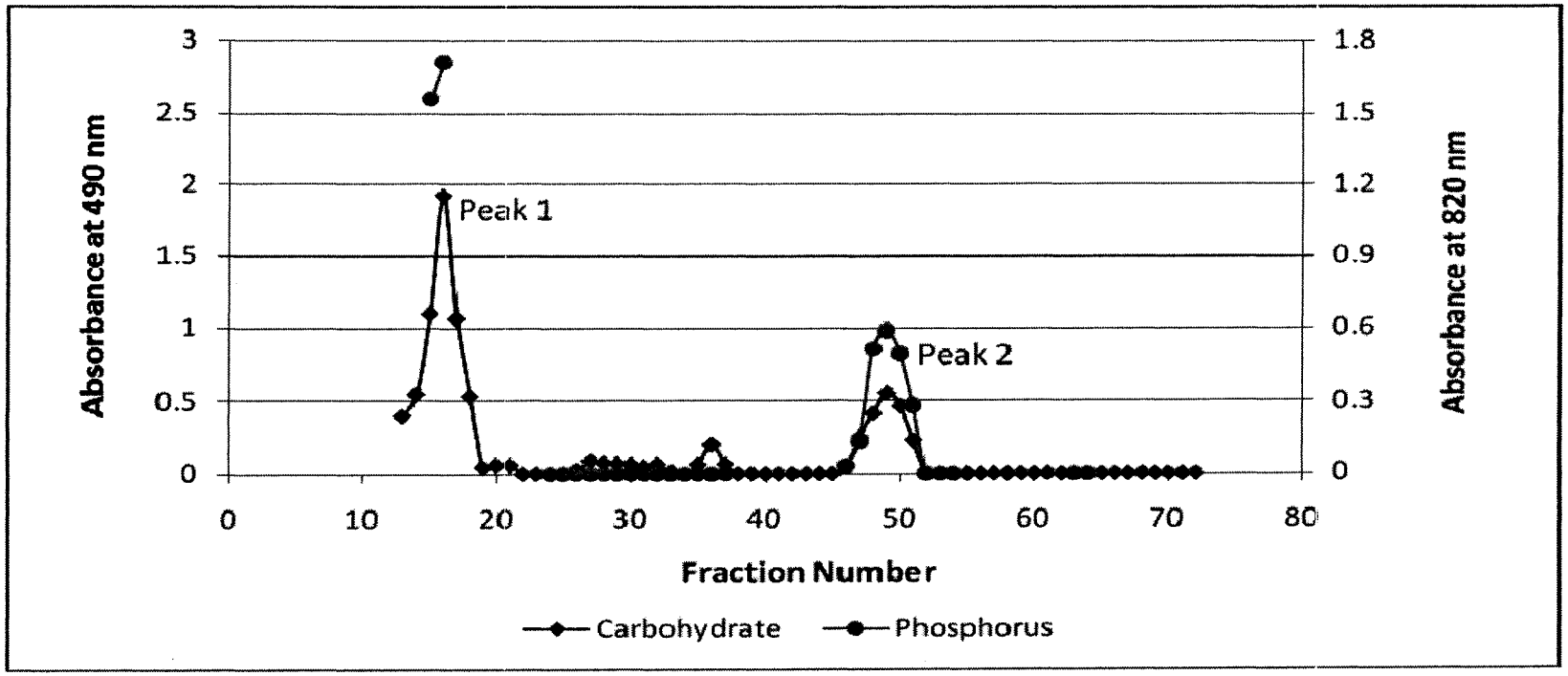

Figure 7.7. HIC-FPLC profile for the purification of a crude phenol extract from *Streptomyces* strain DSM2. The crude extract was loaded to the column with equilibration buffer until fraction 12, after which gradient elution with an increasing concentration of propanol was begun. Column fractions (4 mL) were analyzed for carbohydrate and phosphorus.

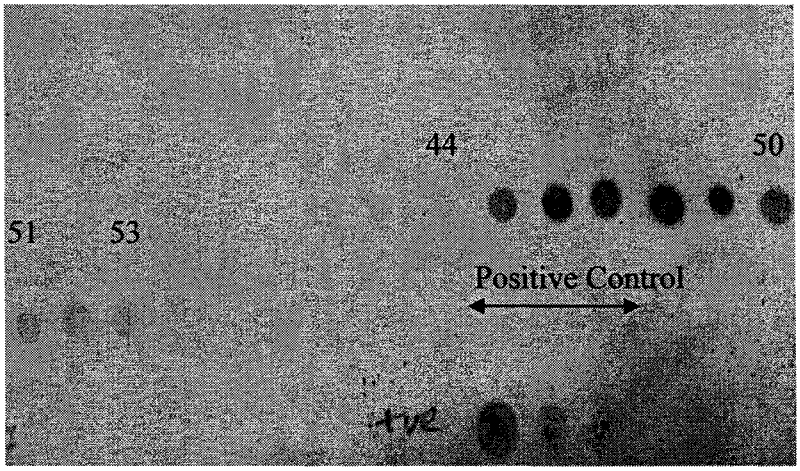

Figure 7.8. Dot immunoblotting with monoclonal anti-LTA against HIC column fractions from the HIC purification of macroamphiphile from *Streptomyces* sp. strain DSM1. The numbers indicates the fraction numbers. Fractions 44-53 showed a positive reaction with the monoclonal anti-LTA which represented the fractions earlier than and across peak 2 of Figure 7.5. Positive control spots are serial 10-fold dilutions of an approximately 1 mg/mL LTA preparation from *Streptococcus agalactiae*.

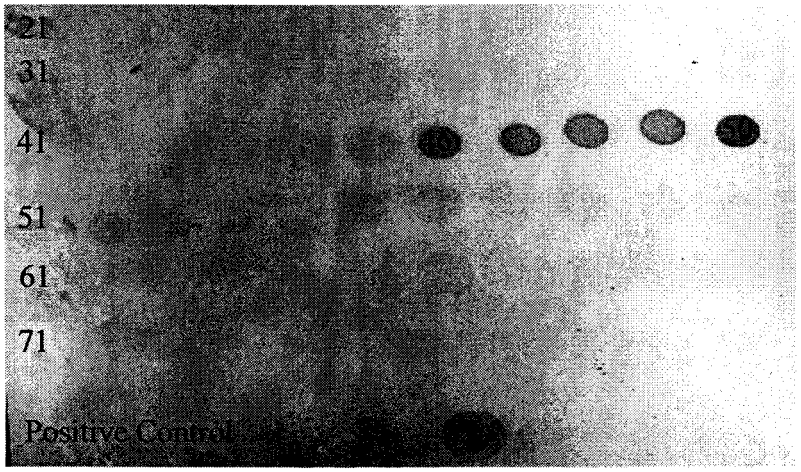

Figure 7.9. Dot immunoblotting with monoclonal anti-LTA against HIC column fractions from the HIC purification of macroamphiphile from *Streptomyces* sp. strain DSM2. The numbers represent the fraction numbers. Fractions 46-50 showed a positive reaction with the monoclonal anti-LTA which represented fractions earlier than and across peak 2 of Figure 7.6. Positive control spots are serial 10-fold dilutions of an approximately 1 mg/mL LTA preparation from *Streptococcus agalactiae.*

7.3.4. Chemical composition of the macroamphiphiles

Chemical analysis indicated the presence of significant amounts of phosphorus in the peak 2 materials from both the strains DSM1 and DSM2.

The fatty acid compositions of the whole cells and macroamphiphiles for both strains of *Streptomyces* sp. were determined by FAME derivatisation and GC analysis (described in Chapter 2, Section 2.2.6.1) and are summarised in Table 7.2 and Figures 7.10 & 7.11.

The fatty acid profiles of the whole bacterial cells for both strains showed similar profile. The major fatty acids were iC14:0, iC15:0, aiC15:0, iC16:0, C16:0, iC17:0, aiC17:0 and an unknown tentatively identified as a branched chain C12:0 fatty acid. Fatty acid profiles were obtained for the macroamphiphilic Peak 2 materials from both strains, which showed a very similar pattern of fatty acids to the respective whole cells and to each other, with minor variations in the relative percentages of some fatty acids (Figs. 7.10 and 7.11; Table 7.2).

The sugar composition of the strain DSM1 macroamphiphile was determined following acid hydrolysis to release monosaccharide components and derivatisation to alditol acetates for GC, as described in Chapter2, section 2.2.6.2. As shown in Figure 7.12 and Table 7.3, the Peak 2 macroamphiphile contained predominantly in glycerol, mannose, galactose and inositol. Lower

amounts of arabinose, glucose and an unknown sugar were present in S1 strain. Unfortunately, the strain DSM2 sugar analysis could not be performed due to lack of sample.

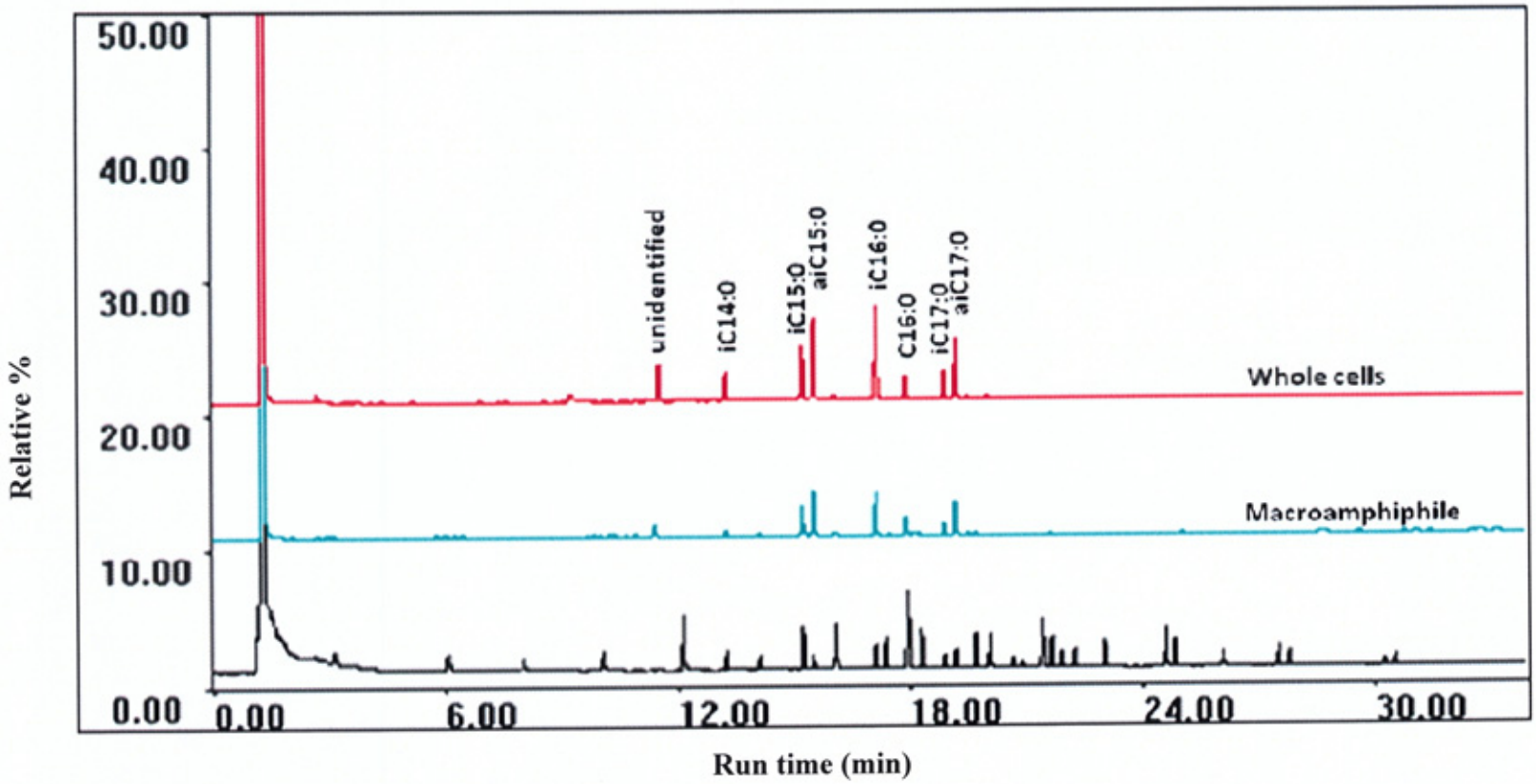

Figure 7.10. FAME analysis results for whole cells and peak 2 macroamphiphilic material *Streptomyces* sp. strain DSM1. The identities of the standard fatty acids are shown in Chapter 2, Figure 2.4.

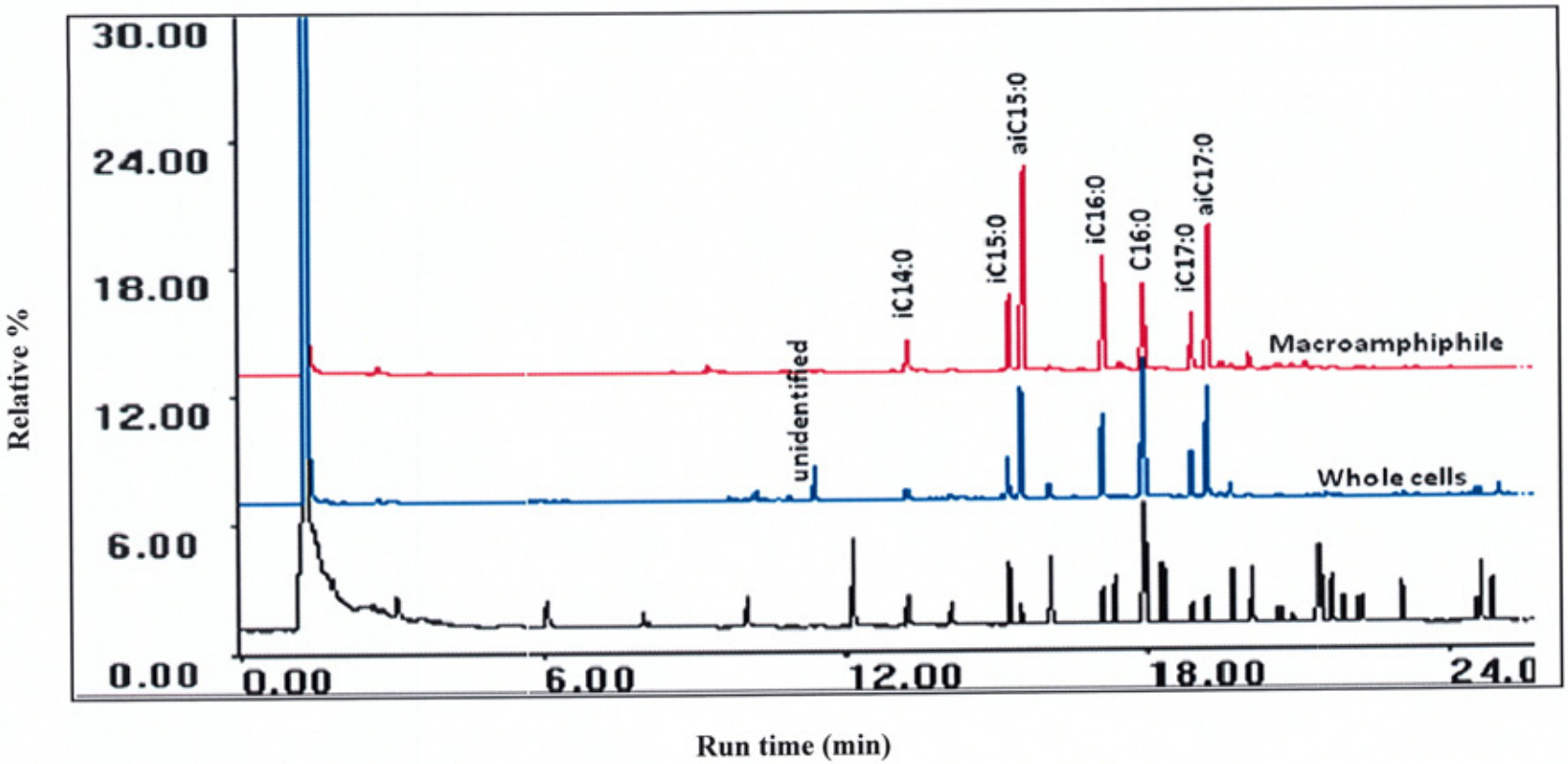

Figure 7.11. FAME analysis results for whole cells and peak 2 macroamphiphilic material *Streptomyces* sp. strain DSM2. The identities of the standard fatty acids are shown in Chapter 2, Figure 2.4.

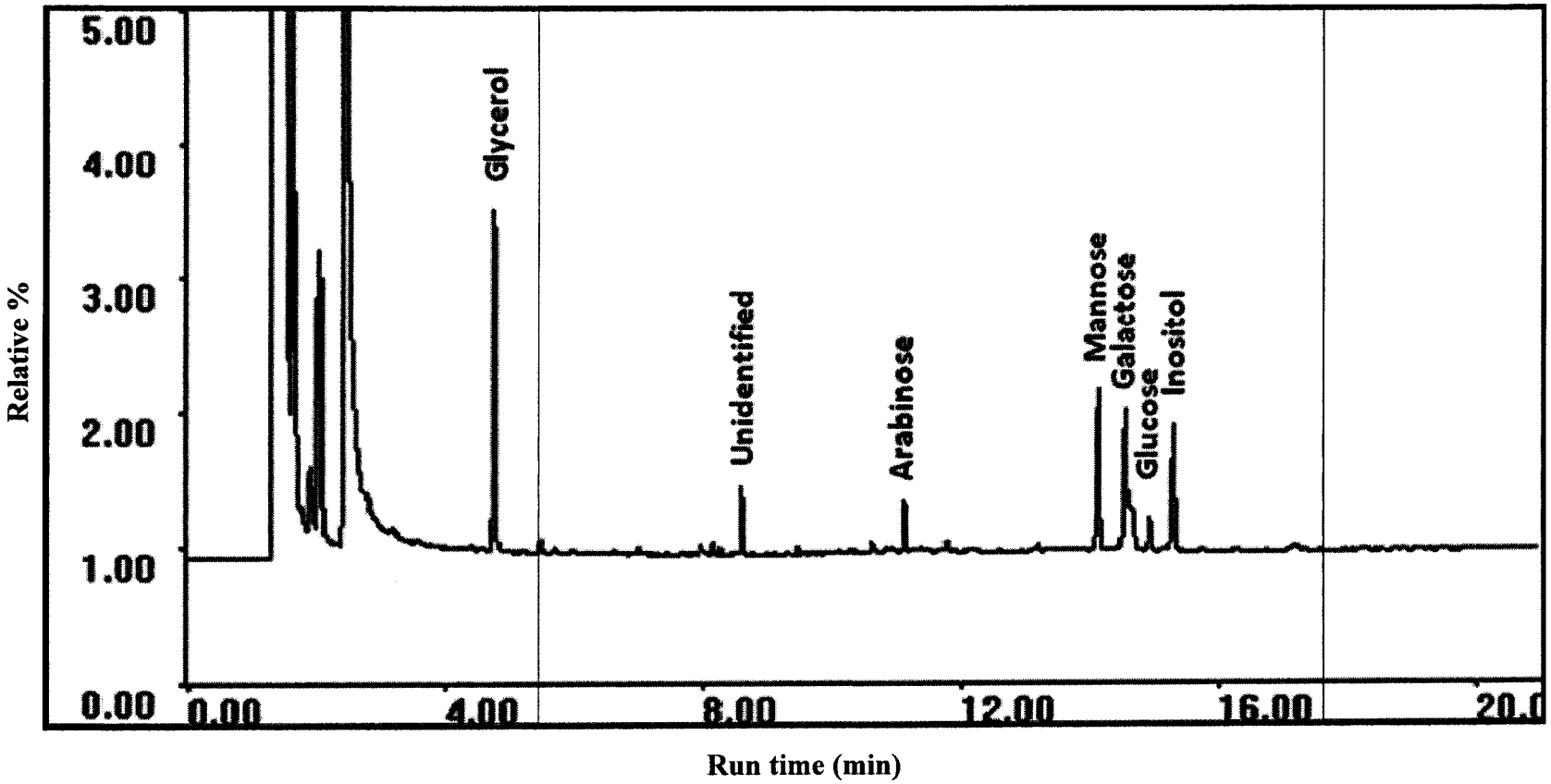

Figure 7.12. Carbohydrate analysis results for peak 2 macroamphiphilic material from *Streptomyces* strain DSM1. The identity of the sugar standards is shown in Chapter 2, Figure 2.5 and Table 2.14.

Table 7.2. Comparison of Peak 2 macroamphiphile fatty acid composition with the whole cell fatty acids of *Streptomyces* strains DSM1 and DSM2.

FAME identified[a]	**Whole cells DSM strain**	**Peak 2 macroamphiphile of DSM1 strain**	**Whole cells DSM2 strain**	**Peak 2 macroamphiphile of DSM2 strain**
Unknown[b]	4.3	Trace	7.91	6.5
iC14:0	1.57	3.0	5.53	trace
iC15:0	5.38	7.8	11.84	13.0
aiC15:0	17.34	33.8	25.61	26.3
C15:0	1.97		trace	trace
iC16:0	14.93	14.9	24.85	21.1
C16:0	25.11	10.2	5.42	9.3
iC17:0	7.04	6.7	4.54	5.6
aiC17:0	20.32	21.9	14.30	18.2
C17:0	1.92	Trace	trace	trace
C17:1	trace	1.8		

[a] Fatty acids were analysed by GC of their methyl esters and identified by comparison with a mixture of 32 authentic standards (Sigma Chemical Co.). Composition is given as the percentage of total integrated chromatographic peak areas. [b]Unknown represents a possible branched chain C12:0 fatty acid.

Table 7.3. Carbohydrate composition of the HIC-purified acid hydrolysed macroamphiphile from *Streptomyces* strain DSM1.

Carbohydrate identified[a]	**Peak 2 macroamphiphile of S2 strain**
Glycerol	38.2
unidentified[b]	5.4
Arabinose	3.4
Mannose	19.4
Galactose	19.4
Glucose	3.0
Inositol	16.7

[a] Carbohydrates were analysed by GC of their alditol acetate derivatives and identified by comparison with a mixture of authentic standards (alditol acetates of glycerol, erythritol, rhamnose, ribose, arabinose, xylose, mannose, galactose, glucose and inositol). Composition is given as the percentage of total integrated chromatographic peak areas. [a] Unidentified means the sugar was not from the standards available.

7.3.5. Electrophoretic analyses of the *Streptomyces* sp. strains DSM1 and DSM2 macroamphiphiles

The macroamphiphiles fractions (phenol extracted, HIC purified) were examined by electrophoresis followed by staining with combined Alcian-Blue 8GX and silver-nitrate staining (Sections 2.2.3.1 and 2.2.3.2). The staining, for both strains, revealed a broad band around 20 KDa and also another broad band around 10 KDa, as in *S. coelicolor* M145 (Figure 7.13, lanes 2 & 3). The latter band runs to the same position as the reference PIM_6 (Figure 7.13, lane 5) and stained intensively with Silver-nitrate stain, as did the reference PIM_6.

Though the Alcian-Blue/silver-nitrate staining didn't detect any macromolecules similar to LTA, on Western blotting the Peak 2 preparations of both strains DSM1 and DSM2 reacted with the monoclonal anti-LTA around 15 KDa (Figure 7.14), similar to the region to which GBS-LTA runs (Figure 7.13, Lane 4). Cumulatively, these data suggested each peak 2 preparation contained LTA with other two macromolecules, as had been also detected for *S. coelicolor* M145 (Figure 6.17).

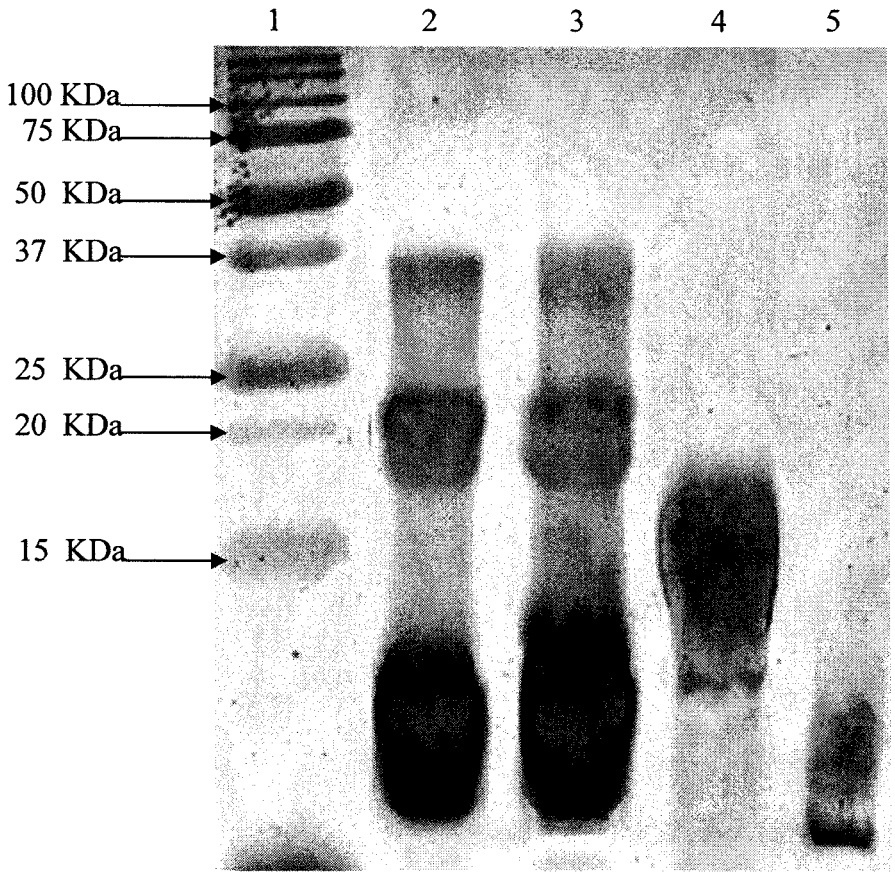

Figure 7.13. Alcian Blue & Silver-nitrate staining of *Streptomyces* sp. macroamphiphiles. Lane 1: Protein standard ladder; Lane 2: Peak 2 of strain DSM1; Lane 3: Peak 2 of strain DSM2; Lane 4: GBS LTA (reference); Lane 5: PIM_6 (reference).

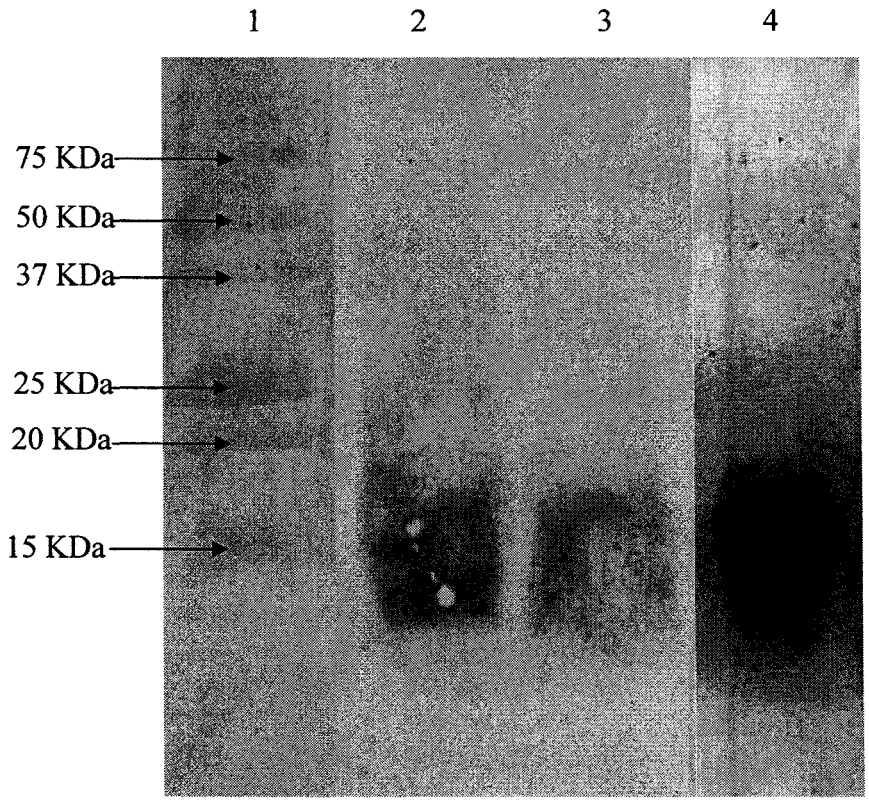

Figure 7.14. Monoclonal anti-LTA blotting of *Streptomyces* sp. DSM1 and DSM2 macroamphiphiles. Lane 1: Protein standard ladder; Lane 2: Peak 2 of strain DSM1; Lane 3: Peak 2 of strain DSM2 and Lane 4: GBS-LTA. Irrelevant sample lanes between the samples shown as lanes 1 and 2; 3 and 4 have been digitally removed.

7.4. Discussion

The present study regarding *Streptomyces* sp. DSM40537 (ATCC 3351) was done to reconfirm the result of Potekhina *et al.* (1983) suggesting the presence of LTA in this strain and to provide a reference result for the macroamphiphile study of *Streptomyces coelicolor* M145.

The characteristic phenotypic (morphological) differences between the two distinct strains DSM1 and DSM2, found after culturing from single stocks led to further morphological, 16S rDNA and chemical studies of both strains. The cultures of the two strains showed two stable and distinct morphological characteristics in different media. From these studies it appears that strain DSM1 closely resembles the described strain in the previous literature (Shirling and Gottlieb, 1972). Further study of the 16S rRNA gene sequences revealed the sequences of both strains showed 100% identity to each other, suggesting both the strains are from same species. Further evidence for the similarity of these strains was provided by fatty acid analysis of the whole cells (Table 7.2) and the macroamphiphile studies. Thus both strains appear to be the same *Streptomcyes* sp. i.e. the *Streptomcyes* sp. DSM 40537 (as received from DSMZ). The fatty acid profiles of these strains were very similar and also consistent with their being members the genus *Streptomyces* (Schauner *et al.*, 1999, Hoischen *et al.*, 1997, Semedo *et al.*, 2004, Lee *et al.*, 2005a, Wang *et al.*, 2007, Li *et al.*, 2005). The distinct phenotypic characteristics observed might therefore have been caused during the first subculturing from the DSMZ stock onto different media, possibly by some sort of developmental mutation in the DSM2 strain, which lead to the morphological changes. *Streptomyces* sp.

are well studied because of their complex life cycles and the ability of mutations to cause developmental phenotypes (such as Bld and Whi, changes in antibiotic and/or pigment production) is well documented (Kieser *et al.*, 2000, Hopwood, 1999, Chater and Chandra, 2006, Gehring *et al.*, 2000). The NCBI Blast with the 16S rRNA gene sequence showed that both the DSM1 and DSM2 strains were closely related to the strain *S. albus* and *S. saprophyticus* NBRC 3422(=ATCC3351=DSM 40537).

Based on the above analyses and comparison with Shirling and Gottlieb (1972) it is considered that the stain investigated here as DSM1 is the truest representative of *Streptomyces* sp. DSM 40537 (=ATCC 3351).

The macroamphiphile study showed the presence of three macroamphiphiles: the major one ran at around 20 KDa on electrophoresis and stained with Alcian Blue/Silver stain (Fig. 7.12); the second macroamphiphile was identifed by Western blotting as an LTA, which ran around 15 KDa (Fig. 7.13); and the final one was the glycolipid-like fraction, which had a similar mobility as the reference PIM_6 on gel electrophoresis and stained with both Alcian Blue and Silver nitrate stain (Fig. 7.12). The results were very similar for both strains DSM1 and DSM2, which further suggest the strains are very closely related. The identification of an LTA is also noted to confirm the findings of Potekhina *et al.* (1983) i.e. that *Streptomyces* sp. can synthesise LTA.

The fatty acid analysis for the macroamphiphiles showed a similar pattern as with the whole cell fatty acid profiles and the fatty acids identified agreed with

the previous study of Potekhina *et al.* (1983). The sugar analysis showed the major carbohydrates present were glycerol, mannose, galactose and inositol with minor amount of arabinose and glucose with an unidentified sugar. Glucose was suggested by Potekhina *et al.* (1983) to be possible component of the LTA lipid anchor. Mannose and inositol, along with some glycerol, may be explained by the presence of a PIM-like glycolipid (as identified by electrophoresis). Potekhina *et al.* (1983) also reported a wall polysaccharide containing mannose and galactose and so the presence of galactose was notable. Together these data suggest the presence of a PIM-like glycolipid, LTA and a lipoglycan or glycan. The present studies showed that the *Streptomyces* sp. strains DSM1 and DSM2 identifed here have a similar macroamphiphile profile as *S. coelicolor* M145 and even the sugar composition of the polymers resembled each other. These findings are significant as they again show that TA-containing *Streptomyces* may possess both LTA as a macroamphiphiles and also contain lipoglycan like macromolecule, along with the presence of glycolipid (possibly PIM–like) molecules. Moreover, the presence of lipoglycan-like molecules along with the anionic polymer LTA has been reported previously and so is itself significant.

These finding are also of significance in correlating the distribution of TA and LTA. Many different types of TA have now been reported in other species of the genus *Streptomyces* (Naumova *et al.*, 1980a). Recently TA was also detected in *Streptomyces fulvissimus* and *Streptomyces spectabilis* with 1,3-poly-GroP backbone with different sugar substituents (Shashkov *et al.*, 2006) and also in the thermophile *Streptomyces thermoviolaceus* subsp

thermoviolaceus VKM Ac-1857 (Kozlova *et al.*, 2006). Ribibol phosphate backbone or complex TA has been identified by Namouva *et al.* (1980) in different strains of the genus *Streptomyces*, whilst recently a teichuronic acid and ribitol TA have been identified in *Streptomyces* sp. VKM Ac-2124 by Shashkov *et al.* (2002). The presence of LTA has always found to be corelating with the presence of TA as the SCWPs. The present result suggests that other species in the genus *Streptomyces* identified as having TA might also contain LTA.

Further studies are needed to separate and purify these macroamphiphiles, which could be then structurally analysed. As a future extension of the present study, *S. coelicolor* M145 could be used as the model organism, with *Streptomyces* DSM 40537 included as another representative of the genus. Moreover, more species of the *Streptomyces* genus should be subjected to studies to understand the full distribution of these macroamphiphiles. The present study not only found the unique distribution of two types of macroamphiphiles in same organism but also challenge the hypothesis of the Fischer (1994) ***"LPS, LTA and lipoglycan do not occur together in the same organism and may replace each other functionally".***

Chapter Eight

Discussion

The present study focussed on the investigation of macroamphiphile composition and biosynthesis in representative Actinomycete bacteria. The present and previous studies regarding macroamphiphiles have tried to establish the distribution pattern of these structurally diverse macromolecules to help clarify their functions. The present study has contradicted the traditional hypothesis regarding the distribution pattern of macroamphiphiles and allowed a significant new hypothesis to be formed.

8.1. Need of macroamphiphiles in thermophilic bacteria

The present study has for the first time investigated the macroamphiphiles of two thermophilic Actinobacteria: *T. fusca* and *R. xylanophilus*. Previous thermophilic organisms studied with regard to their macroamphiphiles, such as *Bacillus coagulans* (Iwasaki *et al.*, 1986) and *Bacillus stearothermophilus* (Card and Finn, 1983) have been Firmicutes identified as synthesising LTA. Consequently the presence of LTA has been found to be compatible with effective membrane function during growth at high temperatures. This result is in agreement with the present finding of LTA in the cell membrane of *T. fusca*, which represents the first thermophilic Actinobacteria found to synthesise this macroamphiphile. Previous studies (Russell and Fukunaga, 1990, Konings *et al.*, 2002) have shown that thermophiles need to regulate their membrane composition to counteract the fluidising effects on membrane lipids of growth at high temperatures. Notably, LTA do not inherently form bilayer lipids and

instead form micelles in aqueous solution (Labischinski *et al.*, 1991, Fischer, 1994b, Gutberlet *et al.*, 1997). However, biophysical studies suggest that appropriately regulated amounts of polyGroP-LTA may help to stabilise the membrane surface due to interactions between the polyGroP and membrane lipid headgroups (Gutberlet *et al.*, 1997). Therefore the present study, along with the previous studies of the thermophilic low G+C Gram-positive bacteria, confirm that the presence of LTA is clearly compatible with effective membrane function during growth at high temperatures. On the other hand, the failure to recover either LTA or lipoglycan from the membranes of *R. xylanophilus* suggests that a macroamphiphile is not *per se* needed as a plasma membrane component in either mesophilic or thermophilic Gram-positive bacteria. This is a significant finding as the only previous reports of the absence of LTA or related macroamphiphile from Gram-positive bacteria are studies of some *Bacillus* spp. *Bacillus* sp. A007 failed to turnover radio-labelled PtdG into PGP-LTA although the presence of an alternative macroamphiphile was not investigated (Koga *et al.*, 1984). Likewise, strains of *Bacillus polymyxa* (now *Paenibacillus polymyxa*) and *Bacillus circulans* lack polyGroP-LTA (Iwasaki *et al.*, 1989). However, neither of these studies used HIC to distinguish macroamphiphiles from other non-lipidated cellular components and so the absence of structurally variant (non-PGP) LTA or lipoglycan in these species needs definitive confirmation.

Further studies are required to investigate the functions of LTA in the cell membranes of thermophilic Gram-positive organism (both Actinobacteria and Firmicutes). As LTA has been found to be distributed in both mesophilic and

thermophilic Firmicutes (Fischer, 1988, Fischer, 1990, Fischer, 1994a, Fischer, 1994b, Fischer *et al.*, 1978b) it is difficult to determine the LTA function based on its distribution pattern in this phylum. However, in the case of Actinobacteria, where lipoglycans predominate as macroamphiphiles (Fischer, 1994b, Sutcliffe, 1994b), the presence of LTA among thermophiles could be significant. The recent studies by Kozlova *et al.* (2006) of the thermophile *S. thermoviolaceus* subsp *thermoviolaceus* VKM Ac-1857 showed the presence of a 1,3-polyGroP back bone TA. This suggests the possibility of an LTA also being present in this organism, since LTA and TA appear to share a similar distribution, as has been discussed in Chapter 6 and later in Section 8.2.3. The investigation of the macroamphiphile present in such an organism, along with the other thermophilic members of the Actinobacteria where there is the possibility of lipoglycan being present, and comparing the biochemical and biophysical characteristics between the macroamphiphiles identified, might give a clearer insight into the functions of macroamphiphiles e.g. in the stability of membrane at higher temperatures.

8.2. Presence of LTA in Actinomycetes

8.2.1. Presence of LTA in *T. fusca*

The present study has, for the first time, identified the presence of LTA in *T. fusca* and detailed its structure (Chapter 3). This LTA is a polyGroP backbone LTA, with an approximate chain length of 19 GroP units, attached to a glycolipid presumed to be a glycosyl-containing diacylglyceride glycolipid. The main chain is substituted with β-glucosyl, acetate and lactyl groups. The presence of β-glucosyl substituents is notable, as the wall TA of *T. fusca* is also substituted with β-glucose residues (Potekhina *et al.*, 2003).

8.2.2. Presence of LTA in *Streptomyces* and other genera of Actinobacteria

The present study has identified the presence of LTA in *S. coelicolor* M145 (Chapter 6) and confirmed the presence of LTA in a reference organism, *Streptomyces* sp. strain DSM 40537 (ATCC 3351; Chapter 7), which has been previously reported by Potekhina *et al.* (1983). However, the LTA present in these organisms might not be the major macroamphiphile and further studies are needed to separate and characterise the different components identified here (Chapters 6 and 7).

The presence of LTA also has been reported in members of the genus *Agromyces* by Gnilozub *et al.* (1994). The study reported that a 1,3-polyGroP backbone LTA, substituted to varying extents with Gal*p* and acetyl groups were present in a strain each of *Agromyces cerinus* subsp. cerinus, *Agromyces cerinus* subsp. nitratus, *Agromyces fucosus* subsp. fucosus and *Agromyces*

fucosus subsp. hippuratus (Gnilozub *et al.*, 1994). The presence of acetyl groups in an LTA was reported for the first time, a finding extended by the finding here of acetyl groups as a substituent in the LTA of *T. fusca* (see above). It is noted that subsequent studies suggest that *A. fucosus* subsp. fucosus and *A. fucosus* subsp. hippuratus are separate species, *Agromyces fucosus* and *Agromyces hippuratus* (Ortiz-Martinez *et al.*, 2004).

8.2.3. Relation between LTA and TA distribution

The distribution of TA and LTA throughout the phylum Firmicutes (Neuhaus and Baddiley, 2003, Fischer, 1994b, Walsh *et al.*, 2004) suggests that the organisms containing LTA as the macroamphiphile also typically contain TA as SCWP. However, a general hypothesis couldn't be developed previously due to the presence of TA in many organisms still needing to be investigated for macroamphiphiles.

Previous and recent studies have identified many structurally diverse TA in Actinobacteria in different genera such as *Agromyces*, *Streptomyces*, *Thermobifida* and many others (Gnilozub *et al.*, 1994a, Naumova *et al.*, 1980a, Potekhina *et al.*, 2003, Shashkov *et al.*, 2006, Kozlova *et al.*, 2006, Shashkov *et al.*, 2004, Streshinskaya *et al.*, 2004, Shashkov *et al.*, 1995). The present study has identified the presence of LTA in the genus *Thermobifida* and *Streptomyces.* Gnilozub *et al.* (1994) identified LTA in *Agromyces* species but the members of many other genera still remain to be studied.

The above discussion demonstrates that where ever an organism has been identified with LTA as a macroamphiphile, TA has also been identified as a SCWP. This distribution pattern again suggests that there may be a functional correlation between these two anionic cell envelope polymers, although the biosynthetic pathway for each type of macromolecules has been found to be notably different (Chapter 1, Section 1.6.2.1 & 1.7.3.3). No SCWPs other than TA have been identified in LTA-producing Actinobacteria.

Thus it is interesting that many TA producing actinomycetes are still to be investigated for macroamphiphiles. The present studies regarding *S. coelicolor* M145 and *Streptomyces* DSM 40537 showed lipoglycan-like molecules may also be present in TA producing organisms, even though LTA has been identified in these species. However, it is notable that the structures of the SCWPs have yet to de defined in *S. coelicolor* as the structure analysis by Naumova *et al.* (1980) did not mention the details of the strain investigated i.e. whether the strain was A3(2) or a *S. coelicolor* sensu stricto strain. Though the presence of ribitol and glycerol has been detected in the TA preparation of strain A3(2) (Figure 6.15) as yet the fine structure remains to be revealed. Moreover, several *Streptomyces* species have been identified with more than one type of SCWPs, such as *Streptomyces* sp. VKM Ac-2534 which has been identified with two types of anionic cell wall polymer, teichuronic acid containing sugar in their backbone and ribitol-phosphate backbone TA with sugar substituents (Tul'skaya *et al.*, 2007). *Streptomyces melanosporofaciens* VKM Ac-1864(T), *Streptomyces hygroscopicus* subsp. hygroscopicus VKM Ac-831(T), *Streptomyces violaceusniger* VKM Ac-583(T), *Streptomyces endus* VKM Ac-1331(T), *S. endus* VKM Ac-129 and *S. rutgersensis* subsp. castelarensis VKM Ac-832(T) have been identified with three types of TAs: (1,3-polyGroP) with N-acetylated alpha-glucosaminyl substituents on the C-2 of glycerol, and minor TAs, 1,3- and 2,3-polyGroP polymers without substitution (Tulskaya *et al.*, 2007), indicating that members of the genus *Streptomyces* may contain more than one TA. Thus the distribution of TA might be complex in this genus, with strains also containing other neutral carbohydrate polymers as SCWPs along with TA, as has been identified in

Streptomyces thermoviolaceus subsp. thermoviolaceus VKM Ac-1857(T) (Kozlova *et al.*, 2006).

Further analyses are therefore required to conclude whether TA producing organism only synthesize LTA, rather than other macroamphiphiles. Moreover, no Actinobacteria containing AG or other non-TA SCWPs have been identified that produce any macroamphiphile other than lipoglycan (for example mycobacteria produce AG and LAM; *Kineococcus* species apparently produce AG and lipoglycan [Chapter V]). So from the above observations, the following hypothesis could be derived:

"LTA containing Actinobacteria contain TA as a SCWP, whilst on the other hand lipoglycan containing Actinobacteria generally contains SCWPs other than TA."

This hypothesis suggests that anionic macroamphiphiles (e.g. LTA) are functionally inter-related to the SCWPs (such as TA), which create an anionic environment at the membrane surface and through the cell envelope. Similarly, uncharged or less charged macroamphiphiles (eg. lipoglycans) are functionally inter-related to uncharged SCWPs (such as AG) and may maintain a more neutral electrostatic environment at the cell envelope, as reviewed recently by Wiedenmaier and Peschel (2008).

8.2.4. LTA biosynthesis genes in Actinobacteria

The biosynthetic pathway for LTA is still to be fully determined as has been described in Chapter one, Section 1.7.3.3. The main gene found to be responsible for LTA biosynthesis is that for the LTA synthase enzyme (LtaS, primary accession number: Q2FIS2) which has been found to be responsible for polymerisation of poly-GroP of LTA in *S. aureus*, as shown in Figure 1.19 (Grundling and Schneewind, 2007a, Grundling and Schneewind, 2007b). LtaS was previously annotated as a sulfatase in GenBank. An NCBI Blast search using the LtaS (SAUSA300_0703, 646 amino acids) sequence of *S. aureus* (strain USA300) as query against some of the known LTA producing Gram-positive Low G+C (phylum Firmicutes) organisms showed the presence of one or more homologous proteins (Table 8.1), but no homologues were found in representatives of the class Mollicutes such as *Mycoplasma mycoides* subsp. mycoides SC str. PG1, *Mycoplasma pneumoniae* M129 and *Ureaplasma parvum* serovar 3 str. ATCC 700970. Mollicutes are known not to produce LTA and rather produce lipoglycans (Smith, 1984). Recently it has been suggested that this class should be moved from the phylum Firmicutes to the phylum "*Tenericutes*" (http://www.bacterio.cict.fr/ classifphyla.html #Tenericutes). Most of the homologous proteins in Table 8.1 have been annotated as sulfatases or as hypothetical proteins. The Blast results showed that LtaS homologues are present in all of the representative LTA producing organisms in the phylum Firmicutes and absent from lipoglycan producing representatives of the class Mollicutes, consistent with the observation of Grundling & Schneewind (2007a; b) on the distribution of the LtaS protein in LTA producing Gram-positive low G+C organisms.

Surprisingly, a Blast search for LtaS homologues in Actinobacteria (investigating fully sequenced genome organisms, with an E cut-off of 0.0001) identified few actinobacterial homologues except for three homologues in *R. xylanophilus* (Chapter 4, Table 4.4) and two bifidobacterial homologues. However, *R. xylanophilus* has been demonstrated not to produce LTA (Chapter 4) and the three homologues are only distantly related to LtaS. Likewise, bifidobacteria synthesise a lipoglucogalactan lipoglycan (section 1.7.4.1). On the other hand, the LTA producing organisms *T. fusca* and *S. coelicolor* M145 were found to lack of clear LtaS homologues by Blast analysis, although SCO7547 and Tfu_1353 both belong to the PF00884 sulfatase family. As a genome sequence is not yet available for any strain of *Agromyces* sp. the comparative Blast search could not be done for this genus. The above observations suggest that LTA biosynthesis in Actinobacteria might proceed by a second, alternative pathway which is independent of LtaS.

Given the above, it also seemed appropriate to re-examine the established the pathway for alanylation (Chapter one, Section 1.7.3.3.4.1) for both LTA and TA, and also the biosynthetic pathway for TA (Chapter One, section 1.6.2.1), between Actinobacteria and Firmicutes.

The search for *dlt* genes that control alanylation of both TA and LTA (Neuhaus and Baddiley, 2003) showed no complete *dlt* operons to be present in any of the Actinobacteria investigated (Table 8.2). In the case of *T. fusca*, this agrees with the known chemical structures of the TA (Potekhina *et al.*, 2003) and

LTA (this study) as no alanine substituents have been found. D-alanine has not yet been reported in the TA of any other Actinobacteria, yet.

Tag proteins are responsible for the biosynthesis of the poly(GroP) backbone TA, as has been described for *B. subtilis* 168 (Figure 1.9). The two gene products responsible for the polymerisation of GroP are TagB and TagF, the first one of which is responsible for initial incorporation of GroP onto the linkage unit and the latter of which is responsible for the continuation of polymerisation, are found to be essential for poly(GroP) TA biosynthesis in Firmicutes (Bhavsar and Brown, 2006; Figure 1.9). Although different sizes, TagB and TagF share a functional domain, described in by Pfam as PF04464 (CDP-Glycerol:Poly(Gro-P)glycerophosphotransferase; http:// pfam. sanger. ac.uk/ family?acc=PF04464). For poly(GroP) backbone TA producing Firmicutes these genes are found to be present as either an individual member or two orthologues belonging to PF04464.

In *T. fusca*, which is known to produce poly(GroP) TA (Potekhina *et al.*, 2003), a single protein, Tfu_2178, showed homology with both the TagB and TagF proteins, and also belongs to PF04464. Tfu_2178 is a large (952 amino acid) protein with the PF04464 domain at its extreme C-terminus. A glycosyltransferase family 2 domain (PF00535) is present at its N-terminus, such that the two domains are separated by a long ca. 600 amino acid internal spacer. This protein may therefore act as a 'mixed function' enzyme, both polymerising the poly(GroP) main chain and adding the β-glucosyl substituents. Tfu_2177, a family 1 glycosyltransferase (PF00534), is apparently

part of an operon with Tfu_2178. This protein may therefore be involved in TA linkage unit biosynthesis such that Tfu_2177 and Tfu_2178 may be sufficient for TA biosynthesis i.e. might be similar to TagE and TagB. The proteins Tfu_2196 and Tfu_2191 are noted to be homologous to TagD family and ABC transport proteins, respectively, and might therefore be assumed to function as TagD and TagGH, which are responsible for CDP-GroP formation and TA transport across the plasma membrane.

In the case of *Streptomyces* the analysis of a TA biosynthesis path is much more complicated, which might be due to production of more complex and/or more than one TA, as discussed in section 8.2.3. This was also found to be the case for *S. coelicolor* M145, where two or three genetic loci that may encode teichoic acid or other carbohydrate polymer biosynthesis proteins appear to be present: six 'mixed function' fused glycosyltransferase and PF04464 (TagB/TagF) domain proteins are present (SCO2589, SCO2590, SCO2981, SCO2982, SCO2983; and SCO2997) as shown in Table 8.3. The first locus contain two homologues, SCO2589 and SCO2590, both of which are bifunctional proteins containing two Pfam-A domains, for a glycosyltransferase (PF00535) and a GroP transferase (PF04464), separated by Pfam-B 1440 and Pfam-B701 domains. The latter domain showed homology to both TagB and TagF. This locus therefore seems to be involved in TA biosynthesis but the specific structure can't be determined as the presence of the glycosyltranferase domains might involve in addition of sugar residues in the backbone of a complex TA or as a substituents to the backbone. The second locus has SCO2981, SCO2982 and SCO2983 homologues of TagB, all of

which are bifunctional proteins containing similar Pfam-A domains as the proteins in the previous locus and similarly separated by 2 to 4 Pfam-B domains. This locus might also be involved in complex TA biosynthesis. The third locus (or which might be the extension of the second locus) has a TagB homologue, SCO2997, similar in structure to the other TagB homologues, adjacent to a putative ABC transporter ATP-binding protein, SCO2996, which might function as a TagGH homologue. Finally, another bifunctional protein, SCO6187, has been found which has a sugar kinase and a CTP-transferase domain. The latter domain is homologue to TagD and might be responsible for CDP-glycerol production. However, SCO6187 belongs to a 'cell wall glycan operon' which is apparently responsible for the synthesis of an as yet uncharacterised cell wall polymer distinct from TA (Hong *et al.*, 2002). The above bioinformatics analysis for *S. coelicolor* TA biosynthesis (Table 8.3) agrees with the conclusion that *S. coelicolor* might produce more than one type of TAs and might also produce other carbohydrate based polymers as SCWP, as discussed in section 8.2.3.

From the above discussion it can be concluded for both *T. fusca* and *S. coelicolor* no full Tag operon comparable to that present in *B. subtilis* can be identified. Moreover, the TagB domains present always seem to be fused to a glycosyltransferase domain which might be required for substitution of glucose in the *T. fusca* TA or for producing more complex structures for TA in *S. coelicolor*. Also separate TagB and TagF proteins are not required, as *T. fusca* has been identified with only one PfamA: PF04464 protein. This suggests TA biosynthesis might be differently co-cordinated in members of the phylum Actinobacteria, though further studies are required to explore this hypothesis.

Table 8.1. LtaS (*S. aureus,* LTAS_STAA3) homologues in representative Gram-positive bacteria.

Firmicutes name	**LtaS homologue(s)**	**Size (a.a)**	**Amino acid identity**	**E number**
Staphylococcus epidermidis ATCC 12228	SE0494	646	579/646 (89%),	0.0
Bacillus subtilis subsp. subtilis str. 168	BSU07260	639	358/625 (57%),	0.0
	BSU07710	649	314/627 (50%),	2e-179
	BSU24840	638	258/631 (40%),	6e-138
	BSU33360	617	249/612 (40%),	6e-129
Listeria monocytogenes EGD-e	lmo0927	653	334/638 (52%)	0.0
	lmo0644	606	168/632 (26%),	6e-6
Enterococcus faecalis V583	EF1264	702	292/645 (45%),	2e-155
	EF1813	686	276/662 (41%),	7e-146
Lactobacillus delbrueckii subsp. bulgaricus ATCC 11842	Ldb1835	690	288/635 (45%),	7e-149
	Ldb0690	740	255/646 (39%),	6e-129
Streptococcus agalactiae A909	SAK_1414	714	268/658 (40%)	2e-132
Lactococcus lactis subsp. lactis Il1403	L13927	722	251/671 (37%),	3e-119
Clostridium botulinum A str. ATCC 19397	CLB_2827	619	184/575 (32%),	6e-87
	CLB_0634	636	181/583 (31%),	3e-77

Table 8.2. Presence of homologues of dlt operon proteins in representative Actinobacteria. BlastP searches were performed with an E cut-off of 0.01.

Actinobacteria	*dltA*	*dltB*	*dltC*	*dltD*
Acidothermus cellulolyticus 11B	Present	Absent	Absent	Absent
Arthrobacter aurescens TC1	Present	Absent	Absent	Absent
Arthrobacter sp. FB24	Present	Absent	Absent	Absent
Bifidobacterium adolescentis ATCC 15703	Present	Absent	Absent	Absent
Bifidobacterium longum DJO10A (unfinished genome)	Present	Absent	Absent	Absent
Bifidobacterium longum NCC2705	Present	Absent	Absent	Absent
Brevibacterium linens BL2 (unfinished genome)	Present	Absent	Absent	Absent
Corynebacterium diphtheriae NCTC 13129	Present	Absent	Absent	Absent
Corynebacterium efficiens YS-314	Present	Absent	Absent	Absent
Corynebacterium glutamicum ATCC 13032	Present	Absent	Absent	Absent
Corynebacterium glutamicum R	Present	Absent	Absent	Absent
Corynebacterium jeikeium K411	Present	Absent	Absent	Absent
Frankia alni ACN14a	Present	Present	Absent	Absent
Frankia sp. CcI3	Present	Present	Absent	Absent
Kineococcus radiotolerans SRS30216	Present	Absent	Absent	Absent
Leifsonia xyli subsp. xyli str. CTCB07	Present	Absent	Absent	Absent
Mycobacterium avium 104	Present	Absent	Absent	Absent
Mycobacterium avium subsp. paratuberculosis K-10	Present	Absent	Absent	Absent
Mycobacterium bovis AF2122/97	Present	Absent	Absent	Absent

Actinobacteria	***dltA***	***dltB***	***dltC***	***dltD***
Mycobacterium bovis BCG str. Pasteur 1173P2	Present	Absent	Absent	Absent
Mycobacterium leprae TN	Present	Absent	Absent	Absent
Mycobacterium smegmatis str. MC2 155	Present	Absent	Absent	Absent
Mycobacterium sp. JLS	Present	Absent	Absent	Absent
Mycobacterium sp. KMS	Present	Absent	Absent	Absent
Mycobacterium sp. MCS	Present	Absent	Absent	Absent
Mycobacterium tuberculosis H37Rv	Present	Absent	Absent	Absent
Mycobacterium ulcerans Agy99	Present	Absent	Absent	Absent
Mycobacterium vanbaalenii PYR-1	Present	Absent	Absent	Absent
Nocardia farcinica IFM 10152	Present	Absent	Absent	Absent
Nocardioides sp. JS614	Present	Absent	Absent	Absent
Propionibacterium acnes KPA171202	Present	Absent	Absent	Absent
Rhodococcus sp. RHA1	Present	Absent	Absent	Absent
Rubrobacter xylanophilus DSM 9941	Present	Absent	Absent	Absent
Saccharopolyspora erythraea NRRL 2338	Present	Present	Absent	Absent
Salinispora tropica CNB-440	Present	Absent	Absent	Absent
Streptomyces avermitilis MA-4680	Present	Absent	Absent	Absent
Streptomyces coelicolor A3(2)	Present	Absent	Absent	Absent
Thermobifida fusca YX	Present	Absent	Absent	Absent
Tropheryma whipplei TW08/27	Present	Absent	Absent	Absent
Tropheryma whipplei str. Twist	Present	Absent	Absent	Absent

Table 8.3. Identification TA biosynthesis loci in *Streptomyces* based on TagB/TagF homologues in *S. coelicolor* A3(2) genome.

Locus	Protein	PfamA (bifunctional)	PfamB	Description
1	SCO2589	• PF00535* • PF004464*	• 1440 • 701	1. Possible TA Biosynthesis locus. 2. Not possible to be specific about structure 3. Might form a complex TA due to the presence of fused glycosyltransferase domains. 4. Not a full Tag operon
	SCO2590	• PF00535* • PF004464*	• 1440 • 701	
2	SCO2981	• PF00535* • PF004464*	• 1440 • 19216 • 178318 • 701	1. Possible TA Biosynthesis locus. 2. Not possible to be specific about structure 3. Might form a complex TA due to the presence of fused glycosyltransferase domains. 4. Not a full Tag operon
	SCO2982	• PF00535* • PF004464*	• 107049 • 19216 • 701	
	SCO2983	• PF00535* • PF004464*	• 19216 • 701	
Locus 3 or extension of locus 2	SCO2997	• PF00535* • PF004464*	• 19216 • 701	1. Adjacent to ABC transporter SCO2996 which might function as a TagGH homologue. 2. Nearby on chromosome and possibly an extension of locus 2 or a 3rd TA locus.
4	SCO6187	• PF01467* • PF00294*	None	1. No TagB type protein and thus might not be responsible for TA biosynthesis. More likely responsible for synthesis of a cell wall polysaccharide (Hong *et al.*, 2002). 2. TagD proteins belong to PF01467 .

* PF00535 function as glycosyltransferase, PF004464 as GroP transferase. PF01467 as CTP transferase and PF00294 as phosphokinase.

8.3. Diversity of macroamphiphiles in Actinobacteria

The generalization that lipoglycans are always present in Actinobacteria (Fischer, 1994; Sutcliffe, 1994) has been shown to be wrong by the discovery of LTA in representatives of the genera *Thermobifida, Streptomyces* and *Agromyces*. More genera still needed to be subjected to macroamphiphile studies, which can be seen in the phylogenetic tree of Figure 8.1. Moreover, much diversity between lipoglycan structures has been observed from genus to genus and even between species to species (Discussed in Chapter One, Sections 1.6.4 & 1.8).

The present study of *K. radiotolerans* showed the likely presence of a novel LAM-like molecule, which requires further structural studies. Moreover bioinformatic studies has revealed the presence of most of the genes required for the biosynthesis of a LAM-like molecule (Table 5.6 and 5.7), in agreement with the present study. The likely presence of arabinoglactan (AG) as the SCWP in this organism, which is also a common characteristics for the Mycolata group, also agrees with the present finding, as Mycolata members also synthesise LAM or LAM-like macroamphiphiles (Sutcliffe, 2006). This is also consistent with the suggestion these macroamphiphiles and SCWPs have a common distribution pattern, which might be necessary for the properties of the cell membrane's outer surface environment.

The findings for *S. coelicolor* M145 and *Streptomyces* DSM40537 are complicated by the identification of up to three macromolecules. The presence of LTA with the presence of TA as SCWP is again consistent with the

proposed relationship between the distribution of macroamphiphiles and SCWP. However, the *S. coelicolor* genome is also noted to have a large operon (SCO6180-SCO6190 and, most likely, other adjacent genes) apparently encoding a non-TA cell wall glycan (Hong *et al.*, 2002). In this context, the apparent presence of a lipoglycan-like molecule along with an LTA is very interesting. Previously, two lipoglycans, LM and LAM, have been identified in several different Mycolata organisms but these are thought to be related in their biosynthesis (section 1.7.5.4). The finding of two macroamphiphiles without any obvious biosynthetic relationship is reported here for the first time.

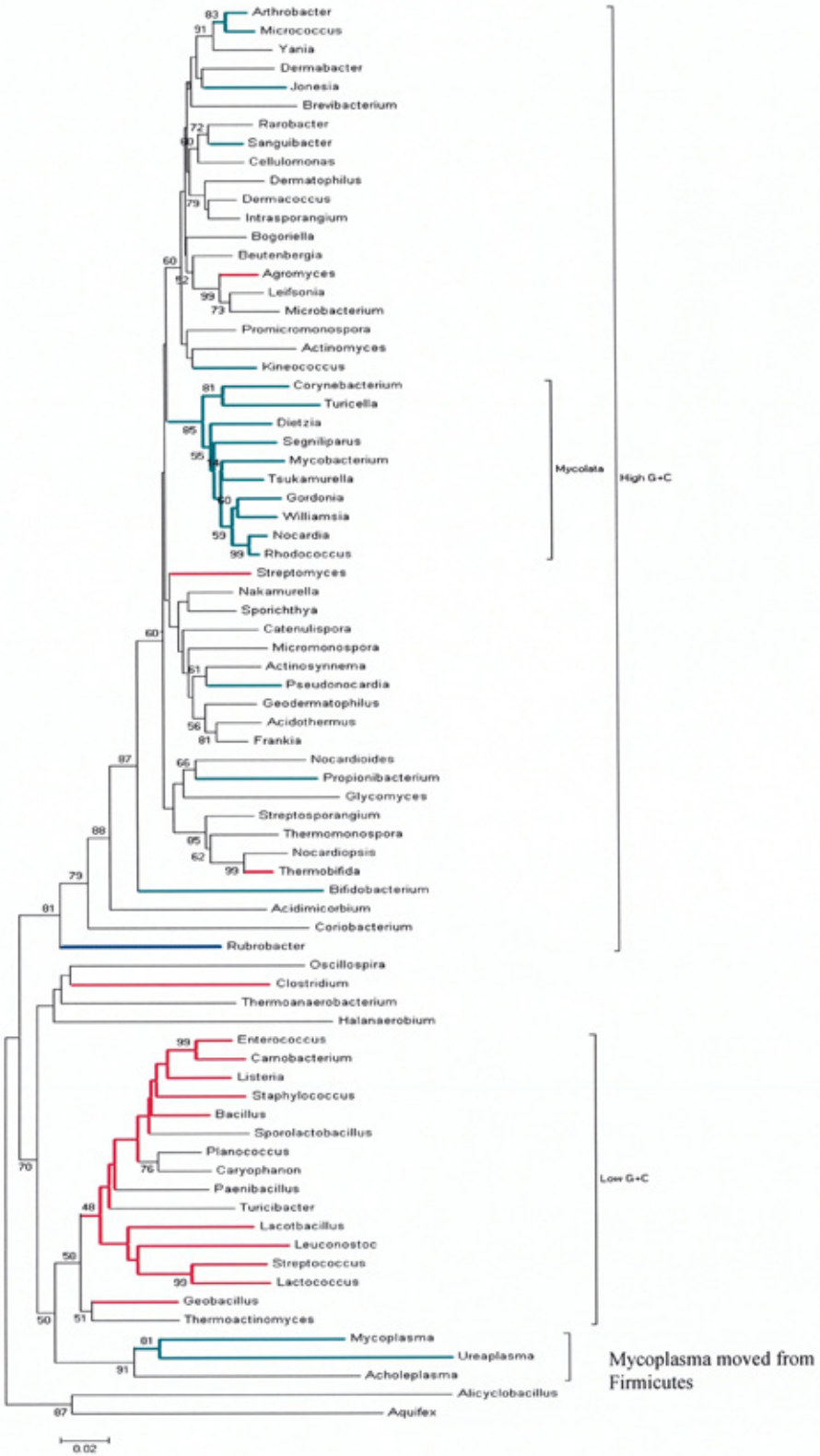

Figure 8.1. Phylogenetic tree of Gram-positive bacteria based on 16S rRNA and the distribution of macroamphiphiles. Green lines indicate lineages known to produce lipoglycans (LM, LAM or LCHO), red lines represent lineages known to produce LTA. The blue line indicates the *Rubrobacter* lineage (apparent absence of macroamphiphiles) and black lines represent lineages that have yet to be investigated.

8.4. Comparative genomic analyses

The comparative genomic analyses in Table 8.4 shows that the four representative Actinobacteria contain homologues of the biosynthetic proteins needed for the biosynthesis of PI and the apolar PIMs (notably to at least PIM_2). The presence of these homologues in *T. fusca, K. radiotolerans* and *S. coelicolor* agrees with the presence of PI or PIM glycolipid in these organisms (Lee, 2006, Lechevalier *et al.*, 1977, Kudo, 1997, Kroppenstedt *et al.*, 1990). The *R. xylanophilus* glycolipid composition has yet to be revealed, although uncharacterised phosphoglycolipids were detected in *R. radiotolerans* and *R. xylanophilus* (Suzuki *et al.*, 1988; Carreto *et al.*, 1998).

The data in Table 8.5 shows that *K. radiotolerans* has homologues of the major proteins required for the biosynthesis of LAM or LAM-like molecules, which agrees with the present analysis of the macroamphiphile content (Chapter 5). Notably, homologues of the mannosyl transferases responsible for mannose translocation (Krad_0328) and extracytoplasmic polymerisation (e.g. Krad_10171) could be identified. Moreover, the bioinformatic analysis for homologue(s) of lipoglycan biosynthesis genes suggests *S. coelicolor* M145 is capable of synthesising PIMs but not LM-like lipoglycan. It is therefore interesting that *S. coelicolor* has clear homologue of the proteins for synthesis of lipid linked arabinose (SCO4841, SCO4842 and SCO4844). However, the absence of an arabinose polymerase (EmbC) homologue suggests that the organism does not have the capability to produce LAM or extensively arabinosylated LAM-like lipoglycan, which reflects the results in Chapter 6. Recent experiments with mutants (supplied by Anpu Varghese/Prof Maggie

Smith, University of Aberdeen) in the MSEG3860 and MSEG3859 homologues SCO1014 and SCO1423 (Table 8.5), and in a putative protein mannosyltransferase, showed no difference in the macroamphiphile profiles when examined by gel electrophoresis (data not shown).

The absence of homologues for enzymes involved in the synthesis of polar PIM, LM and LAM (Table 8.5) are consistent with the present finding of LTA as the single macroamphiphile in *T. fusca* (Chapter 3). It is however interesting that *T. fusca* has clear homologues (Tfu_2460 to Tfu_2462) in operon that apparently allows the synthesis of lipid linked arabinose precursors. A locus SCO4841 – SCO4844 is also present in *S. coelicolor* (Table 8.5). Although containing the pathway for PI and apolar PIM synthesis, *R. xylanophilus* lacks siginficant homologues of proteins needed for LM/LAM bisoynthesis, consistent with the absence of these macroamphiphiles in this organism.

Table 8.4. PI and apolar PIMs biosynthesis genes (*M. tuberculosis*) homologue(s) in *K. radiotolernas, S. coelicolor A3(2), T. fusca* and *R. xylanophilus*

Reactions	**Gene name (*M. tuberculosis*)**	***K. radiotolerans* homologue(s)**	***S. coelicolor* A3(2) homologue(s)**	***T. fusca* homologue(s)**	***R. xylanophilus* homologue(s)**
PI/precursor synthesis					
Phosphomannomutase	Rv3257c (465 a.a.)	Krad_3841(497 a.a.) Identities=282/479 (58%) Expect = 4e-147	SCO3028 (454 a.a.) Identities= 289/458 (63%) Expect= 9e-155	Tfu_2510 (455 a.a.) Identities= 282/453 (62%) Expect = 2e-159	Rxyl_1134 (472 a.a.) Identities = 210/445 (47%) Expect= 2e-106
Ins-1-phosphate synthase	Rv0046, Ino1 (367 a.a.)	Krad_3509 (360 a.a.) Identities=275/352 (78%) Expect = 8e-156	SCO3899 (360 a.a.) Identities= 77/353 (78%) Expect=3e-154	Tfu_3099 (359 a.a.) Identities= 83/352 (80%) Expect = 1e-162	Rxyl_0688 (443 a.a.) Identities = 30/107 (28%) Expect = 6e-04
Inos-1-P phosphatase	Rv1604, ImpA (270 a.a.)	Krad_2135 (260 a.a.) Identities = 72/211 (34%) Expect = 8e-18	SCO5860 (272 a.a.) Identities = 86/273 (31%) Expect = 4e-20	Tfu_1212 (273 a.a.) Identities = 89/258 (34%) Expect = 1e-30	Rxyl_1545 (259 a.a.) Identities = 85/246 (34%) Expect = 2e-25
PI synthase CDP-DAG + inositol → PI	Rv2612c, PgsA (217 a.a.)	Krad_3064 (206a.a.) Identities = 94/192 (48%) Expect = 2e-39	SCO1527 (241 a.a.) Identities = 92/212 (43%), Expect = 8e-42	Tfu_2103 (225 a.a.) Identities = 93/188 (49%), Expect = 2e-44	Rxyl_2978 (201 a.a.) Identities = 63/189 (33%) Expect = 4e-20

Reactions	**Gene name (*M. tuberculosis*)**	***K. radiotolerans* homologue(s)**	***S. coelicolor* A3(2) homologue(s)**	***T. fusca* homologue(s)**	***R. xylanophilus* homologue(s)**
PI/precursor synthesis					
DAG → Phosphatidate	Rv2252 (309 a.a.)	Krad_1884 (293 a.a.) Identities = 118/294 (40%), Expect = 2e-47	SCO0667 (293 a.a.) Identities = 91/294 (30%), Expect = 3e-29	Tfu_1766 (291 a.a.) Identities=117/292 (40%), Expect = 4e-52	Rxyl_1713 (312 a.a.) Identities = 92/304 (30%), Expect = 4e-23
	Rv3218 (321 a.a.)	Krad_0248 (366 a.a.) Identities = 90/337 (26%), Expect = 7e-12	SCO5241 (322 a.a.) Identities = 131/328 (39%), Expect = 6e-55	Tfu_0557 (311 a.a.) Identities = 131/321 (40%), Expect = 1e-54	Rxyl_1713 (312a.a.) Identities = 83/326 (25%), Expect = 9e-09
PI to PIMs cytoplasmic (apolar PIM biosynthesis)					
PI → PIM_1	Rv2610c, PimA (378 a.a.)	Krad_3062 (371 a.a.) Identities = 197/371 (53%) Expect = 3e-97	SCO1525 (387 a.a.) Identities = 196/375 (52%) Expect= 9e-101	Tfu_2101 (379 a.a.) Identities = 194/375 (51%) Expect = 7e-99	Rxyl_2620 (385 a.a.) Identities = 157/393 (39%) Expect = 3e-59
PIM_1 acyltransferase	Rv2611c (316 a.a.)	Krad_3063 (311 a.a.) Identities = 125/306 (40%) Expect = 6e-47	SCO1526 (311 a.a.) Identities = 145/307 (47%) Expect = 5e-62	Tfu_2102 (307 a.a.) Identities = 153/304 (50%) Exect = 1e-72	Absent

Reactions	**Gene name (*M. tuberculosis*)**	***K. radiotolerans* homologue(s)**	***S. coelicolor* A3(2) homologue(s)**	***T. fusca* homologue(s)**	***R. xylanophilus* homologue(s)**
PI to PIMs cytoplasmic (apolar PIM biosynthesis)					
$PIM_1 \rightarrow PIM_2$	Rv2188c, PimB' (385 a.a.)	Krad_3243 (396 a.a.) Identities = 195/383 (50%) Expect = 3e-103	SCO2132 (412 a.a.) Identities = 203/3912 (51%) Expect = 1e-104	Tfu_1764 (398a.a) Identities = 191/379 (50%) Expect = 3e-93	Rxyl_0383 (377 a.a.) Identities = 159/359 (44%) Expect = 6e-61
$PIM_2 \rightarrow PIM_3$/ PIM_4	PimC, MT1800 (381 a.a.) or other Mannosyl transferase	Krad_3070 (403 a.a.) Identities = 108/374 (28%) Expect = 8e-13	SCO2706 (436 a.a.) Identities = 89/326 (27%) Expect = 2e-10	Tfu_2257 (426 a.a.) Identities = 104/365 (28%) Expect = 1e-20	Rxyl_1298 (374 a.a..) Identities = 77/238 (32%) Expect = 2e-19

Table 8.5. Polar PIMs, LM and LAM biosynthesis genes (*M. tuberculosis*) homologue(s) in *K. radiotolernas, S. coelicolor A3(2), T. fusca* and *R. xylanophilus*

Reactions	**Gene name (*M. tuberculosis*)**	***K. radiotolerans* homologue(s)**	***S. coelicolor* A3(2) homologue(s)**	***T. fusca* homologue(s)**	***R. xylanophilus* homologue(s)**
Lipid linked precursor synthesis (for transfer from the inner membrane to outer surface)					
C35P (polyprenol) → C35P-mannose	Rv2051c (874 a.a.)	Krad_1890 (593 a.a.) Identities = 210/545 (38%) Expect = 3e-87	SCO1014 (537 a.a.) Identities = 238/527 (45%) Expect= 5e-110	Tfu_1762 (527a.a.) Identities = 188/513 (36%) Expect = 3e-75	Absent
	MSMEG_3860 (615 a.a.) CN hydrolase domain (≡ N-terminus of Rv2501c)	Krad_1890 (593 a.a.) Identities = 226/532 (42%) Expect = 7e-91	SCO1014 (537a.a.) Identities = 241/509 (47%) Expect = 1e-115	Tfu_1762 (527 a.a.) Identities = 190/517 (36%) Expect = 2e-81	Absent
	MSMEG_3859 (265 a.a..) (≡ C-terminus of Rv2501c)	Krad_ 0328(270 a.a.) Identities = 115/237 (48%) Expect = 1e-53	SCO1423 (302 a.a.) Identities = 148/243 (60%) Expect= 2e-78	Tfu_1850 (258 a.a.) Identities = 103/217(47%) Expect = 6e-50	Rxyl_1238(340 a.a.) Identities = 80/242(33%) Expect = 2e-18

Reactions	**Gene name (*M . tuberculosis*)**	***K. radiotolerans* homologue(s)**	***S. coelicolor* A3(2) homologue(s)**	***T. fusca* homologue(s)**	***R. xylanophilus* homologue(s)**
Lipid linked precursor synthesis (for transfer from the inner membrane to outer surface)					
C35P-ribose synthase	Rv3806 (302 a.a.)	Krad_3882 (300 a.a.) Identities = 158/299 (52%) Expect = 1e-77	SCO4844 (322 a.a.) Identities = 150/292 (51%), EXpect = 2e-75	Tfu_2460 (294 a.a.) Identities = 123/297 (41%) Expect = 2e-53	Rxyl_1966 (301 a.a.) Identities = 95/279 (34%) Expect = 3e-39
C35P-ribose → C35P-arabinose epimerase	Rv3790 (461 a.a.)	Krad_4160 (481 a.a.) Identities = 257/457 (56%) Expect = 2e-147	SCO4842 (457 a.a.) Identities = 213/452 (47%) Expect = 2e-109	Tfu_2461 (452 a.a.) Identities = 201/455 (44%) Expect = 3e-100	Rxyl_3087 (752 a.a.) Identities = 50/187 (26%) Expect = 3e-09
	Rv3791 (254 a.a.)	Krad_3873 (257 a.a.) Identities = 135/255 (52%) Expect = 3e-70	SCO4841 (256 a.a.) Identities = 115/254 (45%) Expect = 2e-57	Tfu_2462 (255 a.a.) Identities = 115/246 (46%) Expect = 2e-54	Rxyl_2474 (263 a.a.) Identities = 63/216 (29%) Expect = 4e-10
Convert apolar PIMs to Polar PIMs or LM (extracytoplasmic)					
LpqW feeds PIM_4 to LM	Rv1166 (635 a.a.)	Krad_3863 (523 a.a.) Identities = 83/385 (21%) Expect = 1e-07	SCO5110 (771 a.a.) Identities = 78/281 (27%) Expect = 7e-22	Tfu_0818 (568 a.a.) Identities = 90/352 (25%) Expect = 2e-23	Rxyl_0872 (541 a.a.) Identities = 57/284 (20%) Expect = 2e-07
PIM_4→ PIM_5 (PIM branch rather than LAM)	Rv1159, PimE (431 a.a.)	Krad_0243 (417 a.a.) Identities = 119/376 (31%) Expect = 2e-33	SCO2335 (761 a.a.) Identities = 87/346 (25%) Expect = 3e-14	Absent	Rxyl_2872 (393 a.a.) Identities = 90/339 (26%) Expect = 6e-07

Reactions	**Gene name (*M. tuberculosis*)**	***K. radiotolerans* homologue(s)**	***S. coelicolor* A3(2) homologue(s)**	***T. fusca* homologue(s)**	***R. xylanophilus* homologue(s)**
Mannan extension	Rv2174, MptA (516 a.a.)	Krad_0171 (473 a.a.) Identities = 138/523 (26%) Expect = 4e-15	SCO5682 (377a.a.) Identities = 77/278 (27%) Expect = 5e-04	Absent	Rxyl_2872 (393 a.a.) Identities = 77/318 (24%) Expect = 6e-06
	Rv1459c (591 a.a.)	Krad_0171 (473 a.a.) Identities = 73/234 (31%) Expect = 5e-12	Absent	Absent	Absent
Convert apolar PIMs to Polar PIMs or LM (extracytoplasmic)					
Mannan branches	Rv2181(427 a.a.)	Krad_0243 (417 a.a.) Identities = 136/425 (32%) Expect = 2e-46	SCO2335 (761 a.a.) Identities = 82/276 (29%) Expect = 7e-21	Tfu_3096 (456 a.a.) Identities = 100/391 (25%) Expect = 4e-08	Rxyl_2872 (393 a.a.) Identities = 93/389 (23%) Expect = 5e-10
Arabinan addition					
LM-Arabinose$_1$→ LAM	Rv3793,EmbC (1094 a.a.)	Krad_0769 (590 a.a.) Identities = 89/331 (26%) Expect = 3e-07	Absent	Absent	Absent
Capping/ substituents					
Mannose capping	Rv1635c (556 a.a.)	Krad_3874,(523 a.a.) Identities = 126/421 (29%) Expect = 1e-26	Absent	Absent	Absent

8.5. Chemotaxonomic value of Macroamphiphiles distribution

8.5.1. Justification of the position of the genus *Rubrobacter* in the 16S rRNA phylogenetic tree on the basis of Macroamphiphiles distribution

The genus *Rubrobacter* has been recently placed in the deepest lineage of Actinobacteria on the basis of 16S rRNA phylogeny by Stackebrandt *et al.* (1997), as shown in Figure 8.1 and 8.2. This position has been confirmed by the study of Gao & Gupta (2005) which showed presence of two indel sequences (for Cox 1 and CTP synthetase) out of four indel signature sequences of Actinobacteria, suggesting the genus is distantly related to the phylum Actinobacteria.

The present studies has unable to identify any LTA or lipoglycan in *R. xylanophilus* (Chapter 4) and the LtaS homologues (Table 4.4) are therefore most likely to be members of the PFAM sulfatase family with alternative functions. The absence of the characteristic macroamphiphiles of the actinobacteria (notably lipoglycans, but also LTA) agrees with the present position of the genus *Rubrobacter* in the 16S rRNA based phylogenetic tree. However, the presence of homologues of the enzymes responsible for PI and apolar PIM biosynthesis (Table 4.6, 4.7, 8.3 and 8.4) is consistent with the classification of the genus within the Actinobacteria, since PIMs are very characteristic of actinobacteria (Kudo *et al.*, 1998, Kremer *et al.*, 2002, Haites *et al.*, 2005, Flaherty and Sutcliffe, 1999).

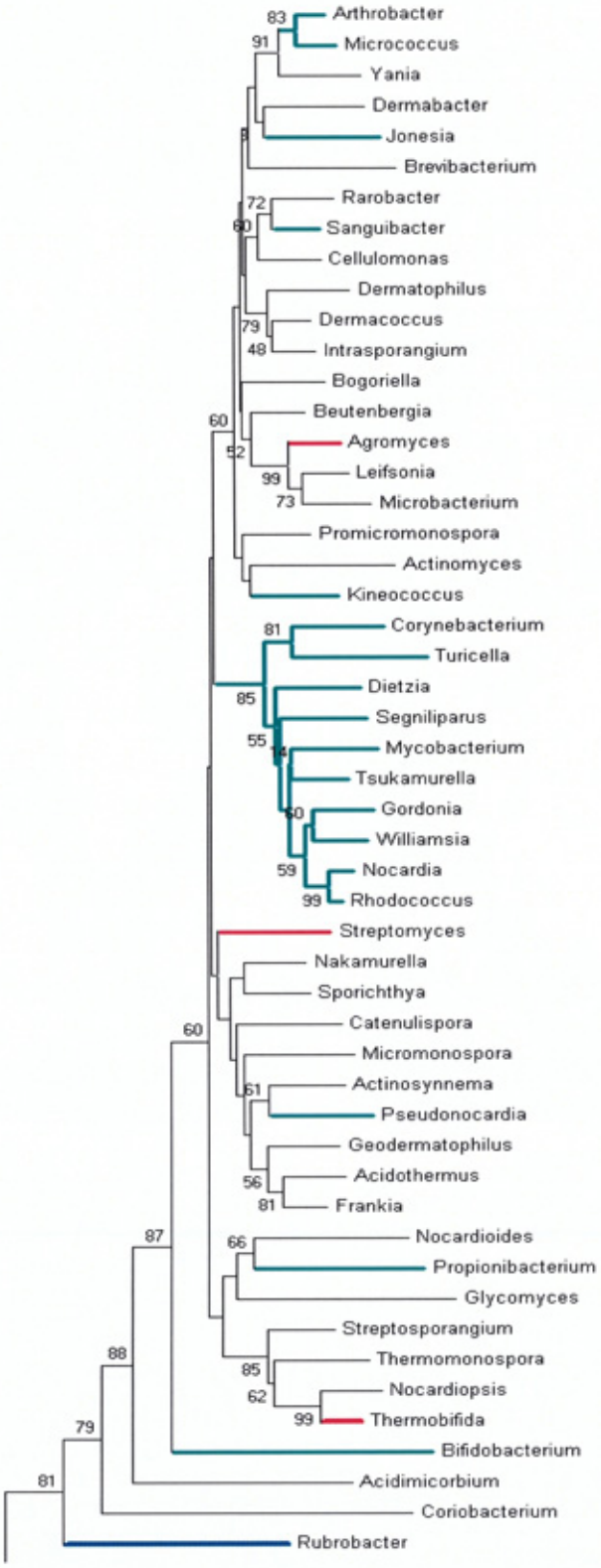

Figure 8.2. Phylogenetic tree of Actinobacteria based on 16S rRNA gene sequence analysis and showing the distribution of macroamphiphiles. Green lines indicate lineages known to produce lipoglycans (LM, LAM or LCHO), red lines represent lineages known to produce LTA. The blue line indicates the *Rubrobacter* lineage (apparent absence of macroamphiphiles) and black lines represent lineages that have yet to be investigated.

8.5.2. Relation between *T. fusca* and *S. coelicolor* based on macroamphiphile studies

Figure 8.1 and 8.2 shows the position of *T. fusca* and *S. coelicolor* A3(2), which demonstrates the quite wide apparent phylogenetic distance between these two genera based on 16S rRNA gene trees. However, morphological comparisons have showed both the organisms are quite closely related as both are filamentous capable of producing spores on aerial hyphae (Chater and Chandra, 2006). Moreover, the comparative genomics studies between *S. coelicolor* and *T. fusca* as discussed in Charter & Chandra (2006), showed comparatively high orthologue values between specific proteins of these organisms, indicating the two genera might be more closely related than suggested by the phylogenetic tree (Figures 8.1 & 8.2). This finding is supported by the present study on the basis of the macroamphiphiles detected, as both the organisms were identified as producing LTA (Chapter 3 & 7), though *S. coelicolor* has also been identified with a lipoglycan as a major macroamphiphile (Chapter 7). Both *T. fusca* and *Streptomyces* spp. have also been found to contain TA as the SCWP (Potekhina *et al.*, 2003, Naumova *et al.*, 1980a).

8.5.3. Macroamphiphiles distribution in Gram-positive bacteria

Figure 8.1 showed the distribution of LTA across the phylogenetic tree of Gram-positive bacteria. The Low G+C Gram-positive bacteria (phylum Firmicutes) show the presence of LTA as a suprageneric characteristic of this phylum (Sutcliffe, 1994; Fisher, 1994). In contrast the Mollicutes (genera Mycoplasma, Ureaplasma) has been shown to produce lipoglycans (Smith, 1984, Plackett, 1967). Consistent with this, recently it has been suggested to move Mollicutes from the phylum Firmicutes to the phylum "*Tenericutes*" and this will be formally published in the next edition of the *Bergey's Manual of Systematic Bacteriology* (http://www.bacterio.cict.fr/classifphyla.html# Tenericutes).

In high (G+C) Gram-positive bacteria (phylum Actinobacteria), most studies previously have been concentrated on the mycolata or their close relatives. All of these studies have identified PI-LM or LAM type lipoglycans (green lines, Fig. 8.1 and 8.2). The present study therefore tried to explore novel areas of the phylogenetic tree and has showed the presence of a LAM-like molecule in *K. radiotolerans* (which contain AG but lacks mycolic acids); that the members of the genus *Streptomyces* likely contain both LTA and lipoglycan; and that *T. fusca* contains LTA. Members of the genus *Agromyces* have also been shown to produce LTA (Gnilozub *et al.*, 1994b). These data extend the previous studies of Sutcliffe (1994) that suggest that the distribution of macroamphiphiles has chemotaxonomic value at the supragenic level.

8.6. Future Study

Future studies should focus on the *S. coelicolor* macroamphiphiles in order to solve the major assumed lipoglycan and LTA structures and also their synthesis pattern at different stage of the organsims life cycle. Moreover the detailed structure of the *K. radiotolerans* macroamphiphile needs to be resolved, as it is considered to be novel LAM-like structure. Furthermore, the 2D gel analysis should be utilized to resolve the isomer structure of the macroamphiphiles in a single organism, which may be important for further insight into the biosynthesis and functions of these macromolecules.

Perhaps most importantly, further analyses are needed to investigate the major lineages which still remain to be investigated as to the nature of their macroamphiphiles (as shown in Fig. 8.1 & 8.2 as black lines). Such studies may help in understanding the phylogeny of the Gram-positive bacteria, as the precise relationship of the *Firmicutes* and the *Actinobacteria* has been difficult to define (for an example, see Cavalier-Smith, 2006). Further studies of their structural diversity may also help understanding of the function of these molecules. In this regard, further understanding is needed of the relationship between the SCWPs and macroamphiphile types present within a particular cell envelope. Moreover further studies of thermophilic Gram-positive organisms' macroamphiphiles may also indicate whether LTA is essential in the cell membrane at higher temperatures.

8.7. Addendum

Result form this thesis has been accepted for publication as the following paper:

1) Rahman, O.; Pfitzenmaier, M.; Poster, O.; Morath, S.; Cummings, S.; Hartung, T.; Sutcliffe, I. (2009) Macroamphiphilic Components of Thermophilic Actinomycetes: Identification of Lipoteichoic Acid in Thermobifida fusca. Journal of Bacteriology. doi:10.11.28/JB.1105-08.

2) Rahman, O.; Cummings, S.; Sutcliffe, I. (2009) Phenotypic variation in Streptomyces sp. DSM40537, a lipotiechoic acid producing actinomycete. Journal of Applied Microbiology.

REFERENCES

ABACHIN, E., POYART, C., PELLEGRINI, E., MILOHANIC, E., FIEDLER, F., BERCHE, P. & TRIEU-CUOT, P. (2002) Formation of D-alanyl-lipoteichoic acid is required for adhesion and virulence of Listeria monocytogenes. *Molecular Microbiology,* 43, 1-14.

ALDERSON, G., GOODFELLOW, M. & MINNIKIN, D. E. (1985) Menaquinone Composition in the Classification of Streptomyces and Other Sporoactinomycetes. *Journal of General Microbiology,* 131, 1671-1679.

ALDERWICK, L. J., RADMACHER, E., SEIDEL, M., GANDE, R., HITCHEN, P. G., MORRIS, H. R., DELL, A., SAHM, H., EGGELING, L. & BESRA, G. S. (2005) Deletion of Cg-emb in corynebacterianeae leads to a novel truncated cell wall arabinogalactan, whereas inactivation of Cg-ubiA results in an Arabinan-deficient mutant with a cell wall galactan core. *Journal of Biological Chemistry,* 280, 32362-32371.

ALEXANDER, D. C., JONES, J. R. W., TAN, T., CHEN, J. M. & LIU, J. (2004) PimF, a mannosyltransferase of mycobacteria, is involved in the biosynthesis of phosphatidylinositol mannosides and lipoarabinomannan. *Journal of Biological Chemistry,* 279, 18824-18833.

ANDERSON, A. J., GREEN, R. S., STURMAN, A. J. & ARCHIBALD, A. R. (1978) Cell-Wall Assembly in Bacillus-Subtilis - Location of Wall Material Incorporated during Pulsed Release of Phosphate Limitation, Its Accessibility to Bacteriophages and Concanavalin a, and Its Susceptibility to Turnover. *Journal of Bacteriology,* 136, 886-899.

ANDERSON, A. S. & WELLINGTON, E. M. H. (2001) The taxonomy of Streptomyces and related genera. *International Journal of Systematic and Evolutionary Microbiology,* 51, 797-814.

ANDERSON, T. B., BRIAN, P. & CHAMPNESS, W. C. (2001) Genetic and transcriptional analysis of absA, an antibiotic gene cluster-linked two-component system that regulates multiple antibiotics in Streptomyces coelicolor. *Mol Microbiol,* 39, 553-66.

ARAKI, Y. & ITO, E. (1989) Linkage Units in Cell-Walls of Gram-Positive Bacteria. *Critical Reviews in Microbiology,* 17, 121-135.

ARCHIBAL, A., BADDILEY, J. & HECKELS, J. E. (1973) Molecular Arrangement of Teichoic Acid in Cell-Wall of Staphylococcus-Lactis. *Nature-New Biology,* 241, 29-31.

ARCHIBALD, A. R., BADDILEY, J. & BUTTON, D. (1968a) The glycerol teichoic acid of walls of Staphylococcus lactis I3. *Biochem J,* 110, 543-57.

ARCHIBALD, A. R., BADDILEY, J. & SHAUKAT, G. A. (1968b) The glycerol teichoic acid from walls of Staphylococcus epidermidis I2. *Biochem J,* 110, 583-8.

ARCHIBALD, A. R., HANCOCK, I. C. & HARWOOD, C. R. (1993) Cell wall structure, synthesis and turnover. IN SONENSHEIN, A. I.,

HOCH, J. A. & LOSICK, R. (Eds.) *Bacillus subtilis and other gram-positive bacteria: biochemistry, physiology, and molecular genetics.* Washington, D.C., American Society for Microbiology.

ATLAS, R. (1997) *Principles of microbiology,* New York, NY, WCB McGrill-Hill.

AZUMA, I., THOMAS, D. W., ADAM, A., GHUYSEN, J. M., BONALY, R., PETIT, J. F. & LEDERER, E. (1970) Occurrence of N-Glycolylmuramic Acid in Bacterial Cell Walls - a Preliminary Survey. *Biochimica Et Biophysica Acta,* 208, 444-&.

BACHMANN, S. L. & MCCARTHY, A. J. (1991) Purification and Cooperative Activity of Enzymes Constituting the Xylan-Degrading System of Thermomonospora-Fusca. *Applied and Environmental Microbiology,* 57, 2121-2130.

BADDILEY, J. (1970) Structure, Biosynthesis, and Function of Teichoic Acids. *Accounts of Chemical Research,* 3, 98-&.

BAGWELL, C. E., MILLIKEN, C. E., GHOSHROY, S. & BLOM, D. A. (2008) Intracellular Copper Accumulation Enhances the Growth of Kineococcus radiotolerans during Chronic Irradiation. *Appl Environ Microbiol.*

BARRY, C. E., LEE, R. E., MDLULI, K., SAMPSON, A. E., SCHROEDER, B. G., SLAYDEN, R. A. & YUAN, Y. (1998) Mycolic acids: Structure, biosynthesis and physiological functions. *Progress in Lipid Research,* 37, 143-179.

BAULARD, A. R., GURCHA, S. S., ENGOHANG-NDONG, J., GOUFFI, K., LOCHT, C. & BESRA, G. S. (2003) In vivo interaction between the polyprenol phosphate mannose synthase Ppm1 and the integral membrane protein Ppm2 from Mycobacterium smegmatis revealed by a bacterial two-hybrid system. *Journal of Biological Chemistry,* 278, 2242-2248.

BAYLIS, H. A. & BIBB, M. J. (1988) Organization of the Ribosomal-Rna Genes in Streptomyces-Coelicolor A3(2). *Molecular & General Genetics,* 211, 191-196.

BEACHEY, E. H. & SIMPSON, W. A. (1982) The Adherence of Group-a Streptococci to Oropharyngeal Cells - the Lipoteichoic Acid Adhesin and Fibronectin Receptor. *Infection,* 10, 107-111.

BEHR, T., FISCHER, W., PETERKATALINIC, J. & EGGE, H. (1992) The Structure of Pneumococcal Lipoteichoic Acid - Improved Preparation, Chemical and Mass-Spectrometric Studies. *European Journal of Biochemistry,* 207, 1063-1075.

BELANGER, A. E., BESRA, G. S., FORD, M. E., MIKUSOVA, K., BELISLE, J. T., BRENNAN, P. J. & INAMINE, J. M. (1996) The embAB genes of Mycobacterium avium encode an arabinosyl transferase involved in cell wall arabinan biosynthesis that is the target for the antimycobacterial drug ethambutol. *Proceedings of the National Academy of Sciences of the United States of America,* 93, 11919-11924.

BENTLEY, S. D., CHATER, K. F., CERDENO-TARRAGA, A. M., CHALLIS, G. L., THOMSON, N. R., JAMES, K. D., HARRIS, D. E., QUAIL, M. A., KIESER, H., HARPER, D., BATEMAN, A., BROWN, S., CHANDRA, G., CHEN, C. W., COLLINS, M., CRONIN, A.,

FRASER, A., GOBLE, A., HIDALGO, J., HORNSBY, T., HOWARTH, S., HUANG, C. H., KIESER, T., LARKE, L., MURPHY, L., OLIVER, K., O'NEIL, S., RABBINOWITSCH, E., RAJANDREAM, M. A., RUTHERFORD, K., RUTTER, S., SEEGER, K., SAUNDERS, D., SHARP, S., SQUARES, R., SQUARES, S., TAYLOR, K., WARREN, T., WIETZORREK, A., WOODWARD, J., BARRELL, B. G., PARKHILL, J. & HOPWOOD, D. A. (2002) Complete genome sequence of the model actinomycete Streptomyces coelicolor A3(2). *Nature,* 417, 141-147.

BERG, S., STARBUCK, J., TORRELLES, J. B., VISSA, V. D., CRICK, D. C., CHATTERJEE, D. & BRENNAN, P. J. (2005) Roles of conserved proline and glycosyltransferase motifs of embC in biosynthesis of lipoarabinomannan. *Journal of Biological Chemistry,* 280, 5651-5663.

BERGELSON, L. D., BATRAKOV, S. G. & PILIPENKO, T. (1970) A new glycolipid from Streptomyces. *Chem Phys Lipids,* 4, 181-90.

BERTRAM, R., SCHLICHT, M., MAHR, K., NOTHAFT, H., SAIER, M. H., TITGEMEYER, J. & TITGEMEYER, F. (2004) In silico and transcriptional analysis of carbohydrate uptake systems of *Streptomyces coelicolor* A3(2). *Journal of Bacteriology,* 186, 1362-1373.

BHAVSAR, A. P. & BROWN, E. D. (2006) Cell wall assembly in Bacillus subtilis: how spirals and spaces challenge paradigms. *Molecular Microbiology,* 60, 1077-1090.

BHAVSAR, A. P., ERDMAN, L. K., SCHERTZER, J. W. & BROWN, E. D. (2004) Teichoic acid is an essential polymer in Bacillus subtilis that is functionally distinct from teichuronic acid. *Journal of Bacteriology,* 186, 7865-7873.

BIERBAUM, G. & SAHL, H. G. (1987) Autolytic System of Staphylococcus-Simulans-22 - Influence of Cationic Peptides on Activity of N-Acetylmuramoyl-L-Alanine Amidase. *Journal of Bacteriology,* 169, 5452-5458.

BIERNE, H. & COSSART, P. (2007) Listeria monocytogenes surface proteins: from genome predictions to function. *Microbiology and Molecular Biology Reviews,* 71, 377-+.

BIRDSELL, D. C., DOYLE, R. J. & MORGENSTERN, M. (1975) Organization of Teichoic-Acid in Cell-Wall of Bacillus-Subtilis. *Journal of Bacteriology,* 121, 726-734.

BOTERO, L. M., BROWN, K. B., BRUMEFIELD, S., BURR, M., CASTENHOLZ, R. W., YOUNG, M. & MCDERMOTT, T. R. (2004) Thermobaculum terrenum gen. nov., sp nov.: a non-phototrophic gram-positive thermophile representing an environmental clone group related to the Chloroflexi (green non-sulfur bacteria) and Thermomicrobia. *Archives of Microbiology,* 181, 269-277.

BOUVET, A., GRIMONT, F. & GRIMONT, P. A. D. (1989) Streptococcus-Defectivus Sp-Nov and Streptococcus-Adjacens Sp-Nov, Nutritionally Variant Streptococci from Human Clinical Specimens. *International Journal of Systematic Bacteriology,* 39, 290-294.

BRENNAN, P. J. & CRICK, D. C. (2007) The cell-wall core of Mycobacterium tuberculosis in the context of drug discovery. *Current Topics in Medicinal Chemistry,* 7, 475-488.

BRIKEN, V., PORCELLI, S. A., BESRA, G. S. & KREMER, L. (2004) Mycobacterial lipoarabinomannan and related lipoglycans: from biogenesis to modulation of the immune response. *Molecular Microbiology,* 53, 391-403.

BROWN, A. D. (1976) Microbial water stress. *Bacteriol Rev,* 40, 803-46.

BUCKLAND, A. G. & WILTON, D. C. (2000) The antibacterial properties of secreted phospholipases A(2). *Biochimica Et Biophysica Acta-Molecular and Cell Biology of Lipids,* 1488, 71-82.

BURGUIERE, A., HITCHEN, P. G., DOVER, L. G., KREMER, L., RIDELL, M., ALEXANDER, D. C., LIU, J., MORRIS, H. R., MINNIKIN, D. E., DELL, A. & BESRA, G. S. (2005) LosA, a key glycosyltransferase involved in the biosynthesis of a novel family of glycosylated acyltrehalose lipooligosaccharides from Mycobacterium marinum. *Journal of Biological Chemistry,* 280, 42124-42133.

CALAMITA, H. G. & DOYLE, R. J. (2002) Regulation of autolysins in teichuronic acid-containing Bacillus subtilis cells. *Molecular Microbiology,* 44, 601-606.

CARD, G. L. & FINN, D. J. (1983) Products of Phospholipid-Metabolism in Bacillus-Stearothermophilus. *Journal of Bacteriology,* 154, 294-303.

CARRETO, L., MOORE, E., NOBRE, M. F., WAIT, R., RILEY, P. W., SHARP, R. J. & DACOSTA, M. S. (1996) *Rubrobacter xylanophilus* sp nov: A new thermophilic species isolated from a thermally polluted effluent. *International Journal of Systematic Bacteriology,* 46, 460-465.

CAVALIER-SMITH, T. (2006) The tiny enslaved genome of a rhizarian alga. *Proceedings of the National Academy of Sciences of the United States of America,* 103, 9379-9380.

CHATER, K. & LOSICK, R. (1997) Mycelial life style of *Streptomyces coelicolor* A3(2) and its relatives. IN SHAPIRO, J. A. & DWORKIN, M. (Eds.) *Bacteria as Multicellular Organisms.* New York, Oxford University press.

CHATER, K. F. (2001) Regulation of sporulation in Streptomyces coelicolor A3(2): a checkpoint multiplex? *Current Opinion in Microbiology,* 4, 667-673.

CHATER, K. F. & CHANDRA, G. (2006) The evolution of development in Streptomyces analysed by genome comparisons. *Fems Microbiology Reviews,* 30, 651-672.

CHATTERJEE, D., HUNTER, S. W., MCNEIL, M. & BRENNAN, P. J. (1992) Lipoarabinomannan. Multiglycosylated form of the mycobacteril mannosylphosphatidylinositols. *The Journal of Biological Chemistry,* 267, 6228-6233.

CHATTERJEE, D. & KHOO, K. H. (1998) Mycobacterial lipoarabinomannan: an extraordinary lipoheteroglycan with profound physiological effects. *Glycobiology,* 8, 113-120.

CHEN, M.-Y., WU, S.-H., LIN, G.-H., LU, C.-P., LIN, Y.-T., CHANG, W.-C. & TSAY, S.-S. (2004) *Rubrobacter taiwanensis* sp. nov., a novel thermophilic, radiation-resistant species isolated from hot springs. *International Journal of Systematic and Evolotionary Microbiology,* 54, 1849-1855.

CHEN, P. S., TORIBARA, T. Y. & WARNER, H. (1956) Microdetermination of phosphorus. *Analytical Biochemistry,* 16, 1-9.

CHIU, T. H., MORIMOTO, H. & BAKER, J. J. (1993) Biosynthesis and Characterization of Phosphatidylglycerophosphoglycerol, a Possible Intermediate in Lipoteichoic Acid Biosynthesis in Streptococcus-Sanguis. *Biochimica Et Biophysica Acta,* 1166, 222-228.

CHUN, J., KANG, S.-O., HAH, Y. C. & GOODFELLOW, M. (1996) Phylogeny of mycolic acid-containing actinomycetes. *Journal of Industrial Microbiology* 17, 205-213.

COLE, S. T., BROSCH, R., PARKHILL, J., GARNIER, T., CHURCHER, C., HARRIS, D., GORDON, S. V., EIGLMEIER, K., GAS, S., BARRY, C. E., TEKAIA, F., BADCOCK, K., BASHAM, D., BROWN, D., CHILLINGWORTH, T., CONNER, R., DAVIES, R., DEVLIN, K., FELTWELL, T., GENTLES, S., HAMLIN, N., HOLROYD, S., HORNSBY, T., JAGELS, K., KROGH, A., MCLEAN, J., MOULE, S., MURPHY, L., OLIVER, K., OSBORNE, J., QUAIL, M. A., RAJANDREAM, M. A., ROGERS, J., RUTTER, S., SEEGER, K., SKELTON, J., SQUARES, R., SQUARES, S., SULSTON, J. E., TAYLOR, K., WHITEHEAD, S. & BARRELL, B. G. (1998) Deciphering the biology of Mycobacterium tuberculosis from the complete genome sequence (vol 393, pg 537, 1998). *Nature,* 396, 190-198.

COLEY, J., TARELLI, E., ARCHIBALD, A. R. & BADDILEY, J. (1978) Linkage between Teichoic-Acid and Peptidoglycan in Bacterial-Cell Walls. *Febs Letters,* 88, 1-9.

COLLINS, L. V., KRISTIAN, S. A., WEIDENMAIER, C., FAIGLE, M., VAN KESSEL, K. P. M., VAN STRIJP, J. A. G., GOTZ, F., NEUMEISTER, B. & PESCHEL, A. (2002) Staphylococcus aureus strains lacking D-alanine modifications of teichoic acids are highly susceptible to human neutrophil killing and are virulence attenuated in mice. *Journal of Infectious Diseases,* 186, 214-219.

COLLINS, M. D., FAULKNER, M. & KEDDIE, R. M. (1984) Menaquinone Composition of Some Sporeforming Actinomycetes. *Systematic and Applied Microbiology,* 5, 20-29.

COLLINS, M. D. & JONES, D. (1981) Distribution of Isoprenoid Quinone Structural Types in Bacteria and Their Taxonomic Implications. *Microbiological Reviews,* 45, 316-354.

COLLMER, A., RIED, J. L. & MOUNT, M. S. (1988) Assay-Methods for Pectic Enzymes. *Methods in Enzymology,* 161, 329-335.

CRAWFORD, D. L. (1975) Cultural, Morphological, and Physiological Characteristics of Thermomonospora-Fusca (Strain 190th). *Canadian Journal of Microbiology,* 21, 1842-1848.

CRONAN, J. E. (2003) Bacterial membrane lipids: Where do we stand? *Annual Review of Microbiology,* 57, 203-224.

CROSS, T. & GOODFELLOW, M. (1973) Taxonomy and classification of the actinomycetes. IN SYKES, G. & SKINNER, F. A. (Eds.) *Actinomycelates: Characteristics and Practical Importance*
London, Academic Press.

D'ELIA, M. A., MILLAR, K. E., BEVERIDGE, T. J. & BROWN, E. D. (2006a) Wall teichoic acid polymers are dispensable for cell viability in Bacillus subtilis. *Journal of Bacteriology,* 188, 8313-8316.

D'ELIA, M. A., PEREIRA, M. P., CHUNG, Y. S., ZHAO, W. J., CHAU, A., KENNEY, T. J., SULAVIK, M. C., BLACK, T. A. & BROWN, E. D. (2006b) Lesions in teichoic acid biosynthesis in Staphylococcus aureus lead to a lethal gain of function in the otherwise dispensable pathway. *Journal of Bacteriology,* 188, 4183-4189.

DA COSTA, M. S., SANTOS, H. & GALINSKI, E. A. (1998) An overview of the role and diversity of compatible solutes in Bacteria and Archaea. *Adv Biochem Eng Biotechnol,* 61, 117-53.

DAFFE, M., MCNEIL, M. & BRENNAN, P. J. (1993) Major Structural Features of the Cell-Wall Arabinogalactans of Mycobacterium, Rhodococcus, and Nocardia Spp. *Carbohydrate Research,* 249, 383-398.

DALEN, A. & KRUIJFF, B. (2004) The role of lipids in membrane insertion and translocation of bacterial proteins. *Biochemica et Biophysica Acta,* 1694, 97-109.

DE SMET, K. A. L., WESTON, A., BROWN, I. N., YOUNG, D. B. & ROBERTSON, B. D. (2000) Three pathways for trehalose biosynthesis in mycobacteria. *Microbiology-Uk,* 146, 199-208.

DENCAMP, H. J. M. O., OOSTERHOF, A. & VEERKAMP, J. H. (1985) Phosphatidylglycerol as Biosynthetic Precursor for the Poly(Glycerol Phosphate) Backbone of Bifidobacterial Lipoteichoic Acid. *Biochemical Journal,* 228, 683-688.

DESVAUX, M. (2005) The cellulosome of Clostridium cellulolyticum. *Enzyme and Microbial Technology,* 37, 373-385.

DESVAUX, M., DUMAS, E., CHAFSEY, I. & HEBRAUD, M. (2006) Protein cell surface display in Gram-positive bacteria: from single protein to macromolecular protein structure. *Fems Microbiology Letters,* 256, 1-15.

DIAMOND, D. L., STROBEL, S., CHUN, S. Y. & RANDALL, L. L. (1995) Interaction of SecB with intermediates along the folding pathway of maltose-binding protein. *Protein Sci,* 4, 1118-23.

DIJKSTRA, A. J. & KECK, W. (1996) Peptidoglycan as a barrier to transenvelope transport. *Journal of Bacteriology,* 178, 5555-5562.

DINADAYALA, P., KAUR, D., BERG, S., AMIN, A. G., VISSA, V. D., CHATTERJEE, D., BRENNAN, P. J. & CRICK, D. C. (2006) Genetic basis for the synthesis of the immunomodulatory mannose caps of lipoarabinomannan in Mycobacterium tuberculosis. *Journal of Biological Chemistry,* 281, 20027-20035.

DMITRIEV, B., TOUKACH, F. & EHLERS, S. (2005) Towards a comprehensive view of the bacterial cell wall. *Trends in Microbiology,* 13, 569-574.

DMITRIEV, B. A., TOUKACH, F. V., SCHAPER, K. M., HOLST, O., RIETSCHEL, E. T. & EHLERS, S. (2003) Tertiary structure of bacterial murein: The scaffold model. *Journal of Bacteriology,* 185, 3458-3468.

DONADIO, S., SOSIO, M. & LANCINI, G. (2002) Impact of the first Streptomyces genome sequence on the discovery and production of bioactive substances. *Appl Microbiol Biotechnol,* 60, 377-80.

DORAN, K. S., ENGELSON, E. J., KHOSRAVI, A., MAISEY, H. C., FEDTKE, I., EQUILS, O., MICHELSEN, K. S., ARDITI, M., PESCHEL, A. & NIZET, V. (2005) Blood-brain barrier invasion by group B Streptococcus depends upon proper cell-surface anchoring of lipoteichoic acid. *Journal of Clinical Investigation,* 115, 2499-2507.

DOWHAN, W. (1997a) CDP-diacylglycerol synthase of microorganisms. *Biochimica Et Biophysica Acta-Lipids and Lipid Metabolism,* 1348, 157-165.

DOWHAN, W. (1997b) Molecular basis for membrane phospholipid diversity: Why are there so many lipids? *Annual Review of Biochemistry,* 66, 199-232.

DOYLE, R. J. & MARQUIS, R. E. (1994) Elastic, flexible peptidoglycan and bacterial cell wall properties. *Trends Microbiol,* 2, 57-60.

DOYLE, R. J., MCDANNEL, M. L., HELMAN, J. R. & STREIPS, U. N. (1975) Distribution of Teichoic-Acid in Cell-Wall of Bacillus-Subtilis. *Journal of Bacteriology,* 122, 152-158.

DOYLE, R. J., MCDANNEL, M. L., STREIPS, U. N., BIRDSELL, D. C. & YOUNG, F. E. (1974) Polyelectrolyte Nature of Bacterial Teichoic-Acids. *Journal of Bacteriology,* 118, 606-615.

ELBEIN, A. D., PAN, Y. T., PASTUSZAK, I. & CARROLL, D. (2003) New insights on trehalose: a multifunctional molecule. *Glycobiology,* 13, 17r-27r.

ELLIOT, M. A. & TALBOT, N. J. (2004) Building filaments in the air: aerial morphogenesis in bacteria and fungi. *Current Opinion in Microbiology,* 7, 594-601.

ELLWOOD, D. C. & TEMPEST, D. W. (1969) Control of teichoic acid and teichuronic acid biosyntheses in chemostat cultures of Bacillus subtilis var. niger. *Biochem J,* 111, 1-5.

EMBLEY, M. T., SMIDA, J. & STACKEBRANDT, E. (1988) The Phylogeny of Mycolate-Less Wall Chemotype-Iv Actinomycetes and Description of Pseudonocardiaceae Fam-Nov. *Systematic and Applied Microbiology,* 11, 44-52.

EMPADINHAS, N., ALBUQUERQUE, L., COSTA, J. & DA COSTA, M. S. (2005) A highly divergent MpgS accounts for the synthesis of mannosylglycerate in the gram-positive bacterium Rubrobacter xylanophilus. *Febs Journal,* 272, 84-85.

EMPADINHAS, N. & DA COSTA, M. S. (2006) Diversity and biosynthesis of compatible solutes in hyper/thermophiles. *International Microbiology,* 9, 199-206.

EMPADINHAS, N., MARUGG, J. D., BORGES, N., SANTOS, H. & DA COSTA, M. S. (2001) Pathway for the synthesis of mannosylglycerate in the hyperthermophilic archaeon Pyrococcus horikoshii - Biochemical and genetic characterization of key enzymes. *Journal of Biological Chemistry,* 276, 43580-43588.

EMPADINHAS, N., MENDES, V., SIMOES, C., SANTOS, M. S., MINGOTE, A., LAMOSA, P., SANTOS, H. & DA COSTA, M. S.

(2007) Organic solutes in Rubrobacter xylanophilus: the first example of di-myo-inositol-phosphate in a thermophile. *Extremophiles,* 11, 667-673.

ENDL, J., SEIDL, H. P., FIEDLER, F. & SCHLEIFER, K. H. (1983) Chemical-Composition and Structure of Cell-Wall Teichoic-Acids of Staphylococci. *Archives of Microbiology,* 135, 215-223.

ENSIGN, J. C. (1978) Formation, Properties, and Germination of Actinomycete Spores. *Annual Review of Microbiology,* 32, 185-219.

ESCUYER, V. E., LETY, M. A., TORRELLES, J. B., KHOO, K. H., TANG, J. B., RITHNER, C. D., FREHEL, C., MCNEIL, M. R., BRENNAN, P. J. & CHATTERJEE, D. (2001) The role of the embA and embB gene products in the biosynthesis of the terminal hexaarabinofuranosyl motif of Mycobacterium smegmatis arabinogalactan. *J Biol Chem,* 276, 48854-62.

EUZÉBY, J. P. (2008) LPSN :List of Prokaryotic names with Standing in Nomenclature

FEDTKE, I., MADER, D., KOHLER, T., MOLL, H., NICHOLSON, G., BISWAS, R., HENSELER, K., GOTZ, F., ZAHRINGER, U. & PESCHELL, A. (2007) A Staphylococcus aureus ypfP mutant with strongly reduced lipoteichoic acid (LTA) content: LTA governs bacterial surface properties and autolysin activity. *Molecular Microbiology,* 65, 1078-1091.

FERREIRA, A. C., NOBRE, M. F., MOORE, E., RAINEY, F. A., BATTISTA, J. R. & DA COSTA, M. S. (1999) Characterization and radiation resistance of new isolates of Rubrobacter radiotolerans and Rubrobacter xylanophilus. *Extremophiles,* 3, 235-238.

FISCHER, W. (1988) Physiology of Lipoteichoic Acids in Bacteria. *Advances in Microbial Physiology,* 29, 233-302.

FISCHER, W. (1990) Bacterial phsphoglycolipids and lipoteichoic acids. IN KATES, M. (Ed.) *Handbook of lipid research.* New York, Plenum Press.

FISCHER, W. (1994a) Lipoteichoic Acid and Lipids in the Membrane of Staphylococcus-Aureus. *Medical Microbiology and Immunology,* 183, 61-76.

FISCHER, W. (1994b) Lipoteichoic acid and lipoglycans. IN GHUYSEN, J.-M. & HAKENBECK, R. (Eds.) *Bacterial Cell Wall.* Elsevier Science B.V.

FISCHER, W., LAINE, R. A. & NAKANO, M. (1978a) Relationship between Glycero-Phospho-Glycolipids and Lipoteichoic Acids in Gram-Positive Bacteria .2. Structures of Glycero-Phospho-Glycolipids. *Biochimica Et Biophysica Acta,* 528, 298-308.

FISCHER, W., NAKANO, M., LAINE, R. A. & BOHRER, W. (1978b) Relationship between Glycero-Phospho-Glycolipids and Lipoteichoic Acids in Gram-Positive Bacteria .1. Occurrence of Phospho-Glycolipids. *Biochimica Et Biophysica Acta,* 528, 288-297.

FISCHER, W. & ROSEL, P. (1980) The Alanine Ester Substitution of Lipoteichoic Acid (Lta) in Staphylococcus-Aureus. *Febs Letters,* 119, 224-226.

FISCHER, W., ROSEL, P. & KOCH, H. U. (1981) Effect of Alanine Ester Substitution and Other Structural Features of Lipoteichoic Acids on Their Inhibitory Activity against Autolysins of Staphylococcus-Aureus. *Journal of Bacteriology,* 146, 467-475.

FLAHERTY, C., MINNIKIN, D. E. & SUTCLIFFE, I. C. (1996) A chemotaxonomic study of the lipoglycans of Rhodococcus rhodnii N445 (NCIMB 11279). *Zentralblatt Fur Bakteriologie-International Journal of Medical Microbiology Virology Parasitology and Infectious Diseases,* 285, 11-19.

FLAHERTY, C. & SUTCLIFFE, I. C. (1999) Identification of a lipoarabinomannan-like lipoglycan in Gordonia rubropertincta. *Syst Appl Microbiol,* 22, 530-3.

FLARDH, K. (2003) Growth polarity and cell division in Streptomyces. *Current Opinion in Microbiology,* 6, 564-571.

FOSTER, S. J. & POPHAM, D. L. (2002) Structure and synthesis of cell wall, spore cortex, teichoic acids, S-layers, and capsules. IN SONENSHEIN, A. L., HOCH, J. A. & LOSICK, R. (Eds.) *Bacillus subtilis and its closest relatives: from genes to cells.* Washington, D.C., American Society of Microbiology.

FOX, G. E., STACKEBRANDT, E., HESPELL, R. B., GIBSON, J., MANILOFF, J., DYER, T. A., WOLFE, R. S., BALCH, W. E., TANNER, R. S., MAGRUM, L. J., ZABLEN, L. B., BLAKEMORE, R., GUPTA, R., BONEN, L., LEWIS, B. J., STAHL, D. A., LUEHRSEN, K. R., CHEN, K. N. & WOESE, C. R. (1980) The Phylogeny of Prokaryotes. *Science,* 209, 457-463.

FOX, J. D. & ROBYT, J. F. (1991) Miniaturization of 3 Carbohydrate Analyses Using a Microsample Plate Reader. *Analytical Biochemistry,* 195, 93-96.

FREYMOND, P. P., LAZAREVIC, V., SOLDO, B. & KARAMATA, D. (2006) Poly(glucosyl-N-acetylgalactosamine 1-phosphate), a wall teichoic acid of Bacillus subtilis 168: its biosynthetic pathway and mode of attachment to peptidoglycan. *Microbiology-Sgm,* 152, 1709-1718.

FURNEAUX, R. H., LANDERSJO, C. L., MCCULLOUGH, J. L. & SEVERN, W. B. (2005) A novel phosphatidylinositol manno-oligosaccharide (dPIM-8) from Gordonia sputi. *Carbohydrate Research,* 340, 1618-1624.

GAO, B., PARAMANATHAN, R. & GUPTA, R. S. (2006) Signature proteins that are distinctive characteristics of Actinobacteria and their subgroups. *Antonie Van Leeuwenhoek International Journal of General and Molecular Microbiology,* 90, 69-91.

GAO, B. L. & GUPTA, R. S. (2005) Conserved indels in protein sequences that are characteristic of the phylum Actinobacteria. *International Journal of Systematic and Evolutionary Microbiology,* 55, 2401-2412.

GARRITY, G. M. (Ed.) (2001) *Bergey's Mannual of Systematic Bacteriology* Berlin Heidelberg, Springer.

GARRITY, G. M. & SEARLES, D. M. (1998) Direct sequence submission to the NCBI GenBank database.

GARTON, N. J., GILLERON, M., BRANDO, T., DAN, H. H., GIGUERE, S., PUZO, G., PRESCOTT, J. F. & SUTCLIFFE, I. C. (2002) A novel lipoarabinomannan from the equine pathogen Rhodococcus equi - Structure and effect on marcophage cytokine production. *Journal of Biological Chemistry,* 277, 31722-31733.

GARTON, N. J. & SUTCLIFFE, I. C. (2006) Identification of a lipoarabinomannan-like lipoglycan in the actinomycete Gordonia bronchialis. *Archives of Microbiology,* 184, 425-427.

GEHRING, A. M., NODWELL, J. R., BEVERLEY, S. M. & LOSICK, R. (2000) Genomewide insertional mutagenesis in Streptomyces coelicolor reveals additional genes involved in morphological differentiation. *Proceedings of the National Academy of Sciences of the United States of America,* 97, 9642-9647.

GIBSON, K. J. C., EGGELING, L., MAUGHAN, W. N., KRUMBACH, K., GURCHA, S. S., NIGOU, J., PUZO, G., SAHM, H. & BESRA, G. S. (2003a) Disruption of Cg-Ppm1, a polyprenyl monophosphomannose synthase, and the generation of lipoglycan-less mutants in Corynebacterium glutamicum. *Journal of Biological Chemistry,* 278, 40842-40850.

GIBSON, K. J. C., GILLERON, M., CONSTANT, P., BRANDO, T., PUZO, G., BESRA, G. S. & NIGOU, J. (2004) Tsukamurella paurometabola lipoglycan, a new lipoarabinomannan variant with pro-inflammatory activity. *Journal of Biological Chemistry,* 279, 22973-22982.

GIBSON, K. J. C., GILLERON, M., CONSTANT, P., PUZO, G., NIGOU, J. & BESRA, G. S. (2003b) Identification of a novel mannose-capped lipoarabinomannan from Amycolatopsis sulphurea. *Biochemical Journal,* 372, 821-829.

GIBSON, K. J. C., GILLERON, M., CONSTANT, P., PUZO, G., NIGOU, J. & BESRA, G. S. (2003c) Structural and functional features of Rhodococcus ruber lipoarabinomannan. *Microbiology-Sgm,* 149, 1437-1445.

GIBSON, K. J. C., GILLERON, M., CONSTANT, P., SICHI, B., PUZO, G., BESRA, G. S. & NIGOU, J. (2005) A lipomannan variant with strong TLR-2-dependent pro-inflammatory activity in Saccharothrix aerocolonigenes. *Journal of Biological Chemistry,* 280, 28347-28356.

GILLERON, M., GARTON, N. J., NIGOU, J., BRADDO, T., PUZO, G. & SUTCLIFFE, I. C. (2005) Characterisation of a truncated lipoarabinomannan from the actinomycete Turicella otitidis. *Journal of Bacteriology,* 187, 854-861.

GILLERON, M., QUESNIAUX, V. F. J. & PUZO, G. (2003) Acylation state of the phosphatidylinositol hexamannosides from Mycobacterium bovis bacillus Calmette Guerin and Mycobacterium tuberculosis H37Rv and its implication in toll-like receptor response. *Journal of Biological Chemistry,* 278, 29880-29889.

GILLERON, M., RONET, C., MEMPEL, M., MONSARRAT, B., GACHELIN, G. & PUZO, G. (2001) Acylation state of the phosphatidylinositol mannosides from Mycobacterium bovis bacillus Calmette Guerin and ability to induce granuloma and recruit natural killer T cells. *Journal of Biological Chemistry,* 276, 34896-34904.

GINSBERG, C., ZHANG, Y. H., YUAN, Y. Q. & WALKER, S. (2006) In vitro reconstitution of two essential steps in wall teichoic acid biosynthesis. *Acs Chemical Biology,* 1, 25-28.

GLASER, P., KUNST, F., ARNAUD, M., COUDART, M. P., GONZALES, W., HULLO, M. F., IONESCU, M., LUBOCHINSKY, B., MARCELINO, L., MOSZER, I., PRESECAN, E., SANTANA, M., SCHNEIDER, E., SCHWEIZER, J., VERTES, A., RAPOPORT, G. & DANCHIN, A. (1993) Bacillus-Subtilis Genome Project - Cloning and Sequencing of the 97kb Region from 325-Degrees to 333 Degrees. *Molecular Microbiology,* 10, 371-384.

GNILOZUB, V. A., STRESHINSKAIA, G. M., EVTUSHENKO, L. I., NAUMOVA, I. B. & SHASHKOV, A. S. (1994a) [1,5-poly(ribitol phosphate) with tetrasaccharide substituents in the cell wall of Agromyces fucosus ssp. Hippuratus]. *Biokhimiia,* 59, 1892-9.

GNILOZUB, V. A., STRESHINSKAYA, G. M., EVTUSHENKO, L. I., SHASHKOV, A. S. & NAUMOVA, I. B. (1994b) Lipoteichoic Acids of Agromyces Species. *Microbiology,* 63, 275-279.

GOLDFINE, H. (1984) Bacterial membranes and lipid packing theory. *J Lipid Res,* 25, 1501-7.

GRANT, W. D. (1979) Cell-Wall Teichoic-Acid as a Reserve Phosphate Source in Bacillus-Subtilis. *Journal of Bacteriology,* 137, 35-43.

GREINERMAI, E., KROPPENSTEDT, R. M., KORNWENDISCH, F. & KUTZNER, H. J. (1987) Morphological and Biochemical-Characterization and Emended Descriptions of Thermophilic Actinomycetes Species. *Systematic and Applied Microbiology,* 9, 97-109.

GRIFFIN, D. W., KELLOGG, C. A., GARRISON, G. A., LISLE, J. T., BORDEN, T. & SHINN, E. A. (2003) Direct sequence submission to the NCBI GenBank database.

GRUNDLING, A. & SCHNEEWIND, O. (2007a) Genes required for glycolipid synthesis and lipoteichoic acid anchoring in Staphylococcus aureus. *Journal of Bacteriology,* 189, 2521-2530.

GRUNDLING, A. & SCHNEEWIND, O. (2007b) Synthesis of glycerol phosphate lipoteichoic acid in Staphylococcus aureus. *Proceedings of the National Academy of Sciences of the United States of America,* 104, 8478-8483.

GUERARDEL, Y., MAES, E., BRIKEN, V., CHIRAT, F., LEROY, Y., LOCHT, C., STRECKER, G. & KREMER, L. (2003a) Lipomannan and lipoarabinomannan from a clinical isolate of Mycobacterium kansasii - Novel structural features and apoptosis-inducing properties. *Journal of Biological Chemistry,* 278, 36637-36651.

GUERARDEL, Y., MAES, E., BRIKEN, V., CHIRAT, F., LEROY, Y., LOCHT, C., STRECKER, G. & KREMER, L. (2003b) Lipomannan and lipoarabinomannan from a clinical isolate of Mycobacterium kansasii: novel structural features and apoptosis-inducing properties. *J Biol Chem,* 278, 36637-51.

GUNTHER, G. R., WANG, J. L., YAHARA, I., CUNNINGHAM, B. A. & EDELMAN, G. M. (1973) Concanavalin A derivatives with altered biological activities. *Proc Natl Acad Sci U S A,* 70, 1012-6.

GUPTA, R. S. (1998) Protein phylogenies and signature sequences: A reappraisal of evolutionary relationships among archaebacteria, eubacteria, and eukaryotes. *Microbiology and Molecular Biology Reviews,* 62, 1435-+.

GUTBERLET, T., FRANK, J., BRADACZEK, H. & FISCHER, W. (1997) Effect of lipoteichoic acid on thermotropic membrane properties. *Journal of Bacteriology,* 179, 2879-2883.

HAGERDAL, B. G., FERCHAK, J. D. & PYE, E. K. (1978) Cellulolytic Enzyme System of Thermoactinomyces sp. Grown on Microcrystalline Cellulose. *Appl Environ Microbiol,* 36, 606-612.

HAITES, R. E., MORITA, Y. S., MCCONVILLE, M. J. & JACOBE, H. B. (2005) Function of phosphatidylinositol in mycobacteria. *Journal of Biological Chemistry,* 280, 10981-10987.

HAMADA, S., TAI, S. & SLADE, H. D. (1976) Selective Adsorption of Heterophile Polyglycerophosphate Antigen from Antigen Extracts of Streptococcus-Mutans and Other Gram-Positive Bacteria. *Infection and Immunity,* 14, 903-910.

HANCOCK, I. C. (1997) Bacterial cell surface carbohydrates: Structure and assembly. *Biochemical Society Transactions,* 25, 183-187.

HANCOCK, I. C. & BADDILEY, J. (1972) Biosynthesis of Wall Teichoic Acid in Bacillus-Licheniformis. *Biochemical Journal,* 127, 27-&.

HATANO, K., TAMURA, T. & NISHII, T. (1994) Taxonomic status of *Streptomyces coelicolor* A3(2) and *Streptomyces lividans* 66. *Actinomycetologica,* 8, 47-50.

HAYHURST, E. J., KAILAS, L., HOBBS, J. K. & FOSTER, S. J. (2008) 'Cell wall peptidoglycan architecture in Bacillus subtilis'. *Poceeding of the National Academy of Sciences of the United States of America,* 105(38), 14603-14608.

HEATON, M. P. & NEUHAUS, F. C. (1994) Role of the D-Alanyl Carrier Protein in the Biosynthesis of D-Alanyl-Lipoteichoic Acid. *Journal of Bacteriology,* 176, 681-690.

HECKELS, J. E., LAMBERT, P. A. & BADDILEY, J. (1977) Binding of Magnesium-Ions to Cell-Walls of Bacillus-Subtilis-W23 Containing Teichoic-Acid or Teichuronic Acid. *Biochemical Journal,* 162, 359-365.

HEIJENOORT, J.-V. (2001a) Formation of the glycan chain inthe synthesis of bacterial peptidoglycan. *Glycobiology,* 11, 25R-36R.

HEIJENOORT, J.-V. (2001b) Recent advances in the formation of the bacterial peptidoglycan monomer unit. *Nat. Prod. Rep.,* 18, 503-519.

HENNEKE, P., MORATH, S., UEMATSU, S., WEICHERT, S., PFITZENMAIER, M., TAKEUCHI, O., MULLER, A., POYART, C., AKIRA, S., BERNER, R., TETI, G., GEYER, A., HARTUNG, T., TRIEU-CUOT, P., KASPER, D. L. & GOLENBOCK, D. T. (2005) Role of lipoteichoic acid in the phagocyte response to group B Streptococcus. *Journal of Immunology,* 174, 6449-6455.

HENSSEN, A. (1957) Beitrage zur Morphlogie and Systematik der thermophilen Actinomyceten. *Arch Midorbiol,* 26, 373-414.

HESKETH, A. R., CHANDRA, G., SHAW, A. D., ROWLAND, J. J., KELL, D. B., BIBB, M. J. & CHATER, K. F. (2002) Primary and secondary

metabolism, and post-translational protein modifications, as portrayed by proteomic analysis of Streptomyces coelicolor. *Molecular Microbiology,* 46, 917-932.

HOELZLE, I. & STREETER, J. G. (1990) Increased Accumulation of Trehalose in Rhizobia Cultured under 1-Percent Oxygen. *Applied and Environmental Microbiology,* 56, 3213-3215.

HOISCHEN, C., GURA, K., LUGE, C. & GUMPERT, J. (1997) Lipid and fatty acid composition of cytoplasmic membranes from Streptomyces hygroscopicus and its stable protoplast-type L form. *Journal of Bacteriology,* 179, 3430-3436.

HOLMES, A. J., BOWYER, J., HOLLEY, M. P., O'DONOGHUE, M., MONTGOMERY, M. & GILLINGS, M. R. (2000) Diverse, yet-to-be-cultured members of the Rubrobacter subdivision of the Actinobacteria are widespread in Australian arid soils. *Fems Microbiology Ecology,* 33, 111-120.

HOLTJE, J. V. & TUOMANEN, E. I. (1991) The Murein Hydrolases of Escherichia-Coli - Properties, Functions and Impact on the Course of Infections Invivo. *Journal of General Microbiology,* 137, 441-454.

HOPWOOD, D. A. (1999) Forty years of genetics with Streptomyces: from in vivo through in vitro to in silico. *Microbiology-Sgm,* 145, 2183-2202.

HOPWOOD, D. A., CHATER, K. F. & BIBB, M. J. (1995) Genetics of antibiotic production in Streptomyces coelicolor A3(2), a model streptomycete. *Biotechnology,* 28, 65-102.

HUANG, H. R., SCHERMAN, M. S., D'HAEZE, W., VEREECKE, D., HOLSTERS, M., CRICK, D. C. & MCNEIL, M. R. (2005) Identification and active expression of the Mycobacterium tuberculosis gene encoding 5-phospho-alpha-D-ribose-1-diphosphate: Decaprenyl-phosphate 5-phosphoribosyltransferase, the first enzyme committed to decaprenylphosphoryl-D-arabinose synthesis. *Journal of Biological Chemistry,* 280, 24539-24543.

HUANG, J., LIH, C. J., PAN, K. H. & COHEN, S. N. (2001) Global analysis of growth phase responsive gene expression and regulation of antibiotic biosynthetic pathways in Streptomyces coelicolor using DNA microarrays. *Genes Dev,* 15, 3183-92.

HUGENHOLTZ, P. & STACKEBRANDT, E. (2004) Reclassification of Sphaerobacter thermophilus from the subclass Sphaerobacteridae in the phylum Actinobacteria to the class Thermomicrobia (emended description) in the phylum Chloroflexi (emended description). *Int J Syst Evol Microbiol,* 54, 2049-51.

HUNTER, S. W., GAYLORD, H. & BRENNAN, P. J. (1986) Structure and Antigenicity of the Phosphorylated Lipopolysaccharide Antigens from the Leprosy and Tubercle-Bacilli. *Journal of Biological Chemistry,* 261, 2345-2351.

IBA, K., GIBSON, S., NISHIUCHI, T., FUSE, T., NISHIMURA, M., ARONDEL, V., HUGLY, S. & SOMERVILLE, C. (1993) A gene encoding a chloroplast omega-3 fatty acid desaturase complements alterations in fatty acid desaturation and chloroplast copy number of the fad7 mutant of Arabidopsis thaliana. *J Biol Chem,* 268, 24099-105.

IMPERI, F., CANEVA, G., CANCELLIERI, L., RICCI, M. A., SODO, A. & VISCA, P. (2007) The bacterial aetiology of rosy discoloration of ancient wall paintings. *Environmental Microbiology,* 9, 2894-2902.

ITOH, T., KUDO, T., PARENTI, F. & SEINO, A. (1989) Amended Description of the Genus Kineosporia, Based on Chemotaxonomic and Morphological-Studies. *International Journal of Systematic Bacteriology,* 39, 168-173.

IWASAKI, H., ARAKI, Y., ITO, E., NAGAOKA, M. & YOKOKURA, T. (1990) Structure of Macroamphiphiles from Several Bifidobacterium Strains. *Journal of Bacteriology,* 172, 845-852.

IWASAKI, H., ARAKI, Y., KAYA, S. & ITO, E. (1989) Structural Studies on the Amino-Acid-Linked Teichuronic Acid of Bacillus-Subtilis Ahu-1219 Cell-Walls. *European Journal of Biochemistry,* 178, 643-648.

IWASAKI, H., SHIMADA, A. & ITO, E. (1986) Comparative-Studies of Lipoteichoic Acids from Several Bacillus Strains. *Journal of Bacteriology,* 167, 508-516.

JACKSON, M., CRICK, D. C. & BRENNAN, P. J. (2000) Phosphatidylinositol is an essential phospholipid of mycobacteria. *Journal of Biological Chemistry,* 275, 30092-30099.

JOE, M., SUN, D., TAHA, H., COMPLETO, G. C., CROUDACE, J. E., LAMMAS, D. A., BESRA, G. S. & LOWARY, T. L. (2006) The 5-deoxy-5-methylthio-xylofuranose residue in mycobacterial lipoarabinomannan. Absolute stereochemistry, linkage position, conformation, and immunomodulatory activity. *Journal of the American Chemical Society,* 128, 5059-5072.

JONQUIERES, R., BIERNE, H., FIEDLER, F., GOUNON, P. & COSSART, P. (1999) Interaction between the protein InlB of Listeria monocytogenes and lipoteichoic acid: a novel mechanism of protein association at the surface of gram-positive bacteria. *Mol Microbiol,* 34, 902-14.

JONSON, A. B., NORMARK, S. & RHEN, M. (2005) Fimbriae, pili, flagella and bacterial virulence. *Contrib Microbiol,* 12, 67-89.

JORASCH, P., WARNECKE, D. C., LINDNER, B., ZAHRINGER, U. & HEINZ, E. (2000) Novel processive and nonprocessive glycosyltransferases from Staphylococcus aureus and Arabidopsis thaliana synthesize glycoglycerolipids, glycophospholipids, glycosphingolipids and glycosylsterols. *European Journal of Biochemistry,* 267, 3770-3783.

JORASCH, P., WOLTER, F. P., ZAHRINGER, U. & HEINZ, E. (1998) A UDP glucosyltransferase from Bacillus subtilis successively transfers up to four glucose residues to 1,2-diacylglycerol: expression of ypfP in Escherichia coli and structural analysis of its reaction products. *Molecular Microbiology,* 29, 419-430.

KARAGOUNI, A. D., VIONIS, A. P., BAKER, P. W. & WELLINGTON, E. M. H. (1993) The effect of soil moisture content on spore germination, mycelium development and survival of a seeded streptomycete in soil. *Micorbiol. Releases,* 2, 47-51.

KAUR, D., BERG, S., DINADAYALA, P., GICQUEL, B., CHATTERJEE, D., MCNEIL, M. R., VISSA, V. D., CRICK, D. C., JACKSON, M. &

BRENNAN, P. J. (2006) Biosynthesis of mycobacterial lipoarabinomannan: Role of a branching mannosyltransferase. *Proceedings of the National Academy of Sciences of the United States of America,* 103, 13664-13669.

KAUR, D., LOWARY, T. L., VISSA, V. D., CRICK, D. C. & BRENNAN, P. J. (2002) Characterization of the epitope of anti-lipoarabinomannan antibodies as the terminal hexaarabinofuranosyl motif of mycobacterial arabinans. *Microbiology,* 148, 3049-57.

KAWAMOTO, S. & OCHI, K. (1998) Comparative ribosomal protein (L11 and L30) sequence analyses of several Streptomyces spp. commonly used in genetic studies. *International Journal of Systematic Bacteriology,* 48, 597-600.

KAWASE, T., YOKOKAWA, S., SAITO, A., FUJII, T., NIKAIDOU, N., MIYASHITA, K. & WATANABE, T. (2006) Comparison of enzymatic and antifungal properties between family 18 and 19 chitinases from S-coelicolor A3(2). *Bioscience Biotechnology and Biochemistry,* 70, 988-998.

KELEMEN, G. H. & BUTTNER, M. J. (1998) Initiation of aerial mycelium formation in Streptomyces. *Current Opinion in Microbiology,* 1, 656-662.

KEMPER, M. A., URRUTIA, M. M., BEVERIDGE, T. J., KOCH, A. L. & DOYLE, R. J. (1993) Proton Motive Force May Regulate Cell Wall-Associated Enzymes of Bacillus-Subtilis. *Journal of Bacteriology,* 175, 5690-5696.

KHOO, K. H., DELL, A., MORRIS, H. R., BRENNAN, P. J. & CHATTERJEE, D. (1995) Structural Definition of Acylated Phosphatidylinositol Mannosides from Mycobacterium-Tuberculosis - Definition of a Common Anchor for Lipomannan and Lipoarabinomannan. *Glycobiology,* 5, 117-127.

KIESER, T., CHATER, K. F., BIBB, M. J., BUTTNER, M. J. & HOPWOOD, D. A. (Eds.) (2000) *Practical Streptomyces genetics,* Norwich, England, Crowes.

KILBANE, J. J., DARAM, A., ABBASIAN, J. & KAYSER, K. J. (2002) Isolation and characterization of Sphingomonas sp GTIN11 capable of carbazole metabolism in petroleum. *Biochemical and Biophysical Research Communications,* 297, 242-248.

KIRIUKHIN, M. Y., DEBABOV, D. V., SHINABARGER, D. L. & NEUHAUS, F. C. (2001) Biosynthesis of the glycolipid anchor in lipoteichoic acid of Staphylococcus aureus RN4220: Role of YpfP, the diglucosyldiacylglycerol synthase. *Journal of Bacteriology,* 183, 3506-3514.

KIRIUKHIN, M. Y. & NEUHAUS, F. C. (2001) D-alanylation of lipoteichoic acid: Role of the D-alanyl carrier protein in acylation. *Journal of Bacteriology,* 183, 2051-2058.

KLEINIG, H., REICHENBACH, H. & ACHENBACH, H. (1970) Carotenoid pigments of Stigmatella aurantiaca (Myxobacterales). II. Acylated carotenoid glucosides. *Arch Mikrobiol,* 74, 223-34.

KLUTTS, J. S., HATANAKA, K., PAN, Y. T. & ELBEIN, A. D. (2002) Biosynthesis of D-arabinose in Mycobacterium smegmatis: Specific

labeling from D-glucose. *Archives of Biochemistry and Biophysics,* 398, 229-239.

KOBAYASHI, K., EHRLICH, S. D., ALBERTINI, A., AMATI, G., ANDERSEN, K. K., ARNAUD, M., ASAI, K., ASHIKAGA, S., AYMERICH, S., BESSIERES, P., BOLAND, F., BRIGNELL, S. C., BRON, S., BUNAI, K., CHAPUIS, J., CHRISTIANSEN, L. C., DANCHIN, A., DEBARBOUILLE, M., DERVYN, E., DEUERLING, E., DEVINE, K., DEVINE, S. K., DREESEN, O., ERRINGTON, J., FILLINGER, S., FOSTER, S. J., FUJITA, Y., GALIZZI, A., GARDAN, R., ESCHEVINS, C., FUKUSHIMA, T., HAGA, K., HARWOOD, C. R., HECKER, M., HOSOYA, D., HULLO, M. F., KAKESHITA, H., KARAMATA, D., KASAHARA, Y., KAWAMURA, F., KOGA, K., KOSKI, P., KUWANA, R., IMAMURA, D., ISHIMARU, M., ISHIKAWA, S., ISHIO, I., LE COQ, D., MASSON, A., MAUEL, C., MEIMA, R., MELLADO, R. P., MOIR, A., MORIYA, S., NAGAKAWA, E., NANAMIYA, H., NAKAI, S., NYGAARD, P., OGURA, M., OHANAN, T., O'REILLY, M., O'ROURKE, M., PRAGAI, Z., POOLEY, H. M., RAPOPORT, G., RAWLINS, J. P., RIVAS, L. A., RIVOLTA, C., SADAIE, A., SADAIE, Y., SARVAS, M., SATO, T., SAXILD, H. H., SCANLAN, E., SCHUMANN, W., SEEGERS, J. F. M. L., SEKIGUCHI, J., SEKOWSKA, A., SEROR, S. J., SIMON, M., STRAGIER, P., STUDER, R., TAKAMATSU, H., TANAKA, T., TAKEUCHI, M., THOMAIDES, H. B., VAGNER, V., VAN DIJL, J. M., WATABE, K., WIPAT, A., YAMAMOTO, H., YAMAMOTO, M., YAMAMOTO, Y., YAMANE, K., YATA, K., YOSHIDA, K., YOSHIKAWA, H., ZUBER, U. & OGASAWARA, N. (2003) Essential Bacillus subtilis genes. *Proceedings of the National Academy of Sciences of the United States of America,* 100, 4678-4683.

KOCH, A. L. (1986) The pH in the Neighborhood of Membranes Generating a Protonmotive Force. *Journal of Theoretical Biology,* 120, 73-84.

KOCH, H. U., HAAS, R. & FISCHER, W. (1984) The Role of Lipoteichoic Acid Biosynthesis in Membrane Lipid-Metabolism of Growing Staphylococcus-Aureus. *European Journal of Biochemistry,* 138, 357-363.

KOEBNIK, R. (2001) The role of bacterial pili in protein and DNA translocation. *Trends Microbiol,* 9, 586-90.

KOGA, Y., NISHIHARA, M. & MORII, H. (1984) Products of Phosphatidylglycerol Turnover in 2 Bacillus Strains with and without Lipoteichoic Acid in the Cells. *Biochimica Et Biophysica Acta,* 793, 86-94.

KOGAN, G., UHRIN, D., BRISSON, J. R., PAOLETTI, L. C., BLODGETT, A. E., KASPER, D. L. & JENNINGS, H. J. (1996) Structural and immunochemical characterization of the type VIII group B Streptococcus capsular polysaccharide. *Journal of Biological Chemistry,* 271, 8786-8790.

KOJIMA, N., ARAKI, Y. & ITO, E. (1985) Structure of the Linkage Units between Ribitol Teichoic-Acids and Peptidoglycan. *Journal of Bacteriology,* 161, 299-306.

KOKEGUCHI, S., KATO, K., OHTA, H., FUKUI, K., TSUJIMOTO, M., OGAWA, T., TAKADA, H. & KOTANI, S. (1987) Isolation and Characterization of an Amphipathic Antigen from Corynebacterium-Diphtheriae. *Microbios,* 50, 183-199.

KOMAGATA, K. & SUZUKI, K.-I. (1987) Lipid and cell-wall analysis in bacterial systematics. *Meth. Microbiol,* 19, 161-207.

KONINGS, W. N., ALBERS, S. V., KONING, S. & DRIESSEN, A. J. M. (2002) The cell membrane plays a crucial role in survival of bacteria and archaea in extreme environments. *Antonie Van Leeuwenhoek International Journal of General and Molecular Microbiology,* 81, 61-72.

KORDULAKOVA, J., GILLERON, M., MIKUSOVA, K., PUZO, G., BRENNAN, P. J., GICQUEL, B. & JACKSON, M. (2002) Definition of the first mannosylation step in phosphatidylinositol mannoside synthesis - PimA is essential for growth of mycobacteria. *Journal of Biological Chemistry,* 277, 31335-31344.

KORDULAKOVA, J., GILLERON, M., PUZO, G., BRENNAN, P. J., GICQUEL, B., MIKUSOVA, K. & JACKSON, M. (2003) Identification of the required acyltransferase step in the biosynthesis of the phosphatidylinositol mannosides of Mycobacterium species. *Journal of Biological Chemistry,* 278, 36285-36295.

KORNWENDISCH, F. & KUTZNER, H. J. (1992) The faimly Streptomycetaceae. IN BARLOWS, A., TURUPER, H. G., DWORKIN, M., HARDER, W. & SCHLEIFER, K. H. (Eds.) *The Prokaryotes.* New York, Springer.

KORNWENDISCH, F. & SCHNEIDER, J. (1992) Phage Typing - a Useful Tool in Actinomycete Systematics. *Gene,* 115, 243-247.

KOVACEVIC, S., ANDERSON, D., MORITA, Y. S., PATTERSON, J., HAITES, R., MCMILLAN, B. N. I., COPPEL, R., MCCONVILLE, M. J. & BILLMAN-JACOBE, H. (2006) Identification of a novel protein with a role in lipoarabinomannan biosynthesis in mycobacteria. *Journal of Biological Chemistry,* 281, 9011-9017.

KOZLOVA, Y. I., STRESHINSKAYA, G. M., SHASHKOV, A. S., SENCHENKOVA, S. N. & EVTUSHENKO, L. I. (2006) Carbohydrate-containing polymers of the cell wall of the thermophilic streptomycete Streptomyces thermoviolaceus subsp thermoviolaceus VKM Ac-1857. *Biochemistry-Moscow,* 71, 775-780.

KREMER, L., GURCHA, S. S., BIFANI, P., HITCHEN, P. G., BAULARD, A., MORRIS, H. R., DELL, A., BRENNAN, P. J. & BESRA, G. S. (2002) Characterization of a putative alpha-mannosyltransferase involved in phosphatidylinositol trimannoside biosynthesis in Mycobacterium tuberculosis. *Biochemical Journal,* 363, 437-447.

KROPPENSTEDT, R. M. & GOODFELLOW, M. (Eds.) (1992) *The Prokaryotes* Berlin, Springer.

KROPPENSTEDT, R. M. & KUTZNER, H. J. (1976) Biochemical Markers in Taxonomy of Actinomycetales. *Experientia,* 32, 318-319.

KROPPENSTEDT, R. M., STACKEBRANDT, E. & GOODFELLOW, M. (1990) Taxonomic Revision of the Actinomycete Genera Actinomadura

and Microtetraspora. *Systematic and Applied Microbiology,* 13, 148-160.

KUDO, T. (1997) Family *Thermonosporaceae.* IN MIYADOH, S. (Ed.) *In Atlas of Actinomycetes.* Tokyo, Asakura Publishing.

KUDO, T., MATSUSHIMA, K., ITOH, T., SASAKI, J. & SUZUKI, K. (1998) Description of four new species of the genus Kineosporia : Kineosporia succinea sp. nov., Kineosporia rhizophila sp. nov., Kineosporia mikuniensis sp, nov. and Kineosporia rhamnosa sp, nov., isolated from plant samples, and amended description of the genus Kineosporia. *International Journal of Systematic Bacteriology,* 48, 1245-1255.

KUKOLYA, J., NAGY, I., LADAY, M., TOTH, E., ORAVECZ, O., MARIALIGETI, K. & HORNOK, L. (2002) Thermobifida cellulolytica sp nov., a novel lignocellulose-decomposing actinomycete. *International Journal of Systematic and Evolutionary Microbiology,* 52, 1193-1199.

KUKOLYA, J., SZABO, L. & HORNOK, L. (2001) Surface structures of new and lesser known species of Thermobifida as revealed by scanning electron microscopy. *Acta Biologica Hungarica,* 52, 211-221.

KUMAR, S., TAMURA, K. & NEI, M. (2003) MEGA3: An integrated software for molecular evolutionary genetic analysis and sequence alignment. *Integrative and Comparative Biology,* 43, 947-947.

KUMAR, S., TAMURA, K. & NEI, M. (2004) MEGA3: Integrated software for molecular evolutionary genetics analysis and sequence alignment. *Briefings in Bioinformatics,* 5, 150-163.

KUNISAWA, T. (2007) Gene arrangements characteristic of the phylum Actinobacteria. *Antonie Van Leeuwenhoek International Journal of General and Molecular Microbiology,* 92, 359-365.

KUTZNER, H. J. & WAKSMAN, S. A. (1959) Streptomyces coelicolor Mueller and Streptomyces violaceoruber Waksman and Curtis, two distinctly different organisms. *J Bacteriol,* 78, 528-38.

LABISCHINSKI, H., GOODELL, E. W., GOODELL, A. & HOCHBERG, M. L. (1991) Direct Proof of a More-Than-Single-Layered Peptidoglycan Architecture of Escherichia-Coli W7 - a Neutron Small-Angle Scattering Study. *Journal of Bacteriology,* 173, 751-756.

LABISCHINSKI, H. & MAIDHOF, H. (1994) Bacterial peptidoglycan: overview and evolving concepts. *New Compr. Biochem.,* 27, 23-38.

LANG, W. K., GLASSEY, K. & ARCHIBALD, A. R. (1982) Influence of Phosphate Supply on Teichoic-Acid and Teichuronic Acid Content of Bacillus-Subtilis Cell-Walls. *Journal of Bacteriology,* 151, 367-375.

LAZAREVIC, V., ABELLAN, F. X., MOLLER, S. B., KARAMATA, D. & MAUEL, C. (2002) Comparison of ribitol and glycerol teichoic acid genes in Bacillus subtilis W23 and 168: identical function, similar divergent organization, but different regulation. *Microbiology-Sgm,* 148, 815-824.

LAZAREVIC, V., SOLDO, B., MEDICO, N., POOLEY, H., BRON, S. & KARAMATA, D. (2005) Bacillus subtilis alpha-phosphoglucomutase is required for normal cell morphology and biofilm formation. *Applied and Environmental Microbiology,* 71, 39-45.

LEA-SMITH, D. J., MARTIN, K. L., PYKE, J. S., TULL, D., MCCONVILLE, M. J., COPPEL, R. L. & CRELLIN, P. K. (2008) Analysis of a new mannosyltransferase required for the synthesis of phosphatidylinositol mannosides and lipoarbinomannan reveals two lipomannan pools in corynebacterineae. *Journal of Biological Chemistry,* 283, 6773-6782.

LECHEVALIER, M. P., DEBIEVRE, C. & LECHEVALIER, H. (1977) Chemotaxonomy of Aerobic Actinomycetes - Phospholipid Composition. *Biochemical Systematics and Ecology,* 5, 249-260.

LECHEVALIER, M. P., STERN, A. E. & LECHEVALIER, H. A. (1981) Phospholipids in the taxonomy of actinomycetes. IN SCHAAL, K. P. & PULVERE, G. (Eds.) *In Actinomycetes.* Stuttgart, Gustav Fischer.

LEE, J. Y., LEE, J. Y., JUNG, H. W. & HWANG, B. K. (2005a) Streptomyces koyangensis sp nov., a novel actinomycete that produces 4-phenyl-3-butenoic acid. *International Journal of Systematic and Evolutionary Microbiology,* 55, 257-262.

LEE, J. Y., LEE, J. Y., JUNG, H. W. & HWANG, B. K. (2005b) Streptomyces koyangensis sp. nov., a novel actinomycete that produces 4-phenyl-3-butenoic acid. *Int J Syst Evol Microbiol,* 55, 257-62.

LEE, S. D. (2006) Kineococcus marinus sp nov., isolated from marine sediment of the coast of Jeju, Korea. *International Journal of Systematic and Evolutionary Microbiology,* 56, 1279-1283.

LI, Y. L., FLOROVA, G. & REYNOLDS, K. A. (2005) Alteration of the fatty acid profile of Streptomyces coelicolor by replacement of the initiation enzyme 3-ketoacyl acyl carrier protein synthase III (FabH). *Journal of Bacteriology,* 187, 3795-3799.

LIM, S. & SALTON, M. R. J. (1985) Comparison of the Chemical-Composition of Lipomannan from Micrococcus-Agilis Membranes with That of Micrococcus-Luteus Strains. *Fems Microbiology Letters,* 27, 287-291.

LISANTI, M. P., TANG, Z. L., SCHERER, P. E., KUBLER, E., KOLESKE, A. J. & SARGIACOMO, M. (1995) Caveolae, Transmembrane Signaling and Cellular-Transformation. *Molecular Membrane Biology,* 12, 121-124.

LYKIDIS, A., MAVROMATIS, K., IVANOVA, N., ANDERSON, I., LAND, M., DIBARTOLO, G., MARTINEZ, M., LAPIDUS, A., LUCAS, S., COPELAND, A., RICHARDSON, P., WILSON, D. B. & KYRPIDES, N. (2007) Genome sequence and analysis of the soil cellulolytic actinomycete Thermobifida fusca YX. *Journal of Bacteriology,* 189, 2477-2486.

MA, Y. F., STERN, R. J., SCHERMAN, M. S., VISSA, V. D., YAN, W. X., JONES, V. C., ZHANG, F. Q., FRANZBLAU, S. G., LEWIS, W. H. & MCNEIL, M. R. (2001) Drug targeting Mycobacterium tuberculosis cell wall synthesis: Genetics of dTDP-rhamnose synthetic enzymes and development of a microtiter plate-based screen for inhibitors of conversion of dTDP-glucose to dTDP-rhamnose. *Antimicrobial Agents and Chemotherapy,* 45, 1407-1416.

MADIGAN, M. T., MARTINKO, J. M. & PARKER, J. (Eds.) (2003) *Bock Biolgy of Microorganisms,* Upper Saddler River, NJ., Pearson Education, Inc.

MANTECA, A., FERNANDEZ, M. & SANCHEZ, J. (2005) Mycelium development in Streptomyces antibioticus ATCC11891 occurs in an orderly pattern which determines multiphase growth curves. *Bmc Microbiology,* 5, -.

MARLAND, Z., BEDDOE, T., ZAKER-TABRIZI, L., LUCET, I. S., BRAMMANANTH, R., WHISSTOCK, J. C., WILCE, M. C. J., COPPEL, R. L., CRELLIN, P. K. & ROSSJOHN, J. (2006) Hijacking of a substrate-binding protein scaffold for use in mycobacterial cell wall biosynthesis. *Journal of Molecular Biology,* 359, 983-997.

MARQUIS, R. E. (1988) Turgor presure, sporulation, and the physical properties of cell walls. IN ACTOR, P., DANEO-MOORE, L., HIGGINS, M. L., SALTON, M. R. J. & SHOCKMAN, G. D. (Eds.) *Antibiotic inhibition of bacterial cell surface assembly and function.* Washington, D.C., American Society of Microbiology.

MARTINS, L. O., EMPADINHAS, N., MARUGG, J. D., MIGUEL, C., FERREIRA, C., DA COSTA, M. S. & SANTOS, H. (1999) Biosynthesis of mannosylglycerate in the thermophilic bacterium Rhodothermus marinus - Biochemical and genetic characterization of a mannosylglycerate synthase. *Journal of Biological Chemistry,* 274, 35407-35414.

MATSUMOTO, K., KUSAKA, J., NISHIBORI, A. & HARA, H. (2006) Lipid domains in bacterial membranes. *Molecular Microbiology,* 61, 1110-1117.

MAUEL, C., BAUDURET, A., CHERVET, C., BEGGAH, S. & KARAMATA, D. (1995) In Bacillus-Subtilis-168, Teichoic-Acid of the Cross-Wall May Be Different from That of the Cylinder - a Hypothesis Based on Transcription Analysis of Tag Genes. *Microbiology-Uk,* 141, 2379-2389.

MAUEL, C., YOUNG, M. & KARAMATA, D. (1991) Genes Concerned with Synthesis of Poly(Glycerol Phosphate), the Essential Teichoic-Acid in Bacillus-Subtilis Strain-168, Are Organized in 2 Divergent Transcription Units. *Journal of General Microbiology,* 137, 929-941.

MAYBERRY, W. R., SMITH, P. F. & LANGWORT.TA (1974) Heptose-Containing Pentaglycosyl Diglyceride among Lipids of Acholeplasma-Modicum. *Journal of Bacteriology,* 118, 898-904.

MC. CARTY, M. (1959) The occurrence of polyglycerophosphate as an antigenic component of various gram-positive bacterial species. *J Exp Med,* 109, 361-78.

MCARTHUR, H. A. I., HANCOCK, I. C., ROBERTS, F. M. & BADDILEY, J. (1980) Biosynthesis of Teichoic-Acid in Micrococcus-Varians Atcc-29750 - Characterization of a Further Lipid Intermediate. *Febs Letters,* 111, 317-323.

MCCARTHY, A. J. & CROSS, T. (1984) A Taxonomic Study of Thermomonospora and Other Monosporic Actinomycetes. *Journal of General Microbiology,* 130, 5-25.

MCCARTHY, T. R., TORRELLES, J. B., MACFARLANE, A. S., KATAWCZIK, M., KUTZBACH, B., DESJARDIN, L. E., CLEGG, S., GOLDBERG, J. B. & SCHLESINGER, L. S. (2005) Overexpression of Mycobacterium tuberculosis manB, a phosphomannomutase that increases phosphatidylinositol mannoside biosynthesis in Mycobacterium smegmatis and mycobacterial association with human macrophages. *Molecular Microbiology,* 58, 774-790.

MCNEIL, M., DAFFE, M. & BRENNAN, P. J. (1991) Location of the Mycolyl Ester Substituents in the Cell-Walls of Mycobacteria. *Journal of Biological Chemistry,* 266, 13217-13223.

MEROUEH, S. O., BENCZE, K. Z., HESEK, D., LEE, M., FISHER, J. F., STEMMLER, T. L. & MOBASHERY, S. (2006) Three-dimensional structure of the bacterial cell wall peptidoglycan. *Proc Natl Acad Sci U S A,* 103, 4404-9.

MESNAGE, S., TOSI-COUTURE, E., GOUNON, P., MOCK, M. & FOUET, A. (1998) The capsule and S-layer: Two independent and yet compatible macromolecular structures in Bacillus anthracis. *Journal of Bacteriology,* 180, 52-58.

MEYER, H. & MEYER, F. (1971) Lipid metabolism in the parasitic and free-living spirochetes Treponema pallidum (Reiter) and Treponema zuelzerae. *Biochim Biophys Acta,* 231, 93-106.

MIKUSOVA, K., HUANG, H., YAGI, T., HOLSTERS, M., VEREECKE, D., D'HAEZE, W., SCHERMAN, M. S., BRENNAN, P. J., MCNEIL, M. R. & CRICK, D. C. (2005) Decaprenylphosphoryl arabinofuranose, the donor of the D-arabinofuranosyl residues of mycobacterial arabinan, is formed via a two-step epimerization of decaprenylphosphoryl ribose. *J Bacteriol,* 187, 8020-5.

MILEYKOVSKAYA, E. (2007) Subcellular localization of Escherichia coli osmosensory transporter ProP: focus on cardiolipin membrane domains. *Molecular Microbiology,* 64, 1419-1422.

MIMS, C., DEREK, W., PLAYFAIR, J., ROITT, I., WALKELIN, D. & WILLIAMS, R. (1998) *Medical Microbiology,* London Mosby Int. Ltd.

MIN, H. & COWMAN, M. K. (1986) Combined Alcian Blue and Silver Staining of Glycosaminoglycans in Polyacrylamide Gels - Application to Electrophoretic Analysis of Molecular-Weight Distribution. *Analytical Biochemistry,* 155, 275-285.

MIRELMAN, D., BECK, B. D. & SHAW, D. R. D. (1970) Location of D-Alanyl Ester in Ribitol Teichoic Acid of Staphylococcus-Aureus. *Biochemical and Biophysical Research Communications,* 39, 712-&.

MISAKI, A., AZUMA, I. & YAMAMURA, Y. (1977) Structural and immunochemical studies on D-arabino-D-mannans and D-mannans of Mycobacterium tuberculosis and other Mycobacterium species. *J Biochem,* 82, 1759-70.

MISHRA, A. K., ALDERWICK, L. J., RITTMANN, D., TATITURI, R. V. V., NIGOU, J., GILLERON, M., EGGELING, L. & BESRA, G. S. (2007) Identification of an alpha(1 -> 6) mannopyranosyltransferase (MptA), involved in Corynebacterium glutamicum lipomanann biosynthesis, and identification of its orthologue in Mycobacterium tuberculosis. *Molecular Microbiology,* 65, 1503-1517.

MONSON, A. M., BRADLEY, S. G., ENQUIST, L. W. & CRUCES, G. (1969) Genetic homologies among Streptomyces violaceoruber strains. *J Bacteriol,* 99, 702-6.

MORATH, S., GEYER, A. & HARTUNG, T. (2001) Structure-function relationship of cytokine induction by lipoteichoic acid from *Staphylococcus aureus. J. Exp. Med.,* 193, 393-397.

MORITA, Y. S., SENA, C. B. C., WALLER, R. F., KUROKAWA, K., SERNEE, M. F., NAKATANI, F., HAITES, R. E., BILLMAN-JACOBE, H., MCCONVILLE, M. J., MAEDA, Y. & KINOSHITA, T. (2006) PimE is a polyprenol-phosphate-mannose-dependent mannosyltransferase that transfers the fifth mannose of phosphatidylinositol mannoside in mycobacteria. *Journal of Biological Chemistry,* 281, 25143-25155.

MORRISON, D. C. & LEIVE, L. (1975) Fractions of Lipopolysaccharide from Escherichia-Coli O111-B4 Prepared by 2 Extraction Procedures. *Journal of Biological Chemistry,* 250, 2911-2919.

MOVAHEDZADEH, F., SMITH, D. A., NORMAN, R. A., DINADAYALA, P., MURRAY-RUST, J., RUSSELL, D. G., KENDALL, S. L., RISON, S. C. G., MCALISTER, M. S. B., BANCROFT, G. J., MCDONALD, N. Q., DAFFE, M., AV-GAY, Y. & STOKER, N. G. (2004) The Mycobacterium tuberculosis inol gene is essential for growth and virulence. *Molecular Microbiology,* 51, 1003-1014.

MURATA, M., PERANEN, J., SCHREINER, R., WIELAND, F., KURZCHALIA, T. V. & SIMONS, K. (1995) Vip21/Caveolin Is a Cholesterol-Binding Protein. *Proceedings of the National Academy of Sciences of the United States of America,* 92, 10339-10343.

MUYZER, G., DEWAAL, E. C. & UITTERLINDEN, A. G. (1993) Profiling of complex microbial-population by denaturing gradient gel-electrophoresis analysis of polymerase chain reaction- amplified genes-coding for 16s rRNA. *Applied and Environmental Microbiology,* 59(3), 695-700.

NAKANO, M. & FISCHER, W. (1978) Trihexosyldiacyl-Glycerol and Acyltrihexosyldiacyl-Glycerol as Lipid Anchors of Lipoteichoic Acid of Lactobacillus-Casei Dsm 20021. *Hoppe-Seylers Zeitschrift Fur Physiologische Chemie,* 359, 1-11.

NANNINGA, N. (1998) Morphogenesis of Escherichia coli. *Microbiology and Molecular Biology Reviews,* 62, 110-+.

NAUMOVA, I. B., KUZNETSOV, V. D., KUDRINA, K. S. & BEZZUBENKOVA, A. P. (1980a) The occurance of teichoic acids in *Streptomycetes. Arch Mirobiol,* 126, 71-75.

NAUMOVA, I. B., KUZNETSOV, V. D., KUDRINA, K. S. & BEZZUBENKOVA, A. P. (1980b) The Occurrence of Teichoic-Acids in Streptomycetes. *Archives of Microbiology,* 126, 71-75.

NAUMOVA, I. B. & SHASHKOV, A. S. (1997) Anionic polymers in cell walls of gram-positive bacteria. *Biochemistry-Moscow,* 62, 809-840.

NAUMOVA, I. B., SHASHKOV, A. S., TUL'SKAYA, E. M., STRESHINSKAYA, G. M., KOZLOVA, Y. I., POTEKHINA, N. V., EVTUSHENKO, L. I. & STACKEBRANDT, E. (2001) Cell wall teichoic acids: structural diversity, species specificity in the genus

Nocardiopsis, and chemotaxonomic perspective. *Fems Microbiology Reviews,* 25, 269-283.

NAVARRE, W. W. & SCHNEEWIND, O. (1999) Surface proteins of gram-positive bacteria and mechanisms of their targeting to the cell wall envelope. *Microbiology and Molecular Biology Reviews,* 63, 174-+.

NESBITT, J. A., 3RD & LENNARZ, W. J. (1968) Participation of aminoacyl transfer ribonucleic acid in aminoacyl phosphatidylglycerol synthesis. I. Specificity of lysyl phosphatidylglycerol synthetase. *J Biol Chem,* 243, 3088-95.

NEUHAUS, F. C. & BADDILEY, J. (2003) A continuum of anionic charge: Structrues and functions of D-alanyl-teichoic acids in gram-positive bacteria. *Microbiology and Molecular Biology reviews,* 67, 686-723.

NEUHAUS, F. C., HEATON, M. P., DEBABOV, D. V. & ZHANG, Q. Y. (1996) The dlt operon in the biosynthesis of D-alanyl-lipoteichoic acid in Lactobacillus casei. *Microbial Drug Resistance-Mechanisms Epidemiology and Disease,* 2, 77-84.

NIGOU, J., GILLERON, M., CAHUZAC, B., BOUNERY, J. D., HEROLD, M., THURNHER, M. & PUZO, G. (1997) The phosphatidyl-myo-inositol anchor of the lipoarabinomannans from Mycobacterium bovis bacillus Calmette Guerin - Heterogeneity, structure, and role in the regulation of cytokine secretion. *Journal of Biological Chemistry,* 272, 23094-23103.

NIGOU, J., GILLERON, M. & PUZO, G. (1999) Lipoarabinomannans: characterization of the multiacylated forms of the phosphatidyl-myo-inositol anchor by NMR spectroscopy. *Biochemical Journal,* 337, 453-460.

NIGOU, J., GILLERON, M. & PUZO, G. (2003) Lipoarabinomannans: from structure to biosynthesis. *Biochimie,* 85, 153-166.

NING, B. & ELBEIN, A. D. (1999) Purification and properties of mycobacterial GDP-mannose pyrophosphorylase. *Archives of Biochemistry and Biophysics,* 362, 339-345.

OCHI, K. (1995a) Taxonomic characterization of Streptomyces coelicolor A3(2) and Streptomyces lividans 66 by analysis of ribosomal proteins. *Actinomycetologica,* 9, 49-52.

OCHI, K. (1995b) A Taxonomic Study of the Genus Streptomyces by Analysis of Ribosomal-Protein at-L30. *International Journal of Systematic Bacteriology,* 45, 507-514.

OCHI, K. & HIRANUMA, H. (1994) A Taxonomic Review of the Genera Kitasatosporia and Streptoverticillium by Analysis of Ribosomal-Protein at-L30. *International Journal of Systematic Bacteriology,* 44, 285-292.

ORTIZ-MARTINEZ, A., GONZALEZ, J. M., EVTUSHENKO, L. I., JURADO, V., LAIZ, L., GROTH, I. & SAIZ-JIMENEZ, C. (2004) Reclassification of Agromyces fucosus subsp hippuratus as Agromyces hippuratus sp nov., comb. nov and emended description of Agromyces fucosus. *International Journal of Systematic and Evolutionary Microbiology,* 54, 1553-1556.

OSHIDA, T., SUGAI, M., KOMATSUZAWA, H., HONG, Y. M., SUGINAKA, H. & TOMASZ, A. (1995) A Staphylococcus-Aureus

Autolysin That Has an N-Acetylmuramoyl-L Alanine Amidase Domain and an Endo-Beta-N-Acetylglucosaminidase Domain - Cloning, Sequence-Analysis, and Characterization. *Proceedings of the National Academy of Sciences of the United States of America,* 92, 285-289.

OSHIMA, M. & YAMAKAWA, T. (1972) Isolation and partial characterization of a novel glycolipid from an extremely thermophilic bacterium. *Biochem Biophys Res Commun,* 49, 185-91.

OU, L. T. & MARQUIS, R. E. (1970) Electromechanical Interactions in Cell Walls of Gram-Positive Cocci. *Journal of Bacteriology,* 101, 92-&.

OWEN, P. & SALTON, M. R. J. (1975) Succinylated Mannan in Membrane System of Micrococcus-Lysodeikticus. *Biochemical and Biophysical Research Communications,* 63, 875-880.

PAKKIRI, L. S., WOLUCKA, B. A., LUBERT, E. J. & WAECHTER, C. J. (2004) Structural and topological studies on the lipid-mediated assembly of a membrane-associated lipomannan in Micrococcus luteus. *Glycobiology,* 14, 73-81.

PAL, M. K., GHOSH, T. C. & GHOSH, J. K. (1990) Studies on the Conformation of and Metal-Ion Binding by Teichoic-Acid of Staphylococcus-Aureus. *Biopolymers,* 30, 273-277.

PARISH, T., LIU, J., NIKAIDO, H. & STOKER, N. G. (1997) A Mycobacterium smegmatis mutant with a defective inositol monophosphate phosphatase gene homolog has altered cell envelope permeability. *Journal of Bacteriology,* 179, 7827-7833.

PATTERSON, J. H., WALLER, R. F., JEEVARAJAH, D., BILLMAN-JACOBE, H. & MCCONVILLE, M. J. (2003) Mannose metabolism is required for mycobacterial growth. *Biochemical Journal,* 372, 77-86.

PEREGO, M., GLASER, P., MINUTELLO, A., STRAUCH, M. A., LEOPOLD, K. & FISCHER, W. (1995) Incorporation of D-Alanine into Lipoteichoic Acid and Wall Teichoic-Acid in Bacillus-Subtilis - Identification of Genes and Regulation. *Journal of Biological Chemistry,* 270, 15598-15606.

PHILLIPS, R. W., WIEGEL, J., BERRY, C. J., FLIERMANS, C., PEACOCK, A. D., WHITE, D. C. & SHIMKETS, L. J. (2002) Kineococcus radiotolerans sp nov., a radiation-resistant, Gram-positive bacterium. *International Journal of Systematic and Evolutionary Microbiology,* 52, 933-938.

PLACKETT, P. (1967) The glycerolipids of Mycoplasma mycoides. *Biochemistry,* 6, 2746-54.

POLLACK, J. H. & NEUHAUS, F. C. (1994) Changes in Wall Teichoic-Acid during the Rod-Sphere Transition of Bacillus-Subtilis-168. *Journal of Bacteriology,* 176, 7252-7259.

POLOTSKY, V. Y., BELISLE, J. T., MIKUSOVA, K., EZEKOWITZ, R. A. B. & JOINER, K. A. (1997) Interaction of human mannose-binding protein with Mycobacterium avium. *Journal of Infectious Diseases,* 175, 1159-1168.

POLOTSKY, V. Y., FISCHER, W., EZEKOWITZ, R. A. B. & JOINER, K. A. (1996) Interactions of human mannose-binding protein with lipoteichoic acids. *Infection and Immunity,* 64, 380-383.

POOLEY, H. M., PASCHOUD, D. & KARAMATA, D. (1987) The Gtab Marker in Bacillus-Subtilis 168 Is Associated with a Deficiency in Udpglucose Pyrophosphorylase. *Journal of General Microbiology,* 133, 3481-3493.

POTEKHINA, N. V., SHASHKOV, A. S., EVTUSHENKO, L. I. & NAUMOVA, I. B. (2003) Teichoic acids in the cell walls of Microbispora mesophila Ac-1953(T) and Thermobifida fusca Ac-1952(T). *Microbiology,* 72, 157-161.

POTEKHINA, N. V., STRESHINSKAYA, G. M., NOVITSKAYA, G. V. & NAUMOVA, I. B. (1983) Isolation of Lipoteichoic Acid from Streptomyces-Levoris. *Microbiology,* 52, 340-343.

POWELL, D. A., DUCKWORT.M & BADDILEY, J. (1974) Acylated Mannan in Membrane of Micrococcus-Lysodeikticus. *Febs Letters,* 41, 259-263.

POYART, C., PELLEGRINI, E., MARCEAU, M., BAPTISTA, M., JAUBERT, F., LAMY, M. C. & TRIEU-CUOT, P. (2003) Attenuated virulence of Streptococcus agalactiae deficient in D-alanyl-lipoteichoic acid is due to an increased susceptibility to defensins and phagocytic cells. *Molecular Microbiology,* 49, 1615-1625.

QIAN, Z. L., YIN, Y. B., ZHANG, Y., LU, L. Y., LI, Y. X. & JIANG, Y. (2006) Genomic characterization of ribitol teichoic acid synthesis in Staphylococcus aureus: genes, genomic organization and gene duplication. *Bmc Genomics,* 7, -.

RAO, P. & PATTABIRAMAN, T. N. (1989) Reevaluation of the Phenol Sulfuric-Acid Reaction for the Estimation of Hexoses and Pentoses. *Analytical Biochemistry,* 181, 18-22.

REEKE, G. N., BECKER, J. W., CUNNINGH.BA, GUNTHER, G. R., WANG, J. L. & EDELMAN, G. M. (1974) Relationships between Structure and Activities of Concanavalin A. *Annals of the New York Academy of Sciences,* 234, 369-382.

ROCOURT, J., WEHMEYER, U. & STACKEBRANDT, E. (1987) Transfer of Listeria Dentrificans to a New Genus, Jonesia Gen-Nov, as Jonesia-Denitrificans Comb-Nov. *International Journal of Systematic Bacteriology,* 37, 266-270.

RUHLAND, G. J. & FIEDLER, F. (1987) Occurrence and Biochemistry of Lipoteichoic Acids in the Genus Listeria. *Systematic and Applied Microbiology,* 9, 40-46.

RUSSELL, N. J. & FUKUNAGA, N. (1990) A Comparison of Thermal Adaptation of Membrane-Lipids in Psychrophilic and Thermophilic Bacteria. *Fems Microbiology Reviews,* 75, 171-182.

SADDLER, G. S., TAVECCHIA, P., LOCIURO, S., ZANOL, M., COLOMBO, L. & SELVA, E. (1991) Analysis of madurose and other actinomycete whole cell sugars by gas chromatography. *J. microb. Meth.,* 14, 185-191.

SANTOS, H. & DA COSTA, M. S. (2002a) Compatible solutes of organisms that live in hot saline environments. *Environ Microbiol,* 4, 501-9.

SANTOS, H. & DA COSTA, M. S. (2002b) Compatible solutes of organisms that live in hot saline environments. *Environmental Microbiology,* 4, 501-509.

SARA, M. (2001) Conserved anchoring mechanisms between crystalline cell surface S-layer proteins and secondary cell wall polymers in Gram-positive bacteria? *Trends in Microbiology,* 9, 47-49.

SCHAEFFER, M. L., KHOO, K. H., BESRA, G. S., CHATTERJEE, D., BRENNAN, P. J., BELISLE, J. T. & INAMINE, J. M. (1999) The pimB gene of Mycobacterium tuberculosis encodes a mannosyltransferase involved in lipoarabinomannan biosynthesis. *J Biol Chem,* 274, 31625-31.

SCHAFFER, C. & MESSNER, P. (2005) The structure of secondary cell wall polymers: how Gram-positive bacteria stick their cell walls together. *Microbiology-Sgm,* 151, 643-651.

SCHAFFER, C., NOVOTNY, R., KUPCU, S., ZAYNI, S., SCHEBERL, A., FRIEDMANN, J., SLEYTR, U. B. & MESSNER, P. (2007) Novel biocatatysts based on S-Layer self-assembly of Geobacillus Stearothermophilus NRS 2004/3a: A nano biotech nologicat approach. *Small,* 3, 1549-1559.

SCHATZ, G. & DOBBERSTEIN, B. (1996) Common principles of protein translocation across membranes. *Science,* 271, 1519-26.

SCHAUNER, C., DARY, A., LEBRIHI, A., LEBLOND, P., DECARIS, B. & GERMAIN, P. (1999) Modulation of lipid metabolism and spiramycin biosynthesis in Streptomyces ambofaciens unstable mutants. *Applied and Environmental Microbiology,* 65, 2730-2737.

SCHERMAN, M., WESTON, A., DUNCAN, K., WHITTINGTON, A., UPTON, R., DENG, L., COMBER, R., FRIEDRICH, J. D. & MCNEIL, M. (1995) Biosynthetic Origin of Mycobacterial Cell-Wall Arabinosyl Residues. *Journal of Bacteriology,* 177, 7125-7130.

SCHIFFER, G. & HOLTJE, J.-V. (1972) Peptidoglycan types of bacterial cell walls and their taxonomic implications. *Bacteriol. Rev.,* 36, 407-477.

SCHNEIDER, E. (2001) ABC transporters catalyzing carbohydrate uptake. *Research in Microbiology,* 152, 303-310.

SEGREST, J. P., TERRY, W., JACKSON, R. L. & MARCHESI, V. T. (1972) Membrane Glycoproteins - Arrangement of Cyanogen Bromide Fragments and Evidence for Bipolarity. *Federation Proceedings,* 31, A736-&.

SEMEDO, L. T. A. S., GOMES, R. C., LINHARES, A. A., DUARTE, G. F., NASCIMENTO, R. P., ROSADO, A. S., MARGIS-PINHEIRO, M., MARGIS, R., SILVA, K. R. A., ALVIANO, C. S., MANFIO, G. P., SOARES, R. M. A., LINHARES, L. F. & COELHO, R. R. R. (2004) Streptomyces drozdowiczii sp nov., a novel cellulolytic streptomycete from soil in Brazil. *International Journal of Systematic and Evolutionary Microbiology,* 54, 1323-1328.

SHAPIRO, L., MCADAMS, H. H. & LOSICK, R. (2002) Generating and exploiting polarity in bacteria. *Science,* 298, 1942-1946.

SHASHKOV, A. S., KOSMACHEVSKAYA, L. N., STRESHINSKAYA, G. M., EVTUSHENKO, L. I., BUEVA, O. V., DENISENKO, V. A., NAUMOVA, I. B. & STACKEBRANDT, E. (2002) A polymer with a backbone of 3-deoxy-D-glycero-D-galacto-non-2-ulopyranosonic acid, a teichuronic acid, and a beta-glucosylated ribitol teichoic acid in the

cell wall of plant pathogenic Streptomyces sp. VKM Ac-2124. *Eur J Biochem,* 269, 6020-5.

SHASHKOV, A. S., POTEKHINA, N. V., EVTUSHENKO, L. I. & NAUMOVA, I. B. (2004) Cell wall teichoic acids of two Brevibacterium strains. *Biochemistry-Moscow,* 69, 658-664.

SHASHKOV, A. S., STRESHINSKAYA, G. M., GNILOZUB, V. A., EVTUSHENKO, L. I. & NAUMOVA, I. B. (1995) Poly(Arabitol Phosphate) Teichoic-Acid in the Cell-Wall of Agromyces-Cerinus Subsp Cerinus Vkm Ac-1340(T). *Febs Letters,* 371, 163-166.

SHASHKOV, A. S., STRESHINSKAYA, G. M., SENCHENKOVA, S. N., KOZOVA, Y. I., ALFEROVA, I. V., TEREKHOVA, L. P. & EVTUSHENKO, L. I. (2006) Cell wall teichoic acids of streptomycetes of the phenetic cluster 'Streptomyces fulvissimus'. *Carbohydrate Research,* 341, 796-802.

SHATALKIN, A. I. (2004) Highest level of division in classification of organisms. 3. Monodermata and Didermata. *Zhurnal Obshchei Biologii,* 65, 195-210.

SHAW, N. (1970) Bacterial glycolipids. *Bacteriol Rev,* 34, 365-77.

SHAW, N. (1975) Bacterial glycolipids and glycophospholipids. *Advances in Microbial Physiology,* 12, 141-167.

SHAW, N. & DINGLINGER, F. (1969) The structure of an acylated inositol mannoside in the lipids of propionic acid bacteria. *Biochem J,* 112, 769-775.

SHIRLING, E. B. & GOTTLIEB, D. (1972) Cooperative description of type strains of *Streptomyces* V. additional discriptions. *International Journal of Systematic Bacteriology,* 22, 265-394.

SHOCKMAN, G. D. & HOLTJE, J.-V. (1994) Microbial peptidoglycan (murein) hydorlases. *New Compr. Biochem.,* 27.

SIMONS, K. & IKONEN, E. (1997) Functional rafts in cell membranes. *Nature,* 387, 569-572.

SINGER, S. J. & NICOLSON, G. L. (1972) Fluid Mosaic Model of Structure of Cell-Membranes. *Science,* 175, 720-&.

SLEYTR, U. B. (1976) Self-Assembly of Hexagonally and Tetragonally Arranged Subunits of Bacterial Surface-Layers and Their Reattachment to Cell-Walls. *Journal of Ultrastructure Research,* 55, 360-377.

SLEYTR, U. B., EGELSEER, E. M., ILK, N., PUM, D. & SCHUSTER, B. (2007) S-Layers as a basic building block in a molecular construction kit. *Febs Journal,* 274, 323-334.

SLEYTR, U. B., PUM, D., SARA, M. & SCHUSTER, B. (2005) S-layer based nanostructures. *Abstracts of Papers of the American Chemical Society,* 229, U638-U638.

SMITH, P. F. (1984) Lipoglycans from Mycoplasmas. *Crc Critical Reviews in Microbiology,* 11, 157-186.

SMITH, P. F. (1985) Detection of Lipoglycans in Ureaplasmas. *Journal of Bacteriology,* 162, 611-614.

SMITH, P. F. (1987) Antigenic Character of Membrane Lipoglycans from Mollicutes - a Review. *Israel Journal of Medical Sciences,* 23, 448-452.

SNEL, B., HUYNEN, M. A. & DUTILH, B. E. (2005) Genome trees and the nature of genome evolution. *Annual Review of Microbiology,* 59, 191-209.

SOLDO, B., LAZAREVIC, V., PAGNI, M. & KARAMATA, D. (1999) Teichuronic acid operon of Bacillus subtilis 168. *Molecular Microbiology,* 31, 795-805.

SOMERHARJU, P., VIRTANEN, J. A. & CHENG, K. H. (1999) Lateral organisation of membrane lipids - The superlattice view. *Biochimica Et Biophysica Acta-Molecular and Cell Biology of Lipids,* 1440, 32-48.

SONENSHEIN, A. L., HOCH, J. A. & LOSICK, R. (Eds.) (1993) *In Bacillus subtilis and other Gram-positive bacteria: Biochemistry, Physiology and Molecular Genetics,* Washington, D.C., American Society of Micorbiol.

STACKEBRANDT, E., RAINEY, F. A. & WARDRAINEY, N. L. (1997) Proposal for a new hierarchic classification system, Actinobacteria classis nov. *International Journal of Systematic Bacteriology,* 47, 479-491.

STRESHINSKAYA, G. M., SHASHKOV, A. S., USOV, A. I., EVTUSHENKO, L. I. & NAUMOVA, I. B. (2004) Cell Wall Teichoic Acids of Actinomycetes of Three Genera of the Order Actinomycetales *Biochemistry (Moscow),* 67, 778-785.

SUTCLIFFE, I. C. (1994a) Identification of a Lipomannan from Rothia-Dentacariosa. *Systematic and Applied Microbiology,* 17, 321-326.

SUTCLIFFE, I. C. (1994b) The lipoteichoic acids and lipoglycan of Gram-positive bacteria: a chemotaxonomic perspective. *System. Appl. Microbiol.,* 17, 467-480.

SUTCLIFFE, I. C. (1995) Identification of a lipoarabinomannan-like lipoglycan in Corynebacterium matruchotii. *Archives of Oral Biology,* 40, 1119-1124.

SUTCLIFFE, I. C. (1997) Macroamphiphilic cell envelope components of *Rhodococcus equi* and closely related bacteria. *Veterinary Microbiology,* 56, 287-299.

SUTCLIFFE, I. C. (1998) Cell envelope composition and organisation in the genus Rhodococcus. *Antonie Van Leeuwenhoek,* 74, 49-58.

SUTCLIFFE, I. C. (2000) Characterisation of a lipomannan lipoglycan from the mycolic acid containing actinomycete Dietzia maris. *Antonie Van Leeuwenhoek International Journal of General and Molecular Microbiology,* 78, 195-201.

SUTCLIFFE, I. C. & ALDERSON, G. (1995) A Chemotaxonomic Appraisal of the Distribution of Lipomannans within the Genus Micrococcus. *Fems Microbiology Letters,* 133, 233-237.

SUTCLIFFE, I. C. & OLD, L. A. (1995a) Stomatococcus-Mucilaginosus Produces a Mannose-Containing Lipoglycan Rather Than Lipoteichoic Acid. *Archives of Microbiology,* 163, 70-75.

SUTCLIFFE, I. C. & OLD, L. A. (1995b) *Stomatococcus mucilaginosus* produces a mannose-containing lipoglycan rather than lipoteichoic acid. *Arch Midorbiol,* 163, 70-75.

SUTCLIFFE, I. C. & RUSSELL, R. R. B. (1995) Lipoproteins of Gram-Positive Bacteria. *Journal of Bacteriology,* 177, 1123-1128.

SUTCLIFFE, I. C. & SHAW, N. (1991) Atypical lipoteichoic acis of Gram-positive bacteria. *Journal of Bacteriology,* 173, 7065-7069.

SUTCLIFFE, L. (2005) Lipoarabinomannans-structurally diverse and functionally enigmatic macroamphiphiles of mycobacteria and related actinomycetes. *Tuberculosis,* 85, 205-206.

SUZUKI, K., COLLINS, M. D., IIJIMA, E. & KOMAGATA, K. (1988) Chemotaxonomic Characterization of a Radiotolerant Bacterium, Arthrobacter-Radiotolerans - Description of Rubrobacter-Radiotolerans Gen-Nov, Comb Nov. *Fems Microbiology Letters,* 52, 33-39.

TAKAYAMA, K. & GOLDMAN, D. S. (1969) Pathway for the synthesis of mannophospholipids in Mycobacterium tuberculosis. *Biochim Biophys Acta,* 176, 196-8.

TARON, D. J., CHILDS, W. C. & NEUHAUS, F. C. (1983) Biosynthesis of D-Alanyl-Lipoteichoic Acid - Role of Diglyceride Kinase in the Synthesis of Phosphatidylglycerol for Chain Elongation. *Journal of Bacteriology,* 154, 1110-1116.

TATITURI, R. V. V., ALDERWICK, L. J., MISHRA, A. K., NIGOU, J., GILLERON, M., KRUMBACH, K., HITCHEN, P., GIORDANO, A., MORRI, H. R., DELL, A., EGGELING, L. & BESRA, G. S. (2007) Structural characterization of a partially arabinosylated lipoarabinomannan variant isolated from a Corynebacterium glutamicum ubiA mutant. *Microbiology-Sgm,* 153, 2621-2629.

THEILACKER, C., KACZYNSKI, Z., KROPEC, A., FABRETTI, F., SANGE, T., HOLST, O. & HUEBNER, J. (2006) Opsonic antibodies to Enterococcus faecalis strain 12030 are directed against lipoteichoic acid. *Infection and Immunity,* 74, 5703-5712.

THWAITES, J. J. & MENDELSON, N. H. (1991) Mechanical-Behavior of Bacterial-Cell Walls. *Advances in Microbial Physiology,* 32, 173-222.

TJALSMA, H., ANTELMANN, H., JONGBLOED, J. D. H., BRAUN, P. G., DARMON, E., DORENBOS, R., DUBOIS, J. Y. F., WESTERS, H., ZANEN, G., QUAX, W. J., KUIPERS, O. P., BRON, S., HECKER, M. & VAN DIJL, J. M. (2004) Proteomics of protein secretion by Bacillus subtilis: Separating the "secrets" of the secretome. *Microbiology and Molecular Biology Reviews,* 68, 207-+.

TJALSMA, H., BOLHUIS, A., JONGBLOED, J. D. H., BRON, S. & VAN DIJL, J. M. (2000) Signal peptide-dependent protein transport in Bacillus subtilis: a genome-based survey of the secretome. *Microbiology and Molecular Biology Reviews,* 64, 515-+.

TON-THAT, H., MARRAFFINI, L. A. & SCHNEEWIND, O. (2004) Protein sorting to the cell wall envelope of Gram-positive bacteria. *Biochimica Et Biophysica Acta-Molecular Cell Research,* 1694, 269-278.

TOON, P., BROWN, P. E. & BADDILEY, J. (1972) Lipid Teichoic Acid Complex in Cytoplasmic Membrane of Streptococcus-Faecalis Ncib 8191. *Biochemical Journal,* 127, 399-&.

TORRELLES, J. B., KHOO, K. H., SIELING, P. A., MODLIN, R. L., ZHANG, N. N., MARQUES, A. M., TREUMANN, A., RITHNER, C. D., BRENNAN, P. J. & CHATTERJEE, D. (2004) Truncated structural variants of lipoarabinomannan in Mycobacterium leprae and an

ethambutol-resistant strain of Mycobacterium tuberculosis. *Journal of Biological Chemistry,* 279, 41227-41239.

TOTSUKA, M., SHIBATA, K. I. & WATANABE, T. (1990) Chemical-Analyses, Local Shwartzman Reactivity, and Body Weight-Decreasing Activity of Aqueous-Phenol Extracts of Mycoplasma-Salivarium Cells - Biological-Activities of Mycoplasma-Salivarium. *Antonie Van Leeuwenhoek International Journal of General and Molecular Microbiology,* 58, 73-77.

TOUHAMI, A., JERICHO, M. H. & BEVERIDGE, T. J. (2004) Atomic force microscopy of cell growth and division in Staphylococcus aureus. *J Bacteriol,* 186, 3286-95.

TRESNER, H. D., DAVIES, M. C. & BACKUS, E. J. (1961) Electron microscopy of *Streptomyces* spore morphology and its role in species differentiation. *Journal of Bacteriology,* 81, 70-80.

TREUMANN, A., FENG, X. D., MCDONNELL, L., DERRICK, P. J., ASHCROFT, A. E., CHATTERJEE, D. & HOMANS, S. W. (2002) 5-methylthiopentose: a new substituent on lipoarabinomannan in Mycobacterium tuberculosis. *Journal of Molecular Biology,* 316, 89-100.

TROPIS, M., LEMASSU, A., VINCENT, V. & DAFFE, M. (2005) Structural elucidation of the predominant motifs of the major cell wall arabinogalactan antigens from the borderline species Tsukamurella paurometabolum and Mycobacterium fallax. *Glycobiology,* 15, 677-686.

TSAI, C. M. & FRASCH, C. E. (1982) A Sensitive Silver Stain for Detecting Lipopolysaccharides in Polyacrylamide Gels. *Analytical Biochemistry,* 119, 115-119.

TUL'SKAYA, E. M., SHASHKOV, A. S., SENCHENKOVA, S. N., AKIMOV, V. N., BUEVA, O. V., STUPAR, O. S. & EVTUSHENKO, L. I. (2007) Anionic polymers of the cell wall of Streptomyces sp VKM Ac-2534. *Russian Journal of Bioorganic Chemistry,* 33, 251-257.

TULSKAYA, E. M., SHASHKOV, A. S., BUYEVA, O. V. & EVTUSHENKO, L. I. (2007) Anionic carbohydrate-containing cell wall polymers of Streptomyces melanosporofaciens and related species. *Microbiology,* 76, 39-44.

TURNBULL, W. B., SHIMIZU, K. H., CHATTERJEE, D., HOMANS, S. W. & TREUMANN, A. (2004) Identification of the 5-methylthiopentosyl substituent in mycobacterium tuberculosis lipoarabinomannan. *Angewandte Chemie-International Edition,* 43, 3918-3922.

UCHIDA, K. & AIDA, K. (1977) Acyl Type of Bacterial-Cell Wall - Simple Identification by Colorimetric Method. *Journal of General and Applied Microbiology,* 23, 249-260.

UCHIDA, K. & AIDA, K. (1979) Taxonomic Significance of Cell-Wall Acyl Type in Corynebacterium-Mycobacterium-Nocardia Group by a Glycolate Test. *Journal of General and Applied Microbiology,* 25, 169-183.

VAN VEEN, H. W. & KONINGS, W. N. (1998) The ABC family of multidrug transporters in microorganisms. *Biochimica Et Biophysica Acta-Bioenergetics,* 1365, 31-36.

VANDENBOGART, H. G. G., VANDENENDE, G., VANLOON, P. C. C. & VANGRIENSVEN, L. J. L. D. (1993) Mushroom Workers Lung - Serologic Reactions to Thermophilic Actinomycetes Present in the Air of Compost Tunnels. *Mycopathologia,* 122, 21-28.

VENTURA, M., CANCHAYA, C., TAUCH, A., CHANDRA, G., FITZGERALD, G. F., CHATER, K. F. & VAN SINDEREN, D. (2007) Genomics of Actinobacteria: Tracing the evolutionary history of an ancient phylura. *Microbiology and Molecular Biology Reviews,* 71, 495-+.

VERCELLONE, A., NIGOU, J. & PUZO, G. (1998) Relationships between the structure and the roles of lipoarabinomannans and related glycoconjugates in tuberculosis pathogenesis. *Front Biosci,* 3, e149-63.

VEREB, G., SZOLLOSI, J., MATKO, J., NAGY, P., FARKAS, T., VIGH, L., MATYUS, L., WALDMANN, T. A. & DAMJANOVICH, S. (2003) Dynamic, yet structured: The cell membrane three decades after the Singer-Nicolson model. *Proceedings of the National Academy of Sciences of the United States of America,* 100, 8053-8058.

WALSH, S., KOKAI-KUN, J., SHAH, A. & MOND, J. (2004) Extended nasal residence time of lysostaphin and an anti-staphylococcal monoclonal antibody by delivery in semisolid or polymeric carriers. *Pharmaceutical Research,* 21, 1770-1775.

WANG, Y. X., ZHI, X. Y., CHEN, H. H., ZHANG, Y. Q., TANG, S. K., JIANG, C. L., XU, L. H. & LI, W. J. (2007) Streptomyces serianimatus sp nov., isolated from a rhizophere soil. *Antonie Van Leeuwenhoek International Journal of General and Molecular Microbiology,* 92, 201-206.

WEIDENMAIER, C., KOKAI-KUN, J. F., KRISTIAN, S. A., CHANTURIYA, T., KALBACHER, H., GROSS, M., NICHOLSON, G., NEUMEISTER, B., MOND, J. J. & PESCHEL, A. (2004) Role of teichoic acids in Staphylococcus aureus nasal colonization, a major risk factor in nosocomial infections. *Nature Medicine,* 10, 243-245.

WEIDENMAIER, C. & PESCHEL, A. (2008) Teichoic acids and related cell-wall glycopolymers in Gram-positive physiology and host interactions. *Nature Reviews Microbiology,* 6, 276-287.

WEIDENMAIER, C., PESCHEL, A., XIONG, Y. Q., KRISTIAN, S. A., DIETZ, K., YEAMAN, M. R. & BAYER, A. S. (2005) Lack of wall teichoic acids in Staphylococcus aureus leads to reduced interactions with endothelial cells and to attenuated virulence in a rabbit model of endocarditis. *Journal of Infectious Diseases,* 191, 1771-1777.

WHALE, G. A., SUTCLIFFE, I. C., MORRISSON, A. R., PRETSWELL, E. L. & EMMISON, N. (2004) Purification and characterisation of lipoglycan macroamphiphiles from Propionibacterium acnes. *Antonie Van Leeuwenhoek International Journal of General and Molecular Microbiology,* 86, 77-85.

WICKEN, A. J., BROADY, K. W., EVANS, J. D. & KNOX, K. W. (1978) New Cellular and Extracellular Amphipathic Antigen from Actinomyces Viscosus Ny1. *Infection and Immunity,* 22, 615-616.

WICKEN, A. J., EVANS, J. D. & KNOX, K. W. (1986) Critical Micelle Concentrations of Lipoteichoic Acids. *Journal of Bacteriology,* 166, 72-77.

WICKEN, A. J. & KNOX, K. W. (1975) Lipoteichoic Acids - New Class of Bacterial Antigen. *Science,* 187, 1161-1167.

WICKEN, A. J. & KNOX, K. W. (1980) Bacterial-Cell Surface Amphiphiles. *Biochimica Et Biophysica Acta,* 604, 1-26.

WILKINSON, S. G. (1969) Lipids of Pseudomonas diminuta. *Biochim Biophys Acta,* 187, 492-500.

WILLIAMS, S. T., SHARPE, M. E. & HOLT, J. G. (Eds.) (1989) *Bergey's Mannual of Systematic Bacteriology,* Baltimore, Maryland, Williams and Wilkins.

WITT, D. & STACKEBRANDT, E. (1990) Unification of the Genera Streptoverticillum and Streptomyces, and Amendation of Streptomyces-Waksman and Henrici-1943, 339al. *Systematic and Applied Microbiology,* 13, 361-371.

WOLF, A., KRAMER, R. & MORBACH, S. (2003) Three pathways for trehalose metabolism in Corynebacterium glutamicum ATCC13032 and their significance in response to osmotic stress. *Molecular Microbiology,* 49, 1119-1134.

WOLUCKA, B. A., MCNEIL, M. R., DEHOFFMANN, E., CHOJNACKI, T. & BRENNAN, P. J. (1994) Recognition of the Lipid Intermediate for Arabinogalactan Arabinomannan Biosynthesis and Its Relation to the Mode of Action of Ethambutol on Mycobacteria. *Journal of Biological Chemistry,* 269, 23328-23335.

WRIGHT, J. & HECKELS, J. E. (1975) Teichuronic Acid of Cell-Walls of Bacillus-Subtilis W23 Grown in a Chemostat under Phosphate Limitation. *Biochemical Journal,* 147, 187-189.

YOKOTA, A., TAMURA, T., NISHII, T. & HASEGAWA, T. (1993) *Kineococcus aurantiacus* Gen-Nov, Sp-Nov, a New Aerobic, Gram-Positive, Motile Coccus with Meso-Diaminopimelic Acid and Arabinogalactan in the Cell-Wall. *International Journal of Systematic Bacteriology,* 43, 52-57.

YOKOYAMA, K., MIZUGUCHI, H., ARAKI, Y., KAYA, S. & ITO, E. (1989) Biosynthesis of Linkage Units for Teichoic-Acids in Gram-Positive Bacteria - Distribution of Related Enzymes and Their Specificities for Udp-Sugars and Lipid-Linked Intermediates. *Journal of Bacteriology,* 171, 940-946.

YOSHINAK.T, YANO, K. & YAMAGUCH.H (1973) Isolation of Highly Radioresistant Bacterium, Arthrobacter-Radiotolerans Nov-Sp. *Agricultural and Biological Chemistry,* 37, 2269-2275.

ZHANG, N., TORRELLES, J. B., MCNEIL, M. R., ESCUYER, V. E., KHOO, K. H., BRENNAN, P. J. & CHATTERJEE, D. (2003) The Emb proteins of mycobacteria direct arabinosylation of lipoarabinomannan and arabinogalactan via an N-terminal recognition region and a C-terminal synthetic region. *Molecular Microbiology,* 50, 69-76.

ZHANG, Y. M. & ROCK, C. O. (2008) Membrane lipid homeostasis in bacteria. *Nature Reviews Microbiology,* 6, 222-233.

ZHANG, Z. S., WANG, Y. & RUAN, J. S. (1998) Reclassification of Thermomonospora and Microtetraspora. *International Journal of Systematic Bacteriology,* 48, 411-422.

ZHOU, W. L., IRWIN, D. C., ESCOVAR-KOUSEN, J. & WILSON, D. B. (2004) Kinetic studies of Thermobifida fusca Cel9A active site mutant enzymes. *Biochemistry,* 43, 9655-9663.

Appendix I

S. agalactiae (GBS)

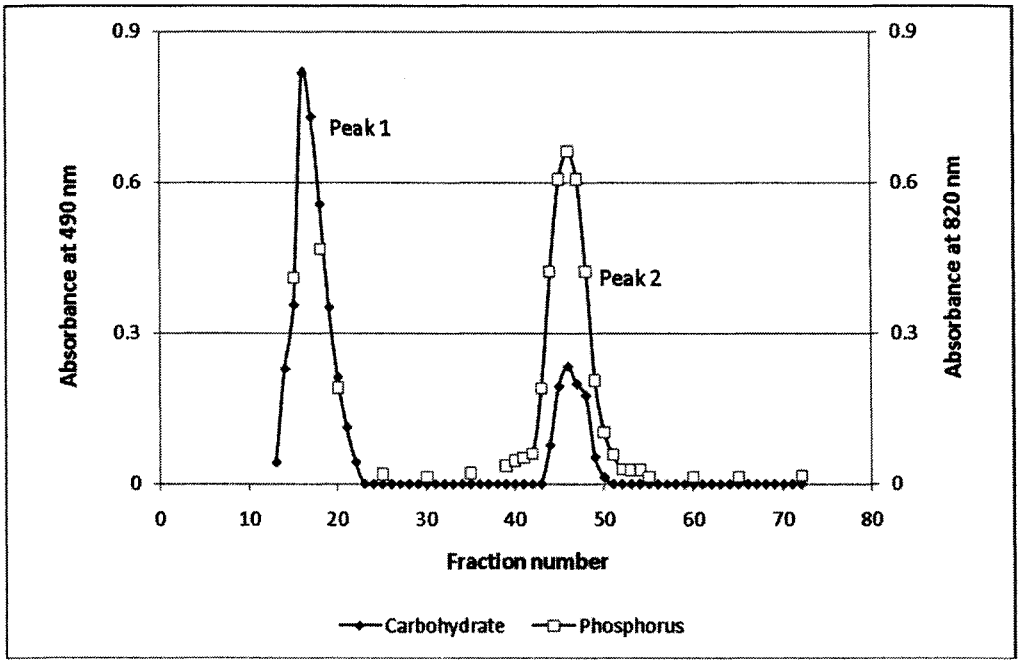

Figure I.1. HIC profile for the purification of a crude phenol extract of FPLC run 1 for GBS. The crude extract was loaded to the column with equilibration buffer until fraction 12, after which gradient elution with an increasing concentration of propanol was begun. Column fractions (4 mL) were analyzed for carbohydrate and phosphorus.

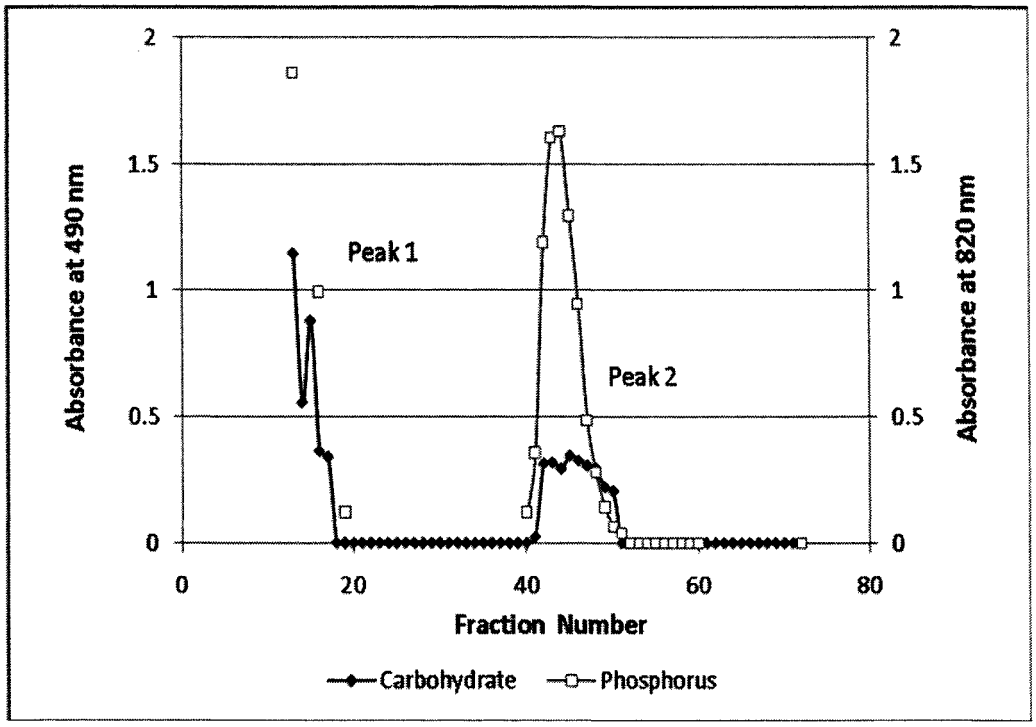

Figure I.2. HIC profile for the purification of a crude phenol extract of FPLC run 2 for GBS. The crude extract was loaded to the column with equilibration buffer until fraction 12, after which gradient elution with an increasing concentration of propanol was begun. Column fractions (4 mL) were analyzed for carbohydrate and phosphorus.

Appendix Two

T. fusca

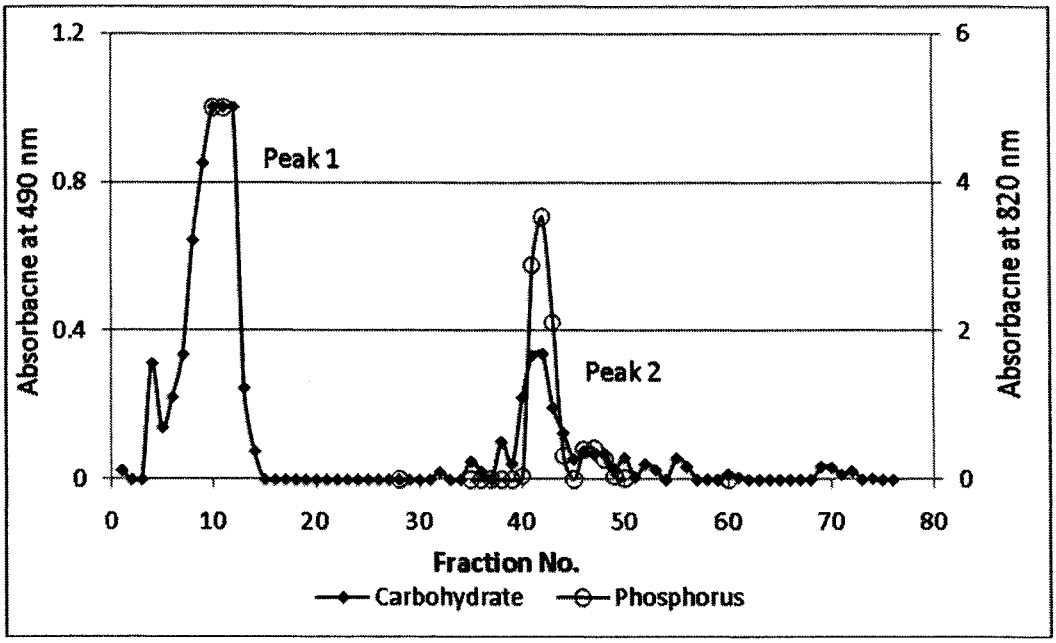

Figure II.1. HIC profile for the purification of a crude phenol extract of FPLC run 1 for *T. fusca*. The crude extract was loaded to the column with equilibration buffer until fraction 12, after which gradient elution with an increasing concentration of propanol was begun. Column fractions (4 mL) were analyzed for carbohydrate and phosphorus.

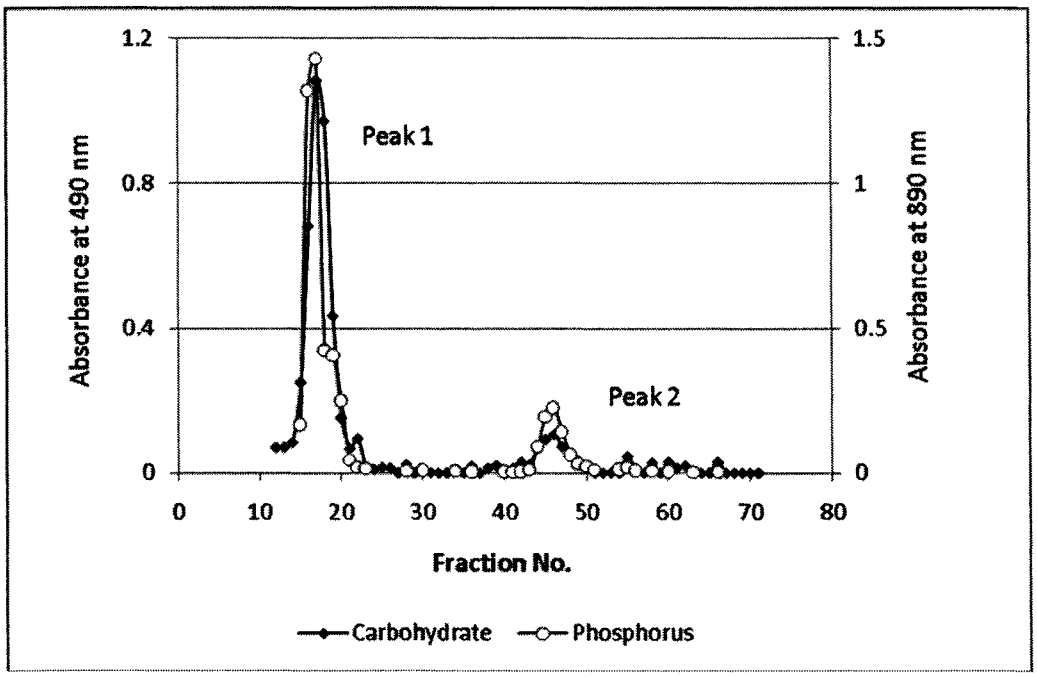

Figure II.2. HIC profile for the purification of a crude phenol extract of FPLC run 2 (cellobiose was used as carbon source in the media) as for *T. fusca*. The crude extract was loaded to the column with equilibration buffer until fraction 12, after which gradient elution with an increasing concentration of propanol was begun. Column fractions (4 mL) were analyzed for carbohydrate and phosphorus.

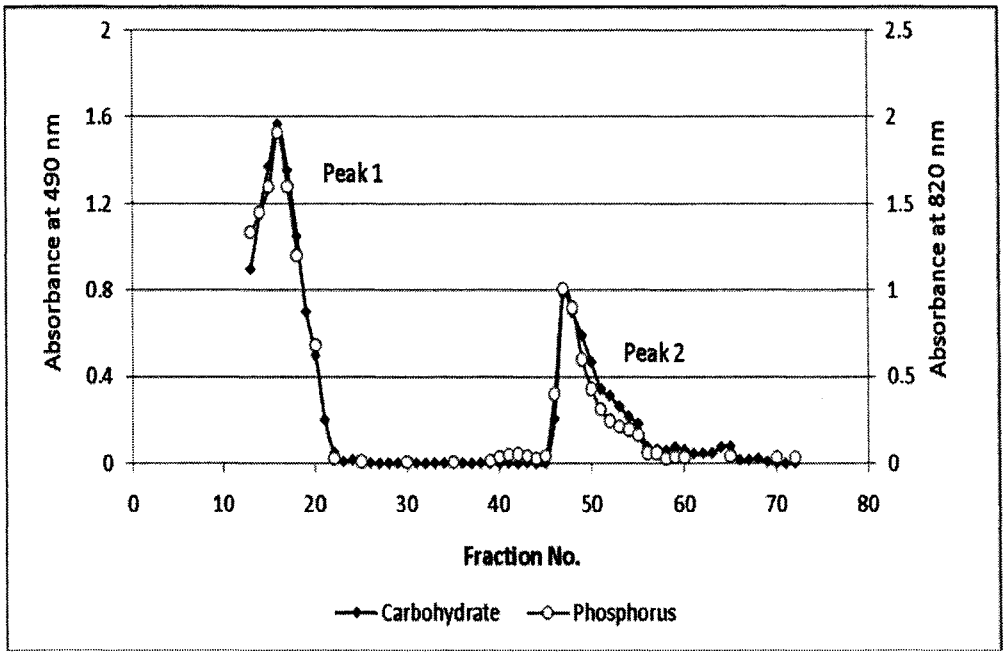

Figure II.3. HIC profile for the purification of a crude phenol extract of FPLC run 6 for *T. fusca*. The crude extract was loaded to the column with equilibration buffer until fraction 12, after which gradient elution with an increasing concentration of propanol was begun. Column fractions (4 mL) were analyzed for carbohydrate and phosphorus.

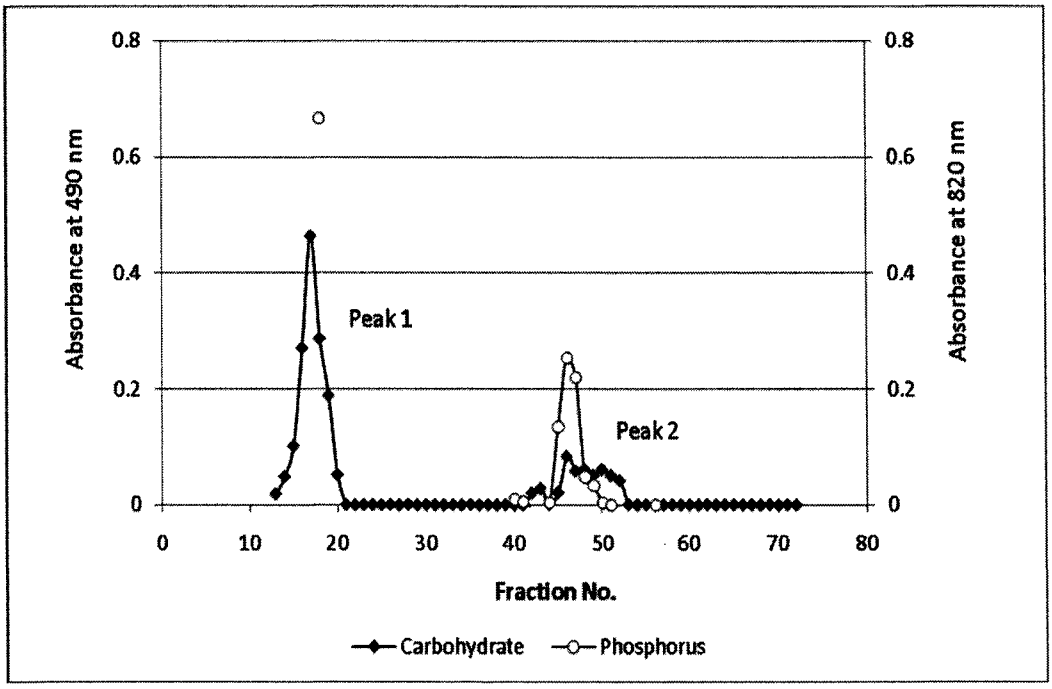

Figure II.4. HIC profile for the purification of a crude phenol extract of FPLC run 7 for *T. fusca*. The crude extract was loaded to the column with equilibration buffer until fraction 12, after which gradient elution with an increasing concentration of propanol was begun. Column fractions (4 mL) were analyzed for carbohydrate and phosphorus.

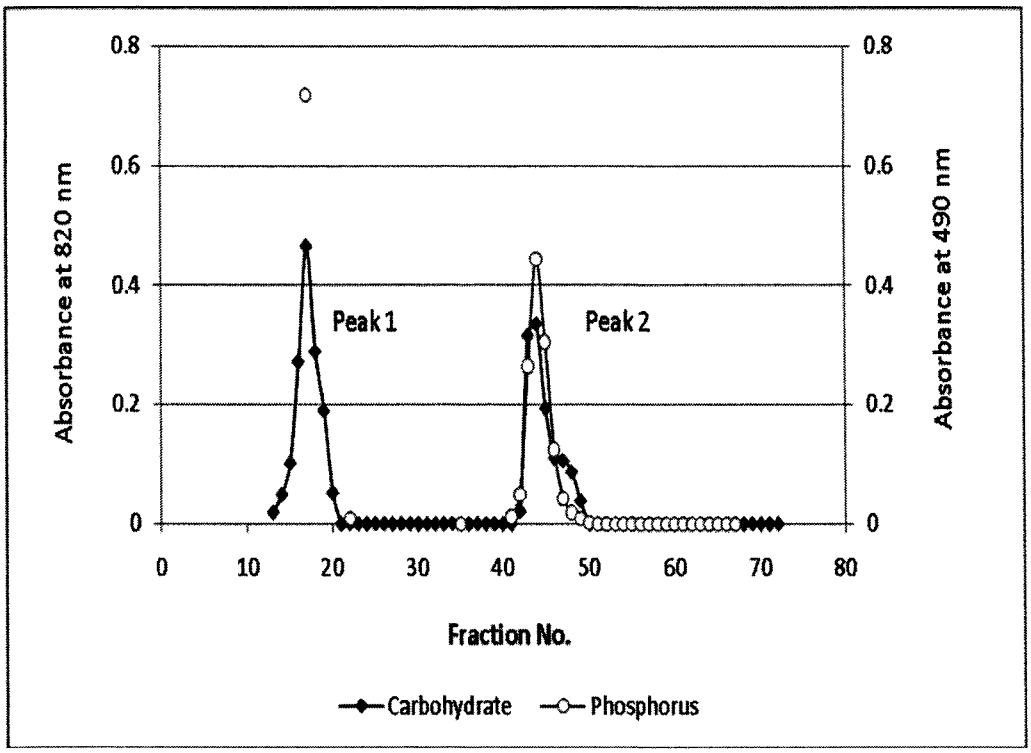

Figure II.5. HIC profile for the purification of a crude phenol extract of FPLC run 8 for *T. fusca*. The crude extract was loaded to the column with equilibration buffer until fraction 12, after which gradient elution with an increasing concentration of propanol was begun. Column fractions (4 mL) were analyzed for carbohydrate and phosphorus.

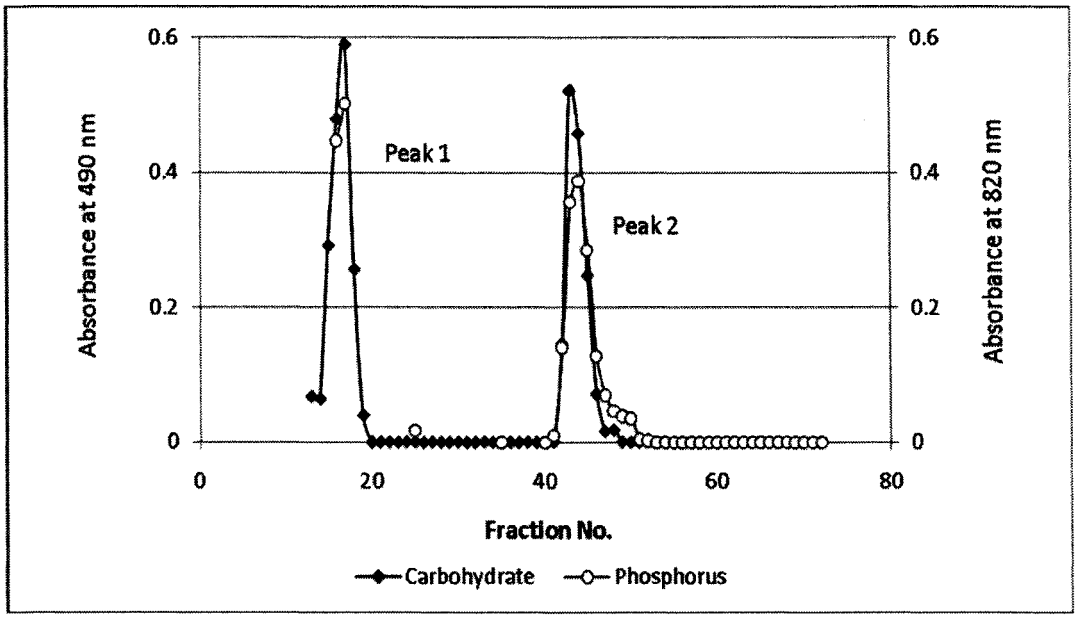

Figure II.6. HIC profile for the purification of a crude phenol extract of FPLC run 9 (cellobiose was used as carbon source in the media) for *T. fusca*. The crude extract was loaded to the column with equilibration buffer until fraction 12, after which gradient elution with an increasing concentration of propanol was begun. Column fractions (4 mL) were analyzed for carbohydrate and phosphorus.

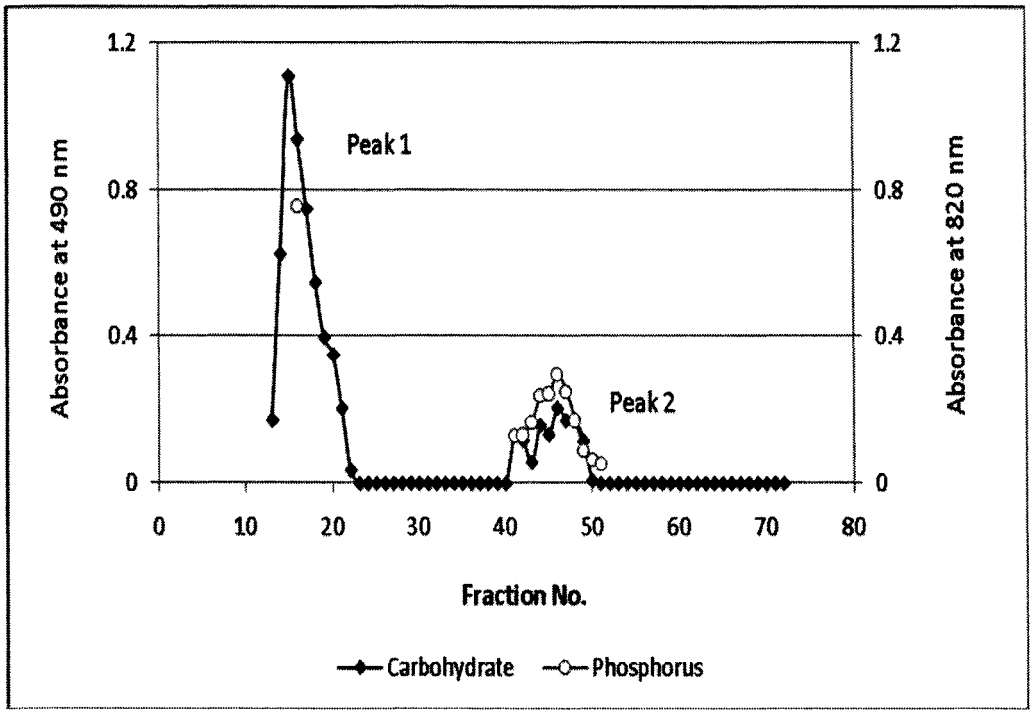

Figure II.7. HIC profile for the purification of a crude phenol extract of FPLC run 10 for *T. fusca*. The crude extract was loaded to the column with equilibration buffer until fraction 12, after which gradient elution with an increasing concentration of propanol was begun. Column fractions (4 mL) were analyzed for carbohydrate and phosphorus.

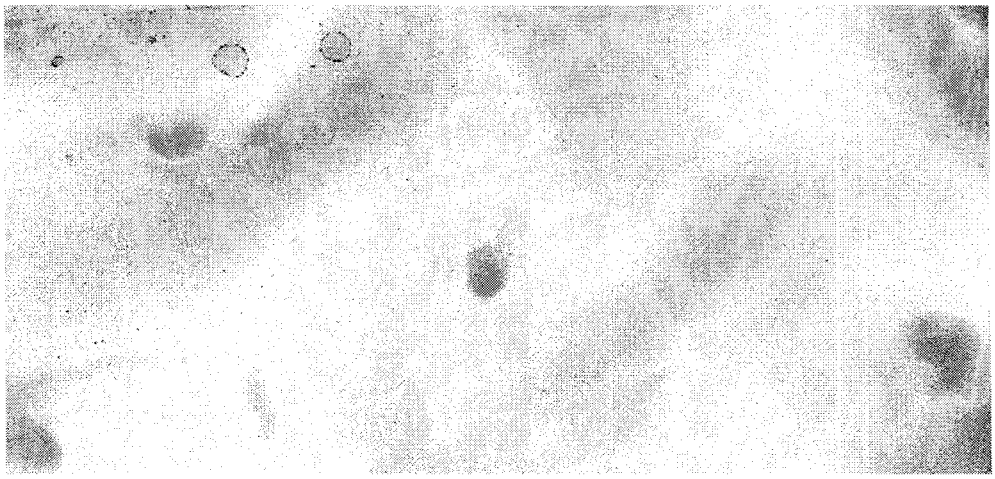

Figure II.8. Two dimensional gels figure for TfuLTA.

Appendix Three

R. xylanophilus

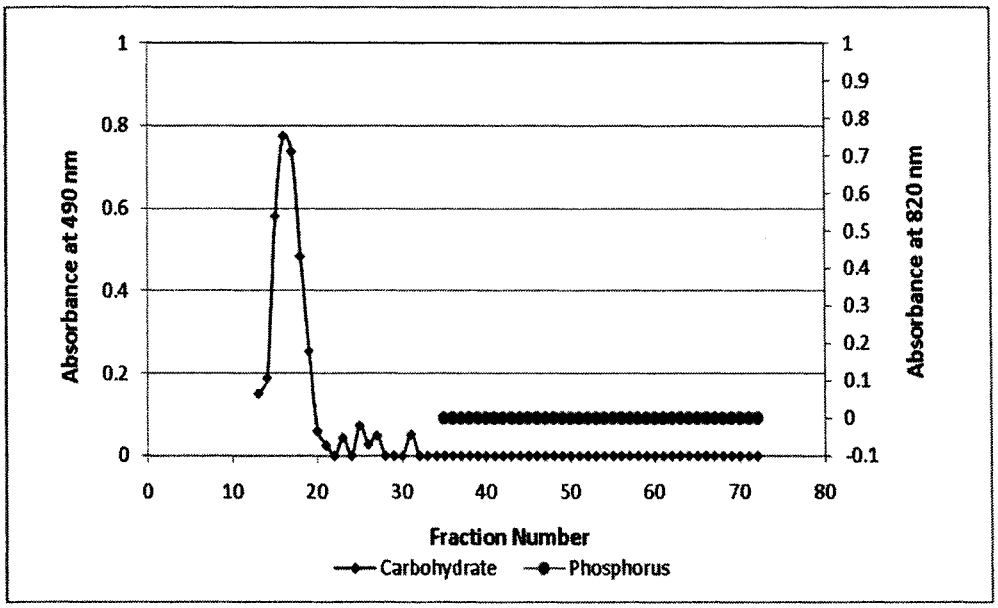

Figure III.1 HIC profile for the purification of a crude phenol extract of FPLC run 3 for *R. xylanophilus*. The crude extract was loaded to the column with equilibration buffer until fraction 12, after which gradient elution with an increasing concentration of propanol was begun. Column fractions (4 mL) were analyzed for carbohydrate and phosphorus.

List of organisms used in the phylogenetic tree in Figure 4.5, 8.1 and 8.2

Out Group:

1) Aquifecae – Aquifox aeolicus	Aa
2) Deinococcus – Deinococcus gethermals Strain 50051	Dg
Firmicutes:	
1) Clostridia – Butyrivibrio fibrisolvens	Bf
2) Mycoplasma – Mycoplasma pneumoniae M129	Mp
3) Bacillus- Bacillus subtilis 168	Bs
Staphylococcus aureus RF122	Sa
4) Lactobacillus – Streptococcus agalactiae A909	GBS
Streptococcus pneumoniae R6	Sp
Lactococcus lactis r1403	Ll
5) Caldithrix – Caldithrix abyssi LF13T	Ca

Actibobacteria:

1) Bifidobacterium – bifidobacterium longum NCC2705	Bl
Gardnerella vaginalis	Gv
2) Acidomicrobiales – Acidomicrobium ferrodoxians	Af
3) Corriobacteriales: Atopobium vaginae	Av
4) Rubrobacter: Rubrobacter xylanophilus DSM9941	Rx
Rubrobacter raiotolerans	Ra
5) Actionomycelates:	
i) Micorcoccus: Micorcoccus luteus	Ml
ii) Nocardiaceae: Rhodococcus equi DSM777	Re
iii) Propionibacterium: Propinobacterium acnes KPA171202	Pa
iv) Pseudonacardiaceae: Saccharopolyspora histura	Sh
v) Gordoniaceae: Gordonia terrae	Gt
vi) Mycobacterium: Mycobacterium tuberculosis	Mt
Mycobacterium bovis	Mb
vii) Dietziaceae: Dietzia maris	Dm
viii) Tsukamurellaceae: Tsukmurella paurometabola	Tm
ix) Corynebacteriaeceae: Corynebacterium diptheriae	Cd
x)Jonesiaceae: Jonesiaceae dentrificans	Jd
xi) Streptomyceae: Streptomyces coelicolor	Sc
Streptomyces avermitillis	Sa
xii) Kineosporiaceae: Kineococcus marinus	Km
xiii) Nocardiopseceae: Thermobifida fusca	Tf
xiv) Actinomyces: Actinomyces viscous	Avi
xv) Agromyces: Agromyces mediolanous	Am
xvi)Frankia: Frankia alni ACN14a	Fa
xvii) Micromonospora: Micromonospora olivoasterospora	Mo1

Appendix Four

K. radiotolerans

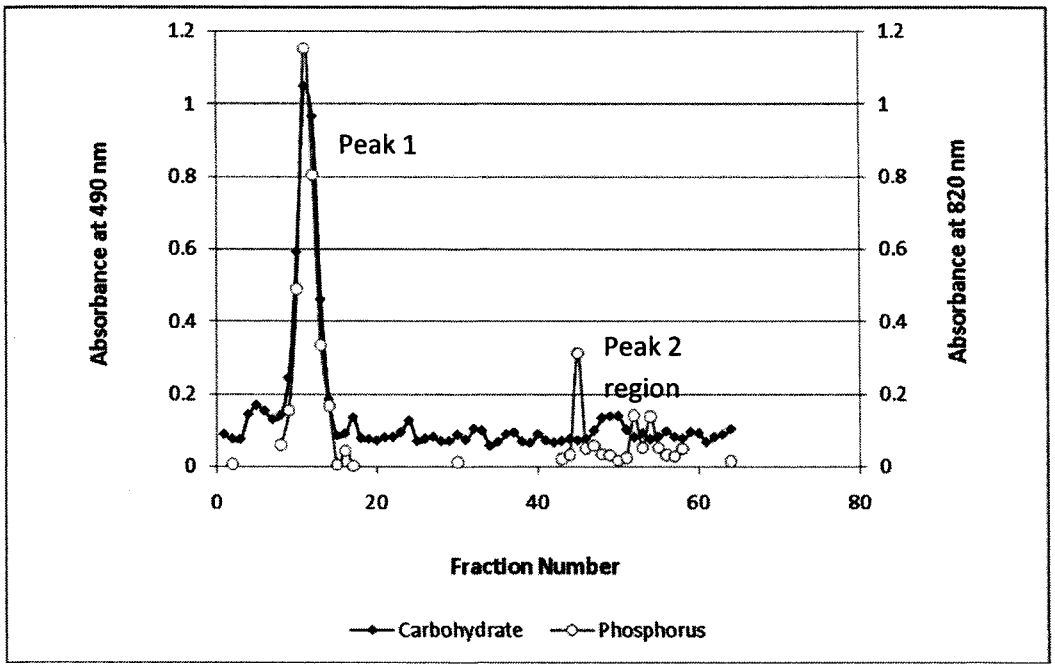

Figure IV.1 HIC profile for the purification of a crude phenol extract of FPLC run 1 for *K. radiotolerans*. The crude extract was loaded to the column with equilibration buffer until fraction 12, after which gradient elution with an increasing concentration of propanol was begun. Column fractions (4 mL) were analyzed for carbohydrate and phosphorus.

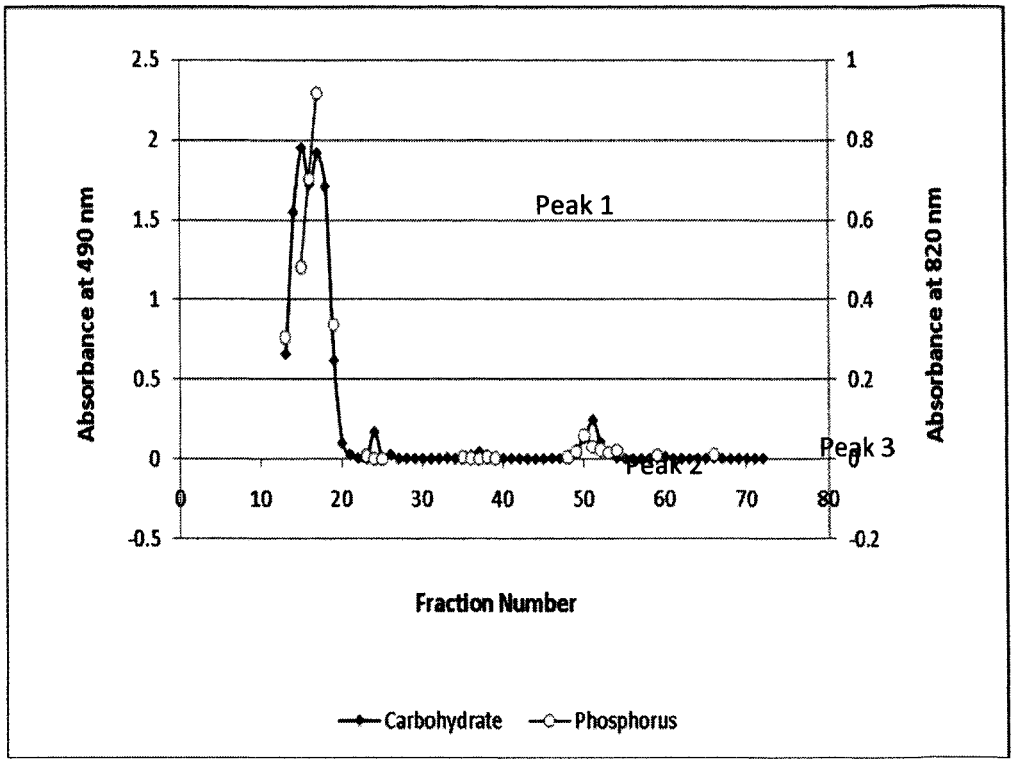

Figure IV.2 HIC profile for the purification of a crude phenol extract of FPLC run 2 for *K. radiotolerans*. The crude extract was loaded to the column with equilibration buffer until fraction 12, after which gradient elution with an increasing concentration of propanol was begun. Column fractions (4 mL) were analyzed for carbohydrate and phosphorus.

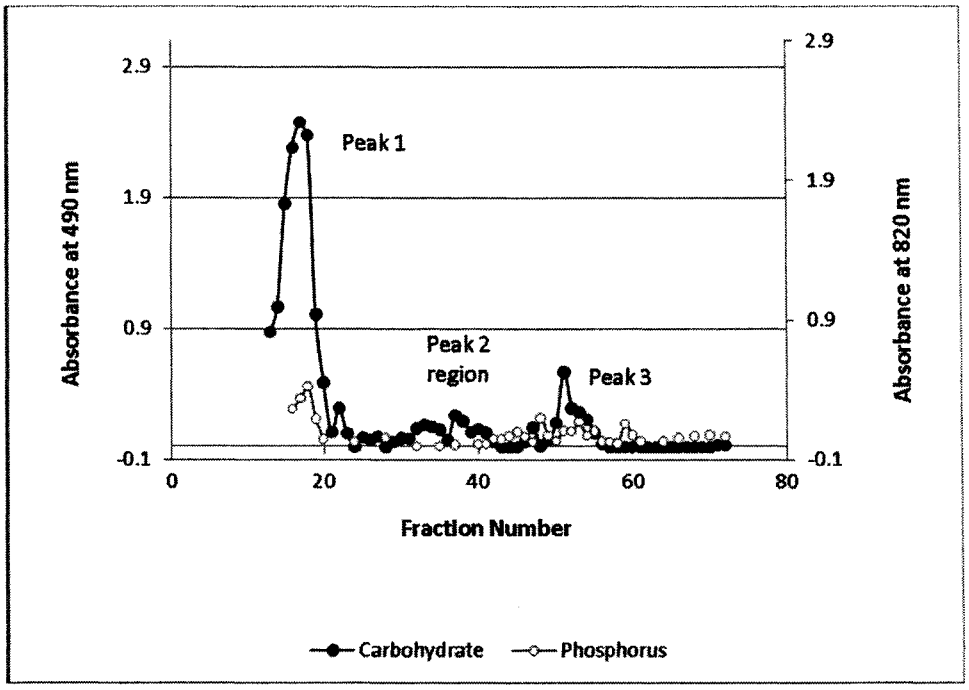

Figure IV.3 HIC profile for the purification of a crude phenol extract of FPLC run 3 for *K. radiotolerans*. The crude extract was loaded to the column with equilibration buffer until fraction 12, after which gradient elution with an increasing concentration of propanol was begun. Column fractions (4 mL) were analyzed for carbohydrate and phosphorus.

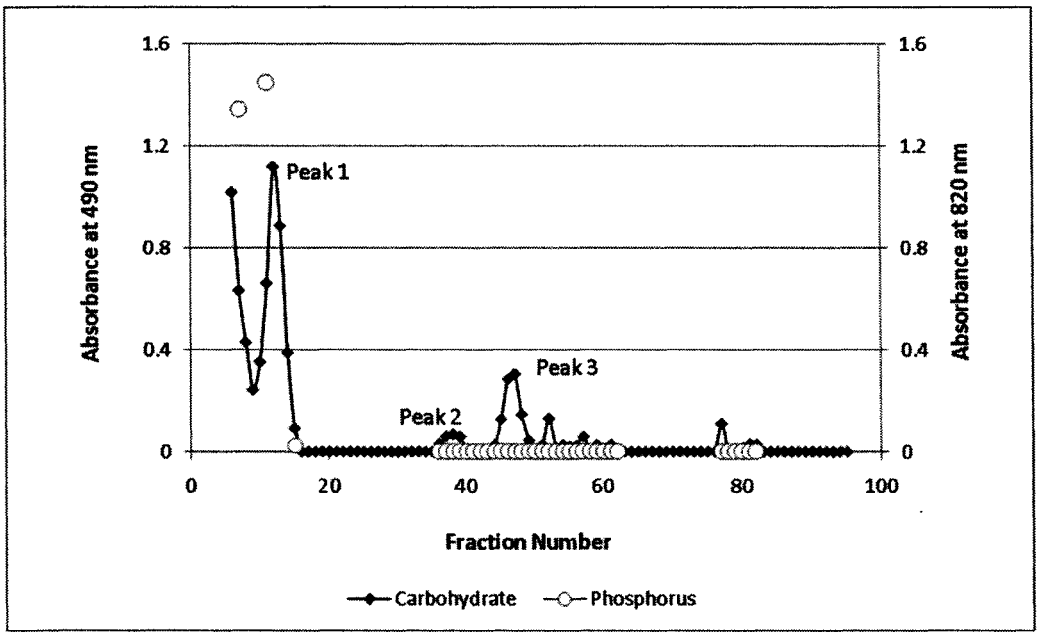

Figure IV.4 HIC profile for the purification of a crude phenol extract of FPLC run 4 for *K. radiotolerans*. The crude extract was loaded to the column with equilibration buffer until fraction 12, after which gradient elution with an increasing concentration of propanol was begun. Column fractions (4 mL) were analyzed for carbohydrate and phosphorus.

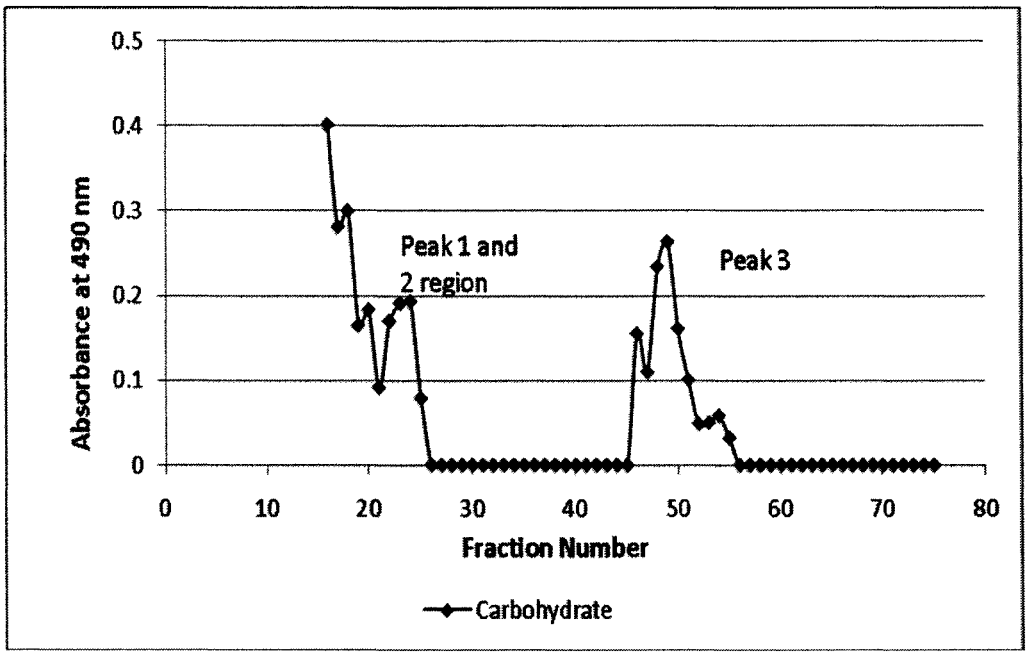

Figure IV.5 HIC profile for the purification of a crude phenol extract of FPLC run 5 for *K. radiotolerans*. The crude extract was loaded to the column with equilibration buffer until fraction 12, after which gradient elution with an increasing concentration of propanol was begun. Column fractions (4 mL) were analyzed for carbohydrate.

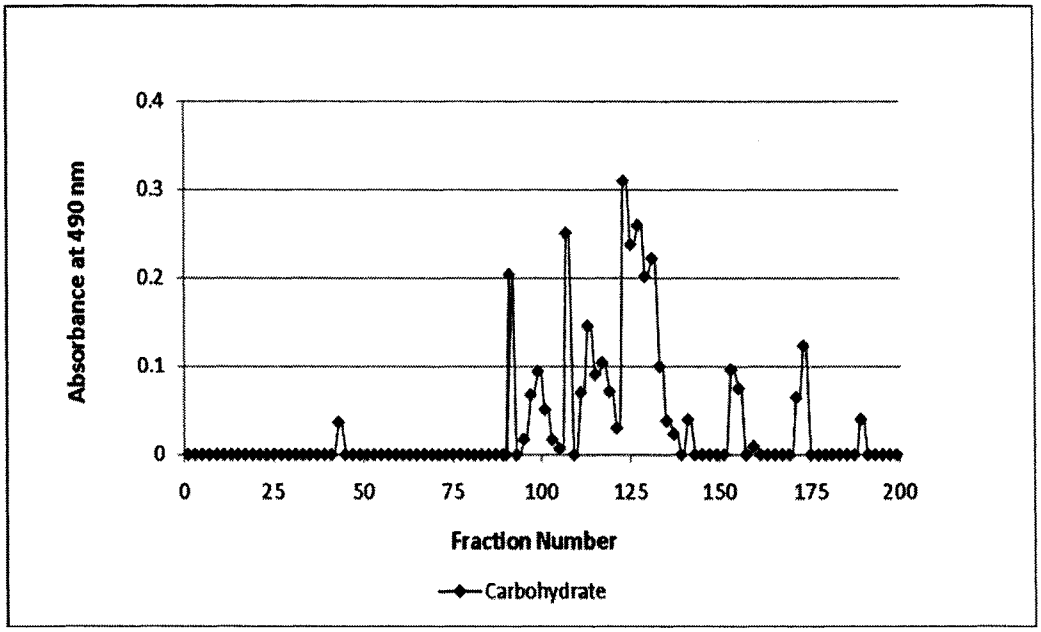

Figure IV.6 Anion exchange profile for the crude phenol extract (peak 3) of FPLC run 5 for *K. radiotolerans*. The crude extract was loaded to the column with equilibration buffer until fraction 12, after which gradient elution with an increasing concentration of propanol was begun. Column fractions (4 mL) were analyzed for carbohydrate.

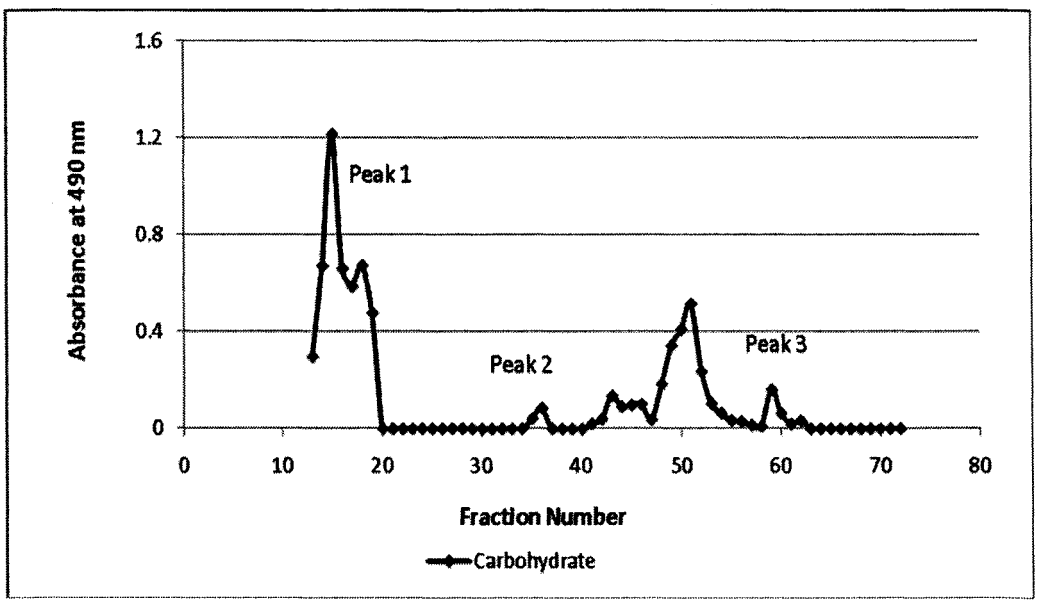

Figure IV.7. HIC profile for the purification of a crude phenol extract of FPLC run 6 for *K. radiotolerans*. The crude extract was loaded to the column with equilibration buffer until fraction 12, after which gradient elution with an increasing concentration of propanol was begun. Column fractions (4 mL) were analyzed for carbohydrate.

Appendix V

S. coelicolor M145

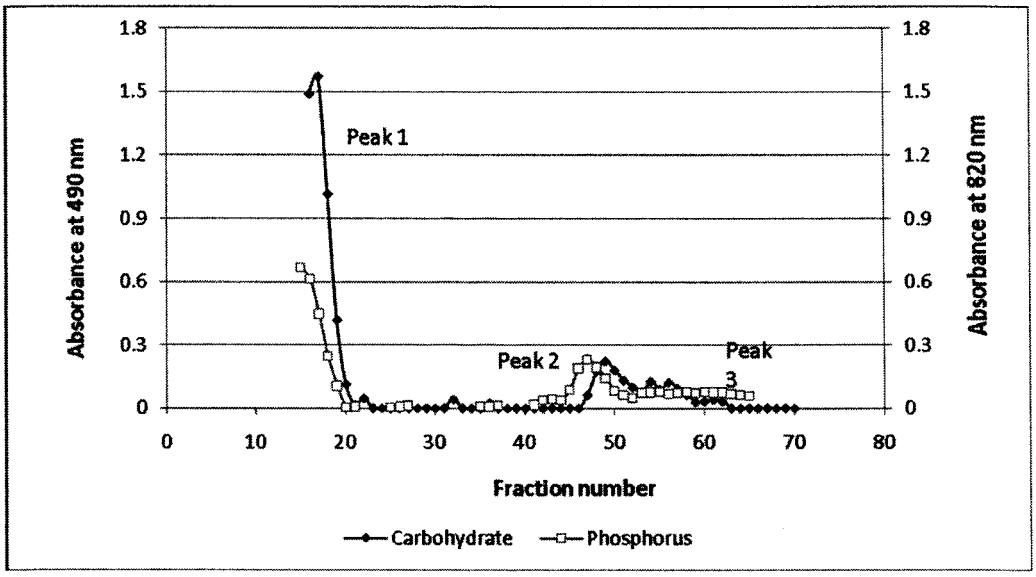

Figure V.1. HIC profile for the purification of a crude phenol extract of FPLC run 2 for *S. coelicolor* M145 . The crude extract was loaded to the column with equilibration buffer until fraction 12, after which gradient elution with an increasing concentration of propanol was begun. Column fractions (4 mL) were analyzed for carbohydrate.

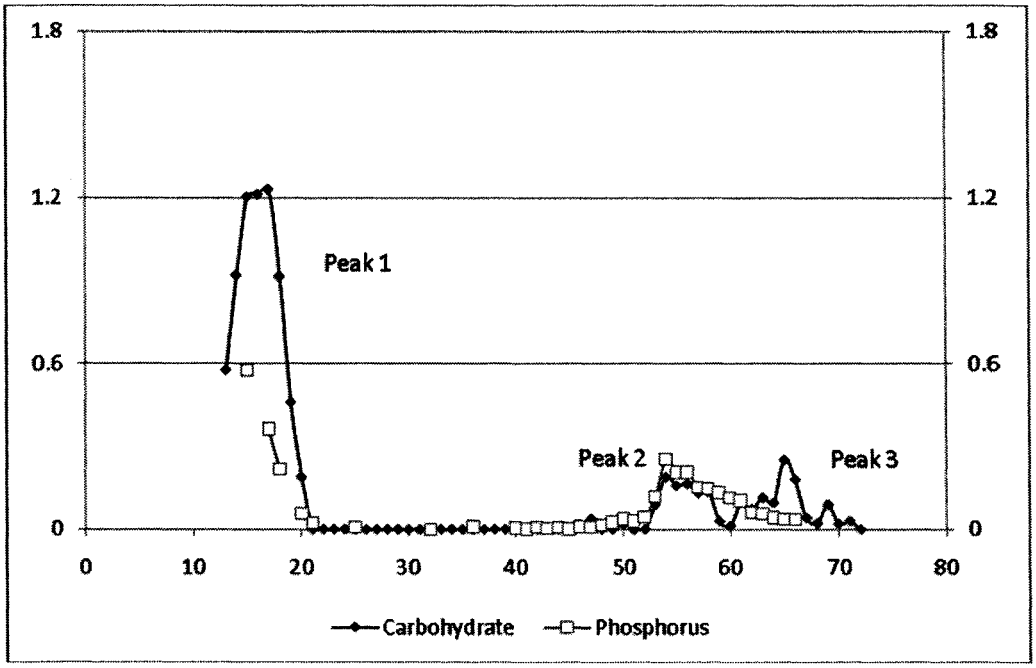

Figure V.2. HIC profile for the purification of a crude phenol extract of FPLC run 3 for *S. coelicolor* M145 . The crude extract was loaded to the column with equilibration buffer until fraction 12, after which gradient elution with an increasing concentration of propanol was begun. Column fractions (4 mL) were analyzed for carbohydrate.

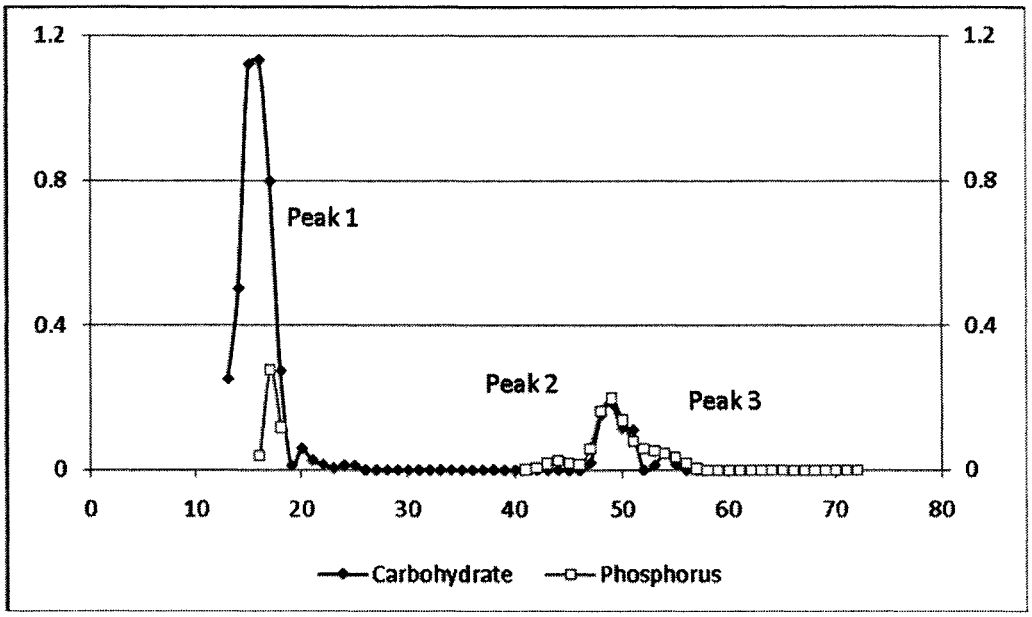

Figure V.3. HIC profile for the purification of a crude phenol extract of FPLC run 4 for *S. coelicolor* M145 . The crude extract was loaded to the column with equilibration buffer until fraction 12, after which gradient elution with an increasing concentration of propanol was begun. Column fractions (4 mL) were analyzed for carbohydrate.

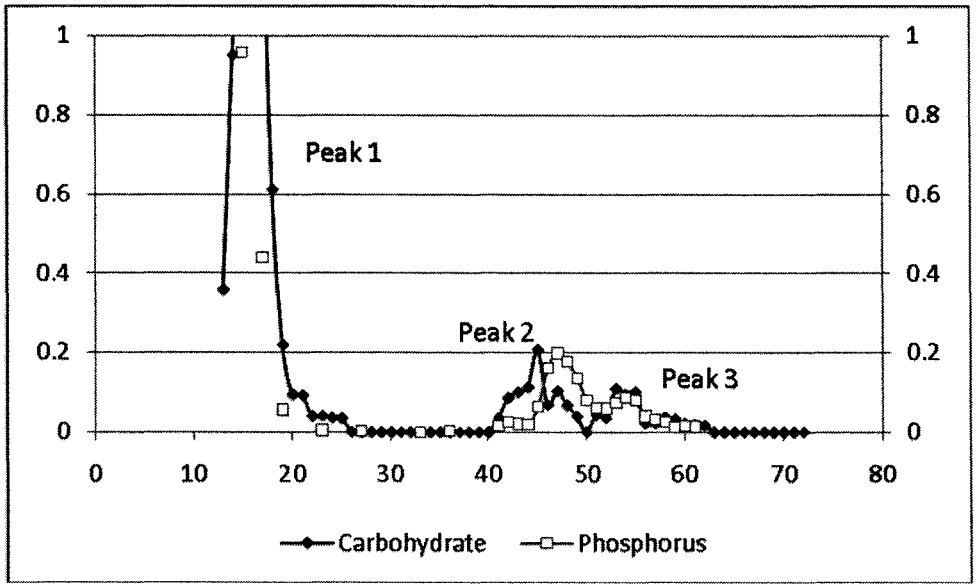

Figure V.4. HIC profile for the purification of a crude phenol extract of FPLC run 5 for *S. coelicolor* M145 . The crude extract was loaded to the column with equilibration buffer until fraction 12, after which gradient elution with an increasing concentration of propanol was begun. Column fractions (4 mL) were analyzed for carbohydrate.

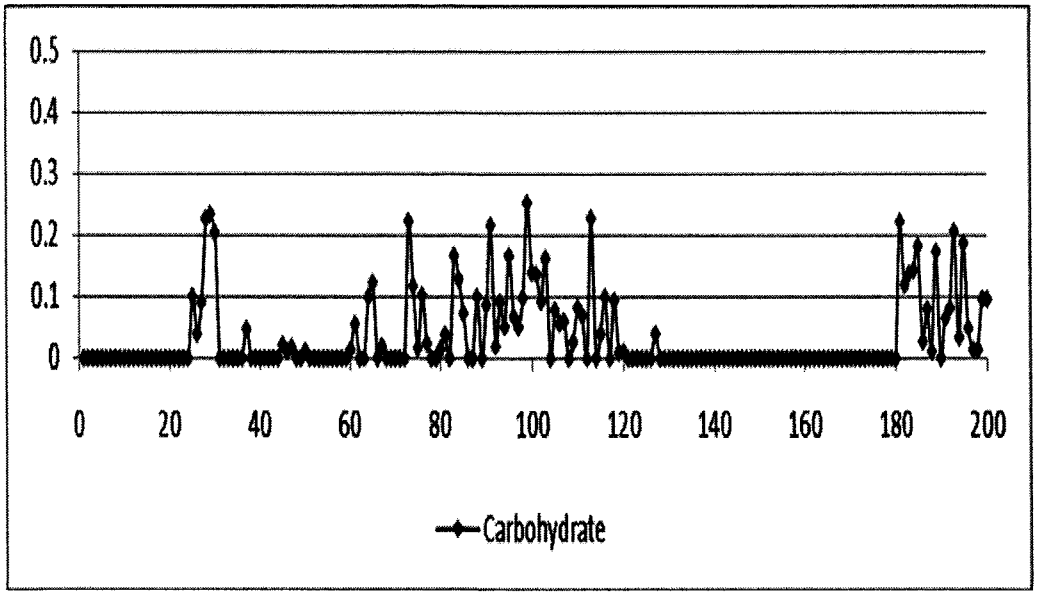

Figure V.5. Anion exchange chromatography profile of FPLC run 5 for *S. coelicolor* M145.

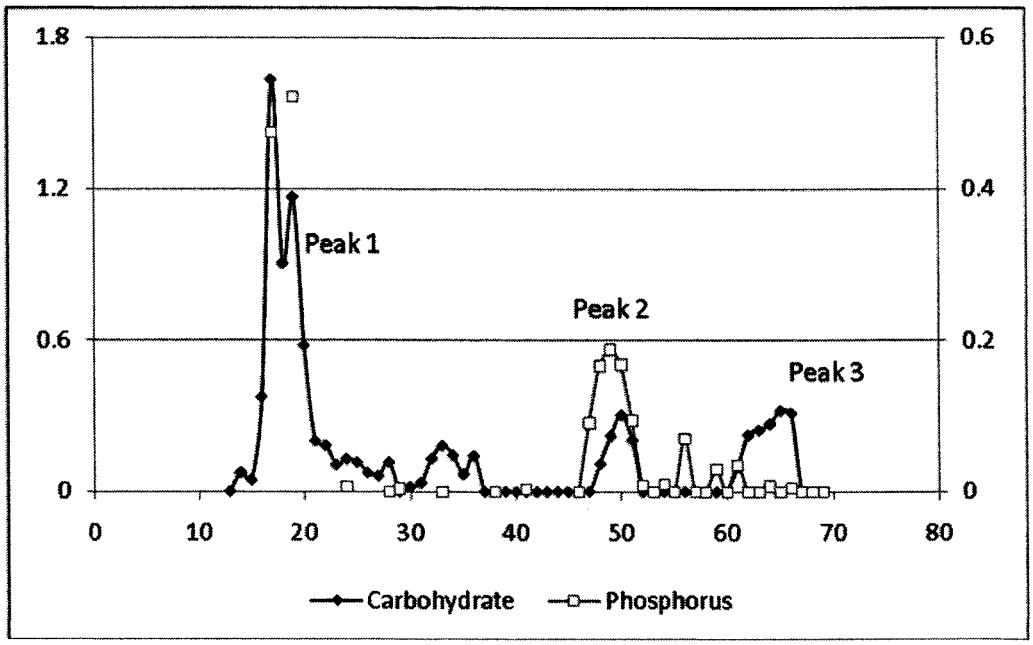

Figure V.6. HIC profile for the purification of a crude phenol extract of FPLC run 6 for *S. coelicolor* M145 . The crude extract was loaded to the column with equilibration buffer until fraction 12, after which gradient elution with an increasing concentration of propanol was begun. Column fractions (4 mL) were analyzed for carbohydrate.

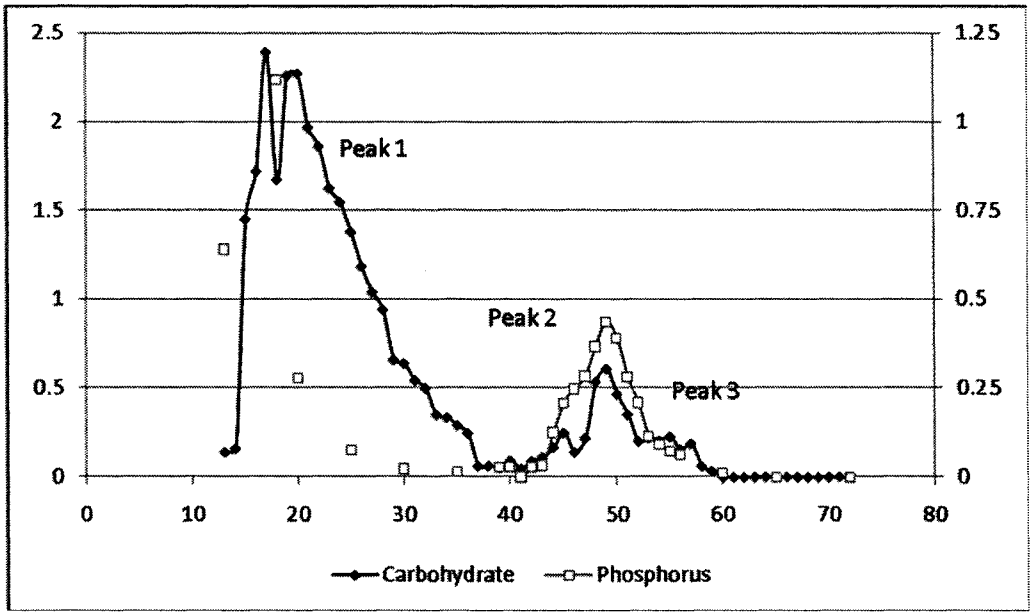

Figure V.7. HIC profile for the purification of a crude phenol extract of FPLC run 8 for *S. coelicolor* M145 . The crude extract was loaded to the column with equilibration buffer until fraction 12, after which gradient elution with an increasing concentration of propanol was begun. Column fractions (4 mL) were analyzed for carbohydrate.

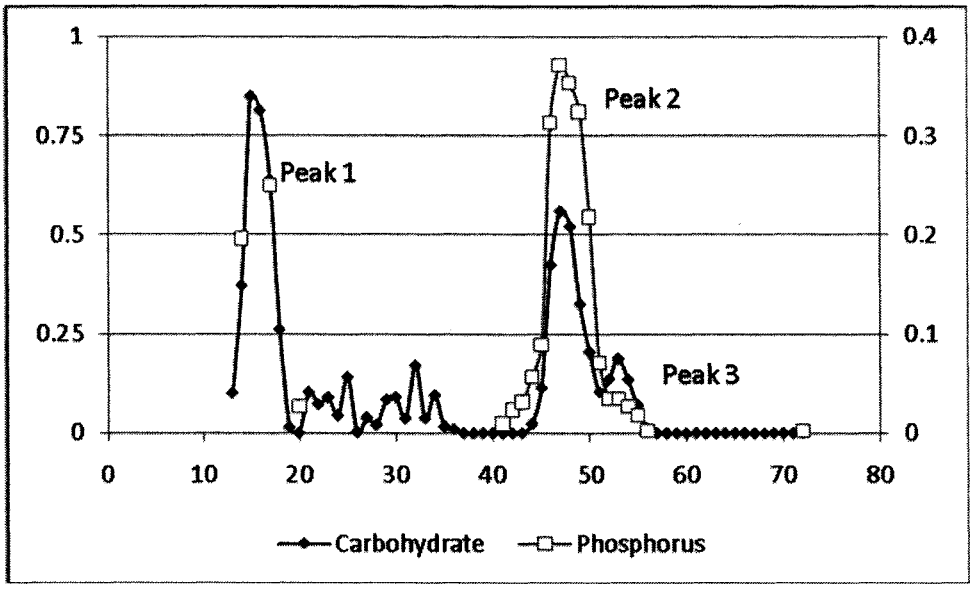

Figure V.8. HIC profile for the purification of a crude phenol extract of FPLC run 9 for *S. coelicolor* M145 . The crude extract was loaded to the column with equilibration buffer until fraction 12, after which gradient elution with an increasing concentration of propanol was begun. Column fractions (4 mL) were analyzed for carbohydrate.

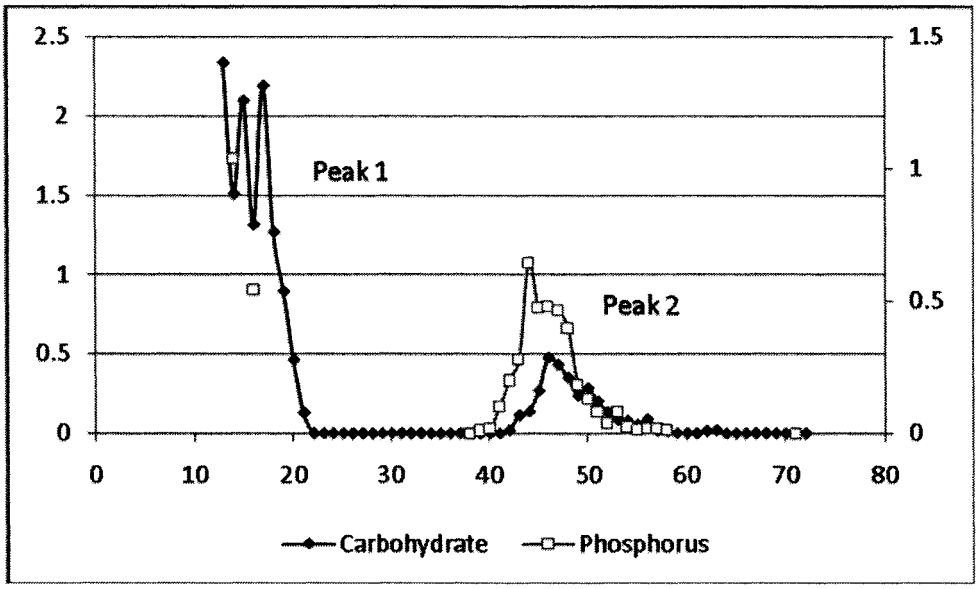

Figure V.9. HIC profile for the purification of a crude phenol extract of FPLC run 10 for *S. coelicolor* M145 . The crude extract was loaded to the column with equilibration buffer until fraction 12, after which gradient elution with an increasing concentration of propanol was begun. Column fractions (4 mL) were analyzed for carbohydrate.

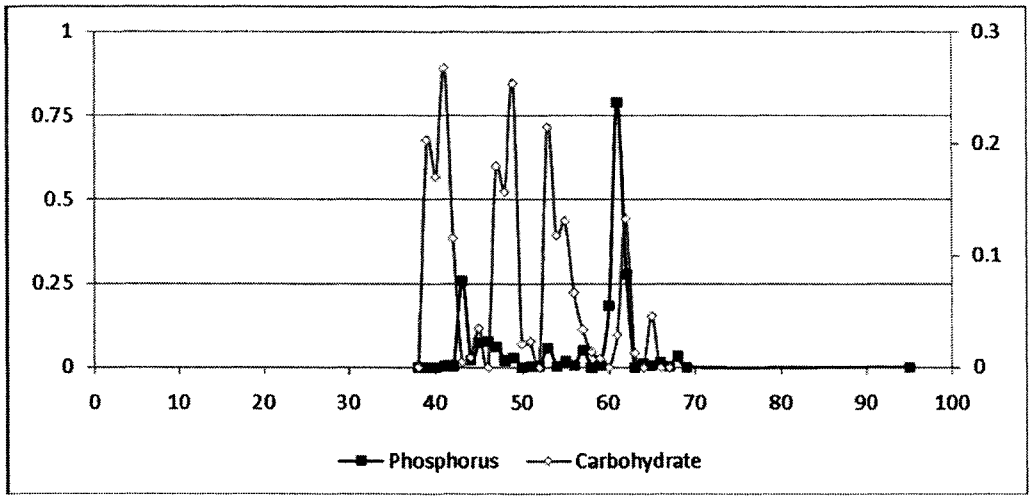

Figure V.10. Anion exchange chromatography profile of FPLC run 11 for *S. coelicolor* M145. The carbohydrate and phosphate assay was done with the fractions which shows positive reaction with anti-LTA in immune dot blotting .

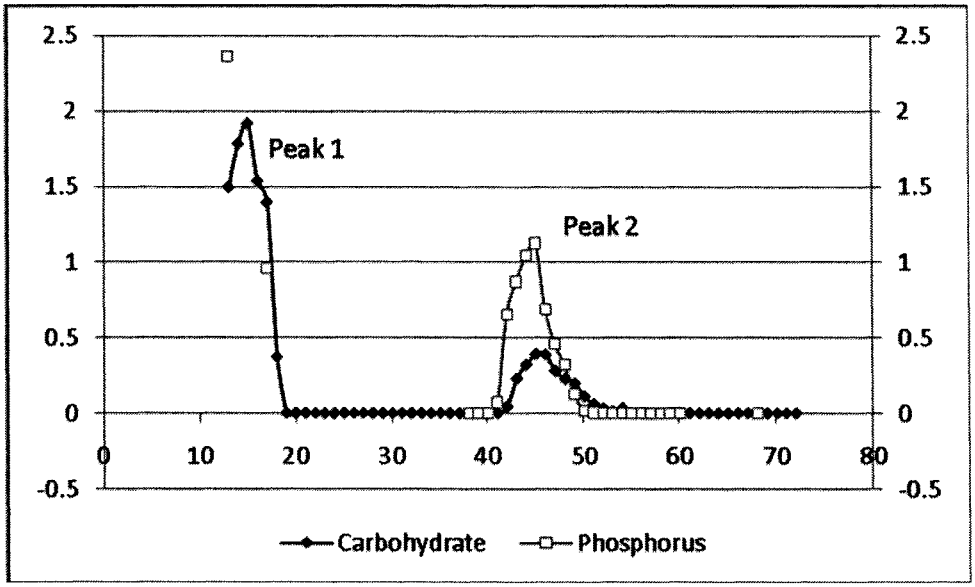

Figure V.11. HIC profile for the purification of a crude phenol extract of FPLC run 11 for *S. coelicolor* M145. Delipidation was done prior to extraction. The crude extract was loaded to the column with equilibration buffer until fraction 12, after which gradient elution with an increasing concentration of propanol was begun. Column fractions (4 mL) were analyzed for carbohydrate.

Appendix Six

Streptomyces DSM 40537

Strain taken for Figure 7.5 Phylogenetic tree from RDP II:

Streptomyces type strains:

- S000000827 Streptomyces arenae (T); ISP 5293; AJ399485
- S000001636 Streptomyces odorifer (T); DSM 40347T; Z76682
- S000001688 Streptomyces somaliensis (T); DSM 40738; AJ007403
- S000001861 Streptomyces kasugaensis (T); M338-M1; AB024441
- S000001870 Streptomyces tauricus (T); JCM 4837; AB045879
- S000002035 Streptomyces chartreusis (T); ISP 5085; AJ399468
- S000002044 Streptomyces virginiae (T); IFO 12827; D85123
- S000002270 Streptomyces mirabilis (T); ATCC27447; AF112180
- S000002402 Streptomyces felleus (T); DSM 40130T; Z76681
- S000002613 Streptomyces venezuelae (T); JCM 4526; AB045890
- S000002792 Streptomyces sparsogenes (T); NRRL 2940T; AJ391817
- S000003179 Streptomyces thermocoprophilus (T); B19; AJ007402
- S000003569 Streptomyces iakyrus (T); ISP 5482; AJ399489
- S000003965 Streptomyces coerulescens (T); ISP 5146; AJ399462
- S000003980 Streptomyces violarus (T); ISP 5205; AJ399477
- S000004208 Streptomyces clavuligerus (T); JCM 4710; AB045869
- S000004385 Streptomyces janthinus (T); ISP 5206; AJ399478
- S000004441 Streptomyces stelliscabiei (T); CFBP4521; AJ007429
- S000004852 Streptomyces cangkringensis (T); D13P3 (S23); AJ391831
- S000005155 Streptomyces griseorubiginosus (T); ISP 5469; AJ399488
- S000005383 Streptomyces platensis (T); JCM 4662; AB045882
- S000005538 Streptomyces afghaniensis (T); ISP 5228; AJ399483
- S000005539 Streptomyces albidoflavus (T); DSM 40455T; Z76676
- S000005595 Streptomyces europaeiscabiei (T); CFBP4497; AJ007423
- S000005612 Streptomyces rhizosphaericus (T); A10P1 (S27); AJ391834
- S000005908 Streptomyces cinnabarinus (T); ISP 5467; AJ399487
- S000005910 Streptomyces intermedius (T); DSM 40372T; Z76686
- S000005912 Streptomyces lanatus (T); ISP 5090; AJ399469
- S000006100 Streptomyces armeniacus (T); JCM 3070; clone21; AB018092
- S000006303 Streptomyces thermoalcalitolerans (T); TA56 (Type strain); AJ000284
- S000006665 Streptomyces limosus (T); DSM 40131T; Z76679
- S000006679 Streptomyces violaceus (T); ISP 5209; AJ399480
- S000007083 Streptomyces indonesiensis (T); A4R2 (S34); AJ391835
- S000007214 Streptomyces rimosus subsp. Rimosus (T); JCM 4667; AB045883
- S000007833 Streptomyces pseudovenezuelae (T); ISP 5212; AJ399481
- S000008561 Streptomyces canescens (T);

DSM 40001T; Z76684

☐ S000008719 Streptomyces phaeochromogenes (T); DSM 40073; AF500071

☐ S000008947 Streptomyces macrosporus (T); DSM 41449 (type strain); Z68099

☐ S000008956 Streptomyces thermovulgaris (T); DSM 40444 (type strain); Z68094

☐ S000008957 Streptomyces violaceusniger (T); NRRL B-1476T; AJ391822

☐ S000009302 Streptomyces longisporus (T); ISP 5166; AJ399475

☐ S000009303 Streptomyces luteogriseus (T); ISP 5483; AJ399490

☐ S000009305 Streptomyces melanosporofaciens (T); NRRL B-12234T; AJ271887

☐ S000009787 Streptomyces puniciscabiei (T); S77; AF361785

☐ S000010498 Streptomyces yogyakartensis (T); C4R3 (S3); AJ391827

☐ S000010499 Streptomyces asiaticus (T); A14P1 (S17); AJ391830

☐ S000010871 Streptomyces hawaiiensis (T); ISP 5042; AJ399466

☐ S000010876 Streptomyces roseoviolaceus (T); ISP 5277; AJ399484

☐ S000011639 Streptomyces coelicolor (T); DSM 40233T; Z76678

☐ S000011833 Streptomyces griseus (T); JCM 4623; AB045872

☐ S000012014 Streptomyces coeruleofuscus (T); ISP 5144; AJ399473

☐ S000012018 Streptomyces gougerotii (T); DSM 40324T; Z76687

☐ S000012074 Streptomyces reticuliscabiei (T); CFBP4531; AJ007428

☐ S000012108 Streptomyces luridiscabiei (T); S63; AF361784

☐ S000012433 Streptomyces thermolineatus (T); DSM 41451 (type strain); Z68097

☐ S000013940 Streptomyces megasporus (T); DSM 41476 (type strain); Z68100

☐ S000014552 Streptomyces griseus (T); ATCC51928; AF112160

☐ S000015759 Streptomyces fumanus (T); ISP 5154; AJ399463

☐ S000015773 Streptomyces thermoviolaceus subsp. Thermoviolaceus (T); DSM 40443 (type strain); Z68096

☐ S000015944 Streptomyces albulus (T); IMC S-0802 (ISP5492); AB024440

☐ S000016102 Streptomyces rutgersensis subsp. Rutgersensis (T); DSM 40077T; Z76688

☐ S000016475 Streptomyces lydicus (T); ATCC 25470; Y15507

☐ S000021803 Streptomyces albofaciens (T); JCM 4342; AB045880

☐ S000022092 Streptomyces peucetius (T); JCM 9920; AB045887

☐ S000022304 Streptomyces thermodiastaticus (T); JCM 4840; clone121; AB018095

☐ S000022378 Streptomyces javensis (T); B22P3 (B26); AJ391833

☐ S000084736 Streptomyces albogriseolus (T); type strain: NRRL B-1305 = DSM 40003; AJ494865

☐ S000085577 Streptomyces flavogriseus (T); type strain: CBS 101.34 = DSM 40323; AJ494864

☐ S000126814 Streptomyces purpurascens (T); DSM 40310, Type strain; AJ310925

☐ S000128654 Streptomyces cyaneus (T); DSM 40108, Type strain; AJ310927

☐ S000129856 Streptomyces coeruleorubidus (T); ISP 5145; AJ306622

☐ S000129857 Streptomyces resistomycificus (T); DSM 40133, Type strain; AJ310926

☐ S000129979 Streptomyces hygroscopicus subsp. Hygroscopicus (T); NRRL 2387T; AJ391820

☐ S000131089 Streptomyces griseochromogenes (T); type strain DSM 40499; AJ310923

☐ S000134752 Streptomyces jietaisiensis (T); FXJ46; AY314783

☐ S000142900 Streptomyces tuirus (T); ICSSB 1017; AF503493

☐ S000143178 Streptomyces coelescens (T); ICSSB 1021; AF503496

☐ S000143381 Streptomyces humiferus (T); DSM 43030; AF503491

☐ S000143382 Streptomyces rubrogriseus (T); DSM 41477; AF503501

☐ S000143706 Streptomyces violaceolatus (T); ICSSB 1022; AF503497

S000266729 Streptomyces rutgersensis subsp. Castelarensis (T); DSM 40830; AY508511

S000269433 Streptomyces ciscaucasicus (T); DSM 40275; AY508512

S000270388 Streptomyces chrestomyceticus (T); type strain: DSM 40545; AJ621609

S000270574 Streptomyces griseocarneus (T); DSM40004; X99943

S000270582 Streptomyces albus subsp. Albus (T); type strain: DSM 40313; AJ621602

S000270583 Streptomyces erumpens (T); type strain: DSM 40941; AJ621603

S000270584 Streptomyces niger (T); type strain: DSM 43049; AJ621607

S000270785 Streptomyces violens (T); type strain: DSM 40597; AJ621605

S000270786 Streptomyces sclerotialus (T); type strain: DSM 43032; AJ621608

S000271004 Streptomyces purpurogeneiscleroticus (T); type strain: DSM 43156; AJ621604

S000271215 Streptomyces chattanoogensis (T); type strain: DSM 40002; AJ621611

S000271817 Streptomyces olivaceiscleroticus (T); type strain: DSM 40595; AJ621606

S000271818 Streptomyces rimosus subsp. Paromomycinus (T); type strain: DSM 41429; AJ621610

S000271819 Streptomyces tubercidicus (T); type strain: DSM 40261; AJ621612

S000271820 Streptomyces catenulae (T); type strain: DSM 40258; AJ621613

S000357416 Streptomyces hebeiensis (T); YIM 001; AY277529

S000381275 Streptomyces mashuensis (T); DSM40221; X79323

S000381276 Streptomyces bluensis (T); ISP5564; X79324

S000381283 Streptomyces bikiniensis (T); DSM40581; X79851

S000381284 Streptomyces galbus (T); DSM40089; X79852

S000381286 Streptomyces lincolnensis (T); NRRL2936; X79854

S000381288 Streptomyces caelestis (T); NRRL 2418; X80824

S000381289 Streptomyces subrutilus (T); DSM 40445; X80825

S000388805 Streptomyces scopiformis (T); A25; AF184081

S000391769 Streptomyces thermospinosisporus (T); AT10; AF333113

S000391846 Streptomyces yatensis (T); DSM 41771T; AF336800

S000392042 Streptomyces yunnanensis (T); YIM 41004; AF346818

S000392846 Streptomyces beijiangensis (T); YIM6; AF385681

S000394172 Streptomyces mexicanus (T); CH-M-1035; AF441168

S000394398 Streptomyces speibonae (T); PK-Blue; AF452714

S000394435 Streptomyces lateritius (T); AS4.1427; JCM4389T; AF454764

S000395644 Streptomyces sanglieri (T); A5843; AY094363

S000395648 Streptomyces laceyi (T); c7654; AY094367

S000395649 Streptomyces aureus (T); B7319; AY094368

S000395651 Streptomyces olivochromogenes (T); DSM 40451; AY094370

S000405816 Streptomyces aureofaciens (T); IMET 43577; AY289116

S000417792 Streptomyces africanus (T); CPJVR-H; AY208912

S000426477 Streptomyces bangladeshensis (T); AAB-4; AY750056

S000428899 Streptomyces yeochonensis (T); CN 732; AF101415

S000429250 Streptomyces malaysiensis (T); ATB-11; AF117304

S000436160 Streptomyces ambofaciens (T); M27245

S000438871 Streptomyces thermocarboxydovorans (T); DSM 44296; U94489

S000438872 Streptomyces thermocarboxydus (T); DSM 44293; U94490

S000439340 Streptomyces scabiei (T); ATCC49173; D63862

S000439343 Streptomyces acidiscabies (T); ATCC49003; D63865

S000439345 Streptomyces diastatochromogenes (T); ATCC12309; D63867

S000439346 Streptomyces bottropensis (T); ATCC25435; D63868

S000439347 Streptomyces neyagawaensis (T); ATCC27449; D63869

S000439348 Streptomyces eurythermus (T); ATCC14975; D63870

S000439349 Streptomyces sampsonii (T); ATCC25495; D63871

S000439350 Streptomyces griseus (T); ATCC25497; D63872

S000439351 Streptomyces tendae (T); ATCC19812; D63873

S000469290 Streptomyces scabrisporus (T); KM-4927; AB030585

S000469461 Streptomyces avermitilis (T); MA-4680; AB078897

S000473202 Streptomyces koyangensis (T); VK-A60; AY079156

S000481156 Streptomyces sp. 1307 (T); AY876940

S000481157 Streptomyces sp. 13c15 (T); 13C15; AY876941

S000481158 Streptomyces sp. 701 (T); AY876942

S000481159 Streptomyces sp. 1413 (T); AY876943

S000484619 Streptomyces ferralitis (T); SFOp68; AY262826

S000484976 Streptomyces glauciniger (T); FXJ14; AY314782

S000544199 Streptomyces atroolivaceus (T); type strain:LMG 19306; AJ781320

S000544200 Streptomyces griseoincarnatus (T); type strain:LMG 19316; AJ781321

S000544201 Streptomyces griseoflavus (T); type strain:LMG 19344; AJ781322

S000544202 Streptomyces massasporeus (T); type strain:LMG 19362; AJ781323

S000544207 Streptomyces erythrogriseus (T); type strain:LMG 19406; AJ781328

S000544208 Streptomyces graminofaciens (T); type strain:LMG 19892; AJ781329

S000544209 Streptomyces globosus (T); type strain:LMG 19896; AJ781330

S000544210 Streptomyces fulvorobeus (T); type strain:LMG 19901; AJ781331

S000544211 Streptomyces glaucus (T); type strain:LMG 19902; AJ781332

S000544212 Streptomyces graminearus (T); type strain:LMG 19904; AJ781333

S000544213 Streptomyces flavovariabilis (T); type strain:LMG 19905; AJ781334

S000544214 Streptomyces gobitricini (T); type strain:LMG 19910; AJ781335

S000544215 Streptomyces lavendofoliae (T); type strain:LMG 19935; AJ781336

S000544216 Streptomyces lilacinus (T); type strain:LMG 19937; AJ781337

S000544217 Streptomyces mashuensis (T); type strain:LMG 19939; AJ781338

S000544219 Streptomyces inusitatus (T); type strain:LMG 19955; AJ781340

S000544221 Streptomyces laurentii (T); type strain:LMG 19959; AJ781342

S000544222 Streptomyces heliomycini (T); type strain:LMG 19960; AJ781343

S000544223 Streptomyces indiaensis (T); type strain:LMG 19961; AJ781344

S000544224 Streptomyces olivoreticuli subsp. Olivoreticuli (T); type strain:LMG 20050; AJ781345

S000544225 Streptomyces lilacinus (T); type strain:LMG 20059; AJ781346

S000544226 Streptomyces malachitofuscus (T); type strain:LMG 20067; AJ781347

S000544227 Streptomyces abikoensis (T); type strain:LMG 20072; AJ781348

S000544230 Streptomyces libani subsp. Rufus (T); type strain:LMG 20087; AJ781351

S000544231 Streptomyces lomondensis (T); type strain:LMG 20088; AJ781352

S000544232 Streptomyces lienomycini (T); type strain:LMG 20091; AJ781353

S000544233 Streptomyces mediolani (T); type strain:LMG 20093; AJ781354

S000544234 Streptomyces nojiriensis (T); type strain:LMG 20094; AJ781355

- S000544235 Streptomyces longwoodensis (T); type strain:LMG 20096; AJ781356
- S000544236 Streptomyces mutomycini (T); type strain:LMG 20098; AJ781357
- S000544237 Streptomyces mauvecolor (T); type strain:LMG 20100; AJ781358
- S000544239 Streptomyces thioluteus (T); type strain:LMG 20253; AJ781360
- S000544241 Streptomyces tanashiensis (T); type strain:LMG 20274; AJ781362
- S000544245 Streptomyces rangoonensis (T); type strain:LMG 20295; AJ781366
- S000544246 Streptomyces torulosus (T); type strain:LMG 20305; AJ781367
- S000544247 Streptomyces sporocinereus (T); type strain:LMG 20311; AJ781368
- S000544248 Streptomyces sporoclivatus (T); type strain:LMG 20312; AJ781369
- S000544249 Streptomyces spororaveus (T); type strain:LMG 20313; AJ781370
- S000544250 Streptomyces variegatus (T); type strain:LMG 20315; AJ781371
- S000544251 Streptomyces viridobrunneus (T); type strain:LMG 20317; AJ781372
- S000544253 Streptomyces violaceorubidus (T); type strain:LMG 20319; AJ781374
- S000544254 Streptomyces netropsis (T); type strain:LMG 20320; AJ781375
- S000544255 Streptomyces spinoverrucosus (T); type strain:LMG 20321; AJ781376
- S000544256 Streptomyces pulveraceus (T); type strain:LMG 20322; AJ781377
- S000544257 Streptomyces cinnamoneus (T); type strain:LMG 20324; AJ781378
- S000544258 Streptomyces rameus (T); type strain:LMG 20326; AJ781379
- S000544259 Streptomyces tricolor (T); type strain:LMG 20328; AJ781380
- S000544262 Streptomyces aurantiacus (T); type strain:LMG 19358; AJ781383
- S000544264 Streptomyces glomeratus (T); type strain: LMG 19903; AJ781754
- S000546611 Streptomyces sodiiphilus (T); YIM 80305; AY236339
- S000549403 Streptomyces pharetrae (T); CZA14; AY699792
- S000570539 Streptomyces olivoverticillatus (T); type strain:LMG 20277; AJ781363
- S000627041 Streptomyces cheonanensis (T); VC-A46; AY822606

Out group:

- S000134750 Streptacidiphilus jiangxiensis (T); 33214; AY314780
- S000428468 Streptacidiphilus neutrinimicus (T); JL 206; DSM 41755; AF074410
- S000428470 Streptacidiphilus carbonis (T); JL 415; DSM 41754; AF074412
- S000428473 Streptacidiphilus albus (T); JL 83; DSM 41753; AF074415
- S000614212 Streptacidiphilus oryzae (T); TH49; DQ208700

CLUSTAL 2.0.5 Multiple Sequence Alignments

Sequence format is Pearson
Sequence 1: gi|90960603|dbj|AB184782.1| 1478 bp
Sequence 2: gi|90960594|dbj|AB184773.1| 1478 bp
Sequence 3: gi|90960220|dbj|AB184404.1| 1475 bp

comparing
paramArg[setSeqNoRange]= off
comparing
Start of Pairwise alignments
Aligning...

Sequences (1:2) Aligned. Score: 100
Sequences (1:3) Aligned. Score: 100
Sequences (2:3) Aligned. Score: 100
Guide tree file created: [/ebi/extserv/clustalw-work/interactive/2008051202/clustalw2-20080512-02485193.dnd]

There are 2 groups
Start of Multiple Alignment

Aligning...
Group 1: Sequences: 2 Score:28025
Group 2: Sequences: 3 Score:28053
Alignment Score 32934

CLUSTAL-Alignment file created [/ebi/extserv/clustalw-work/interactive/2008051202/clustalw2-20080512-02485193.aln]

CLUSTAL 2.0.5 multiple sequence alignment

```
gi|90960603|dbj|AB184782.1|
ACGAACGCTGGCGGCGTGCTTAACACATGCAAGTCGAACGATGAACCGCT 50
gi|90960220|dbj|AB184404.1|    -CGAACGCTGGCGGCGTGCTTAACACATGCAAGTCGAACGATGAACCGCT
49
gi|90960594|dbj|AB184773.1|
ACGAACGCTGGCGGCGTGCTTAACACATGCAAGTCGAACGATGAACCGCT 50
                  **************************************************

gi|90960603|dbj|AB184782.1|
TTCGGGCGGGGATTAGTGGCGAACGGGTGAGTAACACGTGGGCAATCTGC 100
gi|90960220|dbj|AB184404.1|
TTCGGGCGGGGATTAGTGGCGAACGGGTGAGTAACACGTGGGCAATCTGC 99
gi|90960594|dbj|AB184773.1|
TTCGGGCGGGGATTAGTGGCGAACGGGTGAGTAACACGTGGGCAATCTGC 100
                  **************************************************

gi|90960603|dbj|AB184782.1|    CCTGCACTCTGGGACAAGCCCTGGAAACGGGGTCTAATACCGGATATGAC
150
gi|90960220|dbj|AB184404.1|    CCTGCACTCTGGGACAAGCCCTGGAAACGGGGTCTAATACCGGATATGAC
149
gi|90960594|dbj|AB184773.1|    CCTGCACTCTGGGACAAGCCCTGGAAACGGGGTCTAATACCGGATATGAC
150
                  **************************************************

gi|90960603|dbj|AB184782.1|    CGTCTGCCGCATGGTGGATGGTGTAAAGCTCCGGCGGTGCAGGATGAGCC
200
gi|90960220|dbj|AB184404.1|    CGTCTGCCGCATGGTGGATGGTGTAAAGCTCCGGCGGTGCAGGATGAGCC
199
gi|90960594|dbj|AB184773.1|    CGTCTGCCGCATGGTGGATGGTGTAAAGCTCCGGCGGTGCAGGATGAGCC
200
                  **************************************************

gi|90960603|dbj|AB184782.1|    CGCGGCCTATCAGCTTGTTGGTGAGGTAGTGGCTCACCAAGGCGACGACG
250
gi|90960220|dbj|AB184404.1|    CGCGGCCTATCAGCTTGTTGGTGAGGTAGTGGCTCACCAAGGCGACGACG
249
```

gi|90960594|dbj|AB184773.1| CGCGGCCTATCAGCTTGTTGGTGAGGTAGTGGCTCACCAAGGCGACGACG
250
****

gi|90960603|dbj|AB184782.1|
GGTAGCCGGCCTGAGAGGGCGACCGGCCACACTGGGACTGAGACACGGCC 300
gi|90960220|dbj|AB184404.1|
GGTAGCCGGCCTGAGAGGGCGACCGGCCACACTGGGACTGAGACACGGCC 299
gi|90960594|dbj|AB184773.1|
GGTAGCCGGCCTGAGAGGGCGACCGGCCACACTGGGACTGAGACACGGCC 300
****

gi|90960603|dbj|AB184782.1|
CAGACTCCTACGGGAGGCAGCAGTGGGGAATATTGCACAATGGGCGAAAG 350
gi|90960220|dbj|AB184404.1|
CAGACTCCTACGGGAGGCAGCAGTGGGGAATATTGCACAATGGGCGAAAG 349
gi|90960594|dbj|AB184773.1|
CAGACTCCTACGGGAGGCAGCAGTGGGGAATATTGCACAATGGGCGAAAG 350
****

gi|90960603|dbj|AB184782.1| CCTGATGCAGCGACGCCGCGTGAGGGATGACGGCCTTCGGGTTGTAAACC
400
gi|90960220|dbj|AB184404.1| CCTGATGCAGCGACGCCGCGTGAGGGATGACGGCCTTCGGGTTGTAAACC
399
gi|90960594|dbj|AB184773.1| CCTGATGCAGCGACGCCGCGTGAGGGATGACGGCCTTCGGGTTGTAAACC
400
****

gi|90960603|dbj|AB184782.1|
TCTTTCAGCAGGGAAGAAGCGAAAGTGACGGTACCTGCAGAAGAAGCGCC 450
gi|90960220|dbj|AB184404.1|
TCTTTCAGCAGGGAAGAAGCGAAAGTGACGGTACCTGCAGAAGAAGCGCC 449
gi|90960594|dbj|AB184773.1|
TCTTTCAGCAGGGAAGAAGCGAAAGTGACGGTACCTGCAGAAGAAGCGCC 450
****

gi|90960603|dbj|AB184782.1|
GGCTAACTACGTGCCAGCAGCCGCGGTAATACGTAGGGCGCAAGCGTTGT 500
gi|90960220|dbj|AB184404.1|
GGCTAACTACGTGCCAGCAGCCGCGGTAATACGTAGGGCGCAAGCGTTGT 499
gi|90960594|dbj|AB184773.1|
GGCTAACTACGTGCCAGCAGCCGCGGTAATACGTAGGGCGCAAGCGTTGT 500
****

gi|90960603|dbj|AB184782.1| CCGGAATTATTGGGCGTAAAGAGCTCGTAGGCGGCTTGTCACGTCGGTTG
550
gi|90960220|dbj|AB184404.1| CCGGAATTATTGGGCGTAAAGAGCTCGTAGGCGGCTTGTCACGTCGGTTG
549
gi|90960594|dbj|AB184773.1| CCGGAATTATTGGGCGTAAAGAGCTCGTAGGCGGCTTGTCACGTCGGTTG
550
****

gi|90960603|dbj|AB184782.1|
TGAAAGCCCGGGGCTTAACCCCGGGTCTGCAGTCGATACGGGCAGGCTAG 600
gi|90960220|dbj|AB184404.1|
TGAAAGCCCGGGGCTTAACCCCGGGTCTGCAGTCGATACGGGCAGGCTAG 599
gi|90960594|dbj|AB184773.1|
TGAAAGCCCGGGGCTTAACCCCGGGTCTGCAGTCGATACGGGCAGGCTAG 600
****

gi|90960603|dbj|AB184782.1|
AGTTCGGTAGGGGAGATCGGAATTCCTGGTGTAGCGGTGAAATGCGCAGA 650
gi|90960220|dbj|AB184404.1|
AGTTCGGTAGGGGAGATCGGAATTCCTGGTGTAGCGGTGAAATGCGCAGA 649
gi|90960594|dbj|AB184773.1|
AGTTCGGTAGGGGAGATCGGAATTCCTGGTGTAGCGGTGAAATGCGCAGA 650
****

gi|90960603|dbj|AB184782.1|
TATCAGGAGGAACACCGGTGGCGAAGGCGGATCTCTGGGCCGATACTGAC 700

```
gi|90960220|dbj|AB184404.1|
TATCAGGAGGAACACCGGTGGCGAAGGCGGATCTCTGGGCCGATACTGAC 699
gi|90960594|dbj|AB184773.1|
TATCAGGAGGAACACCGGTGGCGAAGGCGGATCTCTGGGCCGATACTGAC 700
                  **************************************************

gi|90960603|dbj|AB184782.1|
GCTGAGGAGCGAAAGCGTGGGGAGCGAACAGGATTAGATACCCTGGTAGT 750
gi|90960220|dbj|AB184404.1|
GCTGAGGAGCGAAAGCGTGGGGAGCGAACAGGATTAGATACCCTGGTAGT 749
gi|90960594|dbj|AB184773.1|
GCTGAGGAGCGAAAGCGTGGGGAGCGAACAGGATTAGATACCCTGGTAGT 750
                  **************************************************

gi|90960603|dbj|AB184782.1|   CCACGCCGTAAACGGTGGGCACTAGGTGTGGGCAACATTCCACGTTGTCC
800
gi|90960220|dbj|AB184404.1|   CCACGCCGTAAACGGTGGGCACTAGGTGTGGGCAACATTCCACGTTGTCC
799
gi|90960594|dbj|AB184773.1|   CCACGCCGTAAACGGTGGGCACTAGGTGTGGGCAACATTCCACGTTGTCC
800
                  **************************************************

gi|90960603|dbj|AB184782.1|
GTGCCGCAGCTAACGCATTAAGTGCCCCGCCTGGGGAGTACGGCCGCAAG 850
gi|90960220|dbj|AB184404.1|
GTGCCGCAGCTAACGCATTAAGTGCCCCGCCTGGGGAGTACGGCCGCAAG 849
gi|90960594|dbj|AB184773.1|
GTGCCGCAGCTAACGCATTAAGTGCCCCGCCTGGGGAGTACGGCCGCAAG 850
                  **************************************************

gi|90960603|dbj|AB184782.1|
GCTAAAACTCAAAGGAATTGACGGGGGCCCGCACAAGCGGCGGAGCATGT 900
gi|90960220|dbj|AB184404.1|
GCTAAAACTCAAAGGAATTGACGGGGGCCCGCACAAGCGGCGGAGCATGT 899
gi|90960594|dbj|AB184773.1|
GCTAAAACTCAAAGGAATTGACGGGGGCCCGCACAAGCGGCGGAGCATGT 900
                  **************************************************

gi|90960603|dbj|AB184782.1|   GGCTTAATTCGACGCAACGCGAAGAACCTTACCAAGGCTTGACATACACC
950
gi|90960220|dbj|AB184404.1|   GGCTTAATTCGACGCAACGCGAAGAACCTTACCAAGGCTTGACATACACC
949
gi|90960594|dbj|AB184773.1|   GGCTTAATTCGACGCAACGCGAAGAACCTTACCAAGGCTTGACATACACC
950
                  **************************************************

gi|90960603|dbj|AB184782.1|   GGAAACGTCTGGAGACAGGCGCCCCCTTGTGGTCGGTGTACAGGTGGTGC
1000
gi|90960220|dbj|AB184404.1|   GGAAACGTCTGGAGACAGGCGCCCCCTTGTGGTCGGTGTACAGGTGGTGC
999
gi|90960594|dbj|AB184773.1|   GGAAACGTCTGGAGACAGGCGCCCCCTTGTGGTCGGTGTACAGGTGGTGC
1000
                  **************************************************

gi|90960603|dbj|AB184782.1|   ATGGCTGTCGTCAGCTCGTGTCGTGAGATGTTGGGTTAAGTCCCGCAACG
1050
gi|90960220|dbj|AB184404.1|   ATGGCTGTCGTCAGCTCGTGTCGTGAGATGTTGGGTTAAGTCCCGCAACG
1049
gi|90960594|dbj|AB184773.1|   ATGGCTGTCGTCAGCTCGTGTCGTGAGATGTTGGGTTAAGTCCCGCAACG
1050
                  **************************************************

gi|90960603|dbj|AB184782.1|   AGCGCAACCCTTGTCCCGTGTTGCCAGCAGGCCCTTGTGGTGCTGGGGAC
1100
gi|90960220|dbj|AB184404.1|   AGCGCAACCCTTGTCCCGTGTTGCCAGCAGGCCCTTGTGGTGCTGGGGAC
1099
gi|90960594|dbj|AB184773.1|   AGCGCAACCCTTGTCCCGTGTTGCCAGCAGGCCCTTGTGGTGCTGGGGAC
1100
                  **************************************************
```

gi|90960603|dbj|AB184782.1|
TCACGGGAGACCGCCGGGGTCAACTCGGAGGAAGGTGGGGACGACGTCAA 1150
gi|90960220|dbj|AB184404.1|
TCACGGGAGACCGCCGGGGTCAACTCGGAGGAAGGTGGGGACGACGTCAA 1149
gi|90960594|dbj|AB184773.1|
TCACGGGAGACCGCCGGGGTCAACTCGGAGGAAGGTGGGGACGACGTCAA 1150
****

gi|90960603|dbj|AB184782.1| GTCATCATGCCCCTTATGTCTTGGGCTGCACACGTGCTACAATGGCCGGT
1200
gi|90960220|dbj|AB184404.1| GTCATCATGCCCCTTATGTCTTGGGCTGCACACGTGCTACAATGGCCGGT
1199
gi|90960594|dbj|AB184773.1| GTCATCATGCCCCTTATGTCTTGGGCTGCACACGTGCTACAATGGCCGGT
1200
****

gi|90960603|dbj|AB184782.1|
ACAATGAGCTGCGATACCGTGAGGTGGAGCGAATCTCAAAAAGCCGGTCT 1250
gi|90960220|dbj|AB184404.1|
ACAATGAGCTGCGATACCGTGAGGTGGAGCGAATCTCAAAAAGCCGGTCT 1249
gi|90960594|dbj|AB184773.1|
ACAATGAGCTGCGATACCGTGAGGTGGAGCGAATCTCAAAAAGCCGGTCT 1250
****

gi|90960603|dbj|AB184782.1| CAGTTCGGATTGGGGTCTGCAACTCGACCCCATGAAGTCGGAGTCGCTAG
1300
gi|90960220|dbj|AB184404.1| CAGTTCGGATTGGGGTCTGCAACTCGACCCCATGAAGTCGGAGTCGCTAG
1299
gi|90960594|dbj|AB184773.1| CAGTTCGGATTGGGGTCTGCAACTCGACCCCATGAAGTCGGAGTCGCTAG
1300
****

gi|90960603|dbj|AB184782.1| TAATCGCAGATCAGCATTGCTGCGGTGAATACGTTCCCGGGCCTTGTACA
1350
gi|90960220|dbj|AB184404.1| TAATCGCAGATCAGCATTGCTGCGGTGAATACGTTCCCGGGCCTTGTACA
1349
gi|90960594|dbj|AB184773.1| TAATCGCAGATCAGCATTGCTGCGGTGAATACGTTCCCGGGCCTTGTACA
1350
****

gi|90960603|dbj|AB184782.1|
CACCGCCCGTCACGTCACGAAAGTCGGTAACACCCGAAGCCGGTGGCCCA 1400
gi|90960220|dbj|AB184404.1|
CACCGCCCGTCACGTCACGAAAGTCGGTAACACCCGAAGCCGGTGGCCCA 1399
gi|90960594|dbj|AB184773.1|
CACCGCCCGTCACGTCACGAAAGTCGGTAACACCCGAAGCCGGTGGCCCA 1400
****

gi|90960603|dbj|AB184782.1|
ACCCCTTGTGGGAGGGAGCTGTCGAAGGTGGGACTGGCGATTGGGACGAA 1450
gi|90960220|dbj|AB184404.1|
ACCCCTTGTGGGAGGGAGCTGTCGAAGGTGGGACTGGCGATTGGGACGAA 1449
gi|90960594|dbj|AB184773.1|
ACCCCTTGTGGGAGGGAGCTGTCGAAGGTGGGACTGGCGATTGGGACGAA 1450
****

gi|90960603|dbj|AB184782.1| GTCGTAACAAGGTAGCCGTACCGGAAGG 1478
gi|90960220|dbj|AB184404.1| GTCGTAACAAGGTAGCCGTACCGGAA-- 1475
gi|90960594|dbj|AB184773.1| GTCGTAACAAGGTAGCCGTACCGGAAGG 1478
****

Abbreviation

A

ABC	ATP Binding Cassette
Act	Actinorhodin
AG	Arabinogalactan
APS	Ammonium persulfate
Ara	Arabinoside
Ara*f*	Arabinosyl furanosyl

B

BHI	Brain Heart Infusion media
BSA	Bovine Serum Albumine

C

$CaCl_2$	Calcium Chloride
CDP	Cytodine diphosphate
CDA	Calcium dependent antibiotic
CDS	Coding sequence
CHAP	3-[(3-chloroimidopropyl)dimethylammino]-1-propane sulfonate
CH_3OH	Methanol
$CHCl_3$	Chloroform
CL	Cardiolipin
CM	Cytoplasmic membrane
Cox1	Cytochrome-c-oxidase subunit 1
CTP	Cyotdine triphosphate

D

DA	Diamino acid
DAG	Diacyl glycerol
DAGAP	di-N-acetyl-glucosamine phosphate
D-Ala	D-Alanine
DIP	di-myo-inositol-phosphate
DPA	Decaprenylphosphoryl-D-Ara*f*
DPPR	5-phospho-α-D-ribose-1-phosphate
DPPG	Dipalmitoyl-sn-glycerol-3-phospho-1-glycerol
DPR	A-D-ribose-phophate-decaprenyl

E

EDTA	Ethylene diamine tetraacetic acid
EtBr	Ethidium bromide
ExPASY	Expert protein analysis system

F

$FeSO_4$	Ferus sulphate
FPLC	Flow-pressure liquid Chromatography

G

Gal*f*	Galactofuranosyl
Gal*p*	Galactopyranosyl
GBS	Group B Streptococcus
GC	Gas chromatography
GDPMP	GDP-mannose pyrophosphorylase
Glc-6-P	Glucose-6-phosphate
GluRS	Glutamyl-tRNA synthetase

Gly	Glycine
gm	Gram
GroP	Glycerol phosphate
GT-A	Glycosyl transferase A
GtaB	A-glucose-1-phosphate uridyl transferase

H

HCl	Hydrochloric acid
HIC	Hydrophobic interaction chromatography
HMW-PBPs	High molecular weight penicillin binding protein
H_2SO_4	Sulfuric acid

I

IAA	Iodoacetamide
IgM	Immunoglubulin M
IMP	Inositol monophosphatase
InlB	Internalin B
Ino	Inositol
Ino-1-P	Inositol-1-phosphate
IPS	Inoitol -3-phosphate synthase
IPTG	Isopropyl-β-D-thioglactopyranoside

K

KH_2PO_4	Potasium bi phosphate

L

L	Litre
LAM	Lipoarabinomannan
LB	Luria-Betani media

LCHO	Lipoglycan
LM	Lipomannan
LPS	Lipopolysaccharide
LPSN	List of Prokaryotic names with Standing in Nomenclature
LTA	Lipoteichoic acid

M

M	Molar
M1P	Mannose-1-phosphate
P6P	Mannose-6-phosphate
MA	Macroamphiphile
mL	Mili litre
Man*p*	Mannosspyranosyl
ManT	Mannosyl transferase
MCS	Multiple cloning site
Mg	Milligram
MG	Mannosyl glycerate
$MgCl_2$	Magnesium chloride
MgS	Mannosyl glycerate synthetase
$MgSO_4$	Magnesium sulfate
Mm	Milimolar
Mmy	Methlenomycin
MP	Membrane protein
MPG	Mannosyl-3-phosphoglycerate

N

NaCl	Sodium Chloride
NAcGlc	N-acetyl-glucosamine
NAcMur	N-acetyl-muramic acid
Na_2HPO_4	Sodium bi phosphate
NCBI	National centre for biotechnology information
$(NH_4)_2HPO_4$	Ammonium bi phosphate
$(NH_4)_2SO_4$	Ammonium sulphate
NMR	Nuclear magnetic resonance

O

ORF	Open reading frame

P

P_i	Phosphate
PA	Phosphatidic acid
PAGE	Polyacralamide gel electrophoresis
PBP	Penicillin binding protein
PBS	Phosphate buffer saline
PBST	Phosphate buffer saline Tween
PC	Phosphatidylcholine
PE	Phosphatidylethanolamine
PEG	Polyethylene glycol
PG	Peptidoglycan
PgcA	α-phosphoglucomutase
PGP	Phosphatidyl glycerol-3-phosphate
pgsA	Phosphatidyl inositol synthase

PI	Phosphatidyl inositol
PIM	Phosphatidyl inositol mannoside
PMI	Phosphomannose isomerise
PMM	Phosphomannomutase
poly(GlcGANac-1-P)	Poly(glucosy-N-acetylglactosamine-1-phosphate
PPM	Polyprenol-phosphate-mannose
pRpp	5-phosphoribose diphosphate
Ptd	Phosphatidyl
PtdG	Phosphatidyl glycerol
PTYG	Peptone-Tryptone-Yeast extract-Glucose media
PS	Phosphatidyl serine

R

RboP	Ribitol phosphate
RDP II	Ribosomal database project II
Red	tripyrrole undecylprodigiosin
rpm	Rotation per minute
RruLAM	*R. ruber* LAM

S

SCWP	Secondary cell wall polymer
SLG	S-layer glycoprotein
SLH	S-layer homology
S-N model	Singer-Nicolson model
SP	S-layer protein

T

TA	Teichoic acid

TAA	Trichloroacetic acid
TEMED	N,N,N',N'-Tetramethylethylenediamine; N,N,N',N'-Di-(dimethylamino)ethane
TGY	Tryptone-Glucose-Yeast extract media
TM	Tripticase syoa medium
Trp	Tryptone

U

UDP	Uridyl diphosphate

Y

YEME	Yeast extract-malt extract media

Z

$ZnSO_4$	Zinc sulphate

Others

µl	Micro litre
µg	Micro gram